The development of tissue explant and embryonic stem cell derived models to investigate the molecular and cellular mechanisms that coordinate vertebrate haematopoiesis and angiogenesis

Amanda Lisabeth Evans

Student Identification Number: 0924547

A thesis in partial fulfilment of the requirements of Anglia Ruskin University for the degree of *Doctor of Philosophy* by published work.

This research was carried out in the laboratories of the University of Cambridge at: The Department of Pathology, Tennis Court Road, Cambridge, CB2 1QP; The Wellcome Trust/Cancer Research UK Gurdon Institute, Tennis Court Road, Cambridge, CB2 1QP and The Division of Transfusion Medicine, Department of Haematology, University of Cambridge, NHSBT Cambridge Centre, Cambridge, CB2 0PT in collaboration with authors acknowledged in this thesis, funded by: The WHO Rockfeller Foundation Trust Grant No: RF99021/115; The British Heart Foundation; The Wellcome Trust; The National Institute for Health Research programme grant to NHSBT (RP-PG-0310-1002).

Submitted: September 2013

I Declaration

"I hereby declare that this submission is my own work and that, to the best of my knowledge and belief, it contains no material previously published or written by another person nor material which to a substantial extent has been accepted for the award of any other degree or diploma of the university or other institute of higher learning, except where due acknowledgment has been made in the text."

Signature ……

Name ……

Date ……

II Abstract

Understanding the processes that control the formation of blood (haematopoiesis), and blood vessels (vasculogenesis and angiogenesis) *in vivo* has huge clinical importance. The complex three-dimensional architecture of blood vessels is dynamic and aberrant regulation of either the growth or function of the vascular system may potentiate the spread of tumours, resulting in failure of physiological processes such as implantation and placental development, leading to a range of angiogenesis associated disorders for example diabetic retinopathy. Both embryonic and adult haematopoiesis are also three-dimensional, dynamic processes in which deregulation may result in blood disorders or leukaemia.

The experiments herein describe my contribution to investigations into the molecular mechanisms involved in haematopoiesis and angiogenesis over a period of approximately 15 years, taking advantage of technical advances as they became available and adapting them to specific cell models. For example, microarray technology has facilitated discovery of new pathways and transcripts implicated in normal and pathological angiogenesis; central to this mechanism is the role of vascular endothelial growth factor (VEGF), a mitogen specific to endothelial cells. Chromosome immunoprecipitation (ChIP) technology subsequently revealed pathways of early mesoderm formation and the importance of gastrulation in this process. Transcriptional targets of the T-box transcription factor *Brachyury* were subsequently determined.

Throughout this work, the human female reproductive tract provided a unique resource, as one of the rare sites of physiological angiogenesis with which to investigate endothelial cell biology and haematopoiesis. Embryonic stem cell-derived embryoid bodies subsequently proved to be an excellent model for the study of early blood vessel development in three dimensions (2003-5), and to follow early mesoderm development (2006-2010). Targets of *Brachyury* revealed the close association between blood vessel development, haematopoiesis and early mesoderm formation via a common haemangioblast precursor for blood and endothelial cell lineages.

Data gathered by myself, and colleagues, from gene expression and transcription factor analysis is now being used to create lineage codes or routemaps for differentiation of stem cells to mature cells *in-vitro* and it is now possible to produce mature megakaryocytes and erythrocytes *in vitro*. The current challenge is to produce fully functional human platelets and enucleated red blood cells. Combined with the use of autologous induced pluripotent stem cells (iPSCs) this makes patient-specific tailoring of cell-based therapies a real possibility.

Keywords: VEGF/Haemangioblast /*Brachyury*/ESC/iPSC

III Acknowledgements

This has been a long journey for me and but I have been lucky enough to work with a number of outstanding scientists and lovely people. Dr Andy Ryan was an early mentor who gave me a fascination with all aspects of molecular biology. At the Rosie three people stand out Dr Andrew Sharkey, Professor Cristin Print and Professor Steve Charnock-Jones. Jim Smith gave me a glimpse into the world of development as well as a master class in the lyrics of Bob Dylan. At the NHSBT Professor Willem Ouwehand, Dr Cedric Ghevaert and Dr Thomas Moreau, and all of Cedric's group with whom I now work closely. To you all, thankyou.

Two others were also responsible in different ways for bringing this to fruition Dr Peter Coussons who somehow believed in me and Dr Elizabeth Callery who first told me of the existence of the degree of *Doctor of Philosophy* by published work.

On a more personal level my everlasting gratitude to my dear parents who have stood by me in so many dark days, only they can tell what it was like to have a daughter fade away from them as a teenager and spend the rest of her life learning to live in the world again. Thanks to Alison, Dr Alison Forster, who shared many of those days when she was probably the stronger one, now as her health is failing I will try to be strong. Also to Mrs Diana Licence, for your friendship and support all these years especially for your strength through the wobbly bits of chemotherapy.

Finally, besides the amazing care I receive from the breast cancer team at Addenbrooks, I can't finish these acknowledgements without mentioning the late Professor of Medicine Ivor Mills (1921-2005) who refused to give up on me. Also, the late Simon Peter Smith (1957-1982) probably one of the few people who knew me truly before our world fell apart. Wish they could see this, not all their efforts were wasted.

"Spring rain is neither high nor low,

but the branches carrying flowers may be short or long"

(1225-1258, The Emperor Thai Tong, Vietnamese Tran Dynasty)

IV Abbreviations

ACH	Atypical Complex Hyperplasia
AE	Anterior endoderm
AIIMS	All India Institute of Medical Sciences
AGM	Aorta-gonad mesonephros
α^{33}P-UTP	[alpha-^{33}P] Uridine 5'-triphosphate
Ang1/2	Angiopoietins 1 and 2, ANGPT1/2
AP	Anterioposterior
APAF1	Apoptosis Protease Activating Factor 1
APC	Adenomatous Polyposis Coli
ARL2	ADP-ribosylation factor like 2
Axin 2	Conductin
BCIP	(5-bromo-4-chloro-3-indolyl-phosphate) is used with NBT
Bcl-2	B-cell lymphoma 2
BHF	British Heart Foundation
bFGF	basic Fibroblast Growth Factor
BMP4	Bone Morphogenetic Protein 4
BM purple	Chromogenic substrate for alkaline phosphatase, ready to use NBT/BCIP (Roche)
bp	base pairs
CD	Cluster of Differentiation, cell surface antigens
CD34	Hematopoietic Progenitor Cell Antigen
CD41a	Alpha integrin GPIIb/IIIa complex on platelets, megakaryocytes and acute megakaryoblastic leukemia cells
CD42b	Platelet GPIb alpha, glycoprotein Ib-alpha, platelet receptor for von Willebrand factor on endothelium and a marker of mature megakaryocytes
CD61	Integrin beta-3 (β3) forms a complex with CD41
CDH1	E-cadherin
cDNA	complementary Deoxyribonucleic acid
CFP	Cyan Fluorescent Protein
CFU-GM	Colony Forming Unit-Granulocyte/Monocyte

IV Abbreviations (continued)

ChIP-on-chip	Chromatin immunoprecipitation or location analysis combined with array technology
ChIP-seq	Chromatin immunoprecipitation combined with massively parallel DNA sequencing
CIP	Calf Intestinal Phosphatase
c-kit	Proto-oncogene, protein kinase Kit, CD117
CLP	Common Lymphoid Progenitor
CMP	Common Myeloid Progenitor
CMV	Cytomegalovirus
c-MYC	Avian Myelocytomatosis Viral Oncogene Homolog
COX2	Cyclooxygenase 2
cPLA2	cystolic phospholipase A2
Cy3-dUTP	Cyanine 3-2´-Deoxyuridine, 5´-Triphosphate
Cy5-dUTP	Cyanine 5-2´-Deoxyuridine, 5´-Triphosphate
DAB	3,3' Diaminobenzidine
DAPI	Diamidino-2-phenylindole
DKK1	Dickkopf 1
dpc	days post coitum
Dvl	Dishevelled
E	Embryonic day
EBs	Embryoid bodies
EC	Endothelial cell
ECM	Extracellular Cell Matrix
ELISA	Enzyme-linked immunosorbent assay
EMT	Epithelial to Mesenchymal Transition
EPCs	Endothelial progenitor cells, cultured from peripheral blood and used in reprogramming to iPSCs
EPO	Erythropoietin
ERa	Oestrogen Receptor alpha
ERb	Oestrogen Receptor beta
ERK	Extracellular signal-regulated protein kinases 1 and 2
ESCs	Embryonic Stem Cells

IV Abbreviations (continued)

hESCs	Human ESCs
ETS	E-twenty-six transcription factor family
FGF8	Fibroblast Growth Factor 8
FIGO	The International Federation of Gynaecology and Obstetrics
FITC	Fluorescein Isothiocyanate
Fli1	Friend leukaemia integration 1 transcription factor
Flt	Fms-like tyrosine kinase
Flk	Fetal liver kinase
FoxA2	Forkhead A2 transcription factor
FS	Forward Scatter (in flow cytometry related to cell size)
FSH	Follicle Stimulating Hormone
FZD1	Frizzled (Drosophila) homolog wnt receptor 1
GAPDH	Glyceraldehyde-3-phosphate dehydrogenase
GATA	Globin transcription factor
GFP	Green Fluorescent Protein
GO	Gene Ontology
GPS	Gray Platelet Syndrome
GRN	Gene Regulatory Network
GSK3β	Glycogen synthase kinase 3 beta
HeLa	The first human immortal cells from **He**nrietta **La**cks
HCG	Human Chorionic Gonadotropin
hESCs	human Embryonic Stem Cells
HIF-1a	Hypoxia Inducible Factor 1 alpha
HLA	Human Leucocyte Antigen
HPA	Human Platelet Antigen
hpf	hours post fertilization
HSC	Haematopoietic Stem Cells
HUVEC	Human Umbilical Vein Endothelial Cells
ICA	Independent Component Analysis
ICM	Inner cell mass
INT	2-(4-iodophenyl)-3-(4-nitrophenyl)-5-phenyltetrazolium chloride
IMAGE	Integrated Molecular Analysis of Genomes and their Expression

IV Abbreviations (continued)

IP	Immunoprecipitation
iPSC	induced Pluripotent Stem Cells
ISSN	International Standard Serial Number
ITG	Integrin
IUGR	Intrauterine growth
JAK/STAT3	Janus kinase 1/ Signal transducer and activator of transcription 3
JNK1	Jun-N terminal kinase
Kb	Kilobase
KDR	Kinase Domain Region
KLF4	Kruppel-like factor 4
LIF	Leukaemia inhibitory factor
LH	Luteinizing hormone
LY294002	A potent inhibitor of phosphoinositide 3-kinases
M2	Alternatively activated Macrophages
Mag	Magenta phosphate used with INT
MEFs	Mouse embryonic fibroblasts
Meis1	Meis homeobox 1
MEP	Megakaryocyte/erythoblast precursor
MK	Megakaryocyte
MMP	Matrix metalloproteinase
MPP	Multipotent progenitor cell
mESCs	Mouse ESCs
MRC	Medical Research Council
Msgn1	Mesogenin1
mRNA	messenger Ribonucleic acid
MVD	microvessel density
MYC	Avian Myelocytomatosis Viral Oncogene Homolog
NBT	(nitro blue tetrazolium) for the colorimetric detection of alkaline phosphatase
NFKβ	Nuclear factor of kappa light polypeptide gene enhancer in B-cells
NHSBT	National Health Service Blood and Transplant
NIK	NFKβ inducing kinase

IV Abbreviations (continued)

NRP	Neuropilin
Oct4/Pou5F1	Octamer-binding transcription factor 4/POU domain, class 5, transcription factor 1
OP9	Mouse mesenchymal cell line
^{33}P-UTP	[alpha-33P] Uridine 5'-triphosphate (UTP)
p38	P38 mitogen-activated protein kinase
PBS	Phosphate Buffered Saline solution
PBMNC	Peripheral blood mononuclear cells
PDGF	Platelet-Derived Growth Factor
PDK1	Pyruvate Dehydrogenase Kinase, isozyme 1
PECAM1	Platelet Endothelial Cell Adhesion Molecule-1, CD31
PGR	Progesterone receptor
PI3K	Phosphatidylinositol-3 Kinase
PlGF	Placental Growth Factor
PKB	Protein kinase-B
PLPs	Platelet-like-particles
PPARα	Peroxisome proliferative activated receptor alpha
PPARβ	Peroxisome proliferative activated receptor gamma
qPCR	quantitative Polymerase Chain Reaction
RACK1	Receptor for Activated Kinase C1/ Gnb2l1
RARb	Retinoic acid receptor, beta
RBCs	Red blood cells
Rex1/Zfr42	RNA exonuclease 1 homolog
RMRG	Reproductive molecular research group
RNA	Ribonucleic acid
Robo 4	Roundabout 4
ROCK	Rho-associated protein kinase
RSAT	Regulatory Sequence Analysis Tools
RT-PCR	Reverse Transcriptase- Polymerase Chain Reaction
Rttn	Rotatin

IV Abbreviations (continued)

RU486	Mifepristone, 11β-[*p*-(Dimethylamino) phenyl]-17β-hydroxy-17-(1-propynyl) estra-4,9-dien-3-one, "RU" stands for Roussel-Uclaf, the name of the pharmaceutical corporation that makes the drug
RXR	Retinoic X Receptor
SAGE	Serial Analysis of Gene Expression
SAM	Significance of Microarrays
Scl/Tal1	T-cell acute lymphocytic leukaemia 1
Slit 2	Slit homolog 2, receptor for Robo 4
Smc	Smooth muscle cell
Sox 2	SRY (sex determining region Y)-box 2
SS	Side Scatter (in flow cytometry linked to the granularity or complexity of the particles)
STEMCCA	A human Cre-excisable Constitutive polycistronic vector encoding human Oct4, Klf4, Sox2, and c-Myc (OKSM)
TAMS	Tumour Associated Macrophages
TAR	Thrombocytopenia with Absent Radius, a rare blood disease with a reduction in the number of platelets and the absence of the radius bone in the forearm
TEK/Tie2	Tyrosine kinase receptor, endothelial/ Tunica Interna Endothelial Cell Kinase 2
TES	Transcription end site
TGFα	Transforming Growth Factor alpha
TGFβ	Transforming Growth Factor beta
TGM2	Transglutaminase 2
TNFα	Tumour Necrosis Factor alpha
T protein	The protein product of the *Brachyury* gene, a transcription factor
TPO	Thrombopoietin
TSS	Transcription start site
VAV2	Guanine nucleotide exchange factor
VE	Visceral endoderm
VEGF	Vascular endothelial growth factor
VEGFR	Vascular endothelial growth factor receptor

IV Abbreviations (continued)

VSMC	Vascular smooth muscle cells
WCE	Whole chromatin extract
WGA	Whole genome amplification
Wisp1	Wnt-1 inducible signalling pathway protein 1
Wnt	Wingless-type MMTV integration site family
Wt	Wildtype
Y27632	A selective ROCK inhibitor

V Table of contents PAGE

Synopsis **PAGE**

PAGE

PAGE

PAGE

VI Preface

After completing my initial training during the late 80's and early 90's at the Department of Zoology, University of Cambridge with the Cancer Research Campaign, Mammalian Cell DNA Repair Group, with Dr. Andy Ryan[a], I was already developing an interest in the blood and vascular system as one of the main routes of cancer metastasis. At the same time I acquired a thorough grounding in cellular and molecular biology skills.

In 1996 I moved to the Molecular Reproductive Medicine Group, then based solely at the Rosie Maternity Hospital Department of Obstetrics and Gyneacology[b]. The attraction was to set up a project using Serial Analysis of Gene Expression (SAGE) to investigate gene expression during placental development and in the cycling human endometrium. The group subsequently expanded to a second location at the Department of Pathology, Tennis Court Road, Cambridge, where most of the work on a tailored angiogenesis array took place, as well as the largescale production of an anti-VEGF antibody. The opportunity arose for a post with a new principal investigator, Dr Cris Print[c], in an offshoot from the group, which meant becoming a research assistant with responsibility for a project to develop 3D cultures of embryonic stem cells as a tool for the study of blood and vascular development. Despite having only a year of BHF funding remaining we were able to show that mouse embryoid bodies provide a means to investigate the effects of anti-angiogenic agents in a three dimensional environment. Vascular Endothelial Growth Factor (VEGF), a key player in both vasculogenesis and angiogenesis featured in much of the work.

Another move in 2005 to the Wellcome Trust/Cancer Research UK Gurdon Institute, and eventually to the MRC National Institute for Medical Research, Mill Hill, provided the opportunity to work with Dr. Jim Smith[d] whose expertise and interest is the molecular basis of mesoderm formation using two frog species, *Xenopus laevis* and *Xenopus tropicalis*, and the zebrafish, *Danio rerio* as model organisms. Jim was interested in building on recent work in the zebrafish by transferring to a mammalian system. Since vertebrate blood and vascular systems emerge with mesoderm induction this was an ideal opportunity to investigate the early stages of their formation. The transcription factor *Brachyury*, was central to this work.

In 2010, I returned to the investigation of human blood and vascular cells at the Division of Transfusion Medicine, Department of Hematology, University of Cambridge, NHSBT Cambridge, where utilization of the same mesodermal pathways involving *Brachyury* and VEGF provided the means by which we can now direct and manipulate the differentiation of haematopoietic progenitors into mature blood cells. This has made it possible to produce human platelet-like particles from human induced pluripotent stem cells (hiPSCs), bringing the technology a step closer to the *in-vitro* production of blood products for transfusion.

[a] Dr Anderson Ryan is now Senior Group Leader, Gray Institute for Radiation Oncology and Biology, University of Oxford, UK
anderson.ryan@oncology.ox.ac.uk

[b] Then led by Professor S.K.Smith DSc, FMedSci, now vice president Research Nanyang Technological University, Singapore
d-po@ntu.edu.sg

[c] Dr Cristin Print is now Associate Professor, Clinical Molecular Medicine & Pathology School of Medical Sciences, The University of Auckland , New Zealand
c.print@auckland.ac.nz

[d] Dr James C Smith is now the director of the MRC National Institute for Medical Research The Ridgeway, Mill Hill, London, UK
jim.smith@nimr.mrc.ac.uk

PAGE

VII List of Figures by Chapter then number

Chapter 1

Chapter 2

PAGE

Chapter 3

Chapter 4

Chapter 5

PAGE

Chapter 6

Chapter 7

PAGE

Chapter 8

Appendix

List of tables by chapter then number

Chapter 2

Chapter 4

Chapter 8

PAGE

Appendix

Publications are reproduced in full in appendices, in order of publication date.
Each is preceded by cover page listing full details of personal contributions and collaborations.
In text where a reference is followed by * then a number 1-12 this refers to publication as listed.

PUBLICATION 1

Evans, A. L., Sharkey, A. S., Saidi, S. A., Print, C. G., Catalano, R. D., Smith,S. K. & Charnock-Jones, D. S. 2003. Generation and use of a tailored gene array to investigate vascular biology. *Angiogenesis,* 6**,** 93-104.

PUBLICATION 2

Holland, C. M., Day, K., **Evans, A.** & Smith, S. K. 2003. Expression of the vegf and angiopoietin genes in endometrial atypical hyperplasia and endometrial cancer. *Br J Cancer,* 89**,** 891-8.

PUBLICATION 3

Catalano, R. D., Yanaihara, A., **Evans, A. L**., Rocha, D., Prentice, A., Saidi, S., Print, C. G., Charnock-Jones, D. S., Sharkey, A. M. & Smith, S. K. 2003. The effect of RU486 on the gene expression profile in an endometrial explant model. *Mol Hum Reprod.* 9, (8), 465-473.

PUBLICATION 4

Holland, C. M., Saidi, S. A., **Evans, A. L.,** Sharkey, A. S., Latimer, J. A., Crawford, R. A., Charnock-Jones, D. S., Print, C. G., and Smith, S. K. 2004. Transcriptome analysis of endometrial cancer identifies peroxisome proliferator-activated receptors as potential therapeutic targets *Mol. Cancer Therapeutics* 3, 993-1001.

PUBLICATION 5

Schoenfeld, J., Lessan, K., Johnson, N., Charnock-Jones, D. S., **Evans, A. L**., Vourvouhaki, E., Scott, L., Stephens, R., Freeman, T., Saidi, S. A., et al. 2004. Bioinformatic analysis of primary endothelial cell gene array data illustrated by the analysis of transcriptome changes in endothelial cells exposed to VEGF-A and PlGF. Angiogenesis 7, 143-156.

PUBLICATION 6

Print, C., R. Valtola, **A. Evans**, K. Lessan, S. Malik, and S. Smith. 2004. Soluble Factors from Human Endometrium Promote Angiogenesis and Regulate the Endothelial Cell Transcriptome. Hum Reprod 19, (10), 2356-66.

PUBLICATION 7

Xu, F., T. M. Hazzard, **A. Evans**, S. Charnock-Jones, S. Smith, and R. L. Stouffer. 2005. Intraovarian Actions of Anti-Angiogenic Agents Disrupt Periovulatory Events During the Menstrual Cycle in Monkeys. Contraception 71, (4), 239-48

PUBLICATION 8

Sharkey, A. M., R. Catalano, **A. Evans**, D. S. Charnock-Jones, and S. K. Smith. 2005. Novel Antiangiogenic Agents for Use in Contraception. Contraception 71, (4), 263-71.

PUBLICATION 9

Evans, A.L., Bryant, J., Skepper, J., Smith, S. K., Print, C. G., and Charnock-Jones, D. S. 2007. Vascular development in embryoid bodies: quantification of transgenic intervention and antiangiogenic treatment. Angiogenesis 10, 217-226.

PUBLICATION 10

Duval, H., N. Johnson, J. Li, **A. Evans**, S. Chen, D. Licence, J. Skepper, D. S. Charnock-Jones, S. Smith, and C. Print. 2007. Vascular Development Is Disrupted by Endothelial Cell-Specific Expression of the Anti-Apoptotic Protein Bcl-2. Angiogenesis 10, (1), 55-68.

PUBLICATION 11

Sengupta, J., P. G. Lalitkumar, A. R. Najwa, D. S. Charnock-Jones, **A. L. Evans**, A. M. Sharkey, S. K. Smith, and D. Ghosh. 2007. Immunoneutralization of Vascular Endothelial Growth Factor Inhibits Pregnancy Establishment in the Rhesus Monkey (Macaca Mulatta). Reproduction 133, (6), 1199 -211.

PUBLICATION 12

Evans, A. L., Faial, T., Gilchrist, M. J., Down, T., Vallier, L., Pedersen, R. L., Wardle F. C., and Smith J.C.et al. 2012. Genomic targets of brachyury (T) in differentiating mouse embryonic stem cells. PLoS One [Online], 7, 3, e33346.

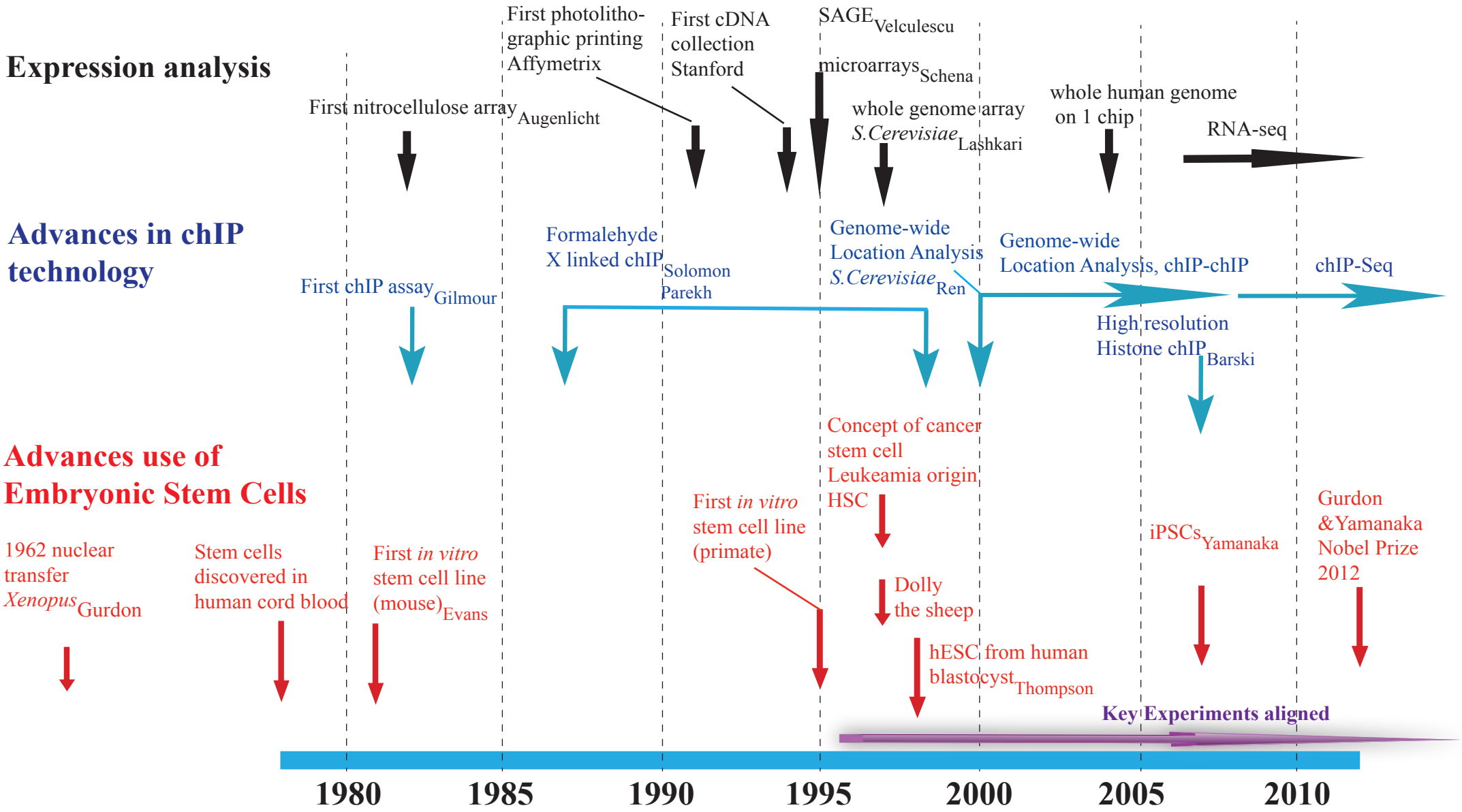

Timelines for significant technological and scientific advances relevant to this work

Abbrv. SAGE Serial Analysis of Gene Expression, cDNA complimentary deoxyribonucleic acid, RNA ribonucleic acid, hESC human Embryonic Stem Cells, chIP-chip chromatin immunoprecipitation on chip, HSC hematopoietic stem cells, iPSCs induced pluripotent stem cells.

Key Experiments

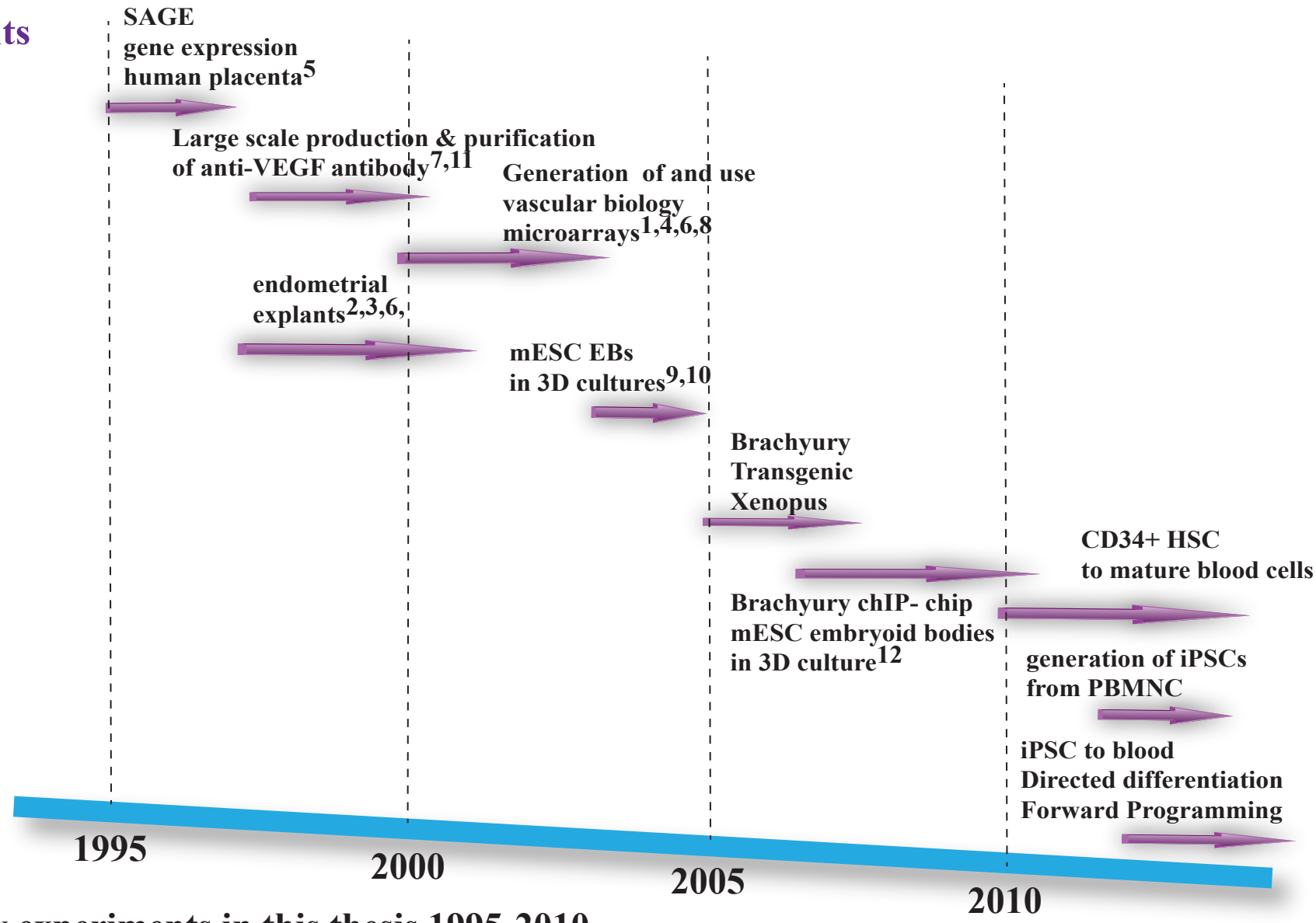

Timelines for key experiments in this thesis 1995-2010

Abbrv. SAGE Serial Analysis of Gene Expression, VEGF vascular endothelial growth factor, mESC mouse embryonic stem cells, chIP-chip chromatin immmunoprecipitation on chip, EBs embryoid bodies, HSC hematopoietic stem cells, iPSCs induced pluripotent stem cells, PBMNC Peripheral blood mononuclear cells. Numbers refer to publications as follows:
[1] Evans et al. 2003, [2] Holland et al. 2003, [3] Catalano et al. 2003, [4] Holland et al. 2004, [5] Schoenfeld et al. 2004, [6] Print et al. 2004, [7] Xu et al. 2007, [8] Sharkey et al. 2005, [9] Evans et al. 2007, [10] Duval et al. 2007, [11] Sengupta et al. 2007, [12] Evans et al. 2012.

VIII Timelines

References to timelines for significant technological and scientific advances that inspired the design of experiments in this thesis

Expression Analysis (Augenlicht and Kobrin, 1982); (Barski et al., 2007); (Takahashi and Yamanaka, 2006); (Schena et al., 1995) (Solomon et al., 1988); (Lashkari et al., 1997)

chIP Technology (Gilmour and Lis, 1984); (Solomon et al., 1988); (Parekh and Maniatis, 1999); (Ren et al., 2000); (Barski et al., 2007)

Advances in embryonic stem cells (Gurdon, 1962); (Evans and Kaufman, 1981); (Thomson et al., 1998); (Takahashi and Yamanaka, 2006)

Bibliography for timelines for significant technological and scientific advances of influence in this work

Augenlicht, L. H. & Kobrin, D. 1982. Cloning and screening of sequences expressed in a mouse colon tumor. *Cancer Research,* 42**,** 1088-93.

Barski, A., Cuddapah, S., Cui, K., Roh, T. Y., Schones, D. E., Wang, Z., Wei, G., Chepelev, I. & Zhao, K. 2007. High-resolution profiling of histone methylations in the human genome. *Cell,* 129**,** 823-37.

Evans, M. J. & Kaufman, M. H. 1981. Establishment in culture of pluripotential cells from mouse embryos. *Nature,* 292**,** 154-6.

Gilmour, D. S. & Lis, J. T. 1984. Detecting protein-DNA interactions in vivo: distribution of RNA polymerase on specific bacterial genes. *Proc Natl Acad Sci U S A,* 81**,** 4275-9.

Gurdon, J. B. 1962. The developmental capacity of nuclei taken from intestinal epithelium cells of feeding tadpoles. *J Embryol Exp Morphol,* 10**,** 622-40.

Holland, C. M., Day, K., Evans, A. & Smith, S. K. 2003. Expression of the VEGF and angiopoietin genes in endometrial atypical hyperplasia and endometrial cancer. *Br J Cancer,* 89**,** 891-8.

Lashkari, D. A., Derisi, J. L., Mccusker, J. H., Namath, A. F., Gentile, C., Hwang, S. Y., Brown, P. O. & Davis, R. W. 1997. Yeast microarrays for genome wide parallel genetic and gene expression analysis. *Proc Natl Acad Sci U S A,* 94**,** 13057-62.

Parekh, B. S. & Maniatis, T. 1999. Virus infection leads to localized hyperacetylation of histones H3 and H4 at the IFN-beta promoter. *Mol Cell,* 3**,** 125-9.

Ren, B., Robert, F., Wyrick, J. J., Aparicio, O., Jennings, E. G., Simon, I., Zeitlinger, J., Schreiber, J., Hannett, N., Kanin, E., Volkert, T. L., Wilson, C. J., Bell, S. P. & Young, R. A. 2000. Genome-wide location and function of DNA binding proteins. *Science,* 290**,** 2306-9.

Schena, M., Shalon, D., Davis, R. W. & Brown, P. O. 1995. Quantitative monitoring of gene expression patterns with a complementary DNA microarray. *Science,* 270**,** 467-70.

Solomon, M. J., Larsen, P. L. & Varshavsky, A. 1988. Mapping protein-DNA interactions in vivo with formaldehyde: evidence that histone H4 is retained on a highly transcribed gene. *Cell,* 53**,** 937-47.

Takahashi, K. & Yamanaka, S. 2006. Induction of Pluripotent Stem Cells from Mouse Embryonic and Adult Fibroblast Cultures by Defined Factors. *Cell,* 126**,** 663-676.

Thomson, J. A., Itskovitz-Eldor, J., Shapiro, S. S., Waknitz, M. A., Swiergiel, J. J., Marshall, V. S. & Jones, J. M. 1998. Embryonic stem cell lines derived from human blastocysts. *Science,* 282**,** 1145-7.

Towards next generation regenerative medicine

The integrity of blood vessel and blood cell formation is essential to human life, forming the driver for exploring the origins and regulation of blood cells and blood vessels. These cells have common developmental origins in nascent mesoderm and overlapping genetic programs. Endothelial and haematopoietic cells differentiate in close proximity, with endothelial cells playing an active role in haematopoiesis. Therefore, knowledge gained from studying the role of angiogenesis in blood vessel development compliments studies reconstructing the route-map to haematopoietic differentiation using embryonic stem cells. The studies presented employ the constant advancement in molecular profiling technologies, allowing an increasingly complete genetic classification of tissue, including transcriptional and epigenetic control.

As a direct consequence of the close overlap in the gene networks controlling differentiation the same basic protocols can be designed for directing cells *in vitro* to haematopoietic lineages or endothelial cells. By modifying the genetic and environmental cues cells are exposed to, we are increasingly able to control the route of terminal differentiation. Adult haematopoiesis occurs in the bone marrow haematopoietic stem cell niche, a complex three-dimensional tissue containing multiple cell types. Current regenerative medicine projects using human induced pluripotent stem cells to produce megakaryocytes, large platelet producing cells, requires recapitulation of the haematopoietic differentiation hierarchy that occurs in the niche. Understanding the developmental origins of these cells together with the biology of closely associated cells in the niche provide the tools to achieve the ultimate goal of *in vitro* produced human blood cell products.

Introduction

Coincidental with size and complexity, humans have evolved a highly developed blood and vascular system to transport oxygen and nutrients to all body cells. The vascular system is formed and maintained by a balance of several mechanisms including vasculogenesis, angiogenesis and apoptosis. During embryogenesis primitive endothelial cells become organised into vessels by vasculogenesis. The vascular system is then maintained by angiogenesis, the sprouting of new vessels from pre-existing ones, and further fined tuned by selective programmed cell death (apoptosis). The vascular endothelial growth factors (VEGFs) are the most prominent family of growth factors influencing the growth and the architecture of these vessels in normal and abnormal angiogenesis (Hoeben et al., 2004). The dynamic nature of these systems is of particular relevance to female reproductive medicine where angiogenesis and apoptosis are part of the cyclic growth and destruction of the endometrial lining, the stratum functionalis (Chapter 1.2).

One of the aims of the experiments described in the first part of this thesis was to establish molecular and morphological changes that result in blastocyst attachment and ask to what extent angiogenesis and apoptosis are a part of the process. Specifically, we wanted to test the hypothesis that implantation could be influenced by anti-angiogenic intervention. Deregulated angiogenesis is a key event in tumour metastasis and we further asked whether the VEGF family and angiogenesis were part of the etiology of endometrial cancer.

To address some of these aims we developed cell-based models (Chapter 1) using endothelial cells and endometrial explants. However, human endometrium was always a limited resource and once removed from the uterus is only suitable for short-term culture (Chapters 3 and 4). Experiments using this model led us to consider exploiting the similarities between neovascularisation in cancer and embryonic vessel development. This led to the development of a spinner culture system to create large numbers of mouse embryonic stem cell-derived embryoid bodies (EBs). Using carefully screened serum batches, EBs provided a supply of developing vessel networks sensitive to intervention (Chapters 1, 5), in particular for experiments using anti-angiogenic agents, not relating to steroidal control of angiogenesis. Anti-angiogenic therapy is relevant to many diseases characterized by excessive or abnormal angiogenesis, for

example diabetic retinopathy (Carmeliet, 2003). These experiments also suggested EBs as a suitable model for early mesoderm development complementing the Zebrafish *Danio rerio* and *Xenopus* models already used in Jim Smith's laboratory, and I went on to use this model at the Gurdon Institute in Cambridge (Chapter 6).

Alongside the cell based models advances in molecular profiling technology were incorporated and adapted to complement the studies (see timelines VIII). Thus, expression arrays (Chapter 2) were developed to discover pathways involved in endometrial cancer, and implantation. Chromatin immunoprecipitation (chIP) was used (Chapters 6 and 7) to elucidate transcriptional targets of *Brachyury,* a T-box transcription factor required for mesoderm induction, gastrulation and subsequent blood and vascular development.

ChIP-chIP produced a list of targets associated with morphogenesis, vascular and endothelial biology and cancer. Selected putative targets were empirically verified in wild type and *Brachyury* mutant mice by *in-situ* hybridisation. Experiments using human embryonic stem cells then suggested the role of *Brachyury* in development appears to be conserved between mouse and human cells.

The debate concerning the origins of the blood and vascular system in early embryonic life is a longstanding one. Evidence points to a common haemangioblast precursor for blood and endothelial cell lineages with a sensitive molecular switch controlling the balance between the two fates (Choi et al., 1998; Eilken et al., 2009; Yue et al., 2012). Invertebrate and vertebrate studies both *in vitro* and *in vivo* have established the cellular sequence from a common progenitor cell (Messner and Jamal, 1993; Stainier et al., 1995; Gering et al., 1998; Meister and Lagueux, 2003; Huber et al., 2004) and evidence from our work in EBs suggests *Brachyury* may play a role in both primitive and definitive haematopoiesis.

The significance of the close relationship between the origins of the blood and vascular systems lies in their overlapping genetic programs. They share common markers; for example VEGFR2 receptor or kinase domain region/ foetal liver kinase (VEGFR2/KDR/FLK1) is found on precursor haemangioblasts (Kubo and Alitalo, 2003) and endothelial progenitors (George et al., 2011). In addition they are influenced by common signals such as VEGF, bone morphogenetic protein 4 (BMP4) and *Brachyury,*

and also influence each other. As a result, the use of differentiation protocols using the same basal media and starting conditions is possible. Protocols can be further manipulated with specific cytokines or transcription factors to produce cells of our choice. Different groups are working on endothelial cell production (Morgan et al., 2013; Samuel et al., 2013) and erythroblast production (Giarratana et al., 2005; Dias et al., 2011), while, together with my colleagues at the NHSBT, I am now concentrating on the myeloid lineage; specifically megakaryopoiesis and the production of platelets, using patient specific induced pluripotent stem cells (iPSCs) (Chapter 8). We now know for example that a wave of *Brachyury* expression, which accompanies mesoderm formation, is a requirement in both mESC and hESC for haematopoietic development. Progenitor cells at this stage are multipotent and can be directed or reprogramed towards different blood lineages, leading to the possibility of patient specific cell therapies in the future.

Chapter 1 The development of cell-based models for vasculogenesis, angiogenesis and haematopoiesis

Experiments performed at the Rosie Maternity Hospital, Department of Obstetrics and Gynaecology, when I joined in 1996, were based on the use of cell lines, and tissue samples for *in-situ* detection of transcripts, immunohistochemistry and ribonucleic acid (RNA) extraction to study individual genes. The primary aim was to investigate causes and possible treatments for reproductive disorders. One of the objectives was to investigate the role of angiogenesis in both endometrial cancer and implantation and the significance of the VEGF family in these processes. Since angiogenesis plays a role in the development of a receptive endometrium (Gordon et al., 1995; Torry and Torry, 1997; Abulafia and Sherer, 1999; Smith, 2001), we believed it could also play a critical role in implantation. In endometrial cancer we hypothesized, that invasion of healthy tissue during malignancy maybe analogous to angiogenic invasion of the decidua during placental development (Jackson et al., 1994).

Many i*n vitro* and *in vivo* models of angiogenesis have been extensively used and reviewed (Vailhe et al., 2001; Auerbach et al., 2003; Hasan et al., 2004; Staton et al., 2009), however, our interest also extended to steroid control of VEGF. Regulation of VEGF occurs at many levels. In the female reproductive tract oestrogen (Mueller et al., 2000) is an important VEGF regulator resulting in endothelial angiogenesis and endometrial growth in the follicular phase. Therefore we were interested in developing a model that incorporated steroid control.

1.1 The female reproductive tract: a unique resource

The human female reproductive tract offers a unique resource to study angiogenesis in the adult vascular system. It is the site of physiological and pathological vasculogenesis, angiogenesis and endothelial apoptosis as the vessel networks undergo cyclic remodelling. Aside from pathology and trauma there are limited opportunities to do this, while in the female reproductive tract angiogenesis occurs normally as part of ovulation, menstruation, implantation and placental development (Demir et al., 1989).

1.1.2 The endothelial cell (EC)

All the blood vessels in the body are lined with endothelial cells (ECs) and endothelial cell biology is central to normal and pathological angiogenesis (Figure 1.2). Human umbilical vein endothelial cells (HUVEC) (Figure 1.1) isolated from the umbilical vein using gentle digestion with collagenase (Jaffe et al., 1973), were used for many of our experiments.

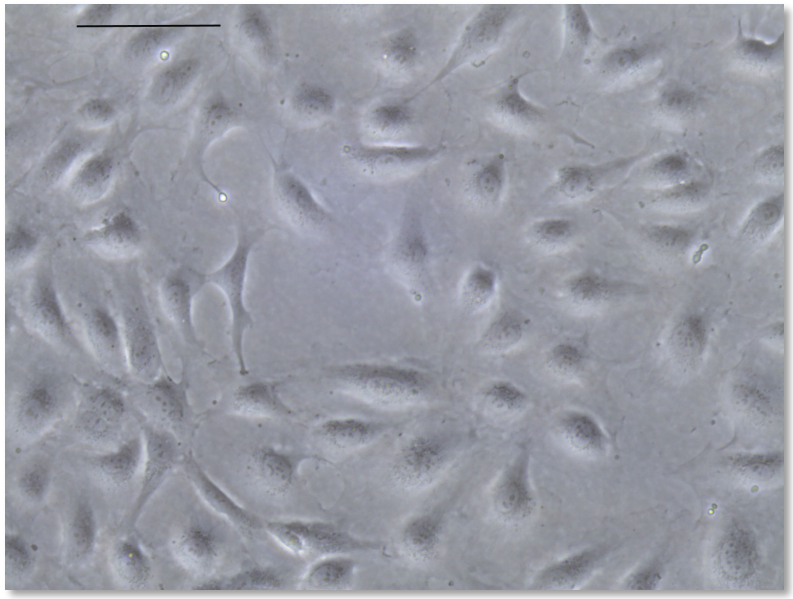

Figure 1.1 Light microscope image of cultured Human Umbilical Vein Endothelial Cells (HUVEC) passage 6 maintained in Endothelial cell basal media-2 (EBM™-2) Clonetics™ (Lonza, Verviers, Belgium) supplemented with 2% FBS, hEGF, Hydrocortisone, GA-1000 (Gentamicin, Amphotericin-B), VEGF, rhFGF-B, R3-IGF-1, Ascorbic Acid, and Heparin. Scale bar =100µm. HUVEC grow as adherent cells on tissue culture plastic and have a typical cobblestone-like appearance but do not form tubes unless seeded in Matrigel (BD Biosciences), a mixture of extracellular and basement membrane proteins,
Abbrvs: foetal bovine serum (FBS), human epidermal growth factor (hEGF), vascular endothelial growth factor (VEGF), recombinant human fibroblast growth factor B (rhFGF-B), recombinant insulin growth factor 1 (R3-IGF-1)
Photographed using a Leica DM IL LED microscope (Leica microsystems, UK).

HUVEC express the VEGF family of receptors (Appendix figure 1), but lack some of the physiological cell contacts, such as basement membranes and supporting

vascular smooth muscle cells (VSMC), or pericytes (Armulik et al., 2005), usually associated with mature endothelial cells (Figure 1.2).

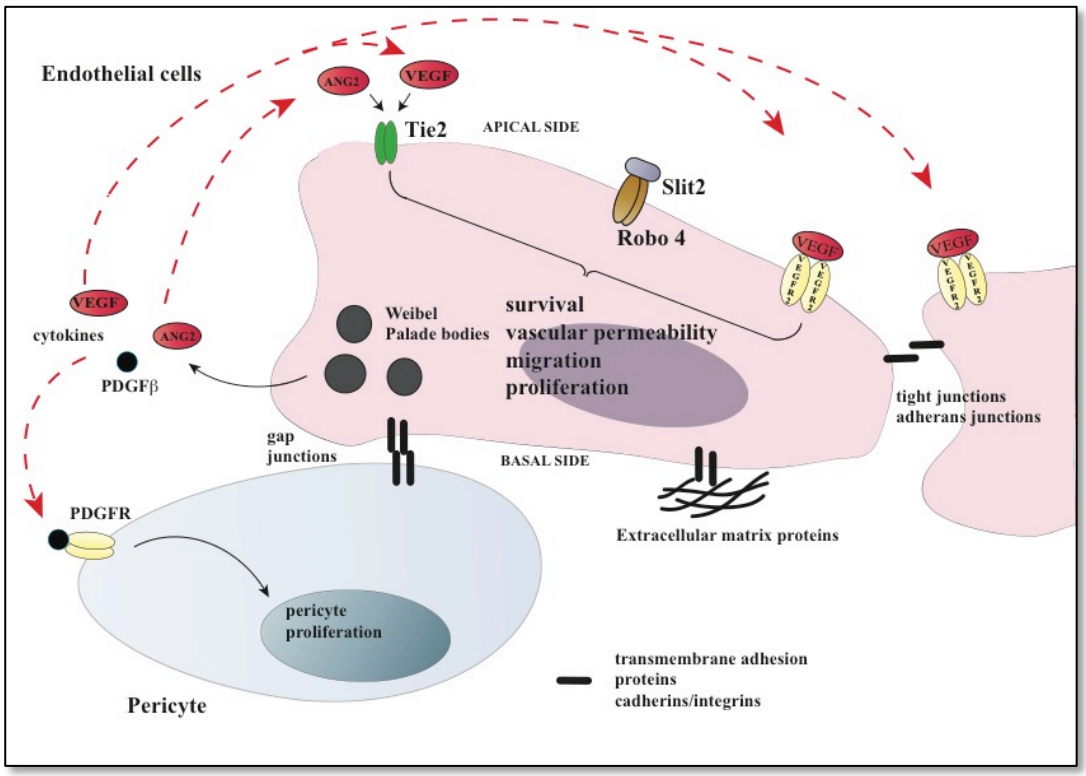

Figure 1.2 Endothelial cells and supporting pericytes

ECs (red) express a number of receptors, the most significant of which are VEGFR1/FLT1 fms- like tyrosine kinase (Quinn et al., 1993), VEGFR2/KDR/FLK1 kinase domain region/fetal liver kinase (Waltenberger et al., 1994) and the TEK tyrosine kinase (Tie2/Tek) receptor, important in haematopoietic and vascular development (Korhonen et al., 1994). Mature ECs are surrounded by supporting vascular smooth muscle cells (VSMC) or pericytes (blue), linked by transmembrane adhesion proteins. Endothelial storage organelles, Weibel-Palade bodies (Weibel and Palade, 1964), secrete cytokines including angiopoietin 2 (ANGPT2, Ang2); platelet derived growth factor β (PDGFβ); vascular endothelial growth factor (VEGF) which act in autocrine and panacrine signalling (red dashed arrows). Robo 4, an endothelial specific guidance receptor stabilises endothelial networks (Acevedo et al., 2008; Jones et al., 2008) and is involved in homing of haematopoietic stem cells (HSCs) to the bone marrow niche (Chapter 8.1).

Key: Platelet-derived growth factor receptor (PDGFR); magic roundabout, axon guidance receptor, homolog 4 (Robo 4); Slit homolog 2, the secreted ligand for Robo 4 (Slit2).

1.2 The endometrium

The endometrium, the inner layer lining the uterus, undergoes extensive remodelling under the influence of steroid hormones (Figure 1.4). A complex and highly dynamic tissue, it contains many closely associated cell types (Figure 1.3).

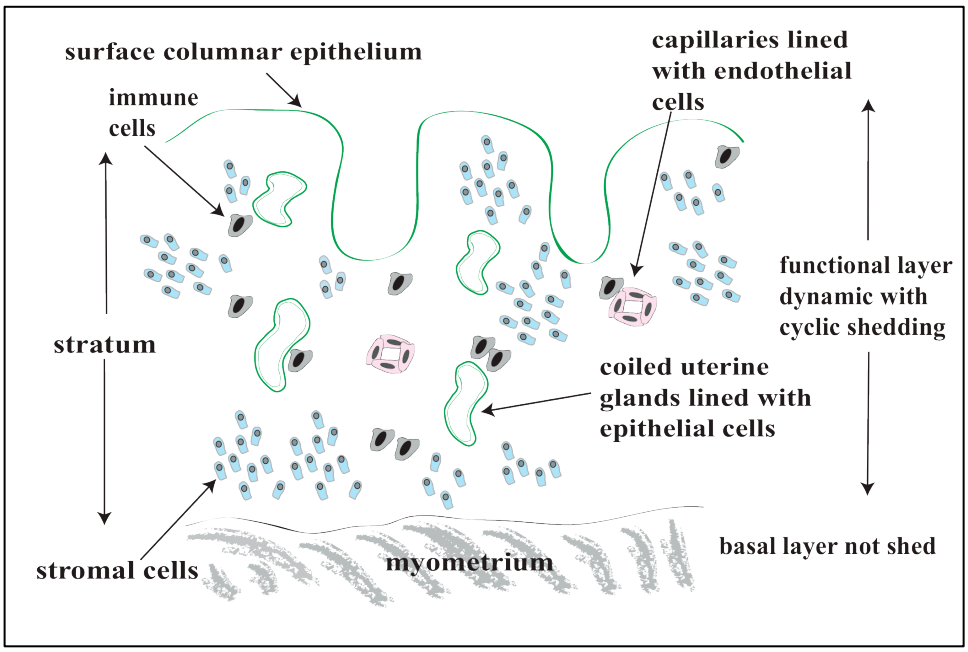

Figure 1.3 The key components of the human endometrium

The functional layer, contains stromal cells (blue), glandular epithelial cells (green), endothelial cells in spiral arteries and sub-epithelial capillary plexus (pink) and immune cells particularly macrophages and natural killer cells (grey). The basal layer or myometrium is not shed and the functional layer develops from it.

Model cell lines such as ECC-1, a human epithelial endometrial cancer cell line (Clarke et al., 1987) and Ishikawa, a glandular epithelial cell line from human endometrial adenocarcinoma (Nishida et al., 1985), although influenced by steroid regulation, are all epithelial cells, and HUVEC do not respond to steroid hormones.

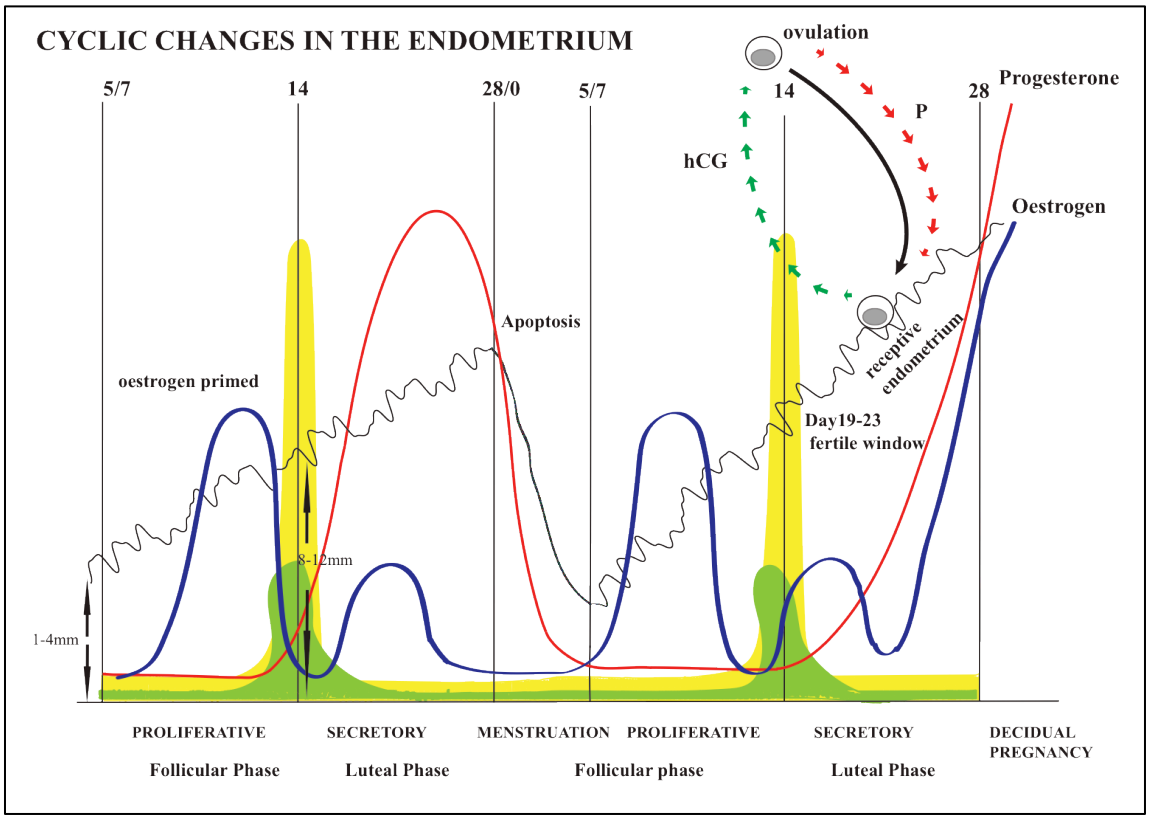

Figure 1.4 Steroid hormone regulation of the endometrium during the Menstrual Cycle
Cyclic regeneration of the spiral arteries of the endothelium in the highly vascularised stratum functionalis associated with menstruation and implantation.
Oestrogen (blue line) induces proliferation (follicular phase) and progesterone (red line), produced by the corpus luteum following follicle release, then results in glandular differentiation of the stroma (luteal phase). In the brain the pituitary gland secretes luteinizing hormone (LH, yellow) and follicle stimulating hormone (FSH, green). FSH stimulates the ovary to ripen an ovule and with the help of a spike in LH, to produce an egg. An average 28 day cycle is shown. On implantation, 5-9 days after ovulation, progesterone further regulates the establishment and maintenance of pregnancy by decidualization. Human chorionic gonadotropin (hCG) secreted by the growing embryonic placental villi signals the corpus luteum to continue producing progesterone (P). Information based on a number of sources.

1.2.1 Endometrial explants

With the aim of investigating active angiogenesis during the secretory phase of the endometrial cycle (Figure 1.4) and how this may influence implantation of the blastocyst we decided to use freshly acquired endometrial biopsies. Short term explants

taken from the endometrial surface survive well in tissue culture provided care is taken to ensure the samples are aseptically biopsied and immediately put into sterile phosphate buffered saline solution (PBS).

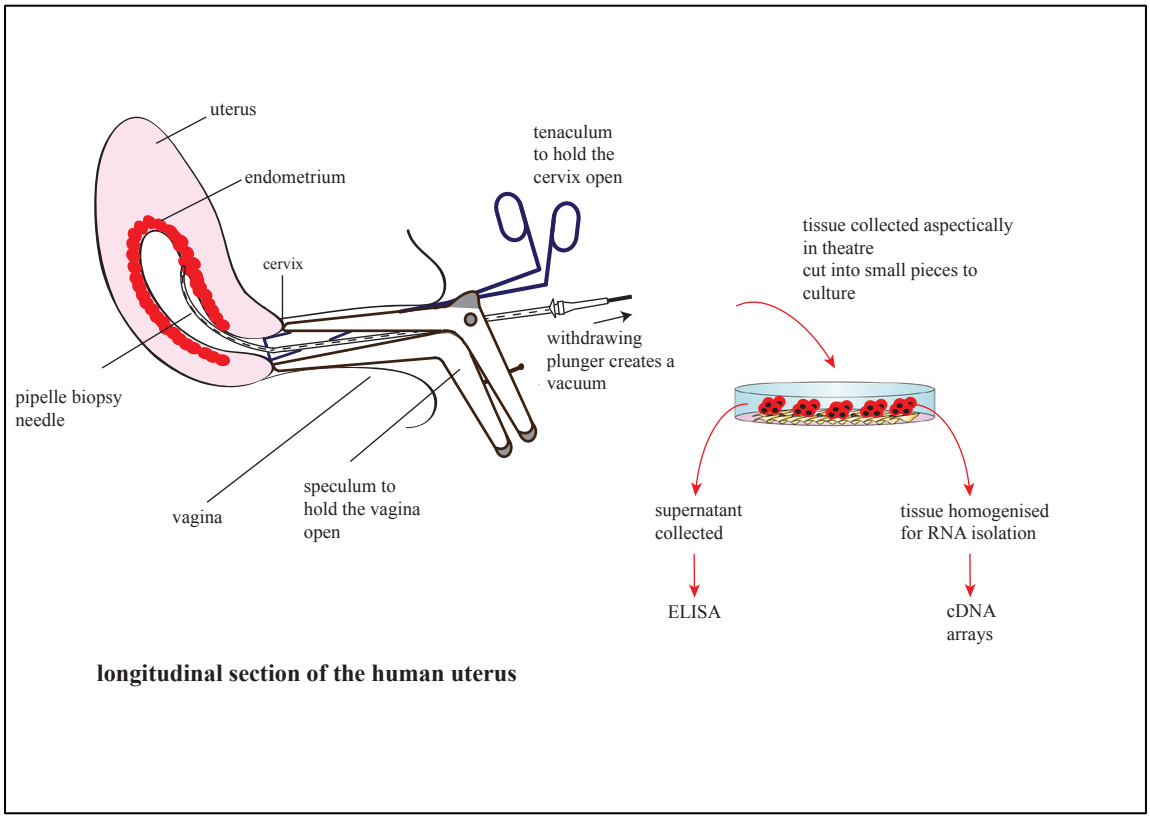

Figure 1.5 Endometrial explants

Image (left) illustrates endometrial sampling in theatre. The surgeon inserts a speculum to open the vagina, and tenaculum forceps to open the cervix and allow the insertion of the pipelle biopsy needle. The pipelle is a piston device to sample the lining of the uterus. Samples are then used in explant culture (right). Enzyme-linked immunosorbent assays (ELISA), and complementary DNA (cDNA) arrays were then performed).

Endometrial biopies were obtained using a pipelle endometrial biopsy instrument at the time of laparoscopy or hysteroscopic examination (Figure 1.5). Biopsies were washed 2-3 times in sterile Dulbecco's modified Eagle media (DMEM)/Ham's F-12 (Life Technologies, UK), to remove blood from the sampling process, before cutting into pieces. If the endometrial explants were not cut into 1-2mm^3 uniform pieces they

became hypoxic at the centre accompanied by VEGF up regulation, before necrosis occurred.

Samples were sent for histological dating of the endometrium. Mid-secretory biopsies were required for implantation experiments. The explants maintain all the correct types and ratios of cells found in the lining of the uterus and to a degree the original *in-vivo* connections between the cells and extracellular matrix (ECM).

1.3 The placenta and umbilical cord

Aside from the study of placental pathologies such as pre-term birth and pre-eclampsia, the placenta and umbilical cord were another important resource both for endothelial cells and an invaluable supply of RNA for cloning transcripts associated with angiogenesis (Chapter 2).

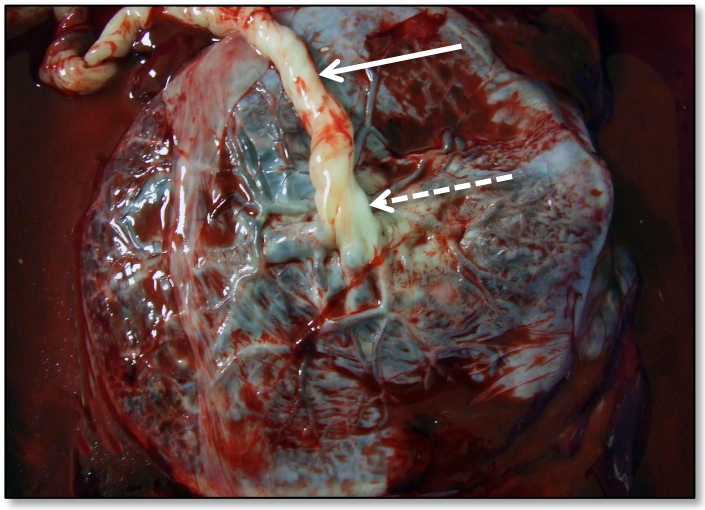

Figure 1.6 A fresh human term placenta

Image from maternal side after delivery of foetus, white arrow indicates the umbilical cord and the dashed white line the amnion: this membrane would have surrounded the foetus. Note the extensive amount of blood from this highly vascularised organ.

Villous endothelial tubes and foetal vessels form the umbilical cord (Demir et al., 1989) and from this HUVEC were isolated as soon as possible following delivery (Chapter 1.1.2).

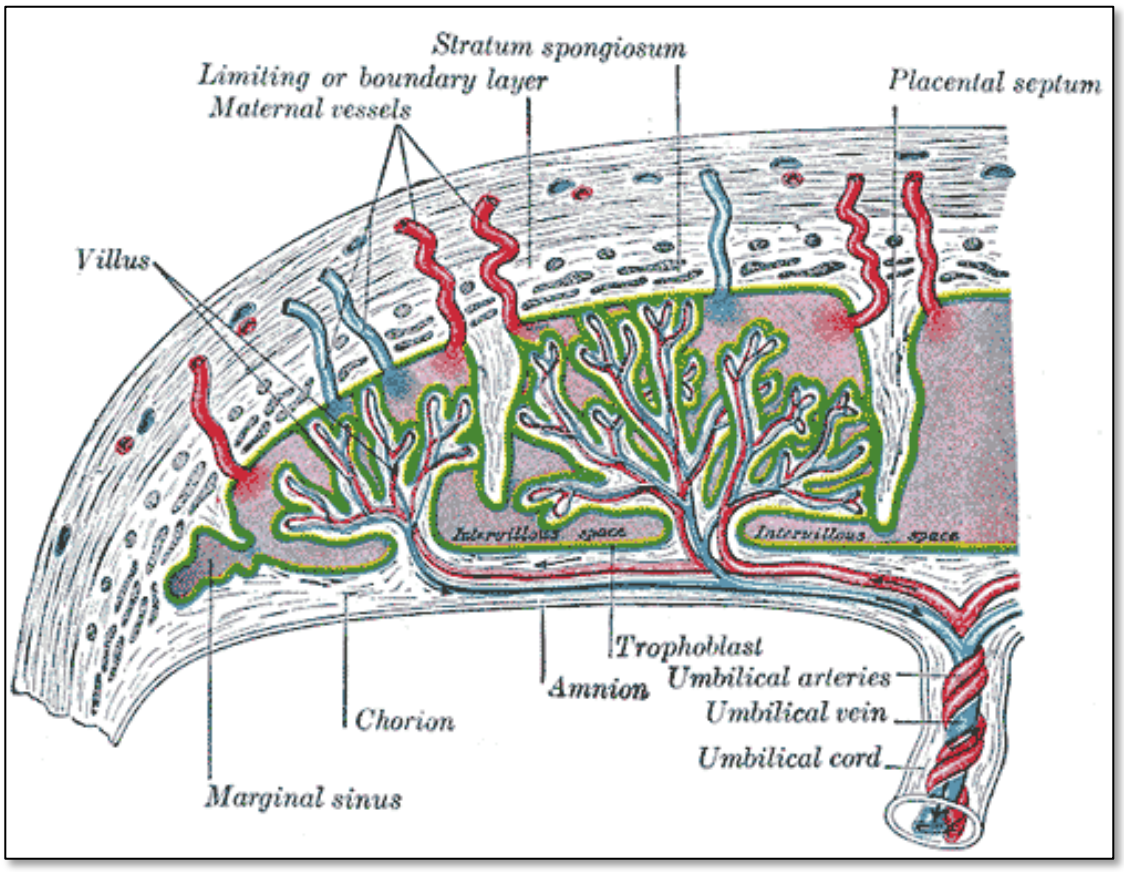

Figure 1.7 The Human Placenta Reproduction of a lithograph plate from the 20th U.S. edition of Gray's Anatomy of the Human Body, published in 1918 *Trophoblast* - cells surrounding the early embryo important in implantation and interaction with the maternal decidualised uterus, *Chorion* - outer extraembryonic membrane of the trophoblast lined with mesoderm, *Amnion*- membrane surrounding the fetus, *Villus*- vascular extensions of membrane increasing surface area of maternal-foetal contact, *Placental septum*- delineates the cotyledons but maternal blood circulates freely.

The umbilical cord (Figures 1.6 and 1.7) and placental blood are also the source of CD34-positive haematopoietic progenitors from which all blood cells can be derived (Figures 1.8, 1.9). Approximately 0.1-0.5% of cord blood cells are CD34-positive, a marker for haematopoietic precursors. Bone marrow contains a relatively high percentage of CD34+ cells (0.5-3%) but requires a highly invasive procedure for collection. Peripheral blood requires whole units of blood to obtain useful numbers having the lowest percent (0.05-0.2).

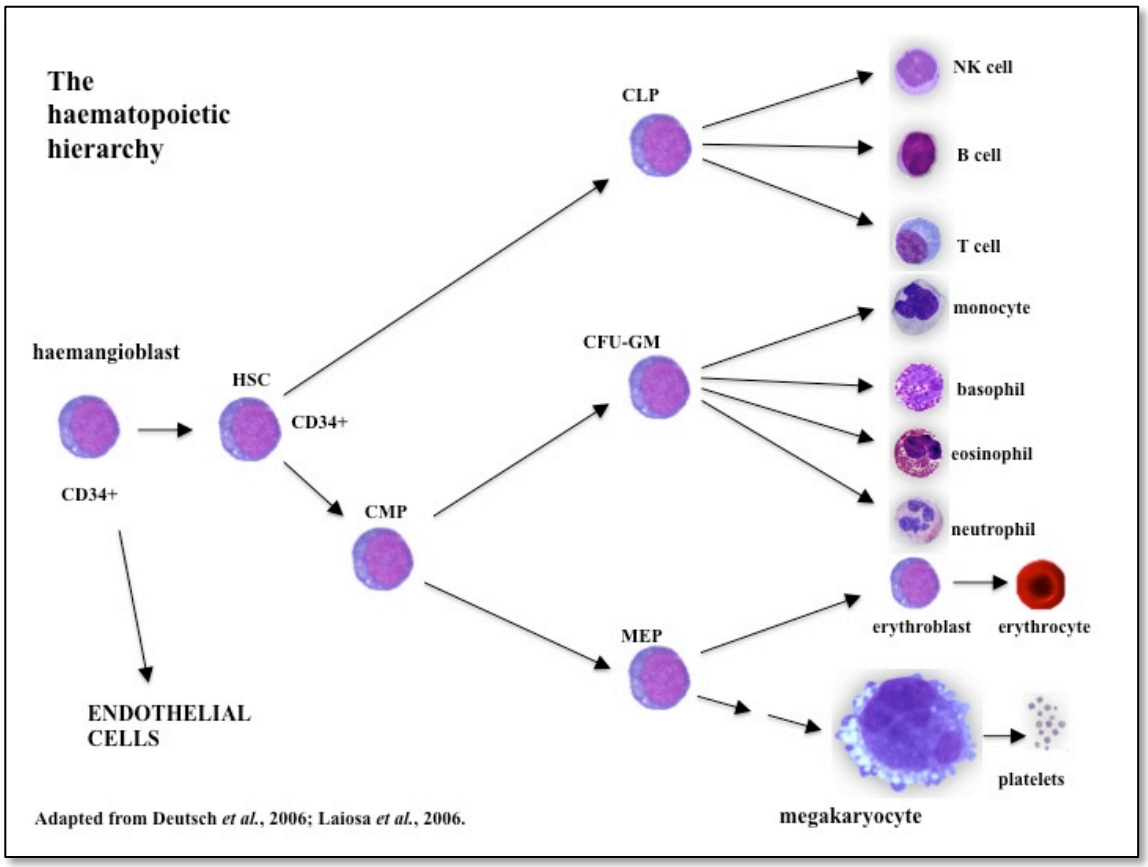

Figure 1.8 The haematopoietic hierarchy.

All blood cells differentiate from a common progenitor, the haematopoietic stem cell (HSC). As cells progress to terminally differentiated cells the potential to become cells of alternate lineages diminishes. Closely related cells, such as megakaryocytes (MK) and erythroblasts (myeloid lineages), or B- and T-cells (lymphoid lineages) share common progenitors restricted to the production of these cells only. Adapted from (Deutsch and Tomer, 2006; Laiosa et al., 2006).

Abbrvs: common myeloid progenitor (CMP); common lymphoid progenitor (CLP); megakaryocyte/erythoblast precursor (MEP); colony forming unit-granulocyte/monocyte (CFU-GM); natural killer (NK).

From experience, an average placenta supplies approximately 90ml of cord blood, which will contain at least a million CD34+ progenitors. By manipulation of the cytokine cocktail and specific culture conditions these progenitors are a valuable source of differentiated cell lineages (Figure 1.8, 8.5).

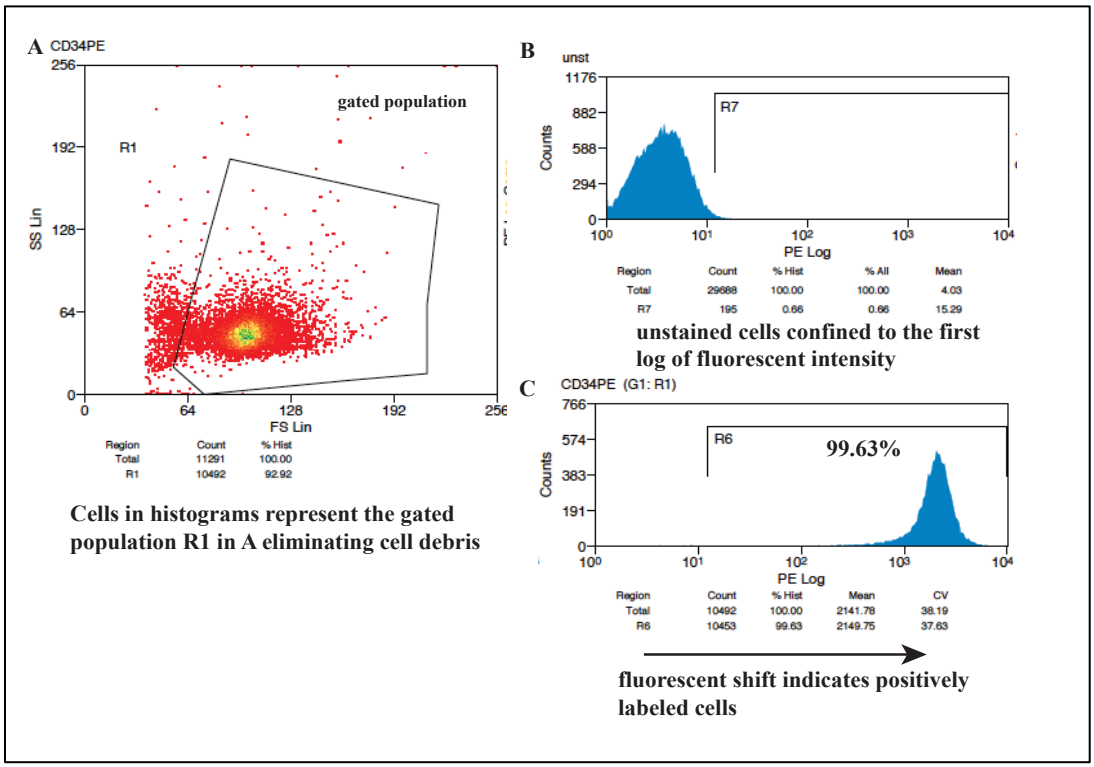

Figure 1.9 Flow cytometry data for isolated cord blood CD34+ progenitor cells

Precursor cells are isolated by positive selection with CD34 magnetically labelled MicroBeads (MACS®) (Miltenyi Biotec, GmbH). Peripheral blood mononuclear cells (PBMNCs) are isolated from anticoagulated cord blood by density gradient centrifugation using Ficoll-Paque™ (GE Healthcare). The cell suspension is then loaded onto a column and placed in a magnetic field. On removal positively selected cells are eluted.

A Dot plot shows linear side scatter (SS lin) against linear forward scatter (FS lin). SS is linked to the granularity/complexity of the particles and FS to cell size. Region R1 is a gated CD34+ population isolated using positive selection.

B Histogram shows number of events or gated cells (y axis) against the log of signal intensity (x axis) for an unstained control sample of sorted cells.

C Cells stained with anti-CD34 labeled phycoerythrin-conjugated (PE) antibody (Beckman Coulter), a marker for haematopoietic precursors, capillary endothelium and the ligand for CD62 (L-selectin).

A CyAn^{TM} Advanced Digital Processing (ADP) Analyser (Beckman Coulter) was used together with Summit 4.3 software. Performed by A. Evans

1.4 Embryoid bodies as a model for endothelial network development

Endometrial explants are only suitable for short-term culture and are not suitable to follow new vessel formation. A mouse embryonic stem cell model was therefore developed to produce networks of endothelial cells, with the aim of testing the efficacy of anti-angiogenic reagents and to quantify these effects by computer based stereological methods.

Embryoid bodies (EBs) are aggregates of embryonic stem cells (ESCs), released from pluripotent culture constraints, which then start the process of differentiation with the potential to form all three germ layers (Bradley et al., 1984).

1.4.1 A three dimensional model for early mouse development

The inner cell mass can generate all the cells of the embryo (Kanatsu and Nishikawa, 1996), and from these cells mouse embryonic stem cells (mESCs) are derived (Evans and Kaufman, 1981). ESCs can be maintained for long periods (Evans and Kaufman, 1981; Brook and Gardner, 1997; Nichols et al., 1998) in the undifferentiated state using appropriate conditions (Ying et al., 2003) enabling expansion of the starting population and a continuous experimental supply.

For these experiments (Evans et al., 2007)[*9] R1 mouse ES cells were (Nagy et al., 1993) maintained in the pluripotent state by culturing on mouse embryonic STO feeder cells (Martin and Evans, 1975), which were genetically modified to produce leukaemia inhibitory factor (LIF) protein. Single ESCs re-aggregate during the first 24-48 hours of feeder-free culture, starting as small spheres of 50-100μM with an irregular surface which becomes smooth by day 3 (see Figure 1.10), resembling morula compaction of the blastocyst *in vivo.* The potential of EBs as embryonic surrogates is explored further in chapter 6.

Culturing EBs in spinner culture (Figure 1.10) produced a homogeneous population of cells in which sustained gradients of cytokines cannot develop due to slow stirring. The media, containing extensively batch tested serum but no additional cytokines, needs regular replenishment and therefore the timing of differentiation stages is unlikely to reflect those seen *in vivo.* Samples are easily withdrawn via side arms in the spinner flasks and either frozen and sectioned, embedded in wax to section or mounted whole for confocal microscopy.

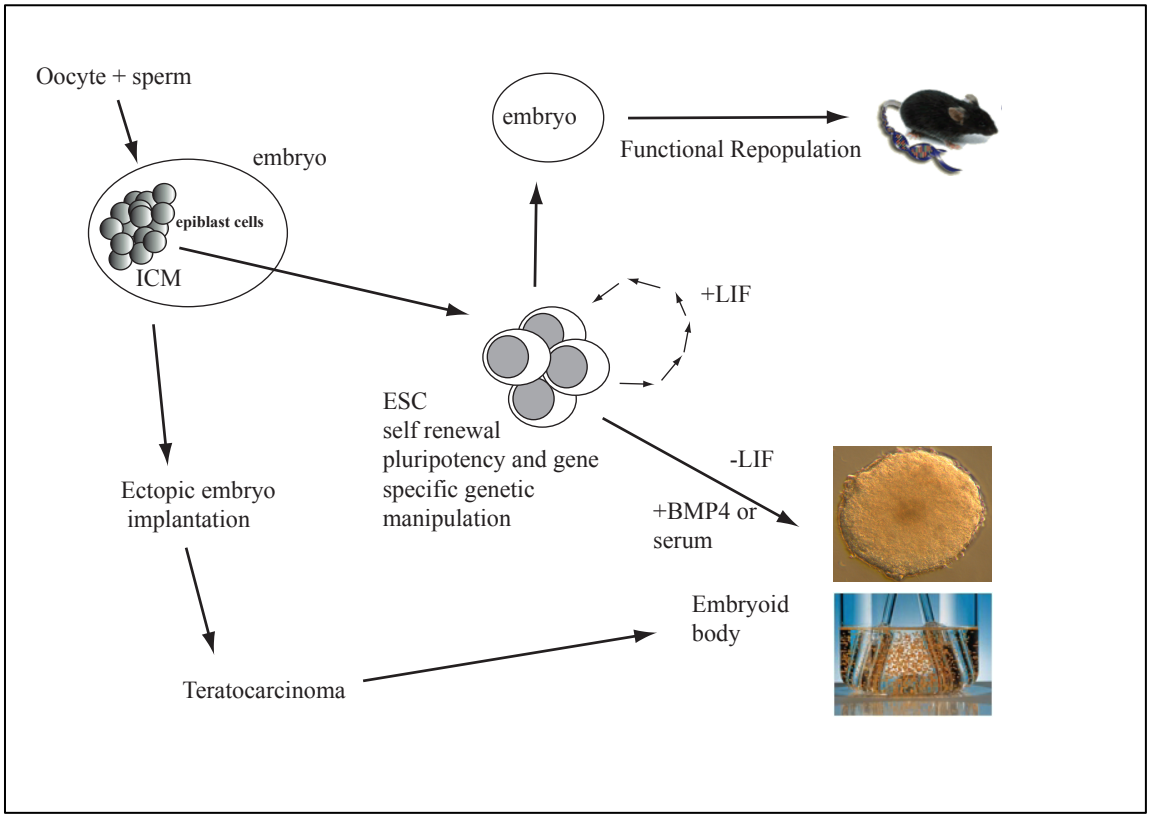

Figure 1.10 Mouse ESCs are derived from the inner cell mass of the embryo and are capable of forming all germ layers. Key: inner cell mass (ICM), embryonic stem cell (ESC), leukaemia inhibitory factor (LIF). Mesoderm induction requires the addition of bone morphogenetic protein 4 (BMP4) or the presence of serum. Insert images are of a single day 3 embryoid body and spinner culture flask used for all these experiments. The flasks are siliconised and are magnetically controlled using glass impellers via an adjustable speed and rotation angle control unit.

Having developed this reliable way of consistent differentiation of EBs, we were confident it could be adapted for use in monitoring anti-angiogenic agents and for transgenic intervention as described later in chapter 5.

Chapter 2 Transcriptome analysis using cDNA expression arrays

The advent of DNA array technology and the availability of cDNA collections led to a progression towards profiling of complete pathways and eventually whole genomes (Lashkari et al., 1997). Commercially produced arrays were expensive, and academically produced generic arrays were of limited availability at the time therefore, the aim was to produce a tailored cDNA based on vasculogenesis, angiogenesis, apoptosis and vascular remodelling. Aiming for a reliable, reproducible and affordable tool, each step was quality controlled to produce a standardized protocol designed for multiple users. Not only did this speed up our research, but we could also address specific issues such as pathways influencing the establishment of a receptive endometrium leading to possible intervention.

2.1 An aside - Serial Analysis of Gene Expression (SAGE)

Before settling on cDNA arrays as the best option for the group, serial analysis of gene expression (SAGE) (Velculescu et al., 1995) was explored as an alternative (Appendix figure 2 for technical details). The attraction was that SAGE is not limited to the arrayed transcripts and would enable a complete inventory of differentially expressed transcripts in placenta and endometrium. However, SAGE required some molecular experience, a large sequencing capacity and downstream computing capacity to extract tags and convert them to transcripts. As a result, SAGE was replaced by cDNA arrays, but components of this elegant technique are now recognisable in parts of the library construction for RNA-sequencing (RNA-seq) using current massively parallel or next generation sequencing.

2.2 The development of a tailored expression microarray to investigate vascular biology

There are two main types of gene arrays, large generic ones and much smaller tailored arrays. With that in mind we set out to create the latter, comprising a gene list of approximately a thousand genes covering all aspects of research at the Rosie. Prior knowledge of angiogenesis, apoptosis, implantation and vascular remodelling produced a list that included a number of in-house clones and others obtained from the IMAGE (Integrated Molecular Analysis of Genomes and their Expression) Consortium (then

based at UK MRC Hinxton Genome Mapping project Resource Centre, Hinxton, Cambridge, UK). The array included many cytokines and growth factors involved in the co-ordinated growth and regression of blood vessels including the VEGF family and its receptors. A number of known oncogenes and transcription factors such as c-myc, and set of blood cell surface antigens were also included (see RMRG genelist following (Evans et al., 2003)[*1] appendices).

Using radiolabeled probes enabled studies with very limited material (5µg total RNA) such as post-menopausal endometrium. Although ^{33}P was more expensive with lower energy particles than the more commonly used ^{32}P, at this time there were good reasons for its choice. The arrays were exposed to low energy phosphor screens as these have a wider dynamic range than X ray film. The spots produced were cleaner and better recognised by automatic grid-placing software during analysis, and the smaller angle of radiation scatter meant better overall spot resolution. In addition, the half-life of ^{33}P is 25.4 days compared to 14 days for ^{32}P.

2.3 Choice of genes, clones and their authentication

The final set of cDNAs printed on the arrays included all the clones already being used in our research and those from the list that were verified as correct after sequencing. In a number of cases this meant inclusion of genes not originally chosen, an example of this is the apoptosis associated gene transglutaminase 2 (TGM-2) (Table 1). TGM-2 is a calcium dependent enzyme found to be upregulated in apoptotic cells and for this reason was included in the final plate layout (Fesus et al., 1989; Taresa et al., 1992; McConkey and Orrenius, 1997). Bacterial stocks of IMAGE clones were then available from Hinxton free of charge. Duplicating complete multiwell plates or individual clones selected from their vast collection was inevitably an error prone process. Plates were sometimes replaced in the wrong orientation compared to the database; bacterial clones were contaminated or failed to grow in culture; and many were also miss-assigned in the database. For some genes, six different clones were sequenced before a correct one was found. Sequencing data was then fed back to continually improve the resource. The collection is currently held by Source BioScience LifeSciences and a single sequence-verified clone now costs £120 (http://www.lifesciences.sourcebioscience.com).

Table 1 Summary table of gene groups included in cDNA array tailored to investigate all aspects of vascular biology

Note as with the complete list categories are not exclusive

For full list in alphabetical order see appendix following (Evans et al., 2003)[*1]

Process /pathway	Example	Gene Name
Apoptosis		
Bcl-2 family	anti-apoptotic pro-apoptotic	Bcl-2, B-cell CLL/lymphoma Bax, Bcl-2 associated protein 2
Bcl-2 interacters	APAF1	Apoptosis protease activating factor 1
Death receptor ligands	TNFα	Tumour necrosis factor alpha
Death receptors	TRAIL/ APO2L	TNF-related apoptosis-inducing ligand
Death receptor associated	TRAF1	TNF receptor associated factor 1
Cytoplasmic signaling molecules		
Signaling/transcription	JNK1	Mitogen activated protein kinase 8
Caspase family programmed cell death	Caspases e.g. caspase1/IL1BCE	Interleukin1 beta converting enzyme, caspase 1
Jak/STAT pathway	STAT1	Signal transducer and activator of transcription-1
wnt pathway	Wnt 11	Wingless-type MMTV integration site 11
NFκβ pathway	1-kB epsilon/ NFκβIE	Nuclear factor of kappa light polypeptide gene enhancer in B-cells inhibitor, epsilon
MAPK pathway	MEK1, MAPKK1	MAP kinase kinase 1
NFκβ pathway	NFκβp65	Nuclear factor κβ p65
Growth factors/ Chemokines /cytokines		
EGF family	BTC	Betacellulin, ligand for EGF receptor
VEGF family	VEGF A	Vascular endothelial growth factor A
Chemokines	MCP-1, CCL2	Monocyte chemoattractant protein 1
Cytokine families eg TGF family	TGFβ	Transforming growth factor beta
Receptors		
Angiogenesis	VEGF family e.g. KDR	Kinase Domain receptor, VEGFR2, Flk-1
Integrins	ITGA1	Integrin alpha 1
cluster of differentiation	CD56	isoform of Neural Cell Adhesion Molecule (NCAM), adhesion molecule
Wnt receptors	FZD1	Frizzled (Drosophila) homolog 1

Process /pathway	Example	Gene Name
Receptors (continued)		
Nuclear receptors	RARA	Retinoic acid receptor, alpha
Tumour associated antigens	MUC1	cell surface associated (MUC1) or polymorphic epithelial mucin (PEM) mucin1
Chemokine receptors	MCP-1R, CCR2	Monocyte chemoattractant protein 1 receptor, chemokine R2
Cytokine receptors eg TGF family	TRFBR3	Transforming growth receptor beta receptor III, betaglycan
Cell division		
Cell division	CDC2	cell division cycle 2
cell cycle checkpoint proteins	RAD1	RAD1 homolog, DNA repair exonuclease REC1
Extracellular matrix molecules		
interstitial collagenases	MMP1	Matrix metalloproteinase
	THBS1	Thrombospondin-1
apical cell adhesion	TRO	Trophinin (trophoblast)
Controls		
Non human exogenous	ATC ab	Arabidopsis thaliana chlorophyll a/b binding
Human endogenous	G3PDH, GAPDH	Glyceraldehyde-3-phosphate dehydrogenase
Unexpected inclusion: Example of an imposter resulting from clone errors		
apoptosis associated	TGM2	Transglutaminase 2

The organisation of the array required some biological knowledge as it was important not to print very highly expressed genes, such as some of the endogenous control transcripts, next to much less well expressing genes and, in addition, to distribute them in different subgrids (as in Figure 1, (Evans et al., 2003)[*1]).

2.4 Quality control

Control spots were included, endogenous normalisation controls and exogenous controls, in this case *Arabidopsis thaliana* cDNAs, to enable monitoring of variability between arrays (Figure 3, p96, (Evans et al., 2003) [*1]). Keeping variation due to technique to a minimum is always a concern when arrays are distributed to different users and laboratories across the world, and this factor was built into the analysis of each experiment. All the genes were spotted as duplicates and the number of strikes of the robotic printing tool was constant, as was the humidity of the robot and concentrations of the spotted templates.

Variable experimental parameters including hybridisation temperature, hybridisation buffer concentration, hybridisation length as well as the duration of

phosphor screen exposure after optimising, were set as constants to enable consistency within and between experiments. The membranes were denatured post-printing rather than the templates, since denatured templates do not store well. For each experiment, a set of filters was allocated and set aside to ensure that only a single printing batch was used. A datasheet was produced for each array hybridised (Figure 2.1).

Array number: 703
RNA sample name: Term Placenta 1 lobule 3C
User: Amanda
Location of expt notes: Amanda 131
PCR products in houseset 6 Batch G (5)
RNA Source: untreated human tissue Tri-reagent/ DNAsed and agilent
Tissue source: placenta/Graham Burton Anatomy
Date of Extraction of RNA : 28.6.02
Spikes labelled: (all 5 spikes 500pg to 1pg) x 2microl
Date of labelling: 20.8.02
Protocol: Endofree RT,
Probe purification method: Pharmacia column
Hyb temp: 65C
Hyb Time: approx. 16 hours
Final Wash: 0.1XSSC +0.1%SDS
Counts of probe: 1.78 x 10^7 per 400 microlitres (NB probs with counter)
Duration of Phosphorimager exposure DRY 48hrs
Image Quality: good
Image File Saved As: combined 703710.gel, indiv as 703.gel
Scanned with 704,705,706,707,708,709,710
Notes on Array:
Matched samples P=periphery, C=centre of lobule

Figure 2.1 An example of a completed technical datasheet

2.5 Data analysis

The data analysis pipeline was another potential source of variation. After verification of linearity of the hardware-software interface for primary data acquisition (Figure 4, p98, (Evans et al., 2003)[*1]), the filtering steps used for image processing were standardised and applied to each array. An analysis grid was created for each batch of arrays (Figure 2.2). Hybridisation intensities were calculated for each spot, and local background subtracted, control spots and positive controls were filtered out, and intra-array noise avoided by excluding outliers with discordance between duplicate pairs.

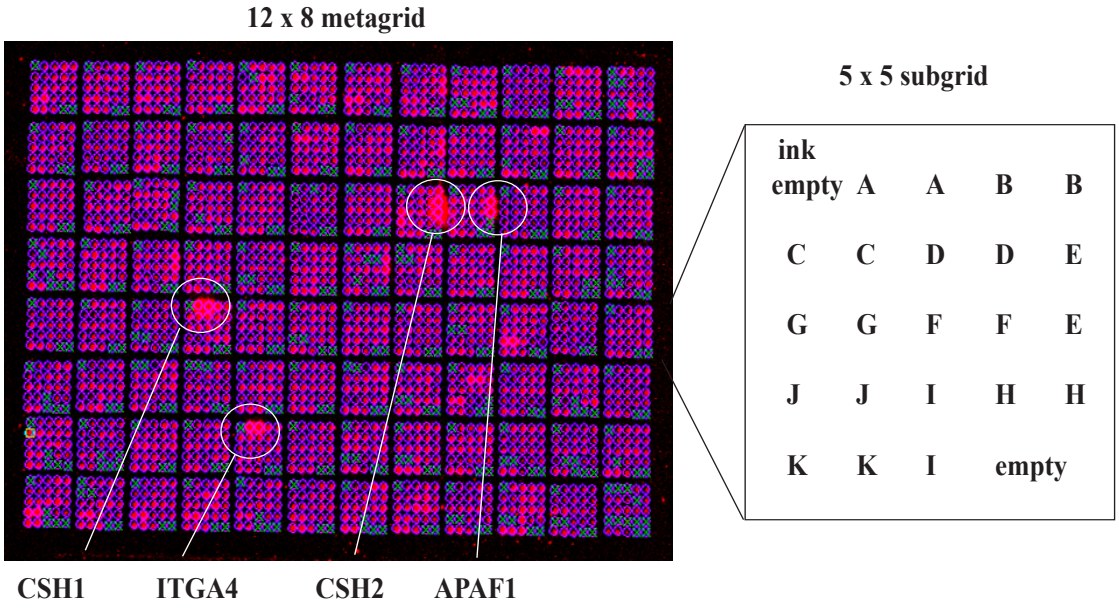

Figure 2.2 Primary data acquisition from hybridised fluorescent intensities
A grid is placed across the array. x indicates empty or blank wells. Poor quality spots are flagged for exclusion by the software package at this stage. The image is coloured red to aid spot-finding during analysis. The complete array forms a 12x8 metagrid made up of 5x5 spots in a subgrid, with a theoretical maximum of 2400 spots. A-K indicates the reference plates storing the clones. Duplicate spots are adjacent. This example is easily recognised as placenta by the characteristic pattern of highly expressed genes circled in white: placental lactogen 1/ chorionic somatomammotropin hormone 1 (CSH1), integrin alpha 4/antigen CD49 (ITGA4), chorionic placental lactogen 2/ somatomammotropin hormone 2 (CSH2), apoptotic protease activating factor 1 (APAF1).

Experiments to assess both intra- and inter-array variability led to the conclusion that to obtain biologically relevant data there was an absolute requirement for technical and biological replicates. At least three independent replicates were needed to define differential expression between samples and to reduce the chance of false positive results.

There are further sources of variation that influence data, including the efficiency of transcription and labelling of probes (see p99, (Evans et al., 2003)*[1]); therefore normalisation in the form of mathematical adjustment needs to be made. Loess normalisation, a type of intensity-dependent normalisation, was used (Figure 2.3).

Following normalisation the datasets were compared by various statistical methods. Cyber T (Baldi and Long, 2001) based on the Student's t-test but including a computational method to account for large sample numbers was used, along with significance analysis of microarrays (SAM) which uses non-parametric analysis, as samples may not be normally distributed (Tusher et al., 2001). Both Cyber T and SAM focus on significance of single genes. Multigene approaches to search for patterns of co-regulated genes are more biologically relevant when dealing with complex tissue samples. To do this independent component analysis (ICA) was used in which the components are statistically independent (Leimeister et al., 2000; Saidi et al., 2004) and provides a global view of trends in expression between samples (see Figure 5, p151 (Schoenfeld et al., 2004)*[5]

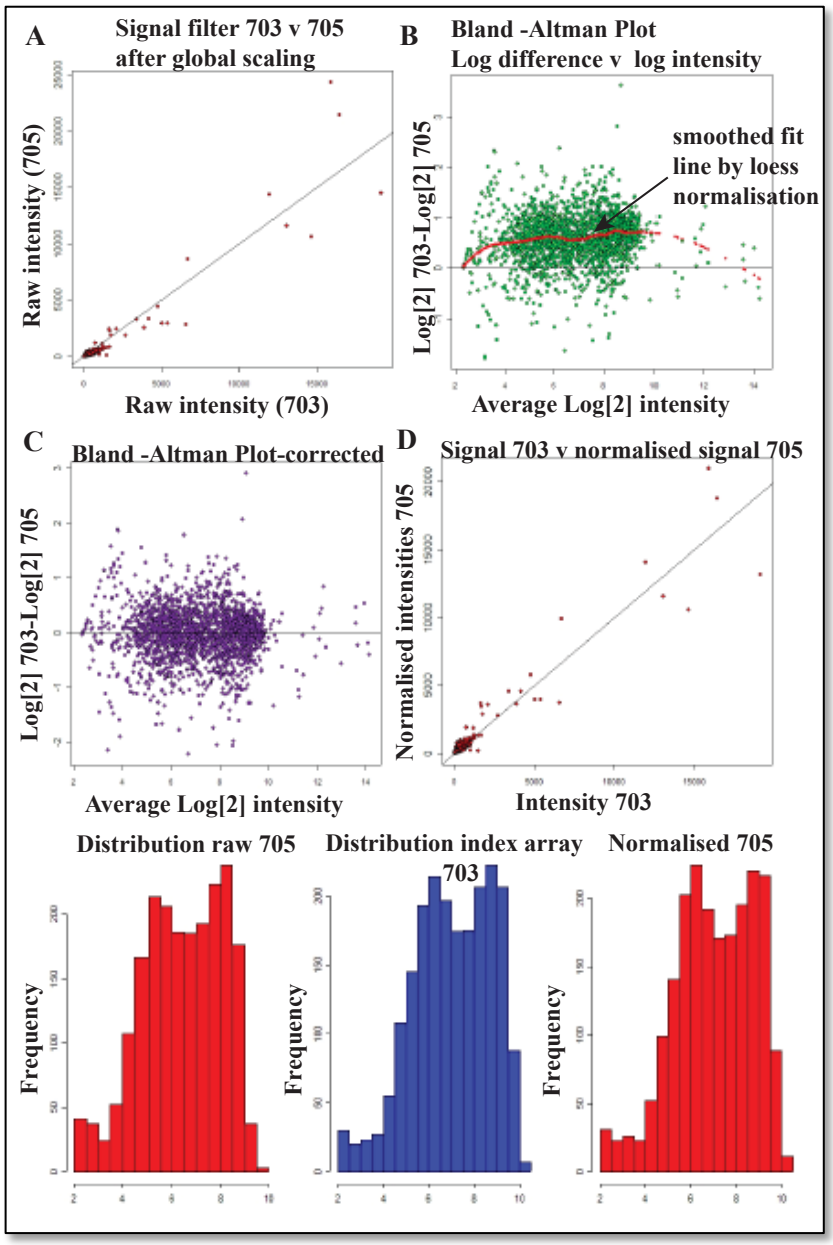

Figure 2.3 Loess Normalisation of intensity dependent errors

A: Signal intensity filter 705 against 703 after global scaling, this fails to completely normalise to the alignment line, although these two filters were hybridised with RNA from different lobules of the same placenta.

B: Rotation and transformation using a Bland-Altman Plot (Bland and Altman.D.G, 1999). Difference in log signal intensity plotted against the mean log signal intensity to demonstrate intensity dependent deviation on the x axis. Loess normalisation is applied (the red smoothing line)

C: Data corrected to filter 703, the most representative by Euclidean distance of a set of six arrays (see Figure 2.1).

D: Data plotted as in **A**

Figure 2.3 legend (continued)

A full description for loess normalisation of gene intensities is available at http://www.obgyn.cam.ac.uk/genearray

Below A-D are frequency histograms**. Left:** The distribution of raw data for filter 705. **Centre:** The distribution for the index array 703, the most representative of the set by Euclidean distance. The reference array is the array closest, in terms of Euclidean distance to the geometric average array (Workman et al., 2002). **Right:** The distribution of normalised data for filter 705. Since the two arrays in this illustration are both from different parts of the same placenta the distribution of signals was already very similar.

Analysis and arrays performed by A. Evans

See also Figure 7, p100, (Evans et al., 2003)[*1]

2.6 Pitfalls and limitations

Unlike SAGE and RNA-seq the analysis is limited to genes already on the array, which in practice are genes already reported or suspected to be involved. Microarrays also cannot detect tissue-specific isoforms, without prior knowledge, which is the real strength of current next generation sequencers. Additionally, half-life variations for mRNA and changes in transcriptional regulation are not considered. Given these limitations, with strict monitoring of the hardware-software pipeline we were nevertheless able to have high confidence in the data produced.

2.7 Use and distribution

The most time-consuming step of the whole process was the assembly and verification of all the clones, so once this was achieved several large printing batches were produced and distributed. At each printing batch, random clones were sequenced to check all the quality control systems were working, and to prevent any errors from the many steps in the production pipeline. These arrays formed the basis of a number of PhD projects (see facing page for publication 1 in appendices). The entire genelist later formed part of a larger generic human array produced on glass slides (Rossi et al., 2005).

By the design and use of a small tailored array system to focus on our research needs we were able create hypothesis driven experiments in the field of angiogenesis and vascular biology. We also demonstrated reliability using individual isolates of HUVEC. During the validation process we concluded there was an absolute requirement

for technical and biological replicates, ideally at least three biological replicates, to maximise experimental power. The requirement for only 5μg of template RNA permitted the discovery of pathways involved in implantation in normal endometrium (Chapter 3), and changes involved in endometrial carcinoma (Chapter 4). For example, we were able to confirm earlier work revealing changes in the expression of VEGFA in endometrial cancer and at the same time a possible mechanism for this via the upregulation of hypoxia-inducible factor 1, alpha (HIF1α) (Chapter 4.2).

Chapter 3 Insights into the role of angiogenesis in implantation and endometriosis using *in vivo* and *in vitro* models

Aspects of birth control and infertility impact all our lives. Therefore, a clear understanding of the molecular and morphological changes that result in blastocyst attachment has huge significance. In humans the endometrial lining is only receptive for a narrow implantation window 5-9 days post-ovulation (Figure 1.4). The action of progesterone on oestrogen-primed endometrium results in morphological and genetic changes rendering the endometrium receptive. Successful implantation also requires the development of a hatched blastocyst. Both processes involve vascular remodelling, and one question we addressed was whether anti-angiogenic intervention alone could prevent implantation, by neutralising antibodies to the principal angiogenic regulator VEGF. Another question was whether direct steroidal control of angiogenesis was part of the process. In a further study designed to examine indirect control mechanisms using soluble factors produced by the endometrium, we included samples from patients with endometriosis, in which endometrial fragments are found in ectopic sites. The cell-based and molecular techniques described in chapters 1 and 2 were used in these studies.

3.1 Angiogenesis and implantation

Attachment and implantation of the blastocyst is critical for the establishment of pregnancy in eutherian mammals. With the hypothesis that in humans and primates implantation involves vascular remodelling of the endometrium, systemic injection of a mouse anti-human VEGF monoclonal antibody was carried out in collaboration with the Oregon National Primate Research Center, USA and colleagues at the All India Institute of Medical Sciences (AIIMS), New Delhi, India (Sengupta et al., 2007)[*11]. My role was the production and purification of monoclonal anti-human VEGF-A and anti-IgG_1 isotype control (see (Xu et al., 2005)[*7] facing page)**.** In both studies the route of administration was subcutaneous injection into fertile, ovulating rhesus monkeys *(Macaca mulatta*).

There are two sites of potential antiangiogenic intervention likely to influence implantation. The first site is the receptive endometrium itself where spiral arterioles develop around the endometrial glands and below the luminal epithelium. On implantation local remodelling and changes in permeability will influence placental

development. The second is the maturing ovary itself, or corpus luteum after the release of the follicle, required for high progesterone release until the placenta is established.

In the first study, systemic injection of the VEGF neutralizing antibody was either in the early follicular phase or mid-cycle (see Figure 1.4) and had little effect on ovarian function, although in the same study, the soluble form of the VEGFR1 receptor (sflt1) intra-follicular injection did reduce serum progesterone levels and ovulation. The placenta produces sflt1 as a VEGF antagonist and natural regulator (Kendall and Thomas, 1993; Clark et al., 1998) and, sflt1 injection would form a sink for VEGF blocking local angiogenesis.

In the AIIMS study (Sengupta et al., 2007)[*11], designed to study the effects of immunoneutralization slightly later during the peri-implantation stage, when the blastocyst is free before recognition and implantation, did show significant ($p<0.04$) inhibition of pregnancy when two doses of antibody were given on day 5 and 10, at 10mg per dose, post-ovulation. This provided proof of principle that in the rhesus monkey, VEGF neutralizing antibody can act as a contraceptive agent.

3.2 The role of the antiprogesterone RU486 in the prevention of implantation and in steroid control of angiogenesis

Steroid hormone regulation of endometrial cycling and implantation is another potential target for intervention. RU486 (mifepristone) is a progesterone analogue binding with high affinity to the progesterone receptor as well as glucocorticoid receptors. It is most well known as an emergency post-coital contraceptive.

The mechanism of action of RU486 is unclear as the progesterone receptor can still bind DNA, but the net result is an unproductive association with no transcription of progesterone target genes such as VEGFA (Leonhardt and Edwards, 2002). It is thought that RU486 changes the conformation of the progesterone receptor to favour corepressor rather than coactivator recruitment (Leonhardt et al., 2003). Studies at AIIMS showed post-coital RU486 prevented pregnancy in the rhesus monkey (Ghosh and Sengupta, 2005) and a single oral 600mg dose will induce abortion in humans (Sarkar, 2002).

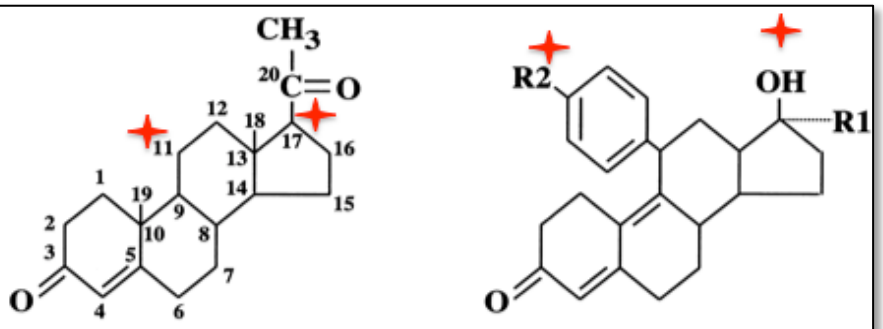

Progesterone **RU486**

Figure 3.1 The chemical structure of the steroid hormone Progesterone and RU486 (Mifepristone) a synthetic analogue of progesterone

(17β−hydroxyl 11β-(-4dimethyl aminophenyl-)-17α-(1propyny11)-estra-4, 9-dien-3-one.

11β and 17α substitutions ✦ create an antogonist

To identify pathways involved in receptivity, endometrial explants (Chapter 1.2.1) from five normal fertile women at mid-secretory phase were cultured in the presence of estradiol and progesterone with or without RU486 for 12 hours (Catalano et al., 2003)[*3]. For short periods of incubation all the normal epithelial to stromal cell interactions remain intact. cDNA probes from the paired endometrial samples were hybridized to the arrays described in Chapter 2 and hybridization signals were quantified.

3.2.1 The JAK/STAT3 and the MAPK signaling pathways are modulated by RU486 treatment

In the presence of RU486, Janus kinase 1 (JAK1) and Jun-N terminal kinase (JNK1), a mitogen-activated protein kinase, were downregulated compared to steroid hormone only treated samples. Results were verified by quantitative PCR (qPCR). This implicates the JNK/p38 MAP kinase (MAPK) signaling pathway in implantation. Mice lacking the p38 kinase had been shown to lack vascularization and have defects in

placental angiogenesis (Mudgett et al., 2000) and since this publication others have shown that inhibition of either the JNK kinase or p38 kinase pathway results in the inhibition of cavity formation in the endometrium at the peri-implantation stage (Maekawa et al., 2005).

JAK1 is expressed in endometrial glands throughout the cycle and also in the stromal cells at the mid-secretory phase (Figure 4, (Catalano et al., 2003)*3). The JAK/STAT (signal transducer and activator of transcription) pathway is activated by a number of cytokines and growth factors, including LIF, important in mouse and human implantation (Charnock-Jones et al., 1994; Arici et al., 1995; Smith et al., 1998; Sharkey et al., 1999). STAT3 is activated in the mouse during implantation and is at its highest at the time of blastocyst attachment (Teng et al., 2004). Reduction of JAK1 signals by RU486 suggests a role for JAK/STAT signaling in successful blastocyst attachment in humans reflecting downstream inflammatory responses, cell survival promotion and angiogenic changes (Figure 3.2).

3.2.2 Immunity, inflammation and the non-canonical NF-κβ2 pathway are regulated by anti-progesterone treatment

Treatment with RU486 also upregulated a number of transcripts including cystolic phospholipase A2 (cPLA2), NFKβ inducing kinase (NIK) and the natural killer cell receptor CD94. Upregulation of NIK, expressed in the glandular epithelium and endothelium implies tight regulation of the non-canonical nuclear factor Kappa 2 (NF-κB2) pathway is required to control inflammatory responses and allow successful implantation (King et al., 2001).

cPLA2, which promotes inflammation by releasing arachidonic acid in a rate-limiting step of prostanoid synthesis, also fits the notion of ovulation and implantation as a controlled inflammatory-like reaction. Inflammation is an inducer of angiogenesis (Carmeliet and Jain, 2000) and deregulation during implantation prevents blastocyst attachment. At the time of the study (2002-3) cPLA2 upregulation by RU486 had already been reported (Kol et al., 1998).

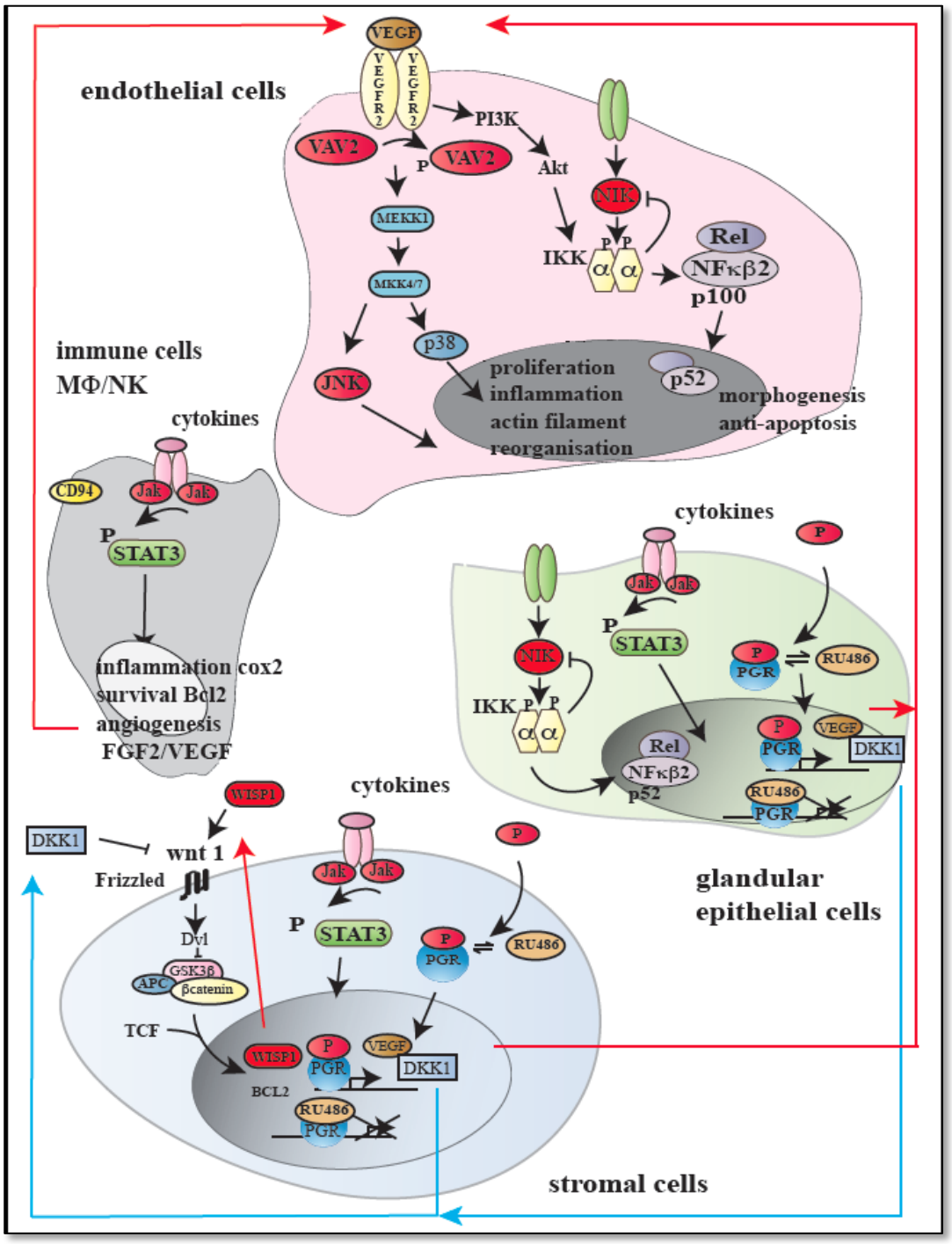

Figure 3.2 Pathways modulated by RU486 treatment of endometrial explants

Genes in red ovals were modulated by the anti-progesterone RU486 implicating the associated cells and pathways in blastocyst implantation. Decreased expression of progesterone targets such as DKK1 (blue line) and VEGF (red line) for example, influences more than one cell type. Cell types as in Figure 1.3**,** immune cells include macrophages (MΦ) and natural killer (NK) cells. The pathways and their components below contribute to the remodelling required for implantation.

Key to Figure 3.2: Phosphorylation (P)**,** progesterone (P in red ovals), progesterone receptor (PGR).

The Wnt pathway: wnt-1 inducible signaling pathway protein 1 (wisp); frizzled receptor ligand (wnt1); dickkopf1 (DKK1) a negative regulator; disheveled (dvl); Glycogen synthase kinase 3 beta (GSK3β); adenomatous polyposis coli (APC); T cell factor (TCF).

The Jak/Stat pathway: Janus kinase 1 (Jak); signal transducer and activator of transcription 3 (STAT3). **Downstream targets:** cyclooxygenase 2 (cox2); B-cell lymphoma 2 anti-apoptotic (Bcl-2); fibroblast growth factor 2 (FGF2).

The non-canonical NFκβ2 pathway: NFKβ inducing kinase (NIK); Ikappa B kinase alpha (IKKα); nuclear factor of kappa light polypeptide gene enhancer in B-cells 2; p100 and p52 subunits (NFκβ2), v-rel reticuloendotheliosis viral oncogene homolog B (RelB), a transcription factor.

The MAPK/ERK pathway: guanine nucleotide exchange factor (VAV2); mitogen-activated protein kinase kinase 1 (MEKK1); mitogen-activated protein kinase kinases 4 and 7 (MKK4/7), extracellular signal-regulated protein kinases 1 and 2 (ERK1/2); c-jun N terminal kinase (JNK); P38 mitogen-activated protein kinase (p38). Down regulation of guanine nucleotide exchange factor (vav2) enhances the reduction in JNK-mediated transcription since vav2 acts upstream of JNK (Abe et al., 2000)

Natural Killer (NK) cells play a role in the prevention of maternal rejection of the foetus and alterations in NK activity are implicated in endometrial receptivity (McGrath et al., 2009), local upregulation of CD94 in the secretory phase may contribute to unexplained infertility. Natural killer cells make up 70-80% of the endometrial leucocyte population, and CD94 with its KIR (Killer cell immunoglobulin-like receptor) partner NKG2A, is a ligand for HLA-E (major histocompatibility complex, class I, E) modulating NK activity, thought to be critical for spiral artery remodelling and trophoblast survival (Rabot et al., 2005).

3.2.3 Wnt pathway modulation by RU486

The Wnt-1 inducible signaling pathway protein 1 (WISP1 or CCN4 CCN family member 4) is upregulated by RU486 treatment. Wisp1 is a wingless-Type MMTV

Integration Site Family, member 1 (Wnt 1) responsive gene and high Wisp1 has since these experiments been associated with poor prognosis in endometrial endometroid carcinoma (Tang et al., 2011), as well as breast (Davies et al., 2007; Faivre and Lange, 2007) and lung cancer (Chen et al., 2007). Secretion of Wisp1 further upregulates the Wnt pathway in stromal cells via autocrine regulation (see Figure 3.2).

Increased blood flow is associated with follicle release and endometrial thickening during the periovulatory phase and the effects of RU486 suggest steroid control of angiogenesis in the endometrium.

3.3 Soluble factors produced by the endometrium promote angiogenesis

Endometriosis, a condition in which ectopic endometrial fragments are found in the peritoneum or scarring the fallopian tubes, is accompanied by elevated VEGF in the peritoneal fluid (McLaren et al., 1996). A major cause of infertility and abdominal pain, endometriosis has a huge impact on quality of life for women with the condition. Endometriosis is a disease of the 20th and 21st centuries, whereas previous generations of woman had in the region of forty menstrual cycles in a lifetime, largely due to pregnancy and lactation, that number is now nearer five hundred. If the attachment of tissue fragments to the peritoneum does contribute to endometriosis, the chances of aberrant angiogenesis caused by menstrual fragments will increase with the number of cycles.

Soluble factors produced by endometrial tissue are thought to promote angiogenesis. In a series of experiments using endometrial supernatants and menstrual effluent, these factors were shown to influence the transcriptome of cultured HUVEC cells (Print et al., 2004)[*6]. When combined in coculture with dermal fibroblasts endometrial supernatants also influenced the sprouting of new vessels in an *in-vitro* angiogenic assay (Figure 3.3), both proliferative and secretary phase supernatants significantly increased vessel formation.

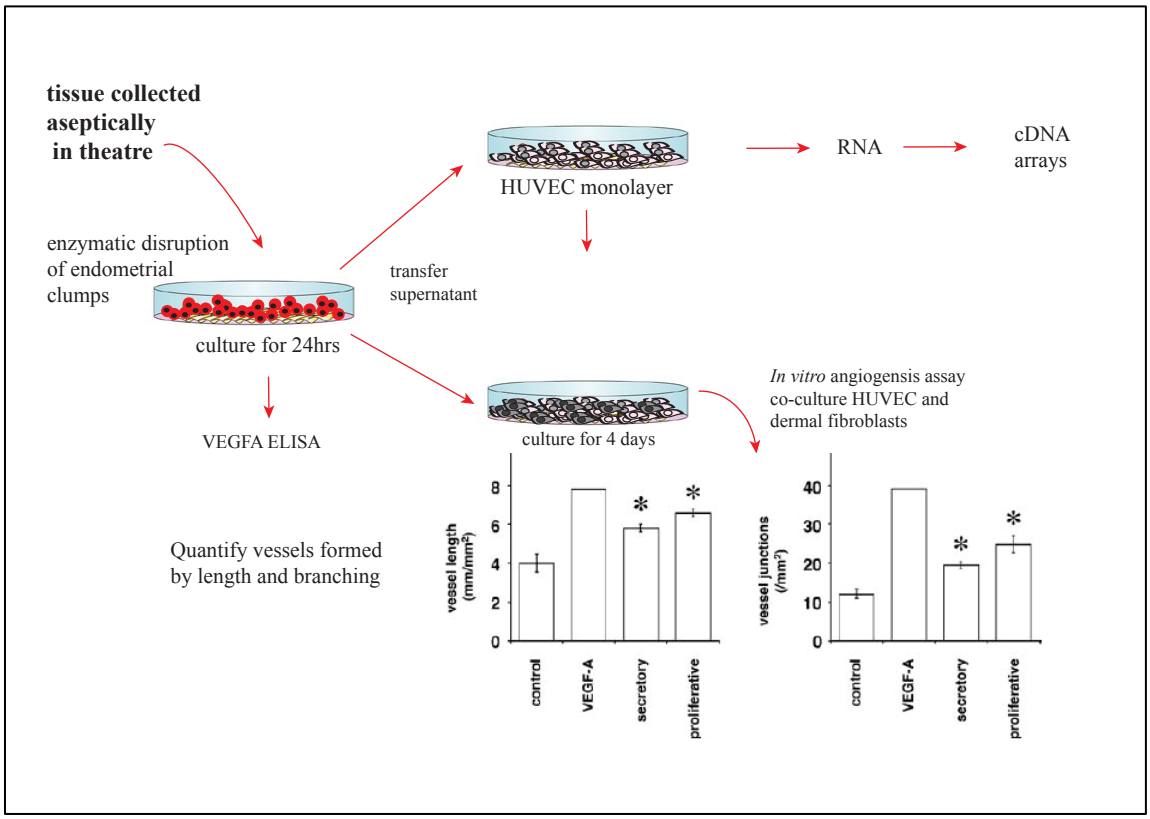

Figure 3.3 Soluble angiogenic factors produced by the endometrium alter gene expression in cultured HUVEC cells

To ensure uniform oxygen tension the tissue samples were dissociated enzymatically since this experiment required longer incubation times than the explant experiments.

Ribonucleic acid preparations (RNA) were transcribed and applied to the tailored cDNA array described (Chapter 2). Coculture with dermal fibroblasts showed a significant increase in vessel length (left graph *) and vessel junctions (right graph*) (Students' t-test $p<0.05$) for both secretory phase and proliferative phase endometrial supernatants compared to the controls. 10ng/ml VEGFA was used as a positive control, graph reproduced from (Print et al., 2004)[*6], Figure 1B, C.

Abbrv. enzyme-linked immunosorbent assay (ELISA).

ELISA confirmed the presence of VEGFA protein in endometrial supernatants and in menstrual effluent. However, there was no detectable difference between supernatants of samples from patients with endometriosis compared to those from normal tissues. Microarray and clustering analysis of HUVEC cells following exposure to proliferative, secretory or endometriotic supernatants Clustering (Figure 4C (Print et al., 2004)[*6]) could not separate the normal samples from those with endometriosis. Clear

proliferative and secretory clusters were distinguishable. In hindsight, perhaps a better experiment for the endometriotic samples may have been to compare eutopic (uterine) and ectopic (peritoneal) tissues directly from the same patient. However, these results provide a clear indication that, in this study group, soluble factors from the lesions themselves, including VEGF, are not the major causal factor in the disease.

The Sampson theory of retrograde menstruation cannot explain cases of endometrial lesions far removed from the peritoneal cavity in the lung or even nasal passage (Sampson, 1927). There is some evidence that excess VEGF and other angiogenic factors are produced by macrophages in the peritoneum (McLaren et al., 1996; McLaren, 2000) and that these macrophages are M2 type, or alternatively activated macrophages, in endometriosis. There are two extremes of macrophage differentiation, classically activated type 1 (M1) or M2 macrophages with similar properties to tumour-associated macrophages (TAMS) in endometrial carcinoma, although TAMS have a more mixed phenotype depending on the cytokine environment (Mantovani et al., 2002).

We demonstrated that anti-angiogenic intervention can prevent implanation in primates (Sengupta et al., 2007)[*11] and provided strong support for an angiogenic role in pre-ovulatory follicle and post-ovulatory corpus luteum development (Xu et al., 2005)[*7]. In addition, we have shown direct steroidal control of at least two important intracellular pathways, the JAK/STAT and JNK pathways in the endometrium (Catalano et al., 2003)[*3] therefore targeting components of these pathways may prevent implanation. Prevention by RU486 of the JAK/STAT promotion of angiogenesis and inflammation points to a controlled angiogenic and inflammatory remodeling as a requirement of successful implantation. Leucocyte involvement in the attachment and survival of the blastocyst is also suggested by our findings. Immunity has important implications in pre-eclampsia, a major complication of pregnancy characterised by shallow cytotrophoblast invasion of decidua, and associated with altered HLA profiles (Le Bouteiller et al., 2003).

Control is perhaps the key word, since the processes described are also features of metastatic tumour growth. Insufficient angiogenesis can alter fertility while altered or excess will lead to cancer and many more disorders. The following experiments explore this further.

Chapter 4 Gene expression analysis implicates angiogenesis and inflammation as key processes in endometrial cancer

Angiogenesis is an important component of the metastatic pathway (Folkman, 1990; Zetter, 1998) and, metastasis is the major cause of death for cancers of solid tumours, accompanied by cell invasion (Tirino et al., 2013). Endometrial cancer, the most common gynaecological malignancy, is associated with poor survival once the disease has progressed to extrauterine sites. We investigated the role of the VEGF family in endometrial cancer and go on to profile the gene expression changes in these tumours with the aim of establishing the molecular basis of the disease and, to search for potential therapeutic targets.

4.1 VEGF upregulation in endometrial cancer

Prior to completing the microarrays described in chapter 2, RT-PCR and *in-situ* hybridisation had shown VEGF upregulation in endometrial cancer (Holland et al., 2003)[*2]. Samples were collected during endometrial curettage or in the case of carcinoma, total hysterectomy. Both benign and atypical complex hyperplasia (ACH) showed no *in-situ* signal for VEGFA, but all the stages of carcinoma were positive. It could be argued that more modern techniques would be more sensitive, but nevertheless our work indicated that increased VEGFA expression may be associated with invasive tumours of the endometrium as with other cancers such as gliomas (Plate et al., 1992), poor outcome in breast cancer (Bando et al., 2005), and many other cancers reviewed by Kut (Kut et al., 2007).

Levels of some of the other VEGF isoforms (Appendix figure 1) showed different patterns of staining. An interesting finding was that VEGFD expression was specific to TAMS (Mantovani et al., 2002) and co-localised with anti-human CD68, a trans-membrane glycoprotein expressed in tissue macrophages (Figure 4.1). This implied a role for TAMS in the promotion of tumour angiogenesis and clinical studies have since shown a correlation between numbers of TAMS and poor prognosis in a number of cancers including endometrial (Hashimoto et al., 2000; White et al., 2002; Ohno et al., 2004; Soeda et al., 2008).

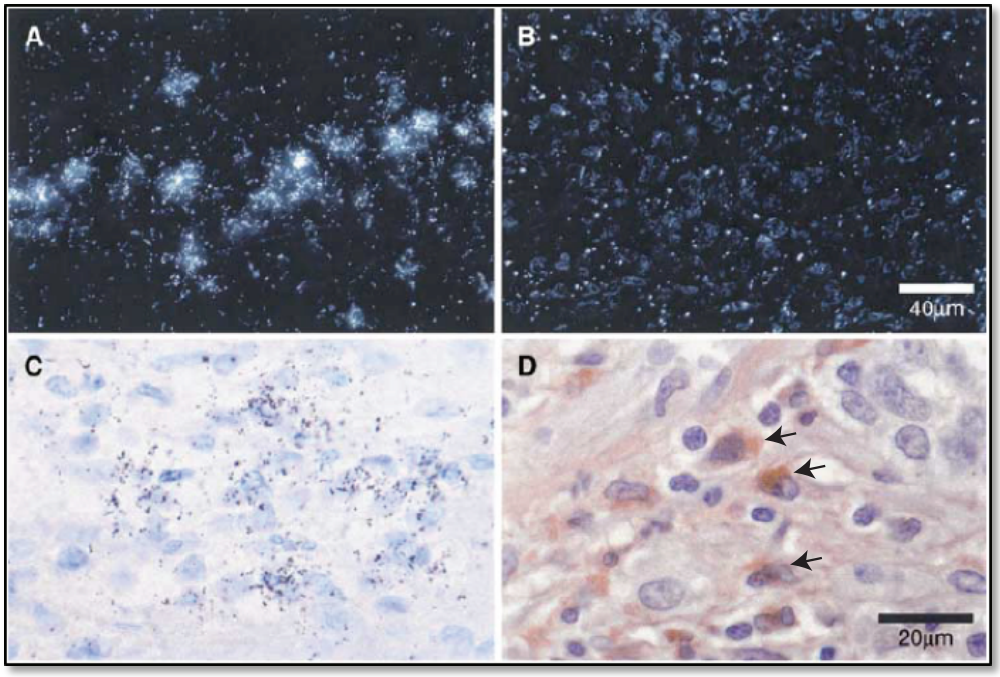

Figure 4.1 Reproduction of Figure 3 A-D p895 (Holland et al., 2003)[*2]
***In situ* hybridisation of a formalin-fixed paraffin-embedded section from a poorly differentiated endometrial carcinoma.** The isoform VEGFD is associated with mature lymphatic endothelial cells.
A dark field VEGFD antisense probe ^{33}P-UTP radiolabeled riboprobes
B dark field VEGFD sense probe no specific hybridisation
C As A but light field conditions
D Immunostaining with anti human CD68 (clone PG-1, Dako Ltd) in a serial section localises silver grains to tumour-associated macrophages (TAMS) (black arrows). White scale bar applies to A, B; black scale bar applies to C, D.
In-situ hybridisation by C. Holland

Angiopoietin 2 (ANGPT2, Ang 2), a ligand for Tie 2 in newly formed vessels, was upregulated in endometrial cancer measured by RT-PCR analysis. In the absence of pericytes around the immature tumour vessels this facilitates vessel sprouting via Tie 2, increased tumour microvessel density (MVD) and tumour invasion. It is also thought to increase vessel sensitivity to VEGFA (Oshima et al., 2004) and promote the angiogenic switch.

Apoptosis or programmed cell death is an important feature of endothelial cell biology (Kerr et al., 1972). As a morphogenetic tool apoptosis allows capillary networks

to be remodelled as they develop for correct vessel patterning and organ size. In normal tissues it is a function of cell turnover but has important implications in the immature vessels of tumours. High Ang 2 would usually cause apoptosis of newly formed tumour vessels (Maisonpierre et al., 1997). However in combination with high VEGF, as we see here, new vessels survive promoting tumour invasion.

Despite the limitations of surveying small numbers of transcripts these experiments identified VEGF and Ang 2 as potential therapeutic targets.

4.2 Transcriptome analysis of endometrial cancer reveals further signalling pathways in human endometrium

Changes in the expression of VEGF isoforms revealed by means of RT-PCR and in-situ (Holland et al., 2003)*2 indicated angiogenesis may contribute to the progression of endometrial cancer. To identify pathways involved in endometrial carcinoma and identify possible therapeutic targets, the cDNA arrays described in Chapter 2 were used to compare malignant samples to atypical complex hyperplasia (ACH) samples and postmenopausal benign tissues. The total sample size, 31 patients in this case, would have been prohibitively expensive at the time if using commercial arrays. By using ICA (see Chapter 2.5) a component consisting of a set of genes representing the "cancer phenotype" was identified.

The upregulation of ANGPT2 and VEGFA in endometrial carcinoma and downregulation of VEGFB agreed with earlier findings (Holland et al., 2003)*2. Table 2 lists key genes that were found to be upregulated in endometrial cancer and are therefore potential therapeutic targets (Figure 4.2 illustrates these changes). The overexpression of cyclooxygenase 2 (cox-2), the rate limiting step in the biosynthesis of prostaglandins (PG) from arachidonic acid, has already been described in cancer (Eberhart et al., 1994; Fosslien, 2000; Costa et al., 2002) including endometrial carcinoma (Tong et al., 2000; Fujiwaki et al., 2002; Tamura et al., 2002). Changes in cox-2 and PPARα indicate altered lipid metabolism in endometrial carcinoma (Littman et al., 2001).

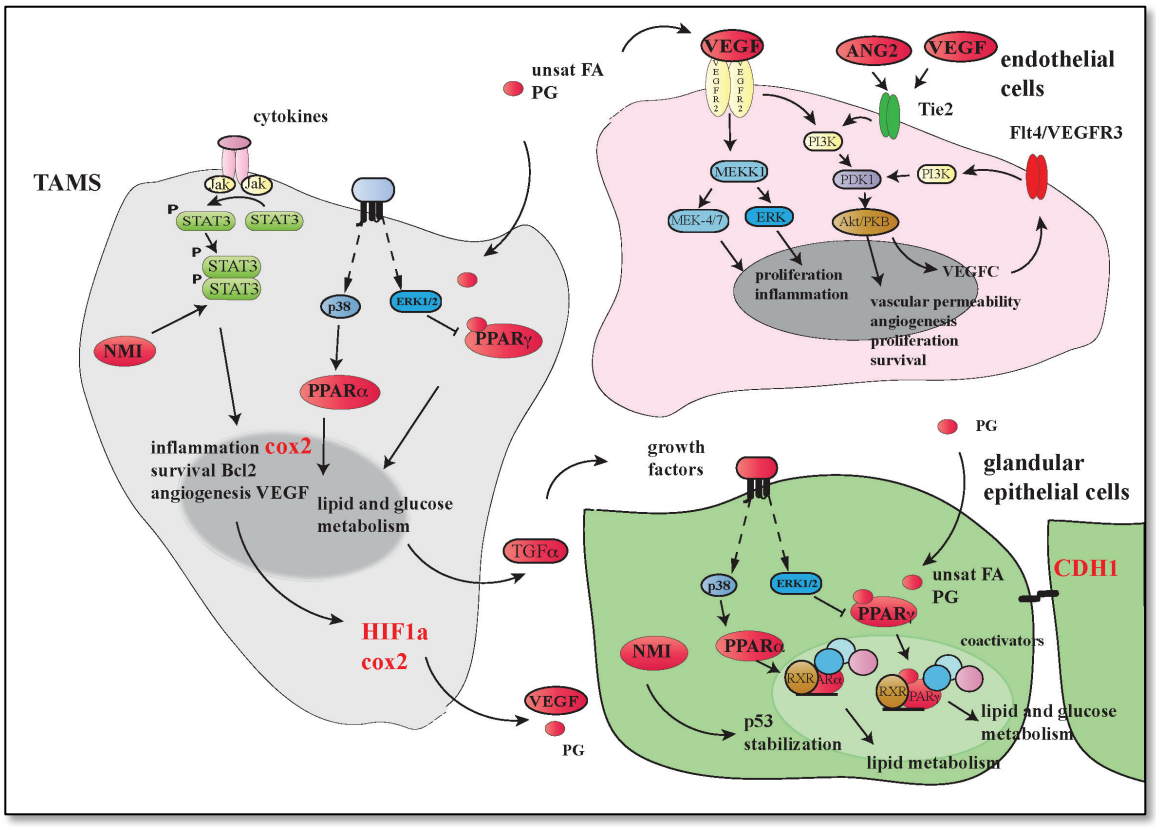

Figure 4.2 Changes in the endometrium in endometrial carcinoma

Glandular epithelial /stromal cell ratio increases in cancer, TAMS (grey) promote tumour growth and matrix remodelling by matrix TGFa and matrix metalloproteinase production. The upregulation of Flt4 (or VEGFR3) increases metastasis by the formation of a positive feedback loop with its specific ligand VEGFC (Su et al., 2006).

Overexpressed transcripts (RED): angiopoietin 2 (Ang2); cyclooxygenase 2 (cox2); E-cadherin (CDH1); Fatty acids (FA); Fms-related tyrosine kinase 4 (Flt4/VEGFR3); hypoxia inducible factor 1 alpha (HIF1α); N-myc (STAT) interactor (NMI); prostaglandin (PG); peroxisome proliferative activated receptor alpha (PPARα); peroxisome proliferative activated receptor gamma (PPARγ)**; transforming growth factor alpha (TGFα).

**PPARγ has since been reported as both upregulated (Knapp et al., 2012) and downregulated (Knapp et al., 2012; Nickkho-Amiry et al., 2012) in endometrial cancer indicating a complex relationship between lipid metabolism and endometrial cancer.

Key: phosphorylation (P); retinoic X receptor (RXR); TEK tyrosine kinase receptor (Tie2); tumour protein 53 (p53). **The Jak/Stat pathway**: Janus kinase 1 (Jak); signal transducer and activator of transcription 3 (STAT3). **The MAPK/ERK pathway:** extracellular signal-regulated protein kinases 1 and 2 (ERK1/2); p38 mitogen-activated protein kinase (p38).

The PI3Kinase Akt/PKB pathway: phosphatidylinositol-3 Kinase (PI3K); pyruvate dehydrogenase kinase, isozyme 1 (PDK1); protein kinase-B (PKB).

4.2.1 Altered oxygen tension in tumours may contribute to the angiogenic switch

Oxygen tension is an important VEGF regulator and VEGF mRNA is rapidly induced by exposure to low oxygen tension. Hypoxia-inducible factor 1 alpha (HIF-1α), the mediator of VEGF transcriptional responses to hypoxia (Wang and Semenza, 1995) was also upregulated. This contributes towards overexpression of both VEGF and ANGPT2 and the angiogenic switch (Figure 4.3) (Sharkey et al., 2000; Holash et al., 1999).

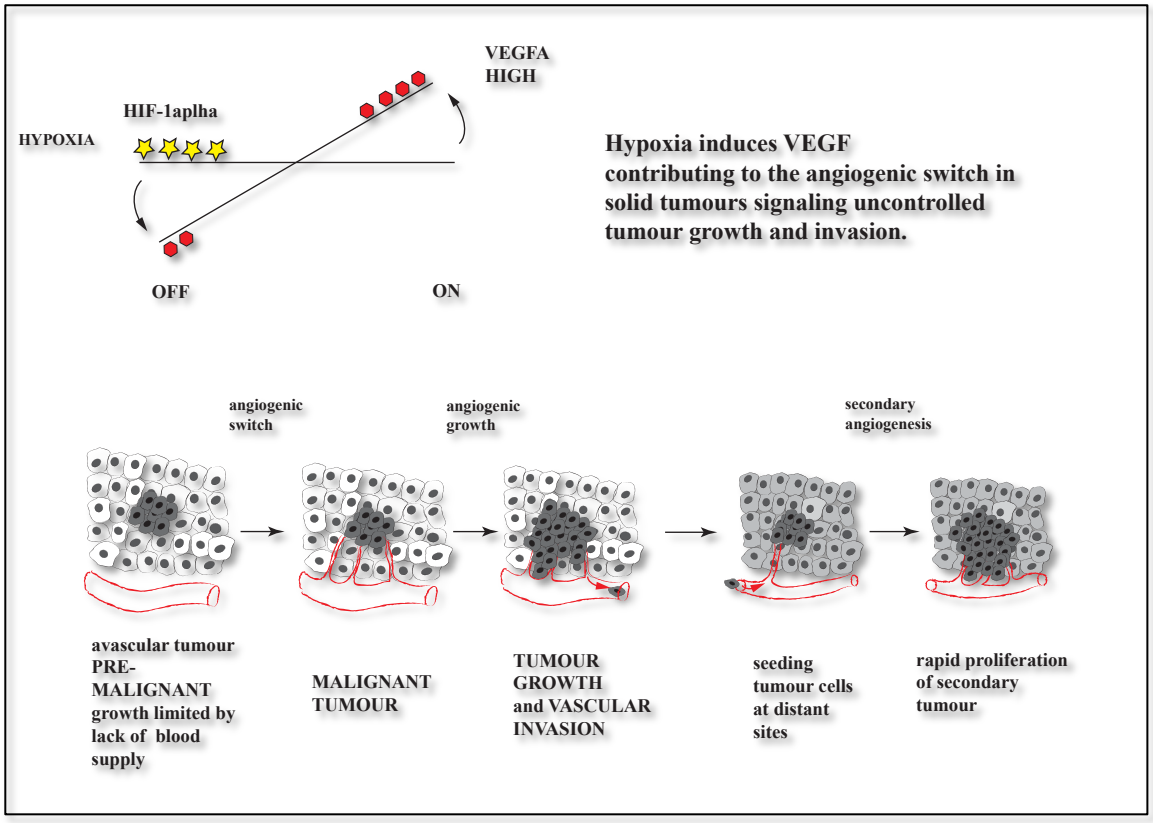

Figure 4.3 Tumour progression and the angiogenic switch

HIF1α is upregulated in endometrial cancer contributing to tumour progression, once the tumour becomes vascularised the possibility of malignant invasion of other sites increases. Anti-angiogenic intervention forms part of many cancer therapies targeting VEGF directly via anti-VEGF (Bevacizumab/Avastin®, Roche) or tyrosine kinase inhibitors (TKIs) (sunitinib/Sutent®,Pfizer)

Abbrvs: Hypoxia inducible factor 1 alpha (HIF-1α)

Table 2 Genes upregulated in endometrial cancer

(see Table 1 p996 (Holland et al., 2004)[*4]), genes from a significantly regulated cancer associated independent component (P<0.001).

GENE ID	GENE	Pathway/Process
Transcription factors/nuclear receptors		
NMI	N-myc (STAT) interactor	Interacts c-myc/n-myc/STATS Mediates ARF (alternate reading frame) tumour suppressor controls p53
PPARα/NRIC1	Peroxisome proliferative activated receptor alpha	Transcription factor complex leads to increased breakdown of triglycerides and fatty acids, expressed endometrial cancer cells not stromal cells
PPARγ/NRIC3	Peroxisome proliferative activated receptor, gamma	Acts in a transcription factor complex anti-inflammatory, high expression endothelial cells
HIF1α	Hypoxia -inducible factor1, alpha subunit	Hypoxia activates HIF1α expression via apurinic apyrimidinic endonuclease redox effector factor-1 (APE1/Ref-1) transactivation domain.
RARβ	Retinoic acid receptor, beta	Receptor for all-trans 9-cis retinoic acid. RAR /RXR (retinoid X receptor) heterodimer required for growth arrest.
Angiogenesis		
$VEGF_{189}$	vascular endothelial growth factor, splice variant 189	Bound to cell surface or extracellular matrix, usually present low amounts compared to $VEGF_{121}$ and $_{165}$ also induces Flt1/KDR
ANGPT2	Angiopoietin 2, Ang 2	Increases vascular permeability, angiogenesis in particular of newly formed vessels
Flt4	Fms-related tyrosine kinase 4 (VEGFR3)	Receptor for VEGFC and D, also up regulates VEGFC by positive feedback
Cell-cell/cell-matrix adhesion		
CDH1	E cadherin, epithelial Cadherin 1, uvomorulin	Its down regulation in most cancers usually associated cellular motility
MMP1	Matrix metalloproteinase 1 (interstitial collagenase)	Involved in matrix remodelling, tumour invasion
MMP3	Matrix metalloproteinase 3 (stromelysin 1, progelatinase)	Breakdown extracellular matrix, associated tumour initiation and enhanced cancer cell invasion
Growth factors		
TGFα	Transforming growth factor alpha	Produced by TAMs contributes to tumour growth
EGFR, c-erbB	Epidermal growth factor receptor	EGFR signalling regulates growth, survival, proliferation and differentiation
Enzymes		
COX2	cyclooxygenase 2, prostaglandin-endoperoxide synthase 2 PTGS2 gene	Rate limiting step in prostaglandin synthesis, expressed TAMS and glandular epithelial cells

4.2.2 Altered cell-cell adhesion may also contribute to the progression of endometrial cancer

The cell-cell adhesion protein, E cadherin, often reduced in cancer (Chen et al., 2003), is associated with the promotion of adenocarcinomas (Pecina-Slaus, 2003; Rodriguez et al., 2012) originating in glandular tissue like many endometrial cancers. E-cadherin over-expression in primary breast carcinomas has also been reported in metastatic tumors of the ductal type derived from glandular epithelium (Kowalski et al., 2003).

Altered expression of matrix metalloproteinases (Park et al., 2001; Hua et al., 2011) indicates breakdown of the extracellular matrix may enhance cancer cell invasion (Table 2).

4.3 Tumour vessels resemble those found during embryonic angiogenesis

The use of explants (Chapter 3) and endometrial samples (Chapter 4) demonstrated that angiogenesis is a major process in the biology of the endometrium. Abnormal angiogenesis forms part of the etiology of reproductive tract disorders including endometriosis and endometrial cancer and increasing MVD is a prognostic indicator in endometrial cancer (Kaku et al., 1997). Endometrial cancer showed altered expression of angiogenic factors: upregulation of both VEGFA and Ang 2 and downregulation of VEGFB. The molecular profile of endometrial cancer revealed an association with lipid metabolism suggesting PPARα as a potential therapeutic target.

One of the hallmarks of cancer is sustained angiogenesis, and the TEK tyrosine kinase receptor (Tie2), on the endothelial cells is a characteristic marker of newly formed immature vessels associated with tumours. Newly formed tumour vessels are vulnerable to intervention without the stabilising effect of supporting cells, much like embryonic vasculature before mesenchyme-derived progenitors form supporting cells (Benjamin et al., 1999; Bergers and Song, 2005) indicating a potential control point for metastasis. The development of newly formed vessels is explored further in chapter 5 by the use of a three-dimensional model for vessel development.

Chapter 5 Embryoid body derived endothelial networks

Endometrial explants were designed to allow all the normal contact-mediated and panacrine signalling to be preserved, with the caveat that function will only be preserved for a few hours. Molecular analysis of endometrial cancer indicated new vessel growth as a potential therapeutic target and to investigate this we moved to the embryoid body (EB) model, maintaining a whole tissue environment in which to manipulate vessel formation. Soluble agents and cell-specific transgenes were tested with minimal intervention during vessel formation. Key questions were whether it was possible to influence vessel progression using this model, to quantify these changes, and to investigate the extent to which apoptosis forms part of vessel formation.

5.1 Haematopoietic and vascular development in embryoid bodies

EBs cultured in spinner flasks (Figure 1.10) for ten days have clearly visible "blood islands" containing red haemoglobin expressing cells (Figure 5.1) indicating mesodermal precursors committed to a haematopoietic fate (Choi et al., 1998).

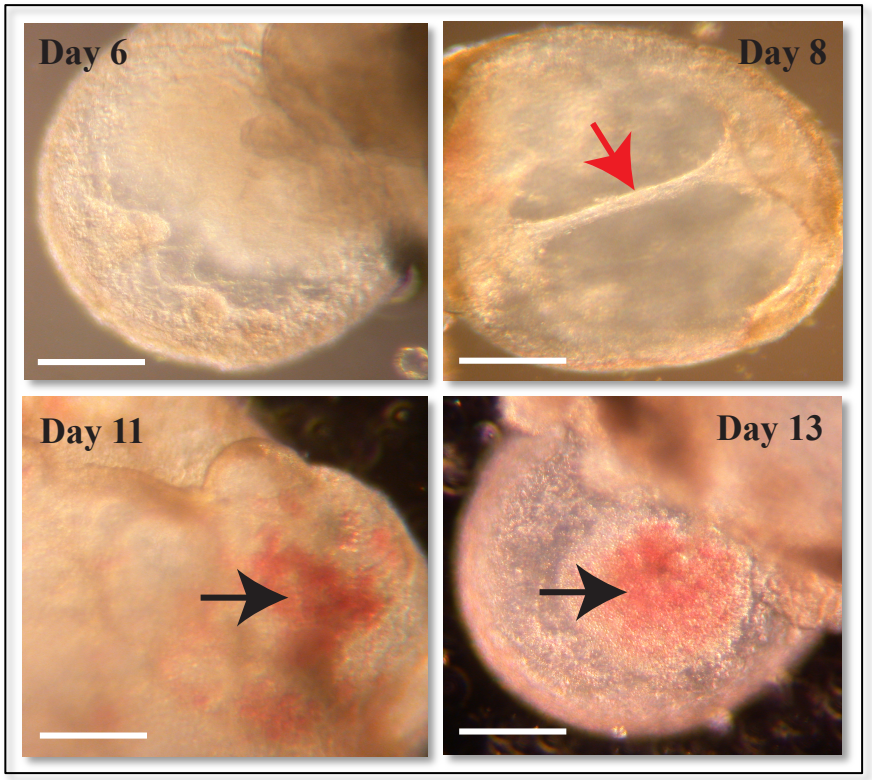

Figure 5.1 Mouse embryoid bodies differentiated in spinner flasks

Legend: Figure 5.1 Mouse EBs differentiated in spinner flasks

Day 6 EB: cystic structures and a central cavity; **Day 8 EB:** the cavity is now septate (red arrow); **Day 11 and 13:** cystic EBs containing haemoglobin-filled blood islands (black arrows). To visualise the three-dimensional networks of endothelial cells requires specific staining. Live cell images captured using a Nikon Coolpix 995. EB experiments, and imaging by A. Evans

White bar is 200µm

The EBs must be fixed and stained or sectioned to show vessel networks around the edges of the cystic cavities. Stained vessels are CD31-positive (PECAM-1, platelet endothelial cell adhesion molecule-1), a marker for endothelial cells (Vecchi et al., 1994).

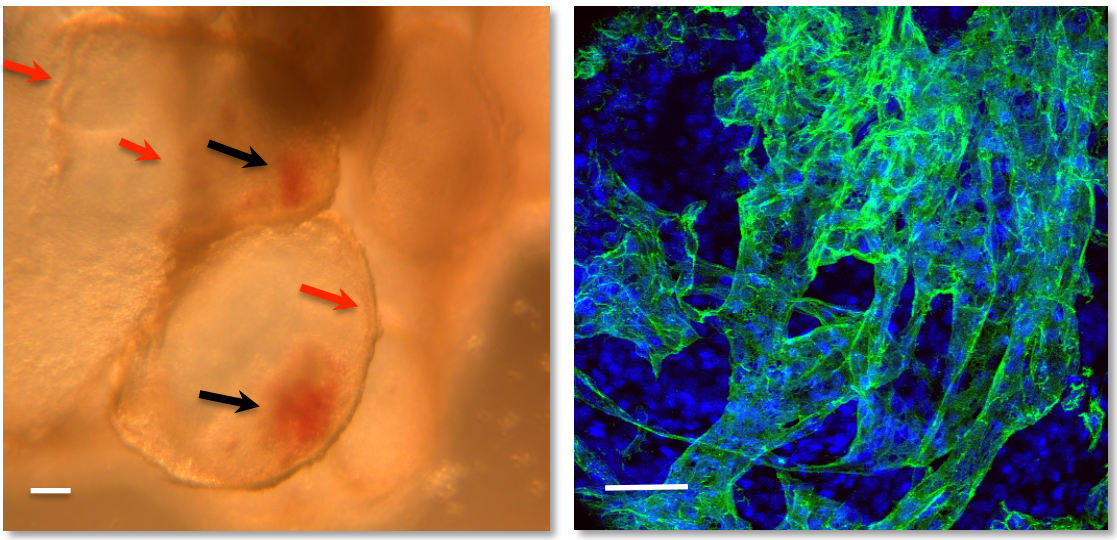

Figure 5.2 Images of a day 14 cystic embryoid body.

Left: Light microscope image of part of a cystic EB captured using a Nikon Coolpix 995. **Red arrows:** indicate regions where endothelial cells form vessels **Black arrows:** indicate groups of haemoglobin containing cells. **Right:** Maximum projection confocal image of a whole mount EB stained with anti-CD31 antibody (clone MEC13.3, Beckon Dickinson) visualised using Alexa Fluor 488 (green) plus Hoechst 33528 nuclear staining (blue). The newly formed vessels are branched, interconnected, and some appear to form lumens. Confocal image captured using a Leica TCS laser scanning confocal microscope.

White bar represents 100µm. Imaging, staining and confocal by A. Evans.

EBs grown in spinner cultures for 14 days using these culture conditions have both haemoglobin- containing cells and endothelial cells forming vessels; however, none of the vessels contained blood cells, as described using quail EBs (Krah et al., 1994), indicating a lack of the correct patterning seen *in vivo*.

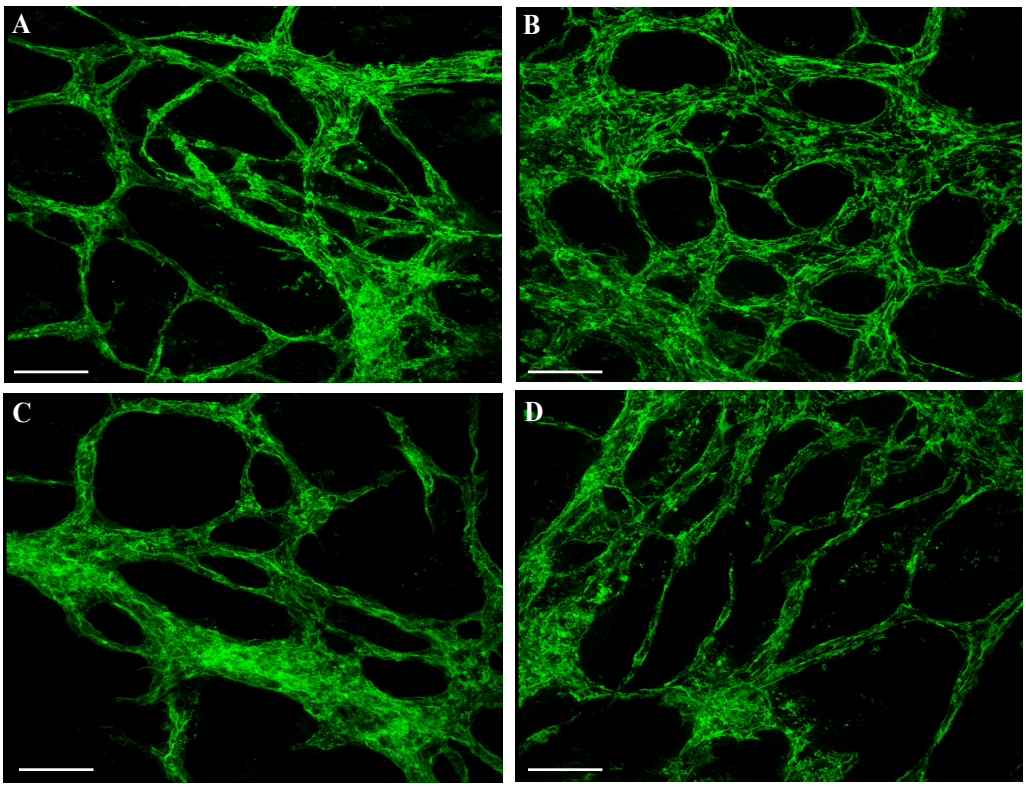

Figure 5.3 Confocal images from a single day 15 whole mount EB

Maximum projection confocal images from a whole mount EB stained with monoclonal CD31 antibody (clone MEC13.3, Beckon Dickinson) visualised using Alexa Fluor 488 (green). The reconstructed Z stacks A-D illustrate the three-dimensional interconnected vessels and the variability in their size and degree of branching. Confocal image captured using a Leica TCS laser scanning confocal microscope.

White bar represents 100µm

Staining and confocal by A. Evans

CD31-positive vessels are variable in diameter and degree of branching (Figures 5.3 and 5.4). Local nutrient and cytokine gradients set up within each EB, in part governed by the distance from the endothelial cells to either a cystic cavity or the

surface of the EB, influence vessel growth and branching. Some larger vessels do appear to possess a lumen (Figure 5.4). There was no evidence of supporting cells or pericytes, all attempts at smooth muscle actin staining were negative unlike in quail EBs (Krah et al., 1994). Vessels are therefore likely to be sensitive to VEGF withdrawal (Benjamin et al., 1999) or anti-angiogenic intervention.

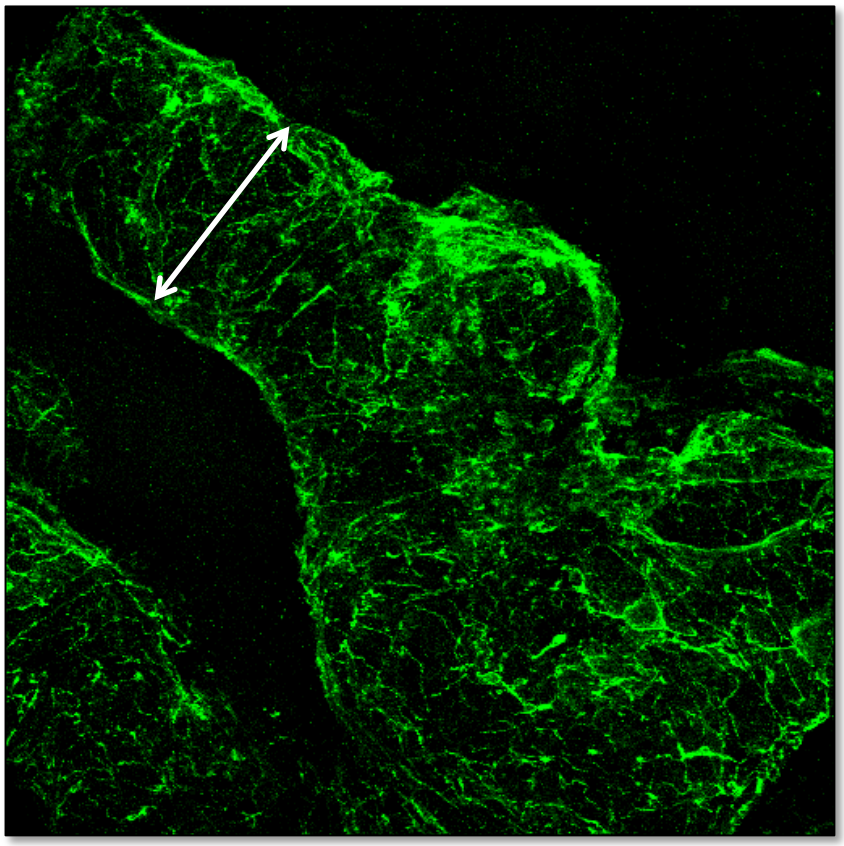

Figure 5.4 A large vessel from a day 11 EB which appears to possess a lumen

Maximum projection confocal image from a whole mount EB stained with monoclonal CD31 antibody (clone MEC13.3, Beckon Dickinson) visualised using Alexa Fluor 488 (green).
Confocal image captured using a Leica TCS laser scanning confocal microscope. White arrow vessel diameter 150µm
EBs fixed whole in zinc fixative (BD Biosciences)
Staining and confocal by A. Evans

5.2 Antiangiogenic agents to modulate vascular development in EBs

The spinner culture system is particularly suited to treatment with antiangiogenic agents. Soluble agents were introduced via side arms in the flasks. Pilot experiments using 100µg/ml Thalidomide (Sauer et al., 2000) had a dramatic effect on EB development. Berberine, a naturally occurring isoquinoline alkaloid from a number of plant species including *Berberis* and *Coptis,* with a wide range of pharmacological activities (Figure 5.5) and uses in traditional Chinese medicine, was chosen to test in the EB system for its reported anti-inflammatory properties (Fukuda et al., 1999).

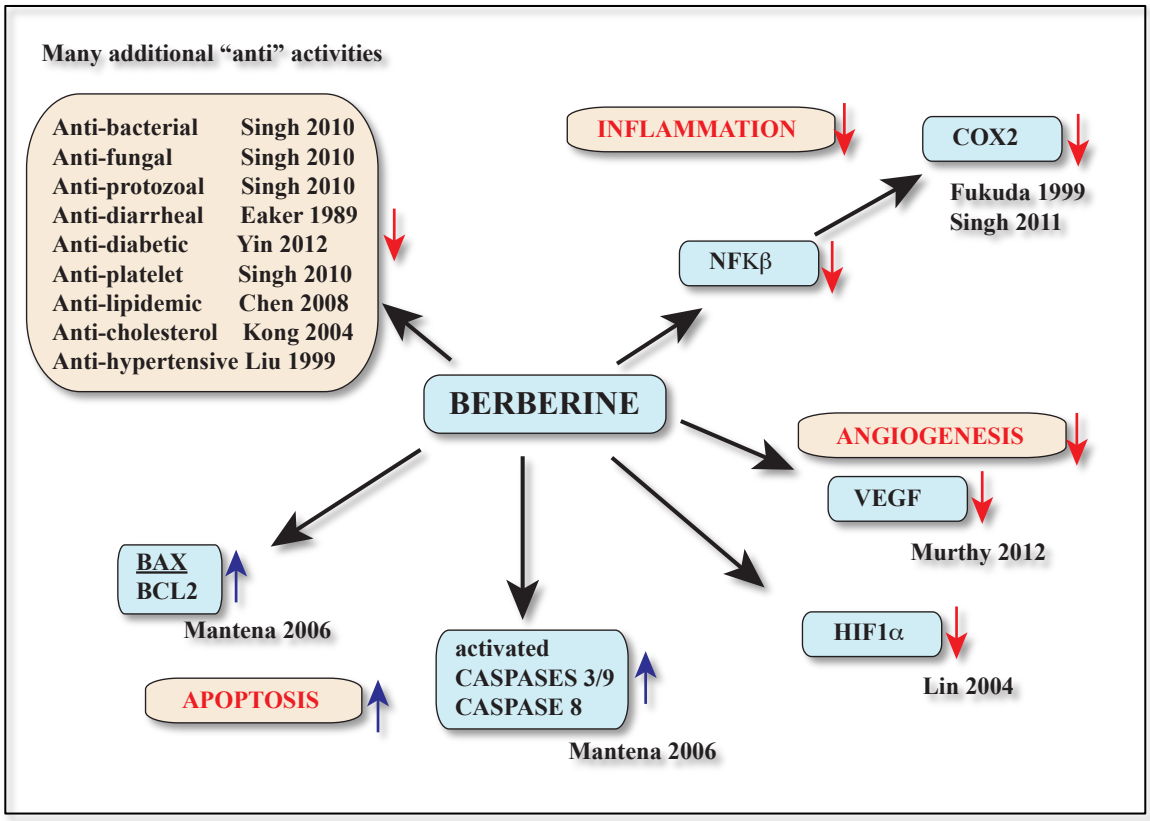

Figure 5.5 The effects of Berberine, a natural alkaloid in mammalian cells

Berberine has a wide range of biological effects for example anti-inflammatory and anti-angiogenic and is in common use in Chinese medicine.

Key: Bcl-2 associated protein 2 (Bax), pro-apoptotic; B-cell CLL/lymphoma (Bcl2), anti-apoptotic; cysteine-dependent aspartate-directed proteases (caspases); cyclooxygenase 2 (cox2); hypoxia inducible factor 1 alpha (HIF1α); nuclear factor κβ (NFKβ).

References for Figure 5.5: (Eaker and Sninsky, 1989; Fukuda et al., 1999; Liu et al., 1999; Kong et al., 2004; Lin et al., 2004; Mantena et al., 2006a; Mantena et al., 2006b; Chen et al., 2008; Singh et al., 2010; Singh et al., 2011; Murthy et al., 2012; Yin et al., 2012)

Treating EBs with 10µM Berberine significantly altered CD31 distribution. EBs failed to become cystic and cavitated, instead dense central staining is seen (Figure 5.6 below and Figure 5 (Evans et al., 2007)[*9]). The differences in CD31 distribution indicate altered angiogenic development of the EBs.

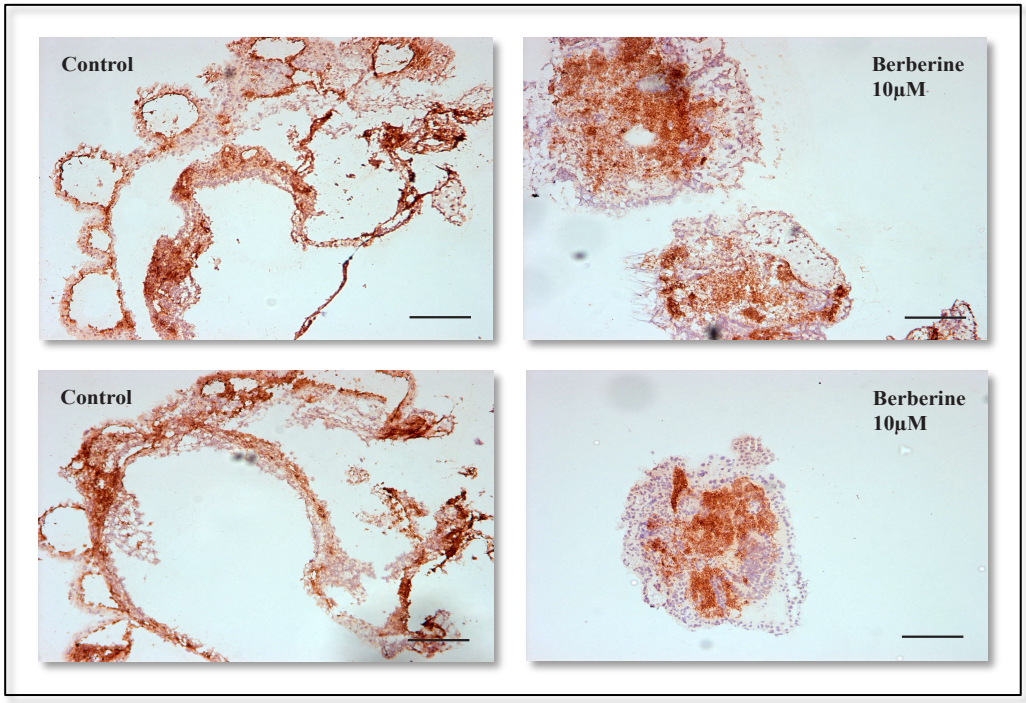

Figure 5.6 Immunohistochemistry of day 15 EB frozen sections

Endothelial cells were stained with monoclonal rat anti-mouse CD31 antibody (clone MEC13.3, Beckton Dickinsion) followed by biotinylated anti-rat IgG (Vector Laboratories) and 3,3' Diaminobenzidine (DAB) chromagen (Dako). Slides were counterstained with Carazzi's haematoxylin (to stain nuclei). Berberine significantly altered regional volume fraction of CD31+ vessels, but not the total volume fraction (Figure 5A, C, D in (Evans et al., 2007)[*9]).

Left: control day15 EBs **Right:** EBs treated with 10µM Berberine.

Black bar represents 200µm

Frozen in optimal cutting compound (OCT, Tissue Tek, Sakura, USA), sectioned and stained by A. Evans.

Berberine has been reported to alter the apoptotic protein ratio of a cell. The pro-apoptotic Bcl-2–associated X protein (Bax) to anti-apoptotic B-cell CLL/lymphoma (Bcl2) ratio increases (Mantena et al., 2006a) and pro-apoptotic activated caspases also increase (Mantena et al., 2006b). Cavitation of EBs and angiogenic growth of vessels is driven by central hypoxia and accompanied by apoptotic remodelling. However, the presence of Berberine at 10μM does not appear to enhance apoptosis in these experiments. This may be due to higher concentrations of Berberine used in the studies citied in Figure 5.5 or the direct down regulation of HIF1α (Lin et al., 2004) and VEGF (Murthy et al., 2012; Hamsa and Kuttan, 2012), which also suggests Berberine may be beneficial in endometrial cancer (Chapter 4.2).

An alternative explanation for the effects seen (Figure 5.6) is that the primary effect seen here is cytostatic rather than cytotoxic, central CD31 staining indicating endothelial progenitor cells which have failed to form or not yet contributed to vessels. Berberine has been shown to reduce cell proliferation in both mouse and human cancer cells (Bonon et al., 2013). Both scenarios may apply to some degree since Berberine's multiphasic effects appear to vary with dose and length of exposure (Serafim et al., 2008).

Since this work, adenosine monophosphate-activated protein kinase (AMPK) activation by Berberine has been described as one mechanism of its action (Lee et al., 2006b). This finding is consistent with its anti-diabetic properties similar to oral hypoglycaemic agents for example Metformin, (Marles and Farnsworth, 1995; Wang and Ng, 1999), which also activates AMPK. Activation of AMPK acts as an energy sensor linking low glucose and resulting G1 cycle arrest to its effects on mitochondrial function and downstream pathways (van den Bogert et al., 1986; Nagata et al., 2003; Cui et al., 2009; Fu et al., 2013). In proliferative disorders these multiphasic actions may be exploited to advantage since arrest of cell growth may be an acceptable outcome alongside additional chemotherapeutics.

5.3 Apoptosis is necessary for normal blood vessel patterning *in vitro* and *in vivo*

To clarify the role of apoptosis during blood vessel development, we created an endothelial specific vector construct containing the Tie2 promoter to drive the

expression of transgenes (Figure 2, (Evans et al., 2007)[*9]), stable mESC clones were generated expressing wild type Bcl2 or a mutant G145E Bcl2 in which the apoptotic function but not the proliferation function was deleted.

In these experiments volume fraction analysis, expressed as percentage of CD31/DAPI, of vessels in differentiating EBs was reduced when wild type Bcl2 was overexpressed compared to the loss of function mutant G145E Bcl2 (Figure 5.7). This finding shows that *in vitro* apoptosis plays a role in the normal development of CD31-positive vessels.

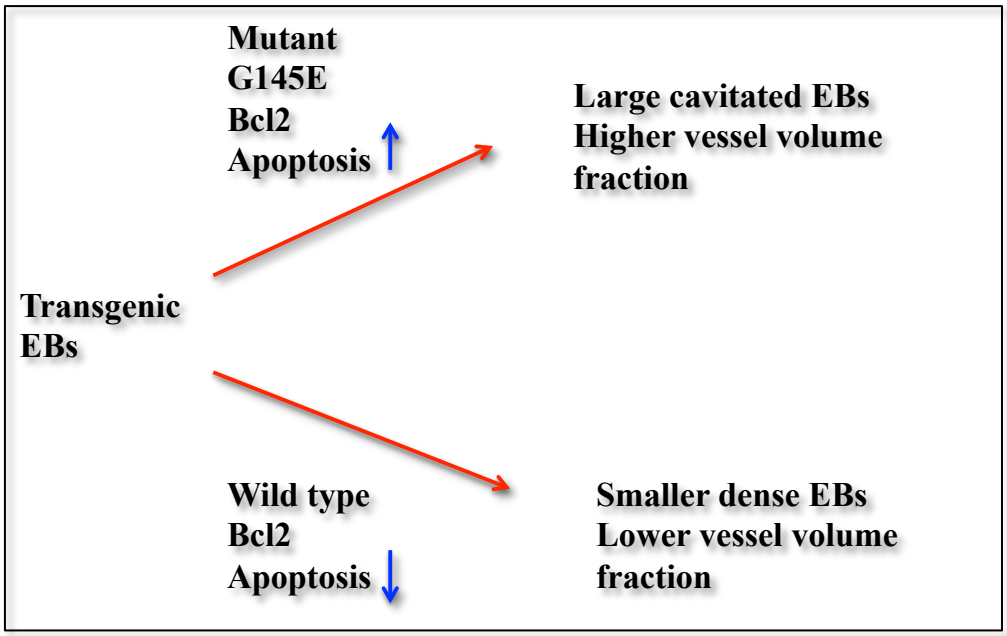

Figure 5.7 Apoptosis is required for normal vessel formation

Summary of the results of CD31/DAPI volume fraction analysis of frozen sections stained with anti-CD31 antibody (clone MEC13.3, Beckon Dickinson) plus Alexa Fluor 488 and Hoechst 33528 nuclear staining. Quantifying the morphological changes in a three dimensional network was achieved by importing images into **C**omputer-**A**ided **S**tereological **T**oolbox (CAST) software (Olympus Denmark) as described (Evans et al., 2007)[*9].

Quantification: point counting of CD31/DAPI staining from 5 random images from each of 5 random sections, slides were numbered and later assigned to their respective experimental groups.

We then used a transgenic approach to elucidate EC apoptosis *in-vivo* shown by others in neonatel vessel remodelling (Kim et al., 2000). When the anti-apoptotic Bcl2

was expressed in transgenic mice under the control of the Tie2 promoter, including the enhancer region, the mice died during gestation (Duval et al., 2007)[*10]. In wild type mice active caspase 3, a key component of the apoptotic programme, was co-expressed with CD31 in the smaller vessels (Figure 1 (Duval et al., 2007)[*10]). When the transgenic mice were examined and compared to wild type littermates there were vascular defects including areas of haemorrhage, excess capillary networks around the face, retarded interdigital cleft formation (Figure 5.8), and abnormalities of placental vasculature. Vessels that were destined to regress in normal embryos persisted.

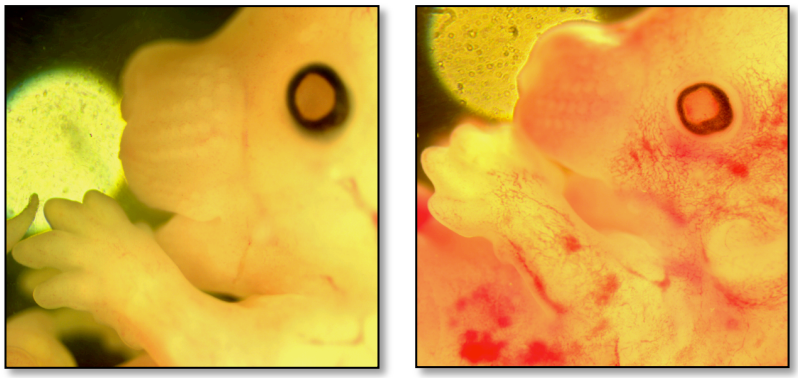

Figure 5.8 Failure of vascular remodelling in embryos overexpressing Bcl-2
14.5 dpc embryos expressing human Bcl2 in endothelial cells appear to have failed vascular remodelling and regression (right) compared to control embryos (left). From figure 4 (Duval et al., 2007)[*10].

EBs proved ideal to model and quantify early vessel development in a complex tissue, demonstrating angiogenic and apoptotic control of vessel development. These experiments further suggest that apoptosis is a normal feature of development, shown *in vitro* and *in vivo*. In addition, the findings indicate that once they are established and invested with support cells, vessels are less vulnerable to intervention, as seen in the transgenic mice where the larger established vessels are less vulnerable to the over-expression of Bcl2. Remodelling of newly formed smaller vessels appears to be an important developmental function of apoptosis. Apoptosis may therefore have important implications in tumour regression, since tumour vessels resemble neovascularisation in development, and also for intrauterine growth restriction (IUGR) defects.

Chapter 6 The emergence of mesoderm and the haemangioblast

More than 80% of known animal phyla develop from three germ layers (Technau and Scholz, 2003). The third layer, mesoderm, is recognised as a widely distributed germ layer in adult organisms (Figure 6.1). Mesoderm forms part of the many adult tissues including cells of the haematopoietic and vascular systems. Given the origins of the vertebrate blood and vascular systems in the emerging mesoderm of the embryo, it was a natural progression from previous work to look closer at their origin.

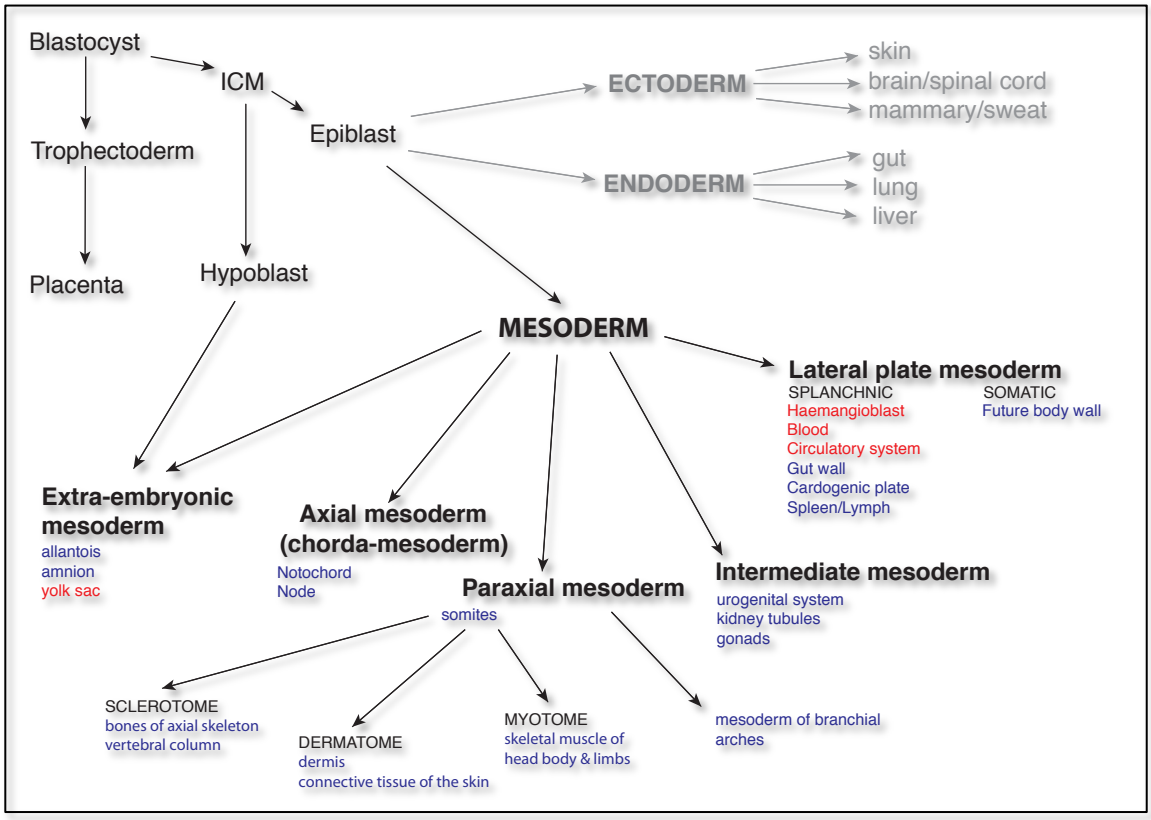

Figure 6.1 The origins of mesoderm from the epiblast. A large number of cells of an adult vertebrate, in many areas of the body, are mesoderm derivatives.
As early as the 1880's (Minot, 1883) it was thought mesoderm was "derived from scattered and isolated cells."
Abbreviations: Inner cell mass (ICM)

It was clear EBs model both vascular and haematopoietic development (Figure 5.1), and that EBs cultured as described (Chapter 1.4.1) may also be suitable to trace mesoderm induction *in-vitro* (Figure 6.1), as one of the early events prior to formation of

the blood and vascular systems. The aim of the work described in this and the following chapter was to review mesoderm specification in a mammal, as an extension to the wealth of knowledge already derived from amphibians and fish.

6.1 *Brachyury*: a key transcription factor in mesoderm development

Brachyury, a T-box transcription factor, found in all bilaterian animals plays a key role in mesoderm development in all vertebrates. The Brachyury protein binds DNA at a specific promoter sequence, the T-box (TCACACCT), and influences the transcription of target genes. T-box genes appeared in evolutionary terms when body plans diversified and this in itself suggests a crucial role. *Brachyury,* or *T*, is expressed in the primitive streak (Figure 6.7), tailbud and notochord (Figure 6.3A, C) of the early mouse embryo (Dobrovolskaïa-Zavadskaïa, 1927; Herrmann et al., 1990; Wilkinson et al., 1990).

Much of the early work on *Brachyury* was carried out using frogs (*Xenopus laevis)* and zebrafish (*Danio Rerio*), and in *Xenopus Brachyury* appears to be sufficient for mesoderm formation (Cunliffe and Smith, 1992). The expression patterns of *Brachyury* homologs for *Xenopus Xbra*, (Smith et al., 1991) and zebrafish no tail ntl (Schulte-Merker et al., 1992; Martin and Kimelman, 2008; Morley et al., 2009), resemble that seen in the mouse (Figure 6.2). These transcripts play similar roles in early development (Schulte-Merker et al., 1994; Conlon et al., 1996; Martin and Kimelman, 2008) indicating conservation of Brachyury protein function.

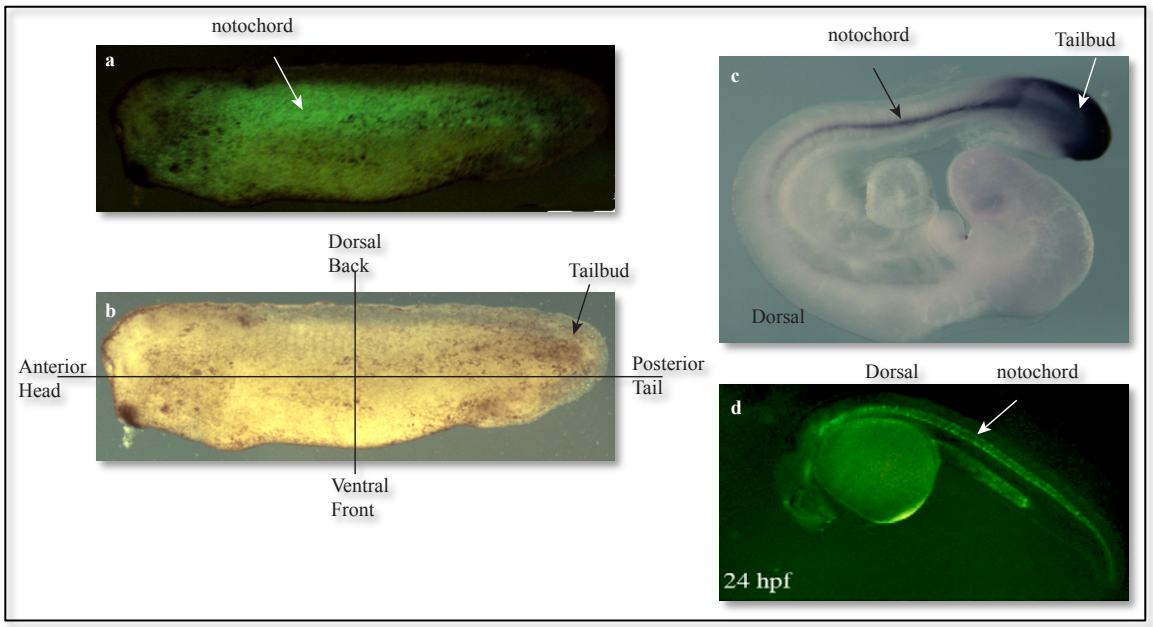

Figure 6.2 *Brachyury* conservation in vertebrate embryos

a. Frog *Xenopus laevis* stage 33-34 (Late tailbud stage, Xenbase). F1 outcross male GFP transgenic frog pSceGFPXbra x wildtype female using the I-SceI meganuclease system, created by A. Evans 2006-7, by cloning the Xenopus *Brachyury Xbra* promoter sequence into pSceGFP. GFP expressed from *Xbra* promoter shows GFP signal in the notochord and tailbud. The meganuclease I-Sce-I is an intron-encoded endonuclease isolated from the yeast *Sacchoromyces cerevisiae* (Thermes et al., 2002).

b. Light microscope image of the same embryo.

c. Mouse *Mus musculus* embryo 9.5 dpc *in-situ* showing *Brachyury* RNA expression in the tailbud and notochord (Figure S6 B from (Evans et al., 2012)[*12]) detected with NBT/BCIP.

d. Zebrafish *Danio rerio* embryo 24 hpf (Zfin) shows expression of notail RNA in ntl: CFP transgenic fish, specific staining for notail in the notochord, image from Steven Harvey (Harvey et al., 2010).

Xenopus developmental data from Nieuwkoop and Faber (1994) Normal Table of *Xenopus laevis* (Daudin) from Xenbase website. Zebrafish embryonic stages are modified from Kimmel (Kimmel et al., 1995) Zfin website.

(see section III for abbreviations and appendix for websites)

Mouse dissection and staining, Xenopus *Xbra* transgenic frog by A. Evans,

Zebrafish transgenic by S.Harvey.

Mouse embryos lacking functional Brachyury protein fail to gastrulate properly, do not form a differentiated notochord, and lack structures posterior to somite seven (Yanagisawa et al., 1981; Wilson et al., 1995; Naiche et al., 2005)(Figure 6.3B). In the mouse, mRNA and protein are detectable by 6.5-7.0 dpc and homozygous embryos lacking T activity die *in utero* around 9.5-10 dpc (Chesley, 1935; Gluecksohn-Schoenheimer, 1944).

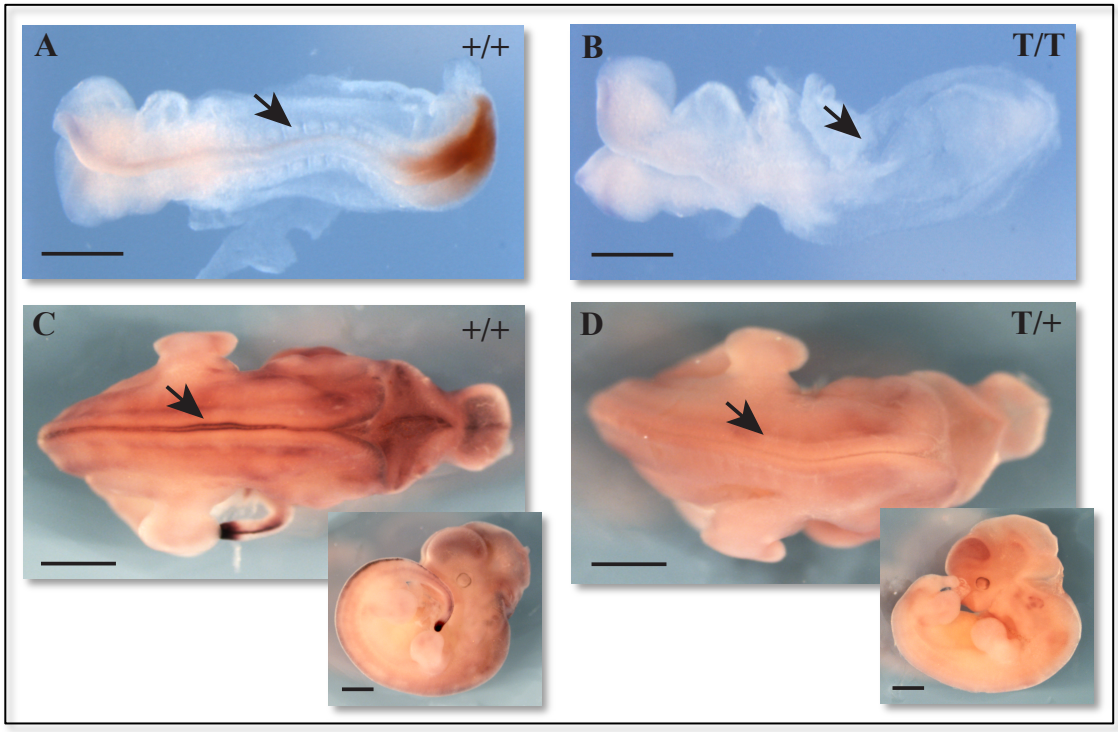

Figure 6.3 *Brachyury* in the mouse embryo

A Wildtype (+/+) 8.5.dpc mouse embryo *in-situ* for digoxigenin-labeled antisense mouse *Brachyury* detected with Mag/INT (brown) shows *Brachyury* staining in the tailbud and notochord, black arrow indicates somites. Somites form in pairs from paraxial mesoderm flanking the notochord and the neural tube.

B Homozygous 8.5 dpc T/T mutant stained as **A** note absence of *Brachyury* staining in the tailbud, lack of notochord and somites (black arrowhead). The embryo in **A** was about to undergo axial rotation but **B** would have died soon after. Black bars **A** and **B** 250µm. Orientation anterior-posterior, dorsal views shown. **C** Wildtype (+/+) 11.5.dpc mouse embryo stained as **A** Note tailbud, notochord staining and straight neural folds, inset lateral view of the same embryo. **D** Heterozygote (T/+) stained as **A** note faint staining, distinctly kinked notochord, inset lateral view shows lack of tail elongation. Black bars 1000µm for 11.5dpc embryos. Orientation for C, D as in A, B. See Appendix Table 1 for mouse staging. Embryo dissection and *in-situ* hybridisation A. Evans.

Using mouse EBs to reveal mammalian *Brachyury* binding targets was a means of establishing the contribution of gastrulation and mesoderm induction on the formation of the blood and vascular systems. Culturing EBs in suspension (Evans et al., 2007)[*9] allowed the production of sufficient quantities of cross-linked chromatin from *Brachyury* expressing cells to carry out chromatin immunoprecipitation or chIP (Figure 6.4). To obtain sufficient *Brachyury* positive cells *in vivo* would have required large numbers of experimental animals at a high cost.

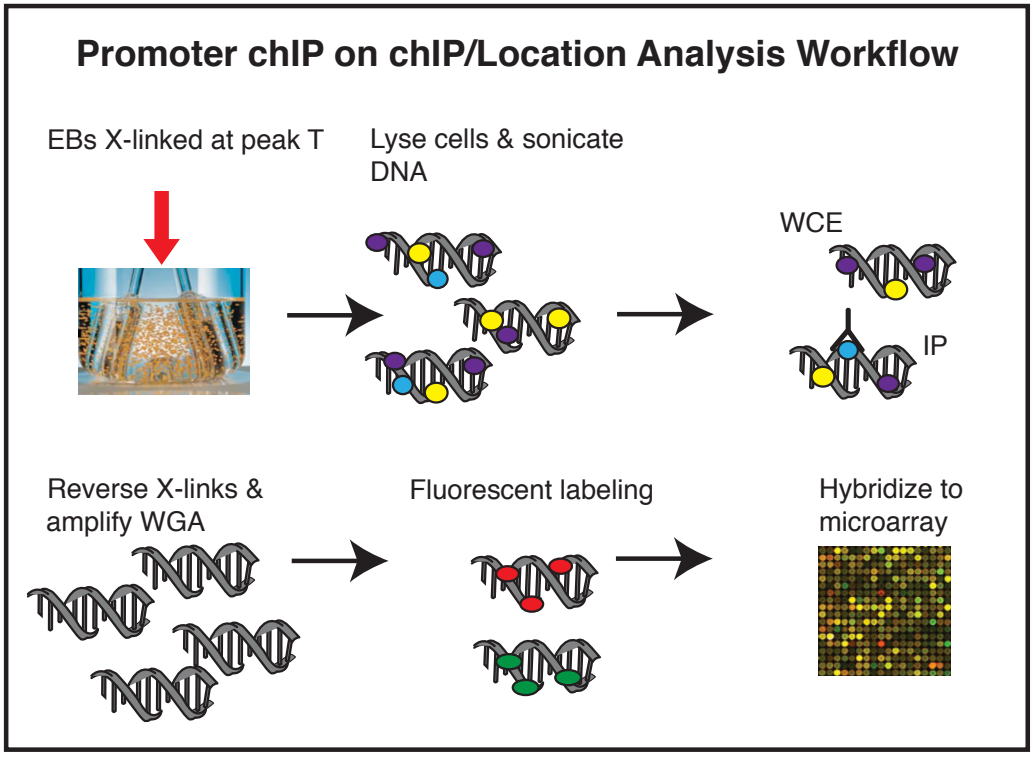

Figure 6.4 Chromatin Immunoprecipitation or Location Analysis

A: ChIP on chIP workflow EBs grown in spinner culture as described (Chapter 1) are cross-linked (X-linked) using formaldehyde at the peak of *Brachyury* expression. EBs are lysed and the chromatin sonicated to 100-200 bp. Samples are divided, one labeled with antibody specific to Brachyury protein or an isotype control (IP) and the other is the whole chromatin extract (WCE) sample, cross-links are reversed and the DNA amplified using whole genome amplification (WGA). Samples are fluorescently labelled and hybridised to promoter chips. For more details see materials and methods (Evans et al., 2012)*[12].

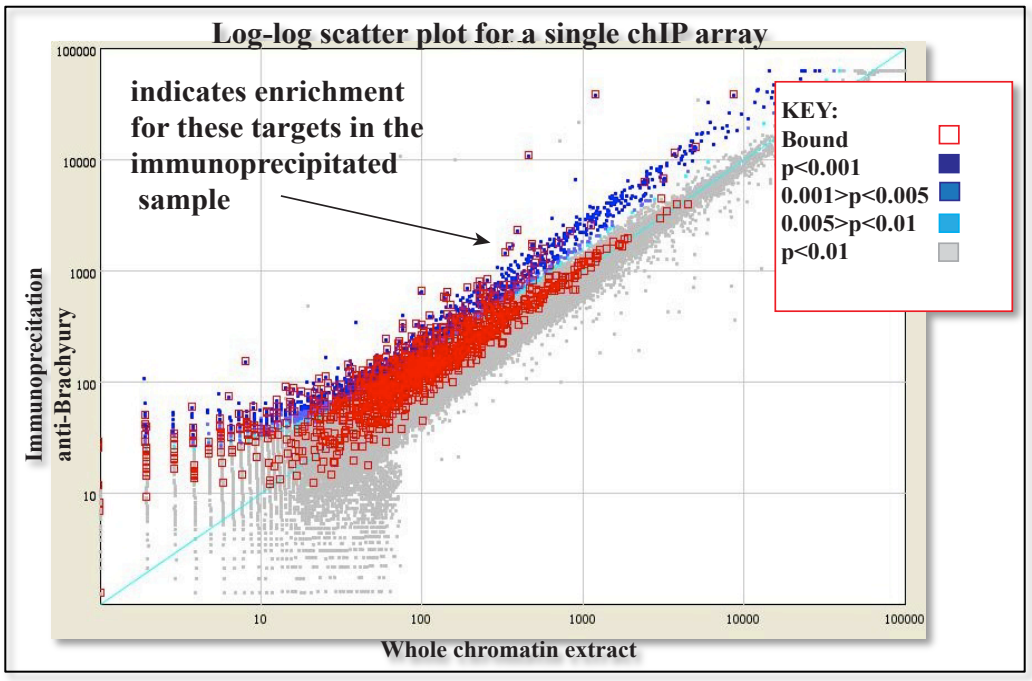

Figure 6.4 Chromatin Immunoprecipitation or Location Analysis

B: A log-log scatter plot of immunoprecipitated (IP) chromatin using anti-Brachyury antibody (y axis) labelled with Cy5-dUTP, against whole chromatin extract for that sample (x axis) labelled with Cy3-dUTP. Arrow indicates region of genes that are significantly enriched in the Brachyury IP samples.

All chIP-chip experiments were performed by A. Evans.

Key: Cyanine 3-2′-Deoxyuridine, 5′-Triphosphate (Cy3-dUTP); Cyanine 5-2′-Deoxyuridine, 5′-Triphosphate (Cy5-dUTP), fluorescent nucleotide analogs

6.2 The embryoid body as an *in-vitro* surrogate for mouse gastrulation and mesoderm formation

Pilot experiments in spinner cultures showed *Brachyury* mRNA peaking consistently on day 4-5 of differentiation (Figure 6.6). This finding indicated EBs may mimic the early stages of eutherian embryo development acting as surrogates for the embryo at a stage where it becomes inaccessible once implanted.

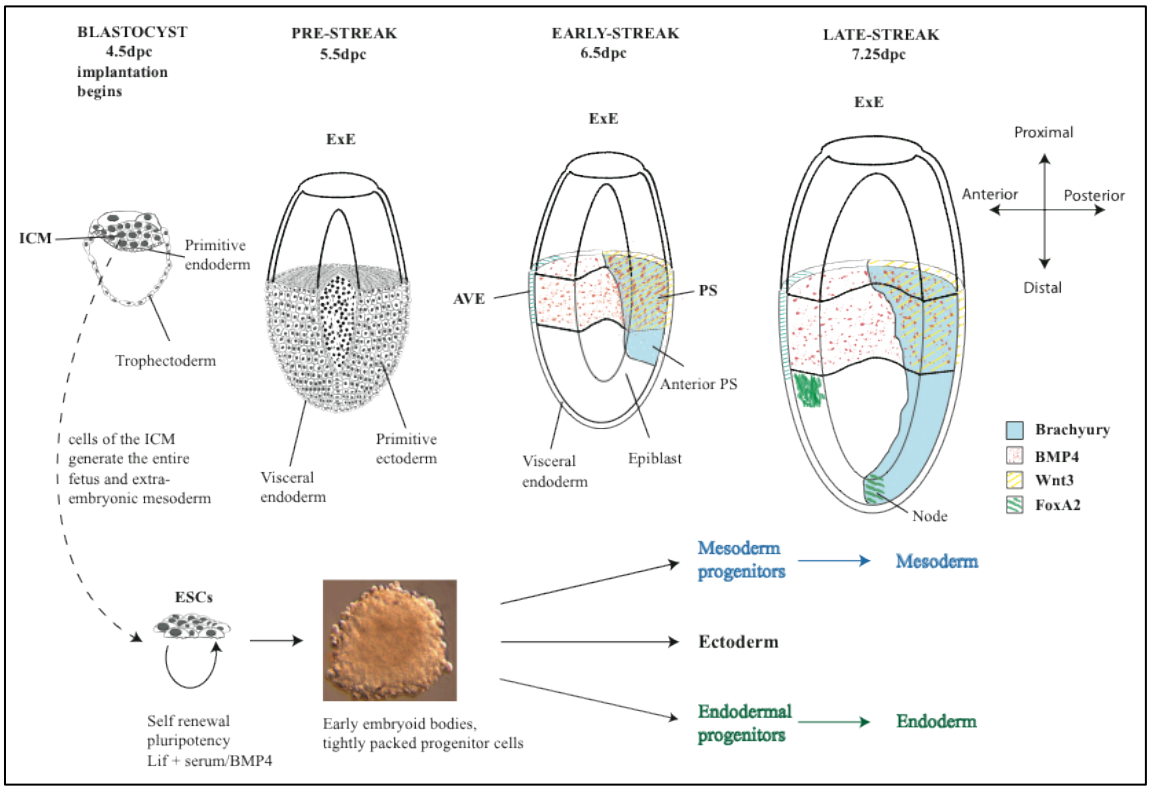

Figure 6.5 Schematic representation of mouse embryo development

Development of the three germ layers from the blastocyst, and the key signaling genes involved. ESCs derived from the ICM can form all three germ layers *in vitro*

Mesoderm and definitive endoderm are established in mouse embryos during gastrulation. At the start of gastrulation, the primitive streak (PS) forms from the epiblast-extraembryonic border and will become the posterior of the embryo (6.5dpc above).

Key: extraembryonic ectoderm **(**ExE); days post coitus (dpc); embryonic stem cells (ESC); anterior visceral endoderm (AVE); primitive streak (PS); inner cell mass (ICM); bone morphogenetic protein 4 (BMP4); leukaemia inhibitory factor (LIF); forkhead box A2 (foxa2) transcription factor; wingless-type MMTV integration site family, member 3 (wnt3). Based on (Gadue et al., 2005).

Late primitive streak mouse embryos (Figure 6.7) possess polarity and have their own three-dimensional geometry (Figure 6.5). *Brachyury*-positive posterior primitive streak cells undergo epithelial-to-mesenchymal transition (EMT). In using the EB as a model, one of the important questions was whether the differentiation events seen *in vivo* will be faithfully reproduced without these precise morphological movements.

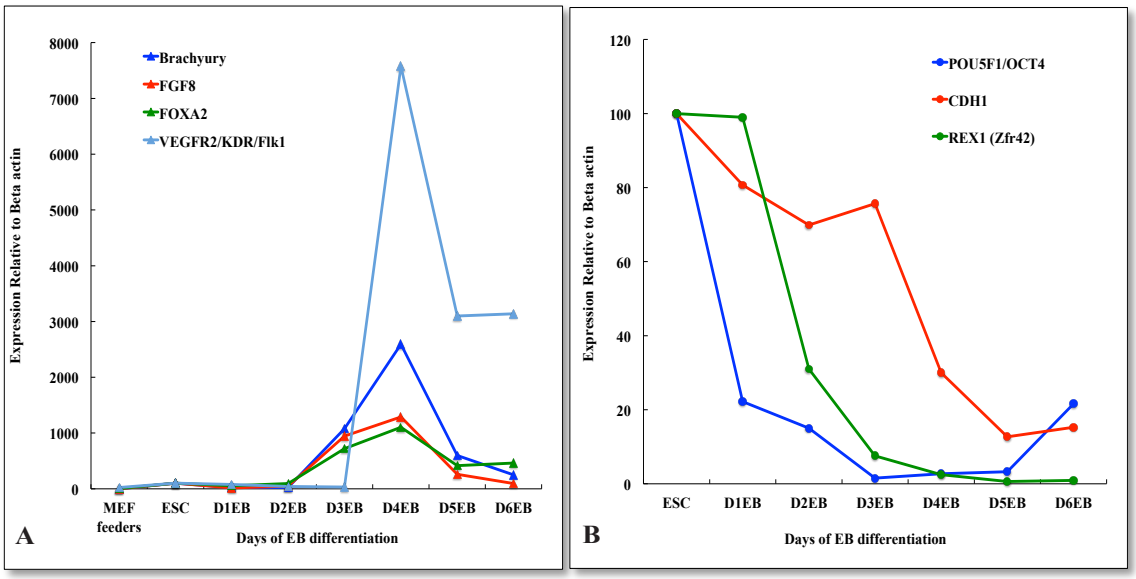

Figure 6.6 Expression of stage-specific markers in mouse EB differentiation

Quantitative PCR data expressed relative to β actin (endogenous control), and undifferentiated ESC as 100%. **Key:** mouse embryonic fibroblasts (MEF); undifferentiated embryonic stem cells (ESC); Day 1-6 differentiating EBs (D1-D6 EBs).

A: <u>A wave of mesoderm induction occurs in early vertebrate development.</u> *Brachyury* marking early mesoderm; fibroblast growth factor 8 (FGF8) expressed in embryonic ectoderm and mesoderm; forkhead A2 (foxa2/HNF3beta) regarded as a marker for endoderm, expressed in the primitive streak and node *in vivo;* vascular endothelial growth factor receptor 2 (VEGFR2/KDR/Flk1) indicates presence of early haemangioblast progenitors.

B: **<u>A decrease in stem cell/ pluripotency markers occurs on differentiation</u>**.

E cadherin (CDH1) down regulation is associated with epithelial-mesenchymal transition and cell movements, octamer-binding transcription factor 4/POU domain, class 5, transcription factor 1 (Oct4/Pou5F1) a marker for undifferentiated cells and RNA exonuclease 1 homolog (Rex1) or Zfr42 is a transcription factor highly expressed in embryonic stem cells.

Performed by A. Evans from a timecourse sampling experiment and the Roche LightCycler®480 System (Roche Diagnostics).

Primer sequences are listed in Appendix Table 2.

At day 3 cells expressing *Brachyury* and other mesoderm markers (Figure 6.6A) (Keller et al., 1993) and markers for definitive endoderm such as forkhead box A2 (Foxa2) are detectable in EBs. At the same time markers of pluripotency rapidly

decrease (Figure 6.6B), for example, octamer-binding transcription factor 4/POU domain, class 5, transcription factor 1 (Oct4/Pou5F1) a marker for undifferentiated cells. Changes in cell adhesion molecules also occur for example, E-cadherin (CDH1) downregulation, associated with EMT.

6.3 Origins of the blood and vascular system from a haemangioblast progenitor

Following the proposal by Sabin (Sabin, 1917) of the existence of a bipotent haematopoietic and endothelial precursor, Murray used the term haemangioblast (Murray, 1932) to describe a common precursor.

Blood and vascular development occur following a wave of *Brachyury* expression associated with the expression of BMP4 and fibroblast growth factor 2, basic (FGF2). Mouse haemangioblast commitment occurs in the posterior primitive streak (Figure 6.7) in *Brachyury*-positive VEGFR2/KDR/Flk1-positive cells (Huber et al., 2004; Shalaby et al., 1995; Shalaby et al., 1997).

6.4 Developmental noise or chaos in embryoid bodies

The patterning and development of an embryo requires intricate transcriptional and cellular interactions but nevertheless EBs are capable of spontaineous, rhythmical contractions after 7-8 days of culture. If allowed to attach, EBs do show a degree of axis formation and form assymetric sacs of attached cells. A key question for lineage progression of haematopoietic cells is whether primitive blood islands progress through definitive haematopoiesis to mature lineages. EB differentiation does not appear completely chaotic, although local gradients within the EBs may cause a high degree of stochastic patterning.

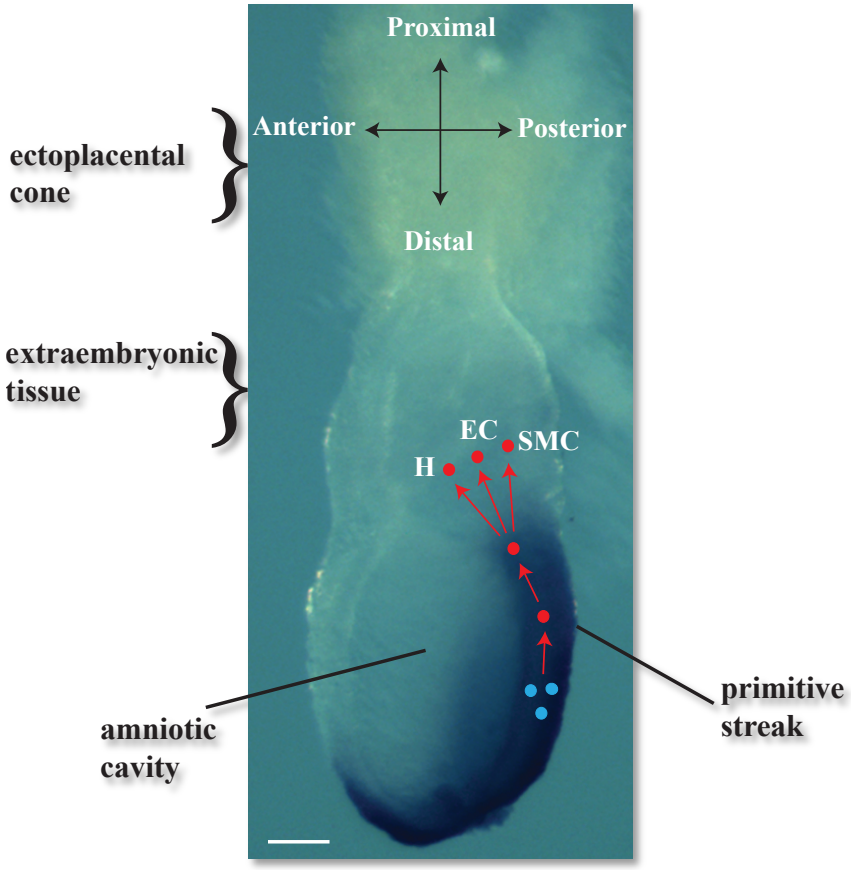

Figure 6.7 A model for haemangioblast formation in the mouse late primitive streak embryo.

Brachyury expressing EBs act as *in-vitro* surrogates for these events.

Image shows a 7.5 dpc wild type 129 mouse embryo *in-situ* using digoxigenin-labeled antisense mouse *Brachyury* RNA visualised with BM purple. Specific staining in the node and primitive streak was observed. Staining was absent in a sense control. Mesoderm cells (blue dots) in the posterior primitive streak migrate and differentiate into haemangioblasts (red dots) that are Brachyury + and VEGFR2/KDR/Flk-1+. Primitive endothelial cells (EC), smooth muscle cells (smc) and haemangiopoietic cells (H) are formed, and a blood band and endothelial plexus will form around the border of the extra embryonic and embryonic mesoderm. Embryo dissection and *in-situ* hybridisation by A. Evans. Scheme based on Huber (Huber et al., 2004).

White bar indicates 200µm.

We investigated use of EBs as a model system for early mesoderm and by using chIP-chIP analysis of cultures cross-linked at peak *Brachyury* expression this led to the discovery of previously unknown *Brachyury* targets (Chapter 7). The faithful recapitulation of the key events of early development fits the principal of the 3Rs (Replacement, Refinement and Reduction) regarding the use of mouse embryos.

Chapter 7 *Brachyury* target genes

Transcriptional targets form the basis of a *Brachyury*-driven regulatory network involving a complex interplay of genes and transcription factors directing the establishment of mesoderm. After testing the efficacy of the model (chapter 6) we were able to successfully achieve the main aim of discovering unknown *Brachyury* targets in the mouse. Even in the rather chaotic form of an embryoid body, elements of the key systems of the developing embryo are present, as illustrated by their ability to form networks of endothelial cells (Chapter 5.1).

7.1 ChIP-on-chip technology

The technique of chromatin immunoprecipitation (chIP) or location analysis appeared about the same time as expression arrays (Timeline 2). ChIP-chip (or chIP-on-chip) using immobilized oligonucleotides, from known promoter sequences, on glass chips was the most affordable option at this time (2006-7) (Figure 6.2). The most important requirement is an antibody of high specificity to recognise the crosslinked epitope (Figure S1 (Evans et al., 2012)*[12]).

7.2 *Brachyury* binding targets reflect a key role in development

Evans et al., 2012 describes components of the wingless-type MMTV integration site family (wnt) pathway and other binding targets, for example, fibroblast growth factor 8 (fgf8), consistent with the role of *Brachyury* in mesoderm formation. A number of further well-documented signalling pathways are also targeted by *Brachyury* including the MAPK, c-Jun N-Terminal Kinase (JNK), TGFβ, Hedgehog, integrin, Jak/STAT and ubiquitination pathways ((Evans et al., 2012)*[12] (Table S2)). Gene ontology and motif analysis was performed as described (p12(Evans et al., 2012)*[12]) (see appendix websites). Targets emphasize the links between embryonic morphogenesis (Chapter 7.2.2) and tumour associated cell migration (Chapter 7.3). Both of these processes are dependent on the establishment of the vascular and haematopoietic systems (Chapter 7.2.1) in a growing embryo. *In situ* hybridisation performed using wild type embryos and heterozygote crosses of a *Brachyury* mutant mouse (King et al., 1998) confirmed the *in vivo* expression pattern in relation to that of *Brachyury* for some of these targets.

7.2.1 *Brachyury* binding targets associated with haematopoietic and endothelial biology

Genes associated with the developing blood and vascular systems appear in close association with mesoderm formation (Figure 7.3) and among these are putative direct binding targets of *Brachyury* (Appendix table 3), including the E-twenty-six (ETS) related gene, (Erg) a transcription factor known to be important in self-renewal of HSC in embryos (Ng et al., 2011). Together with the transcription factor friend leukaemia integration 1 (Fli1), Erg is involved in lineage specification via regulation of the balance of erythroid-megakaryocyte differentiation from bipotential megakaryocyte-erythroid progenitors (MEP) (Figure 2.6), (Kruse et al., 2009) and is essential for definitive haematopoiesis (Loughran et al., 2008). The bZIP transcription factor, CCAAT/ enhancer binding protein alpha, Cebpa (C/EBPa) initiates myelopoiesis (Chen et al., 2009) and influences lineage decisions (Reddy et al., 2002).

Central to the biology of the *Brachyury*-positive haemangioblast (Figure 6.7) is the coincident expression of VEGFR2/KDR/Flk1, and a number of targets are associated with VEGF and its action. Fucosyltransferase 8 (Fut 8) is required for the expression of VEGFR2 (Wang et al., 2009) and magic roundabout protein (Robo4). Robo 4 is expressed in the dorsal aorta and intersomitic vessels in 9.5dpc mouse embryos (Brose et al., 1999), but is restricted to HSCs and ECs in adults. Robo 4 functions as a guidance molecule for localisation of adult HSC to the bone marrow (Huminiecki et al., 2002) (see also Figure 8.1).

Another target myeloid ecotropic viral integration site 1 (Meis1), a homeodomain transcription factor (Moskow et al., 1995) is associated with HSC self-renewal and essential for definitive haematopoiesis and vascular patterning in the mouse embryo (Azcoitia et al., 2005) (Figure 7.1 A, B). Meis1-mutant mice have defects in haematopoiesis and angiogenesis (Cai et al., 2012).

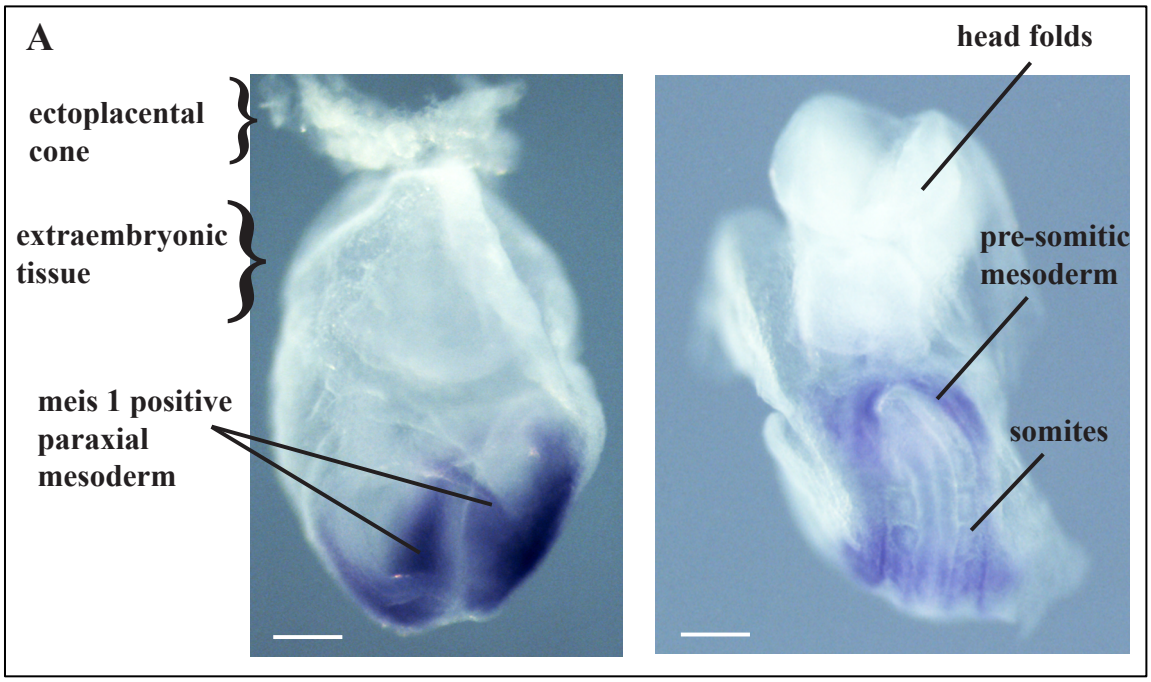

Figure 7.1 A: *In-situ* staining for wildtype 8.5dpc mouse embryos showing Meis 1 staining in the paraxial mesoderm

Embryos are viewed from the posterior. **Left:** 8.5dpc embryo still contained in the extraembryonic membranes. **Right**: 8.5dpc embryo dissected away from all extraembryonic membranes. Embyro shown has reached the seven somite stage, just prior to axial rotation. Stained using digoxigenin-labeled antisense mouse meis 1 RNA visualised with BM purple, see abbrvs. (Roche).

Embyro dissection *in-situ* hybridisation by A. Evans. White bars indicate 250µm

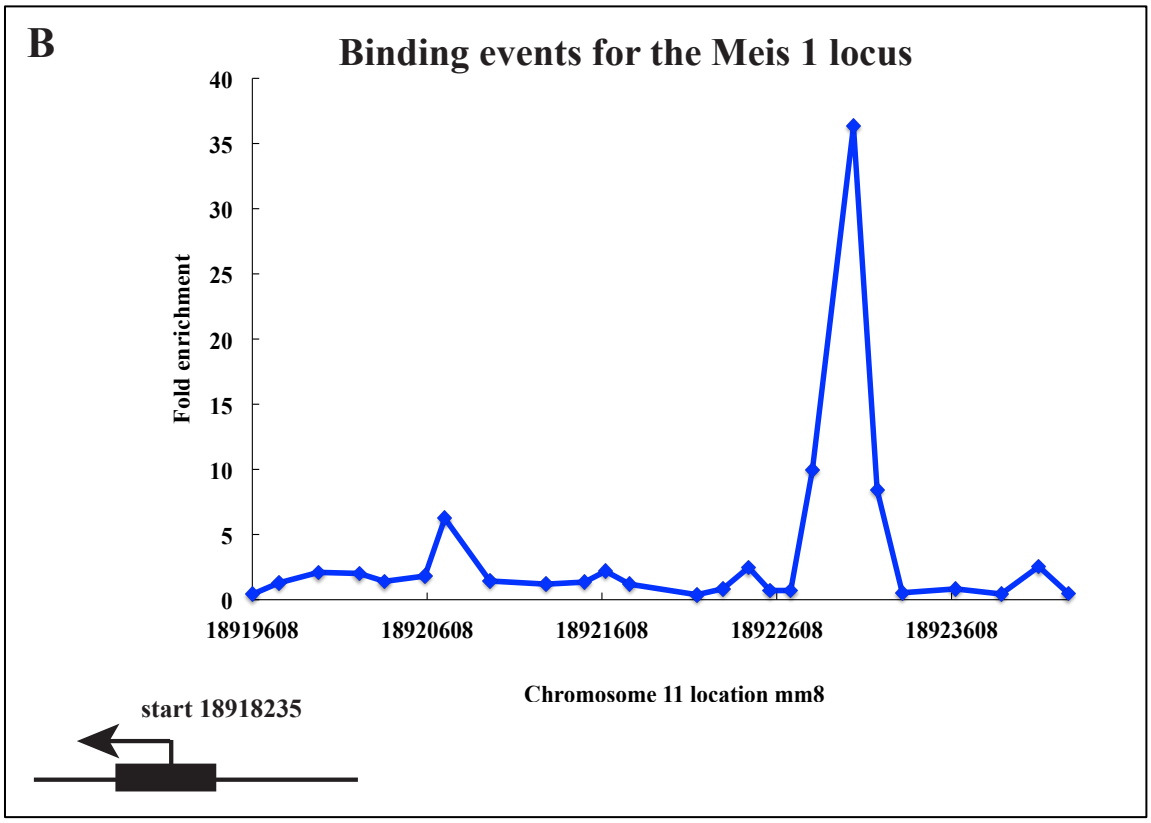

Figure 7.1 B: Binding events at the Meis 1 promoter

Peak data generated from Agilent chIP Analytics 1.3 software showing fold enrichment (y axis) for combined array data from three chIPs against Meis1 chromosomal location (x axis). Bound peak is upstream of transcription start site for Meis1. See also Figure 2 (Evans et al., 2012)*[12] for the expression profile in differentiating EBs. The software uses the whitehead error model (Lee et al., 2006a) taking the p value of the probe in question as well as its neighbours, comparing groups of three probes and computing a combined p value.

Haematopoiesis occurs in distinct waves in both human and mouse embryos (Figure 7.2) and the site of haematopoiesis changes during development. The first wave of primitive haematopoieis in the embryonic yolk sac, which occurs at around 7 dpc, can be considered equivalent to the blood islands described in the EB system (Silver and Palis, 1997) producing primitive nucleated erythroblasts (Kennedy et al., 1997). By 8-8.5 dpc circulation begins in the embryo and yolk sac then at 9 dpc intra-embryonic mesoderm cells give rise to the aorta-gonad mesonephros (AGM), the site of the second wave of definitive haematopoiesis. The AGM of mouse and human embryos is a cluster

of CD34+ haematopoietic cells associated with the ventral floor of the dorsal aorta. Long-term repopulation potential is possible once cells migrate to liver and spleen, then to the bone marrow (Muller et al., 1994).

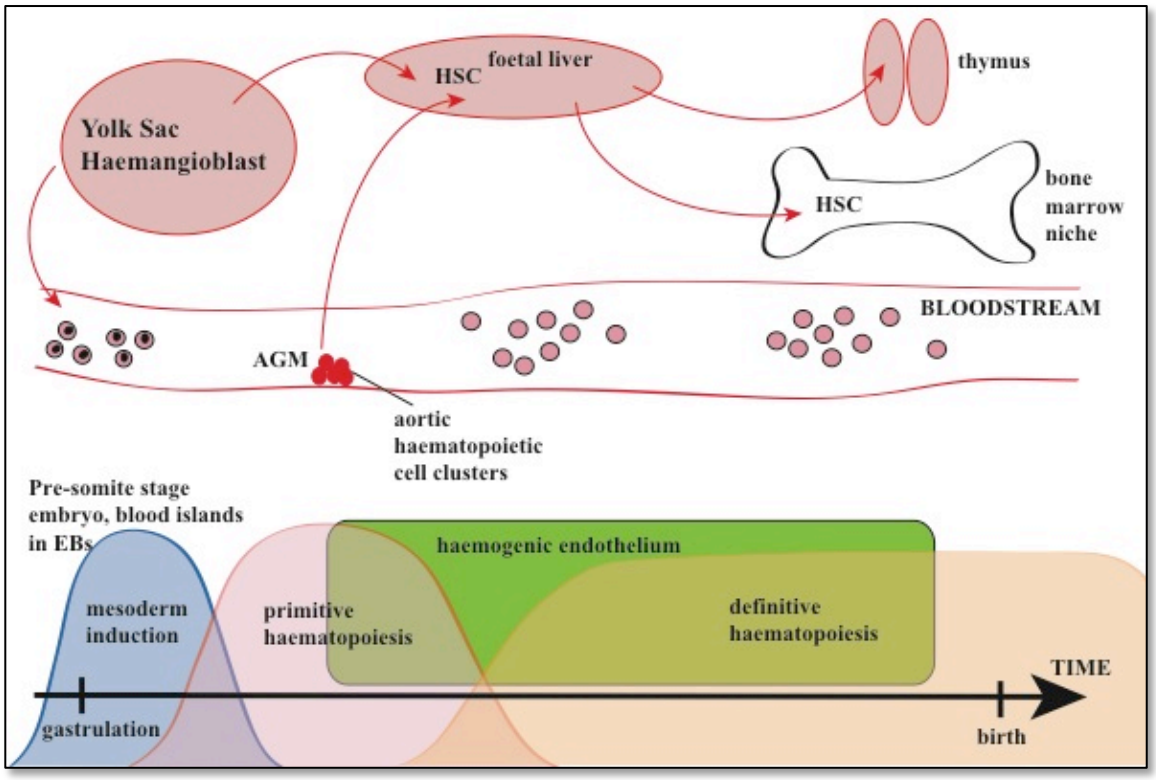

Figure 7.2 Waves of haematopoiesis occur in embryonic development, and the site of haematopoiesis changes as development progresses

Mesoderm induction is followed by the first wave of primitive haematopoiesis in the yolk sac *in vivo* and EB blood islands *in vitro*. Primitive, nucleated erythroblasts containing foetal haemoglobin, macrophages and megakaryocytes are formed and circulation begins in the embryo. A wave of definitive haematopoiesis follows as AGM-derived stem cells migrate to the liver and eventually bone marrow for long-term haematopoiesis. Erythroblasts are now enucleated and stem cells have lymphomyeloid potential.

Key: aorta-gonad-mesonephros (AGM); embryoid bodies (EBs); haematopoietic stem cells (HSC). Based on data from published models (McGrath and Palis, 2005; Tavian and Peault, 2005; Eilken et al., 2009; Kardel and Eaves, 2012).

Despite the lack of correct embryonic patterning it appears that the EB does faithfully reproduce lineage progression for haematopoietic cells from a subset of *Brachyury* expressing cells *in vitro* (Figure 7.3).

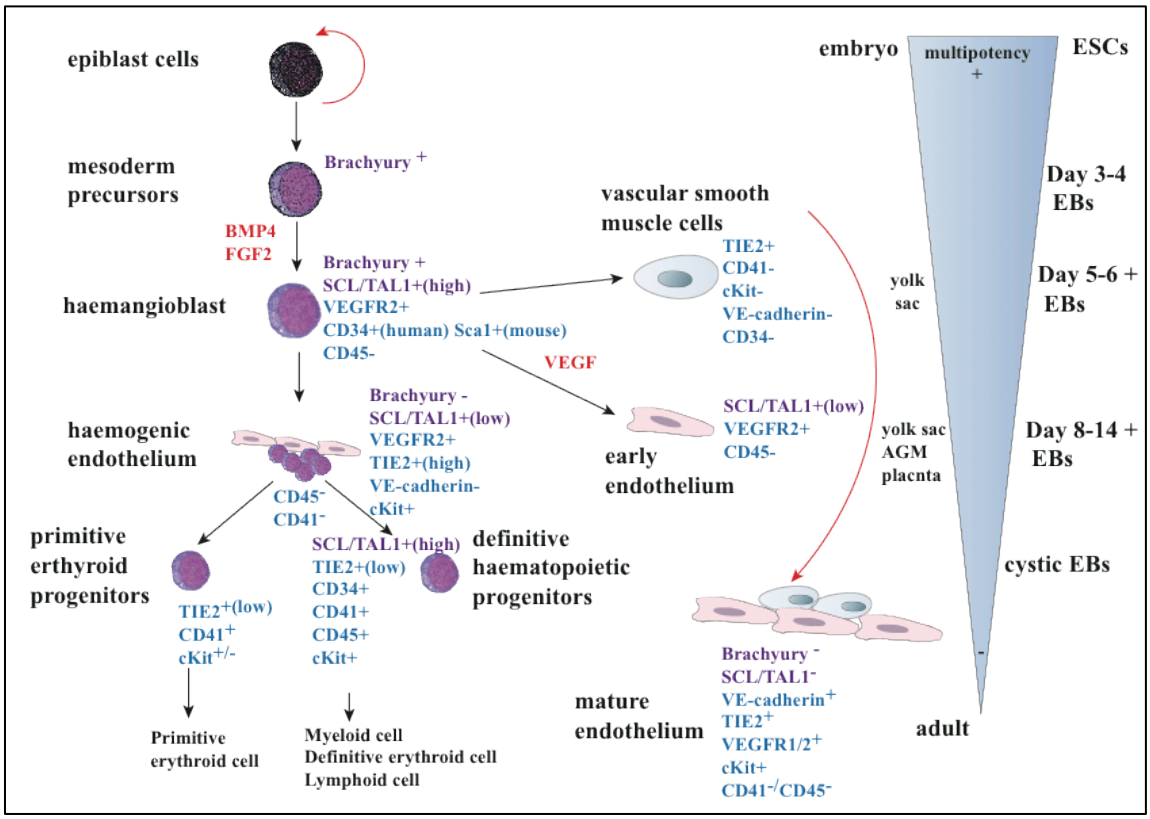

Figure 7.3 A model for the formation of blood cells and endothelium from a common progenitor, the haemangioblast

Early mesoderm is *Brachyury* +, a subset becomes VEGFR2/FLK1/KDR+ and expresses SCL in response to cytokines. This haemangioblast then gives rise to both endothelial and blood cell lineages in response to cytokines and transcription factors. Phenotypes are based on data from flow cytometry and expression. Key surface markers (blue), cytokines (red) and transcription factors (purple) are indicated. The model is based on that of Lancrin (Lancrin et al., 2009). **As differentiation proceeds the pluripotent potential decreases**. The approximate stages in embryos and mouse EBs are also shown.

Key: bone morphogenetic protein 4 (BMP4); fibroblast growth factor 2 (FGF2); T-cell acute lymphocytic leukaemia protein 1(TAL1/SCL); integrin, alpha 2b (CD41); vascular endothelial growth factor Receptor 2 (VEGFR2/FLK1/KDR); protein tyrosine phosphatase, receptor type, C (PTPRC/CD45); TEK tyrosine kinase receptor (Tie2/TEK); cadherin 5, type 2 or VE-cadherin (vascular endothelial) also known as CD144; proto-oncogene c-Kit or tyrosine-protein kinase Kit (CD117/ ckit); haematopoietic progenitor cell antigen CD34 (CD34); aorta-gonad-mesonephros (AGM) region.

7.2.2 *Brachyury* binding targets associated with epithelial-mesenchymal transition (EMT), cell migration, adhesion and left-right determination

Targets that influence cell surface properties reflect the migration potential of mesoderm (Appendix table 4). It is well established that the extracellular matrix of *Brachyury* mutants differs from wildtype embryos (Jacobs-Cohen et al., 1984). *Brachyury* positive cells undergo EMT, accompanied by upregulation of the transcription factor snail 2 /slug resulting in a decrease in E cadherin expression (Bolos et al., 2003). Rack1, highly expressed in ECs, influences cell-matrix adhesion at focal adhesions (Mochly-Rosen et al., 1995; Cox et al., 2003) while camello-like 4 or N-acetyltransferase 8 (Cml4, Nat 8) is thought to be involved in gastrulation movements (Popsueva et al., 2001).

One of the consequences of the processes occuring during gastrulation is the possession of two body axes by bilaterians. In vertebrates a third additional left-right asymmetry aligns with respect to the anterioposterior (AP). The first breaking of symmetry occurs with right-sided heart looping and then axial rotation or turning of the embryo accompanied by twisting with respect to the dorsal-ventral axis (Appendix figure 3). *Brachyury* mutants have consistent abnormalities in heart looping and 50% of embryos have inverted heart *situs* (King et al., 1998). The *Brachyury* target rotatin (Rttn) (Figure 7.4B) is required for the correct asymmetric expression of genes associated with left-right patterning (Figure 7.4A) and axial rotation (Faisst et al., 2002).

It is reassuring to note that despite the absence of the polarity seen in *in-vivo* and the stochastic patterning in the EB, the model is still capable of revealing *Brachyury* regulated transcripts associated with patterning *in-vivo.*

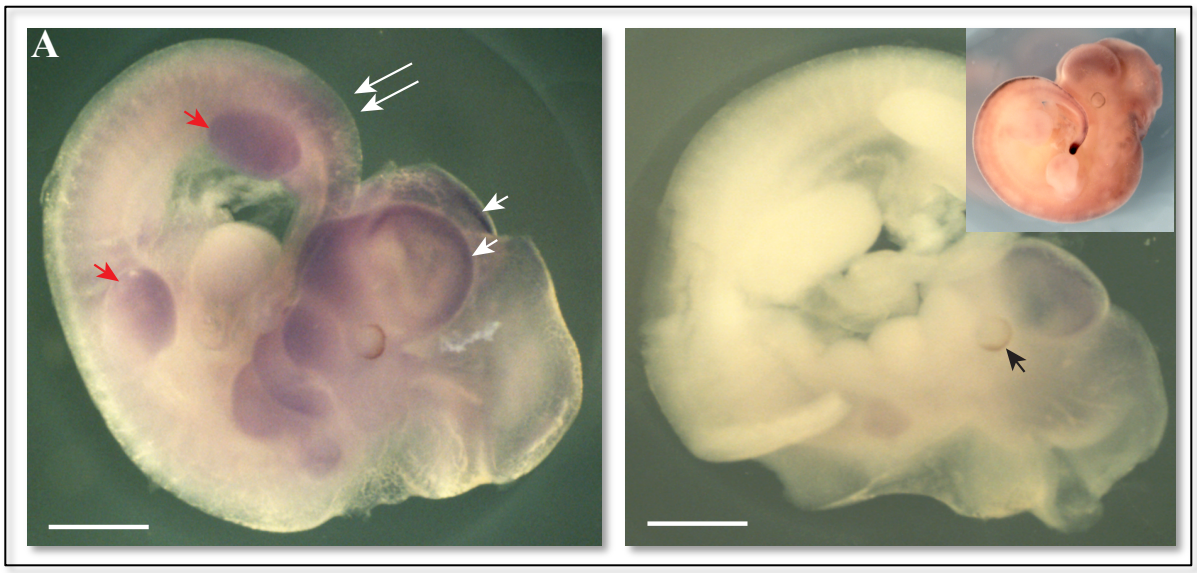

Figure 7.4 A: *In-situ* of wildtype 10.5dpc mouse embryos showing Rttn staining

Lateral views. **Left:** Digoxigenin-labeled antisense mouse Rttn RNA visualised with BM purple (Roche). **White arrowheads:** Telencephalon staining in the developing brain. **Red arrowheads:** Forelimb and hindlimb bud staining. **White arrows:** Staining in somites.

Right: Digoxigenin-labeled sense mouse Rttn RNA visualised with BM purple (Roche). **Black arrowhead:** The optic pit. **Inset image top:** The same stage embryo stained with digoxigenin-labeled antisense mouse *Brachyury* RNA visualised with magenta/INT (brown) shows *Brachyury* is still present in the tail tip and notochord. Embyro dissection and *in-situ* hybridisation A. Evans. White bars indicate 1000µm

B

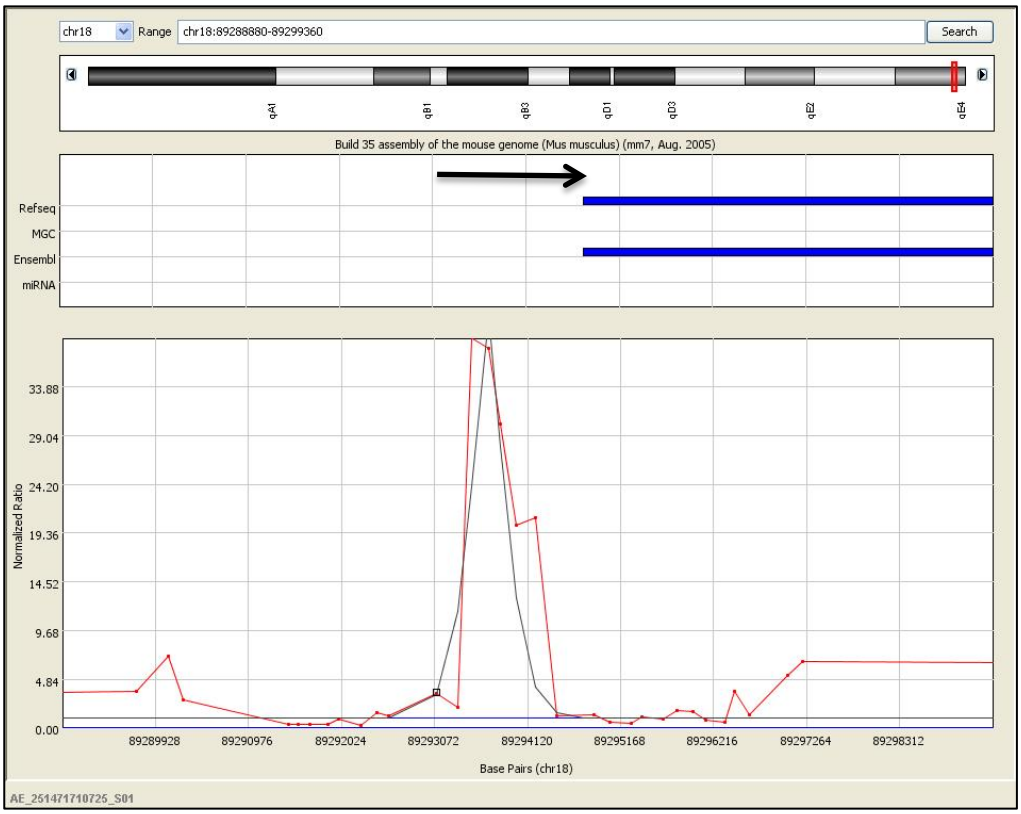

Figure 7.4 B: Binding events for Rttn promoter

The Brachyury binding peak is upstream of the transcription start site (Rttn gene in blue) this image was exported from chIP Analytics 1.3.software (Agilent Technologies). Fold enrichment (y axis) for combined array data from three chIPs against Rttn chromosomal location (x axis). The software uses the whitehead error model (Lee et al., 2006a) taking the p value of the probe in question as well as its neighbours, comparing groups of three probes and computing a combined p value.

7.3 *Brachyury* and cancer

Brachyury is not expressed in adult tissues but is in many human cancers (Palena et al., 2007). Induction of EMT is an important step in the progression of primary tumours, for example in colorectal and lung cancer (Roselli et al., 2012; Sarkar et al., 2012). Brachyury is expressed in haemangioblastomas, rare tumours in blood vessels of the brain and spinal cord (Tirabosco et al., 2008), and chordoma, a rare malignant tumour in bone (Yang et al., 2009; Pillay et al., 2012; Nelson et al., 2012). *Brachyury*

expression is also linked to poor prognosis in colorectal cancers, particularly when expressed in primary tumours prior to metastasis (Kilic et al., 2011). During normal development, the control of cellular plasticity is under tight control, as the epithelial phenotype tends to be polarised while the mesenchymal phenotype is highly motile. In cancer the control of genes associated with EMT and migration are deregulated highlighting the links between embryogenesis and a cancer phenotype (Fernando et al., 2010).

7.4 Brachyury targets in human development, lessons from the mouse

Analysis of early mesoderm development in the mouse embryo and in mESC - derived EBs has provided many insights into cell specification. As the mouse experiments were almost completed, culture protocols were being developed for repeating the experiments in hESCs using chIP-seq technology. FlyB chemically defined media (CDM) plus FGF2 (F), LY294002 (ly) a potent inhibitor of phosphoinositide 3-kinases (PI3Ks) and BMP4 (B) was used to induce mesoderm formation (Bernardo et al., 2011). *Brachyury's* role in development appears to be conserved between mouse and human cells. *Brachyury* regulation was verified in human ESCs for the target genes Axil/Conductin (Axin 2), wnt3a, fgf8 and junction plakoglobin or gamma catenin (JUP) (Figure 7, (Evans et al., 2012)[*12]). Given the data comes from two different technical platforms and analysis pipelines there is a high degree of overlap (Figure 7.5). Platform differences add to other variables including the dynamic nature of transcription factor occupancy and percentage of *Brachyury*-positive cells in the population.

Human *Brachyury* chIP-seq targets also include BMP4, VEGF, Fli1 and Notch1, of particular relevance to mesoderm induction and haematopoietic development (Tiago Faial, manuscript in preparation). In mouse these transcripts were just outside significance, but the human data does suggest they are bona fide targets (see Appendix table 6).

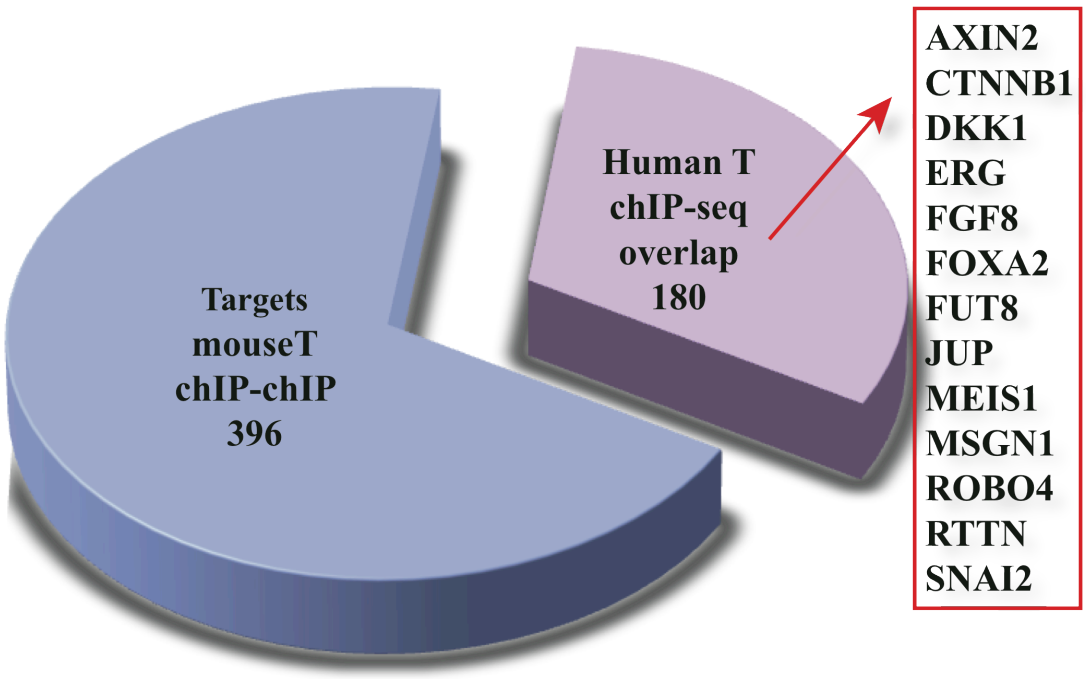

Figure 7.5 Pie chart indicating mouse *Brachyury* targets from chIP-chIP also common to human chIP-seq *Brachyury* data.

396 target transcripts were identified from the chIP-chIP experiments for mouse *Brachyury* and 180 of those targets were also present in the targets from human *Brachyury* chIP-seq data. For the human experiments hESCs were cultured in chemically defined Fly B mesoderm media containing Fgf2 (F), LY294002 (ly) a potent inhibitor of phosphoinositide 3-kinases (PI3Ks) and BMP4 (B) (Bernardo et al., 2011). Common target genes may be higher since overlap is limited to comparing genes and isoforms found on the mouse arrays. Of the transcripts common to both hESCs and mouse EBs are transcripts described in (Evans et al., 2012)[*12] and in Chapter 7 of this work as indicated: conductin (Axin2), β catenin (Ctnnb1); dickkopf homolog 1 (Dkk1); E-twenty-six (Ets) related gene (Erg); fibroblast growth factor 8 (fgf8); forkhead box A2 (Foxa2); Fucosyltransferase 8 (Fut 8); Junction plakoglobin (Jup); myeloid ecotropic viral integration site 1 (Meis1); mesogenin 1 (Msgn1); magic roundabout, axon guidance receptor, homolog 4 (Robo 4); rotatin (Rttn); snail homolog 2b (Drosophila) Slug, Snail2 (Snai2).

Mouse chIP-chip data A. Evans. Human chIP-seq data T. Faial.

7.5 The elusive T-box

The T-box domain, found in all T-box proteins binds DNA in a sequence specific manner. Morley et al showed enrichment of the canonical T-box binding site TCACACCT for no tail (ntl), the zebrafish *Brachyury* ortholog (Morley et al., 2009). Since the original random oligomer binding experiments by Kispert (Kispert and Hermann, 1993), revealing a preference of *Brachyury* for a palindromic form of the consensus sequence, the assumption was for many years that the same would apply *in vivo* for the mouse with speculation that dimer binding involved each monomer binding a half site. No enrichment for the TCACACCT site was found in the mouse EB experiments and we now believe this is due to the limitation of promoter length available, in this case 5.5kb upstream and 2.5kb downstream of the transcription start site (TSS).

The three dimensional arrangement of the chromatin may hold the key to the control of transcription by *Brachyury* and involve co-operation with other transcription factors or enhancers, since the binding sites from the hESC chIP-seq were in many genes far upstream from the TSS (manuscript in preparation by Tiago Faial). Some support for this idea comes from recent data using *Brachyury* expressing chordomas (Nelson et al., 2012), where only 11% of targets were within +/- 2kb of the TSS and 58% of targets within -50kb of the TSS to + 5kb of the transcription end site (TES). Bending and looping of enhancer regions may explain the lack of T box sites found close to many promoters for *Brachyury* targets (Petrascheck et al., 2005). Unravelling the topological organisation of *Brachyury* promoter complexes will require the analysis of long-range interactions using techniques such as chromosome conformation capture (3C) (Dekker et al., 2002).

ChIP-chIP technology has now largely been superseded by chIP-sequencing (ChIP-Seq). ChIP-seq, in which immunoprecipitated DNA is analysed by massively parallel sequencing, has the huge advantage that there is no restriction to a limited length of promoter arrayed on the chips (Barski et al., 2007). To fully resolve the complex picture of mesoderm induction combinational analysis of *Brachyury,* together with closely related transcription factors in the embryo such as Eomesodermin (Eomes), required for trophoblast and paraxial mesoderm specification (Russ et al., 2000), and Tbx 6 downstream of *Brachyury* and required for somitogenesis (Chapman and

Papaioannou, 1998), may be necessary. It is possible many *Brachyury* targets are controlled by more than one T-box gene (Wilson and Conlon, 2002) and other transcription factors as seen in the complex control of haematopoietic differentiation (Wilson et al., 2010). For example mesogenin 1 (msgn1), required for somitogenesis, is a target of both Tbx6 and *Brachyury* (Wittler et al., 2007).

7.6 A wave of mesoderm induction is required for blood and vascular development

Despite unanswered questions concerning the exact role of the T box in mouse we have shown that *Brachyury* has a crucial role during the establishment of mesoderm and its derivatives. The expression of an embryonic transcript in adult tumours also highlights the importance of correct, co-ordinated, transcriptional control of gene expression.

To create robust protocols for the *in-vitro* production of haematopoietic stem cells for blood or endothelial cell differentiation (Tan et al., 2013) requires a peak of *Brachyury* expression, which accompanies mesoderm formation, in both mESC and hESC.

Chapter 8 Translational medicine: the future

The use of EB differentiation *in vitro* provided insights into the reconstruction of the routemap to blood and vascular cells via mesoderm induction. It is now conceivable to develop cell-based therapies in many fields of research and part of this success is due to global sharing of knowledge, from its roots in developmental biology, to the advent of ESC and induced pluripotent stem cell (iPSC) technology (Takahashi and Yamanaka, 2006; Takahashi et al., 2007), leading now to the ability to reprogram cells.

Red blood cell (RBC) transfusions are the oldest form of cell-based therapy but remain dependant on healthy volunteer donations. Platelet transfusions are even more vulnerable to availability having a shelf life of only 5-7 days. Platelets have a central role in haemostatic plug formation and thrombosis (Clemetson, 2012), and angiogenesis via the release of PDGF, VEGF, FGF2 and other stored growth factors. Humans produce approximately 10^{11} platelets daily from terminally differentiated multinucleated, megakaryocytes (MKs) (Kaushansky, 2008) (see Figure 8.5). Chemotherapy, organ or bone marrow transplant, bleeding from trauma or surgery, and inherited blood disorders may all require blood or platelet transfusions. Availability and storage is especially challenging in developing nations. Both platelets and erythrocytes are anucleate therefore can be subjected to gamma irradiation to prevent teratomas from any residual undifferentiated iPSCs and, therefore, are promising targets for the translational process. Recent work concentrates on the *in-vitro* derivation of cells of the myeloid lineage, in particular platelet-producing MKs.

Cord blood CD34+ progenitor cells have provided the gold standard in the production of blood cell lineages (Chapter 1.3) and are used routinely used to produce mature MKs. However, this is a limited resource whereas ESC and iPSC can in theory provide a continuous supply for differentiation. In addition, cord blood derived cells are of foetal origin whereas adult haematopoiesis occurs mainly in the bone marrow (Figure 7.2).

8.1 Translating complex tissue environments to *in-vitro* production protocols: modelling the adult bone marrow niche

Endothelial and haematopoietic cells differentiate in close proximity and, endothelial cells play an active role in haematopoiesis, producing cytokines such as VEGF. The transition of VEGFR2+ progenitors (see Figure 7.3) depends on VEGF for endothelial cells (Samuel et al., 2013) and either low or absent VEGF for haematopoietic development (Eichmann et al., 1997). Adult haematopoiesis occurs in the bone marrow HSC niche (Schofield, 1978; Hawkins and Lo Celso, 2013) closely associated with bone development or osteogenesis (Patt and Maloney, 1972; Maloney and Patt, 1975) (Figure 8.1). This is the site of maturation of platelet producing MKs supported by cells and cytokines of the bone marrow niche.

Thrombopoietin (TPO) and its receptor Mpl, the regulators of megakaryopoiesis, are also regulators of HSCs in the osteoblastic niche (Qian et al., 2007; Yoshihara et al., 2007), as are the receptor roundabout 4 (Robo4), and its ligand slit homolog 2 (Slit 2), in the vascular niche (Sugiyama et al., 2006). To model the functioning bone marrow niche *in-vitro* successfully will require the correct cues, which may include physiological, structural, and topographical components. Modelling the shear force of blood flow through the vascular niche may be a particular requirement of MK maturation since this is known to enhance platelet formation (Machlus and Italiano, 2013).

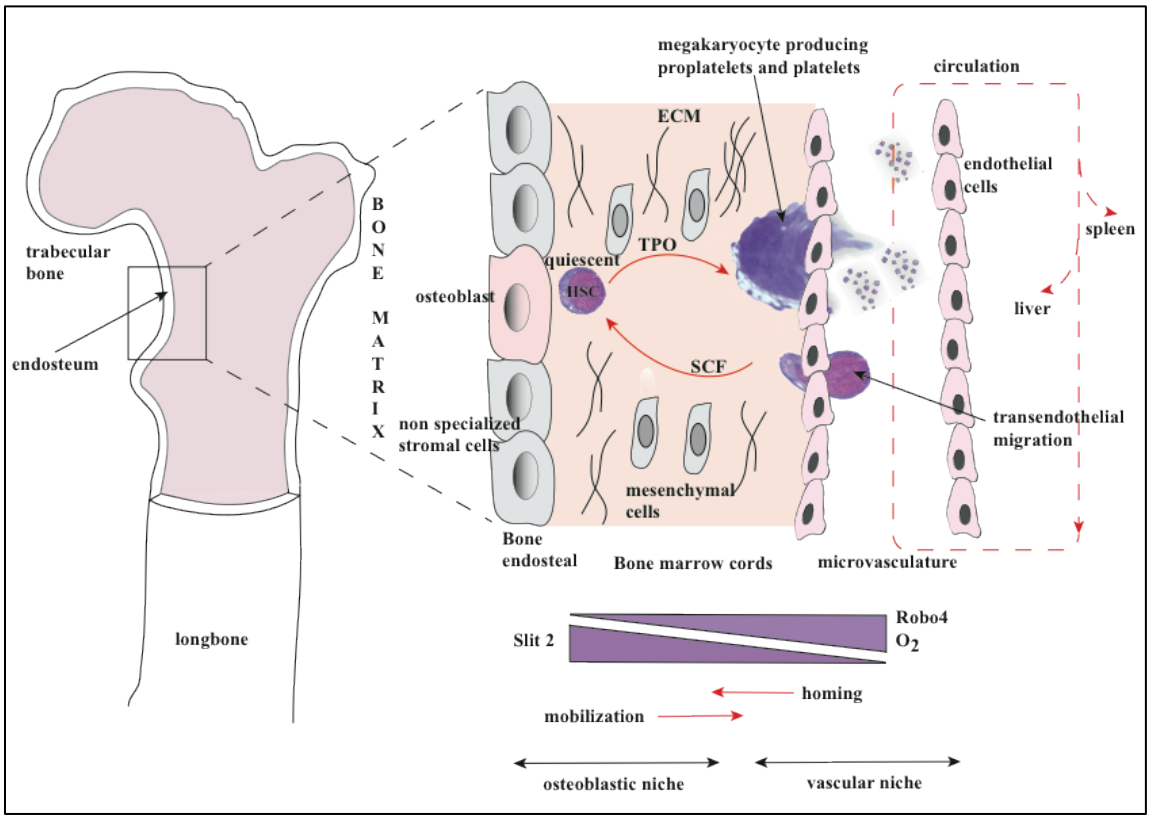

Figure 8.1 The haematopoietic stem cell niche, the site of terminal differentiation of platelets

The challenge to produce fully mature cells may rest on the ability to recreate this niche. Quiescent HSC are closely associated with osteoblasts. Many signals then influence the balance between self-renewal, mobilization and differentiation. Both homing and mobilization also involve close association with endothelial cells (EC).

SCF binds proto-oncogene (c-kit) on HSC and is required for stem cell maintenance. Osteoblasts express membrane bound SCF and, secrete angiopoietin 1 which binds the Tie2 receptor ligand on HSCs. TPO directs cells to the myeloid lineage.

Mature megakaryocytes release platelets into the bloodstream by extending proplatelets via fenestrations in the sinusoidal vessels.

The osteoblast niche is also hypoxic compared to the vascular niche (low O_2). Robo4 is high is the vascular niche (Chapter 7.2.1) and acts as a guidance molecule for its ligand slit 2 expressed by stromal/mesenchymal cells (Smith-Berdan et al., 2012). OP9 cells used in MK differentiation protocols (Takayama et al., 2008) also express slit 2.

Key: Roundabout 4 (Robo4) receptor and its ligand slit homolog 2 (slit 2); stem cell factor (SCF); extracellular matrix (ECM); Thrombopoietin (TPO). Based on (Wilson and Trumpp, 2006).

8.2 Manipulating cell fate

Development has been likened to a progression via regulatory states defining specific phenotypes (Waddington, 1957; Pimanda and Gottgens, 2010). The input is a series of transcription factors and expressed genes, and the output or cell fate is determined by whether target genes are active or repressed. So, at the molecular level, the journey from pluripotency to terminal differentiation requires constant lineage decisions by individual cells. Multiple, distinct, terminally differentiated cells are formed from branched and interconnected routes. Waddington's metaphor for development implies the landscape and route consists of a fixed set of routes to terminal differentiation. However, knowledge of the molecular input for specific lineages provides the means to manipulate either the landscape or route followed (Figure 8.2). This applies to both translational medicine therapies and the control of metastatic invasion such as that described in endometrial cancer (Chapter 5).

8.2.1 Directed differentiation towards terminally differentiated cells

In directed differentiation protocols using hESCs, or patient specific iPSCs, cells are guided by means of cytokines towards specific fates, for example, via the myeloid lineage to megakaryocytes (blue arrows in Figure 8.2). To produce platelets *in-vitro,* progenitor cells are directed along the myeloid lineage using protocols based on those of Hiromitsu Nakauchi (Takayama et al., 2008). Combined in co-culture with the mouse bone marrow stromal cell line OP9 and exogenous cytokines it is possible to direct progenitor cells to a MK (thrombopoietin, blue arrow in Figure 8.2) or erythrocyte fate (erythropoietin) fate (Gao et al., 2010). However, this method has proved both expensive and inefficient even after much tweaking of the protocols the best results from 2 x 10^6 iPSCs produced 4.5 x 10^5 CD34+ haematopoietic progenitors (96% purity) and finally 10^6 megakaryocytes (99% CD41a+CD42b+, see Figure 8.5).

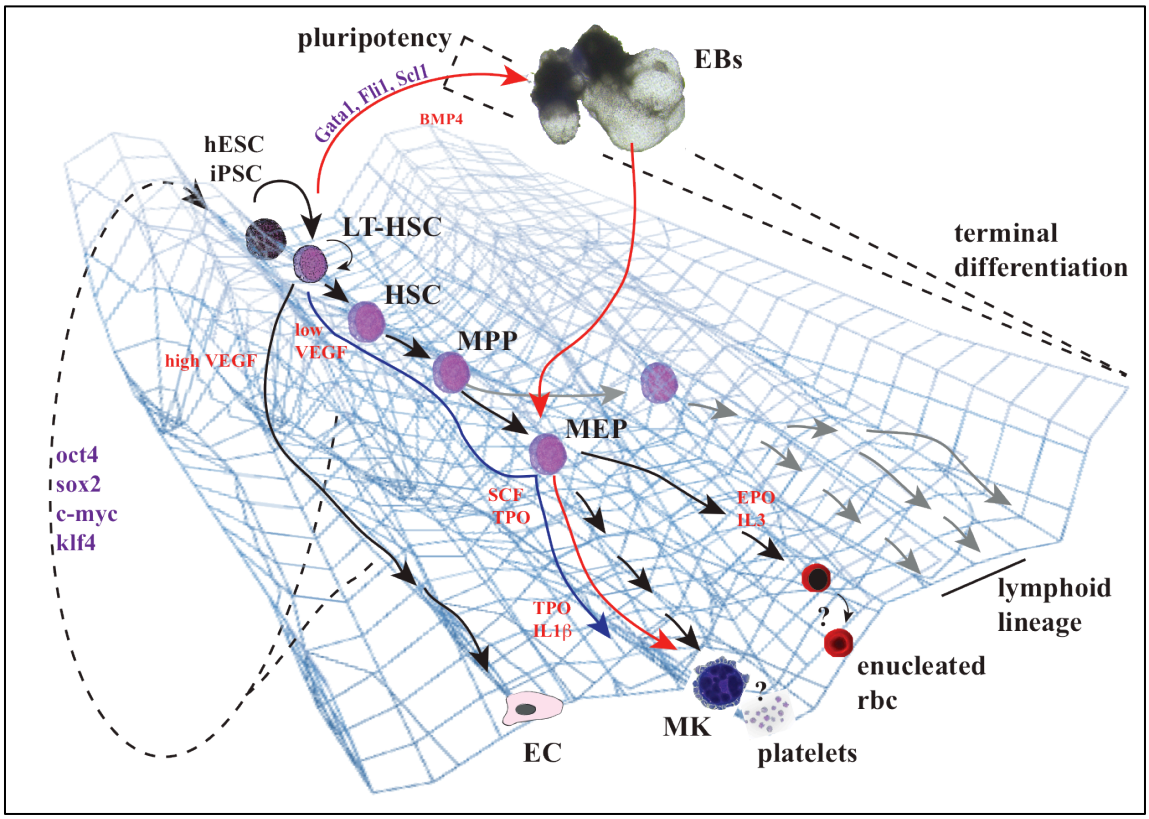

Figure 8.2 Routes to differentiation using Waddington's metaphor for development

→ Directed differentiation based on (Takayama et al., 2008) using co-cultures
Cytokines: erythropoietin (EPO); Interleukin 3 (IL3); Thrombopoietin (TPO); Stem Cell Factor, Kit ligand or steel factor (SCF); Interleukin1β (IL1β).

→ Forward programming (Moreau et al in preparation) Lentiviral transcription factors: globin transcription factor 1 (Gata 1); Friend leukaemia virus integration1 (Fli1); T-cell acute lymphocytic leukaemia 1 (TAL1, Scl1). Cytokines: bone morphogenetic protein 4 (BMP4)

- - → Reprogramming from peripheral blood progenitors to induced pluripotent cells using the four Yamanaka transcription factors (Takahashi and Yamanaka, 2006) also involves viral transduction using oct4 , sox2, c-myc, klf4

⇒ Routes to endothelial cells and other blood lineages

? ? Final maturation steps from MK to PLT and fully enucleated RBC remain elusive

Abbrvs: human embryonic stem cells (hESC); induced pluripotent stem cells (iPSC); embryoid bodies (EBs); long-term haematopoietic stem cells self renewing (LT-HSC); haematopoietic stem cells (HSC), multipotent progenitors (MPP), megakaryocyte/erythoblast precursor (MEP); megakaryocyte (MK); endothelial cell (EC); red blood cell (rbc).

Transcription factors: purple

Cytokines; red

8.2.2 Forward programming towards terminally differentiated cells

Haematopoiesis is controlled by a core group of transcription factors, shown by multiple transcription factor mapping, using genome wide sequencing data (Gottgens et al., 2002; Pimanda et al., 2007a; Pimanda and Gottgens, 2010). By manipulation of the transcription factor input it is possible to push progenitors forward to a myeloid phenotype and at the same time increase the efficiency of the differentiation process *in-vitro* by programming the cells to myeloid precursors, in a way analogous to that of iPSC production using the four Yamanaka transcription factors (Takahashi and Yamanaka, 2006) (Figure 8.2). In effect, this manipulation causes re-wiring of the local gene regulatory network using combined ectopic expression of transcription factors and environmental stimuli.

By comparative analysis of the hESC line H9 (WA09, University of Wisconsin, USA) and cord blood MKs a set of key transcription factors were identified as candidates for lineage progression. Cloning of the transcription factors into lentiviral vectors, followed by transduction of hESCs and iPSCs, eventually led to three factors globin transcription factor 1(Gata1), Fli1 and T-cell acute lymphocytic leukaemia 1 (Tal1, Scl1) which we now use to forward programme pluripotent iPSCs to the myeloid lineage (Thomas Moreau, in preparation) (Figure 8.2 red arrows). The three factors fit closely with the core regulatory circuit for haematopoiesis in the mouse, identified as a fully connected triad (Pimanda et al., 2007b) of the transcription factors: Gata 2, Fli1 and Tal1/ Scl1 (Figure 8.3). All three factors are expressed in the dorsal aorta AGM (Figure 7.2) when HSC are formed, in the fetal liver where they are amplified (Dzierzak, 2005), and in MKs highlighting a number of links between MK maturation and HSC development in the AGM (Gottgens et al., 2002; Huang and Cantor, 2009).

If the system is then made three-dimensional by the introduction of a human embryoid body (hEB) step the recovery of mature megakaryocytes is increased further.

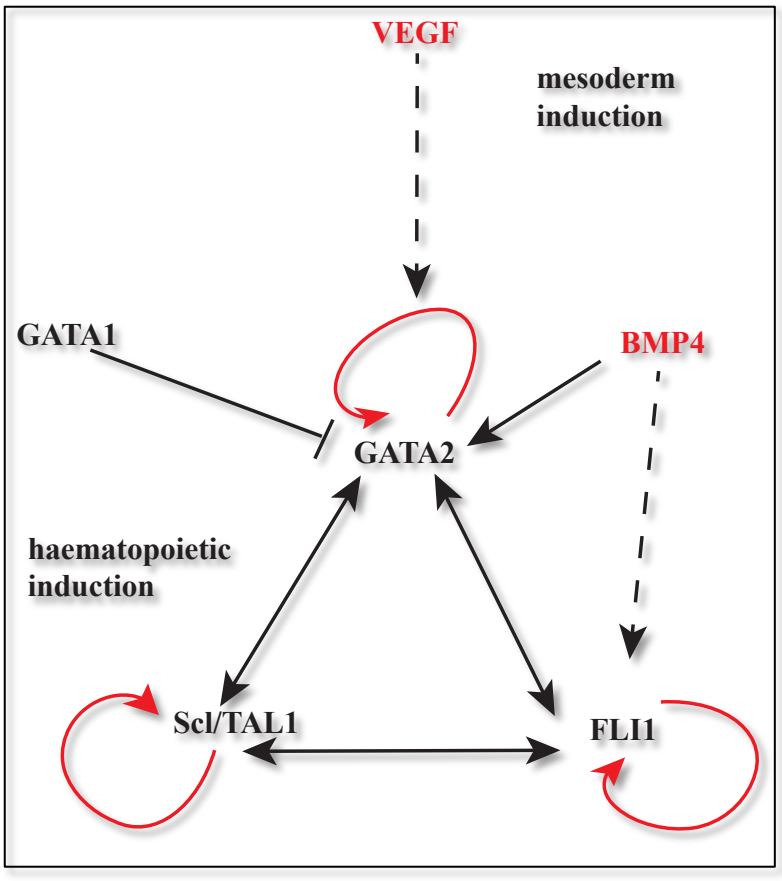

Figure 8.3 The kernel gene regulatory network (GRN) responsible for early haematopoietic and endothelial development

Part of a larger transcriptional network beginning with mesoderm induction, all but that of GATA1 involve positive interactions, GATA 1 interrupts GATA 2-positive autoregulation pushing cells to differentiate.

Gata 2 is required for early stages of myeloid differentiation and is overlapping with Gata 1, which is required for terminal differentiation (Chang et al., 2002). Fli 1 is an Ets transcription factor and in knockout mice vascular integrity and megakaryocyte differentiation are impaired (Spyropoulos et al., 2000). Scl/Tal1 is a basic loop helix transcription factor required for specification HSC and the differentiation of erythroid and megakaryocyte lineages (Porcher et al., 1996). **Transcription factors:** globin transcription factor 1 (Gata 1); globin transcription factor 2 (Gata 2); Friend leukaemia virus integration1 (Fli1); T-cell acute lymphocytic leukaemia 1 (TAL1, Scl1). **Cytokines:** bone morphogenetic protein 4 (BMP4); vascular endothelial growth factor (VEGF). Adapted from (Pimanda et al., 2007b). Solid lines indicate direct binding. Red arrows indicate autoregulation.

The size of hEBs now appears to be of particular relevance to the direction of stem cell development (Ng et al., 2005; Hwang et al., 2009). Recent technologies such as Aggrewell™ (Stem Cell Technologies) allow for uniformity of size and shape of the hEBs, together with improved cell viability and transduction efficiency (Ungrin et al., 2008). Manipulation of cell number per hEB, can alter potential fate, for example, 500 cells per hEB favours the formation of haematopoietic cells (Figure 8.4). This applies to hEBs in particular which usually are more heterogenous in size than mouse EBs described in chapters 5 and 6.

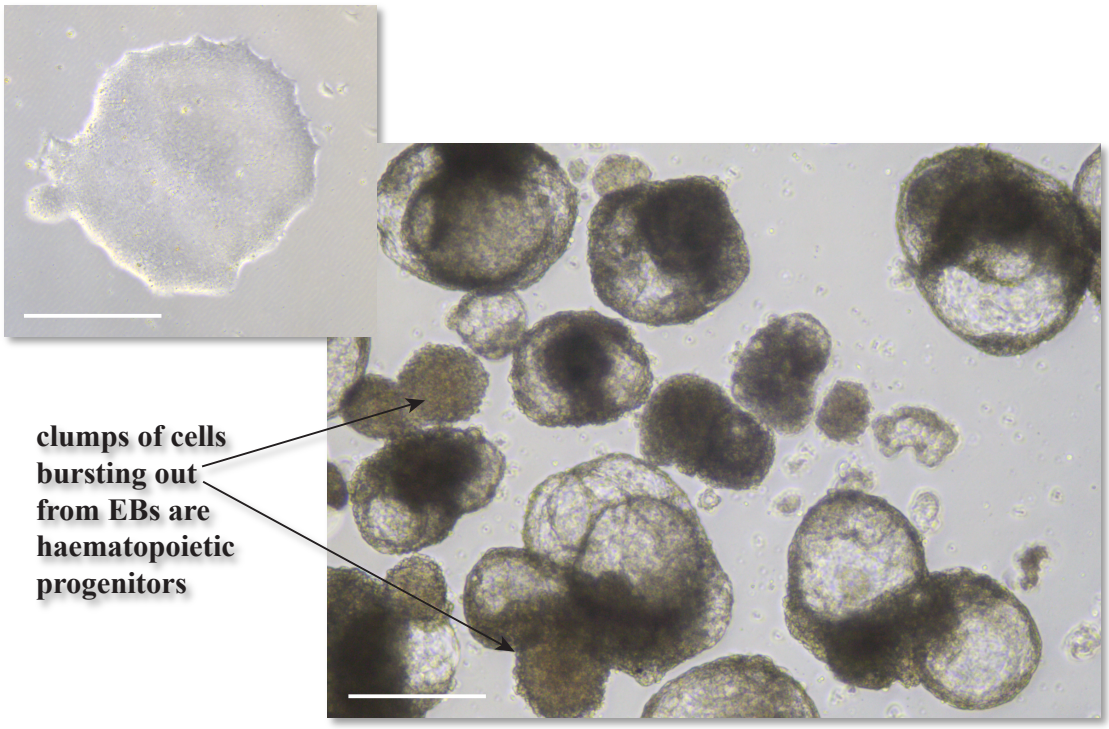

Figure 8.4 Going three-dimensional: Day 8 hEBs produced using Aggrewell™

Images captured using a Leica DM IL LED microscope (Leica microsystems, UK). The cells are Bob iPSCs (originally from Ludovic Vallier, The laboratory of Regenerative Medicine, Cambridge). **Top left:** A single undifferentiated colony grown in feeder free conditions. **Main Image:** Day 8 cystic hEBs, formed using Aggrewell™ plates with 400µm microwells, contain haematopoietic progenitors. Each EB was created from 500 iPSCs cells using TrypLE™ (Life Technologies) to dissociate colonies, in the presence of a ROCK inhibitor Y27632 (Sigma) plus Gata 1, Fli1 and Tal 1 lentivirus. Y27632 inhibits rho-associated protein kinase (ROCK) signaling allowing iPSC survival as single cells (Watanabe et al., 2007), by preventing apoptosis. White bars represent 500µM.

Table 3 Numbers of megakaryocytes from different *in-vitro* differentiation methods

Source of Cells	Mononuclear cell number	iPSCs	CD34+* Progenitors (positive selection)	CD41a/CD42b* MK (positive selection)	Expansion
Cord blood 75ml	5.5×10^8		2×10^6	4.4×10^7	x 22 from CD34+
Mobilised peripheral blood 1ml	3.0×10^8		2×10^6	2×10^7	x 10 from CD34+
Directed differentiation using OP9 feeders then feeder free maturation	N/A	2×10^6	$4.5. \times 10^5$	1.1×10^6	x 2.4 from CD34+ x 0.5 from iPSCs
Forward programming using 3 TFs, EBs and feeder free conditions	N/A	1×10^6	N/A via EBs	1.9×10^7	x 19 from iPSCs

Table 3 Key: N/A Not Applicable; transcription factors (TFs); * absolute numbers of live purified cells; OP9 a murine stomal cell line established from newborn B6C3F1 op/op mouse (Kodama et al., 1994). The same iPSC line was used for directed differentiation and forward programming. **The inclusion of both a brief mesoderm and an EB step have increased efficiency, contributing to the reduction of this bottleneck in production**. On the basis of 10^6 iPSCs (equivalent to half a well from a six well plate of cells) producing 1.9×10^7 MKs, and if 100% of these (highly improbable at this point) produced 10^3 platelets each then 10 times this would be required for a single dose of 10^{11} platelets.

Forward programming increases efficiency compared to directed differentiation. From a starting population of 10^6 undifferentiated iPSCs it is possible to obtain nearly 20 million double positive (for the MK antigens CD41a+CD42+) MKs, ~ 40 times the number obtained with directed differentiation protocols.

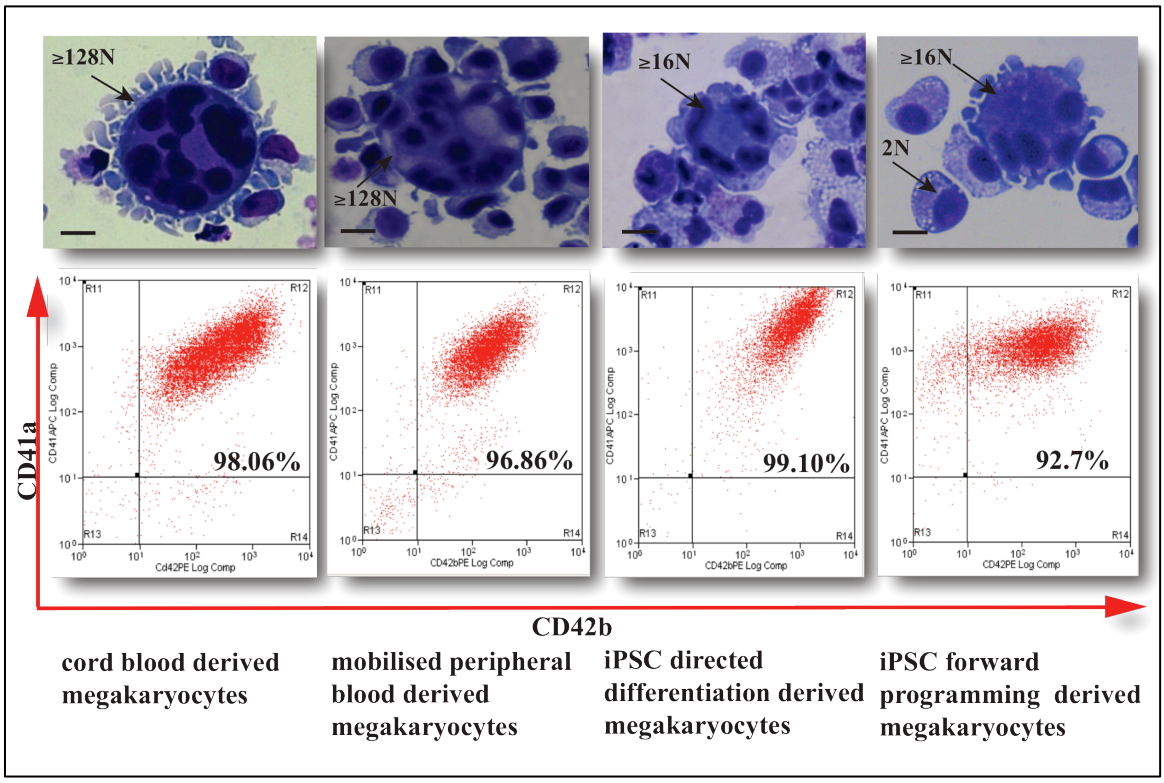

Figure 8.5 Sources of *in-vitro* derived megakaryocytes

From left to right: cord blood derived MKs from CD34+ isolated progenitors (see chapter 1.3); mobilised peripheral blood derived MKs isolated in the same way; iPSC derived MK by directed differentiation (Chapter 8.2.1); iPSC derived MK by forward programming using lentivirus (Chapter 8.2.2), using the same iPSC line.

Top panel: Cytospins from sorted populations using EasySep PE positive selection kit (Stem Cell Technologies), of cultured megakaryocytes (MKs) stained with Rapid Romanisky (a mixture of cationic modified methylene blue nuclear stain and anionic eosin Y). Black Bars =10µm, numbers indicate ploidy, all four populations contain large multinucleated cells.

Bottom panel: Flow cytometry plots of sorted MKs. Top right quadrants show positive staining for anti-CD41a APC (allophycocyanin conjugated), y axis and anti-CD42b PE (phycoerthrin conjugated), x axis. CD41a is integrin, alpha 2b, which is non-covalently associated with CD61 or GPIIIa (the integrin beta 3 chain) to form the GPIIb/IIIa complex, which binds fibrinogen, fibronectin, von Willebrand factor and thrombospondin. CD42b is the more mature marker of the two and reacts with GPIb (integrin I beta), which binds von Willebrand factor.

Percentages are of CD41a/CD42b + sorted cells, all are gated on MK window by isotype control and are diamidino-2-phenylindole (Dapi) negative (live gate).

All experimental data by A. Evans at the NHSBT Centre, Cambridge.

8.3 Cell - based therapies

Using screened iPSCs it is conceivable that on-demand, controllable and biocompatible stocks of human leucocyte antigen (HLA) and human platelet antigen (HPA) phenotyped platelets can be made available to reduce the incidence of alloimmunization following transfusion.

In addition, iPSC derived cells provide opportunities for drug screening and targeted gene repair for example in specific platelet disorders such as gray platelet syndrome (GPS) (Cramer et al., 1985) and thrombocytopenia with absent radius (TAR) (Hall et al., 1969) where the genetic defects have been identified. Mutations in Neurobeachin-like 2 (NBEAL 2), which encodes a BEACH/ARM/WD40 domain protein, are responsible for GPS (Albers et al., 2011; Kahr et al., 2011) and in RBM8A, encoding the Y14 subunit of exon-junction complex (EJC), cause TAR (Albers et al., 2012). Using PBMNCs as the source, iPSC lines have been established for both GPS and TAR syndrome as the first step in the experiments depicted in Figure 8.6.

The impact of reprogramming on the genomic and epigenetic integrity of iPSCs needs to be determined (Lister et al., 2011; Gore et al., 2011; Hussein et al., 2011). We now know the genetic code itself is not sufficient to determine gene expression or phenotype of a cell. A large consortium (BLUEPRINT http://www.blueprint-epigenome.eu/) is currently deciphering both the epigenetic, and expression blueprint, of every cell type in the blood to provide a huge resource of data for researchers and clinicians. The source of the iPSC used may also prove to be a factor in the differentiation potential towards some cell types (Figure 8.6) and use of viral-free and non-integrating approaches are being explored (Warren et al., 2010). It is considered standard to assess generated induced pluripotent stem cells (iPSCs) for use in differentiation protocols by RNA-seq to profile global gene expression, bisulpite sequencing to assess epigenetic status and also chIP-seq using histone markers to give a profile of active and inactive genes (Rada-Iglesias et al., 2011).

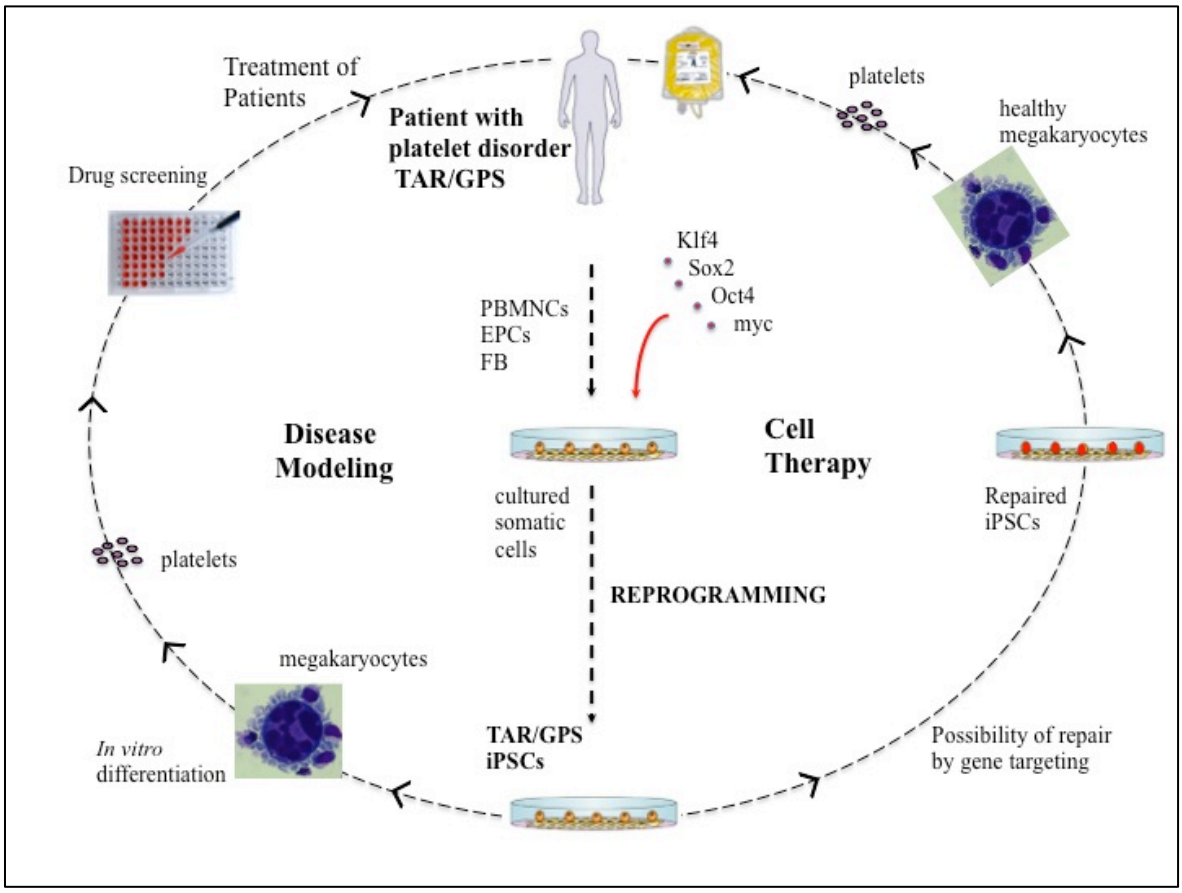

Figure 8.6 Disease modeling and cell therapy using patient specific iPSC

Creating patient specific stem cells allows disease modeling and drug screening in a human cell setting. It also allows the possibility of targeted gene repair. Inherited blood disorders for example gray platelet syndrome (GPS) an abnormality of platelet alpha storage granules, and thrombocytopenia absent radius (TAR) associated with thrombocytopenia and bilateral radial aplasia.

Sources of iPSC include: peripheral blood mononuclear cells (PBMNCs); endothelial progenitor cells (EPCs), EPC are rare bone marrow derived cells that are recruited into the peripheral blood in situations of vascular repair/angiogenesis or vascular stress (Geti et al., 2012); fibroblast cells (FBs) from dermal fibroblasts (using punch biopsies).

Reprogramming to iPSCs using the four Yamanaka transcription factors (Takahashi and Yamanaka, 2006): Octamer-binding transcription factor 4 (Oct4); SRY (sex determining region Y)-box 2 (Sox2); Avian Myelocytomatosis Viral Oncogene Homolog (c-Myc); Kruppel-like factor 4 (Klf4). For GPS iPSCs both a polycistronic lentivirus STEMCCA (A.Evans) or individual retroviral constructs (A.Evans and The laboratory of Regenerative Medicine, Cambridge) were used. For TAR iPSCs STEMCCA (Somers et al., 2010) or Sendai virus (Nishimura et al., 2011) were used (The Childrens Hospital of Philadelphia, USA).

8.4 Scale-up

Translation to the clinic requires many technical, ethical, regulatory and financial hurdles to be overcome. More than 200,000 units of 10^{11} platelets per unit are supplied annually (NHSBT, 2011) and each megakaryocyte produces around 10^3 platelets (Kaufman et al., 1965) in a self limiting process, since the megakaryocytes fragment during this process forming proplatelet extensions which bud platelets at their tips. Estimates for the required number of *in-vitro* produced megakaryocytes vary widely from 6 x 10^6 (about 60 culture plates) to 10^9 (about 1000 culture plates) (Lambert et al., 2013) per unit of platelets for transfusion, clearly a huge challenge.

8.4.1 Moving towards fully defined and xeno-free culture

Most "chemically defined media" contain animal derived lipids and bovine serum albumin so the next challenge is to convert entirely to xeno-free culture. Conversion to feeder-free conditions is another requirement, both for ESC and iPSC culture and in differentiation protocols, and work is underway to establish exactly what feeder lines such as OP9 provide.

Complete profiling of any cells likely to be used in the translational process will be needed to follow good manufacturing process (GMP) criteria (The HipSCi, Human-Induced Pluripotent Stem Cells Initiative, Wellcome Trust Sanger Institute).

8.4.2 Preservation or recreation of normal physiological cues

Tissue culture has come a long way since the establishment of the first human immortal cells in 1951 from tissue cut from the cervix of Henrietta Lacks (Skloot, 2010), starting an explosion in the use of *in vitro* cultured human cells. A PubMed search (August 2013) for HeLa, the acronym by which these cells are known, yielded > 75,000 articles, producing masses of data relevant to our collective understanding of cell biology. But, this is tempered by the knowledge that in practice we are trying to describe and ultimately recapitulate three dimensional, *in vivo,* events.

In vitro culture may lack biological relevance to the whole organism since life is in three dimensions where cells are ellipsoids, with their surface area either in touch

with other cells or with extra cellular matrix rather than flat with 50% of their surface touching a culture dish. Stem cell and replacement therapy may require another revolution in the adaption of biological matrices (Taylor, 2007) to resemble the *in vivo* state (Chiang et al., 2010).

Most cells, like those in the bone marrow niche where MKs mature, are in contact with ECM to which they adhere by surface receptors such as integrins, and are able to sense mechanical cues. Stem cell signalling can be altered by exposure to different porosity and stiffness of hydrogels (Watt and Huck, 2013). Modular bioreactor chambers are now manufactured under the patent name Quasi-vivo® (Kirkstall Ltd, Sheffield, UK) to mimic the dynamic flow of nutrients in tissues and can incorporate scaffolds or tissue slices to create organ like chambers.

8.5 The roadmap from stem cells to terminal differentiation:

Concluding remarks

Taking advantage of new technologies as they appear and adapting these to specific questions, such as those described earlier for endometrial biology and then mesoderm induction, has left the overwhelming impression that to be able to achieve cell therapies of the future, we need to fully understand cells in the context of complex tissues. In addition, both normal and abnormal physiology gives us the boundaries within which we can manipulate the environment in which we produce *in-vitro* surrogates that are fit for purpose. In endothelial cell biology, control of the angiogenic switch is crucial to prevent metastatic invasion. In haematopoiesis, specifically myeloid differentiation, a pivotal point is in the decision to follow the megakaryocyte or erythrocyte route.

The close overlap in the hierarchal development and gene networks controlling the differentiation of haematopoietic cells and endothelial cells allow us to use the same basic protocols to drive cells towards the cell lineage of our choice. By modifying the genetic and environmental cues cells are exposed to, we are increasingly able to control the route of terminal differentiation.

The greatest hurdle still to be overcome is the final maturation steps of both megakaryocyte platelet production and the enucleation of erythroid cells (Niwa et al.,

2009; Dias et al., 2011). A few authors have published claims of having achieved platelet production *in-vitro,* but the evidence is not strong (Takayama et al., 2010 ; Nakagawa et al., 2013) and both directed differentiation and forward programming so far have produced far fewer platelet-like-particles (PLPs) or proplatelet extensions compared to cord blood-derived megakaryocytes. Efficient production of PLPs may require recapitulation of the bone marrow niche by use of three dimensional functionalised scaffolds with a mix of the cells types from the niche (Figure 8.1). RNA-seq profiling and chIP-seq of these cells is allowing us to address these issues as the protocol evolves. Both cell types provide a huge challenge particularly in the final crucial stages of maturation, but the goal is production of a fully functional alternative to donated blood and platelets.

Future experiments, will include establishment of the final maturation steps of platelet formation to improve yield and activity, in the first instance, via creation of lentiviral vectors for genes differentially expressed in mature cord blood MKs and iPSC generated cells. Generating mesenchymal precursors and ECs in parallel from the same iPSCs (Eberle et al., 2012) may be a practical way to recapitulate the bone marrow niche in xeno-free conditions. Since, *in-vivo,* the vascular niche (Figure 8.1) of the bone marrow is the site of MK maturation, the timing of co-culture may be critical for this to be a positive effect on maturation.

Many exciting challenges lay ahead. It may prove judicious, for example, to exploit the bipotential precursor origins of blood and vascular cells and expand stocks of multipotential cells as the starting point for patient specific endothelial tubules, RBCs or platelets (Lu et al., 2007). Advances in molecular profiling techniques and in somatic cell reprogramming have opened the door to potential new therapies and discoveries to improve human health. Alongside the use of autologous induced pluripotent stem cells (iPSCs), my hope is that I may contribute to the development of patient specific treatments and cell therapies using knowledge gained from these studies.

Appendices

Web addresses

Blueprint epigenome: http://www.blueprint-epigenome.eu

Cyber T: http://cybert.ics.uci.edu

GOToolBox: http://genome.crg.es/GOToolBox/

HipSci: http://www.hipsci.org

Mouse Atlas: The Medical Research Council and The University of Edinburgh.

http://www.emouseatlas.org/

NestedMICA: http://www.sanger.ac.uk/resources/software/nestedmica/

RMRG genelist:

http://www.obgyn.cam.ac.uk/genearray/supplementary/RMRG_genelist.xls

RSAT: http://rsat.ulb.ac.be

SAM: http://www-stat.stanford.edu

Source BioScience LifeSciences:

http://www.lifesciences.sourcebioscience.com

WebLogo: http://weblogo.berkeley.edu

Xenbase: http://www.xenbase.org/anatomy/alldev.do

Zfin: https://zfin.org/zf_info/zfbook/stages/stages.html

Appendix figure 1 VEGF Growth factor family and its receptors on endothelial cells display isoform specific functions

Key: Vascular endothelial growth factor A and some of its 9 isoforms ($VEGFA_{121, 145, 165)}$, 165 being the most abundant splice variant; Vascular endothelial growth factor B/C/D (VEGFB/C/D); Placental growth factor 2 (PlGF2); Vascular endothelial growth factor receptor 2 (VEGFR2)/ Fetal liver kinase (Flk1)/ Kinase domain receptor (KDR); Vascular endothelial growth factor receptor1 (VEGFR1) /Fms-like tyrosine kinase (Flt1); soluble Flt1 (sFlt1); Semaphorin (SEMA), a ligand for neuropilin-1 (NRP1), and neuropilin-2 (NRP2) transmembrane non-tyrosine kinase glycoproteins; angiopoietins 1/2 (ANGPT1/2, Ang1/2) ligands for the TEK tyrosine kinase (Tie2/TEK) receptor; Extracellular regulated kinase pathway (Erk) (mitogen activated protein kinase, MAPK); Phosphatidylinositol 3' kinase (PI3K) activating protein kinase B (Akt/PKB). Based on a number of sources.

VEGFD, also known as C-fos induced growth factor (FIGF) is associated with lymphatic endothelial cells and signals via VEGFR2 and vascular endothelial growth factor receptor 3 or Fms-related tyrosine kinase 4 (VEGFR3, Flt4) usually found on lymphatic endothelium (Achen et al., 1998)

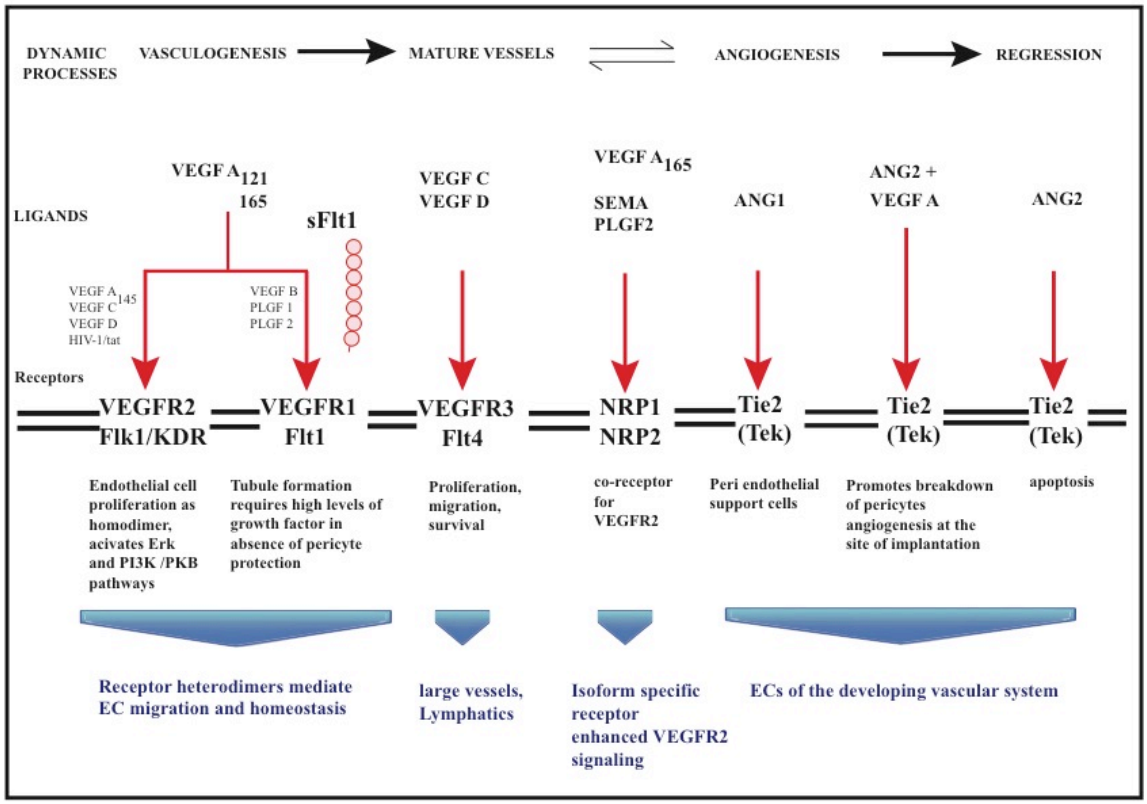

Appendix Figure 2 Serial Analysis of Gene Expression (SAGE)

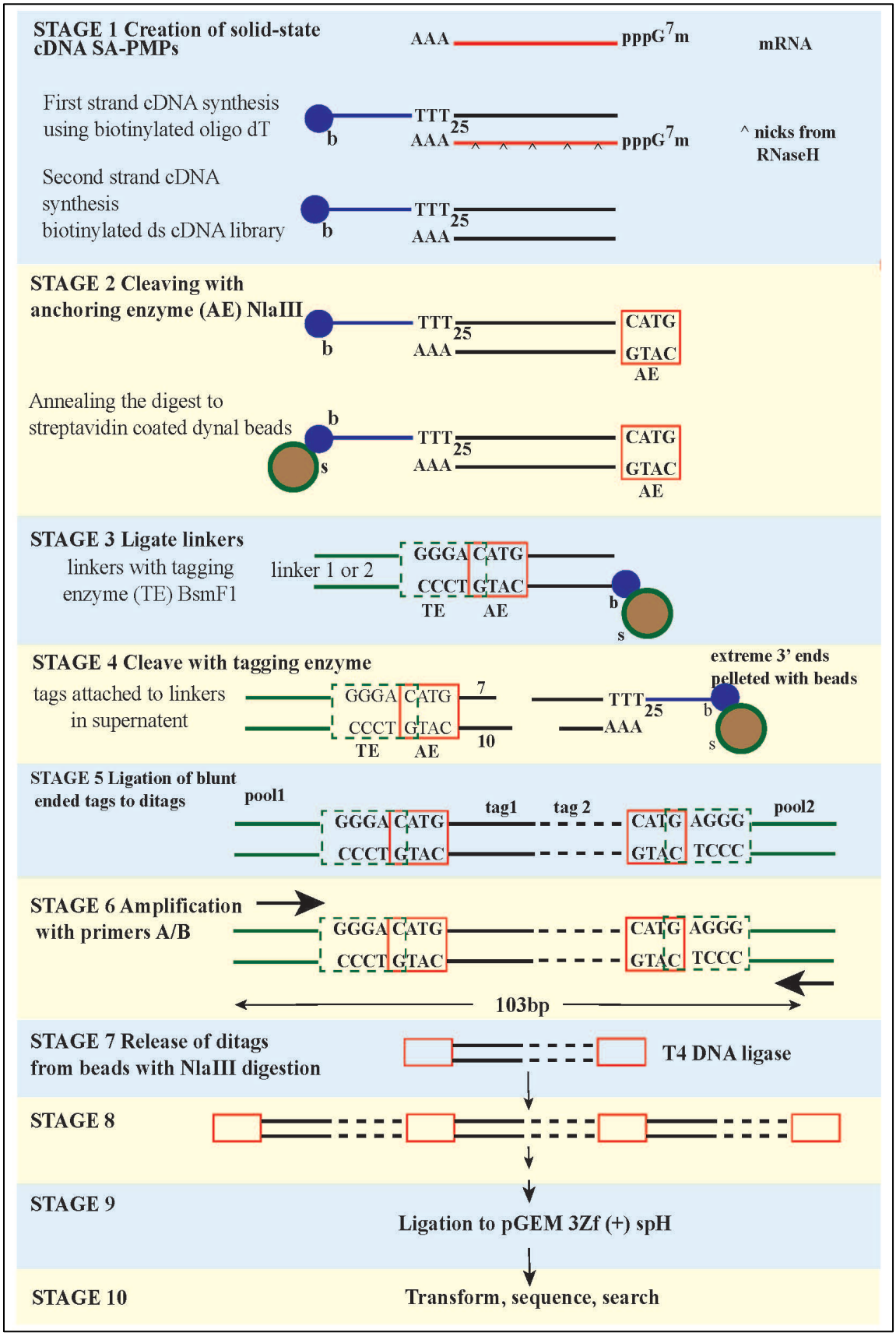

Appendix figure 2 Serial analysis of gene expression (SAGE)

Illustrating the stages of SAGE, each of which needs to be optimised.

SAGE is based on two principles. Firstly, short nucleotide sequence tags of 9-10 base pairs (bp) contain sufficient information to uniquely identify a transcript provided it is from a defined position within the transcript, for this purpose at the 3' non-coding end of a transcript. A 9bp sequence can distinguish 262144 (4^9) transcripts. Secondly, concatenation of the short sequence ditags (when the tags have been ligated head to head) allows efficient analysis of transcripts in a serial manner by sequencing multiple tags within a single clone, ideally 10-20 tags per clone.

Clones were sequenced using the ABI373 fluorescent DNA sequencer or the ABI PRISM 310 genetic analyser (PE Biosystems). Each machine could run 48 samples per run therefore requiring 60-120 runs per sample of 3000-6000 clones for representative data.

Key: pppG^{7}m-5'-triphosphate 7 methylguanosine cap; oligo dT 5' biotin-NH $(T)_{25}$-oligonucluotide primer; RNase H enzyme to allow second strand synthesis by nick translation, b biotin; s Streptavidin Paramagnetic Particles (SA-PMPs); AE-anchoring enzyme Nla III recognizing the sequence CATG, which cleaves approximately every 2^4 (256) bp; TE-tagging enzyme BsmF1 which cuts 10/14 bp from its recognition site; pGEM 3Zf (+) sph1/CIP-the cloning vector (Promega, UK) linearized with the enzyme SpH1 and treated with calf intestinal phosphatase

The technique of SAGE uses multiple enzymatic, amplification, purification, and cloning steps. Unlike cDNA arrays, no prior knowledge of transcripts is necessary and the frequency of each tag provides quantitative expression data. SAGE can reliably detect rare transcripts but this requires the sequencing of many tags; 60,000 tags per sample for robust statistics means sequencing 3000-6000 clones.

SAGE libraries were generated from serum-starved HUVEC treated with or without 10ng/ml VEGFA (Schoenfeld et al., 2004)[*5]. Sequencing cloned ditags on a small scale (5400) identified the same most abundant endothelial transcripts for example, the receptor for activated kinase C1 (Rack1), as Affymetrix Human U95A gene-chips (Affymetrix UK Ltd, UK) but did not identify VEGF regulated transcripts. This illustrates the need for large numbers of sequenced tags, in the tens of thousands,

for each experiment. The technique required some molecular experience, a large sequencing capacity and downstream computing capacity to extract tags and convert them to transcripts.

A disadvantage for studies of human endometrium was that SAGE required 5µg mRNA whereas the nylon cDNA arrays described in chapter 2, using alpha-^{33}P deoxycytidine 5' triphosphate (α-^{33}P dCTP) labelled complex probes, required only 0.5µg mRNA or approximately 5µg total RNA.

Appendix figure 3 Axial rotation in the mouse embryo

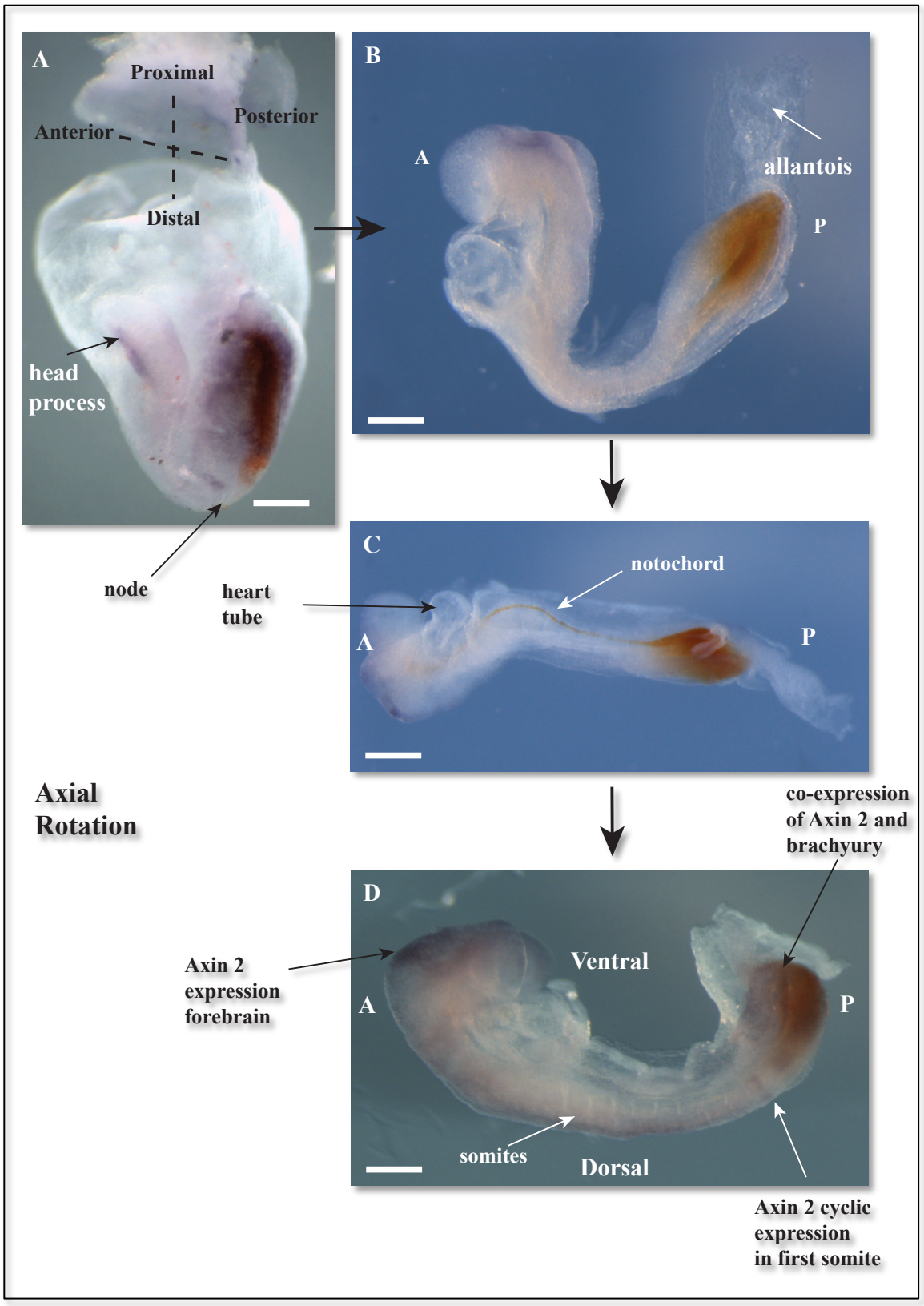

Appendix figure 3 Axial Rotation of the mouse embryo

Wildtype mouse embryo *in-situ* digoxigenin-labeled antisense mouse Brachyury detected with Mag/INT (brown) and FITC labelled antisense mouse axin 2 detected with BCIP/NBT (purple).

A 8.5 dpc unturned embryo in embryonic sac shows specific staining in the node and primitive streak for Brachyury mRNA and for Axin 2 additional head process and paraxial mesoderm staining.

B Before turning, dorsal side in concavity embryo dissected from embryonic sac

C Embryo in process of axial rotation with respect to the dorsal ventral axis, the notochord clearly visible stained with Brachyury

D 8.75 dpc turned embryo with dorsal surface in convexity and the developing heart on the ventral surface

Black bar indicates 250µm. Staining was absent in sense controls

Embryo dissection and staining by A.Evans

Appendix table 1 Mouse developmental stages

Theiler Stage	dpc (range) / Embryonic Day E	Somite No	cell number	Description
1 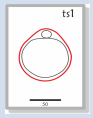	0-0.9 (0-2.5)		1	One-cell egg
2	1 (1-2.5)		2-4	Dividing egg
3	2 (1-3.5)		4-16	Morula
4 	3 (2-4)		16-40	Blastocyst, Inner cell mass ICM apparent
5	4 (3-5.5)			Blastocyst (zona-free)
6	4.5 (4-5.5)			Attachment of blastocyst, primary endoderm covers blastocoel surface of ICM
7	5 (4.5-6)			Implantation, formation of egg cylinder Ectoplacental cone appears, enlarged epiblast, primary endoderm lines mural trophectoderm
8	6 (5-6.5)			Differentiation of egg cylinder. Implantation sites 2x3mm. Ectoplacental cone region invaded by maternal blood, Reichert's membrane and proamniotic cavity form
9a 	6.5(6.257.25)			Pre-streak (PS), advanced endometrial reaction, ectoplacental cone invaded by blood, extraembryonic ectoderm, embryonic axis visible,
9b 				Early streak (ES), gastrulation starts, first evidence of mesoderm
10a 	7 (6.5-7.75)			Mid streak (MS), amniotic fold appears

Theiler Stage	dpc (range)	Somite No	cell number	Description
10b 				Late streak, no bud (LSOB), exocoelom
10c				Late streak, early bud (LSEB), allantoic bud first appears, node, amnion closing
11a	7.5 (7.25-8)			Neural plate (NP), head process developing, amnion complete
11b				Late neural plate (LNP), elongated allantoic bud
11c				Early head fold (EHF)
11d				Late head fold (LHF), foregut invagination
12a 	8 (7.5-8.75)	1-4		**1-4 somites**, allantois extends, 1st branchial arch, heart starts to form, foregut pocket visible
12b		5-7		**5-7 somites**, allantois contacts chorion at the end of TS12 **Absent** 2nd arch, >7 somites
13 	8.5 (8-9.25)	8-12		**Turning of the embryo,** 1st branchial arch has maxillary and mandibular components, 2nd arch present **Absent** 3rd branchial arch
14 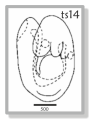	9 (8.5-9.75)	13-20		**Formation & closure of ant. neuropore**, otic pit indented but not closed, 3rd branchial arch visible **Absent** forelimb bud
15	9.5 (9-10.25)	21-29		**Formation of post. neuropore**, forelimb bud, forebrain vesicle subdivides **Absent** hindlimb bud, Rathke's pouch
16	10 (9.5-10.75)	30-34		**Posterior neuropore closes**, Formation of hindlimb & tail buds, lens plate, Rathke's pouch; the indented nasal processes start to form **Absent** thin & long tail
17	10.5 (10-11.25)	35-39		**Deep lens indentation**, brain tube, tail elongates and thins, umbilical hernia starts to form **Absent** nasal pits

Theiler Stage	dpc (range)	Somite No	cell number	Description
18	11 (10.5-11.25)	40-44		**Closure of lens vesicle**, nasal pits, cervical somites no longer visible **Absent** auditory hillocks, anterior footplate
19	11.5 (11-12.25)	45-47		**Lens vesicle completely separated from the surface epithelium**. Anterior, but no posterior, footplate. Auditory hillocks visible **Absent** retinal pigmentation and sign of fingers
20	12 (11.5-13)	48-51		**Earliest sign of fingers** (splayed-out), posterior footplate apparent, retina pigmentation apparent, tongue well-defined, brain vesicles clear **Absent** 5 rows of whiskers, indented anterior footplate
21	13 (12.5-14)	52-55		**Anterior footplate indented**, elbow and wrist identifiable, 5 rows of whiskers, umbilical hernia now clearly apparent **Absent** hair follicles, fingers separate distally
22	14 (13.5-15)	56-~ 60		**Fingers separate distally**, only indentations between digits of the posterior footplate, long bones of limbs present, hair follicles in pectoral, pelvic and trunk regions **Absent** open eyelids, hair follicles in cephalic region
23	15			**Fingers & Toes separate**, hair follicles in cephalic region but not at periphery of vibrissae, eyelids open **Absent** nail primordia, fingers 2-5 parallel
24	16			**Reposition of umbilical hernia**, eyelids closing, fingers 2-5 are parallel, nail primordia visible on toes **Absent** wrinkled skin, fingers & toes joined together
25	17			**Skin is wrinkled**, eyelids are closed, umbilical hernia is gone **Absent** ear extending over auditory meatus, long whiskers
26	18			Long whiskers, eyes barely visible through closed eyelids, ear covers auditory meatus
27 	19			Newborn Mouse
28				Postnatal development

Mouse embryos can be staged according to a variety of criteria, the most general of which are those described by Theiler in "The House Mouse: Atlas of Mouse Development" (Springer-Verlag, New York, 1989).

Embryos of the same gestational age may differ in their stage of development. Included in the table an indication of the expected range of gestational ages (days of gestation, dpc) over which each developmental stage may be found. Images are from the mouse atlas website to illustrate key stages discussed in text.

Adapted from emap edinburgh mouse atlas project.

days post coitum (dpc)/Embyonic Day E

From the mouse Atlas: The Medical Research Council and The University of Edinburgh. http://www.emouseatlas.org/

Appendix table 2 PCR primers used for quantitative RT-PCR analysis

For Chapter 6, Figure 6.6

Markers of differentiation

Primer	Type	Sequence 5' ➔3'	Amplicon bp
β actin F	Endogenous control	AGG TCA TCA CTA TTG GCA ACG A	117
β actin R	Endogenous control	CAC TTC ATG ATG GAA TTG AAT GTA GTT	
Brachyury F	Mesoderm/primitive streak	GCT TCA AGG AGC TAA CTA ACG AG	117
Brachyury R	Mesoderm/primitive streak	CCA GCA AGA AAG AGT ACA TGG C	
FOXA2F/ HNF3β	Anterior primitive streak	TAG CGG AGG CAA GAA GAC C	150
FOXA2R/ HNF3β	Anterior primitive streak	CTT AGG CCA CCT CGC TTG T	
FGF8F	Mesoderm marker	GTC CTG CCT AAA GTC ACA CAG	206
FGF8R	Mesoderm marker	CTT CCA AAA GTA TCG GTC TCC AC	
VEGFR2/KDR/FLK1	VEGF receptor	GGA CCT CAG ACT GCA AGG AG	181
VEGFR2/KDR/FLK1	VEGF receptor	TCT TGG AGG ACA GAG CCA CT	

Markers of pluripotency

Primer	Type	Sequence 5' ➔3'	Amplicon bp
CDH1 F/E-cadherin	Pluripotency marker	CAG CCT TCT TTT CGG AAG ACT	140
CDH1 R/E-cadherin	Pluripotency marker	GGT AGA CAG CTC CCT ATG ACT G	
Oct 4 F/Pou5f1	Pluripotency marker	GGC TTC AGA CTT CGC CTC C	211
Oct 4 R/Pou5f1	Pluripotency marker	AAC CTG AGG TCC ACA GTA TGC	
Zfp42F/Rex1	Pluripotency marker	CCC TCG ACA GAC TGA CCC TAA	117
Zfp42R/Rex1	Pluripotency marker	TCG GGG CTA ATC TCA CTT TCA T	

Appendix table 3 *Brachyury* targets associated with key developmental processes leading to cell migration and cell specification

Genes associated with to haematopoietic and endothelial development

*Transcripts also occur in list of *Brachyury* targets associated with cancer Appendix Table 4

Abbrvs: Endothelial cells (EC); Epithelial-mesenchymal transition (EMT); Natural killer cells (NK); Primitive streak (PS); T-cell factor (TCF); basic Leucine Zipper Domain (bZIP).

GENE	Common Name/s	Accession numbers	Gene Ontology Molecular Function/Biological Process/Expression	Related Reference
Bcl6*	B-cell leukemia lymphoma 6, Bcl5	NM_009744	BCL6-deficient mice have reduced numbers of haematopoietic progenitor cells (HPC) BCL-6 is a transcriptional repressor	(Kawamata et al., 1994)
Bmp1	Bone morphogenetic protein 1	NM_009755	Expressed in cardiomyocyes, placenta and smooth muscle	(Suzuki et al., 1996)
Capns1	calpain, small subunit 1, Capa4, Capn4	NM_009795	Embryonic lethal 11.5 dpc, cardiac developmental defects, accumulation of nucleated erythroid cells in the heart chambers, blood vessels, and developing liver.	(Fairfax et al., 2010)
Ccl1	chemokine (C-C motif) ligand 1 Scya1, Tca-3, CCR8 ligand	NM_011329	Chemotaxis, attracts blood cells, an inflammatory cytokine in developing ECs.	(Gombert et al., 2005)
Cd300e	CD300e antigen, Cd300le, Clm2, Trem5	NM_172050	Cell surface receptor expressed on myeloid cells.	(Brckalo et al., 2010)
Cebpa*	CCAAT/enhancer binding protein (C/EBP), alpha	NM_007678	CEBPA is a bZIP transcription factor expressed in myeloid cells and drives granulocytic differentiation.	(Reddy et al., 2002)
Clnk	cytokine-dependent hematopoietic cell l linker MIST		Regulation of immunoreceptor signalling in T cells, NK cells, and mast cells	(Cao et al., 1999)
DppIV*	dipeptidylpeptidase 4, CD26, THAM	NM_172256	Expressed from 7.5 dpc umbilical artery, heart and somites, regulation of cell-cell adhesion	(Broxmeyer et al., 2012)

GENE	Common Name/s	Accession numbers	Gene Ontology Molecular Function/Biological Process/Expression	Related Reference
Ebf1	early B-cell factor 1 O/E-1, Olf1	NM_007897	B cell differentiation	(Hesslein et al., 2009)
Ebf2	early B-cell factor 2, D14Ggc1e, Mmot1	NM_010095	Homozygous null mutants show decreased viability	(Rajakumari et al., 2013)
Epb4.1l 4a	erythrocyte protein band 4.1-like 4a /NBL4	NM_013512	Cytoskeletal protein involved EMT transition PS.	(Ishiguro et al., 2000)
Erg*	avian erythroblastosis virus E-26 (v-ets) E-twenty-six (ETS) related gene	NM_133659	Vascular tissue from 8 dpc, regulation of angiogenesis, interacts beta catenin and gamma catenin, self renewal of embryonic HSCs.	(Gitton et al., 2002)
Fut8	fucosyltransferase 8, alpha (1,6) fucosyltransferase	NM_016893	Required for VEGFR2 expression, regulates ECM proteins	(Wang et al., 2009)
Fyb	FYN binding protein, ADAP, FYB-120/130		7.5 dpc expressed developing HSC, adult T cells and thymus	(Hunter et al., 2000)
Gcnt2	glucosaminyl (N-acetyl) transferase 2	NM_133219	Expressed from 8 dpc allantois, blood islands, PS and mesoderm	(Inaba et al., 2003)
Il6	Interleukin 6, Interferon, beta 2	NM_031168	Acts on B-cells, T-cells, hepatocytes, HPCs, stimulates megakaryopoiesis in the bone marrow, increasing platelet numbers in circulation.	(Barnes et al., 2011)
Krt8	Card2, cytokeratin 8, EndoA, K8, Krt-2.8, Krt2-8	NM_031170	Intermediate filament protein, mice homozygous for a null allele show placental defects, impaired female fertility, abnormal haematopoiesis	(Jaquemar et al., 2003)
Lama4	laminin, alpha 4	NM_010681	7 dpc blood vessel development, cell adhesion and migration during embryonic development	(Liu and Mayne, 1996)
Laptm5 / E3*	lysosomal-associated protein transmembrane 5 Clast 6	NM_010686	Expressed 9.5d pc yolk sac and in resting mature B cells	(Seimiya et al., 2003)

GENE	Common Name/s	Accession numbers	Gene Ontology Molecular Function/Biological Process/Expression	Related Reference
Meis1*	Meis homeobox 1	NM_010789	7dpc found paraxial mesoderm, required for haematopoiesis	(Cai et al., 2012)
Pax5*	paired box gene 5, B cell-specific activator protein EBB-1 BSAP	NM_008782	Essential for B cell development.	(Busslinger and Urbanek, 1995)
Ptn	pleiotrophin, HBGF-8, heparin-binding growth factor 8,	NM_008973	Bone mineralization, cell proliferation, potent secreted regulator of HSC expansion and regeneration	(Himburg et al., 2010)
Robo4	roundabout homolog 4 (Drosophila), magic roundabout	NM_028783	Restricted HSCs and ECs, thought to counteract VEGF signalling via slit 2. Guidance molecule, localization of HSC to bone marrow niche	(Huminiecki et al., 2002)
Sema4a	semaphorin 4A Semab, SemB	NM_013658	7.5 dpc haematopoietic progenitor cells, suppresses angiogenesis	(Toyofuku et al., 2007)
Syk	spleen tyrosine kinase	NM_011518	Myeloid differentiation, positive selection of developing B cells.	(Henderson et al., 2010)
Tcl1b2	T-cell leukemia lymphoma 1B, 2	NM_013775	Participates in embryonic stem (ES)-cells proliferation and during lymphoid differentiation	(Ragone et al., 2009)
Uqcrh	ubiquinol-cytochrome c reductase hinge protein	NM_025641	From 7.5 dpc haematopoietc progenitors, also heart and skeletal muscle.	(Easterday et al., 2003)
Wasf1	WASP family 1,Scar, WAVE, WAVE-1	NM_001024 936.1	Robo 4 activation Wiskott-Aldrich Syndrome Protein Family, lack of T cells and functional B cells	(Yamazaki et al., 2003)

Appendix table 4 *Brachyury* targets associated with key developmental processes leading to cell migration and cell specification

Genes associated with EMT, migration, adhesion and left-right determination

*Transcripts also occur in *Brachyury* targets associated with cancer Appendix Table 5

** Transcript also occurs in list of *Brachyury* targets associated with hematopoietic development Appendix Table 3

Abbrvs: Epithelial-mesenchymal transition (EMT); human embryonic stem cells (hESC); protein kinase C (PKC).

GENE	Common Name/s	Accession numbers	Gene Ontology Molecular Function/Biological Process/Expression	Related Reference
B4galnt 2	beta-1,4-N-acetyl-galactosaminyl transferase 2 Dlb1	NM_008081	Down regulation of cell-cell adhesion, maybe required implantation mice.	(Li et al., 2011)
Bapx1	NK3 homeobox 2 Nkx-3.2, Nkx3-2, Bagpipe	NM_007524	9.5 dpc to adult, expressed first in the somites, marker of ventral domain sclerotome, involved left/right signalling	(Hecksher-Sorensen et al., 2004)
Cml4	camello-like 4, Nat8 N-acetyltransferase 8	NM_023455	7.5 dpc overexpression prevents gastrulation *Xenopus leavis*. Integral to membrane, negative regulation of cell adhesion	(Popsueva et al., 2001)
Ctnnb1 *	catenin (cadherin associated protein), beta 1 Catnb, Mesc	NM_007614	Homozygous null embryos show A-P axis anomalies. Part of adherens junction complex, key component of the canonical wnt pathway.	(Zhang et al., 2012)
Dlx5	distal-less homeobox 5	NM_010056	6 dpc embryonic limb development.	(Simeone et al., 1994)
Dync2li 1	dynein cytoplasmic 2 light intermediate chain 1, , D2lic, LIC3	NM_172256	7dpc cilium biogenesis, determination of left/right symmetry	(Vandenberg and Levin, 2013)
Elmod1	ELMO/CED12 domain containing 1	AK164094	GTPase activating protein interacts Rac1	(Johnson et al., 2012)
Epb4.1l 4a	erythrocyte protein band 4.1-like 4a /NBL4	NM_013512	Widely expressed component of the β catenin / TCF pathway. Involved EMT transition PS.	(Ishiguro et al., 2000)

GENE	Common Name/s	Accession numbers	Gene Ontology Molecular Function/Biological Process/Expression	Related Reference
Fgf8	Fibroblast growth factor 8 Aigf	NM_010205	Left determination. I*n vitro* hESC culture for mesoderm formation.	(Crossley and Martin, 1995)
Foxa2	forkhead box A2 Hnf-3b, HNF3-beta, Hnf3b, HNF3beta, Tcf3b	NM_010446	From 5.5 dpc visceral endoderm then PS and node, required anterior axial mesoderm and definitive endoderm.	(Ang and Rossant, 1994)
Gcnt2*	glucosaminyl (N-acetyl) transferase 2, I-branching enzyme	NM_133219	Expressed from 8 dpc allantois, blood islands, PS and mesoderm.	(Inaba et al., 2003)
Gnb2l1/ Rack1*	RACK1, receptor for activated kinase C1	NM_008143	Expressed from 10.5 dpc at least, regulates anchorage independent growth.	(Mochly-Rosen et al., 1995)
Jup	Junction plakoglobin gamma-catenin, CTNNG, ARVD12	NM_010593	Homozygous null mutants die with severe heart defects.	(Asimaki et al., 2007)
Kif23	kinesin family member 23 CHO1, MKLP1	NM_024245	Essential for cytokinesis.	(Nislow et al., 1992)
Lmx1b	LIM homeobox transcription factor 1 beta LMX1.2	NM_010725	7.5 dpc cell specification and morphogenesis particularly of dorsal limb structures	(Chen et al., 2011)
Mapre2	microtubule-associated protein, RP/EB family, member 2 EB2	NM_153058	7 dpc involved proliferation & migration of normal cells	(Tirnauer et al., 2002)
Rttn	rotatin (no turning)	NM_175542	7.5- 8.5 dpc telencephalon, mesoderm, somites, notochord 9.5 dpc forelimb bud. Failure of axial rotation in Rttn mutant	(Faisst et al., 2002)
Snai2*	snail homolog 2b (Drosophila) Slug, Slugh, Snail2	NM_011415	7.5 dpc in PS, 8dpc notochord and somites. Migration of neural crest cells, controls cardiac EMT via Notch/TGF beta-BMP pathways and represses E cadherin	(Nelson and Nusse, 2004)
Vangl1*	vang-like 1 (van gogh, Drosophila) Kitenin, Lpp2, mStbm, stbm 2	NM_177545	Cell polarity and migration, Associated neural tube defects and spina bifida	(Kibar et al., 2007)

Appendix table 5 *Brachyury* targets associated with key developmental processes leading to cell migration and cell specification

***Brachyury* targets associated with a cancer phenotype**

Many of these genes reflect similarities between cancer cell migration and the gene profile of cells involved in the cell movements of gastrulation and mesoderm formation and embryonic development.

Abbrvs: acute myeloid leukemia (AML); acute lymphoblastic leukemia (ALL); v-erb-b2 erythroblastic leukemia viral oncogene homolog (ErbB2, Her2, Neu); small-cell lung cancer (SCLC); non-small cell lung cancer (NSCLC).

GENE	Common Name	Accession numbers	Gene Ontology/Cancer Association	Related Reference
Bcl6	B-cell leukemia/lymphoma 6 Bcl5	NM_009744	BCL-6 represses lymphocyte differentiation, Diffuse large B cell lymphomas (DLBCL)	(Shaffer et al., 2000)
Cebpa	CCAAT/enhancer binding protein (C/EBP), alpha	NM_007678	CEBPA is involved in cell cycle arrest, repression of self-renewal and myeloid differentiation during normal hematopoiesis. In AML mutations in *CEBPA* result in a cellular differentiation block	(Grossmann et al., 2012)
Ctnnb1	catenin (cadherin associated protein), beta 1 Catnb; Mesc	NM_007614	Component canonical wnt pathway Considered an oncogene many cancers	(Polakis, 2000)
DppIV	dipeptidylpeptidase 4, CD26, THAM, adenosine deaminase complexing protein 2 (ADCP 2)	NM_010074	Expressed in many kinds of human malignancy, including mesothelioma, renal cell carcinoma, and T cell leukemia/lymphoma	(Masur et al., 2006)
Erg	E-twenty-six (ETS) related gene	NM_133659	ERG deregulation associated prostate cancer and rare myeloid and lymphoid leukemias.	(Narod et al., 2008)
Gm879	Gene model 879, Shisa 6 homolog 6(Xenopus laevis)	NM_001034874	p53 inducible gene, pro-apoptotic and possible anti cancer target	(Furushima et al., 2007)
Gnb2l1/ RACK1	RACK1 receptor for activated kinase C1	NM_008143	Localized to the endothelium of tumor neovascularization. *In vivo* associated with angiogenesis and carcinoma.	(Berns et al., 2000)

GENE	Common Name	Accession numbers	Gene Ontology/Cancer Association	Related Reference
Junb	Jun-B oncogene/AP-1 activator protein 1		Limits HSC proliferation and differentiation, reduced expression metastatic prostate cancer.	(Santaguida et al., 2009)
Laptm5 /E3	lysosomal-associated protein transmembrane 5 Retinoic acid-inducible E3	NM_010686	Transmembrane receptor associated with lysosomes, hematopoietic cell-specific transcript induced by retinoic acid, loss is a key event multiple myeloma	(Hayami et al., 2003)
Map2k 5	mitogen activated protein kinase kinase 5, MEK5 MAPK/ERK kinase 5, Mapkk5,	NM_011840	Homozygous mutants die at 10.5 dpc and exhibit abnormal cardiac development, MEK5 overexpression is associated with metastatic prostate cancer.	(Mehta et al., 2003)
Meis1	Meis homeobox 1	NM_010789	From 7 dpc paraxial mesoderm, required for haematopoiesis transcriptional regulation Pax 6 acute myeloid leukemia AML and ALL	(Argiropoulos et al., 2007)
Mov10	Moloney leukemia virus 10	NM_008619	Involved polycomb repression of INK4a tumour suppressor.	(El Messaoudi-Aubert et al., 2010)
Ovgp1	oviductal glycoprotein 1, Chit5, MOGP, MUC 9, OGP, Ovgp1, oviductin	NM_007696	Overexpressed human endometrial hyperplasia and associated with ovarian cancer.	(Maines-Bandiera et al., 2010)
Pax2	paired box gene 2	NM_011037	Mediator of ER repression of erbB2 by the anti-cancer drug tamoxifen, loss is associated with endometrial adenocarcinoma	(Silberstein et al., 2002)
Pax5	paired box gene 5, B cell-specific activator protein EBB-1 BSAP	NM_008782	Deregulated expression in many cancers specifically SCLC. Pax 5 expression correlates with increasing malignancy in human astrocytomas.	(Kanteti et al., 2009)

GENE	Common Name	Accession numbers	Gene Ontology/Cancer Association	Related Reference
Snai2	snail homologmeis1 2b (Drosophila) Slug, Slugh, Snail2	NM_011415	EMT associated cancer metastasis, and induction of Snail2 is essential for Twist 1 to induce EMT by E- cadherin down regulation	(Chakrabarti et al., 2012)
Stmn1	stathmin 1 19K, Lag, Lap18, leukemia associated phosphoprotein p18, metablastin,	NM_019641	Involved EC differentiation and angiogenesis, high expression in leukemic cells and B cells. Prognostic marker associated colorectal cancer metastasis	(Karst et al., 2011)
Trim28	tripartite motif protein 28, KAP-1, KRIP-1, Tif1b	NM_011588	DNA binding and regulation of transcription, transcriptional co-repressor, involved EMT	(Fitzgerald et al., 2013)
Vangl1	vang-like 1 (van gogh, Drosophila) KITENIN, Lpp2, mStbm, stbm 2	NM_177545	Cell polarity and migration, associated with breast cancer progression	(Anastas et al., 2012)
Wt1	wilms tumor (Nephroblastoma) homolog	NM_144783	WT protein required for embryonic development, implicated hematologic disorders. Co-expressed with pax2 in breast cancer, associated leukemia and solid tumours	(Silberstein et al., 2002)

Appendix table 6 Notable/putative *Brachyury* target genes just outside statistical significance using the whitehead error model

When triplicate chIP arrays are analysed these genes were just outside the strictest criteria but called as bound when arrays are analysed individually (combined p values are very close to the p values set of < 0.01 for central bound probes to < 0.05 for the neighbouring probe. Of particular note are VEGF, BMP4, FLI-1 and Notch1. Using either chIP Analytics software (Agilent Technologies) or direct plotting from the data all these genes showed evidence of being genuine mouse T targets.

Abbrvs: Acute lymphoblastic leukaemia (ALL); anterior-posterior axis (A-P axis); β catenin (ctnnb1); Extracellular matrix (ECM); epithelial-mesenchymal transition (EMT); E-twenty six (ETS); Natural Killer (NK).

GENE	Common Name/s	Gene Ontology/Expression	Reference
Bmp4	Bone Morphogenetic Protein 4	Morphogen for mesoderm induction, expressed before *Brachyury*	(Winnier et al., 1995)
Dll1	Delta-like 1 (Drosophila)	Notch Ligand, cell-cell communication 7-7.5dpc paraxial mesoderm and somites	(Bettenhausen et al., 1995)
Fgfbp1	Fibroblast Growth Factor Binding Protein 1	Associated adenocarcinoma, cell proliferation, enhances Fgf signalling.	(Czubayko et al., 1997)
Fgfr2	Fibroblast Growth Factor Receptor 2, Bek	Receptor for fgf, implicated breast and endometrial cancer	(Ingersoll et al., 2001)
Fli1	Friend leukaemia integration 1 EWSR2, Fli-1, Sic1	Transcriptional activator, required for myeloid differentiation, ALL associated	(Watson et al., 1992)
Hhex	homeobox, haematopoietically expressed	Transcriptional repressor expressed specific haematopoietic lineages B Cells and myleloid cells	(Bedford et al., 1993)
Lef1	Lymphoid Enhancer Binding Factor 1, TCF1α	Activation of transcription with ctnnb1 in wnt pathway (Figure 3A Evans et al [*12]), overexpressed colon cancer	(Hovanes et al., 2001)
Notch1	Notch gene homolog1 (Drosophila)	Receptor for jagged and delta. Left-right patterning and haematopoietic differentiation	(Bigas et al., 2010)
Vegfa	Vascular Endothelial Growth Factor A	Vascular growth factor and mitogen (see Chapter 1)	(Ferrara and Davis-Smyth, 1997)

Ethics

The endometrial explant study was approved by: The Cambridge Local Regions Ethics Committee and, written informed consent was obtained from all patients.

Mouse embryo experiments were carried out under the licence awarded to Professor James Smith then director of the Gurdon Institute, Cambridge. The same applies to the Xenopus and Zebrafish experiments.

Cord blood and peripheral blood collections at the NHSBT, Cambridge were approved by the Cambridgeshire 4 Research Ethics Committee. REC ref no 07/MRE5/44 under the title: The causes of clonal blood cell disorders held by Professor Tony Green, Head, Department of Haematology, Level 6, CIMR, Cambridge, CB2 2XY.

Publications

PUBLICATION 1

Evans, A. L., Sharkey, A. S., Saidi, S. A., Print, C. G., Catalano, R. D., Smith,S. K. & Charnock-Jones, D. S. 2003. Generation and use of a tailored gene array to investigate vascular biology. *Angiogenesis,* 6**,** 93-104.

Cited by 17, Impact Factor 6.063

ISSN: 0969-6970

Journal Type

Angiogenesis is an international peer-reviewed journal devoted to the publication of original articles and reviews on the cellular and molecular mechanisms that regulate angiogenesis in physiological and pathological conditions. This journal publishes innovative experimental studies using molecular, in vitro, animal model systems and clinical investigations of angiogenic diseases. Angiogenesis also reports on novel therapeutic approaches for promoting or inhibiting angiogenesis as well as new markers and techniques for disease diagnosis and prognosis.

Personal Contribution

This was the first paper to which I contributed the majority of writing and experimental work. When I joined this project there were about half of the final set of clones already obtained from the IMAGE consortium but none had been sequenced. I sequenced each clone using a capillary ABI system, amplified the DNA by PCR followed by printing and processing of the arrays. In the region of 1500 arrays were printed. The bioinformatics expert was Dr. Sam Saidi who was very helpful in teaching me the details of analysis. All the authors were involved in the decision making about gene choice.

PhD Students who benefited from these microarrays

Dr Catherine Holland (Holland et al., 2004)[*5], now a clinical senior lecturer in gynaecological oncology at Manchester University, Dr. Reija Valtola (Print et al., 2004)[*6], and Dr Samir A Saidi (Saidi et al., 2004) now a gynaecological oncology consultant for BUPA® in Spire Leeds Hospital. Also indirectly as a result of array data generated: Dr Norfilza Mohd Mokhtar (Mokhtar et al., 2010) now at the National University of Malaysia Department of Physiology, and Dr. Tanweer Omer Beleil who has since returned to the Sudan.

Angiogenesis **6**: 93–104, 2003.

Review

Generation and use of a tailored gene array to investigate vascular biology

Amanda L. Evans[1,2], Andrew S. Sharkey[1,2,*], Samir A. Saidi[1,3,*], Cristin G. Print[1,2,*], Roberto D. Catalano[1,2], Stephen K. Smith[1,3] & D. Stephen Charnock-Jones[1,3]

[1]*Reproductive Molecular Research Group,* [2]*Department of Pathology, University of Cambridge, Tennis Court Rd, Cambridge, UK;* [3]*Department of Obstetrics and Gynaecology, The Rosie Hospital, Robinson Way, Cambridge, UK*

Received 2 April 2003; accepted in revised form 4 June 2003

Key words: angiogenesis, array, HUVEC, normalisation, transcript

Abstract

Vasculogenesis, angiogenesis and vascular remodelling are complex processes where the fate of several cell types is determined by different signalling networks. Many of these networks ultimately function by changing the abundance of RNA transcripts within the cells which constitute blood vessel walls. Researchers can now map these transcript abundance changes using gene array technology. In this review, we describe the design, production and use of a gene array specifically tailored to investigate vascular biology. We describe the advantages of tailored gene arrays, and give detailed protocols based on our experience to allow the reader to use such gene arrays to generate meaningful data. We list the issues to consider when choosing and verifying the genes and splice variants included in an array, and describe our use of *Arabidopsis* sp. RNA spikes for quality control. We present data that illustrates the absolute necessity for both technical and biological replicates to be incorporated in the design of gene array experiments using primary cells such as HUVECS. Finally, we describe methods for the normalisation and interpretation of the data that gene arrays produce. The approach to gene array technology described here is easily within reach of the budget and expertise of most academic research groups.

Abbreviations: QC – quality control; HUVEC – human umbilical vein endothelial cells; PCR – polymerase chain reaction

Introduction

The recent development of DNA array technology has substantially altered the conduct of angiogenesis research. This technology allows the abundance of a large number of transcripts within complex RNA populations to be determined simultaneously. For the first time this offers researchers the prospect of understanding the subtle interactions between multiple genes that may underlie complex cellular behaviours. For example, vasculogenesis, angiogenesis and vascular remodelling are complex processes involving interaction between several cell types within and outside the vessel wall [1–3]. We are using gene arrays to determine the transcript abundance regulation that underlies these processes.

Gene arrays come in two main types: large generic arrays and small tailored arrays. Large generic gene arrays, are available commercially or by collaboration with dedicated gene array laboratories. One well established large generic technology is the Affymetrix Genechip system (Affymetrix Inc. Santa Clara, California, USA, http://www.affymetrix.com) [4] in which two-dimensional arrays of synthetic oligonucleotides are synthesised using a combination of photolithography and solid phase DNA synthesis [5, 6]. Affymetrix gene chips allow thousands of transcripts to be analysed in a single hybridisation, and are ideal for experiments in which researchers wish to search for unexpectedly regulated genes. While we, and others have shown that this approach can be extremely informative for angiogenesis research [7], it is inappropriate for many experimental designs. Commercial generic arrays are expensive and academically produced generic arrays of limited availability. Therefore, generic gene arrays may be impractical when a large number of experimental replicates are required. In addition, the genes included in most generic arrays are inflexible, and frequently omit genes and splice variants of interest. An alternative approach is for individual research laboratories to construct relatively small tailored gene arrays focussed on their specific research interests. These have the advantage of low cost, which allows researchers to

*Authors contributed equally to the work described in this publication.

Correspondence to: Dr Stephen Charnock-Jones, Reproductive Molecular Research Group, Department of Obstetrics and Gynaecology, The Rosie Hospital, Cambridge, CB2 2SW, UK. Tel: +44-1223-336875; Fax: +44-1223-215327; E-mail: dscj1@cam.ac.uk

perform sufficient replicates to maximise experimental power. In addition, tailored gene arrays encourage researchers to perform well planned, hypothesis driven experiments investigating a focused set of transcripts. New genes and splice variants can be added whenever required, and detailed quality control (QC) performed.

Small tailored gene arrays also offer the option to use radioactively labelled complex cDNA probes. These have been used successfully since 1983 [8], and require as little as 3–5 μg of total RNA. In contrast most fluorescent labelling techniques require 20–50 μg of total RNA [9]. Although cDNA amplification methods such as the SMART™ system (BD Biosciences, Clontech, Oxford, UK) allow fluorescent arrays to be used with small amounts of starting material, they are yet to gain wide acceptance due to concerns about linearity and representation. The ability to use small amounts of starting material is essential for many studies involving angiogenesis. In the female reproductive tract for example, only small samples of tissue or cells are available from biopsies.

To perform studies requiring multiple replicates with limited amounts of RNA, at reasonable cost, we have designed and produced a tailored gene array focused on the processes involved in vascular biology (endothelial and smooth muscle cell proliferation, apoptosis, migration, differentiation, activation and morphogenesis). This tailored array currently comprises 988 unique cDNAs (1171 total cDNAs including controls and multiple sequences from some genes) generated by PCR and spotted in duplicate onto a nylon membrane. These membranes are hybridised with ^{33}P-labelled complex cDNA probes derived from 5 μg of total cellular RNA. We have validated the production, hybridisation and analysis steps required to utilise this tool (Figures 1a, b). This approach brings the ability to monitor the abundance of hundreds of transcripts within reach of any academic research group. The aim of this review is to promote the use of gene arrays by vascular biologists who have no previous genomics experience. Therefore, we will describe the gene array methods developed in our laboratory in simple terms, but we will provide sufficient detail to allow our methods to be easily replicated.

Clone selection and verification

The array method described here is based on spotting cDNA fragments generated by PCR onto nylon membranes. The selection of the cDNA fragment to be amplified is a crucial step, since fragments must show little or no homology to other genes. For closely related gene families (such as the VEGF family), we have generated specific fragments which can distinguish family members [10, 11], but for most genes we have obtained appropriate fragments from the IMAGE consortium (http://www.hgmp.mrc.ac.uk). Ideally, cDNA fragments should be relatively short (0.6–2 kb). The inclusion of 3′ non-coding regions often allows discrimination between related transcripts that share close homology within their coding regions. Careful attention was also given to selection of cDNAs that would hybridise either to every splice variant of a transcript, or to individual splice variants of interest. We have found that web-based software provided by Compugen (http://www-labonweb.com/) is helpful to predict splice variants. The 988 cDNAs chosen for the array were selected to include the molecular pathways believed to be important in vascular biology. These include cell adhesion, apoptosis, signalling, cell cycle regulation, extracellular matrix remodelling and angiogenesis. The entire list can be seen at http://www.obgyn.cam.ac.uk/genearray. A significant proportion of the clones held by the IMAGE consortium have been miss-assigned therefore, all the clones included on the array have been validated by re-sequencing.

Generation of PCR products

Amplification of cDNA clones requires a robust protocol to amplify hundreds of different inserts of varying sizes using a universal primer set (see Protocol 1). A variety of PCR conditions and enzymes were tested to optimise the yield of PCR product in a 96 well format (Figure 2). Biotaq DNA polymerase (Bioline, London, UK) consistently generated the most PCR product at the lowest cost. Randomly chosen wells from each plate were checked on 1.2% agarose gels (Figure 1a, Protocol 2); the results forming part of the QC information for each batch of arrays. In order to produce enough purified cDNA to print a large batch of nylon membranes (approx. 600), with sufficient cDNA to achieve satisfactory sensitivity, approximately 40–50 μg of each purified PCR product was prepared in 100 μl of water. Eight PCR reactions each of 50 μl were sufficient to provide this amount from each clone. The PCR products were pooled, purified and concentrated using the Millipore Multiscreen 96 system (Millipore, Watford, UK) with a vacuum manifold as described in Protocol 2.

Quantification of PCR products prior to spotting

PCR products were quantified with SYBR® Green I (Sigma, Poole, UK), an ultrasensitive stain for double stranded DNA. This method uses Blue Fluorescence Imaging on a Molecular Dynamics (Buckinghamshire, UK) Storm 860® Phosphoimager and required only 2 μl of each product [see protocol 2]. This method was rapid and contributed to the archive of QC data relating to each batch of nylon membranes. The concentration of each cDNA product was adjusted to approximately 400 μg/ml to ensure even spotting.

Printing of nylon membranes

Contact printing was carried out using a BioRobotics MicroGrid robot (BioRobotics Inc., a subsidiary of

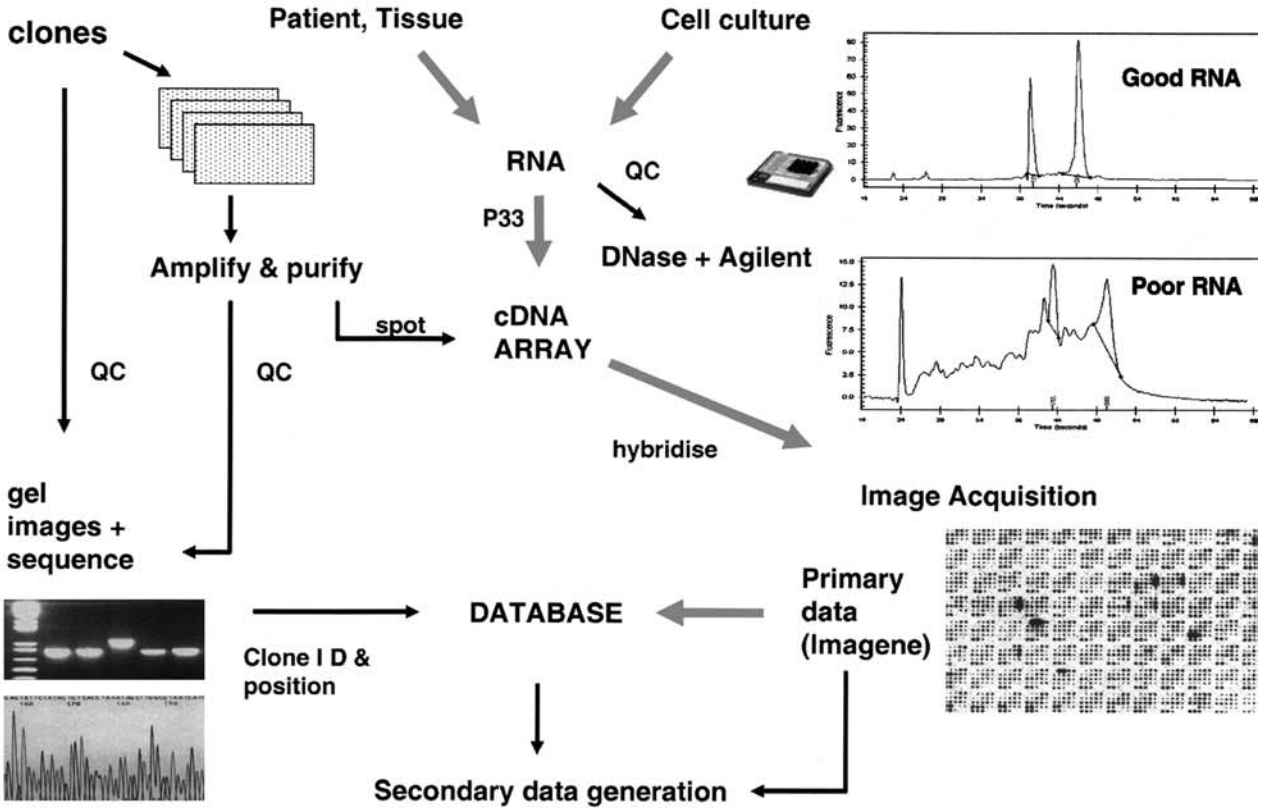

(a)

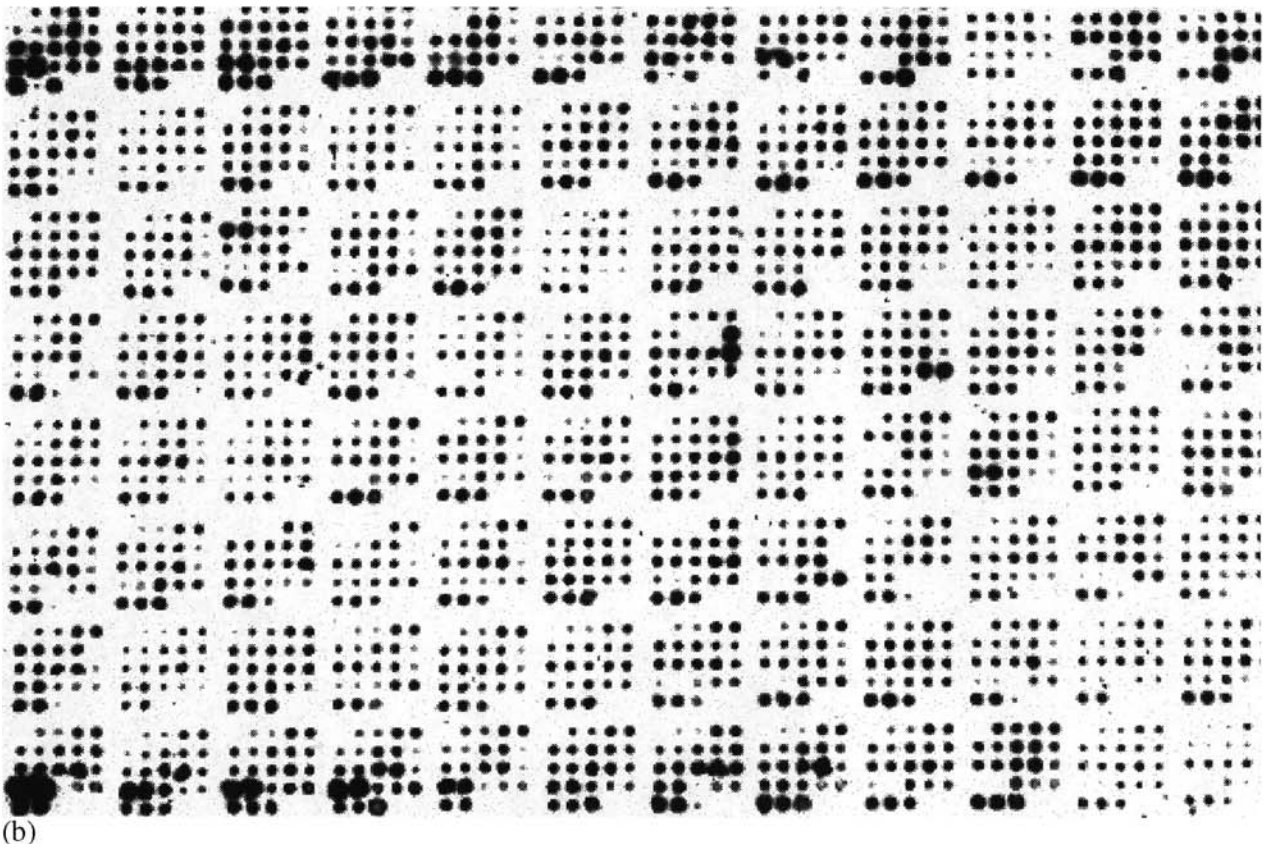

(b)

Figure 1. (a) Production and use of the angiogenesis array, (b) array image produced by probing with radiolabelled cDNA produced from 5 μg total human secretory phase endometrium RNA.

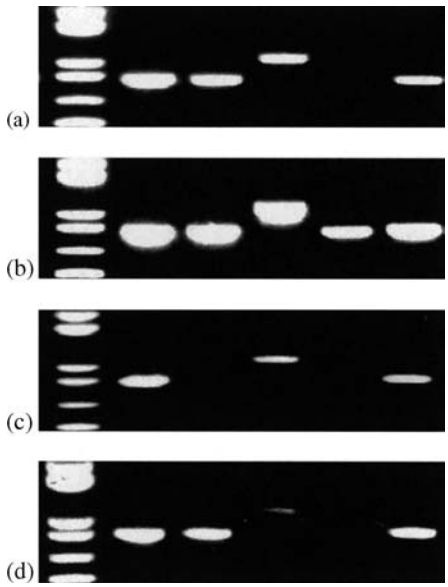

Figure 2. Testing DNA polymerases for efficiency of amplification. PCR amplification of five IMAGE clones carried out under identical conditions, using four different polymerises using the protocol described in protocol 1. Bioline taq DNA polymerase gave consistently the best yield. (a) YieldAce® Stratagene 2.5 U/reaction, (b) Biotaq® Bioline 1.25 U/reaction, (c) ABgene 2 × Master Mix 1.25 U/reaction, (d) Promega 2 × Master Mix 1.25 U/reaction.

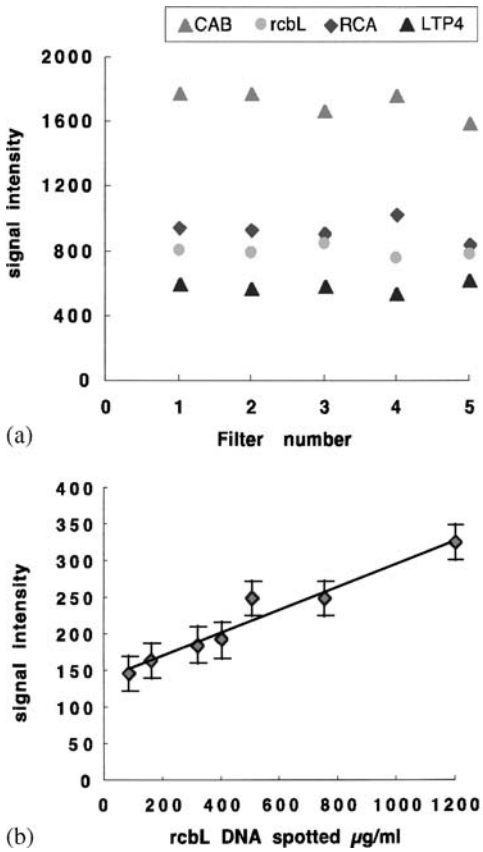

Figure 3. (a) Reliable detection of *Arabidopsis* sp. RNAs. Radiolabelled cDNA was produced from five separate aliquots of 5 μg human placental RNA. Prior to labelling each was spiked with *Arabidopsis* sp., RNA (500 pg to 1 pg as protocol 3). Following hybridisation, image analysis and normalisation the means of each spike duplicate across the five membranes was plotted. The low coefficients of variance for each spike RNA indicates close agreement between the five hybridisations.

	coefficient of variance
Spike 1 CAB Chlorophyll a/b binding protein	0.056
Spike 2 RCA RUBISCO activase	0.078
Spike 3 rbcL Ribulose-1 -5-biphosphate carboxylase/ oxygenase	0.050
Spike 4 LTP4 lipid transfer protein	0.057
Spike 5 LTP6 lipid transfer protein (not shown)	0.046.

(b) Linearity of signal intensity to the amount of DNA spotted is maintained after reverse transcription. rbcL ribulose-1-5-biphosphate carboxylase/oxygenase dilution series of DNA spotted in addition to the set of *Arabidopsis* sp. in 3a, each point is the mean signal intensity of 10 spots. Five membranes were hybridised to a radiolabelled mix of 50 pg rbcL RNA spiked into 5 μg human placental RNA. Errors ± 1 SE.

Apogent Discoveries, Hudson, New Hampshire, USA) and a 96 pin tool to create a 12 × 8 metagrid, 5 × 5 subgrid matrix yielding a theoretical maximum of 25 × 96 (2400) individual spots (Figure 1b). The purified PCR products were spotted in water in duplicate onto pre-cut (12 × 8 cm) Hybond N^+ (Amersham Pharmacia Biotech UK Limited, Buckinghamshire, UK). Each spot was printed with two strikes of a 0.4 mm diameter solid pin. and contained approximately 14 ng of DNA product. After printing, the membranes were air dried, soaked in a denaturing solution (0.5 M NaOH, 1.5 M NaCl for 10 min at room temp.), neutralised (0.5 M Tris pH 7.4, 1.5 M NaCl for 4 min at room temp.), air dried, cross linked (70,000 $\mu J/cm^{-2}$) using a Stratalinker® UV Crosslinker model 1800 (Stratagene, La Jolla, California, USA) and stored dry at room temperature. This protocol is superior to either baking or air drying [12].

Validation and sensitivity

To enable QC and validation of the hybridisation we have incorporated several controls into the design of the array. These comprised:

(i) negative controls, (i.e. target DNAs that should not hybridise to complex cDNA generated from total RNA) such as salmon sperm DNA. Poly dA(40–60), and human Cot-1 DNA (enriched with Alu and Kpn repeats, [13]) were also spotted to confirm that hybridisation to these sequences was efficiently blocked by the prehybridisation step.

(ii) targets which may be used as normalisation controls (β-actin, cyclophilin, 18S ribosomal RNA, hypoxanthine ribosyl transferase, glyceraldehyde-3-phosphate dehydrogenase, ubiquitin and histidyl tRNA synthetase). This enable a suitable endogenous control to be chosen for subsequent real-time PCR confirmation of transcript abundance changes.

(iii) Exogenous cDNA clones from Stratagene's Spot Report® Exogenous Array Validation System (Stratagene, California, USA). These cDNAs from *Arabidopsis*

thaliana show no cross-hybridisation to human sequences. They provide a convenient method to monitor interarray variability and the sensitivity of the arrays. For example known amounts of cRNA corresponding to each of the spot report cDNAs were 'spiked' into five separate 5 μg aliquots of the same placental total RNA. The amounts of each spike RNA used are shown in Protocol 3. The spiked total RNA samples were then labelled and hybridised to five separate arrays. Following image analysis and normalisation, the mean intensity of the cDNA spots corresponding to each of the spikes was determined (Figure 3). As expected the CAB RNA, which was added at 500 pg, gave the strongest signal. The results for each spike exhibited low coefficients of variance (Figure 3) indicating reliable detection of these RNAs in the placental RNA sample. We were also able to determine the sensitivity of the arrays using this data. By depositing 14 ng cDNA per spot on the membrane we were able to detect 10 pg of mRNA (LTP4) at a signal intensity five times above background. Thus we are able to detect transcripts at an abundance of approximately 0.01% with good consistency.

RNA preparation and QC

High quality RNA is essential for efficient labelling and optimal hybridisation. Several issues need to be considered: labelling of degraded RNA or RNA contaminated with protein or carbohydrate will be variable, producing misleading results. In addition, contaminating genomic DNA may increase the background signal and therefore should be eliminated. Finally, when limited amounts of tissue or cells are available, the method chosen should produce a high RNA yield [14]. Of a wide variety of methods tested, Trizol® (Gibco, Life Technologies, Paisley, UK) produced the highest yield with acceptable purity. After isolation, all RNAs are treated with DNAse (using DNase I at 8 units/100 μl RNA for 30 min at 37 °C, Ambion, Inc., Texas, USA), followed by a further Trizol® extraction. Samples were checked for genomic DNA contamination by PCR using primers for the Histydyl tRNA Synthase gene (forward 5′ CCGCAGGTCGAGACAGC 3′, reverse 5′ TCATCAGGACCCAGCTGTGC 3′; 94 °C 4 min (1 cycle); 94 °C 30 s, 65 °C 30 s, 72 °C 30 s (30 cycles); 72 °C 3 min (1 cycle)). PCR products of 186 and 270 bp are produced from cDNA and genomic DNA respectively. The integrity and purity of the RNA are determined using an Agilent Technologies 2100 Bioanalyser, (Agilent technologies UK Limited, Cheshire, UK). This instrument gives detailed information about RNA quality and quantity and requires only a 50–500 ng of sample. Inspection of the electrophoretograms produced reveals any RNA degradation or genomic DNA contamination present in the samples and ensures that only high quality RNAs are labelled (Figure 1a).

Production of labelled cDNA from total RNA samples

Reverse transcription is used to produce cDNA from total cellular RNA (5 μg) labelled to high specific activity with ^{33}P-dCTP (Amersham PLC, Amersham, UK). To minimise non-specific priming the reaction is performed at 48 °C with an anchored Oligo d(T) primer using the EndoFree Reverse Transcriptase (RT)™ system (Ambion®, Texas, USA). EndoFree RT produces greater signal intensities and better sensitivity compared to Superscript™ II RT (Gibco, Life Technologies, Paisley, UK) [15]. Residual RNA is removed and the probes purified using NICK columns (Amersham Pharmacia Biotech) [Protocol 3]. Incorporation is checked using a scintillation counter (Tri-Carb1600Tr Liquid Scintillation Analyser Packard Instrument Company, Connecticut, USA).

Hybridisation

We have tested a number of different buffers and hybridisation conditions. The best results were obtained using ExpressHyb© Hybridisation Solution (BD Biosciences Clontech, USA) (Figure 1b). Membranes are hybridised in 15 cm × 4 cm roller bottles in a Hybridisation Oven (Hybaid Limited, Middlesex, UK) enabling continual mixing in a small volume. Both prehybridisation and hybridisation buffer include non-specific blocking agents [Protocol 4]. Stripping and re-use of membranes has been suggested as a way to reduce costs [16]; however, this can lead to loss of signal. We have not tested the performance of stripped membranes. We recommend drying the membranes by baking at 60 °C for 1 h prior to exposure to phosphor screens [Protocol 4].

Image processing and primary data acquisition

Membranes are exposed to Low Energy Storage Phosphor Screens (Amersham Pharmacia Biotech UK Limited, Buckinghamshire, UK) optimised for use with ^{33}P, and scanned at high resolution (50 μm) using a Molecular Dynamics Storm® 860 Phosphoimager (Molecular Dynamics Inc, California, USA). Images are then transferred directly to IMAGENE 5® (BioDiscovery, California, USA) software, which provides sophisticated tools for spot finding, quantitation and data export.

Linearity

Image generation and data acquisition are complex repetitive tasks and therefore software automation to assist in this progress is advantageous. However, this leads to many of the underlying processes and data manipulations being hidden from the user. Along with others [17], we have found that scanner and phosphorimager software compress the data using non-linear

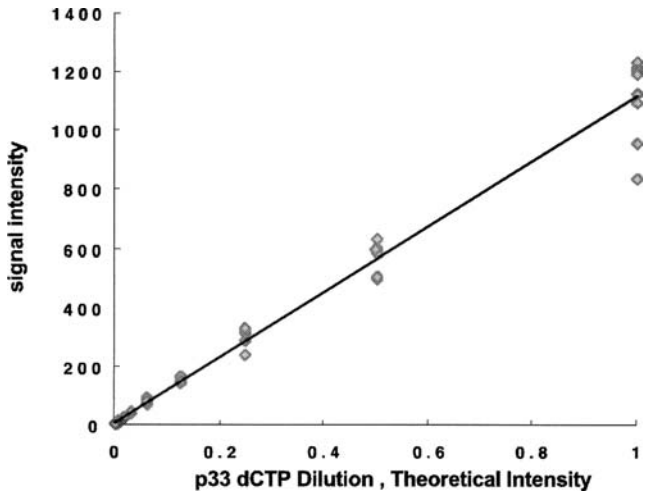

Figure 4. Validation of phosphorimager and image analysis software compatability. A 2 fold dilution series of ^{33}P-dCTP from 1×10^{-3} μCi/μl to 4×10^{-6} μCi/μl was produced. Eight spots of 1 μl of each dilution were manually deposited onto a nylon membrane, which was exposed to a phosphor screen for 48 h and the mean signal intensity for each spot determined. These values were plotted against the theoretical ^{33}P-dCTP dilution. The combination of Imagequant 4 and Imagene 5.1 produced the expected linear response indicating correct image processing.

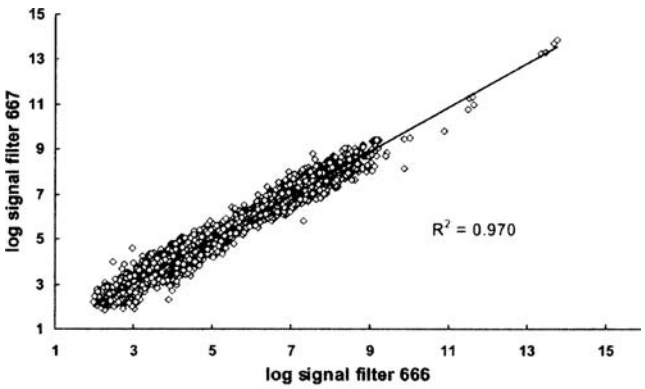

Filter	663	664	665	666	667
663	1.000	0.979	0.970	0.978	0.983
664	0.979	1.000	0.979	0.982	0.980
665	0.970	0.979	1.000	0.980	0.980
666	0.978	0.982	0.980	1.000	0.985
667	0.983	0.980	0.980	0.985	1.000

Figure 5. Determination of Inter-array variability. Five aliquots of the same human placental RNA were labelled and hybridised to five membranes. Inter-array variability was assessed using scatter plots of mean signal intensity for each membrane against any other, as presented above for filters 666 and 667, for all filter combinations. There is a high degree of correlation.

transformations (e.g. square-root) and that some image processing software packages do not correct for this. This can introduce catastrophic artefacts into the data and so is a serious concern. We strongly recommend that the performance of the phosphorimager and image analysis software are validated. To do this we produced an artificial 'array' by manually spotting 2-fold serial dilutions of ^{33}P-dCTP onto a nylon membrane. Each dilution was spotted eight times. The mean signal intensity for each set of eight spots was determined and showed a direct relationship with the dilution factor.

The combination of Molecular Dynamics Storm® 860 Phosphorimager and ImageQuant 4 or Imagene 5.1 faithfully replicated the serial dilution curves of the input ^{33}P-dCTP (Figure 4). We found other image analysis software packages for which this was not the case.

Reproducibility and technical replication

Gene arrays are of little use if the data they produce is so noisy that only very large changes in transcript abundance can be detected above the noise. To reduce the effects of noise, each cDNA represented on the array is spotted in duplicate. In addition, for a small subset of genes, multiple cDNA sequences from distinct regions of the gene are spotted. When five aliquots of the same placental RNA were labelled and hybridised to five different arrays we found that less than 4% of the duplicates on each array differed by >50% (Table 1, Intra-array variability).

To determine inter-array variability, each membrane was compared to the other four. When the mean log signal intensity for each spot in an array is plotted against the results of another array as shown in Figure 5, regression coefficients were close to 1, indicating a close positive correlation. Figure 6 shows that the percentage of array elements in each pairwise comparison of these membranes (technical replicates) which appear to be regulated up or down by more than 2-fold. These 'apparent' changes (given that the same RNA was used for all experiments) represent false positive rates due to technical 'noise' and ranged between 0.5% and 5.0%. Combined with the data presented in Figure 5, this demonstrates that our tailored array is reproducible. However, averaging the results of two or more arrays (technical replication) reduces the impact of chance or technical differences between arrays.

Table 1. Intra – array variability within each of the arrays in Figure 5 less than 4% of the duplicated spots differed by greater than 50%.

Filter	Percentage of duplicates with errors >50%
663	2.9
664	3.3
665	2.4
666	1.8
667	3.1

Biological replicates

There is considerable variation in the behaviour of individual isolates of human umbilical vein endothelial cells (HUVEC) ([18] and our unpublished Affymetrix data). This is also likely to be true of other primary cells.

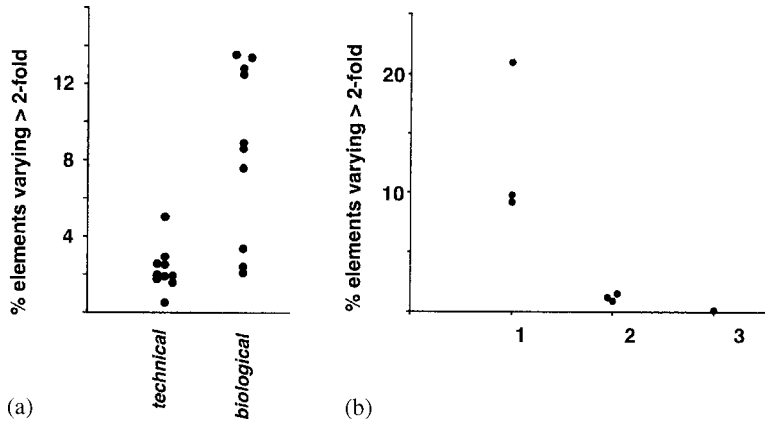

Figure 6. (a) Comparing of the degree of technical and biological variation evident when using our tailored gene arrays, 'technical' designates technical variation, where complex probes were prepared from a single RNA and hybridised to five separate filters. For each possible combination of any two filters, the % of array elements which varied >2-fold (up or down) is shown, *'biological'* designates biological variation, where RNA was isolated from five separate primary HUVEC cultures each collected from a different individual. Radiolabelled cDNAs prepared from each separate RNA were hybridised to five separate filters. For each possible combination of any two filters, the percentage of array elements which varied >2-fold (up or down) is shown. (b) Biological replicates are essential to reduce the incidence of false-positive results. HUVEC from 3 separate individuals were cultured for 24 h in the presence or absence of a low concentration of growth factor, which had no statistically significant effect on transcript abundance in these cells. RNAs were prepared from these cultures and used to generate radiolabelled cDNAs that were hybridised to filters. Averaging the results of any two or all three biological replicates reduced the % of false positives' (array elements that appeared to be regulated >2-fold (up or down) due to the idiosyncratic properties of a single HUVEC culture or due to chance).

Therefore, experiments using primary cells from a single individual donor may reveal idiosyncratic results that cannot be generalised. To illustrate this problem, we prepared RNA from HUVEC obtained from five different individuals. Labelled cDNA was generated from these RNAs and hybridised to our arrays. Pairwise comparisons between the different patients were performed. The percentage of array elements that appear to be regulated by more than 2-fold (up or down) between any two of these 'biological replicates' ranges between 2% and 13.5% (Figure 6a). Since no treatment has been applied to the HUVEC cultures used in this experiment, these differences represent genetic differences, as well as technical differences between cultures or hybridisations. There is approximately five times more variation between biological replicates (where labelled cDNAs are generated from cells from different individuals) than there is between technical replicates (where separate labelled cDNAs are generated from a single RNA).

To demonstrate the importance of biological replicates in a real experiment, HUVEC isolated from three individuals (three biological replicates) were treated with a low dose of a growth factor, and RNA collected after 24 h. Hybridisation of these RNAs to our tailored arrays showed that none of the 998 genes present on our array were regulated significantly in the cells derived from all three individuals. This was confrimed using Affymetrix genechips. However, if the experiment had been conducted only once using HUVECs donated by any one of the three individuals, we would have been mislead into concluding that a significant percentage of the transcripts interrogated by the arrays were regulated in response to the growth factor (Figure 6b, x-axis = 1). When the results for any two biological replicate experiments were averaged, the number of apparently regulated transcripts is substantially reduced (Figure 6b, x-axis = 2). Averaging all three biological replicate experiments further reduced the number of 'false positives' to zero (Figure 6b, x-axis = 3). Therefore, we believe that two, and preferably three or more biological replicates is essential for any gene array experiment. This is particularly true of experiments in which primary cell cultures or tissues from different individuals are used.

When planning complex experiments, a critical consideration is the number of replicates required, to ensure sufficient statistical power to distinguish between genuinely regulated genes and false positive results, due to biological variation [19]. Additionally, randomising the order of tissues (or operators) during the hybridisation process is fundamental to minimising bias [20].

Data normalisation and analysis

One of the biggest problems in extracting biologically relevant data from gene array experiments is making valid comparisons between arrays. Numerous factors influence the signal generated for any particular spot. Some of these relate to the specimen quality (protein contamination, RNA degradation), others to array quality and image processing (spotting efficiency signal quantification, and 'background' correction). Finally there is variation due to reverse transcription efficiency, hybridisation specificity and most importantly the specific activity of labelled RNA.

To obtain meaningful comparisons between data sets it is necessary to make some mathematical adjustment to the data. Although this is commonly termed normalisation, scaling is more often applied in practice. There are several normalisation methods currently in use for

microarray data. Internal reference methods utilise a set of predetermined genes expected to give consistent signal intensities across different experiments [21]. Internal globalisation methods allow normalisation to be dictated by the observed data rather than by the expression level of genes determined *a priori* to be expressed at consistent levels. There are a number of ways this can be done. Global scaling applies a constant scaling factor based on first-order statistics (e.g. the mean or median) to define a scaling quotient. Applying a constant factor, however, is not always appropriate when the error is non-linear. Rank transformation of data can deal with differing data distributions but is insensitive and may lead to data loss.

In most gene array experiments, only a few transcripts are regulated by the treatment or experimental condition under investigation, and the abundance of the majority of transcripts on the array is unchanged. In a graph comparing the abundance of transcripts in the two RNAs we would therefore expect the majority of transcripts (those which are not regulated) to lie on a diagonal line (e.g. Figure 5). However, this is frequently not the case following global scaling. Small differences in probe labelling, hybridisation and scanning may cause intensity-dependant errors, where all transcripts of a particular intensity are shifted off the diagonal (Figure 7a). If not corrected, this can lead to the mistaken conclusion that these transcripts are more abundant in one RNA population than another. An approach for dealing with this type of distribution discrepancy, as well as global scaling errors, is to use a smoothing function aiming to return the position of all unregulated transcripts to the diagonal. This is known as intensity-dependant normalisation. The effect is seen easily in a Bland–Altmann plot [22, 23], shown in Figure 7b, where the difference between the log signal intensities of transcripts within two RNA populations is plotted against the average of the log signal intensities. The majority of transcripts, which are not differentially expressed, should lie along the *x*-axis. Transcripts more abundant in one RNA, than the other, will lie above or below the *x*-axis. Any intensity-dependent deviation

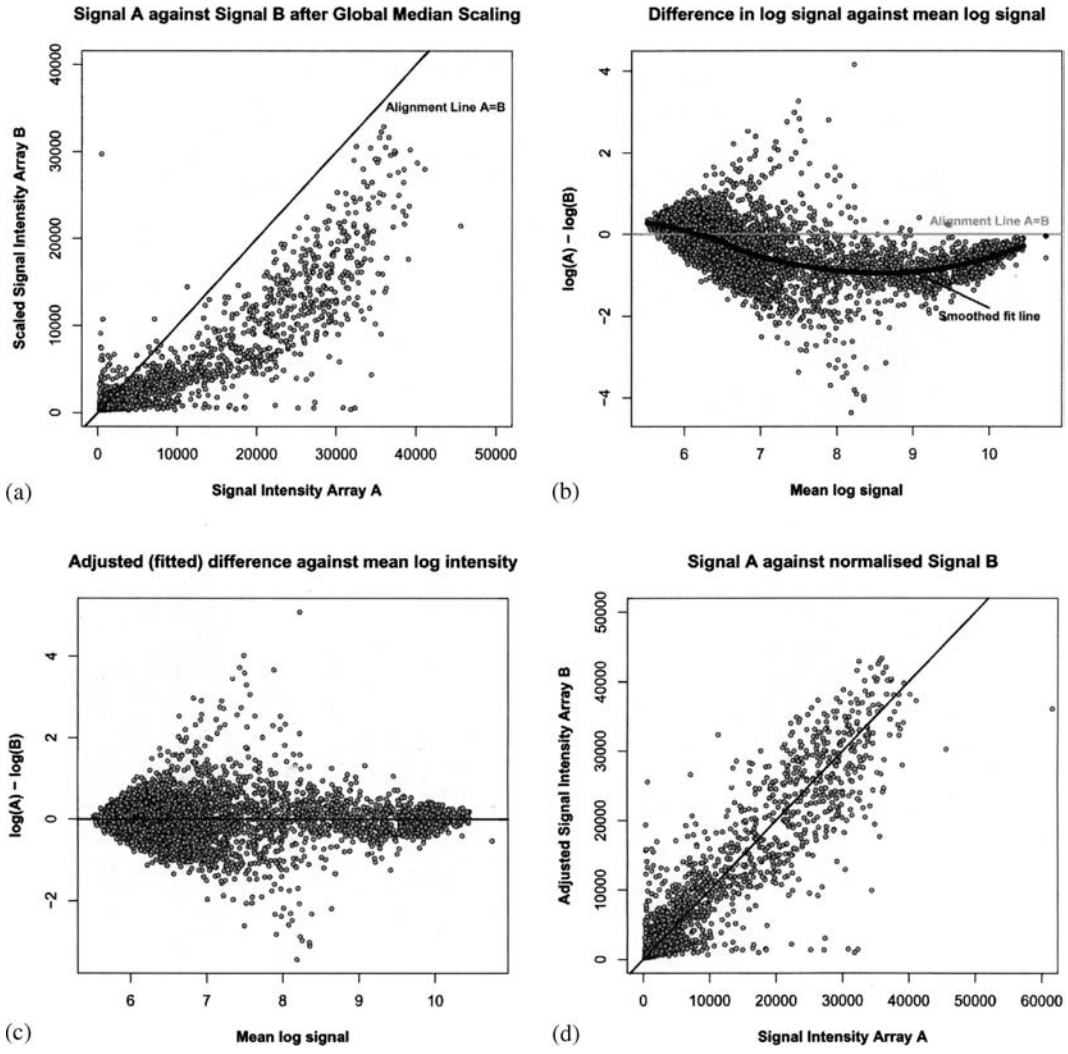

Figure 7. Loess normalisation to correct intensity dependent errors. Two closely related samples were labelled and hybridised. (a) Global scaling fails to correct intensity-dependent scaling errors, (b) rotation and log transformation. Difference in log signal intensity is plotted agains mean log signal intensity, (a Bland–Altman plot), demonstrates intensity-dependent deviation from the x-axis. A Loess smoothing regression is applied (red line) to correct the intensity-dependent deviation from the *x*-axis. (c) Corrected data and (d) transformed back to the original scale.

from this axis can be seen by applying a smoothing fit line as shown in Figure 7b. This allows the data points to be adjusted back to the *x*-axis to correct for the intensity-dependant error (Figure 7c). In most cases the smoothing function applied is derived from the 'Lowess' function [24] of the S statistical package (or its R equivalent, 'Loess'). The disadvantage of this method is that there is a tendency to over-fit data where there are few data points, typically at the upper range of expression values. This may have the effect of reducing fold-change values, even when these represent true biological differences. It is important, therefore to appreciate the effect of such normalisations on reducing the observed fold change in gene expression.

The aim of all normalisation methods is essentially to reduce inter-array variance due to noise, whilst maintaining the ability to detect significant biological differences in gene expression. More sophisticated methods have recently been developed to enhance sensitivity to identify significant change, despite normalisation. The methods of Yang [25], and Huber [26] attempt to improve the sensitivity of detection of differentially expressed genes over Loess-based normalisation alone. However, these methods are complex. We have therefore chosen to adopt the Loess approach to normalisation described above.

There is a further issue arising from the use of Loess for unpaired data sets, the concept of a reference array. Loess normalisation must be applied sequentially between arrays, typically against a standard reference array. For paired experiments the control array in each pair is a natural reference but there is no such natural reference in unpaired data sets (e.g. tumour and normal tissue from different patients). One approach [27] is to use an 'average array', comprising the geometric mean of the data (by genes), as a reference array, to which to normalise all the array data. An alternative approach is to select, as the reference array, the array which is closest (in terms of Euclidean distance) to this average array. A full description of this approach with an example of its application is available at http://www.obgyn.cam.ac.uk/genearray.

Following normalisation, advanced statistical methods are typically required to generate a list of candidate genes for validation by quantitative PCR. Student's *t*-test is often inappropriate in the context of gene array data, due to the large number of genes tested simultaneously. This leads to the problem of multiple comparisons [28] and susceptibility to a high false positive rate. Cyber-T [29] employs a Bayesian modification of the *t*-test, and SAM [30] uses a permutation-based approach to identify the false discovery rate for individual genes. Packages such as Bioconductor (http://www.bioconductor.org) or Genespring (Silicon Genetics, California, USA) can be used for data visualisation and clustering [31]. Reducing the data to a minimal number of components by the use of principal components analysis (PCA) or, more recently, independent component analysis (ICA) [32, 33] may lead to the identification of gene signatures involved in vascular remodelling.

Clearly the production of nylon filters requires multiple steps each of which incurs consumable costs. We have determined these and made allowances for possible failures of some of the steps and therefore the cost per filter is the maximum foreseeable. Thus to produce a batch of 400 filters the cost works out at £19.35 per filter. This compares very favourably with similar commercial filters which cost approximately £1200 for four (however, this does include the cost of some of the labelling reagents as well). We have also costed our optimised labelling and hybridisation protocols and the cost of the isotope, labelling and hybridisation reagents works out at £40 per hybridisation. Since a major portion of the labelling and hybridisation cost is attributable to the purchase of ^{33}P-dCTP, volume discounts may reduce this. The personnel cost associated with the generation of the filters has not been included in the figure above however once the protocols have been developed and optimised it is possible to produce the PCR products necessary and to generate the filters in approximately 6–8 weeks. In fact the most time consuming step is the assembly and verification of the cDNA clone collection. All in all using our optimised protocols we believe it is feasible for modest size laboratories to produce large number of filters which allow many biological replicates to be analysed.

Summary

Over 2000 microarray papers have been published in the last few years. The majority are now fluorescence based studies using commercially produced arrays of tens of thousands of features, but the range also includes a 59 gene rat array [34].

We believe small targeted gene arrays such as our angiogenesis array has an important place in this range, especially in situations where limited RNA is available (such as investigations into reproductive angiogenesis using small tissue samples) or when the use of primary cells and tissues necessitates multiple biological replicates. The array methods presented here are targeted, sensitive, flexible and relatively inexpensive. This type of array is well within the funding and expertise of many laboratories, but generation of meaningful results depends on careful validation of every step in the process. If this is done, tailored gene arrays provide a reliable tool to address the complex regulation of RNA transcript abundance that underlies much of vascular biology.

Acknowledgements

Amanda L. Evans, and Roberto Catalano were supported by WHO Rockfeller Foundation grant number RF99021/115. Andrew S. Sharkey was supported by a Meres Studentship from St. John's College, Cambridge. Sam Saidi was supported by MRC programme grant

Protocol 1. Amplification of cDNA inserts for spotting.

ANGIOGENESIS GENE ARRAY

- 11 × Master Plates glycerols −70 °C
- Grow fresh cultures 96 well plates 37 °C/48 h in LB/Amp 50 μg/ml
- Heat 25 μl culture + 75 μl dH_20 95 °C/10 min
- Lysates stored −20 °C

Spin 5 min 1000 rpm to pellet debris prior to use
Use supernatent as PCR template

96 well PCR

PCR mix	1 × 50 μl	100 × 50 μl
10 × Bioline buffer	5	500
2 mM dNTPs	5	500
M13F 10 μM	2.5	250
M13R 10 μM	2.5	250
50 mM $MgCl_2$	1.5	150
dH_20	31.25	3125
Bioloine Taq5 u/μl	0.25	25

Template (boiled lysate) 2

Parameters for PCR
(94 °C 1 min) × 1,
(94 °C 30 s, 55 °C 30 s, 72 °C 1 min) × 30,
(72 °C 7 min) × 1
Hold 4 °C

M13F (-20) GTA AAA CGA CGG CCA GTG
M13R (-48) AGC GGA TAA CAA TTT CAC AC
Random empty wells serve as negative controls

Protocol 3. Labelling of cDNA using EndoFree RT.

Reverse Transcription (EndoFree RT)

RNA 3–5 μg (cone., ≥0.7μg/μl)
1 μl 10 μM Anchored Oligo(dT) Primer
1 μl RNA Spike mix (below)
μl RNase-free H_2O upto to 8 μl total volume

70 °C, 5 min
48–50 °C, 5 min

2 μl 10X RT Buffer
4 μl dNTPs (2.5 mM dATP, dTTP, dGTP, 10 μM dCTP)
1 μl RNase Inhibitor
3 μl [α-^{33}P] dCTP 10 μCi/μl, 2500 Ci/mmol

48–50 °C for 5 min.
1 μl of Reverse Transcriptase
Incubate at 48–50 °C for 2 h.

RNA SPIKE MIX

1 μl spike mix contains	Spike pg	CAB	RCA	rbcL	LTP4	LTP6
		500	100	50	10	1

Remove RNA
Add
2 μl 10% SDS
1 μl 0.5 M EDTA pH 8.0
3 μl 3M NaOH (fresh)
68 °C 20 min
RT 10 min
Add
10 μl 1 M Tris pH 7.5
3 μl 3 M HCI
Remove unincorporated dNTPS using Nick column (Amersham)

Protocol 2. Purification of amplified cDNA inserts for spotting.

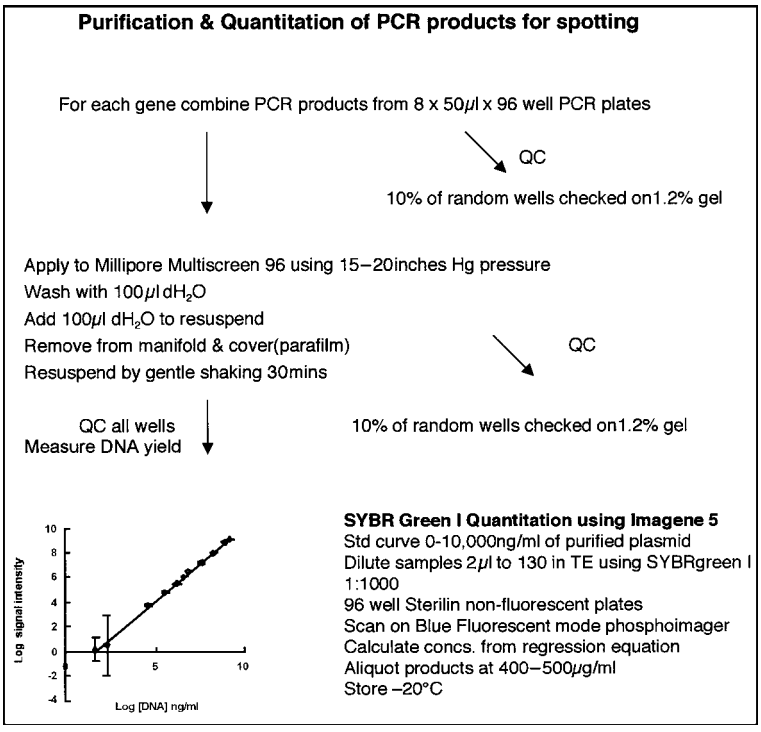

number G9623012 awarded to SK. Smith and DS Charnock-Jones of The Molecular Reproductive Medicine Group. Cristin G. Print was supported by The Wellcome Trust fellowship number 59522.

Protocol 4. Hybridisation and washing nylon membrane.

Pre-Hybridisation of nylon membranes

Pre wet membranes in dH_2O
Pre-heat Express Hyb© buffer at 68 °C
Heat – denature at 95 °C, 5 min the following
10 µl human Cot-1 DNA (1 mg/ml)
10 µl polyA (1 mg/ml)
200 µl salmon sperm DNA (5 mg/ml)

Add to 10 mls Express Hyb.© pre-warmed
Pre-Hybridise at 65 °C 3 h at 5–7 rpm in a roller bottle

Hybridisation

Heat denature at 95 °C, 5 min the following
400 µl purified radiolabelled cDNA
10 µl MEDTA
5 µl human Cot-1 DNA (1 mg/ml)
5 µl poly A (1 mg/ml)
100 µl salmon sperm DNA (5 mg/ml)
Add to 4.5 ml pre-warmed Express Hyb©
Replace the.Pre-Hyb. Buffer with the hyb. Mix.
Hybridise 65 °C 16 h 5–7 rpm

Washing

Pour off the hyb. buffer		
2 × SSC/0.5% SDS	30 min 60 °C	Twice
0.1 × SSC/0.1% SDS	30 min 60 °C	Twice
Rinse dH_20 for 5 sec only		
Bake 60 °C for 1 h		
Expose to Molecular Dynamics LE screen 48 h		
Scan at 50 µm resolution		

We thank Khashayar Lessan, supported by Wellbeing grant number PG/282, for his contribution to the apoptosis gene set, and Nicola Johnson for use of the HUVEC data. We also thank Kate Day for excellent technical support.

Appendix A

Agilent	http://www.agilent.com/chem/labonachip
Apogent	http://www.apogentdiscoveries.com
Amersham	http://amershambiosciences.com
Bd Biosciences	http://bdbiosciences.com
Caliper	http://www.calipertech.com
Genespring	http://www.silicongenetics.com
Imagequant	http://www.mdyn.com/products/lmageQuant/default.htm
Imagene	http://www.biodiscovery.com/products/lmagene/imagene.html
SpotReport	http://www.stratagene.com

A comprehensive list of array web sites is available from Molecular Cloning, A Laboratory Manual, Volume 3, Sambrook and Russel. Cold Spring Harbor Laboratory Press, Cold Spring Harbor, New York.

References

1. Folkman J, D'Amore PA. Blood vessel formation: What is its molecular basis? Cell 1996; 87: 1153–55.
2. Hanahan D, Folkman J. Patterns and emerging mechanisms of the angiogeneic switch during tumorigenesis. Cell 1996; 86: 353–64.
3. Risau W. Mechanisms of angiogenesis. Nature 1997; 386: 671–4.
4. Lipshutz R, Fodor S, Gingeras TR, Lockhart DJ. High density synthetic oligonucleotide arrays. Nat Genet Sup 1999; 21: 20–4.
5. Lockhart DJ, Dong H, Byrne MC et al. Expression monitoring by hybridisation to high density oligonucleotide arrays. Nat Biotechnol 1996; 14(1112): 1675–80.
6. Adessi C, Matton G, Ayala G et al. Solid phase DNA amplification: Characterisation of primer attachment and amplification mechanisms. Nucleic Acids Res 2000; 28(20e87): 1–8.
7. Borthwick JM, Charnock-Jones DS, Tom BD et al. Determination of the transcript profile of human endometrium. Mol Hum Reprod 2003; 9(1): 19–33.
8. Sargent TD, David IB. Differential gene expression in the gastula of Xenopus Laevis. Science 1983; 222(4620): 135–9.
9. Duggan D, Bittner M, Chen Y et al. Expression profiling using cDNA microarrays. Nat Genet Sup 1999; 21: 10–4.
10. Clark DE, Smith SK, He Y et al. A vascular endothelial growth factor antagonist is produced by the human placenta and released into the maternal circulation. Biol Reprod 1998; 59: 1540–48.
11. Sowter HM, Corps AN, Evans AL et al. Expression and localization of the vascular endothelial growth factor family in ovarian epithelial tumors. Lab Invest 1997; 77(6): 607–14.
12. English D, Parker B. Methods for Preparing PCR Based Arrays. Scleicher & Schuell Applications Notes for Biomolecular Screening, 1999.
13. Britten RJ, Graham DE, Neufeld BR. Meth Enzymol 1974; 29: 363–418.
14. Khodarov NN, Yu J, Nodzenski JS et al. Method of RNA purification from endothelial cells for DNA Array Experiments. Biotechniques 2002; 52: 72–4.
15. Hegde P, Qi R, Abernathy C et al. A concise guide to cDNA microarray analysis. Biotechniques 2000; 29: 548–62.
16. Bao Z, Wenli M, Rong S et al. Re-use of a stripped cDNA microarray. Br J Biomed Sci 2002; 59(2): 118–9.
17. Ramdas L, Coombes KR, Baggerly K et al. Sources of nonlinearity in cDNA microarray expression measurements. Genome Biol 2001; 2(11): 0047.1–7.
18. Novak JP. Characterisation of variability in large-scale gene expression data: Implications for study design. Genomics 2002; 79: 104–13.
19. Kerry S, Bland JM. Sample size in cluster randomisation. BMJ 1998; 316(7130): 549.
20. Draghici S, Kuklin A, Hoff B, Shams S. Experimental design, analysis of variance and slide quality assessment in gene expression arrays. Curr Opin Drug Discov Dev 2001; 4(3): 332–7.
21. Kroll T, Wolfl S. Ranking: A closer look on globalisation methods for normalisation of gene expression arrays. Nucleic Acids Res 2002; 30(11): e50.
22. Bland JM, Altman DG. Measuring agreement in method comparism studies. Stat Meth Med Res 1999; 8: 135–40.
23. Dunn G. Statistical methods in laboratory medicine. Stat Meth Med Res 1999; 8(2): 91.
24. Cleveland W. Robust Locally Weighted regression and Smoothing Scatterplots. J Am Stat Assoc 1979; 74: 829–36.
25. Yang Y, Dudoit S, Luu P et al. Normalization for cDNA microarray data: A robust composite method addressing single and multiple slide systematic variation. Nucleic Acids Res 2002; 30(4): e15.
26. Huber W, Van Heydebreck A, Sültmann H et al. Variance stabilization applied to microarray data calibration and to the quantification of differential expression. Bioinformatics 2002; Suppl 1: S96–104.
27. Workman C, Jensen L, Jarmer H et al. A new non-linear normalization method for reducing variability in DNA microarray experiments. Genome Biol 2002; 3(9): research0048.
28. Bland JM, Altman DG. Multiple significance tests: The Bonferroni method. BMJ 1995; 310(6973): 170.
29. Baldi P, Long A. A Bayesian framework for the analysis of microarray expression data: Regularized *t*-test and statistical inferences of gene changes. Bioinformatics 2001; 17(6): 509–19.

30. Tusher V, Tibshirani R, Chu G. Significance of microarrays applied to the ionizing radiation response. Proc Natl Acad Sci USA 2001; 98(18): 10515.
31. Eisen MB, Spellman PT, Brown PO, Botstein D. Cluster analysis and display of genome-wide expression patterns. Proc Natl Acad Sci USA 1998; 95(25): 14863–8.
32. Liebermeister W. Linear modes of gene expression determined by independent component analysis. Bioinformatics 2002; 18(1): 51–60.
33. Martoglio A, Miskin J, Smith SK, Mackey D. A decomposition model to track gene expression signatures: Preview on observer-independent classification of ovarian cancer. Bioinformatics 2002; 18(12): 1617–24.
34. De longueville F, Surry D, Meneses-Lorente G et al. Gene expression profiling of drug metabolism and toxicology markers using a low-density DNA microarray. Biochem Pharmacol 2002; 64(1): 137–49.

Reproductive Molecular Research Group Genelist

Gene ID	IMAGE	Gene	Abbrev	clone source list	Acc.No./Unigene ID	clone details	other information & changes to list name
1-kB epsilon	1580042	I-kB epsilon, NFKBIE nuclear factor of kappa light polypeptide gene enhancer in B-cells,inhibitor, epsilin	NFKBIE, IKBe	apoptosis array	U91616 /Hs.91640	0.6 kb, NO 5's, 3's, NO pA, no sig O/L	
1-TRAF	2731092	I-TRAF (TANK)	TANK	apoptosis array	U63830/Hs146847	unknown size, 3's, NO 5's, pA, no sig O/L	
14-3-3eta	357633	14-3-3 eta ,tyrosine-3-monooxygenase/tryptophan -5-monooxygenaseactivation protein,eta polypeptide	14-3-3 eta,YWHAH	apoptosis array	L20422 /Hs.349530	0.6 kb, pA, 5's3's, no extraneous o/l	
14-3-3zet	195321	14-3-3 zeta,tyrosine-3-monooxygenase/tryptophan -5-monooxygenase	YWHAZ	apoptosis array	NM_003406/Hs.75103	0.8 kb, pA, 5's3's, no extraneous o/l	
A-Raf	1350927	A-raf 1 oncogene putative raf related protein	A-Raf	apoptosis array	L24038	0.8 kb, NO 5's, 3's, pA, no sig O/L	stimulates the Raf/MAPK pathway
A1(Bfl-1)	686515	Bcl -2 related protein A1 (Bfl-1 / GRS)	A1,BCL2A1,Bfl-1,GRS	apoptosis array	U29680 /Hs227817	0.8 kb, pA, 5's3's, no extraneous o/l	
A20	714022	A20,TNFAIP3 tumour necrosis factor,alpha-induced protein 3	A20	apoptosis array	Hs.211600	0.7 kb, 5's, 3's, pA, no sig O/L	TNFalpha-induced protein-3, zinc finger protein, inhibitor of apoptosis in endothelial cells
A2M	878182	alpha macroglobulin 2	A2M	Implantation array	M11313/Hs74561		
ACP5	125101	uteroferrin, acid phosphatase type 5	ACP5	Implantation array	J04430/Hs.1211		tartrate-resistant acid phosphatase
ACTB	324822	actin beta	ACTB	endogenous control	X00351		last 0.5kb
ACVR1	343354	activin A receptor, type I	ACVR1	apoptosis array	Z22534/Hs.150402	0.7 kb, 5's, 3's, pA, no sig O/L	
ACVR2	344197	activin A receptor Type II	ACVR2	Implantation array	M93415		
ACVR2B	2516456	activinA receptor type IIB	ACVR2B	apoptosis array	Hs.23994/X77533	0.9 kb, 3's, NO 5's, NO pA, no sig O/L	
AES	145324	Amino -terminal enhancer of split	AES	unknown	AF269289/Hs.244		aka pp2150 mRNA, BUT BAD CLONE AS ALSO MATCHES Hs.248156 HBOA histone acetyltransferase
AIF	122860	Apoptosis Inducing factor	AIF	apoptosis array	NM_004208	0.7 kB, 5's, 3' s, pA, no unwanted homology	PCD8, flavoprotein
Akt (PKB)	486251	Akt (PKB) protein kinase B	Akt	apoptosis array	M63167	1.0 kB, 5's, 3' s, pA, no unwanted homology	Rac PK alpha, prosurvival signal downstream of PI3K, implicated in the phosphorylation of Bad
ALOX5	132574	Arachidonate -5- lipoxygenase	ALOX5	Implantation array	Hs.89499/J03571		
alphaNAC	589666	Nascent-polypeptide associated complex alpha polypeptide	NACA	in-house clone	X80909/Hs32916	0.9kb	
ALPP	131419	alkaline phosphatase, placental (Regan isozyme)	ALPP	Implantation array	X53279		
Ang 1	34	Angiopoetin 1	ANG-1	in-house clone		pCR-Script	
Ang 2		Angiopoetin 2	ANGPT2	in-house clone	Hs.115181/AB009865	pCR-Script	
ANGPT1	252787	Angiopoietin 1	ANGPT1	Implantation array	U83508		last 0.3 kb
ANGPT2	668204	Angiopoietin 2	ANGPT2	Implantation array	AF004327		last 0.5kb
ANGPTL4	1188593	Angiopoietin -like 4	ANGPTL4	in-house clone	Hs.9613/AF202636		
angtenaseC	2018808	Angiotensinase C,	PRCP	Implantation array	L13977		
ANPEP	625609	alanyl (membrane) aminopeptidase, aminopeptidase N or M	ANPEP	Implantation array	AI685221		CD13,p130
ANXA5	1665821	Vascular anticoagulant protein, annexin A5	ANXA5	in-house clone	AI042581/Hs300711	3's, no 5's,0.8kb	anticoagulant protein PAP, annexin A6
Apaf-1	253554	Apoptosis protease activating factor 1	APAF-1	apoptosis array	Hs.77579/AF013263	0.4 kb, pA, 5's3's, no extraneous o/l	Drosophilsa homologue = "DARK" NB clone also contains some repetitive seq
APAF1	244146	apoptotic protease activating factor	APAF1	Implantation array	AF013263		
APC	470992	adenomatosis polysis coli	APC	Implantation array	M74088		
APG5	134320	APG5 (autophagy 5)	APG5	apoptosis array	NM_004849	0.7 kb, 5's, 3's, pA, no sig O/L	expressed after induction of apoptosis
Arabidops		Arabidopsis Thaliana		exogenous control			
ARF-2	449487	ADP ribosylation factor-like 2	ARF-2	Implantation array	L13687		
ARNT-3	1939053	aryl hydrocarbon receptor translocator-3	ARNT-3	apoptosis array	Hs.74515/U51627	0.8 kb, 3' no 5', pA no sig O/l	"=MOP3 =BMAL1"

Gene ID	IMAGE	Gene	Abbrev	clone source	Acc.No./Unigene ID	clone details	other information & changes to list name
ATCab	46916	Arabidopsis thaliana chlorophyll a/b binding	ATCab	exogenous control	At.23982		
ATM	1868266	Ataxia Telangiestasia Mutated (cluster includes complementation groups A,C &D)	ATM	apoptosis array	AI262879/Hs194382	3'0.6kb	
ATM(2)	1864692	Ataxia Telangiestasia Mutated	ATM	apoptosis array	Hs.194328		
ATP6S14	1758635	ATPase vascuolar 14KD	ATP6V1F	was not listed	Hs.78089/BF314603		Component of vacuolar ATPase (V-ATPase), a multisubunit enzyme that mediates acidification of eukaryotic intracellular organelles.Protein sorting, zymogen activation, receptor-mediated endocytosis, and synaptic vesicle proton gradient generation.
ATR (1)	1879175	Ataxia Telangiestasia and rad 3 related	ATR	apoptosis array	Hs.77613	0.6 kb, 3', pA	some homology to Human FRAP-related protein (FRP1) mRNA
ATR (2)	2339873	Ataxia telangiestasia & Rad 3 related	ATR	apoptosis array	Hs.77613/NM_001184	0.6 kb, 3', pA	some homology to Human FRAP-related protein (FRP1) mRNA
AXIN 1	158891	axin	AXIN1	Implantation array	Hs.184434/AF009674		
B-Raf	1878531	B-Raf,v-raf murine sarcoma viral oncogene homolog B1	BRAF	apoptosis array	Hs.622/M21001	0.7 kb, 3's, NO 5's, pA, no O/L	95kDa b-Raf serine/threonine kinase
B12	2325878	Tumour necrosis factor,alpha -induced protein-1(endothelial)	B12 = TNFAIP1	apoptosis array	Hs.76090	0.5kb, no5's, 3's, pA, no O/L	Tumor necrosis factor, alpha-induced protein 1 (endothelial), induced in HUVEC by TNFalpha, no known function
B7-1	2723769	B7-1, CD80 antigen ligand	B7-1	apoptosis array	Hs.838	3's, NO 5's, no sig O/L, size unknown	CD80 ligand
B7 -2	1634297	B7-2 antigen, CD86 ligand	B7 -2	apoptosis array	Hs.27954	0.8 kb, 3's, NO 5's, pA, no sig O/L	CD86 also CTLA4 counter receptor
Bad (1)	2108212	Bcl-2 antagonist of cell death	Bad	apoptosis array	U66879 /Hs76366	0.6 kb, pA, 5's3's, no extraneous o/l	
Bad (2)	2068876	Bcl-2 antagonist of cell death	Bad	apoptosis array		pA, 3'seq, no 5'seq	
BAG-1	1046695	Bcl2-associated athanogene -1	BAG-1	apoptosis array	Hs.41714	0.6 kb, NO pA, 3's, no extraneous o/l	transduces anti-apoptotic function of cytokines
Bak	235938	BAK1,Bcl-2 antagonist/ killer 1	Bak	apoptosis array	U23765/Hs93213	0.9 kb, pA, 5's3's, no extraneous o/l	
BAR	2046408	BAR,apoptosis regulator LOC51283	BAR	apoptosis array	Hs.168159	0.7 kb, 3' read, pA, search -> no homol	apoptosis regulator which binds pro-caspase 8 and bcl-2
basigin	756533	Basigin (OR blood group)	BSG	Implantation array	Hs.74631/BF316943		
basigin	756533	Basigin (OR blood group)	BSG	Implantation array	Hs.74631/BF316943		
Bax(1)	2049495	BCL-2 associated protein X	Bax	Implantation array	L22473/4/Hs159428		mito protein/pro-apoptotic/alpha-beta, same clone as H/G10
Bax(2)	2049495	Bcl-2 associated protein X	Bax	apoptosis array	L22474 /Hs159428	0.6 kb, pA, NO 5' but has 3',	EST from whole embryo, same clone as D/E7
Bcl-2	1554409	bcl-2	Bcl-2	apoptosis array	NM_004050	0.7 kb, pA, NO 5' but has 3', no extraneous o/l, not in limited cds	
BCL-2	667231	B-cell CLL/lymphoma 2	BCL2	Implantation array	M14745		mito protein/CED9 C.elegans/anti-apoptotic
Bcl-2	667231	Bcl-2,B cell CLL lymphoma 2	Bcl-2	apoptosis array	M14745 /Hs.79241	0.8 kb, pA, 5's3's, no extraneous o/l	
Bcl-XL	1518718	Bcl-2 like	Bcl-xL,Bcl2L1	apoptosis array	Z23115/Hs.305890	0.6 kb, pA, 5's3's, no extraneous o/l	
Bid	2330073	Bid, BH3 interacting domain death agonist	Bid	apoptosis array	AF042083/Hs.172894	0.9 kb, 3's, NO 5's, pA, no sig O/L	
BID	627125	BH3 interacting domain death agonist	BID	Implantation array	AF042083		
Bik (NBK)	685783	Bik (NBK),Bcl-2 interacting killer(apoptosis-inducing)	Bik (NBK)	apoptosis array	U34584/Hs155419	0.7 kb, pA, 5's3's, no extraneous o/l	
Bim	2488679	BCL2-likeII(apoptosis facilitator)	Bim(Bod)	apoptosis array	AF032457/Hs202657	0.7 kb, 3' seq, no 5' seq, pA unknown, no sig O/L	BOD Bcl-2 related ovarian death gene,not verified
BLK	2027963	B lymphoid tyrosine kinase	BLK	apoptosis array	AA465174	3' NO 5', 1.1KB, pA, NO EXTRANEOUS O/L	
BPI	2130568	Bactericidal/permeability-increasing protein	BPI	apoptosis array	Hs.89535	0.7 kb	
BRAC1	241474	breast cancer 1, early onset	BRCA1	Implantation array	U14680		
BRCA2	415529	Breast cancer 2 ,early onset	BRAC2	Implantation array	Hs34012		
BTC	1535554	Betacellulin	BTC	implantation array	Hs.73105/S55606		
BTK	2014424	Bruton agammaglobulinemia tyrosine kinase	BTK	apoptosis array	Hs.159494/AF153764	0.6 kb, 3's, NO 5's, pA, no sig O/L	Bruton agammaglobulinemia tyrosine kinase

Gene ID	IMAGE	Gene	Abbrev	clone source	Acc.No./Unigene ID	clone details	other information & changes to list name
bystin	564538	bystin-like	BYSL	Implantation array	L36720/Hs.106880		
c-abl	284452	v-ablAbelson murine leukemia viral oncogene homolog1	c-abl	apoptosis array	X16416 /Hs146355	0.8 kB, 5's, 3' s, pA, no unwanted homology	multifunctional, regulates DNA damage-induced apoptosis, integrin ligation recruits abl from the nucleus
c-fos(1)	1594287	c-fos, V-fos FBJ murine osteosarcoma viral oncogene homolog	FOS	apoptosis array	Hs.25647/K00650	0.7kb, 3's, NO 5's, pA, no sig O/L	
c-jun	345170	c-jun proto oncogene	c-jun	Implantation array	U65928		
c-myc	739849	c-myc, avian myelocytomatosis viral oncogene homolog	c-myc	Implantation array	V00568/Hs.79070		
c-raf	489327	c-raf (Raf1) V-raf murine leukeamia viral oncogene homolog 1	RAF 1	apoptosis array	X03484 /Hs 85181	0.6 kb, 3's no 5', pA, no sig O/L	downstream of Ras, upstream of MAP kinases
C1orf29	754479	Hypothetical protein, expressed osteoblasts	C1orf29	in-house clone	AB000115/Hs.75470	3's & 5's, no pA,	chromosome 1 open reading frame 29
C3	489327	C3 complement component	C3	Implantation array	K02765/Hs284394		
CA125	117106	CA125, membrane component chr.17 surface marker 2	CA125, M17S2	Implantation array	X76952		ovarian carcinoma antigen CA125
CA4	unknown	carbonic anhydrase 4	CA4	Implantation array	Hs.89485/M83670		
CAB	spike 1	Arabidopsis Thaliana,Photosystem 1chlorophyll a/b binding protein	CAB	exogenous control	X56062	pGEMT, 500bp	
CAB (1)	667409	Arabidopsis thaliana chlorophyll a/b/binding protein	CAB	exogenous control	X56062		
CAB (2)		Arabidopsis thaliana chlorophyll a/b/binding protein	CAB	exogenous control	X56062		
CAB (3)		Arabidopsis Thaliana CAB mRNA for photosystem I	CAB	exogenous control	X56062		
CAB (5)		Arabidopsis Thaliana CAB mRNA for photosystem I	CAB	exogenous control	X56062		
Cadherin-13	1509342	Cadherin-13,cadherin H(heart)	CDH13	in-house clone	L34058/Hs.63984	3's, no 5's,0.8kb	Adhesion
CALCB	1268215	calcitonin-related polypeptide beta	CALCB	Implantation array	X02404		hom. Alpha
CALCR (1)	3033121	Calcitonin receptor	CALCR	apoptosis array	Hs.640/X69920	unknown size, 3's, NO 5's,	
CALCR (2)	2115715	calcitonin receptor	CALCR	Implantation array	U26553		
CASP1	120106	interleukin1 beta converting enzyme, caspase 1	IL1BCE, CASP 1	Implantation array	Hs.2490/U13698		apoptosis related cysteine protease
caspase 3 (1)	429574	caspase 3, apoptosis-related cysteine protease	casp 3	Implantation array	NM_004346		
caspase 3 (2)	30772	caspase-3,apoptosis-related cysteine protease	CASP3	apoptosis array	U13737 /Hs74552	0.9 kb, pA, 5's3's, no extraneous o/l	short prodomain = class II; YAMA PROTEIN; CPP-32
caspase 4	131502	caspase-4, ICH-2	caspase-4	apoptosis array	Hs.74122/U25804	0.8 kb, 5's, 3's, pA	TX PROTEASE (Mih1), note homol with caspase 13 and 1
caspase 5	341763	caspase 5, apoptosis-related cysteine protease,ICE rel III,TY protease	CASP5	apoptosis array	U28015/Hs.3257		
caspase 7	1651252	cysteine protease cleaving an aspartic acid residue 7	caspase-7,Mch-3	apoptosis array	U67320/Hs.9216	0.6 kb, NO 5's, 3's, pA, no sig O/L	short prodomain = class II; MCH3, ICE-LAP3
caspase 8(1)	594361	caspase-8,apoptosis-related cysteine protease	CASP 8	apoptosis array	Hs.19949/NM_033356	0.6 kb, 5's, 3's, pA, note some homol to unidentified database sequnces	long prodomain = class I; MCH-5, MACH, FLICE
caspase 8(2)	594361	caspase 8 ,apoptosis related cysteine protease	CASP8	apoptosis array	Hs.19949/X98173	0.6 kb, 5's, 3's, pA, note some homol to unidentified database sequnces	long prodomain = class I; MCH-5, MACH, FLICE
caspase 8(3)	782488	caspase 8, apoptosis-related cysteine protease, Mach alpha 2 protein	caspase 8	Implantation array	NM_001228		
caspase 9	705110	caspase 9, apoptosis-related cysteine protease	Casp 9/Mch 6	Implantation array	AB015653		
caspase 9	121693	cysteine protease cleaving an aspartic acid residue 9	caspase-9	apoptosis array	Hs.100641/U60521	1.0 kb, 5's, 3's, pA, no sig homol	long prodomain = class I; APAF3, ICE-LAP-6, MCH-6
caspase 10 (1)	241481	caspase-10,apoptosis related cysteine protease	casp10	apoptosis array	U60519 /Hs5353	0.8 kb, NO pA, 5's3's, no extraneous o/l	long prodomain = class I; FLICE2, MCH-4,NB same clone as implantation array E/H11
caspase 10 (2)	241481	caspase10, apoptosis-related cysteine protease	casp10/Mch 4	Implantation array	U60519/Hs.5353		same clone as apoptosis array G/E2
catalase		catalase 1	CAT	in-house clone	Hs.76359/X04076	B/S11 KS +/-, sense, Exons 1-4	

Gene ID	IMAGE	Gene	Abbrev	clone source	Acc.No./Unigene ID	clone details	other information & changes to list name
Cathepsin S	687875	Cathepsin S	CTSS	in-house clone	M90696/Hs181301	0.4 kb,3' & 5's, 0.4kb	Proteolytic enzyme,homology to colon human cDNA clone
cathepsinB	2595361	cathepsin-B	CTSB	apoptosis array	Hs.249982	size unknown	
cathepsinH		cathepsin H	CTSH	in-house clone	Hs.288181/AA973763X07549	pCMVSPORT 2	
CCNB1	531805	cyclin B1	CCNB1	Implantation array	M25753/Hs.23960	3'end	
CD9	727251	CD9 antigen p24	CD9	Implantation array	M38690		
CD10	471700	CD10 (membrane metallo-endopeptidase)	CD10/MME/CALLA	Implantation array	J03779		
CD28	1711889	CD28 antigen (Tp44)	CD28	apoptosis array	Hs.1987/J02988	1.3 kb, 3's, NO 5's, pA, no sig O/L	T cell costimulatory molecule
CD31	134521	platelet endothelial cell adhesion molecule	PECAM-1/CD31	Implantation array	M28526		
CD34	364487	CD34 antigen	CD34	apoptosis array	M81104 /Hs.85289	0.7 kb, pA, 5's3's, no extraneous o/l	
CD36	1739990	CD36 antigen	CD36				thrombospondin receptor
CD40	152683	CD40,TNF receptor superfamily member 5	TNFRSF5	apoptosis array	X60592 /Hs.25648	0.7 kb, pA, 5's3's, no extraneous o/l	expressed on EC (Mach et al, UI 97203164)
CD44	265052	CD44/H-CAM/p80 /GP90	CD44	Implantation array	U40373		
CD56 (1)	1883065	NCAM-1 (CD56)	CD56	apoptosis array	Hs.167988	3's, 0.6 kb, NO 5's, pA, no sig O/L	neural cell adhesion molecule
CD56 (2)	276764	neural cell adhesion molecule 1	NCAM1 (CD 56)	Implantation array	U63041/Hs167988		
CD58	287620	CD58 antigen, lymphocyte function-associated antigen -3 LFA-3	CD58	Implantation array	Y00636		
CD59	1735518	CD59 antigen p18-20	CD59	in-house clone	M34671/Hs.278573	3's, no 5's	Complement restriction, Ly-6-like protein, MEM43
CD63	471872	CD63 antigen (melanoma 1 antigen)	CD63	Implantation array	M59907		
CD69	2130345	CD69antigen,(p60,early T-cellactivation antigen)	CD69	apoptosis array	Hs.82401/L07555	1.3 kb, 3's, NO 5's, pA, no sig O/L	early T-cell activation antigen, also part of NK gene complex
CD84	2099041	CD84antigen(leukocyte antigen)	CD84	apoptosis array	Hs.137548	0.8 kb, 3' no 5', no pA, no extran o/l	MAX.3
CD94	1901363	CD 94,killer cell lectin-like receptor subfamily D,member1	KLRD1,CD 94	apoptosis array	U30610 /Hs.41682	1.5 kb, NO 5's, 3's, pA, no sig O/L	KLRD1, associates with one of five different NKG2 isoforms, part of NK gene complex
CDC 6	204214	cell division cycle 6 homolog, S.cerevisiae	CDC6	Implantation array	U77949		
CDC2 (1)	712505	cell division cycle 2 ,G1 to S and G2 to M	CDC2	apoptosis array	X05360/Hs334562	0.6 kb, 3's, 5's, pA, no sig O/L	
CDC2 (2)	712505	cell division cycle 2 ,G1 to S and G2 to M	CDC2	apoptosis array	Hs.334562/Y00272	3', pA, 0.6 kb, no o/l	
CDC25A	204301	Cell division cycle 25A	CDC25A	apoptosis array	M81933	0.6 kb, 3's, 5's, NO pA, no sig O/L	dephosphorylates, and activates the cell cycle kinase cyclin E-cdk2
CDC25B	172466	Cell division cycle 25B	CDC25B	apoptosis array	M81934/Hs153752	0.6 kb, 3's, 5's, pA, no sig O/L	dephosphorylates p34(cdc2)
CDC25C	1878149	cell division cycle 25C	CDC25C	apoptosis array	M34065 /Hs 656	0.6 kb, 3's, pA, no sig O/L	activates the p34cdc2 protein kinase at mitosis
CDC37	111650	cell division cycle 37(S.cerevisiae),Homolog	CDC37	apoptosis array	U63131 /Hs.160958	0.6 kb, 3's, 5's, pA, no sig O/L	
CDC6	1089493	cell division cycle 6	CDC6	apoptosis array	Hs.69563	1.0 kb, 3' no 5', pA, note great homology to CDC 18	CDC6 (cell division cycle 6, S. cerevisiae) homolog
CDH1	WHO cl.4	cadherin E (uvomorulin)	CDH 1	Implantation array	L08599	pGEMT	homology with N-cadherin/primers7/8
CDH3	359051	cadherin P (placental) also cadherin 3	CDH 3	Implantation array	X63629		hom. cadherin E
CDI-1	843110	GDP-dissociation inhibitor 1	CDI-1	Implantation array	Hs.74576		
CDK4	842806	cyclin dependent kinase 4	CDK4	apoptosis array	M14505 /Hs.95577	0.7 kb, 5's, 3's, NO pA, no sig O/L	
CDK5	220505	cyclin dependent kinase 5	CDK5	apoptosis array	X66364 /Hs.166071	0.8kb, 5's, 3's, NO pA, no sig O/L	
CDK6	1646946	cyclin dependent kinase 6	CDK6	apoptosis array	X66365 /Hs.38481	1.0 kb, 3's, 5's, pA, no sig O/L	
CDK7	1516792	Cyclin dependent kinase 7(homolog of Xenopus MO15 cdk-activating kinase)	CDK7	apoptosis array	Hs.184298	0.7 kb, 3', pA, no o/l	
CdKn2a (1)	15523215	cyclin -dependent kinase inhibitor 2A,p16, inhibits CDK4	CdKn2a		Hs1174		

Gene ID	IMAGE	Gene	Abbrev	clone source	Acc.No./Unigene ID	clone details	other information & changes to list name
CdKn2a (2)	2242420	cyclin -dependent kinase inhibitor 2A,p16, inhibits CDK4	CdKn2a		Hs.1174		
CERB	135178	CREB binding protein (Rubinstein-Taybi syndrome)	CERB (CREBBP)	Implantation array	U47741		
CFL1	625792	cofilin 1(non-muscle)	CFL1	apoptosis array	Hs.180370	5's, 3's, pA, 0.6 kb, no sig O/L	previously listed as cofilin
CGI-134 (2)	1639562	novel protein conserved C.Elegans by comparative proteomics	CGI-134	Implantation array	AAD34129		
Chk1	206717	Chk1 checkpoint (S.pombe) homolog	CHK1	apoptosis array	Hs.20295/AF016582	1.0 kb, 3' and 5', pA, no o/l	
Chk2	2349044	Chk2,checkpoint s.pombe homolog	CHK2/CHEK2	apoptosis array	Hs.146329	0.6 kb, 3', pA, no o/l	Rad53,protein kinase
CHST1	1853818	keratan sulphotransferase 1/chondroitin 6	CHST 1	Implantation array	U65637	hom last 0.6	
CIS4 (1)	668977	Supressor of cytokine signalling 4, STAT induced STAT inhib. 5	STATI-4, CIS5	Implantation array	AB006968		
CIS4 (2)	668977	Supressor of cytokine signalling 4, STAT induced STAT inhib. 7	STATI-4, CIS7	Implantation array	AB006968		
CKN1	2881290	Cockayne's syndrome 1(classical)	CKN1	Implantation array	Hs32967		
Clathrin	79364	Clathrin, heavy chain,Hc	CLTC	in-house clone	D21260/Hs178710	3's, no 5's,0.5kb	Membrane trafficking
CLK1	727344	CDC-like kinase 1	CLK1	apoptosis array	L29222	0.8 kb, 3's, 5's, pA, no sig O/L	CDC-like kinase 1
CLK2	668070	CDC like kinase 2	CLK2	apoptosis array	L29216	0.5 kb, 3's, 5's, pA, no sig O/L	CDC-like kinase 2
CLK3	1187803	CDC-like kinase 3	CLK3	apoptosis array	L29220 /Hs73987	0.6 kb, 3's, 5's, pA, no sig O/L	CDC-like kinase 3
CLU	246127	apolipoprotein J, clusterin, complement lysis inhibitor	CLU	Implantation array	Hs.75106/AL048744		
Clusterin	344538	Clusterin,Complement lysis inhibitor,SP-40,40,sulfated glycoprotein2,testosterone - repressed prostate message 2,apolipoprotein J	CLU	apoptosis array	M74816	0.6 kb, pA, 5's, 3's, no signif O/L	multifunctional secreted protein, initiates apoptosis
CNTFR	156431	ciliary neurotrophic factor receptor	CNTFR	Implantation array	M73238		
COL4A1	359084	collagen IV alpha 1	COL4A1	Implantation array	M11315		last 0.3kb
COL4A2	726808	collagen,type IV alpha 2(canstatin)	COL4A2	Implantation array	Hs.75617/X05610	last 0.5kb	
COL4A4	562397	collagen IV alpha 4	COL4A4	Implantation array	X81053		last 1kb
COL4A5	284501	collagen IV alpha 5 (Alport syndrome)	COL4A5	Implantation array	NM_000495		last 0.8kb
COL4A6	2070789	collagen IV alpha 6	COL4A6	Implantation array	U04845		last 1kb
COL5A2	489919	COL5A2 Collagen, type V, alpha 2	COL5A2	Implantation array	Hs.82985/AA725207		
COL6A1	152687	collagen VI alpha 1	COL6A1	Implantation array	X15880/Hs.108885		
COL6A2	365455	collagen VI alpha 2	COL6A2	Implantation array	M34570 (3'end)		
connexin	201273	Connexin 32/gap junction protein beta 1	GJB1	Implantation array	X04325		Charcot-Marie_Tooth neuropathy
COPA	843200	coatomer protein alpha	COPA	in-house clone	U20105	0.7kb	
cox1(1)	703713	cyclooxygenase 1, prostaglandin-endoperoxide synthase 1	cox 1/PTGS1	Implantation array	M59979		different clone from cox[2]&[3] H/B1 & F/E5
cox1(2)	1589081	cyclooxygenase 1, prostaglandin-endoperoxide synthase 1	cox 1/PTGS1	apoptosis array	U63846	0.7 kb, pA, 3's, NO 5's, No sig O/L	cyclooxygenase-1,same clone as F/E5 cox1[3] not same as A/d2
cox1(3)	1589081	cyclooxygenase 1, prostaglandin-endoperoxide synthase 1	cox 1/PTGS1	apoptosis array	U63846/M59979	0.7 kb, pA, 3's, NO 5's, No sig O/L	cyclooxygenase-1,same clone as H/B1 cox1[2] not same clone as cox1[1] A/D2
cox2 (1)	147050	cyclooxygenase 2, prostaglandin-endoperoxide synthase 2	cox 2/PTGS2	apoptosis array	M90100/U04636	0.5 kb, 5's, 3's, pA, no sig O/L	cyclooxygenase-2; prostaglandin endoperoxidase synthase2,same clone as B/B3
cox2 (2)	147050	cyclooxygenase 2, prostaglandin-endoperoxide synthase 2	cox 2/PTGS2	Implantation array	M90100		same clone as H/A12
cPLA2	1676293	phospholipase A2 cytoplasmic	cPLA2	Implantation array	M68874		
CRABP1	357838	retinoic acid BP CRABP1(cellular)	CRABP1	Implantation array	S74445		
CRABP2	739913	retinoic acid BP CRABP2 (cellular)	CRABP2	Implantation array	M68867		
CRADD	700353	CASP2 and RIPK1 domain containing adapter with death domain	CRADD	apoptosis array	U84388 /Hs155566	1.1 kb, pA, 5's3's, no extraneous o/l, NOTE SIZE	interacts with RIP (DD)& caspase2, constitutively expressed
CRH	143383	corticotropin releasing hormone	CRH	Implantation array	NM_000756/Hs.75294		
CRHR1	178169	corticotrophin releasing factor receptor1	CRHR1	Implantation array	L23332		

Gene ID	IMAGE	Gene	Abbrev	clone source	Acc.No./Unigene ID	clone details	other information & changes to list name
CRYAA	190072	crystallin alpha A	CRYAA	Implantation array	U66584		
CRYAB	172505	crystallin alpha B	CRYAB	Implantation array	S45630/Hs,1940		
CSF1R	142323	colony stimulating factor 1 receptor (c-fms)	CSF1R (c-fms)	Implantation array	Hs.174142/R70654/X03663		feline sarcoma viral (v-fms) oncogene homolog
CSF2	1601601	Colony stimulating factor 2	CSF2	Implantation array	M11220		granulocyte-macrophage
CSF2RA	140352	colony stimulating factor 2 receptor alpha,low affinity granulocyte macrophage	CSF2RA	Implantation array	M37435/Hs.182378	0.5 kb, 5's, NO 3's, NO pA	same clone as G/G8 apoptosis array
CSF2RA	140352	colony stimulating factor 2 receptor alpha	CSF2RA	apoptosis array	Hs.182378/X54935	0.5 kb, 5's, NO 3's, NO pA	
CSF2RB	141115	colony stimulating factor 2 receptor B	CSF2RB	Implantation array	M59941		
CSF3	1074540	Colony stimulating factor 3 (granulocyte)	CSF3	Implantation array	M17706/Hs.2233		
CSF3R	247087	colony stimulating factor 3 receptor (granulocyte)	CSF3R	Implantation array	M59820		
CSFRA	289342	colony stimulating factor 2 receptor A (granulocyte-macrophage)	CSF2RA	Implantation array	L29348		
CSH1	60749	placental lactogen, chorionic somatomammotropin hormone 1	CSH1	Implantation array	J00118		from SAGE set
CSH2	140370	chorionic somatomammotropin hormone 2	CSH2	Implantation array	Hs.3344372/NM_020991		
cst3	949938	cystatin C,amyloid angiopathy & cerebral hemorrhage	CST3	Implantation array	X05607		homology with CST…
CTF1	1562882	cardiotrophin 1	CTF1	Implantation array	U43030		
CTGF	2142125	connective tissue growth factor	CTGF	apoptosis array	Hs.75511	0.7kb, No 5's, 3's, pA, no sig O/L	cysteine-rich mitogen secreted by human vascular endothelial cells (U14750)
CTNA	203313	catenin alpha	CTNA	apoptosis array	D13866	1.0 kb, 5's, 3's, pA, no sig O/L	
CTNNB1	415546	catenin,beta 1 (cadherin associated protein)	CTNNB1	Implantation array	X87838		
CTP	unknown	mitochrondrial citrate transporter,citrate transport protein	CTP,SLC25A1	Implantation array	Hs.111024/BC004980		
CTSB	898035	cathepsin B	CTSB	Implantation array	L16510		
CTSL	130796	cathepsin L	CTSL	Implantation array	NM_001912		
CXC-R4	713888	CXC-R4 = fusin,chemokine (C-X-C) motif ,receptor 4	CXC-R4 = fusin	apoptosis array	Hs.89414	0.3' pA, 0.6 kb, note great homology to H.sapiens mRNA for neuropeptide Y-like receptor	
cyclin A	683100	cyclin A	CCNA	apoptosis array	X51688	0.8 kb, 3's, 5's, pA, no sig O/L	
cyclin C (1)	163424	cyclin C	CCNC	apoptosis array	M74091 /Hs118442	0.8 kb, 3's, no5's, pA	
cyclin C (2)	503756	cyclin C	CCNC	apoptosis array	Hs.118442	0.6 kb, 3's, 5's, pA, no sig O/L	
cyclin D1(1)	325020	cyclinD1	CCND1	apoptosis array	X59798/Hs.82932	0.7 kb, 3's, 5's, pA, no sig O/L	bcl-1, PRAD1: parathyroid adenomatosis 1
cyclin D1(2)	unknown	cyclin D1	CCND1	Implantation array	Hs.82932/M64349		bcl-1, PRAD1: parathyroid adenomatosis 1
cyclin D2	366412	cyclin D2	CCND2	apoptosis array	D13639	0.9 kb, 3's, 5's, pA, no sig O/L	
cyclin D3	1877087	cyclin D3	CCND3	apoptosis array	M92287 /Hs.83173	0.6 kb, 3's, pA, no sig O/L	
cyclin E	68950	cyclin E	CCNE	apoptosis array	M73812	0.6 kb, 3's, 5's, pA, no sig O/L	
cyclin G1	2115540	cyclin G1	CCNG1	apoptosis array	U47413	0.6 kb, NO 5's, 3's, pA, no sig O/L	
cyclin G2	1637315	cyclin G2	CCNG2	apoptosis array	U47414/Hs79069	1.0kb, 3's, NO 5's, pA, no sig O/L	
cyclin H	730411	cyclin H	CCNH	apoptosis array	U11791	1.4 kb, 3's, 5's, pA, no sig O/L	
CYP11A	69087	cytochrome P450 subfamily XIA,17, 20-desmolase	CYP11A	Implantation array	M14565/Hs.76205		
cyt C	264845	cytochrome C	HCS	apoptosis array	Hs.169248/M22877	1.0 kB, 5's, no 3' s, no unwanted homology	unigene cluster listed Hs.697 now "retired"

Gene ID	IMAGE	Gene	Abbrev	clone source	Acc.No./Unigene ID	clone details	other information & changes to list name
Cyt C Ox	79597	cytochrome C oxidase,subunit IV isoform 1	COX4I1,COX4	in-house clone	M21575/Hs347969	0.7kb	
DAD-1	139702	Defender against cell death-1	DAD-1	apoptosis array	D15057 /Hs.82890	0.7kb, 3's5's, pA, note some homol with TCR	component of oligosaccharyltransferase which inhibits apoptosis of BHK21-derived tsBN7 cell line
DAK-P	1607097	death associated protein kinase 2 related protein	DAPK2	apoptosis array	AF052941/Hs.129208	0.5 kb, NO 5's, 3's, pA, no sig O/L	
DAP1	208557	death associated protein1	DAP1	apoptosis array	Hs.75189/X76105	1.0 kB, 5's, 3' s, pA, no unwanted homology	mediates IFN-gamma-induced cell death
DAPK1	364934	Death-associated protein kinase 1	DAPK1	apoptosis array	X76104 /Hs153924	0.7 kB, 5's, 3' s, pA, no unwanted homology	thymidine kinase II, calmodulin-dependent serine/threonine kinase, mediator of gamma IF-induced apoptosis
DAPK3	2107336	DAPK 3 (ZIP kinase) death associated protein kinase 3	DAPK3	apoptosis array	NM_001348/Hs25619	0.7 kb, NO 5's, 3's, pA, no sig O/L - watch for homol with DAPK-rel-prot	cytoskeletal reorganisation in apoptosis
DCC	1540499	deleted in colon carcinoma	DCC	Implantation array	X76132		
DCL1	869233	deleted in liver cancer 1	DLC1	Implantation array	AF035119		
destrin	152271	Destrin,actin depolymerising factor	DSTN	apoptosis array	Hs.82306	0.6 kb, 5's, 3's NO pA, no sig O/L, but there is a pseudogene	(actin depol factor)
DFFA	841357	DNA fragmentation factor,45KD alpha polypeptide	DFFA	apoptosis array	NM_004401/hs.105658	0.8 kb, NO pA, 5's3's, no extraneous o/l	ICAD (p40)
DFFB	1030349	DNA fragmentation factor beta,40KD caspase -activated Dnase	DFFB	apoptosis array	NM_004402/Hs133089	0.6 kb, pA, NO 5', has3's, no extraneous o/l	probably human CPAN homologue of mouse CAD (p45)
DIO2		deiodinase iodothyonine type II	DIO2	in-house clone	U53506/Hs.154424	pCMVSPORT 2	
DLX4	134789	distal-less homeobox 4	DLX4	Implantation array	NM_001934		hom DLX3 but not last 0.8kb
DLX4	252364	distal-less homeobox 4,distal-less homeobox 7&also BP1	DLX4	Implantation array	Hs.172648/BE883924		hom DLX4/DLX7 100%
DNA PK	1301908	DNA-activated protein kinase catalytic polypeptide	DNA-PK,PRKDC	apoptosis array	Hs.155637/U47077	0.6 kb, 3', pA, some homology to Human HepG2 3' region cDNA, clone hmd3h01	catalytic subunit, Ser/Thr kinase, ? tethers DNA strands as additional function, mutation-> SKID
DNHC	116552	dynein,cytoplasmic, heavy chain 1	DNHC1	Implantation array	Hs.7720/AB002323		
DRAK1	687542	DRAK1,Serine/threonine kinase 17a(apoptosis -inducing)	STK17A,DRAK1	apoptosis array	NM_004760/Hs.9075	0.6 kB, 5's, 3' s, pA, no unwanted homology	]ubiquitous, nuclear, pro-apoptotic
DRAK2	594966	DRAK2,serine/threonine kinase 17B	DRAK2,STK17B	apoptosis array	NM_004226	1.4 kB, 5's, 3' s, no pA	pro-apoptotic
DVL	147182	dishevelled 3	DVL3	Implantation array	U75651/Hs.174044	last 1.2kb	phosphoprotein
E-cadherin	900290	E-cadherin, cadherin 1, type1	CDH1	apoptosis array	Z13009	0.6 kb, 3's, NO 5's, pA, no sig O/L	(uvomorulin UVO, L-CAM, cell-CAM 120/80, Arc-1)
E-selectin	1518164	E-Selectin (ELAM1)	ELAM-1	apoptosis array	M24736	0.7 kb, 3's, NO 5's, pA, no sig O/L	transcription induced by TNF alpha or IL1 beta, mediates leucocyte rolling on endothelial cells, Survival function
E2F1	768260	E2F transcription factor 1	E2F1	endogenous control	M96577		
E2F2	2112387	E2F transcription factor 2	E2F2	apoptosis array	Hs.121487	5' no 3', 0.7 kb, some homology to E2F3	
E2F3	1627984	E2F transcription factor 3	E2F3	apoptosis array	Hs.1189	0.6kb, 3's, NO 5's, pA, no sig O/L	
E2F4 (1)	700683	E2F transcription factor 4,p107/p130-binding	E2F4	apoptosis array	Hs.108371	1.0 kb, 5's, 3's, NO pA, no sig O/L	
E2F4 (2)	768048	E2Ftranscription factor4, p107/p130-binding	E2F4	Implantation array	U15641		
E2F5 (1)	701492	E2F transcription factor 5,p130 binding	E2F5	apoptosis array	U15642 /Hs.2331	1.0 kb, 5's, 3's, NO pA, some O/L with E2F4	
E2F5 (2)	809828	E2Ftranscription factor 5, p130-binding	E2F5	Implantation array	U31556		
E2F6	1557277	E2Ftranscription factor 6	E2F6	Implantation array	AF059292		
EDG-2	1624490	Endothelial differentiation G coupled protein receptor 2	EDG-2	apoptosis array	Hs.75794	0.7kb, 3's, NO 5's, pA, no sig O/L	is VZG-1, lysophosphatidic acid receptor
EDG-4	2312192	Endothelial differentiation gene 4	EDG-4	apoptosis array	Hs.122575	0.6kb, 3's, NO 5's, NO pA, no sig O/L	lysophosphatidic acid receptor G protein coupled
EDG-5	1844972	Endothelial differentiation gene 5	EDG-5	apoptosis array	Hs.202672	1kb, 5's, no 3's, no pA, no sig O/L	
EDN1	40813	endothelin 1	EDN1	Implantation array	NM_001955		

Gene ID	IMAGE	Gene	Abbrev	clone source	Acc.No./Unigene ID	clone details	other information & changes to list name
EDN2	1693357	endothelin 2	EDN2	Implantation array	M65199/Hs.1407		
EDN3	341732	endothelin 3	EDN3	Implantation array	J05081/Hs.1408		
EDNRA	489571	endothelin receptor type A	EDNRA	Implantation array	L06622		
EDNRB	264557	endothelin receptor type B	EDNRB	Implantation array	L06623		
EEF1A1	1412228	Eukaryotic translation factor 1 alpha 1	EEF1A1	apoptosis array	Hs.181165/BG177198	SIZE UNKNOWN (all known sizes were 1.8 kb and above), 3' no 5', pA, no O/L	
EEF1B2	unknown	Eukaryotic translation elongation factor 1 beta 2	EEF1B2	Implantation array	Hs.275959/BC000211		
EEF2	34849	eukaryote translation elongation factor 2	EEF2	Implantation array	Z11692/Hs 75309		
EEF2	2096525	Eukaryotic translation elongation factor 2	EEF2	apoptosis array	Hs.75309/X51466	0.6 kb, 3', pA, no O/L	Eukaryotic translation elongation factor 2
EGF	2092678	Epidermal growth factor (beta-urogastrone)	EGF	Implantation array	Hs.2230/X04571	0.9kb,3',pA	
EGF-LIKE	470706	heparin-binding EGF-like GF,Diptheria toxin receptor	DTR	Implantation array	M60278/Hs.799		
EGFR	149925	epidermal growth factor receptor (c-erb B)	EGF-R	Implantation array	X00588/Hs.77432		
EGR-1	68041	Early growth response 1	EGR-1	apoptosis array	M62829 /Hs.326035	0.7 kb, 5's, 3's, pA, no sig O/L	
ELF 1a(2)		eukaryotic translation elongation factor 1 alpha 1	EEF1A1	Implantation array	Hs.181165/BF700509		
ELF 1a(3)		eukaryotic translation elongation factor 1 alpha 1	EEF1A1	Implantation array	Hs.181165/BF700509		
ELF 1a(4)		eukaryotic translation elongation factor 1 alpha 1	EEF1A1	Implantation array	Hs.181165/BF700509		
ELF 1a(5)		eukaryotic translation elongation factor 1 alpha 1	EEF1A1	Implantation array	Hs.181165/BF700509		
ELF 1a(6)		eukaryotic translation elongation factor 1 alpha 1	EEF1A1	Implantation array	Hs.181165/BF700509		
Elf 1alpha		eukaryotic translation elongation factor 1 alpha 1	EEF1A1	Implantation array	X16869		
endoglin	72461	endoglin,Osler-Rendu-Weber syndrome	ENG	apoptosis array	X72012/Hs.76753	0.7 kb, pA, 5's3's, no extraneous o/l	implicated in embryonic vascular assembly
ENG	134791	endoglin (Oster-Rendu-Weber syndrome 1)	ENG	Implantation array	X72012/Hs.76753		
enigma		enigma (LIM domain protein)	ENIGMA	Implantation array	NM_005451		image ID unknown
ENPEP	1714899	aminopeptidase A, glutamyl aminopeptidase	ENPEP	Implantation array	L12468		
EphA1	591828	ephrin type-A receptor 1	EPHA1	apoptosis array	M18391/Hs89839	0.9 kb, 3's, NO 5's, pA, no sig O/L	
EphA2	592634	ephrin type-A receptor 2	EPHA2	apoptosis array	M59371/Hs171596	0.8 kb, pA, 5's3's, no extraneous o/l	
EphB1		ephrin receptor 1 type B	EpHB1	in-house clone		pCR-Script	EpH like receptor kinase (also NET PTK)
EphB2		ephrin receptor 2 type B	Eph B2	in-house clone		pCR-Script,	
EPHB2	2062345	EphB2,ephrin type-B receptor 2	EPHB2	apoptosis array	L41939/Hs.125124	0.8 kb, no pA, 3's	erk protein tyrosine kinase some o/l with receptor protein-tyrosine kinase (HEK5)
EphB2	2062345	ephrin type-B receptor 2	EPHB2	apoptosis array	L41939/Hs 125124	0.8 kb, no pA, 3's,	some o/l with receptor protein-tyrosine kinase (HEK5)
EPHB3	796057	Ephrin type-B receptor 3,EphB3, HEK1	EPHB3	apoptosis array	X75208/Hs 2913	length not determined, pA, 5's3's	also Hek-2 note some o/l with other Eph's
EphB4		erythropoietin producing hepatocellular ,ephrin receptor B4	EpHB4	in-house clone		pCR-Script, antisense,	homolgy ACHE,TRIP6 ,CIP1, ZAN zonadhesion
ephrinB1		EphrinB1,EPLG2(LERK-2) ligand eph related kinase	EFNB1	in-house clone			EpH like receptor tyrosine kinase
ephrinB2		Ephrin B 2	EFNB2	in-house clone			
ErbB2	365147	V-erb-b2 avian erythroblastic leukemia viral oncogene hom.	ErbB2	Implantation array	X03363		last 1.8kb
ErbB4	79829	V-erb-a avian erythroblastic leukemia viral oncogene hom.4	ErbB4	Implantation array	L07868		

Gene ID	IMAGE	Gene	Abbrev	clone source	Acc.No./Unigene ID	clone details	other information & changes to list name
EREG	1256213	epiregulin	EREG	Implantation array	D30783		
Erk1	927361	Erk1,extracellular-signal related kinase 1	MAPK3	apoptosis array	X60188	0.6 kb, 3's, no 5's, pA, no sig O/L	mitogen activated protein kinase 3
Erk2	195122	Erk2, MAPK1 mitogen-activated protein kinase 1	Erk2	apoptosis array	M84489 /Hs.324473	0.7 kb, 5's, 3's, pA, no sig O/L	(MAP K 1)
Erk3(1)	1129873	MAPK6, Erk3 mitogen-activated protein kinase 6	MAPK6,Erk3	apoptosis array	X80692 /Hs.271980	0.7kb, 3's, pA, no sig O/L	(p97 MAP K6)
Erk3(2)	1129873	Erk3, mitogen-activated protein kinase 6	Erk3,MAPK6	apoptosis array	X80692	0.7kb, 3's, pA, no sig O/L	(p97 MAP K6)
Erk4	32410	mitogen activated protein kinase kinase 4	Erk4	apoptosis array	Hs.75217/L36870	0.6 kb, 3' only, pA, no O/L	(MAP2 K 4), Mitogen-activated protein kinase kinase 4
Erk5	472099	Erk5 ,mitogen-activated protein kinase 7	MAPK7,Erk5	apoptosis array	U25278 /Hs.3080	0.6 kb, NO 5's, 3's, no Pa, no sig O/L	BMK1 (big map kinase 1), MAPK7
Erk6 (2)	2467159	Erk6, MAPK12 mitogen -activated protein kinase 12	Erk6	apoptosis array	X79483	0.7 kb, 3's, NO 5's, no pA, no sig O/L	SAPK3, MAPK12
Erk6(1)	2467159	MAPK12, mitogen -activated protein kinase 12, extracellular signal related kinase 6, Erk6	MAPK12,Erk6	apoptosis array	X79483 /Hs.55039	0.7 kb, 3's, NO 5's, no pA, no sig O/L	SAPK3, MAPK12
ESM1	324122	endothelial cell specific molecule 1	ESM 1	Implantation array	X98426		
ESPN		ESPIN	ESPN	Implantation array	Hs.251216/BM017262		
ESR2	Who cl.15	estrogen receptor 2 (ER beta)	ESR2	Implantation array	AF051427		primers29/30
ESRA	WHO cl.14	estrogen receptor alpha	ESRA	Implantation array	M12674		primers 27/28
ESRR	WHO cl.6	estrogen R related-protein	ESRR	Implantation array	M69296		primers 11/12
EST 1	1553406	EST 1		implantation array			uterus-specific EST
EST 2	15383778	EST 2		implantation array			uterus-specific EST
EST 3	14750	EST 3,maybe poor clone CCND1		implantation array			seq poor but partial match to CCND1,Hs.82932/M74092
EST 4	595154	EST 4		implantation array			uterus-specific EST
EST 5	2204189	EST 5		Implantation array			uterus
EST 6	2207731	EST 6		Implantation array			uterus
EST 7	487548	EST 7		Implantation array	AA045001		uterus
EST 8	2493987	EST 8		implantation array			uterus-specific EST
EST 9	470067	EST 9		Implantation array	AA029063		uterus
EST 10	469652	EST 10		Implantation array	AA027953		uterus
EST 11	486325	LOC51241,hypothetical protein	LOC51241	implantation array	Hs.171566/AF151037		uterus-specific EST
EST 13	1697909	EST 13		Implantation array			uterus
EST 14	2276569	EST 14(SEE NOTES col R)		Implantation array	Hs.37106/BC004479		MAGEA11 Melanoma Antigen,family,A
EST15		EST expressed in CD34+ hematopoietic stem/progenitor cells		Implantation array		5'end	
EST16		EST16		Implantation array			listed as MUC1(590873) is EST found germinal center B cells and differentiated psot mitotic neurones
EST17	725124	EST17,cDNA expressed CD34+ hematopoietic stem/progenitor cells	EST17	Implantation array	M34225		NOT KRT8 keratin as previously listed
EST18	1742759		EST	Implantation array			sequence has similarity to laminin binding protein (receptor) but NO match pairwise BLAST to laminin receptor Hs.181357
EST19		EST19 good match EST fetal brain		Implantation array	AL565639		
EST20		EST20		Implantation array			
EST21	unknown	EST21,not strictly an EST BAC clone on chr.14		Implantation array	AC009469		NB also contains repetitive elements
EST22	145503	lysosome associated membrane glycoprotein 1 precursor	EST22	Implantation array	AI201935		
EST23	247281	EST23	EST23	apoptosis array		3', pA, 0.7 kb, no sign. O/l	
EST24	150685	Hypothetical protein	EST24	Implantation array	Hs.319946/AB051514		
EST25	954771	EST25	EST25	Implantation array			
EST26		EST26		in-house clone			
EST27	2218885	EST27	EST27	apoptosis array		size unknown, 3's No 5', pA unknown	

Gene ID	IMAGE	Gene	Abbrev	clone source	Acc.No./Unigene ID	clone details	other information & changes to list name
EST28	1101471	EST28,MGC18386 similar to RIKEN cDNA 2610036L13	EST28	apoptosis array	Hs.23044	3', 0.6 kb, pA, no o/l	previously listed as RAD-51
EST29	212059	partial match to enoyl-co hydratase,Alu elements similar to TNF alpha induced protein1		Implantation array	L07077,Hs.119683		
EST30	147628	DKFZP56600424 hypothetical protein		Implantation array	Hs.226770/AI669519		in IMAGE database as PDGFRA originally
EST31		part matches novel EST & part of sequence matches ribosomal proteins	EST31	Implantation array	not assigned		
EST31		part matches novel EST & part of sequence matches ribosomal proteins	EST31	Implantation array	not assigned		
EST32	2435972	uterus ESTs	EST32	Implantation array	Hs.345027		previously listed as MAGEA11
EST33	131044	EST33		Implantation array	BG289550		miss-assigned clone was listed as CTNND1 catenin
EST34	546171	EST 34		apoptosis array		0.8 kb, pA, 3's, NO 5's, no extraneous o/l	
EST35	1523225	EST35	EST35	Implantation array	AV734688		
EST36	unknown		EST36	Implantation array			
EST37	WHO cl.2	unclassified,unidentified	EST37	Implantation array		pGEMT	
EST38	2016609	EST38 very similiar to retinoblastoma protein 3	EST38	apoptosis array		1.3 kb	
EST39	591683	EST39	EST39	Implantation array	BF526248		
EXO1	1523478	exonuclease 1	EXO1	apoptosis array	Hs.47504/AF060479	0.9 kb, 3', no pA, great homology to hex1	
F3	136590	tissue factor , thromboplastin, coagulation factor III	F3	Implantation array	J02931/Hs62192		
FADD	2428304	FAS associated via death domain	FADD	apoptosis array	U24231/Hs.86131	0.6 kb, pA, 3's no 5', no extraneous o/l	DD-containing adapter between Fas/TNFR1&caspase8, aka MORT-1 mediator of receptor induced cytotoxicity
FAF1	344282	Fas (TNFRSF6) associated factor 1	FAF1	Implantation array	NM_007051		
FAK-1	343717	Focal adhesion kinase 1	FAK-1	apoptosis array	Q05397/Hs740	0.7 kB, 5's, 3' s, pA, no unwanted homology	PTK2, non-receptor TK, suppresses apoptosis following adhesion, cleaved by caspases during apoptosis
FAK-2	739904	PTK2B protein tyrosine kinase 2 beta	FAK-2	apoptosis array	L49207/Hs.20313	1.3 kB, 5's, no 3' s, no unwanted homolog, NOTE SIZE	PYK2
FAS	1949870	Fas,Apo1 fas soluble protein,TNF superfamily member6	FAS,TNFRSF6	apoptosis array	Z70519	0.6 kb, pA, NO 5' but 3', no extraneous o/l	key death receptor/CD95
FASTK	127525	FAST Kinase	FASTK	apoptosis array	X86779 /Hs75087	0.8 kb, pA, 5's3's, no extraneous o/l	
FAU	783057	Finkel-Biskis-Reilly murine sarcoma virus	FAU (MNSF beta)	Implantation array	X65923/Hs.177415		monoclonal nonspecific repressor factor
FBN5	WHO cl.7	fibrillin 5	FBN5	Implantation array	X62009		primers 13/14,NB note homology to FBN2 Hs.79432/X6200
FGF R1	154472	fibroblast growth factor receptor 1	FGF R1	Implantation array	Hs.748/M60485		fms-related tyrosine kinase 2,pfeiffer syndrome
FGF-1	30869	fibroblast growth factor 1, acidic	FGF1	Implantation array	X51943		
FGF-2	323776	fibroblast growth factor 2, basic	FGF2	Implantation array	M27968		
FGF7	365515	keratinocyte GF (FGF 7)	FGF 7	Implantation array	M60828		last 0.5kb
FGFR3	669416	FGF receptor-III,achondroplasia,thanatophoric dwarfism	FGFR3	apoptosis array	Hs.1420	0.9 kb, 5's, 3's, no sig O/L	
FHIT	681997	fragile histidine triad gene	FHIT	Implantation array	U46922/Hs.77252		DXL5
fibulin		fibulin-1CX53743	FBLN1	in-house clone	X53743/Hs.79732	pCMVSPORT 2	
FKBP3		FK506 binding protein 3 (25KD)	FKBP3	in-house clone	Hs.350402/NM_002013	pCMVSPORT 2, Clones from J&J	previously listed as RBP
FLIP	2096139	FLIP (casper, CLARP, FLAME-1)	FLIP	apoptosis array	AF010127	0.7 kb, pA, 3's, homologies to caspase-like apoptosis protein 2 (clarp), CASH beta protein, FLICE-like inhibitory protein	antiapoptotic, interacts with FADD, caspase-8, caspase-3, TRAF1, and TRAF2, DED and caspase-like domains
FLJ20886	130951	HSP22 like hypothetical protein	FLJ20886	apoptosis array	Hs.6289/AF302079	0.7 kb, 3's, 5's, pA, no O/L	previously listed as GRB2 miss-assigned
Flt	UD2	FLT 1, Fms-related tyrosine kinase 1 (vascular endothelial growth factor)	FLT	in-house clone	Hs.138671	B/S11 KS +/- 5'end all flt	
Flt 1		Fms-related tyrosine kinase 1	Flt 1	in-house clone	X51602/Hs.138671	pCMVSPORT 2	

Gene ID	IMAGE	Gene	Abbrev	clone source	Acc.No./Unigene ID	clone details	other information & changes to list name
flt4	1716286	flt 4(VEGFR-3) Fms related tyrosine kinase 4	Flt 4	apoptosis array	Hs.74049/X69878	0.7 kb, pA, 3's, no 5' sequence, no extraneous o/l	fms-related tyrosine kinase 4,some homology to MHC I
FLT4 (1)	25	Fms-related tyrosine kinase 4 (VEGFR3)	Flt 4	in-house clone	Hs.74049/U43143	pCR-Script, 3' end	
flt4 (2)	5	Fms-related tyrosine kinase 4	Flt 4	in-house clone	Hs74049	pCR-Script, 3' end	
Flt4 (3)	3	Fms-related tyrosine kinase 4	Flt 4	in-house clone		B/S11 KS +/-, 5'end	seq matches chr.8 ESTs & partially vimentin but unconfirmed as flt4 (chr.5),ED6 clone 25 verified
flt4 (4)	15	Fms-related tyrosine kinase 4	flt-4	in-house clone		B/S11 KS +/-, full length Kendal	ED6 clone 25 verified
FN1	550038	fibronectin 1	FN1	Implantation array	X02761		
Fork 01A	1572033	Forkhead box O1A(rhabdomyosarcoma)	FOXO1A	in-house clone	Hs170133/AF032885	3's, no 5's,0.6kb	FKHR forkhead protein
Fork 03A	594389	Forkhead box O3A	FOXO3A	in-house clone	Hs169277/AA169707	3's & 5's,0.7kb	forkhead protein FKHRL1
FR2	214573	thrombin receptor (coagulation factor 2)	F2R	Implantation array	M62424		
friz7	162847	frizzled homolog 7 (drosophila)	FZD7	Implantation array	AB017365		last 1.2kb
frizzled1	1881856	frizzled1	FZD1	apoptosis array	Hs.94234/AB017363	0.7 kb, 3' no 5', pA, No sig O/L	
FRZB	364200	frizzled related protein	FRZB,fritz	Implantation array	U24163		
FSHB	WHO cl 1	follicle stimulating hormone beta	FSHB	Implantation array	NM_000510	pGEMT	WHO cl.1 primers 1/2(444bp)
FSHB	2177805	follicle stimulating hormone beta	FSHB	Implantation array	NM_000510		
FST	124543	follistatin	FST	Implantation array	NM_006350		
FTH1	68958	ferritin heavy polypeptide 1	FTH1	Implantation array	M11146		
FZD1		frizzled (Drosophila) homolog 1	FZD1	in-house clone	AB017363/Hs.94234		
FZD2	2288713	frizzled 2	FZD2	Implantation array	AB017364		hom friz 1 7 3 5 9
FZD2	1574734	frizzled (Drosophila) homolog 2	FZD2	apoptosis array	Hs.81217		
FZD3	756467	frizzled 3	FZD3	Implantation array	U82169		hom friz 6
FZD4 (1)	2171485	frizzled homolog 4 (Drosophilla)	FZD4	Implantation array	AB032417/Hs.19545		
FZD 4 (2)		frizzled (Drosophila) homolog 4	FZD4	in-house clone	Hs.19545/AB032417		
FZD5	1076089	frizzled homolog 5 (Drosophilla)	FZD5	Implantation array	U43318		last 0.4kb
FZD6	283451	frizzled homolog 6 (drosophila)	FZD6	Implantation array	AB012911		
FZD6		frizzled (Drosophila) homolog 6	FZD6	in-house clone	Hs.114218/AB012911		
FZD7		frizzled (Drosophila) homolog 7	FZD7	in-house clone	Hs.173859/AB017365		
FZD8	219666	frizzled homolog 8 (drosophila)	FZD8	Implantation array	AF086500/Hs302634		
FZD 9	2338452	frizzled (Drosophila) homolog 9	FZD9	apoptosis array	Hs.158335	0.7 kb, 3's, NO 5's, NO pA, notice homology with frizzled 3	
FZD10		frizzled (Drosophila) homolog 10	FZD10	in-house clone	Hs.31664/AB027464		
G3PDH	2166731	glyceraldehyde-3-phosphate dehydrogenase	G3PDH, GAPD	Implantation array	M17851		
GADD34	2019582	GADD34,PPP1R15A protein phosphatase 1,regulatory (inhibitor)subunit 15A	GADD34	apoptosis array	Hs.76556/U83981	0.6 kb, 3', pA, some homology to junB	
GADD45(1)	135381	Growth arrest and DNA damage -inducible	GADD45	apoptosis array	U83981/L24498	0.7 kb, 3's, 5's, pA, no sig O/L	
GADD45(2)	415112	Growth arrest and DNA damage -inducible alpha	GADD45	apoptosis array	M60974/Hs80409	0.8 kb, 3's, 5's, pA, no sig O/L	NB same gene diff clone I/E3
GAPDH		Glyceraldehyde-3-phosphate dehydrogenase	GAPD	in-house clone	Hs.169476/M33197	B/S11 KS +/-	
GBE1	2140558	glucan 1,4-alpha,branching enyzme 1 (glycogen branching enzyme, Andersen disease, glycogen storage disease type (IV)	GBE1	in-house clone	L07956/Hs.1691	3's, no 5's,0.9kb	
GDH	1873366	glutamate dehydrogenase	GDH	apoptosis array	Hs.149155	0.6 kb, 3' read, pA, search -> no O/L	Originally assigned for VDAC-1 by Image
gDNA	857612	genomic clone chr. 19	gDNA	Implantation array			miss-assigned
GHR	2692010	growth hormone receptor	GHR	apoptosis array	Hs.125180/X06562	3' no 5', unknown size, pA, no sig o/l	
GJA1	132891	gap junction protein, alpha 1, Connexin 43	GJA1	Implantation array	M65188		

Gene ID	IMAGE	Gene	Abbrev	clone source	Acc.No./Unigene ID	clone details	other information & changes to list name
GP130	429893	gp130, interleukin 6 signal transducer,oncostatin m receptor	GP130/IL6ST	Implantation array	M57230		subunit il 6
GPR49	2149968	G-protein coupled receptor 49,orphan G protein	GPR49	Implantation array	Hs.285529/G51260		
GPX		Glutathione peroxidase	GPX	in-house clone	Hs76686/AA074470	B/S11 KS +/-	
GRB10	137049	Growth factor receptor-bound protein 10	GRB10	apoptosis array	U69276/Hs81875	0.7 kB, 5's, 3' s, pA, no unwanted homology	binds insulinR and IGF-1 R and suppresses receptor survival activity
GRL	140925	Glucocorticoid receptor alpha and beta	GRL	apoptosis array	Hs.75772/U80947	3's, 5's, pA, 0.7 kb, no sig O/L	alpha and beta are alternative splice variants
GRO 2	841361	GRO2 oncogene	GRO 2	Implantation array	M36820		hom GRO1/3
GRO1	323238	GRO1oncogene	GRO 1	Implantation array	X12510		hom GRO2/3
GRP58	261497	phospholipase C alpha,glucose regulated protein,58KD	GRP58	Implantation array	D16234/Hs289101		
GSK3B	1072113	GSK3B glycogen syntyetase 3 beta	GSK3B	Implantation array	Hs.78802/AA641950		
GSK3B	1853459	glycogen synthase kinase 3 beta	GSK3B	Implantation array	L33801		
GSR	1056796	glutathione reductase	GSR,GRD1	apoptosis array	X15722 /Hs.121524	0.7 kb, NO 5's, 3's, NO pA, no sig O/L	detoxication of xenobiotics
GST P1	2224433	Glutathione S transferase pi	GSTP1	apoptosis array	Hs.226795/U12472	0.6 kb, 3's, pA, no sig O/L	detoxication of xenobiotics
GST T1	125180	Glutathione S transferase,theta	GSTT1	apoptosis array	X79389 /Hs77490	0.8 kb, 5's, 3's, pA, no sig O/L	detoxication of xenobiotics, theta
GSTA1	1573402	Glutathione S-transferase A1 (contains gene for A2)	GST A1	apoptosis array	M14777 /Hs89552	0.7kb, 3's, pA, no sig O/L	detoxication of xenobiotics, A1 and A2 homologous
H-Ras	2114795	HRAS,v-Ha-ras Harvey rat sarcoma viral oncogene homolog	HRAS	apoptosis array	Hs.37003	0.6 kb, 5's, 3's, pA, no sig O/L	Harvey Ras
Harikari	1519582	Harakiri Bcl-2 interacting protein	HRK	apoptosis array	U76376/Hs87247	0.4 kb, NO pA, NO 5's but has 3's, no extraneous o/l	an activator of apoptosis,DR5
HBA1	unknown	alpha globulin ,hemoglobin	HBA1	Implantation array	NM_000558		
HCG alpha	13184	human chorionic gonadotrophin, alpha polypeptide	HCG alpha	Implantation array	V00518		
HCGbeta	252284	human chorionic gonadotrophin, beta polypeptide	HCG beta (CGB)	Implantation array	J00117		hom LH beta
HDAC1	898976	histone deacetylase 1	HDAC1	Implantation array	U50079	last 0.3kb	last 0.3kb
HDAC1	898976	histone deacetylase 1	HDAC1	Implantation array	U50079	last 0.3kb	last 0.3kb
HDAC2	491639	histone deacetylase 2	HDAC2	Implantation array	U31814/Hs.3352	last 0.5kb	likely to have been a miss-assigned clone
HDAC3	144052	histone deacetylase 3	HDAC3	Implantation array	Hs.350277/U66914	last 0.7kb	
HDAC4	2177805	Histone deacetylase 4, KIAA0288	HDAC4	Implantation array	AI491868/Hs.91400	1.6kb	
HDAC4	1606829	KIAA0288, histone deacetylase 4	HDAC4	Implantation array	Hs.91400/AB006626	0.4kb,3' ,poly A	
HDAC6	669295	histone deacetylase 6	HDAC6	Implantation array	AB020708/Hs.6764		
HEC/SS24	WHO cl.9	Retinoblastoma associated protein HEC	HEC/SS24	Implantation array	AF017790		with WHO 17/18/primers (OKA FSHR primers)
HEXB	251802	hexosaminidase B(beta polypeptide)N-acetyl-beta-glucosaminidase	HEXB	in-house clone	M13519/Hs.51043	3's, no 5's, some homology to alpha subunit	
HGF(1)		Hepatocyte growth factor,hepapoietinA,scatter factor	HGF	in-house clone	Hs809/M29145	pCR-Script	hepapoietin A:scatter factor
HGF(2)	375833	hepatocyte growth factor (hepapoietin, scatter factor)	HGF	Implantation array	M60718/Hs.809		homologous to HGF heavy chain & has homolgy to CD34+
HIF1-alpha	142934	Hypoxia inducible factor1 alpha subunits (basic helix-loop-helix transciption factor)	HIF 1 alpha	apoptosis array	Hs.197540/U22431	0.9 kb, 5's, 3's, pA, no O/L	MOP1, ARNT interacting protein
HIF2 alpha	1733081	Hypoxia inducible factor 2 alpha	EPAS1	apoptosis array	Hs.8136/U51626	0.6 kb, 3' no 5' pA no sig. O/L	MOP2, HLF, EPAS1 endothelial PAS domain protein 1
HIFIA	897806	hypoxia -inducible factor1, alpha subunit	HIF1A	Implantation array	U22431		
HIFIA	897806	hypoxia -inducible factor1, alpha subunit	HIF1A	Implantation array	U22431		
His		Histidyl tRNA synthase	HIS	in-house clone	X05345/Hs.77798		
Histone	899722	H2A histone family member.X	H2AFX	apoptosis array	Hs.147097	0.6 kb, 3', pA, no o/l	phosphorylated by ATM after DNA damage
HLA-C	725228	major histocompatibility complex, class 1, C	HLA-C	Implantation array	M26429/Hs.277477		
HMGIY	701054	high mobility group (nonhistone chromosomal)proteins I&Y	HMGIY	apoptosis array	Hs.139800/AA287531	0.8 kb, pA, NO 5' but 3', no extraneous o/l	

Gene ID	IMAGE	Gene	Abbrev	clone source	Acc.No./Unigene ID	clone details	other information & changes to list name
HNRPA3	192262	Heterogeneous nuclear ribonucleoprotein A3	HNRPA3	Implantation array	Hs.249247/BM458287		previously listed as INHBC ,miss-assigned
Homocyst	545222	homocysteine-responsive gene		in-house clone		0.7kb	
HOXA10	487978	homeo box A10	HOXA10	Implantation array	AF040714/Hs.110637		
HOXA11	491209	homeobox A11	HOXA11	Implantation array	NM_005523		
HOXA13	591699	homeobox A13	HOXA13	Implantation array	NM_000522		
HOXA9	897497	homeo box A9	HOX A9	Implantation array	U82759		
HP	595154	Haptoglobin	HP	Implantation array	Hs 75990		
HPRT	727246	hypoxanthine phosphoribosyltransferase 1 (Lesch-Nyhan)	HPRT	Implantation array	M31642		
HSCPCO34	2045711	CD34+ hematopoietic stem/progenitor cell	HSPCO34	in-house clone	X79302	3's, no 5's,0.7kb	should really be listed as an EST think same as E/G3 EST15
HSD17B1	136491	hydroxysteroid (17-beta) dehydrogenase 1	HSD17B1	Implantation array	M36263		
HSDB	1759603	3-beta-hydroxy-5-ene steroid dehydrogenase (beta)	HSDB	Implantation array	M27137		
hsp60	69928	heat shock protein 60 kD protein 1 (chaperonin)	HSP60,HSPD1	Implantation array	M22382/Hs.79039		
hsp70	72831	heat shock protein 70 kD	HSP70	Implantation array	NM_005345		
HSP90	595057	Heat Shock Protein 90	HSP90	in-house clone	M16660	3's, no 5's,0.7kb	
HUS-1	1751692	HUS1(S.pombe) checkpoint homolog	HUS1	apoptosis array	Hs.152983/AF076844	0.6kb, 3', no pA, no o/l	
HXB	484707	tenascin C,hexabrachion,cytotactin	HXB	Implantation array	M55618/Hs.28914		
Hyp prot	2252160	GS3686 hypothetical protein expressed in osteoblast		in-house clone	AB000115/Hs75470	0.8kb	C1orf 29
I-kBalpha	358896	I-kB alpha,nuclear factor of kappa light polypeptide gene enhancer in Bcells inhibitor alpha	I-kB alpha, NFKB1A	apoptosis array	M69043/Hs.81328	0.7 kb, 3's, 5's, pA, no sig O/L	
ICAM-1	1535767	Intercellular adhesion molecule 1,ICAM-1 (CD54)	ICAM-1	apoptosis array	J03132 /Hs.168383	0.6 kb, 3's, NO 5's, NO pA, no sig O/L	expressed endothelium, binds LFA-2
ICAM1	145112	intercellular adhesion molecule 1 (CD54)	ICAM1	Implantation array	J03132		
ICAM2	127191	ICAM-2,intercellular adhesion molecule 2	ICAM2	Implantation array	Hs.347326/X15606		ligand for LFA-1
IEX-IL	588382	IEX-1L (DIF2) anti-death protein,also IER3 immediate early response protein	IER3,IEX-1L,DIF2	apoptosis array	AF09067/Y14551	0.8 kB, 5's, 3' s, pA, no unwanted homology	promotes NF-kappaB-mediated cell survival
IFN alpha5	WHOcl.10	interferon alpha-5	IFN alpha-5	in-house clone	Hs.37113/V00541	pGEMT	primers 19/20/424bp,chromosome 9
IFNG	1579639	interferon gamma	IFNG	Implantation array	M29383		
IFNGR1	151378	interferon gamma receptor 1	IFNGR1	Implantation array	J03143/Hs.180866		
IFNGR2	310905	interferon gamma receptor 2	IFNGR2	Implantation array	U05877		
IGF1	287327	insulin-like growth factor 1 (somatomedin C)	IGF 1	Implantation array	M29644		
IGF1R(1)	148379	insulin-like growth factor 1 receptor	IGF1R	Implantation array	X04434		last 1kb
IGF1R(2)	148379	insulin-like growth factor 1 receptor	IGF1R	Implantation array	X04434		last 1kb
IGF2	206372	insulin-like growth factor 2 (somatomedin A)	IGF 2	Implantation array	Hs.349109/X06159		
IGF2R(1)	668002	insulin-like growth factor 2 receptor	IGF2R	Implantation array	Y00285		
IGFBP1	469216	insulin-like growth factor binding protein 1	IGFBP1	Implantation array	NM_000596		NB contains repeat seqs
IGFBP2	2163663	insulin-like growth factor binding protein 2	IGFBP2	Implantation array	M35410		
IGFBP3	138707	insulin-like growth factor binding protein 3	IGFBP3	Implantation array	NM_000598		
IGFBP4	70980	insulin-like growth factor binding protein 4	IGFBP4	Implantation array	M62403		
IGFBP5	150555	Insulin-like growth factor binding protein 5	IGFBP5	Implantation array	Hs.180324/L27560		correct gene but recently assigned to different cluster
IgH	2178483	EST similiar to Ig Gamma-1 chain C	IgH	Implantation array			
IL1alpha	1645252	interleukin 1 alpha	IL1alpha	Implantation array	M28983		
IL1R2	137575	interleukin 1 receptor type II	IL1R2	Implantation array	X59770		

Gene ID	IMAGE	Gene	Abbrev	clone source	Acc.No./Unigene ID	clone details	other information & changes to list name
IL1RL1	486393	interleukin 1 receptor like 1	IL1RL1	Implantation array	NM_003856/Hs.66		
IL3	WHO cl.12	interleukin 3/mast cell growth factor	IL 3/MCGF	Implantation array	M14743		primers 23/24
IL6	2148410	Interleukin 6 (B-cell stimulatory factor-2)	IL6	Implantation array	Hs.93913/M18403		
IL6	1508411	interleukin 6 (interferon, beta 2)	IL6	Implantation array	M14584		
IL6R	80474	interleukin 6 receptor	IL6R	Implantation array	X58298		alpha chain + GP130
IL8	1651203	interleukin 8	IL8	Implantation array	M26383		
IL8 (2)	unknown	interleukin 8	IL8	Implantation array	M26383		
IL11	310124	interleukin 11	IL11	Implantation array	M57765		
IL11RA	182152	interleukin 11 receptor, alpha	IL11RA	Implantation array	U32324/Hs.64310		
IL11RA	182152	IL11 receptor alpha	IL11RA	apoptosis array	Hs.64310	0.9 kb, 5's, 3's, NO pA	
IL15	2064047	interleukin 15	IL15	Implantation array	U14407/X91233		
ILIRN	152577	interleukin 1 receptor antagonist	IL1RN	Implantation array	Hs.81134/X52016		
ILK	194179	integrin linked kinase	ILK	apoptosis array	U40282	0.6 kb, 5's, 3's, pA, no sig O/L	(beta1-integrin-linked protein kinase)
ING1	1641423	inhibitor of growth family,member1	ING1	apoptosis array	AF001954 /Hs46700	0.9 kb, 3's, NO 5's, pA, no sig O/L	cooperates with p53-indcued apoptosis
INHA	1711449	inhibin alpha	INHA	Implantation array	M13981		
INHBA	1723823	inhibin Beta A	INHBA	apoptosis array	Hs.727/M13436	0.7 kb, 3's, 5's, pA, no sig O?L	activin A, activin AB alpha polypeptide
INHBB (1)	323599	inhibin beta B (also Activin B)	INHBB	Implantation array	Hs.1735/BM31682		
INHBB (2)	1074867	inhibin beta B (also Activin B)	INHBB	Implantation array	M13437		last 0.7kb
INHBB (3)	415058	Inhibin beta B	INHBB	apoptosis array	Hs.1735/AL355334	0.4kb,3',pA unknown	previously listed as CLAP but not confirmed seq is INHBB
INK-4	1523215	p16/INK-1,CDK4- inhibitor =cyclin - dependent kinase inhibitor 2A	CDKN2A	apoptosis array	Hs1174	0.6 kb, 3', pA, no O/L	
INSR (1)	427812	insulin receptor	INSR	Implantation array	M10051		last 0.6kb
INSR (2)	427812	insulin receptor	INSR	Implantation array	M10051		last 0.6kb
IRF1	685033	Interferon regulatory factor 1	IRF1	Implantation array	NM_002198		
IRF2	122308	Interferon regulatory factor 2	IRF2	in-house clone	X15949	3's, no 5's,0.5kb	
ITGA1	2028225	integrin alpha 1	ITGA1	Implantation array	X68742		
ITGA2	687871	integrin alpha 2/CD49B	ITGA2	Implantation array	X17033		
ITGA3	505285	integrin alpha 3/CD49C	ITGA3	Implantation array	M59911/Hs.265829		
ITGA4	341922	integrin alpha 4/antigenCD49D	ITGA4	Implantation array	AI769736/Hs.40034		
ITGA5	135671	integrin alpha 5,fibronectin receptor	ITGA5	Implantation array	Hs.149609/X06256	last 1.7kb	alpha polypep.fibronectin receptor
ITGA6	182431	integrin alpha 6	ITGA6	Implantation array	X59512		last 1.8 kb
ITGA8	198557	integrin alpha 8	ITGA8	Implantation array	Hs.91286/L36531	(3'end)	
ITGAM	2216556	Integrin alpha-M,complement component receptor 3,macrophage antigen alpha polypeptide	ITGAM	apoptosis array	Hs.172631/NM_000632	0.6 kb, 3's, NO 5's, pA, no sig O/L	alpha-M = CD11b,p170
ITGAV	488512	integrin alpha V/vitronectin R/CD51	ITGAV	Implantation array	M14648/Hs.295726		
ITGB1	505555	integrin beta 1(fibronectin receptor, CD29)	ITGB1	Implantation array	X07979		
ITGB2	704517	integrin beta 2 (CD18)	ITGB2	Implantation array	M15395		
ITGB3	1715386	Integrin beta-3	ITGB3	apoptosis array	Hs.87149/M25108	0.7 kb, 3's, NO 5's, pA, no sig O/L	glycoprotein IIIa
ITGB3	134103	Integrin beta 3	ITGB3	Implantation array	Hs.87149/M20311		platelet glycoprotein IIIa, antigen CD61
ITGB4	726248	Integrin beta 4	ITGB4	Implantation array	AF011375		
ITGB5	486216	integrin beta 5	ITGB5	Implantation array	J05633		
ITNB7	2107532	Integrin beta-7	ITNB7	apoptosis array	Hs.1741	0.7 kb, no 5's, 3's, pA, no sig O/L	
JAK1	177471	janus kinase 1	JAK1	Implantation array	M64174		
JAK2	789379	janus kinase 2	JAK2	Implantation array	AF005216		
JAK3	2043964	janus kinase 3	JAK3	Implantation array	U09607		last 0.6kb

Gene ID	IMAGE	Gene	Abbrev	clone source	Acc.No./Unigene ID	clone details	other information & changes to list name
JNK1	119133	JNK1, mitogen activated protein kinase8	JNK1/MAPK8	apoptosis array	L26318 /Hs190913	0.4 kb, 5's, NO 3's, NO pA, watch for homology withn JNK3	MAPK8, (SAP K 1)
JNK2	1030968	JNK2, Mitogen -activated protein kinase 9	JNK2,MAPK9	apoptosis array	L31951 /Hs.246857	0.9 kb, 3's, NO 5's, pA, no sig O/L	MAPK9, C-JUN N-TERMINAL KINASE 2
JNK3	2168302	c-JUN N-terminal kinase 3	JNK3	apoptosis array	Hs.151051/ U34819	0.7 kb, 3's, NO 5's, pA, no sig O/L	MAPK10, C-JUN N-TERMINAL KINASE 3 alpha
junB	153369	junB (transcription factor)	JunB	Implantation array	NM_002229/Hs198951	last 0.8kb	proto-oncogene, previously listed as ID 143369
junD	155061	junD proto oncogene	junD	Implantation array	X51346		
K-Ras2	1286258	K-Ras2 Kirsten rat sarcoma 2 viral oncogene homolog	K-RAS2	apoptosis array	Hs.351221/M54968	0.7 kb, 5's, 3's, pA, no sig O/L	
KDR	2148038	Kinase Domain receptor,VEGF R2,Flk-1	KDR	Implantation array	X61656		last 1.5kb
KDR (1)	UC1	Kinase Domain receptor,VEGF R2,Flk-1	KDR	in-house clone	Hs.12337/AF035121	B/S11 KS +/-	
KIAA0929	unknown	KIAA0929,SHARP nuclear receptor transcription cofactor,SMART/HDAC1associated repressor protein		Implantation array	Hs.184245/AB023146		miss-assigned clone
KIAAO27	unknown	KIAA027		Implantation array	Hs.78851		
kinectin	1643645	kinectin 1,kinesin receptor	KTN1	apoptosis array	Hs.211577/Z22551	0.6 kb, pA, 3', no sign. O/l	kinesin binding adapter, coiled-coiled transmembrane protein
KISS-1	812955	KiSS-1 metastasis-suppressor	KISS-1	Implantation array	U43527		
KPNB1	684634	Karyopherin (importin beta1)nuclear factor p97(NTF97)	KPNB1	in-house clone	L38951/Hs.180446	3's, 0.7kb	Nuclear import
KPNB2	2055326	Karyopherin (importin beta2), also transportin (TRN)	KPNB2	in-house clone	U72069/Hs.168075	3's, no 5's, n pA, 0.8kb	Nuclear import,beta 2a & beta 2b homology
Ku-70	1571080	Thyroid autoantigen 70KDKu-antigen	G22P1	apoptosis array	Hs.197345/M32865	0.6 kb, 3', pA, no o/l	DNA end-binder, dimerises with Ku-80, recriuts DNA-PK, mutation-> SKID
Ku-80	268333	Ku autoantigen 80KD, XRCC5 Xray repair complementing defective repair CHO cells (ds break re-joining)	Ku-80	apoptosis array	Hs.84981/NM021141	pA, 3'seq, no 5'seq	DNA end-binder, dimerises with Ku-70, recriuts DNA-PK, mutation-> SKID
L-myc	1860279	L-myc,similar to lung carcinoma myc related oncogene 1	L-myc	apoptosis array	Hs.169252	0.9 kb, 3's, NO 5's, pA, no sig O/L	
LAMA2	131358	laminin alpha 2 (merosin,congenital muscular dystrophy)	LAMA2	Implantation array	Z26653		
LAMA3	156183	laminin alpha 3 (nicein 150 KD)(Kalinin 165Kd) (BM600 150KD)	LAMA3	Implantation array	L34155/Hs.83450		
LAMA3	591760	laminin alpha 3 (nicein 150 KD)(Kalinin 165Kd) (BM600 150KD)	LAMA3	Implantation array	L34155/Hs.83450		
LAMB1	253043	laminin beta 1	LAMB1	Implantation array	M61916		
LAMB2	74984	laminin beta 2 (laminin S)	LAMB2	Implantation array	X79683		
LAMB3	841907	laminin beta 3	LAMB3	Implantation array	L25541		
LAMC1	364544	LAMININ GAMMA 1	LAMC1	Implantation array	Hs 214982		
LAMC2	1057687	laminin gamma 2	LAMC2	Implantation array	NM_005562		
LAMP1		lysosomal-associated membrane protein 1	LAMP 1	Implantation array	Hs.150101/J04182		
LEP1	139081	leptin (murine obesity homolog)	LEP	Implantation array	U43653		part of EXON 3 Ob gene/human LEP homolog 3' end contains ALU repeats so beware if it is positive !!!!!!
LEPR	142069	leptin receptor	LEPR	Implantation array	U43168		
LHCGR	1735495	luteinizing hormone/chriogonadotropin receptor	LHCGR	Implantation array	M73746		
LIF (1)	2510878	Leukemia inhibitory factor,cholinergic differentiation factor	LIF	apoptosis array	Hs.2250	3's, 0.6kb, pA, no sig O/L	also called HILDA
LIF (2)	1942528	leukemia inhibitory factor	LIF	Implantation array	NM_002309		cholinergic differentiation factor
LIFR	137437	LIF receptor	LIFR	Implantation array	Hs.249247/BM458287		
LIG3	1847306	DNA ligase III,DNA,ATP-dependent	LIG3	apoptosis array	Hs.100299	0.7 kb, 3', no pA, no o/l	
ligase1	525777	DNA ligase I,ATP dependent	LIG1	apoptosis array	Hs.1770/M36067	0.6 kb, 3', 5' also, pA, no o/l	
Lipocortin 1	1553687	Annexin A1 or Lipocortin 1	ANXA1	in-house clone	X05908/Hs.78225	3's, no 5's, 0.6kb	PLA2 inhibitor
LTF	160749	lactoferrin/lactotransferrin	LTF	Implantation array	Hs.105938/X53961		

Gene ID	IMAGE	Gene	Abbrev	clone source	Acc.No./Unigene ID	clone details	other information & changes to list name
LTP 6	spike 5	Arabidopsis Thaliana,lipid transfer protein 6	LTP6	exogenous control	AF159803	pGEMT,537 bp	
LTP4	spike 4	Arabidopsis Thaliana,lipid transfer protein 4	LTP4	exogenous control	AF159801	pGEMT,527 bp	
M-CSF	68599	M-colony stimulating factor	M-CSF	apoptosis array	Hs.173894	0.7 kb, pA, 5', 3', no extraneous o/l	CSF-1, expressed by EC, (Kosaki et al UI 98220910)
MAD	788421	MAD, mothers against decapentaplegic, homolog 4	MADH4/DPC4	Implantation array	U44378		
MAdCAM-1	1564705	MAdCAM-1,mucosal vascular addressin, cell adhesion molecule 1	MADCAM-1	apoptosis array	U82483/Hs.102598	0.7 kb, no 5's, 3's, pA, no sig O/L	LPAM-1ligand expressed on HEV, ? Survival function/mucosal vascular adhesion mol1
MADD	135635	MAP-kinase activating death domain	MADD	apoptosis array	U77352/Hs82548	0.8 kb, pA, 5's3's, no extraneous o/l (=DENN + cardiac myosin binding prot C)	TNFR1-interacting also called DENN
MAG	32444	myelin associated glycoprotein	MAG	Implantation array	M29273		
MAT2A	287608	Methionine adenosyltransferase II, alpha	MAT2A	in-house clone	L43509/Hs77502	3's & 5's,0.7kb	S-adenosylmethionine synthetase
MBD1(2)	324205	methyl CpG binding protein 1	MBD1	Implantation array	Y10746		matches NADPH dependant retinol dehydrogenase /reductase was a missassigned clone
Mcl-1	711870	Myeloid cell leukemia sequnce 1(bcl 2 related)	MCL-1	apoptosis array	L08246 /Hs.86386	0.9 kb, pA, 5's3's, no extraneous o/l	
MCM-5	213756	minichromosome maintenance deficient,CDC46	MCM 5	apoptosis array	Hs.77171	0.7kb, 3' no 5', pA, no sig o/l other than CDC56 (syonym?)	Minichromosome maintenance deficient (S. cerevisiae) 5 (cell division cycle 46)
MCP-1	147207	monocyte chemotactic protein-1, small inducible cytokine A2	MCP-1	Implantation array	M28226		Chemokine (C-C motif) ligand 2 (CCL2) small inducible cytokine A2
MCP-1	1388786	monocyte chemoattractant protein 1 (MCP-1)	MCP-1	apoptosis array	Hs.340	0.6 kb	Chemokine (C-C motif) ligand 2 (CCL2) small inducible cytokine A2
MCP-1R	430027	monocyte chemoattractant protein 1 receptor, chemokine R2	MCP-1R, CCR2	Implantation array	D29984		last 0.5kb
MCP-2	2179757	monocyte chemotactic protein-2, small inducible cytokine A8	MCP-2, SCYA8	Implantation array	Y16645		last 0.3kb
MCP3	322873	monocyte chemotactic protein-3, small inducible cytokine A7	MCP-3, SCYA7	Implantation array	X72308		Chemokine (C-C motif) ligand 7 (CCL7) is a small cytokine known as a chemokine
MCP4	1257779	monocyte chemotactic protein-4, small inducible cytokine A13	MCP-4, SCYA13	Implantation array	U59808		last 0.7kb
MCP4	1257779	monocyte chemotactic protein-4, small inducible cytokine A13	MCP-4, SCYA13	Implantation array	U59808		last 0.7kb
MDB2	1011311	methyl CPG binding protein 2	MBD2	Implantation array	AF072242		
MDM2	147075	mouse double minute 2	MDM2	apoptosis array	Z12020 /Hs170027	0.5kb, 5's, NO 3's, NO pA, no sig O/L	human homolog of, p53 binding protein
MDMx	2615020	homolog mouse double minute	MDMx	apoptosis array	AF007111	size unknown, 3's, NO 5's, pA, no sig O/L	human homologue of mouse double minute 2, upregulated by p53, binds to p53 and promotes p53 inactivation
MEK	unknown	MEK BP partner 1,mitogen activated protein kinase kinase 1 binding protein	MEK,MAP2KIIP 1	Implantation array	AI142363/Hs.6361		homology to AV711984 expressed human dendritic cells
MEK K5	1604803	MAP3K5,mitogen activated protein kinase kinase kinase 5	MEKK5,ASK1	apoptosis array	D84476	0.6kb, 3's, NO 5's, pA, no sig O/L	(ASK1)
MEK1	712732	MAP kinase kinase 1(MAP2K1)	MEK1	apoptosis array	L05624 /Hs.3446	0.7 kb, 5's, 3's, pA, no sig O/L	MAPKK 1
MEK5	343871	mitogen activated kinase kinase 5	MEK5	apoptosis array	U25265	1.0 kb, 5's, 3's, pA, no sig O/L	MAPKK5
MEK6	2805416	Mitogen activated protein kinase kinase 6	MEK6,MAP2K6	apoptosis array	U39657 /Hs118825	unknown size, 3's, NO 5's, pA, no sig O/L	MAPKK6
MET (1)		Met proto-oncogene (hepatocyte growth factor receptor)	MET	in-house clone	Hs 285754/M54559	pCR-Script	
MET (2)	754509	HGF receptor (met, proto-oncogene)	HGFR (MET)	Implantation array	J02958/Hs285754		
MGC5618	346860	hypothetical protein	MGC5618	in-house clone	Hs.177781/C05030	3's, no 5's, 0.7kb	
MGST1	564980	microsomal glutathione S-transferase 1	MGST1	apoptosis array	J03746 /Hs.790	0.7 kb, 5's, 3's, pA, no sig O/L	membrane-bound GST (GST 12)
MHC		MHC classI proline rich	MHC1	Implantation array	U63336		
MIF	592998	macrophage migration inhibitory factor	MIF	Implantation array	M25639		

Gene ID	IMAGE	Gene	Abbrev	clone source	Acc.No./Unigene ID	clone details	other information & changes to list name
MIHA	1593929	MIHA (XIAP, API 3, ILP) X-linked inhibitor of apoptosis protein,IAP like protein ILP	MIHA	apoptosis array	U45880/hs172777	1.3 kb, pA, NO 5's, 3's, no extraneous o/l, NOTE SIZE	BIRC4 Baculoviral IAP repeat containing 4
MIHB	132713	MIHB (IAP2),BIRC2 Baculoviral IAP repeat containing 2 inhibitor of apoptosis protein homolog B	MIHB	apoptosis array	U45879 / Hs.289107	0.6 kb, pA, 5's3's, no extraneous o/l	
MIHC	926254	MIHC = API2 = IAP1,Baculoviral IAP repeat containing 3	MIHC,BIRC3	apoptosis array	Hs.127799/U37546 / L49431	0.3 kb, 3;s, NO 5's, pA, note short size to attempt to avoid MIHB homology	binds TRAF1, TRAF2, caspases 3 and 8
MIP1alpha	1898671	macrophage inflammatory protein 1 alpha, small inducible cytokine A3	SCYA3	Implantation array	M23452/Hs.73817		
MIP1beta	205633	macrophage inflammatory protein 1 beta, small inducible cytokine A4	SCYA4	Implantation array	J04130/Hs.75703	last 0.4kb	Hom. to mouse MIP 1b
MK167	769513	Ki 67, antigen identified by monoclonal antibody	MKI67	Implantation array	X65551		
MLC-B	139375	myosin light chain regulator,nonsarcomeric	MLC-B	apoptosis array	AA772131/Hs.180224	0.6 kb, pA, 5's3's	
MLH-1	2311591	MutL (E.coli) homolog 1,colon cancer /nonpolyposis type 2	MLH1	Implantation array	Hs.57301/U07343	0.7kb,3',pA	
MMP1	309938	matrix metalloproteinase 1(interstitial collagenase)	MMP1	Implantation array	M13509		interstitial collagenase NB same clone asH/B12
MMP-1	309938	Matrix metalloproteinase 1	MMP-1	apoptosis array	Hs.83169	0.6 kb	Matrix metalloproteinase 1 (interstitial collagenase)NB same clone asB/A8
MMP-2	2347072	matrix metalloproteinase 2	MMP-2	apoptosis array	Hs.111301	0.6 kb	gelatinase A, 72kD type IV collagenase
MMP2	486460	matrix metalloproteinase 2 (gelatinase A)	MMP2	Implantation array	M55593		
MMP-3	323977	Matrix metalloproteinase 3	MMP-3	apoptosis array	Hs.83326	0.6 kb	stromelysin 1, transin-1
MMP3	324700	matrix metalloproteinase 3 (stromelysin 1, progelatinase)	MMP3	Implantation array	J03209		
MMP7(1)	471134	Matrix metalloproteinase 7	MMP-7	apoptosis array	Hs.2256	0.9 kb	matrilysin, COG-7 NB same clone asC/E10
MMP7(2)	471134	matrix metalloproteinase 7 (matrilysin, uterine)	MMP7	Implantation array	X07819		homolog to stromelysin (pump-1)NB same clone as H/C2
MMP9	2522550	MMP9 = type 4 collagenase	MMP9	apoptosis array	Hs.151738	0.6 kb	COG9, gelatinase B
MMP10(1)	1664074	matrix metalloproteinase 10 (stromelysin 2)	MMP10	Implantation array	Hs 2258/X07820	0.6kb	
MMP10(2)	1664074	matrix metalloproteinase 10 (stromelysin 2)	MMP-10	apoptosis array	Hs.2258	0.6 kb	stromelysin 2
MMP11(1)	133842	matrix metalloproteinase 11 (stromelysin 3)	MMP11	Implantation array	X57766		
MMP-11(2)	71651	Matrix metalloproteinase 11	MMP-11	apoptosis array	Hs.155324	0.8 kb	stromelysin-3
MMP12	2062289	matrix metalloproteinase 12 (macrophage elastase)	MMP12	Implantation array	L23808/Hs.1695		macrophage elastase
MMP13	1555874	matrix metalloproteinase 13 (collagenase 3)	MMP13	Implantation array	X75308		
MMP14	1661893	matrix metalloproteinase 14 (membrane - inserted)	MMP14/MT-MMP	Implantation array	Hs.2399/Z48481	last 1.1kb	
MMP15	284428	matrix metalloproteinase 15 (membrane inserted)	MMP15	Implantation array	NM_002428/Hs.80343		last 2kb
MMP16	46916	matrix metalloproteinase 16 (membrane - inserted)	MMP16/MT3 MMP	Implantation array	AB009303		
MMP17	30850	matrix metalloproteinase 17 (membrane - inserted)	MMP17/MT2-MMP	Implantation array	X89576		poor match from random seq 7.2.02/12
MMP19	149932	matrix metalloproteinase 19	MMP19	Implantation array	U38320/Hs154057		MMP18,RASI-1
MMP23B	1579964	matrix metalloproteinase 23B	MMP23B	Implantation array	NM_004659		
Mn SOD		Manganese-containing superoxide dismutase	SOD2	in-house clone	Hs.318885/X14322		mitohondrial
MRE-11A	1879728	Meiotic recombination (S.cerevisiae) 11 homolg A	MRE-11A	apoptosis array	Hs.20555/U37359	0.7 kb, 3', pA, some homology to MRE-11A	
MSH2	2295786	MutS (E.coli) homolog 2 / colon cancer nonpolyposis type1	MSH2	apoptosis array	Hs.78934/U04045	0.6 kb, 3', pA, no o/l	(homologue of bacterial MutS), implicated in most HNPPC
MSH3	738899	mismatch repair protein homolog 3	MSH3	Implantation array	J04810/Hs.42674		(homologue of bacterial MutS), implicated in some HNPPC

Gene ID	IMAGE	Gene	Abbrev	clone source	Acc.No./Unigene ID	clone details	other information & changes to list name
msh5	795640	mismatch repair protein homolog 5	MSH5	Implantation array	AF048986		
MSH6(1)	841478	mismatch repair protein homolog 6	MSH6	Implantation array	U54777		
MSH6(2)	2463136	mismatch repair protein homolog 6	MSH6	apoptosis array	Hs.3248/U54777	0.6 kb, 3', pA, some homology to VIT-1	(homologue of bacterial MutS)
MSP		Macrophage stimulating protein (hepatocyte growth factor -like)	MST1	in-house clone	Hs.349110/L11924	pCR-Script,	ligand for RON
MSX1	135694	Msh (drosophila) homeo box homolog 1	MSX1	Implantation array	M97676/Hs1494		last 0.8kb, formerly homeo box 7 now Msh hom. 1
MT2A	1711581	metallothionein 2A	MT2A	Implantation array	X97260		
MT3	2104626	metallothionein 3 (growth inhibitory factor)	MT3	Implantation array	NM_005954		hom M1,product seq sim to MT3
MT6AA	487441	metallothionein 6AA	MT6AA	Implantation array	AA046711		
MTA1	298963	Metastasis -associated 1	MTA1	Implantation array	Hs101448/U35113		
MUC1	590873	mucin 1, transmembrane	MUC1	Implantation array	NM_002456/Hs.89603		
MUC2	1871480	mucin 2,intestinal/tracheal	MUC2	Implantation array	L21998/Hs.315	last 1kb	
MUC4	2173976	mucin 4, tracheobronchial	MUC4	Implantation array	AJ010901(partial)		
MUC5B(1)	592592	mucin 5B, tracheobronchial, placental	MUC5B	Implantation array	AJ001403		
MUC5B(2)	937208	mucin 5B tracheobronchial, gallbadder	MUC5B, partial	Implantation array	U06711(partial)		
MUC6	2095547	Mucin 6, gastric	MUC6	Implantation array	U97698(partial)		
MUT L	128493	mutL (E.coli) homolog 1, colon cancer nonpolyposis type 2	Mut L/MLH1	Implantation array	U07343		
MUTS	630013	mismatch repair protein homolog 2, colon cancer nonpolyposis 1	MutS/MSH2	Implantation array	U04045		
MYD88	486287	myeloid differentiation primary response gene	MYD88	Implantation array	U70451		
MYO1C		myosin 1C	MYO1C	in-house clone	Hs.286226/X98507	pCR-Script,	
MYST1		histone acetyltransferase MYST1	MYST1	implantation array			previously listed as ILBRbeta MISSASSIGNED also homology to SW_MOF_DROME males absent on the first protein
N-cadherin	1737662	N-Cadherin(neuronal),cadherin 2	CDH2	apoptosis array	Hs.161	0.9 kb, pA, 3', no extraneous o/l	Cadherin-2
N-myc	2006037	N-myc,V-myc avian myelocytomatosis viral related oncogene ,neuroblastoma derived	MYCN	apoptosis array	Hs.25960/M13228	1.0 kb, 3's, NO 5's, pA, no sig O/L	
N-Ras	839623	N-Ras related gene,D1S155SE	N-Ras	apoptosis array	Hs.69855/NM_007158	0.6 kb, 5's, 3's, pA, no sig O/L	Neuroblastoma Ras,NB related to N-ras
NAIP	1734928	NAIP,neuronal apoptosis inhibitory protein	NAIP,BIRC1	apoptosis array	NM_004536/Hs.79019	1.4 kb, pA, NO 5's, 3's, no extraneous o/l, NOTE SIZE	a mammalian IAP implicated in SMA,Baculoviral IAP repeat containing 1
Nbs1	153757	Nijmegen breakage syndrome 1(nibrin)	NBS1	apoptosis array	Hs.25812	0.7 kb, 3', no pA, no o/l	Nijmegen breakage syndrome gene, part of endo/exo-nuclease complex, signals DNA damage to cell cycle, regulates MRE11 / Rad50 complex (homologous to yeast Xrs2)
NCKAP1	135176	NCK-associated protein 1	NCKAP1	in-house clone	Hs.278411/AB014509	3's & 5's	Apoptosis NOTE NOT NAP1 pronapsin Hs 322854
NDUFS5	343461	NADH-dehydrogenase (ubiquinone) Fs.S protein 5 (15KD)NADH coenzyme Q reductase	NDUFS5	in-house clone	Hs.80595/AF020352	0.6kb	
Neu1		Neuropilin 1	NRP1	in-house clone	Hs.69285/AF016050	pCR-Script,	
Neur2		Neuropilin 2	NRP2	in-house clone	Hs.17778/AF022860	pCR-Script,	
NF kappa	154818	NF kappa B transcription factor p65	NF k B	Implantation array	L19067/Hs.75567	0.7 kb, 3' seq, 5' seq, pA, no extra o/L	V-rel hom A,same clone as I/C4 apoptosis
NF-kbp105	1670273	NF-kB p105 (pre p50)	NF-KB	apoptosis array	M58603	0.5 kb, 3' seq, no 5' seq, pA, no extra o/L	(pre-p50)
NF-KBp65	154818	NF-kB p65, V-rel avian reticuloendotheliosis viral oncogene homolog A(nuclear factor of kappa light polypeptide gene enhancer in B cells 3 (p65)	RELA, NF-KBp65	apoptosis array	L19067/Hs.75567	0.7 kb, 3' seq, 5' seq, pA, no extra o/L	(Rel A),same clone as B/C9
NICE-3	595099	DKFZP586G1722 hypothetical protein	NICE-3	Implantation array	Hs.31989/BG260819		

Gene ID	IMAGE	Gene	Abbrev	clone source	Acc.No./Unigene ID	clone details	other information & changes to list name
NIK	342349	serine -threonine protein kinase MAP3K14 mitogen activating protein kinase kinase kinase 14	NIK, MAP3K14	apoptosis array	Y10256 /Hs.47007	1.2 kb, pA, 5's3's, no extraneous o/l, NOTE SIZE	
NIP3	504930	BNI3 Bcl2 adenovius E1B 19 kd interacting protein 3	BNIP3	in-house clone	Hs79428/AF002697	0.7kb,5's & 3's	
NIX	196582	Bcl2 interacting protein 3 like	NIX	apoptosis array	AF067396/Hs132955	0.8 kB, 5's, 3' s, pA, no unwanted homology	pro-apoptotic mitochondrial protein (BCL2/adenovirus E1B 19kD-interacting protein 3-like)
NKG2	2469790	Est highly similar to human NKG2-d type II integral membrane protein,NKG2-A/NKG2-B	NKG2	apoptosis array	Hs.311389	0.6 kb, 3's, NO 5' s, no pA	associates with CD94 - note homology to other NKG2 family members
NKR-P1A	2298045	NKR-P1A (CD 161, human homologue of NK1.1)	KLRB1,NKR-P1A	apoptosis array	Hs. 169824	0.8 kb, NO 5's, 3's, pA, no sig O/L	KLRB1, part of NK gene complex, killer cell lectin like receptor subfamily B member 1
NMI	704532	N-myc (STAT) interactor	NMI	Implantation array	U32849		
Nod1	668297	caspase recruitment domain 4	Nod-1,CARD4	apoptosis array	NM_006092/Hs.19405	0.6kb	APAF-1-like
NOS1	277404	nitric oxide synthase 1 (neuronal)	NOS1	Implantation array	U17327		5'end only 1 x image clone
NOS2A	1086482	nitric oxide synthase 2A (inducible, hepatocytes)	NOS2A	Implantation array	U31511		hom NOS1
NOS3	2002673	nitric oxide synthase 3 (endothelial cell)	NOS3	Implantation array	M93718/Hs.16673	last 0.5kb	homology to Hs.278222
NPR2L	1508338	tumor suppr. gene 21 candidate,homologous to yeast nitrogen permease	NPR2L	Implantation array	AF040708/Hs.356137		
NRP1	254408	neuropilin I	NRP1	apoptosis array	Hs.69285/AF145712	0.6 kb, 3' no 5', No sig O/L	VEGF 165 receptor,previously listed as neuropil 1
NRP2	1689788	neuropilin 2	NRP2	apoptosis array	Hs.17778/NM003872	0.6 kb, pA, 3' no 5', no extran. O/l	VEGF165 receptor 2
OSM	1677457	oncostatin M	OSM	Implantation array	M27288/Hs.248156		
OXT	unknown	oxytocin	OXT	in-house clone	M25650		
OXT	WHO cl.16	oxytocin, prepro - (neurophysin I)	OXT	Implantation array	Hs.113216/M25650		primers 31/32
OXTR	470101	oxytocin receptor	OXTR	Implantation array	X64878		
P-450	146270	P450 aromatase,CYP19	P-450	Implantation array	M28420/Hs.79946		aromatization of androgens ,estrogen synthetase
P1	214255	alpha-1-antitrypsin, protease inhibitor 1	PI	Implantation array	X01683		
p27 KIP1	202710	CDKN1B cyclin dependent kinase inhibitor 1B	p27 KIP1	apoptosis array	Hs.238990	5's, 3's, pA, no extra o/l, no direct homology to cDNA, linked thru gen. Cl.	
p38MAPK	34416	p38 MAP K,mitogen -activated protein kinase 14	MAPK14	apoptosis array	L35253/Hs.79107	0.7 kb, 5's, 3's, pA, some homology to Human CSaids binding protein (CSBP1)	SAPK2A, MAPK14, CSaids binding protein1 = CSBP1, MXI2
p53(1)	24415	tumour protein p53 Li-fraumeni syndrome	TP53	apoptosis array	M14694 /Hs.1846	1.4 kb, 5's, 3's, NO pA, no sig O/L	same clone as E/E10
p53(2)	24415	tumour protein p53 , Li-Fraumeni syndrome	TP53	Implantation array	M14694		same clone as I/D3 so seq confirmed
p53(3)	2573232	tumour protein p53 , Li-Fraumeni syndrome	TP53	apoptosis array	M14694	unknown size, 3's, no 5', pA, no sig O/L	
P73(1)	1486099	Tumour protein p73	TP73	apoptosis array	Hs.247753/NM_005427	3', no pA, no sig o/l	anti-apoptotic, inhibits expression of VEGF gene, asscociates with p53
P73(2)	1486099	tumuor protein P73	TP73	apoptosis array		1.2kb,pA, 3'seq, no 5'seq	
PA11	70891	Plasminogen activating inhibitor 1	PAI1	Implantation array	M16006/Hs.54576		
PAFAHIB3	26467	platelet activating factor acetylhydrolase isoform1b,gamma subunit	PAFAH1B3	Implantation array	D63391/Hs6792		3 end 0.9kb
PAFAHIBI	201664	platelet activating factor acetylhydrolase alpha	PAFAH1B1	Implantation array	L13386		lissencephaly protein
PAI-1	324165	Plasminogen activator inhibitor 1	PAI-1	apoptosis array	Hs.82085/M14083	0.7 kb, 5's 3's, pA, (some homol with alpha PAI-1	
PAI2(1)	138654	Plasminogen activating inhibitor 2/arg-ser	PAI2	Implantation array	M18082		same clone as I/H10
PAI2(2)	138654	Plasminogen activating inhibitor 2/arg-ser	PAI-2	apoptosis array	Hs.75716	0.9 kb	arginine-serpin,same clone as C/C12
PAM	490409	Peptidylglycine alpha-amidating monooxygenase	PAM	in-house clone	M37721/Hs83920	3's, no 5's	
PAPPA	241368	pregnancy-associated plasma protein A	PAPPA	Implantation array	U28727		
PARP	1013951	poly(ADP-ribose) polymerase-1	PARP	apoptosis array	Hs.177766/J03473	0.6 kb, 3', pA, no o/l	poly(ADP-ribose) polymerase-1

Gene ID	IMAGE	Gene	Abbrev	clone source	Acc.No./Unigene ID	clone details	other information & changes to list name
PARP-2	2014562	poly(ADP-ribose) polymerase-2	PARP-2	apoptosis array	Hs.271742	0.6 kb, 3' no 5', no pA, some homology NAD+ ADP-ribosyltransferase 3 (ADPRT3)	
PAX6	230882	paired box gene 6 (aniridia, keratitis)	PAX6	Implantation array	M93650		
PCNA	340634	Proliferating cell nuclear antigen	PCNA	apoptosis array	M15796/Hs78996	0.7 kB, 5's, 3' s, pA, no unwanted homology	multifunctional; p21, Fen1, MCMT and XPG compete to bind PCNA
PCTK1	267308	PCTAIRE protein kinase 1	PCTK1	apoptosis array	X66363 /Hs171834	0.8 kb, 3's, 5's, NO pA, no sig O/L	PCTAIRE protein kinase 1
PCTK2	2471125	PCTAIRE protein kinase 2	PCTK2	apoptosis array	Hs.123063		PCTAIRE protein kinase 2
PCTK3	2327552	PCTAIRE protein kinase 3	PCTK3	apoptosis array	Hs.2994/H51577	unknown size, 3's, NO 5's, no pA, no sig O/L, homology not long	PCTAIRE protein kinase 3
PDCD2	172057	PDCD2 (Prog. Cell death 2)	PDCD2	apoptosis array	S78085	0.7 kb, 5's, 3's, pA, no sig O/L	homologous to Rp8, a rat gene associated with apoptosis
PDGF-A(1)	1877285	platelet derived growth factor alpha polypep.	PDGF-A	apoptosis array	X06374	0.7 kb, pA, NO 5' but 3', no extraneous o/l	PDGF-1
PDGF-beta	145844	Placental derived growth factor-B	PDGF-B	apoptosis array	X02811	1.9 kb, 5' only, NO 3', NO pA, no extraneous o/l, Note length (will need to trim)	PDGF-2
PDGFRA	147628	platelet derived growth factor receptor alpha polypep.	PDGFRA	Implantation array	L27560/Hs.180324		previously listed as PDGFA but it's the receptor !!!
PDGFRA	376499	Platelet derived growth factor -A receptor	PDGFRA	apoptosis array		0.8kb, 5's + 3's, pA, no O/L	previously listed as PDGF-A[2] it's the receptor
PDGFRB	344874	platelet derived growth factor receptor beta	PDGFRB	Implantation array	NM_002609/Hs.76144		hom PDGFRA except last 2kb
PEG10	111654	Paternally expressed 10	PEG10	in-house clone	Hs.137476/T84579	3's, no 5's,1kb	
PG12R	1553933	prostagladin I2 (prostacyclin) receptor	PTGIR	Implantation array	D25418/Hs.393		
PGDH		NAD+dependent 15-hydroxyprostaglandin dehydrogenase(PGDH)	PGDH	unknown origin			
PGR	WHO cl.13	progesterone receptor B 392	PGR	Implantation array	M15716		primers 25/26 match for PGR and a splice variant of PGR
PGR (2)		progesterone receptor B180	PGR	Implantation array	Hs.20905/AF016381	B.Vivellecl.17	(none of three specific for A only)
PIG3	1928657	Quinone oxidoreductase homolog 3	PIG3	apoptosis array	AF010309/Hs50649	0.6 kb, NO 5's, 3's, pA, no sig O/L	induced by p53 expression before the onset of apoptosis, quinone oxidoreductase homolog
PIG7	376814	PIG7, LPS-induced TNF-alpha factor	PIG7	apoptosis array	AF010312 /Hs.76507	0.6 kb, 5's, 3's, pA, no sig O/L	induced by p53 expression before the onset of apoptosis
PIG8	2017310	etoposide induced mRNA	PIG8	apoptosis array	Hs.343911/NM_004879	0.7 kb, NO 5's, 3's, pA, no sig O/L	induced by p53 expression before the onset of apoptosis, etoposide-induced mRNA
PIG 10	345985	PIG10, ENC1 Ectodermal -neural cortex (with BTB -like domain)	PIG10	apoptosis array	AF010314 /Hs.104925	0.6 kb, 5's, 3's, pA, no sig O/L	induced by p53
PIG11	667514	PIG11, p53 induced protein	PIG11	apoptosis array	AF010315 /Hs.96908	0.6 kb, 5's, 3's, pA, no sig O/L	induced by p53 expression before the onset of apoptosis
PIK3R1	178034	PI3Kinase p85,phosphoinositide -3-kinase ,regulatory subunit,polypeptide 1(p85 alpha)	PIK3R1	apoptosis array	M61906 /Hs.6241	0.6 kB, 5's, 3' s, pA, no unwanted homology	86 kDa regulatory subunit, is induced in response to oxidative stress, mediating cell death via p53
PK1_3	435024	gene from NF2/meningioma region of 22q12	PK1.3	Implantation array	NM_003678		
PKA	155556	protein kinase A (CATALYTIC SUBUNIT alpha)	PKA	apoptosis array	Hs.77271	0.9 kb, pA, 5's3's, no extraneous o/l	cAMP-dependent protein kinase
PKCA	469954	protein kinase C alpha	PRKCA	Implantation array	X52479/Hs.169449		
PLA2G4C	1677250	phospholipase A2 gamma, groupIVC	PLA2G4C	apoptosis array	Hs.18858	0.6 kb, 3', pA, no sign. O/l	cytosolic, calcium-independent phospholipase A3
plakoglobin	1089321	plakoglobin,Junction plakoglobin	PLAK/JUP	apoptosis array	M23410 /Hs2340	0.7 kb, 3's, NO 5's, pA, no sig O/L	component of the cadherin-catenin complex, associates with the cytoplasmic region of desmoglein I
PLAT	321838	tissue-type plasminogen activator	tPA, PLAT	Implantation array	M15518		
PLAU	714106	urokinase, plasminogen activator	PLAU	Implantation array	M15476/Hs.77274		
PLD1	327355	Phospholipase D1,phosphatidylcholine specific	PLD1	apoptosis array	U38545	0.5 kB, 5's, 3' s, no pA, unwanted homology	phosphorylation induces binding to Grb2
PLGF (1)		Placental growth factor 2	PLGF 2	in-house clone		pCR-Script,	

Gene ID	IMAGE	Gene	Abbrev	clone source	Acc.No./Unigene ID	clone details	other information & changes to list name
PLGF (2)	133339	placental growth factor	PGF	Implantation array	Hs.2894/X54936		vascular -endothelial growth factor related protein
PLK	124700	Polo,drosophila -like kinase	PLK	apoptosis array	Hs.77597/U01038	0.8 kb, 3', pA , no o/l	Polo (Drosophia)-like kinase
PLOD2	1702704	procollagen-lysine, 2 oxoglutarate 5 -dioxygenase,Lysyl hydroxylase 2	PLOD2	in-house clone	U84573/Hs.41270	3's, no 5's,0.6kb	
PML	2206977	Promyelocytic leukaemia	PML	apoptosis array	Hs.589633	0.6 kb, 3' read, pA, search -> no O/L	promyelocytic leukaemia protein - see Wyllie insight review
PMS1	825726	post meiotic segregation increased 1 (S.crevisiae)	PMS1	Implantation array	NM_000534		
PMS1	1456997	post meiotic segregation increased (S.cerevisiae) 1	PMS1	apoptosis array	Hs.111749/U13695	0.7 kb, 3', pA, no o/l	(homologue of yeast MutL), implicated in some HNPPC
PMS2	1981063	post meiotic segregation increased (S.cerevisiae) 2	PMS2	apoptosis array	Hs.177548/U14658	0.6 kb, 3', pA?, no o/l	(homologue of yeast MutL), implicated in some HNPPC
PODXL	365040	Podocalyxin-like protein	PODXL	in-house clone	U97519/Hs16426	3's, no 5's,	Adhesion
POLD2	2161249	DNA polymerase delta 2regulatory subunit 50KD	POLD2	apoptosis array	Hs.74598/U21090	0.6 kb, 3', pA, no o/l	delta 2, regulatory subunit (50kD)
POMC	1565052	proopiomelanocortin	POMC	Implantation array	M38297/J00292		beta endorphin
POR	416159	P 450 cytochrome oxidoreductase	POR	apoptosis array	S90469 /Hs.167246	0.7 kb, 5's, 3's, pA. No sig O/L	P450 (cytochrome) oxidoreductase
POR1	2144971	Partner of RAC1	POR1	apoptosis array	Hs.75139	1.0 kb, 3' no 5', pA, no o/l	
PP14	235906	Placental Protein 14	PP14	Implantation array	M34046/Hs.82269		also called PAEP progestagen-associated endometrial protein
PPAR	2386312	Peroxisome proliferative activated receptor, gamma	PPAR gamma	apoptosis array	Hs.100724	0.6 kb, 3' no 5', pA, no sig o/l	
PPAR alpha	2106983	peroxisome proliferative activated receptor alpha	PPAR alpha	apoptosis array	Hs.998/S74349	0.8 kb, 3's, NO 5's, NP pA, no sig O/L	peroxisome proliferative activated receptor alpha
PPARA	2106983	peroxisome proliferative activated receptor alpha	PPARA	Implantation array	Y07619		
PPARD	726134	peroxisome proliferative activated receptor delta	PPARD	Implantation array	L07592		
PPARG	160060	peroxisome proliferative activated receptor gamma	PPARG	Implantation array	L40904/Hs.100724		
PPP2R5A	1169776	Protein phosphatase 2, regulatory-subunit B(B56) alpha isoform	PPP2R5A	apoptosis array	L42373 /Hs.155079	0.4 kb, pA, NO 5'	
PRG1	1664152	proteoglycan I, secretory granule	PRG1	in-house clone	J03223/Hs.1908	0.8kb	
PRL	219552	prolactin	PRL	Implantation array	V00566/Hs.1905		
PRLR(1)	WHO cl.2	prolactin rel. peptide receptor	PRLR	Implantation array	AB015745	pGEMT	WHO primers 3/4
PRLR(1)	WHO cl.2	prolactin rel. peptide receptor	PRLR	Implantation array	AB015745	pGEMT	WHO primers 3/4
PRLR(2)	1650749	prolactin receptor	PRLR	Implantation array	M31661/AF091859		seq matches promoter region 7 alt exon 2
Prog rec	17	Progesterone Receptor	PGR	in-house			
PSMA3	664613	proteosome (prosome, macropain) subunits,alpha type,3	PSMA3	in-house clone	D00762/Hs346918	1kb	
PTAFR	853625	platelet activating factor receptor	PTAFR	Implantation array	D10202		
PTEN	1535806	phosphatase & tensin homolog	PTEN	Implantation array	U93051		
PTGDR	WHO cl.11	prostaglandin D2 receptor	PTGDR, PGRD2	in-house clone	U31099/Hs.158326	pGEMT	primers 21/22,401bp insert
PTGDR (2)	WHO cl.11	prostaglandin D2 receptor	PTGDR,PGRD2	in-house clone	U31099/Hs.158326	pGEMT	previously listed as prolactin[1],
PTGDS	725673	prostaglandin D2 synthase gene	PTGDS	Implantation array	M61900/Hs.8272		
PTGER2	470821	prostaglandin E receptor 2 (subtype EP2)	PTGER2	Implantation array	U19487		
PTGER3	2131660	prostaglandin E receptor 3 (subtype EP3)	PTGER3	Implantation array	D86098		
PTGER4	WHO cl.5	prostaglandin E receptor 4 (subtype EP4)	PTGER4	Implantation array	NM_000958		hom. EP2/primers 9/10
PTGES	2097177	PIG12,prostaglandin E synthase	PTGES	apoptosis array	AF010316 /Hs.146688	0.7 kb, No 5's, 3's, pA, ? 2 genes (see notes)	induced by p53 expression before the onset of apoptosis, microsomal glutathione S-transferase 1-like
PTGFR	1639562	prostaglandin F receptor	PTGFR	Implantation array	Hs.89418/L24470		
PTGFR	151011	prostaglandin F receptor	PTGFR	Implantation array	L24470		
PTGIS	469275	prostaglandin 12 (prostacyclin) synthase	PTGIS	Implantation array	D38145		
PTGRF	2140347	prostaglandin F2 alpha receptor	PTGRF	Implantation array	AF004021/Hs89418	1.2kb	**NB partial match to JAM1 (Hs.286218/AF172398)**

Gene ID	IMAGE	Gene	Abbrev	clone source	Acc.No./Unigene ID	clone details	other information & changes to list name
PTN	284476	pleiotrophin/heparin binding growth factor 8	PTN	Implantation array	X52946		
PTP1C		Protein -tyrosine phosphatase 1C, PTP non-receptor type 6	PTPN6	in-house clone	U47924/Hs.63489	pCMVSPORT 2	
PZR	2470870	protein zero related,MPZL1 myelin protein zero -like 1	PZR	apoptosis array	Hs287832/BC007881	3' no 5', pA, 0.5 kb, no sign. O/l	
Rac1(1)	364305	Ras- related C3 botulinum toxin substrate 1(rho superfamily,small GTP binding rac-1)	RAC-1	apoptosis array	Hs 173737	0.6kb, 3's, NO 5's, pA, no O/L	rho family, small GTP binding protein Rac2
Rac1(2)	364305	Rac1,ras -related C3 botulinum toxin susbtrate 1(p21-rac1)	Rac1	apoptosis array	Hs.268134	0.6kb, 3's, NO 5's, pA, no O/L	rho family, small GTP binding protein Rac1
RAC2	195765	Ras related C3 botulinum toxin substrate 2	RAC2	apoptosis array	Hs.173466	1.4kb , 5's only, no pA, some homology to Rac3	Ras-related C3 botulinum toxin substrate 2
RAD1	2429435	checkpoint control protein, exonucleaseRAD1	RAD1	apoptosis array	Hs.7179	0.6 kb, 3', pA, some homology to REC1	human homolog of s.pombe RAD1
Rad9	1523435	Rad9(S.Pombe) homolog	Rad9	apoptosis array	Hs.240457/U53174	0.6 kb, 3', pA	cycle checkpoint control protein
RAD27	1454849	RAD2, Fen-1 flap structure specific endonuclease 1	RAD27	apoptosis array	Hs.4756/X76771	0.8 kb, 3', pA, no o/l	FEN1
Rad50	684652	RAD50 (S.cerevisiae)homolog	RAD50	apoptosis array	Hs.41587/U63139	0.7 kb, 3' and 5', no pA, no o/l	part of endo/exo-nuclease complex
RAD52	2429897	RAD52(S.cerevisiae)homolog	RAD52	apoptosis array	Hs89571	unknown size, 3' pA, no O/L	DNA repair & recombination
RAD54	2498030	RAD54(S.cerevisiae)homolog like	RAD54L	apoptosis array	Hs.66718	0.9 kb, 3', pA, no o/l	homology to mouse RAD54
Rap1	2261011	Ras associated protein 1	Rap1	apoptosis array	Hs.47225	0.6 kb, 3' no pA, no sign. o/l	Ras-associated protein Rap1 = Rab2
RARA	153166	retinoic acid receptor, alpha	RARA	Implantation array	X06614		last 1kb
RARB	1620270	retinoic acid receptor, beta	RARB	Implantation array	X07282		last 0.4kb
RARG	1865257	retinoic acid receptor, gamma	RARG	Implantation array	M38258/Hs.1497	last 1kb	
RASA1	485864	ras p21 protein activator	RASA1	Implantation array	M23379		
RB1	267763	retinoblastoma 1,including osteosarcoma	RB1	Implantation array	M33647/Hs.75770		
rbcl 0		empty well 0 for rcbl std curve		exogenous control			
rbcL	spike 3	Arabidopsis Thaliana, RUBISCO, ribulose 1,5-bisphosphate carboxylase/oxygenase	rbcL	exogenous control	U91966	pGEMT,526 bp	
rbcL80	spike 3	Arabidopsis Thaliana, RUBISCO, ribulose 1,5-bisphosphate carboxylase/oxygenase	rbcL	exogenous control	U91966	pGEMT,526 bp	
rbcL160	spike 3	Arabidopsis Thaliana, RUBISCO, ribulose 1,5-bisphosphate carboxylase/oxygenase	rbcL	exogenous control	U91966	pGEMT,526 bp	
rbcL320	spike 3	Arabidopsis Thaliana, RUBISCO, ribulose 1,5-bisphosphate carboxylase/oxygenase	rbcL	exogenous control	U91966	pGEMT,526 bp	
rbcL400	spike 3	Arabidopsis Thaliana, RUBISCO, ribulose 1,5-bisphosphate carboxylase/oxygenase	rbcL	exogenous control	U91966	pGEMT,526 bp	
rbcL500	spike 3	Arabidopsis Thaliana, RUBISCO, ribulose 1,5-bisphosphate carboxylase/oxygenase	rbcL	exogenous control	U91966	pGEMT,526 bp	
rbcL750	spike 3	Arabidopsis Thaliana, RUBISCO, ribulose 1,5-bisphosphate carboxylase/oxygenase	rbcL	exogenous control	U91966	pGEMT,526 bp	
rbcL1000	spike 3	Arabidopsis Thaliana,RUBISCO,ribulose 1,5-bisphosphate carboxylase/oxygenase	rbcL	exogenous control	U91966	pGEMT,526 bp	
rbcL1200	spike 3	Arabidopsis Thaliana, RUBISCO, ribulose 1,5-bisphosphate carboxylase/oxygenase	rbcL	exogenous control	U91966	pGEMT,526 bp	
RBL2	321247	Retinoblastoma-like 2 (p130)	RBL2	apoptosis array	X74594 /Hs79362	0.8 kb, 3', 5', pA, no sig O/L	Retinoblastoma susceptibility gene
RBP2	80086	retinol -binding protein 2	RBP2	Implantation array	T63266		
RCA	spike 2	Arabidopsis Thaliana, RUBISCO activase	RCA	exogenous control	X14212	pGEMT, 513bp	
relaxin1	940909	relaxin 1(H1)	RLN1	Implantation array	NM_006911		rel 1/2 90%
requiem	212756	requiem	REQ	apoptosis array	Hs.13495/AF001433	0.6 kb, 5's, 3's, pA, no sig O/L	a ubiquitous zinc finger protein required for the apoptosis response
RFC2	1930725	replication factor C (activator1)	RFC2	apoptosis array	Hs.139226	3', pA, 0.5 kb, no O/l	40 kDa subunit
Rho7	383898	Rho 7, GTP binding protein	RHO7	Implantation array	Hs.99034/X95456		
Gene ID	IMAGE	Gene	Abbrev	clone source	Acc.No./Unigene ID	clone details	other information & changes to list name

Gene ID	IMAGE	Gene	Abbrev	clone source	Acc.No./Unigene ID	clone details	other information & changes to list name
RhoA	511607	RhoA,Ras homolog gene family	ARHA	apoptosis array	L25080 /Hs.77273	0.9 kb, 5's, 3's, pA, no sig O/L (care with homology between Rho's)	involved in actin organisation and beta 3 integrin signalling
RhoE (1)	923460	RhoE,Ras homolog gene family member E	RhoE/ARHE	apoptosis array	X95282 /Hs6838	0.6 kb, 3' no pA, no sign. O/l	also called Rho8,GTPase
RhoE (2)	923460	Ras homolog family member ,E,RhoE	ARHE	apoptosis array	X95282 /Hs 6838	0.6 kb, 3' no pA, no sign. O/l	Rho9
RhoG (1)	2066382	RhoG, Ras homolog gene family member G	RhoG	apoptosis array	X61587	0.6 kb, 3's, pA, no sig O/L	same clone as F/F1but different from B/E11
RhoG (2)	2066382	RhoG, Ras homolog gene family member G	RhoG/ARHG	apoptosis array	X61587 /Hs75082	0.6 kb, 3's, pA, no sig O/L	same clone as H/A2,B/E11 is a different clone
RhoG (3)	38398	Rho G ras homolog gene family, GTP binding protein	ARHG	Implantation array	L11317		same gene diff clone as H/A2 &F/F2
RIP K1	2687218	Receptor (TNFRSF) interacting serine threonine kinase 1	RIP (RIP K1)	apoptosis array	AW236421/Hs.296327	size unknown, pA unknown, 3' No 5', **Some homology to Sequences 14 and 16 od US patent 5674734**	kinase domain and death domain
RIP2	1304251	Receptor interacting protein 2,receptor interacting serine-threonine kinase 2,RICK,CARD containing ICE	RIP2 ,RIPK2	apoptosis array	NM_003821/Hs.103755	0.6 kb, pA, 3's, NO 5's, no extraneous o/l	kinase domain and CARD domain
RIP3	2505147	Receptor interacting serine/threonine kinase 3	RIP3	apoptosis array	NM_006871/Hs.268551	757 nt, 3 No 5', pA unknown	kinase, associates with death receptor complex
Rob band	11	Rob band 11/LOC51316 hypothetical protein	band 11	Implantation array	Hs.107139/AF208846		
RON		proto-oncogene RON tyrosine kinase receptor for MSP	MST1R	in-house	Hs.2942/X70040	pCR script	homolgy to MET,Macrophage stimulating 1 receptor (c-met-related tyrosine kinase)
RP_S7	1574779	ribosomal protein S7	RPS7	Implantation array	NM_001011		
RPA3	1524402	Replication Protein A3(14KD)	RPA3	apoptosis array	Hs.1608/L07493	0.6 kb, 3', pA, no o/l	Replication protein A
RPL23	2139225	ribosomal protein L23	RPL23	apoptosis array	Hs.234518/AI831644	0.6kb	
RPS 9	549925	ribosomal protein S9	RPS9	Implantation array	U14971		
RPS27		ribosomal protein S27	RPS27	Implantation array	U57847		
RXRB	357763	retinoic acid receptor,beta	RXRB	Implantation array	M84820		hom RXRA
RYR1	1375309	ryanodine receptor 1 (skeletal)	RYR1	in-house clone	J05200/Hs.89631	0.5kb,3's, no 5's, pA,bhomology to type2 and type 3 receptors	Ca2+ release channel of sarcoplasmic reticulum
RYR2	39296	ryanodine receptor 2 (cardiac)	RYR2	in-house clone	X98330/Hs90821	3's & 5's,0.8kb	Ca2+ release
RYR3	72497	ryanodine receptor 3	RYR3	in-house clone	AJ001515/Hs9349	1.1kb,3's & 5's	Ca2+ release,homology to brain ryanodine
Sag	430330	SAG (CKBBP1)ring finger 7,spliced valant of SAG	CKBBP1	apoptosis array	AF092878	0.4 kb, 5's, 3's, pA, no sig O/L	zinc RING finger protein
Scaffold	2207622	Scaffold protein, Syndecan binding protein,syntenin	SDCBP	in-house clone	U83463/Hs8180	3's, no 5's, 0.6kb	homology to syndecan binding protein (syntenin) also called Pbp1 scaffold protein
SELL	416087	selectin L (lymphocyte adhesion molecule 1)	SELL/LAM-1	Implantation array	M25280	last 1.3kb	
SELP	2004780	P-selectin,granule membrane protein 140kd,CD62	SELP	apoptosis array	Hs.73800/M25322	0.7 kb, NO 5's, 3's, pA, no sig O/L	(PAGEM, GMP-140, CD62), Survival function
SELPLG	471805	selectin P ligand	SELPLG	Implantation array	U02297		
Sem 3 (2)		Semaphorin III (Hsema1)	SEMA3A	in-house clone	L26081/Hs.2414	pCR-Script	previously listed as semaIV but seq shows to be III
Sem3	14	semaphorin 111(HSEMA1)	SEMA3A	in-house clone	Hs.2414/L26081	pCR-Script,	sema domain,immunoglobulin domain (Ig) short basic domain,secreted ,sem 3A
sentrin		sentrin, ubiquitin-like 1 protein	UBL1	Implantation array	U83117/Hs.81424		
SERPIN A5	341272	serpin A5 serine (or cysteine) proteinase inhibitor,clade A	SERPIN A5	Implantation array	Hs.76353		
sflt Ken (1)		sFLT Kendal	sFLT[1]	in-house clone		B/S11 KS +/- full length Kendal	
sflt Ken (2)		sFLT Kendal	sFLT[2]	in-house clone		B/S11 KS +/-full length Kendal	
sflt ken3	3	sFLT Kendal	sFLT[3]	in-house clone	Hs.138671/X51602	pCR-Script, 3' end of kendal	soluble VEGFR receptor
sfriz 1		proteasome)subunit,alpha type,4	PSMA3	in-house clone	Hs.346918/AU100193		
SFRP1	162330	secreted frizzled-related protein 1	SFRP1	Implantation array	AF056087		

Gene ID	IMAGE	Gene	Abbrev	clone source	Acc.No./Unigene ID	clone details	other information & changes to list name
sfrp2	1559823	secreted frizzled-related protein 2	SFRP2	Implantation array	AA927991/Hs.31386		
SFRP4	725269	secreted frizzled-related protein 4	SFRP4	Implantation array	AF026692/Hs.105700		hom fritz except last 1.6 kb
SFRS2	150062	splicing factor,arginine/serine-rich 2, SC35	SFRS2	Implantation array	M90104/Hs.73965		splicing factor SC35
SHC	310534	SHC1,SHC(Src homology) tranforming protein 1	SHC	apoptosis array	X68148/Hs81972	0.6 kb, 3's, pA, no sig O/L	SH2 domain-containing adapter
SHIP2	2074867	SH2 containing inositol phosphatase 2	SHIP2	apoptosis array	X66360/Hs155939	0.8 kb, 3's, NO 5's, NO pA, no sig O/L	was misassigned, now in unigene as INPP5D inositol polyphosphate 5 phosphatase,145KD
Sir2	1705202	Sirtuin silent mating type information regulation 2 hom 2 transcipt variant 2	SIR2,SIRT2	apoptosis array	Hs.112306/AF083107	0.6 kb, 3', pA, no o/l	
SIRT3	2012070	Sirtuin silent mating type information regulation 2 hom 3	SIRT3	apoptosis array	Hs.19306	0.6 kb, 3', pA ?, some homology to Homo sapiens sirtuin type 3 (SIRT3) mRNA	Sir2-like protein (sir2-like 3), check out sir2 at H/E8
SIVA	632137	SIVA,CD27 binding (SIVA)protein	SIVA	apoptosis array	AF033111/Hs 112058	0.9 kb, pA, 5's3's, no extraneous o/l	DD, ring finger, and zinc finger, pro-apoptotic, binds CD27 note that 100% homol to alt spliced SIVA-2
SLC25A1	262516	SLC25A1 Solute carrier family 25 (mitochondrial carrier; citrate transporter) member 1	SLC25A1	Implantation array	Hs.111024/L75823		
SLC6A8	488505	solute carrier 6 (neurotransmitter transporter,creatinine) member 8	SLC6A8	in-house clone	Hs.187958/L31409	0.8 kb,3's, no 5's,	
SLP1	378813	secretory leukocyte protease inhibitor	SLP1	Implantation array			
SLP1	378813	secretory leukocyte protease inhibitor	SLP1	Implantation array			
Smac(1)	1947740	diablo, Second Mitochondria Derived activator of caspase	SMAC	apoptosis array	Hs169611	3' end 0.6kb	
Smac(2)	2400050	diablo, Second Mitochondria Derived activator of caspase	DIABLO/SMAC	apoptosis array	Hs169611	pA, 3'seq, no 5'seq	see also KG5/JA3/KE6 same gene different clones
Smac(3)	266339	diablo, Second Mitochondria Derived activator of caspase	SMAC	not listed	Hs169611/AF262240		see also KG5/JA3/JC9 same gene different clones
Smac(4)	1737818	Second mitochondria -derived activator of caspase	SMAC	not listed	Hs.169611/AK001399		see also KE6/JA3/JC9 same gene different clones
SNX12		sorting nexin 12,endosome-localized proteins	SNX12	Implantation array	Hs.287867/AF171229		
SOCS2(2)	131550	Supressor of cytokine signalling 2, STAT induced STAT inhib. 2	SOCS2, STATI2	Implantation array	AF020590		
SOCS3(1)	152398	Supressor of cytokine signalling 3, STAT induced STAT inhib. 3	SOCS3,SSI3	Implantation array	AB004904		prevoiusly listed as SOCS3 now SOCS3[1]
SOCS3(2)	152398	Supressor of cytokine signalling 3, STAT induced STAT inhib. 3	SOCS3, SSI3	Implantation array	AB004904		prevoiusly listed as SOCS3 now SOCS3[2]
SOCS5	135058	Supressor of cytokine signalling 5, KIAA0671	SOCS5	Implantation array	AB014571		
SOD1	135618	superoxide dismutase 1	SOD1	Implantation array	K00065		
SOD1		CU/ZN Superoxide dismutase 1 soluble, amyotrophic	SOD1	in-house clone	Hs.75428/BG762708	B/S11 KS +/-Exons 1-4	
solute 7	115419	Solute carrier family 7	SLC7A7	apoptosis array	Hs.194693/NM_003982	0.6 kb	cationic amino acid transporter, glycoprotein-associated
SPARC	250654	secreted protein, acidic, cysteine-rich (osteonectin)	SPARC	apoptosis array	Hs.111779/NM003118	1.6 kb, 5's, 3's, NO pA, seq by nhgri	also known as BM-40 extracellular matrix protein, see E/E6 different clone
SPARC(1)	1987468	secreted protein, acidic, cysteine-rich (osteonectin)	SPARC	Implantation array	J03040		
SPOCK	488409	sparc/osteonectin,cwcv&kazal -like domains proteoglycan (TESTICAN-1)	SPOCK	Implantation array	Hs.93029/X73608		previously listed as CTSD, miss-assigned
SPP1	121165	osteopontin, secreted phosphoprotein 1	SPP1	Implantation array	J04765/Hs313		see also in house clone F/D11
SRD5A1	843277	steroid 5-alpha-reductase, alpha polypeptide1	SRD5A1	Implantation array	AF052126		
SSI-1	712481	JAK binding protein, supressor of cytokine signalling	SSI-1	Implantation array	U88326		suppressor of cytokine signalling
SSP1		osteopontin, secreted phosphoprotein 1	SSP1	in-house clone	X13694/Hs313	pCMVSPORT 2, Clones from J&J	see also image clone B/E9, previously listed as osteo

Gene ID	IMAGE	Gene	Abbrev	clone source	Acc.No./Unigene ID	clone details	other information & changes to list name
St calcin2	2113336	Stanniocalcin-2	STC2	apoptosis array	Hs.155223	0.9 kb	calcium-regulated glycoprotein hormone, ?role in Ca2+ homeostasis? - fish relatives
STAT1	471667	signal transducer and activator of transcription-1	STAT1	apoptosis array	M97935	0.8 kb, 5's, 3's, pA, no sig O/L	signal transducer and activator of transcription-1 = ISGF-3
STAT3	612444	signal transducer and activator of transcription-3	STAT3	apoptosis array	L29277	0.9kb, 5's, 3's, pA, no sig O/L	
STAT4(1)	1524207	Signal transducer and activator of transcription 4	STAT4	apoptosis array	Hs.80642/AI700201	0.6 kb, 3's, NO 5's, NO pA, no sig O/L	
STAT5A		signal transducer & activator of transcription 5A	STAT5A	Implantation array	U43185/Hs 1674503	0.8kb	
STAT6		Interleukin 4 induced signal transducer & activator of transcription 6	STAT6	Implantation array	Hs.181015/NM_003153		
STAT6	358375	STAT6	STAT6	apoptosis array	Hs.181015	0.7 kb, 3's, NO 5's, pA, no sig O/L	
stathmin		Stathmin 1 ,oncoprotein 18	STMN1	Implantation array	Hs.250811	0.8kb,3'	
STE	211956	sulfotransferase, estrogen-preferring	STE	Implantation array	U08098		
STM2		Alzheimers disease (STM2) presenilin 2	STM2	Implantation array	U50871		
survivin	109857	survivin,baculoviral IAP repeat containing 5	BIRC5	apoptosis array	U75285 /Hs.1578	0.7 kb, NO pA, 3's, 5's, no extraneous o/l	expressed in G2/M, binds to and inhibits caspases 3 and 7,aka EPR1 effector cell protease 1
TALL-1	593690	TALL-1 (Thank / Blys)	TALL-1	apoptosis array	NM_006573	0.5 kb, pA, NO 5' but 3', no extraneous o/l	transmembrane TNFR ligand, expressed in macropahges, downregulated by PMA
TBXAS1	418423	thromboxane A synthase 1	TBXAS1	Implantation array	M80646		
TCF7L2	752652	transcription factor 7-like 2	TCF7L2	Implantation array	Hs.348412/AA417665		
telo ass	2206426	telomerase-associated protein 1	TEP1	apoptosis array	Hs.232070	unknown size, NO 5's, 3's, pA, no sig O/L	
TERT	2304672	telomerase reverse transcriptase (hTRT)	TERT	apoptosis array	AF015950 /Hs.115256	o.4kb, 3's, NO 5's, pA, no sig O/L	human telomerase catalytic subunit (hTRT/hEST2)
TFPI2	67508	tissue factor pathway inhibitor-2	TFPI2	apoptosis array	Hs.295944/L27624	0.6 kb,3'&5'	placental protein 5 (PP5)
TGF beta	2138946	transforming growth factor beta 1	TGFbeta	apoptosis array	X02812	0.6 kb	
TGFA	1839392	transforming growth factor alpha	TGFA	Implantation array	M31172		
TGFB1	132031	transforming growth factor beta 1	TGFB1	Implantation array	X02812/Hs 1103		last 0.6kb
TGFB3	485709		TGFB3	Implantation array	J03241		
TGFB4 (1)	137335	transforming growth factor beta 4, endo.bleeding associated factor	TGFB4, EBAF	Implantation array	U81523		
TGFB4 (2)	137335	transforming growth factor beta 4, endo.bleeding associated factor	TGFB4, EBAF	Implantation array	U81523		
TGFBR3	143723	transforming growth receptor beta receptor III, betaglycan	TRFBR3	Implantation array	L07594		betaglycan
TGM2	was empty	human transglutaminase 2	TGM-2	an imposter not listed	not empty !		transglutaminase 2 (C polypeptide, protein-glutamine-gamma-glutamyltransferase) apoptosis associated
THBS1	1964654	Thrombospondin 1	THBS1	not listed	Hs.87409/X14787		natural inhibitor of neovascularization and tumorigenesis in healthy tissue mediates cell-to-cell and cell-to-matrix interactions,roles in platelet aggregation, angiogenesis, and tumorigenesis
Tie1		Tie 1,tyrosine kinase with IgG&EGF homology domains	TIE	in-house clone	Hs.78824/X60957	pCR-Script,	
TIE1	376677	TIE 1,tyrosine kinase with immunoglobulin & EGF homology domains	TIE	Implantation array	Hs.78824/X60957/NM_005424	last 0.6kb	
Tie2		Tie 2,tyrosine kinase ,endothelial	TEK	in-house clone	Hs.89640/L06139	pCR-Script,	
TIE2	183661	TIE 2 ,TEK tyrosine kinase, endothelial	TIE 2	Implantation array	L06139		last 0.5kb
TIMP1	740655	tissue inhibitor of metalloproteinase 1	TIMP1	Implantation array	X03124		
TIMP2	138147	tissue inhibitor of metalloproteinase 2	TIMP2	Implantation array	J05593		
TIMP3	469940	tissue inhibitor of metalloproteinase 3	TIMP3	Implantation array	U67195		sorsby fundus dystrophy
Titin	1475648	Titin	TTN	in-house clone	X69490/Hs.172004	3's, no 5's,0.7kb	
TLN	435642	talin	TLN	Implantation array	AF078828		
TMP-1	341328	Tropomyosin 1 alpha	TMP-1	in-house clone	M19267/Hs77899	3's & 5's, 0.5kb	Cell motility,skeletal muscle alpha tropomyosin
TMSB10	840788	thymosin beta 10	TMSB10	Implantation array	M20259		

Gene ID	IMAGE	Gene	Abbrev	clone source	Acc.No./Unigene ID	clone details	other information & changes to list name
TMSB4X	511921	thymosin beta-4	TMSB4X	apoptosis array	Hs.75968/M17733	3' and 5', pA, 0.6kb, homology to Human interferon-inducible mRNA	actin-sequestering protein
TNF-beta	1846402	TNF-beta (=LT-alpha) = (TNF superfamily, member 1)	TGF-B	apoptosis array	D12614	1.0 kb, pA, NO 5' but 3', no extraneous o/l	activated lymphocyte-secreted pro-apoptotic cytokine
TNF-C (2)	701054	high mobility group (nonhistone chromosomal) proteins I&Y	HMGIY	apoptosis array	Hs.139800/AA287531	0.8 kb, pA, NO 5' but 3', no extraneous o/l	
TNF4	2001553	TNFSF4 = OX40 LIGAND = GP34	TNFSF4	apoptosis array		3' read, 1.1 kb, no sig O/L	
TNFA	214060	TNF-alpha	TNFA	apoptosis array	X01394 /Hs241570	0.5kb, pA, 5'3', no extraneous o/l	macrophage-secreted pro-apoptotic cytokine (TNF superfamily, member 2)
TNFB	1672927	tumour necrosis factor beta/lymphotoxin alpha	TNFB	Implantation array	D12614		
TNFR2	153751	tumour necrosis factor receptor 1B	TNFR2 (TNFRSF1B)	Implantation array	M32315		hom TNFR1
TNFR2(1)	1896559	TNF receptor superfamily member 1B	TNFR2	not listed	Hs.256278/AI880380		NB same gene different clone as K/D6
TNFR2(2)	2336400	TNF receptor superfamily member 1B	TNFR2	not listed	Hs.256278/AI880380		NB same gene different clone as K/B6
TNFRSF1A	2326094	TNF receptor superfamily,member 1A	TNFRSF1A	apoptosis array	M33294 /Hs.159	0.5 kb, pA, 3's no 5', no extraneous o/l	caspase activation and also STAT/JAK activation
TNFRSF6B	2506835	TNF receptor superfamily,member 6b, also decoy receptor 3 DcR3	TNFRSF6B	not listed	Hs.348183/AF104419	0.5kb,3',pA	
TNNC2	627935	Troponin C2,fast	TNNC2	in-house clone	X07898/Hs182421	3's, no 5's,0.7kb	fast skeletal muscle troponin
TNR	175767	tenascin R (restrictin,janusin)	TNR	Implantation array	X98085		
TOSO	1653122	TOSO, regulator of FAS-induced apoptosis	TOSO	apoptosis array	NM_005449/AW401870/Hs.58831	0.7 kb , 3' no 5', no extran. O/l	inhibits caspase8 processing, may upregulate FLIP
TPI1	2279444	Triosephosphate isomerase-1	TPI1	in-house clone	M10036/Hs83848	3's, no 5's, 0.5kb	
TR6(DR3)	2108163	TR6 (DR3),TNFRSF6B TNF superfamily,member6b, decoy	TR6 (DR3)	apoptosis array	AF134240/Hs348183	0.5 kb, pA, 3' no 5', no extraneous o/l	supresses LIGHT-mediated apoptosis
TRA 1	2328129	Tumour rejection antigen (gp96)1	TRA-1	in-house clone	X15187/Hs82689	3's, no 5's,0.8kb	Tumour rejection, heat shock protein
TRADD(1)	1455700	TNFRSF1A associated via death domain	TRADD	apoptosis array	L41690 /Hs89862	0.5 kb, pA, 5's, NO 3's, no extraneous o/l	
TRADD(2)	1473788	TNFRSF1A-associated via death domain	TRADD	Implantation array	L41690		
TRAF-1(1)	unknown	TNF receptor associated factor 1Epstein Barr virus induced mRNA	TRAF-1	in-house clone	U19261/Hs.2134		
TRAF-1(2)	2962961	TNF receptor associated factor 1Epstein Barr virus induced mRNA	TRAF-1	apoptosis array	U19261/Hs.2134		
TRAF-2	1014600	TNF receptor -associated factor 2	TRAF-2	apoptosis array	U12597 /Hs200526	0.7 kb, pA, 3's, NO 5's, no extraneous o/l	also called TRAP3, see E/G12 same gene diff clone
TRAF-3	2062637	TRAF-3 (CRAF1)	TRAF-3	apoptosis array	U21092	0.7 kb, NO pA, 3's, NO 5's, no extraneous o/l	CD40 associated factor, =TRAF3
TRAF-4	1855433	TNF receptor -associated factor 4	TRAF-4	apoptosis array	AF082185/Hs8375	0.6 kb, pA, 3's no 5', no extraneous o/l ; some homology to MLN62	CART1
TRAF-5	145410	TNF receptor-associated factor 5	TRAF-5	apoptosis array	U69108 /Hs29736	0.8 kb, no pA, 3's, NO 5's, no extraneous o/l	TNF-receptor family members
TRAIL	139039	TNF-related apoptosis-inducing ligand	TRAIL APO2L	apoptosis array	U57059	0.7 kb, 5's, 3's pA, no sig O/L	tumor necrosis factor ligand superfamily member 10, Apoptosis ligand TRAIL, TRAIL, TL2, TRAIL-PEN, Ly81, Apo-2 ligand, (APO2L)
TRAIL-R-2	2348250	TRAIL-R-2 (DR5 / KILLER),TNFRSF10B TNF superfamily 10B	TRAIL-R-2	apoptosis array	Hs.51233	0.8 kb, 3's, no extraneous o/l	Transcription activated by NFkB, associates with DR5, FADD and TRADD, also utilises RIP
TRAIL-R4/3	1406602	TRAIL-R-3, decoy receptor 1,TNFRSF10D with homology toTRAIL-R-4 (TRUNDD)	TRAIL-R4/3	apoptosis array	AF012536/AF023849	size unknown, 3' no 5', pA unknown, some O/L with others of family	no intracytoplasmic domain, 89% homologouos to TRID
TRAMP	769981	Translocating chain-associating memebrane protein (Apo3, LARD,DDR3,TNFRSF12)	TRAMP	apoptosis array	Hs.180338	0.7 kb, pA, 5's3's, no extraneous o/l,	signals through TRADD, TRAF2, FADD, and FLICE, activates NFkB.769981 **no longer in unigene list (5.1.02)**
TRAP3	770804	TNF receptor-associated factor 2	TRAF2	Implantation array	U12597/Hs200526		see G/E12 TRAF2 same gene diff clone
TRFBR2	469876	transforming growth receptor beta receptor II(70-80KD)	TRFBR2	Implantation array	Hs.82028/M85079		
TRHR		Thyrotrophin-releasing hormone receptor	TRHR	in-house clone	X72089/Hs3022	pCMVSPORT 2	

Gene ID	IMAGE	Gene	Abbrev	clone source	Acc.No./Unigene ID	clone details	other information & changes to list name
TRICK2	1133411	TNF receptor superfamily,member 10b,TNFRSF10b	TRICK2,TRAIL-R2,Killer	apoptosis array	AF018658	0.4kb, pA, no o/l, 3' seq only	pro-apoptotic trail receptor2, Tumor necrosis factor receptor superfamily, member 10b,Apo-2L,death receptor 5
TRIP	2307972	TRAF interacting protein	TRIP	apoptosis array	U77845/Hs21254	no pA, NO 5's, 3's, no extraneous o/l	inhibits TRAF2-mediated NF-kappaB activation
TRO	649344	trophinin	TRO	Implantation array	U04811		MAGED3
TROAP	731099	tastin/trophinin-associated protein	TROAP	Implantation array	U04810/Hs.171955		
TRPC2	unknown	transient receptor potential channel 2	TRPC2	Implantation array	Hs.131910/X89067		
TRPC2	unknown	transient receptor potential channel 2	TRPC2	Implantation array	Hs.131910/X89067		
TRPD3	unknown	transient receptor potential D3,tetratricopeptide repeat domain 3	TTC3,TRPD3	Implantation array	Hs.118174.D83077		
Tsp-1	2440915	Thrombospondin-1	THBS1	apoptosis array	Hs.87409	0.6 kb, 3', pA, no o/l	no verified seq ref, from apoptosis pending list
Tsp-2	416134	Thrombospondin-2	THBS2	apoptosis array	Hs.108623	0.6 kb, 3', pA, no o/l	
Tsp-4 (1)	2070678	Thrombospondin-4	THBS4	apoptosis array	Hs. 75774	0.6 kb, 3', pA, some homology to Tsp-3 and clk2 kinase	
Tsp-4 (2)	2070678	Thrombospondin-4	THBS4	apoptosis array	Hs. 75774	0.6 kb, 3', pA, some homology to Tsp-3 and clk2 kinase	
Tsp3	2362163	Thrombospondin-3	THBS3	apoptosis array	Hs.169875	0.6 kb, 3', pA, some homology to clk2 kinase (CLK2)	
TTR	82063	transthyretin, prealbumin, amyloidosis type 1	TTR	Implantation array	M10605		
TUBB2	1636876	Beta-tubulin 2	TUBB2	in-house clone	X02344/Hs.251653	1kb	
Tweak	154742	TWEAK,tumour necrosis factor,superfamily member12	TWEAK,TNFSF12	apoptosis array	NM_003809/Hs26401	0.7 kb, pA, 5's3's, no extraneous o/l	widely expressed TNFR ligand, secreted, weakly pro-apoptotic
TYK2	212292	tyrosine kinase 2	TYK2	Implantation array	X54637/Hs.75516	last 0.7kb	
ubiqutinC	137024	ubiquitin C	UBC	Implantation array	M26880/Hs.183704		
UGB	118085	uteroglobin	UGB	Implantation array	X13197/Hs.2240		
UPA	714106	Urokinase plasminogen activator (PAI2)	UPA	apoptosis array	Hs.77274/X02419	0.7 kb	Urokinase plasminogen activator (PLAU)
USA-CYP	73425	cyclophilin H, U-snRNP-associated cyclophilin,peptidyl proplylisomerase H	USA-CYP,PPIH	Implantation array	AF036331/Hs9880		
UTS2	926809	urotensin 2	UTS2	Implantation array	AF104118		
vav	80384	VAV1 oncogene	VAV1	apoptosis array	X16316 /Hs.116237	0.7 kb, 5's, 3's, pA, no sig O/L	haemopoietic-specific exchange factor for Rac-1
vav2	2386937	vav2 oncogene	VAV2	apoptosis array	S76992/ AI797805Hs.104005	07 kb, 3' no 5', no pA,	homologue of the vav, note that this is not the TSC1 gene
vav3	2435565	VAV3 oncogene	VAV3	apoptosis array	Hs267659/AF067817	0.6kb	
VCAM1	44477	vascular cell adhesion molecule 1	VCAM1	Implantation array	M30257		last 0.4kb
VDAC-2	994448	Voltage-dependent anion channel 2	VDAC-2	apoptosis array	Hs.78902	0.7 kb, 3' read, pA, search -> no O/L	Voltage-dependent anion channel 2
VE Cad	135239	VE-Cadherin	CDH5	apoptosis array	X79981	1kb, 5'3, 3's, pA, no sig O/L	binds AKT, may regulate Bcl-2 expression (cadherin 5)
vegf 121	B1	vascular endothelial growth factor	VEGF	in-house clone	Hs.73793/AB021221	mouse	NB BLAST matches human
vegf 165	7B	vascular endothelial growth factor	VEGF	in-house clone	Hs.73793/AB021221	B/S11 KS +/-splice variant 165	
vegf 189	13B	vascular endothelial growth factor	VEGF	in-house clone	Hs.73793/AB021221	B/S11 KS +/-splice variant 189	
VEGF A		vascular endothelial growth factor A	VEGF A	in-house clone	Hs.73793/AB021221	B/S11 KS +/-,Exons 1-4	
VEGF B	18	vascular endothelial growth factor B	VEGF B	in-house clone	Hs.78781/U52819	pCR-Script	
VEGF C		Vascular endothelial growth factor C	VEGFC	in-house clone	Hs.79141/X94216	pCR-Script,	
VEGF D		Vascular endothelial growth factor D	FIGF	in-house clone	Hs.11392/D89630	pCR-Script,	aka FIGF C-fos induced growth factor
VEGFA	245379	Vascular endothelial growth factor A	VEGF A	Implantation array	AF022375/Hs.73793		
VEGFB	181724	Vascular endothelial growth factor B	VEGF B	Implantation array	U48801/Hs.78781		

Gene ID	IMAGE	Gene	Abbrev	clone source	Acc.No./Unigene ID	clone details	other information & changes to list name
VEGFC	503189	Vascular endothelial growth factor C	VEGF C	Implantation array	X94216		Flt4 ligand
VEGFD	160946	Vascular endothelial growth factor D (c-fos induced gf)	VEGF D/FIGF	Implantation array	D89630		
VEGFD(1)		Vascular endothelial growth factor D (c-fos induced gf)	VEGF D/FIGF	Implantation array	Hs.11392/D89630		
VHL	41607	Von Hippel-Lindau syndrome	VHL	Implantation array	NM_000551		
VIM	119599	vimentin	VIM	Implantation array	NM_003380/Hs.297753		
VIP2R	2164744	Vasoactive intestinal polypeptide receptor 2	VIP2R	apoptosis array	Y18424	IMAGE:2164744, 3's, appears to have pA, no sig O/L	
vWF	127595	von Willebrand factor	VWF	Implantation array	K03028/Hs.110802		
WAF1	309880	WAF1,p21,CDKN1A cyclin- dependent kinase inhibitor 1A,Cip1	WAF1	Implantation array	U03106/Hs.179665		
WIF1(1)	40908	wnt inhibitory factor 1	WIF-1	Implantation array	AF122922		
WISP1	2125289	WNT1 inducible signalling pathway protein 1	WISP1	Implantation array	AF100779		
WISP1	2125289	WNT1 inducible signalling pathway protein 1	WISP1	Implantation array	AF100779		
WISP2	1632487	WNT1 inducible signalling pathway protein 2	WISP2	Implantation array	AF100780		
WISP3	1076664	WNT1 inducible signalling pathway protein 3	WISP3	Implantation array	Hs.194678/AF100781		
wnt2	122762	wingless-type MMTV integration site family 2	wnt2	Implantation array	X07876/Hs.89791		hom wnt13 except last 1kb.aka human irp
wnt3	1706460	wingless-type MMTV integration site family 3	wnt3	Implantation array	AI159968		last 1.5kb
wnt5A	132333	wingless-type MMTV integration site family 5A	wnt5a	Implantation array	L20861/Hs.152213		
wnt5b	2094005	wingless-type MMTV integration site family 5B	wnt5b	Implantation array	AI424438		last 0.3kb
wnt6	2115315	wingless-type MMTV integration site family 6	wnt6	Implantation array	AI474287		
wnt7a	WHO cl.8	wingless-type MMTV integration site family 7a	wnt7a	Implantation array	U53476		hom wnt8b except last 0.45kb/primers15/16
wnt10a	1935064	wingless-type MMTV integration site family 10a	wnt10a	Implantation array	Hs.121540/AI366749		
WNT10B	1708905	wingless-type MMTV integration site family 10B	wnt10b	Implantation array	U81787		
wnt11	501862	wingless-type MMTV integration site 11	wnt11	Implantation array	Y12692		
XRCC4(1)	1991768	X-ray repair complementing defective repair in CHO cells 4	XRCC4	apoptosis array	Hs.150930	0.8 kb, 3' no5', pA, no o/l	assocsiates with DNA POL 4, substrate of DNA-PKcs, (yeast homologue is LIF1p) seeH/E10 same clone
XRCC4(2)	1991768	X-ray repair complementing defective repair in CHO cells 4	XRCC4	apoptosis array	Hs.150930/U40622	0.8 kb, 3' no5', pA, no o/l	see J/E3 same clone
ZNF313	1693595	zinc finger protein 313	ZNF313	Implantation array	M10988		

KEY

	Implanatation array, many genes involved in angiogenesis are incorporated into this set
	Genes implictaed or known to be involved in apoptosis
	Exogenous control spots eg *Arabidposis Thaliana* with no known cross hybridisation with human sequences
	Endogenous control
	Genes cloned in -house
	Origins of the clone unknown

The original file also contained a link to the sequence and the metagrid/subgrid layout which has been omitted from this table
Assignment to a list does not mean they are exclusive to other groups

PUBLICATION 2

Holland, C. M., Day, K., **Evans, A.** & Smith, S. K. 2003. Expression of the vegf and angiopoietin genes in endometrial atypical hyperplasia and endometrial cancer. *Br J Cancer,* 89**,** 891-8.

Citd by 39, Impact factor 5.042

ISSN: 0007-0920

Journal Type

British Journal of Cancer (BJC) covers all aspects of cancer from a number of disciplines including clinical, pharmaceutical and physical sciences. It provides a forum for original research findings that have relevance to understanding the etiology of cancer and to improving the treatment and survival of patients. Once accepted, papers are published rapidly in print and online. This paper was published under the section: Molecular and Cellular Pathology.

Personal Contribution

My contribution to this publication was collection of the benign and atypical complex hyperplasia endometrial samples from theatre followed by processing to RNA, cDNA and quantitative PCR. I was also involved in the cloning of the angiopoietins 1 and 2 previously published in:

Sowter, H. M., Corps, A. N., Evans, A. L., Clark, D. E., Charnock-Jones, D. S. & Smith, S. K. 1997. Expression and localization of the vascular endothelial growth factor family in ovarian epithelial tumors. *Laboratory Investigation,* 77**,** 607-614.

British Journal of Cancer (2003) 89, 891 – 898

www.bjcancer.com

Expression of the VEGF and angiopoietin genes in endometrial atypical hyperplasia and endometrial cancer

CM Holland*[,1,2], K Day[2], A Evans[1] and SK Smith[1,2]

[1]Department of Pathology, University of Cambridge, Tennis Court Road, Cambridge CB1 1QP, UK; [2]Department of Obstetrics and Gynaecology, University of Cambridge, The Rosie Hospital, Robinson Way, Cambridge CB2 2SW, UK

Angiogenesis is critical for the growth and metastasis of endometrial cancer and is therefore an important therapeutic target. Vascular endothelial growth factor-A (VEGF-A) is a key molecule in angiogenesis, but the identification of related molecules and the angiopoietins suggests a more complex picture. We investigated the presence of transcripts for VEGF-A, VEGF-B, VEGF-C, VEGF-D, Angiopoietin-1 and Angiopoietin-2 in benign endometrium, atypical complex hyperplasia (ACH) and endometrioid endometrial carcinoma using *in situ* hybridisation. We confirmed the presence of VEGF-A mRNA in the epithelial cells of cancers examined (13 out of 13), but not in benign endometrium or ACH. We also demonstrate, using quantitative polymerase chain reaction, that levels of VEGF-B mRNA are significantly lower in endometrial cancer than benign endometrium. We conclude that loss of VEGF-B may contribute to the development of endometrial carcinoma by modulating availability of receptors for VEGF-A.
British Journal of Cancer (2003) **89,** 891 – 898. doi:10.1038/sj.bjc.6601194 www.bjcancer.com

Keywords: VEGF-B; angiopoietins; endometrial cancer; endometrial hyperplasia; *in situ* hybridisation

Angiogenesis is a critical event in the growth and spread of tumours (Folkman, 1990). The vascular endothelial growth factor family (VEGFs) and the angiopoietins are key factors in this process (Fong *et al*, 1995; Shalaby *et al*, 1995; Ferrara *et al*, 1996; Maisonpierre *et al*, 1997; Thurston *et al*, 1999). Vascular endothelial growth factor-A is a dimeric glycoprotein existing as four main isoforms by alternative splicing from a single gene. The coding regions of the VEGF gene comprise eight exons. The first four are conserved but alternative splicing of the last four gives rise to mRNAs of 121, 145, 165, 189 and 206 amino acids, respectively ($VEGF_{121}$, $VEGF_{145}$, $VEGF_{165}$, $VEGF_{189}$, $VEGF_{206}$) (Houck *et al*, 1991; Tischer *et al*, 1991; Charnock-Jones *et al*, 1993). The VEGF-A isoforms bind the tyrosine kinase receptors VEGFR-1 (flt-1) and VEGFR-2 (KDR/flk-1) to promote endothelial cell proliferation, migration and increased vascular permeability. Elevated levels of VEGF-A are found in many tumours including cancers of the endometrium (Doldi *et al*, 1996; Fujimoto *et al*, 1998) and ovarian epithelium (Olson *et al*, 1994; Boocock *et al*, 1995; Abu-Jawdeh *et al*, 1996). When VEGF-A signalling is blocked with VEGF-neutralising antibodies (Olson *et al*, 1996) or dominant-negative receptors (Millauer *et al*, 1994), tumour angiogenesis and growth are impaired.

However, the family of VEGF genes has expanded with the discovery of other VEGFs, for example, VEGF-B (Olofsson *et al*, 1996a), VEGF-C (Joukov *et al*, 1996) and VEGF-D (Achen *et al*, 1998), which share significant sequence homology with VEGF-A. VEGF-B exists as two splice variants, a heparin binding isoform of 167 amino acids ($VEGF\text{-}B_{167}$) and a secreted isoform of 186 amino acids ($VEGF\text{-}B_{186}$) (Olofsson *et al*, 1996b). Whereas VEGF-A binds to both the VEGFR-1 and VEGFR-2 receptors, VEGF-B binds only to the VEGFR-1 receptor (flt-1) (Olofsson *et al*, 1998). Vascular endothelial growth factor-B forms homodimers and can heterodimerise with VEGF-A (Olofsson *et al*, 1996a) to promote endothelial cell proliferation *in vitro* (Olofsson *et al*, 1996a).

Both VEGF-C and VEGF-D are ligands for VEGFR-2 (KDR) and the third VEGF receptor VEGFR-3 (flt-4) (Joukov *et al*, 1996; Achen *et al*, 1998). VEGFR-3 is expressed by adult lymphatic endothelial cells but not by adult vascular endothelium. There is a strong association between lymphovascular density and VEGF-C expression in human malignant mesothelioma, suggesting this pathway as an important therapeutic target (Ohta *et al*, 1999).

A second family of growth factors, the angiopoietins, are ligands for the tyrosine kinase receptor Tie-2 (Davis *et al*, 1996; Maisonpierre *et al*, 1997). The two ligands share 60% sequence homology and bind with equal affinity to Tie-2. Angiopoietin-1 (Ang-1) maintains pericyte/endothelial cell interactions (Hanahan, 1997; Thurston *et al*, 1999) while Angiopoietin-2 (Ang-2) is a functional antagonist of Ang-1 and leads to marked vessel regression in tumours in the absence of VEGF-A (Holash *et al*, 1999). Compared to Ang-1, which is widely expressed in adult tissues, Ang-2 is selectively expressed at sites of active angiogenesis, for example, the corpus luteum of the ovary (Goede *et al*, 1998) and endometrium (Li *et al*, 2001).

Angiogenesis is an important feature of endometrial cancer as microvessel density is an independent prognostic indicator of both progression and overall survival (Kaku *et al*, 1997). Furthermore, there is a progressive increase in microvessel density from benign

*Correspondence: Dr CM Holland, Box 223, Department of Obstetrics and Gynaecology, University of Cambridge, The Rosie Hospital, Robinson Way, Cambridge CB2 2SW, UK;
E-mail: cath.holland@obgyn.cam.ac.uk
Received 21 November 2002; revised 9 June 2003; accepted 24 June 2003

endometrium through the cancer precursor, atypical complex hyperplasia (ACH) to invasive disease (Abulafia *et al*, 1995).

While VEGF-A mRNA and protein are present in endometrial cancer (Doldi *et al*, 1996; Guidi *et al*, 1996; Fujimoto *et al*, 1998), its expression in ACH is unknown. Vascular endothelial growth factor-C (Hirai *et al*, 2001) and VEGF-D (Yokoyama *et al*, 2003) have both been correlated with a poor prognosis in endometrial cancer, but the expression of VEGF-B has not been described. In order to further investigate a possible role for other angiogenic factors in endometrial cancer, we investigated the presence of transcripts for VEGF-A, VEGF-B, VEGF-C, VEGF-D, Ang-1 and Ang-2 in benign postmenopausal endometrium, ACH and endometrioid endometrial carcinoma by *in situ* hybridisation and used quantitative polymerase chain reaction (PCR) to determine the levels of VEGF-B and Ang-2 mRNA in benign and malignant endometrium.

MATERIALS AND METHODS

Patients

A total of 13 carcinoma specimens were examined using *in situ* hybridisation. All were endometrioid-type carcinomas. Five benign postmenopausal endometrial specimens and five complex atypical hyperplasias were also examined for comparison. The age range of the patients was 51–87 years (median 57 years). Histopathological findings and clinical data are shown in Table 1. Presence or absence of lymphovascular space involvement is indicated, where reported, in the table. The survival status for each patient was noted at the time of preparation of this manuscript. Ethical committee approval was obtained from the committee of Addenbrookes Hospital NHS Trust.

Tissue samples

In situ hybridisation and immunohistochemistry were performed on formalin-fixed, paraffin-embedded endometrial tissue. Tissue used for reverse transcription–PCR (RT–PCR) and quantitative PCR was snap-frozen from endometrium removed during endometrial curettage or total hysterectomy, after examination by a histopathologist.

Production of radiolabelled riboprobes for *in situ* hybridisation

Antisense and sense (control) RNA probes were generated against VEGF-A, VEGF-B, VEGF-C, VEGF-D, angiopoietin-1 and angiopoietin-2 (Sowter *et al*, 1997). For VEGF-A, probes were designed to span the first four exons thus detecting the four commonly occurring isoforms. The sequences were amplified in pCRscript SK (Stratagene Ltd., Cambridge, UK) and pBluescript II KS vectors (Stratagene Ltd., Cambridge, UK). Radioactive, single-stranded probes incorporating ^{33}P-UTP (Amersham International plc, Little Chalfont, Buckinghamshire, UK) were carried out with 1 μg plasmid template using the Ambion MAXIscript transcription kit (Ambion Inc., Austin, TX, USA) before phenol extraction and ethanol precipitation.

Identification of mRNA encoding VEGF-A, VEGF-B, VEGF-C, VEGF-D, angiopoietin-1 and angiopoietin-2 by *in situ* hybridisation

Tissue sections (6 μm) were cut onto slides coated with 3-aminopropyltriethoxy-silane (Sigma Chemical, Poole, Dorset, UK). The hybridisation procedure was performed as described by Clark *et al* (1996). The riboprobe was incubated with the tissue sections for 18 h at 55°C. The sections were washed and treated with RNAse A (Sigma Chemicals, St Louis, USA), before being coated with autoradiographic emulsion (Amersham Pharmacia Biotech UK Ltd, Aylesbury, UK) and exposed for 21 days at 4°C. Sections were developed with photographic developer (Kodak D19) and counterstained with Mayer's haemalum (BDH Chemicals, Lutterworth, UK) before viewing.

Immunohistochemistry for cytokeratin and CD-68

Immunohistochemistry was performed on serial sections to identify the cell types expressing the transcripts. Mouse antibodies to human cytokeratin (clone MNF116; Dako, Ltd., High Wycombe,

Table 1 Clinical and histopathological details for patient samples used in the study

Patient	Histology	Age	Status	FIGO stage	Grade	LVS involved	Tamoxifen use
1	Benign	51	Alive	—	—	—	N
2	Benign	57	Alive	—	—	—	N
3	Benign	80	Alive	—	—	—	N
4	Benign	63	Alive	—	—	—	N
5	Benign	68	Alive	—	—	—	N
6	ACH	56	Alive	—	—	—	N
7	ACH	58	Alive	—	—	—	N
8	ACH	52	Alive	—	—	—	N
9	ACH	69	Alive	—	—	—	N
10	ACH	52	Alive	—	—	—	N
11	Endometrioid cancer	41	Alive	1C	1	N	N
12	Endometrioid cancer	56	Alive	2B	2	N/R	N
13	Endometrioid cancer	48	Alive	2B	2	Y	N
14	Endometrioid cancer	46	Alive	1B	2	N	N
15	Endometrioid cancer	71	Alive	3A	3	N/R	N
16	Endometrioid cancer	87	Alive	1B	3	N	N
17	Endometrioid cancer	54	Alive	1B	3	N	Y
18	Endometrioid cancer	78	Deceased	1C	3	N	N
19	Endometrioid cancer	84	Deceased	4A	3	Y	N
20	Endometrioid cancer	56	Alive	3B	3	N/R	N
21	Endometrioid cancer	52	Alive	1B	3	N/R	Y
22	Endometrioid cancer	68	Deceased	4A	3	Y	Y
23	Endometrioid cancer	81	Alive	1B	3	Y	N

ACH = atypical complex hyperplasia; LVS = lymphovascular space involvement N/R = not reported N = never, Y = yes.

Buckinghamshire, UK) and human CD68, a macrophage marker, (clone PG-1; Dako, Ltd.) were used as described previously (Clark *et al*, 1996). Mouse IgG (Dako, Ltd.) incubated with serial sections provided negative controls.

Reverse transcription – PCR

RNA from benign postmenopausal endometrium, ACH and endometrioid endometrial carcinoma was analysed by RT – PCR to determine whether mRNA for VEGF-C was present (Figure 1). Total RNA was extracted from snap-frozen tissue using acid phenol purification (Chomczynski and Sacchi, 1987). Samples for PCR were unrelated to those used for *in situ* hybridisation. RNA was annealed with oligo-dT primers (Pharmacia Biotech LTD., St Albans, UK) and cDNA was synthesised using reverse transcriptase (HT Biotechnology LTD., Cambridge, UK). Polymerase chain reaction for VEGF-C was performed using the upstream primer 5′-TGCCGATGCATGTCTAAACT-3′, and the downstream reverse complement primer 5'-TGAACAGGTCTCTTCATCCAGC-3′ for 40 cycles (15 s at 95°C and 60 s at 60°C).

Quantitative PCR

RNA was extracted and purified and cDNA was prepared as above. Quantitative, real-time PCR was performed in triplicate using the ABI PRISM 7700 Sequence Detector (Applied Biosystems, Warrington, UK) according to the manufacturer's instructions and the resultant data were averaged. Non-template controls were included in each experiment. Specific oligonucleotide primers and probes were designed for VEGF-B using Primer Express® 1.5 software (Applied Biosystems, Warrington, UK). Specific primers and probe for Ang-2 were a gift from Mrs K Day of The Reproductive Molecular Research Group at the University of Cambridge Department of Obstetrics and Gynaecology. Details for VEGF-B primers and probe are shown below.

Forward primer, 5′ – AGCACCAAGTCCGGATG – 3′
Reverse primer, 5′ – GTCTGGCTTCACAGCACTG – 3′
Probe, 5′-6FAM – AGATCCTCATGATCCGGTACCCGT – 3′

A 1 μl volume of each cDNA was amplified using PCR Master Mix (Applied Biosystems, Warrington, UK) under the following PCR conditions: 50°C for 2 min, 95°C for 10 min, followed by 40 cycles of 95°C for 15 s and 60°C for 1 min. β-Actin and 18 s RNA were used as endogenous control sequences for VEGF-B and Angiopoietin-2, respectively. Preliminary experiments confirmed that the endogenous control sequences were amplified at the same rate as the target sequences (data not shown). The threshold cycle (C_T) was determined for each sample. C_T value is the cycle number at which the level of reporter fluorescence rises above a preset threshold level. Normalisation was achieved by subtracting the mean C_T value for each endogenous control triplicate from the mean C_T value for each target gene triplicate. Target gene abundance was calculated for each tissue type.

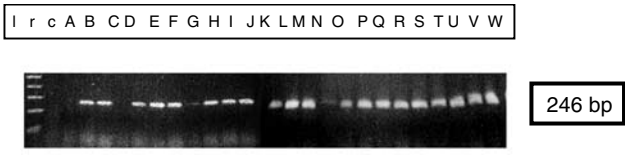

Figure 1 Reverse transcription PCR analysis of VEGF-C in samples of benign endometrium (A–G), ACH (H–J) and endometrioid endometrial carcinoma. Well differentiated carcinoma (K–M), moderately differentiated carcinoma (N–S) and poorly differentiated carcinoma (T–W). Lane r represents an RNA control in which the RT step was omitted and lane c represents a negative control in which the cDNA was replaced by water. The size of the transcripts (shown on the right of the figure) was estimated by co-electrophoresis of a 1 kb ladder (lane l).

Statistical analyses

The presence or absence of specific *in situ* hybridisation for each transcript was compared across the different histological categories using the two-tailed Fisher's exact probability test. This was computed using the *R* statistical computing programme (www.r-project.org). Statistical significance was accepted as $P<0.05$. For results of quantitative PCR, normalised log-transformed transcript levels were compared between groups using the unpaired Student's *t*-test (two-tailed).

RESULTS

Expression of members of the VEGF family and angiopoietins by *in situ* hybridisation

The presence of VEGF-A was detected in all cases of endometrioid endometrial cancer (Table 2 and Figure 2) and was increased near areas of necrosis. Hybridisation for VEGF-A was not seen in cases of ACH or in sections of benign postmenopausal endometrium.

In contrast, hybridisation of the VEGF-B riboprobe was seen in all the five cases of ACH (Table 2 and Figure 2). There was continued expression for VEGF-B in low-grade tumours that diminished as the grade of the tumour increased. Vascular endothelial growth factor-B mRNA was also present in epithelial and stromal compartments (Figure 2), although, unlike VEGF-A, there was no apparent increase in hybridisation near areas of necrosis.

Messenger RNA encoding VEGF-C was not detected in any of the tissues examined using *in situ* hybridisation (Table 2 and Figure 1). A specimen of human lymphoma was used as a positive control and demonstrated specific hybridisation (Figure 2). However, PCR amplification of VEGF-C cDNA was seen in all the samples of endometrial cancer (13 out of 13) and ACH (three out of three) examined (Figure 1), in addition to six out of 7 benign postmenopausal endometria. These findings confirm the presence of VEGF-C in benign, premalignant and malignant endometrium (Hirai *et al*, 2001), although at levels beneath the detection threshold for *in situ* hybridisation.

Messenger RNA encoding VEGF-D was present in three of the five ACH specimens and in six of the 13 carcinomas (one moderately differentiated tumour and five poorly differentiated tumours). The distribution of silver grains did not correspond with epithelial tumour cells but did co-localise with tumour-associated macrophages (CD-68 positive cells) in serial sections (Figure 3).

Hybridisation for Ang-1 mRNA was seen in only one benign and one ACH specimen. Similarly, mRNA encoding Ang-2 was seen in no benign tissues and in only one of the five hyperplastic samples. In contrast, while hybridisation was absent in well/moderately differentiated cancers, hybridisation for Ang-2 mRNA was clearly demonstrated in four out of nine of the poorly differentiated tumours examined. Hybridisation was most marked in macrophage-rich regions of these tumours and was seen to correspond with tumour-associated macrophages (CD-68) upon immunostaining of serial sections (Figure 3). In all of the experiments described, there was no specific hybridisation when the sense probes were used on adjacent sections.

Transcript abundance of VEGF-B and Ang-2 in benign endometrium and endometrial carcinoma assessed by quantitative PCR

Real-time, quantitative PCR was carried out using cDNA generated from benign postmenopausal endometria and endometrioid-type endometrial adenocarcinoma. The abundance of VEGF-B transcript was greater in benign endometrium ($n=7$) than in atypical hyperplasia ($n=3$) ($P=0.13$) and endometrial cancer ($n=17$) ($P=0.04$) (Figure 4A). Conversely, cDNA encoding Ang-2 was

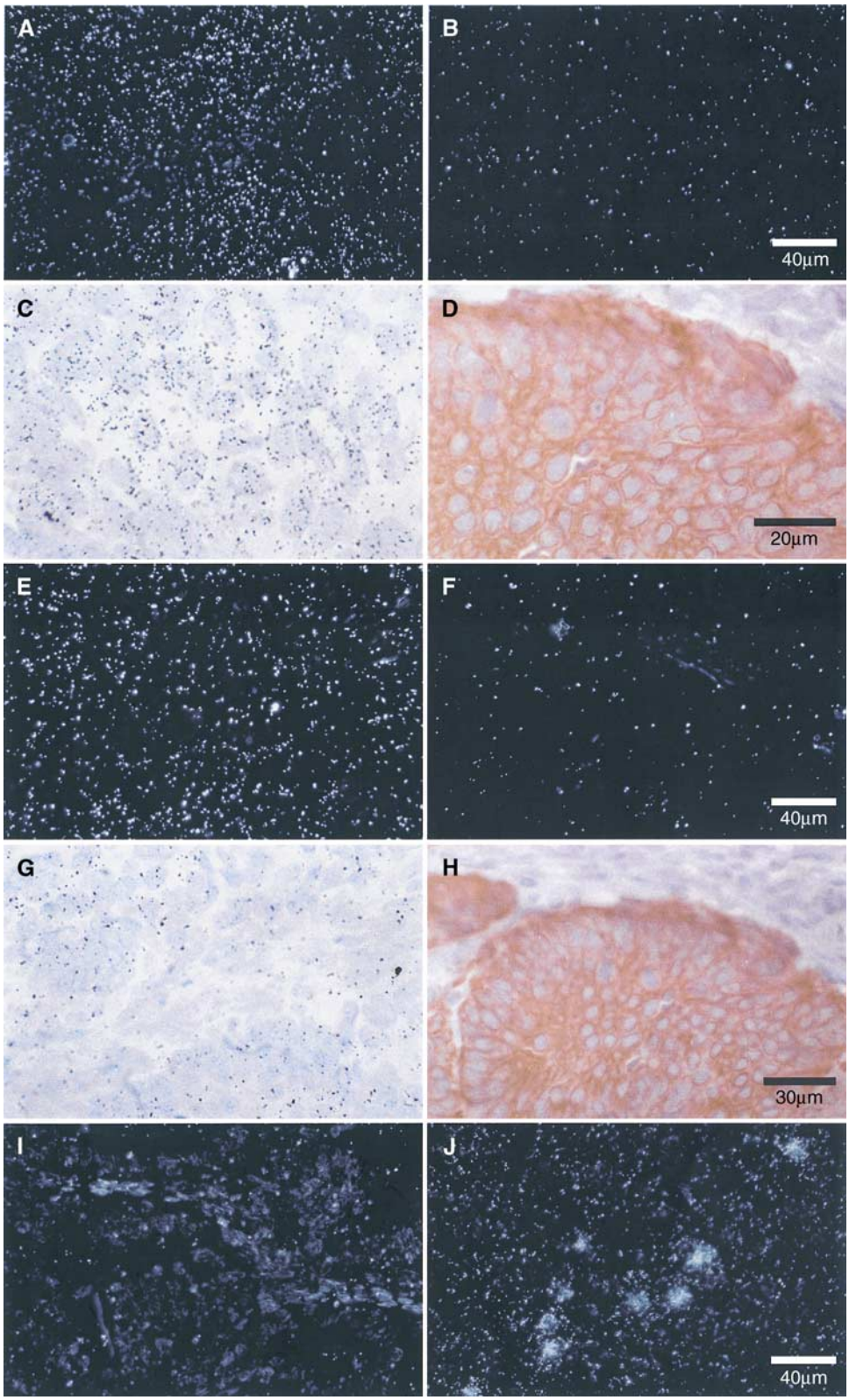

Figure 2 Expression of mRNA encoding VEGF-related factors in the epithelial cells of endometrioid endometrial carcinoma and ACH. *In situ* hybridisation with VEGF-A antisense probe in a moderately differentiated (FIGO grade 2) carcinoma shown under dark-field (**A**) and light-field (**C**) conditions shows hybridisation in epithelial carcinoma cells. There is no specific hybridisation when a sense probe (negative control) is used (**B**). The scale bar in (**B**) applies to (**A**), (**B**), (**E**), (**F**), (**I**) and (**J**). Immunostaining of a serial section with anti-human cytokeratin confirms the epithelial localisation of silver grains (**D**) (scale bar applies to ACH (**C**) and (**D**). *In situ* hybridisation with VEGF-B antisense probe in ACH shown under dark-field (**E**) and light-field (**G**) conditions shows diffuse hybridisation in epithelial and stromal cells. There is no specific hybridisation when a sense probe (negative control) is used (**F**). Immunostaining with anti-human cytokeratin (**H**) identifies the epithelial and stromal cells (**H**) (scale bar applies to (**G**) and (**H**). *In situ* hybridisation with VEGF-C antisense probe in a poorly differentiated (FIGO grade 3) carcinoma shown under dark-field conditions (**I**) shows no specific hybridisation when compared with a human B-cell lymphoma (**J**).

Table 2 Expression of VEGF-A, VEGF-B, VEGF-C, VEGF-D, Ang-1 and Ang-2 detected by *in situ* hybridisation in sections of endometrium

Endometrial histology	***n***	VEGF-A	VEGF-B	VEGF-C	VEGF-D	ANG-1	ANG-2
Benign	5	0/5	0/5	0/5	0/5	1/5	0/5
ACH	5	1/5	5/5*	0/5	3/5	1/5	1/5
FIGO G1/2 carcinoma	4	4/4*	3/4	0/4	1/4	0/4	0/4
FIGO G3 carcinoma	9	9/9*	4/9	0/9	5/9	0/9	4/9

*$P < 0.05$.

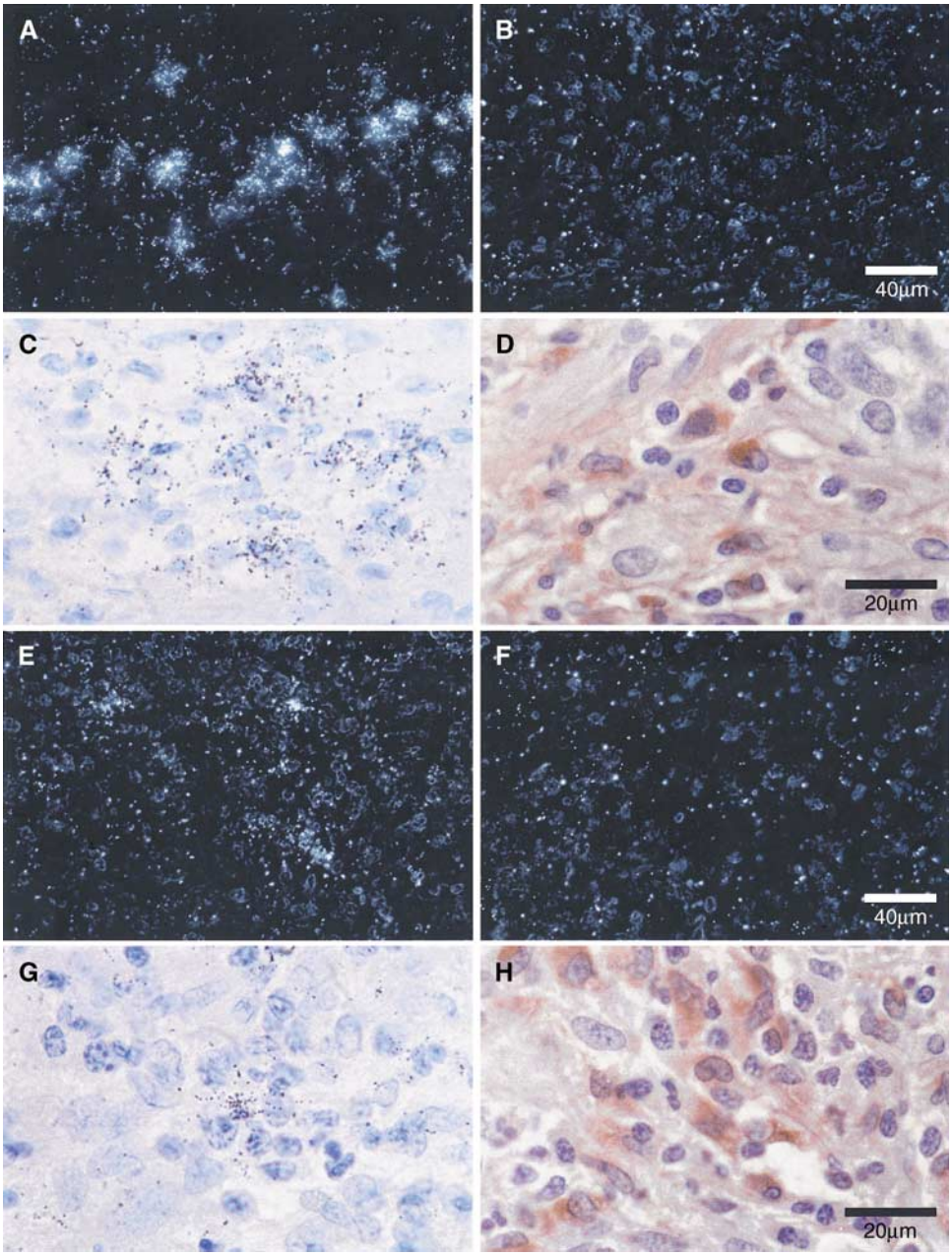

Figure 3 Expression of mRNA encoding VEGF-D and Ang-2 in macrophages infiltrating a poorly differentiated (FIGO grade 3) endometrioid endometrial carcinoma. *In situ* hybridisation with VEGF-D antisense probe shown under dark-field (**A**) conditions and light-field conditions (**C**). *In situ* hybridisation with VEGF-D sense (control) probe shows no specific hybridisation (**B**) (scale bar applies to (**A**), (**B**), (**E**) and (**F**)). Immunostaining with anti-human CD68 in a serial section (**D**), localises the silver grains to tumour associated macrophages (TAMs) (scale bar applies to (**C**), (**D**), (**G**) and (**H**)). *In situ* hybridisation with Ang-2 antisense probe shown under dark-field (**E**) and light-field (**G**) conditions. *In situ* hybridisation with Ang-2 sense (control) probe (**F**) shows no specific hybridisation. Anti-human cytokeratin staining (**H**) localises the hybridisation to TAMs.

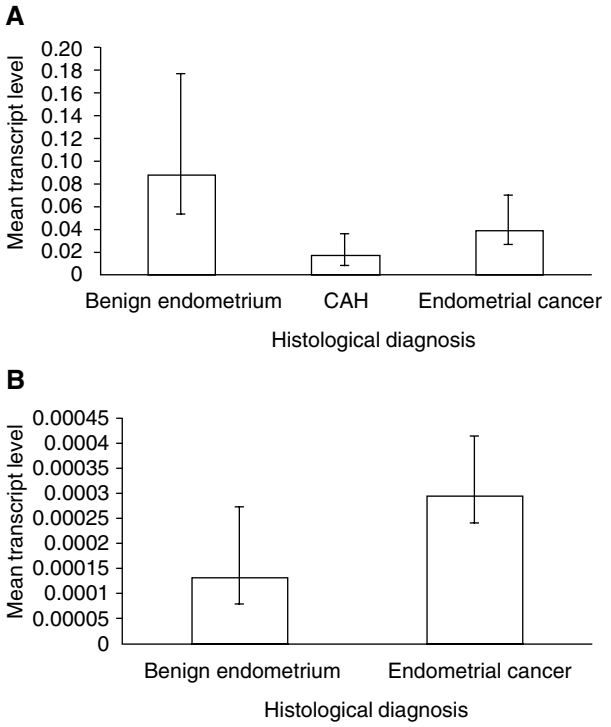

Figure 4 Quantitative PCR for gene transcripts in benign and malignant endometrium. Levels of gene transcript are shown normalised to an endogenous control sequence. Transcript levels are expressed as arbitrary units and represent the mean for each histological group. Experiments for each sample were performed in triplicate. (**A**) The level of mRNA encoding VEGF-B is generally higher in benign postmenopausal endometrium than in CAH ($P = 0.13$) and endometrial cancer ($P = 0.04$). (**B**) mRNA encoding Ang-2 is generally present at higher levels in endometrial cancer than in benign postmenopausal endometrium.

more abundant in the cancer samples ($n = 17$) than in benign postmenopausal endometrium ($n = 4$) (Figure 4B), although this did not reach statistical significance ($P = 0.49$).

DISCUSSION

These findings confirm the expression of VEGF-A in endometrial cancer (Doldi *et al*, 1996; Guidi *et al*, 1996; Fujimoto *et al*, 1998; Fine *et al*, 2000), although in contrast to other published reports (Fujimoto *et al*, 1998; Fine *et al*, 2000), we did not demonstrate VEGF-A mRNA in benign specimens. This may be explained by the inclusion of both pre- and postmenopausal endometrium in other studies (Fujimoto *et al*, 1998). Messenger RNA for VEGF-A is abundant in premenopausal endometrium (Charnock-Jones *et al*, 1993). Our findings support those of Guidi *et al* (1996), who demonstrated little or no mRNA expression in benign atrophic endometrium. We demonstrated VEGF-A mRNA in only one out of 5 specimens of ACH compared with 13 out of 13 endometrioid cancers. These differences may be due to necrosis within the malignant tissue. Hypoxia, in necrotic areas of cancer, leads to the upregulation of transcription (Tischer *et al*, 1991) and increased stability of VEGF-A mRNA (Levy *et al*, 1996).

Messenger RNA and protein for the related growth factor VEGF-B have previously been identified in other tumours including ovarian carcinoma (Sowter *et al*, 1997). We demonstrate, using quantitative PCR, that mRNA encoding VEGF-B is more abundant in benign postmenopausal endometrium than in endometrial adenocarcinoma. The results also suggest that there may be a relative loss of VEGF-B mRNA in ACH although this was not statistically significant and may reflect small sample numbers. We show, using *in situ* hybridisation, that where present, VEGF-B mRNA is expressed in both epithelium and stroma of ACH and some endometrial cancers. These findings contrast with the overexpression of VEGF-A seen in endometrial cancers (Doldi *et al*, 1996; Fujimoto *et al*, 1998). The distribution of VEGF-B in both epithelial and stromal compartments of atypical hyperplasia and some cancers is similar to that observed in ovarian cancer (Sowter *et al*, 1997), but in contrast to VEGF-A, hybridisation was not increased near areas of necrosis. Vascular endothelial growth factor-B is not upregulated by hypoxia (Silins *et al*, 1997) and this may explain the differences seen here.

The function of VEGF-B is not clear. Vascular endothelial growth factor-1 binds VEGFR-1 (flt-1) but not VEGFR-2 (KDR) (Olofsson *et al*, 1998), both of which are present in peritumoral endothelial cells of endometrial cancers (Guidi *et al*, 1996). Mouse 'knockout' experiments suggest that the VEGFR-1 plays a role in endothelial differentiation and/or interactions between the endothelium and extracellular matrix (Fong *et al*, 1995), whereas signalling through VEGFR-2 leads to endothelial cell proliferation and migration (Waltenberger *et al*, 1994). Vascular endothelial growth factor-B is therefore unlikely to promote endothelial cell proliferation or migration directly. However, VEGF-B signalling via VEGFR-1 may participate in the organisation of endothelial–matrix interactions as VEGF-B increases the expression of both uPA (urokinase-type plasminogen activator) and PAI-1 (plasminogen activator inhibitor-1) in endothelial cell cultures (Olofsson *et al*, 1996a). These play a role in matrix degradation and its inhibition, respectively.

Vascular endothelial growth factor-B could contribute to the maintenance of host–tumour responses. Vascular endothelial growth factor-A, produced by tumour cells, inhibits the functional maturation of immune dendritic cells from haemopoietic progenitor cells (Gabrilovich *et al*, 1996). This effect is mediated by binding to VEGFR-1 (Oyama *et al*, 1998). Therefore, loss of VEGF-B may contribute to the escape of tumour cells from the host immune response by making more VEGFR-1 binding sites available for binding by VEGF-A. Vascular endothelial growth factor-B may thus act to suppress changes that favour the development of endometrial cancer.

We confirmed the presence of VEGF-C mRNA in endometrial carcinoma shown by Hirai *et al* (2001), but did not demonstrate this by *in situ* hybridisation. Intense hybridisation for VEGF-C mRNA is seen in endometrial natural killer cells (Li *et al*, 2001), hence the VEGF-C transcript may be present in non-tumour cells that were under-represented in our endometrial tissues.

Vascular endothelial growth factor-D binds to VEGFR-2 and VEGFR-3 (Achen *et al*, 1998), both of which are present in endometrial cancer (Guidi *et al*, 1996). In colon cancer, VEGFR-3 is associated with inflammatory infiltrates of TAMs (White *et al*, 2002) although VEGF-D has not been demonstrated in TAMs themselves. We have shown hybridisation for VEGF-D mRNA in ACH and both well differentiated and poorly differentiated tumours (Table 2), although not all cases in each group were positive. Recently, positive immunostaining for VEGF-D has been demonstrated in both epithelium and stroma of endometrial cancers with some cases of ACH also displaying immunopositivity (Yokoyama *et al*, 2003). In the latter study, 42 and 87% of stage I/II and stage III/IV tumours, respectively, showed significant immunostaining. These findings may reflect differences in the degree of inflammatory infiltration between individual tumours as well as increased expression of VEGF-D by the tumour cells. There is a tendency to higher TAM density in microvessel-rich tumours (Salvesen and Akslen, 1999), and our findings indicate that TAMs may assist in promoting angiogenesis in endometrioid endometrial carcinoma by the secretion of VEGF-D.

Angiopoietin-1 and Ang-2 are previously unreported in endometrial cancer. We demonstrated higher levels of Ang-2

mRNA in endometrial cancers than benign endometrium, although this did not reach statistical significance. The latter may reflect the small numbers of samples in the benign group. Nonetheless, the distribution of mRNA for Ang-2, assessed by *in situ* hybridisation, was similar to that of VEGF-D in TAMs (Figure 3). Both Ang-2 and VEGF-D were only seen in association with CD68-positive cells, although CD68-positive cells, without hybridisation for either of these factors were also present.

Angiopoietin-2 is an antagonist of Ang-1, acting through the Tie-2 receptor and disrupting pericyte-endothelial cell interactions. In the presence of VEGF-A, Ang-2 facilitates vessel sprouting while in its absence, regression of vessel sprouts occurs (Maisonpierre *et al*, 1997). However, in active tumour angiogenesis, a large proportion of the blood vessels lack pericytes and can be selectively ablated by withdrawal of VEGF-A alone (Benjamin *et al*, 1999). In our series, survival did not differ significantly where hybridisation for both VEGF-A and Ang-2 was seen and this may reflect a high proportion of immature tumour vessels lacking pericyte coverage. Angiopoietin-2 may also alter the response of destabilised endothelial cells to cytokines, thus modulating angiogenesis (Laurén *et al*, 1998).

We have shown that gene transcripts for the related growth factors, VEGF-A and VEGF-B, are differentially expressed in benign postmenopausal endometrium and endometrioid endometrial cancer. The reduced expression of VEGF-B in endometrial cancers compared with benign endometrium suggests that VEGF-B may play a role in maintaining normal cellular interactions in endometrium and that loss of expression could contribute to endometrial tumorigenesis.

ACKNOWLEDGEMENTS

This work was supported by a MRC Clinical Training Fellowship, Award number G84/5733; an MRC Programme Grant, Grant number G9623012 and an MRC Cooperative Group Grant number G9722567. We are grateful to Mr Robin Crawford, Mr John Latimer and Dr Robin Moseley, Addenbrookes Hospital, Cambridge, for assistance with tissue collection. We also acknowledge Dr Mark Arends, Department of Pathology, University of Cambridge, for histopathological assessment and Dr Heidi Sowter for technical advice and support.

REFERENCES

Abu-Jawdeh GM, Faix JD, Niloff J, Tognazzi K, Manseau E, Dvorak HF, Brown LF (1996) Strong expression of vascular permeability factor (vascular endothelial growth factor) and its receptors in ovarian borderline and malignant neoplasms. *Lab Invest* **74:** 1105 – 1115

Abulafia O, Triest WE, Sherer DM, Hansen CC, Ghezzi F (1995) Angiogenesis in endometrial hyperplasia and stage I endometrial carcinoma. *Obstet Gynecol* **86:** 479 – 485

Achen MG, Jeltsch M, Kukk E, Makinen T, Vitali A, Wilks AF, Alitalo K, Stacker SA (1998) Vascular endothelial growth factor D (VEGF-D) is a ligand for the tyrosine kinases VEGF receptor 2 (Flk1) and VEGF receptor 3 (Flt4). *Proc Natl Acad Sci USA* **95:** 548 – 553

Benjamin LE, Golijanin D, Itin A, Pode D, Keshet E (1999) Selective ablation of immature blood vessels in established human tumors follows vascular endothelial growth factor withdrawal. *J Clin Invest* **103:** 159 – 165

Boocock CA, Charnock-Jones DS, Sharkey AM, McLaren J, Barker PJ, Wright KA, Twentyman PR, Smith SK (1995) Expression of vascular endothelial growth factor and its receptors flt and KDR in ovarian carcinoma. *J Natl Cancer Inst* **87:** 506 – 516

Charnock-Jones DS, Sharkey AM, Rajput-Williams J, Burch D, Schofield JP, Fountain SA, Boocock CA, Smith SK (1993) Identification and localization of alternately spliced mRNAs for vascular endothelial growth factor in human uterus and estrogen regulation in endometrial carcinoma cell lines. *Biol Reprod* **48:** 1120 – 1128

Chomczynski P, Sacchi N (1987) Single-step method of RNA isolation by acid guanidinium thiocyanate – phenol – chloroform extraction. *Anal Biochem* **162:** 156 – 159

Clark DE, Smith SK, Sharkey AM, Sowter HM, Charnock-Jones DS (1996) Hepatocyte growth factor /scatter factor and its receptor c-met: localisation and expression in the human placenta throughout pregnancy. *J Endocrinol* **151:** 459 – 467

Davis S, Aldrich TH, Jones PF, Acheson A, Compton DL, Jain V, Ryan TE, Bruno J, Radziejewski C, Maisonpierre PC, Yancopoulos GD (1996) Isolation of angiopoietin-1, a ligand for the TIE2 receptor, by secretion-trap expression cloning. *Cell* **87:** 1161 – 1169

Doldi N, Bassan M, Gulisano M, Broccoli V, Boncinelli E, Ferrari A (1996) Vascular endothelial growth factor messenger ribonucleic acid expression in human ovarian and endometrial cancer. *Gynecol Endocrinol* **10:** 375 – 382

Ferrara N, Carver-Moore K, Chen H, Dowd M, Lu L, O'Shea KS, Powell-Braxton L, Hillan KJ, Moore MW (1996) Heterozygous embryonic lethality induced by targeted inactivation of the VEGF gene. *Nature* **380:** 439 – 442

Fine BA, Valente PT, Feinstein GI, Dey T (2000) VEGF, flt-1, and KDR/flk-1 as prognostic indicators in endometrial carcinoma. *Gynecol Oncol* **76:** 33 – 39

Folkman J (1990) What is the evidence that tumors are angiogenesis dependent? *J Natl Cancer Inst* **82:** 4 – 6

Fong GH, Rossant J, Gertsenstein M, Breitman ML (1995) Role of the Flt-1 receptor tyrosine kinase in regulating the assembly of vascular endothelium. *Nature* **376:** 66 – 70

Fujimoto J, Ichigo S, Hirose R, Sakaguchi H, Tamaya T (1998) Expressions of vascular endothelial growth factor (VEGF) and its mRNA in uterine endometrial cancers. *Cancer Lett* **134:** 15 – 22

Gabrilovich DI, Chen HL, Girgis KR, Cunningham HT, Meny GM, Nadaf S, Kavanaugh D, Carbone DP (1996) Production of vascular endothelial growth factor by human tumors inhibits the functional maturation of dendritic cells. *Nat Med* **2:** 1096 – 1103

Goede V, Schmidt T, Kimmina S, Kozian D, Augustin HG (1998) Analysis of blood vessel maturation processes during cyclic ovarian angiogenesis. *Lab Invest* **78:** 1385 – 1394

Guidi AJ, Abu-Jawdeh G, Tognazzi K, Dvorak HF, Brown LF (1996) Expression of vascular permeability factor (vascular endothelial growth factor) and its receptors in endometrial carcinoma. *Cancer* **78:** 454 – 460

Hanahan D (1997) Signaling vascular morphogenesis and maintenance. *Science* **277:** 48 – 50

Hirai M, Nakagawara A, Oosaki T, Hayashi Y, Hirono M, Yoshihara T (2001) Expression of vascular endothelial growth factors (VEGF-A/VEGF-1 and VEGF-C/VEGF-2) in postmenopausal uterine endometrial carcinoma. *Gynecol Oncol* **80:** 181 – 188

Holash J, Maisonpierre PC, Compton D, Boland P, Alexander CR, Zagzag D, Yancopoulos GD, Wiegand SJ (1999) Vessel cooption, regression, and growth in tumors mediated by angiopoietins and VEGF. *Science* **284:** 1994 – 1998

Houck KA, Ferrara N, Winer J, Cachianes G, Li B, Leung DW (1991) The vascular endothelial growth factor family: identification of a fourth molecular species and characterization of alternative splicing of RNA. *Mol Endocrinol* **5:** 1806 – 1814

Joukov V, Pajusola K, Kaipainen A, Chilov D, Lahtinen I, Kukk E, Saksela O, Kalkkinen N, Alitalo K (1996) A novel vascular endothelial growth factor, VEGF-C, is a ligand for the Flt4 (VEGFR-3) and KDR (VEGFR-2) receptor tyrosine kinases. *EMBO J* **15:** 1751

Kaku T, Kamura T, Kinukawa N, Kobayashi H, Sakai K, Tsuruchi N, Saito T, Kawauchi S, Tsuneyoshi M, Nakano H (1997) Angiogenesis in endometrial carcinoma. *Cancer* **80:** 741 – 747

Lauren J, Gunji Y, Alitalo K (1998) Is angiopoietin-2 necessary for the initiation of tumor angiogenesis? *Am J Pathol* **153:** 1333 – 1339

Levy AP, Levy NS, Goldberg MA (1996) Post-transcriptional regulation of vascular endothelial growth factor by hypoxia. *J Biol Chem* **271:** 2746 – 2753

Li XF, Charnock-Jones DS, Zhang E, Hiby S, Malik S, Day K, Licence D, Bowen JM, Gardner L, King A, Loke YW, Smith SK (2001) Angiogenic growth factor messenger ribonucleic acids in uterine natural killer cells. *J Clin Endocrinol Metab* **86:** 1823 – 1834

Maisonpierre PC, Suri C, Jones PF, Bartunkova S, Wiegand SJ, Radziejewski C, Compton D, McClain J, Aldrich TH, Papadopoulos N, Daly TJ, Davis S, Sato TN, Yancopoulos GD (1997) Angiopoietin-2, a natural antagonist for Tie2 that disrupts *in vivo* angiogenesis. *Science* **277:** 55 – 60

Millauer B, Shawver LK, Plate KH, Risau W, Ullrich A (1994) Glioblastoma growth inhibited *in vivo* by a dominant-negative Flk-1 mutant. *Nature* **367:** 576 – 579

Ohta Y, Shridhar V, Bright RK, Kalemkerian GP, Du W, Carbone M, Watanabe Y, Pass HI (1999) VEGF and VEGF type C play an important role in angiogenesis and lymphangiogenesis in human malignant mesothelioma tumours. *Br J Cancer* **81:** 54 – 61

Olofsson B, Korpelainen E, Pepper MS, Mandriota SJ, Aase K, Kumar V, Gunji Y, Jeltsch MM, Shibuya M, Alitalo K, Eriksson U (1998) Vascular endothelial growth factor B (VEGF-B) binds to VEGF receptor-1 and regulates plasminogen activator activity in endothelial cells. *Proc Natl Acad Sci USA* **95:** 11709 – 11714

Olofsson B, Pajusola K, Kaipainen A, von Euler G, Joukov V, Saksela O, Orpana A, Pettersson RF, Alitalo K, Eriksson U (1996a) Vascular endothelial growth factor B, a novel growth factor for endothelial cells. *Proc Natl Acad Sci USA* **93:** 2576 – 2581

Olofsson B, Pajusola K, von Euler G, Chilov D, Alitalo K, Eriksson U (1996b) Genomic organization of the mouse and human genes for vascular endothelial growth factor B (VEGF-B) and characterization of a second splice isoform. *J Biol Chem* **271:** 19310 – 19317

Olson TA, Mohanraj D, Carson LF, Ramakrishnan S (1994) Vascular permeability factor gene expression in normal and neoplastic human ovaries. *Cancer Res* **54:** 276 – 280

Olson TA, Mohanraj D, Carson LF, Ramakrishnan S (1996) *In vivo* neutralization of vascular endothelial growth factor (VEGF)/vascular permeability factor (VPF) inhibits ovarian carcinoma-associated ascites formation and tumor growth. *Int J Oncol* **8:** 505 – 511

Oyama T, Ran S, Ishida T, Nadaf S, Kerr L, Carbone DP, Gabrilovich DI (1998) Vascular endothelial growth factor affects dendritic cell maturation through the inhibition of nuclear factor-kappa B activation in hemopoietic progenitor cells. *J Immunol* **160:** 1224 – 1232

Salvesen HB, Akslen LA (1999) Significance of tumour-associated macrophages, vascular endothelial growth factor and thrombospondin-1 expression for tumour angiogenesis and prognosis in endometrial carcinomas. *Int J Cancer* **84:** 538 – 543

Shalaby F, Rossant J, Yamaguchi TP, Gertsenstein M, Wu XF, Breitman ML, Schuh AC (1995) Failure of blood-island formation and vasculogenesis in Flk-1-deficient mice. *Nature* **376:** 62 – 66

Silins G, Grimmond S, Egerton M, Hayward N (1997) Analysis of the promoter region of the human VEGF-related factor gene. *Biochem Biophys Res Commun* **230:** 413 – 418

Sowter HM, Corps AN, Evans AL, Clark DE, Charnock-Jones DS, Smith SK (1997) Expression and localization of the vascular endothelial growth factor family in ovarian epithelial tumors. *Lab Invest* **77:** 607 – 614

Thurston G, Suri C, Smith K, McClain J, Sato TN, Yancopoulos GD, McDonald DM (1999) Leakage-resistant blood vessels in mice transgenically overexpressing angiopoietin-1. *Science* **286:** 2511 – 2514

Tischer E, Mitchell R, Hartman T, Silva M, Gospodarowicz D, Fiddes JC, Abraham JA (1991) The human gene for vascular endothelial growth factor. Multiple protein forms are encoded through alternative exon splicing. *J Biol Chem* **266:** 11947 – 11954

Waltenberger J, Claesson-Welsh L, Siegbahn A, Shibuya M, Heldin CH (1994) Different signal transduction properties of KDR and Flt1, two receptors for vascular endothelial growth factor. *J Biol Chem* **269:** 26988 – 26995

White JD, Hewett PW, Kosuge D, McCulloch T, Enholm BC, Carmichael J, Murray JC (2002) Vascular endothelial growth factor-D expression is an independent prognostic marker for survival in colorectal carcinoma. *Cancer Res* **62:** 1669 – 1675

Yokoyama Y, Charnock-Jones DS, Licence D, Yanaihara A, Hastings JM, Holland CM, Emoto M, Sakamoto T, Maruyama, H, Sato S, Mizunuma H, Smith SK (2003) Expression of vascular endothelial growth factor (VEGF)-D and its receptor, VEGF Receptor 3, as a prognostic indicator in endometrial carcinoma. *Clin Cancer Res* **9:** 1361 – 1369

PUBLICATION 3

Catalano, R. D., Yanaihara, A., **Evans, A. L**., Rocha, D., Prentice, A., Saidi, S., Print, C. G., Charnock-Jones, D. S., Sharkey, A. M. & Smith, S. K. 2003. The effect of RU486 on the gene expression profile in an endometrial explant model. *Mol Hum Reprod.* 9, (8), 465-473.

Cited by 44, Impact factor 3.852

ISSN: 1360-9947

Journal Type

Molecular Human Reproduction publishes articles on the molecular aspects of reproductive physiology and pathology, endocrinology, andrology, gonad function, gametogenesis fertilization, embryo development, implantation, pregnancy, contraception, oncology and infectious disease. The diagnosis and investigation of genetic disease is also covered in the scope of Molecular Human Reproduction. Published papers include peer-reviewed original research reports review articles and debates on topical areas. It is published on behalf of the European Society of Human Reproduction and Embryology. The paper above was published under the section Molecular Events in the Endometrium.

Personal Contribution

For this publication I collected and processed endometrial samples from theatre. This included culture of explants followed by extraction of RNA and microarrays as described in (Evans et al., 2003)[*1], and included the verification of results by quantitative PCR. Rob Catalano and Andrew Sharkey did the immunohistochemistry for Figure 4.

Molecular Human Reproduction Vol.9, No.8 pp. 465–473, 2003 DOI: 10.1093/molehr/gag060

The effect of RU486 on the gene expression profile in an endometrial explant model

R.D.Catalano[1,3], A.Yanaihara[1], A.L.Evans[1], D.Rocha[1], A.Prentice[2], S.Saidi[2], C.G.Print[1], D.S.Charnock-Jones[2], A.M.Sharkey[1] and S.K.Smith[2]

[1]Reproductive Molecular Research Group, Department of Pathology, University of Cambridge, Cambridge CB2 1QP and [2]Department of Obstetrics and Gynaecology, University of Cambridge Clinical School, The Rosie Hospital, Robinson Way, Cambridge CB2 2SW, UK

[3]To whom correspondence should be addressed. E-mail: rc296@cam.ac.uk

Administration of RU486 *in vivo* during the receptive phase rapidly renders the endometrium non-receptive to the implanting embryo. In order to identify key pathways responsible for endometrial receptivity we have used cDNA arrays to monitor gene expression changes in short-term endometrial explants in response to RU486. Endometrial biopsies from five normal fertile women at mid-secretory phase were cultured in the presence of estradiol and progesterone with or without RU486 for 12 h. cDNA arrays were produced containing ~1000 sequence-verified clones which included genes known to be important in angiogenesis, apoptosis, cell signalling, extracellular matrix remodelling and cell cycle regulation. cDNA probes from the paired endometrial samples were hybridized to the arrays and hybridization signals were quantified. A total of 12 genes displayed significant changes in expression; six were up-regulated and six down-regulated following RU486 treatment. For five of these genes this is the first report suggesting that they are regulated by steroids in the endometrium. *JAK1* and *JNK1* were two of the genes shown by the arrays to be down-regulated in RU486-treated endometrial explants. This was confirmed by real time RT–PCR. JAK1 immunoreactivity was localized to both glandular epithelium and the stroma of normal endometrium and staining was much stronger in the luteal phase of the cycle. These results show that components of two important signalling pathways in endometrium—the JAK/STAT pathway, and the JNK pathway—are altered by RU486. Genes whose expression is controlled by these pathways are likely to be involved in the mechanism by which steroids render the endometrium receptive to the implanting embryo.

Key words: cDNA array/endometrium/gene profiling/implantation/steroids

Introduction

In humans the uterus is receptive to blastocyst implantation between 5 and 9 days post-ovulation, a period known as the implantation window (Wilcox *et al*., 1999). During this period the endometrium becomes functionally receptive to the embryo, which is reflected by its structural and biochemical transformation (Tabibzadeh and Babaknia, 1995). The action of progesterone on an estrogen-primed endometrium results in a particular gene expression profile which renders the endometrium receptive (Giudice *et al*., 1999; Salamonsen *et al*., 2001). If the action of progesterone is antagonized, or progesterone levels fall, the endometrium rapidly reverts to a non-receptive state. This is followed by other changes such as focal haemorrhage and degradation of extracellular matrix (ECM) resulting in menstruation (Papp *et al*., 2000). Based on this paradigm, several approaches have been used to identify genes that are required for a functionally receptive endometrium. The first has been to identify structural and molecular changes that coincide with the transition from a non-receptive state (LH+3), to a receptive state (LH+7). As well as morphological changes, the expression of many proteins alters during this time. These include mucin 1 (Hey *et al*., 1994) placental proteins 12 and 14 (Julkunen *et al*., 1986; Rutanen *et al*., 1986), prolactin (Maslar *et al*., 1979), various integrins (Lessey *et al*., 1992), cytokines (Tabibzadeh *et al*., 1995) and heat shock proteins (Gruidl *et al*., 1997). A recent microarray study reported >600 genes whose mRNA expression levels altered between these two time-points (Carson *et al*., 2002). The second approach has been to try to identify genes that are directly regulated by the action of progesterone on endometrium (Kumar *et al*., 1998; Okulicz and Ace, 1999).

An alternative approach has been to study the effects of antiprogestins such as RU486 (mifepristone). RU486 competes with progesterone for binding to the progesterone receptor and alters its DNA binding characteristics (Jackson *et al*., 1997). It has both antagonist and agonist activities on the action of progesterone in regulating gene transcription and also exhibits anti-glucocorticoid, anti-estrogenic and anti-androgenic activity (Beck *et al*., 1993; McDonnell and Goldman, 1994; Hackenberg *et al*., 1996; Elger *et al*., 2000). A single dose of RU486 (200 mg) administered to normal cycling women 2 days after ovulation produces peak plasma levels of ~0.3–0.4$\times 10^{-6}$ mol/l within 2 h (Sarkar *et al*., 2002). This renders the endometrium non-receptive (Hegele-Hartung *et al*., 1992; Gemzell-Danielsson *et al*., 1993). RU486 has an effect on gene expression in the uterus as early as 6 h after oral administration (Critchley *et al*., 1996). This effect is likely to be due to the direct action of RU486 on endometrium, since there is no significant effect on serum progesterone levels (Swahn *et al*., 1990). This is supported by the fact that RU486 has been shown to suppress expression of leptin receptor in endometrial explants after only 6 h in culture (Koshiba *et al*., 2001).

Many studies have used antiprogestins to analyse the expression of individual endometrial factors that might be important for implantation (Danielsson *et al*., 1997; Schatz *et al*., 1997; Marions *et al*., 1998; Taylor *et al*., 1998; Critchley *et al*., 1999). However, most of these factors have been studied in isolation. To date, no attempt has been made to study the global changes in gene expression caused by RU486 in human endometrium as it changes from a receptive to a non-receptive state.

In order to identify endometrial factors that are important for implantation, we have used an endometrial explant model to identify genes regulated by the action of RU486 on endometrium from the receptive phase. Many previous studies using endometrial explants have shown that they retain their steroid responsiveness *in vitro* for ⩾24 h and respond to steroids in a similar way to endometrium *in vivo* (Dudley *et al*., 1992; Ilouz *et al*., 2000; Koshiba *et al*., 2001). These results suggest that cultures of endometrial explants are a valid model for studying the effects of steroid treatment in the endometrium. We cultured mid-secretory endometrial explants with RU486 for 12 h at a concentration similar to peak plasma levels after oral administration of 200 mg. Total RNA was isolated and used to probe cDNA arrays containing ~1000 genes selected to include the molecular pathways believed to be important for receptivity. These include cell adhesion, apoptosis, signalling, cell cycle regulation, ECM remodelling and angiogenesis. This has enabled the monitoring of early gene expression changes in secretory phase endometrium in response to RU486. The aim was to identify genes whose expression may be involved in the loss of endometrial receptivity.

Materials and methods

Tissue collection

This study took place with the approval of the Cambridge Local Region Ethics Committee. Written informed consent was obtained from all patients. Endometrial biopsies were obtained from seven normally cycling fertile women at the mid-secretory phase (day 19–23) who underwent curettage or hysterectomy for benign gynaecological disorders. The patients were healthy women (aged 28–38 years, with a body mass index between 19 and 25 kg/m^2). They had regular menstrual cycles (27–30 days) and had not received hormone therapy for the last 2 months prior to surgery. Each specimen was assessed as normal by histological examination. Endometrial dating was performed using published criteria (Noyes *et al*., 1950). Biopsies for immunohistology were collected from similar patients throughout the menstrual cycle and confirmed as normal by histological examination.

Explant culture

Endometrial biopsies were washed several times in Dulbecco's minimum essential medium (DMEM)/Ham's F-12 without Phenol Red (Life Technologies, UK) to remove blood. The endometrial tissues were chopped into 1–2 mm^2 pieces and divided into two equal samples. These were placed in a 4-well plate (Nunc) and incubated with 5 ml media (DMEM/F-12 without Phenol Red), 1% L-glutamine (Life Technologies), 1% penicillin G/streptomycin (Life Technologies) for 1 h to allow recovery, culture medium was then changed (Wang *et al*., 1987). One part of the sample was treated with 5 ml of DMEM/F-12 (as above) containing 10^{-9} mol/l estradiol + 10^{-7} mol/l medroxyprogesterone acetate (all steroids purchased from Sigma, UK). These steroid concentrations have previously been shown to elicit responses in endometrial explant cultures (Koshiba *et al*., 2001) and closely resemble plasma concentrations reported during the mid-secretory phase of the endometrium (reviewed in Chabbert Buffet *et al*., 1998). The other half of the endometrial sample was incubated with the same medium to which RU486 (10^{-6} mol/l) (Sigma) was added. Incubations were performed in a humidified atmosphere at 37°C in 5% CO_2. The paired endometrial samples treated with and without RU486 were flash-frozen after 12 h and stored at –70°C.

RNA extraction

Total RNA was extracted using Trizol reagent (Life Technologies) according to the manufacturer's instructions and treated with RQ1 DNase I (Promega, UK) for 30 min at 37°C, then re-extracted with Trizol. RNA quality was assessed by loading 300 ng of total RNA onto an RNA Labchip (Agilent Technologies) and analysed on an A2100 Bioanalyser (Agilent Technologies, Germany). Two biopsies did not yield sufficient RNA for hybridization to arrays, but were used for the subsequent RT–PCR analysis.

Array production

cDNA arrays were produced containing ~1000 sequence-verified clones spotted in duplicate on an 8×12 cm nylon Hybond N+ membrane (Amersham Pharmacia Biotech, UK). The DNA used for spotting was produced by amplification using PCR from the corresponding IMAGE cDNA clones. Specific cDNA clones were chosen that showed little or no homology to other known genes to reduce cross-hybridization and clones were sequenced prior to PCR to confirm the clone identity. To check for any cross-contamination, PCR products were electrophoresed prior to spotting on the array to ensure that each was a single band and 50% of the PCR products used for spotting were resequenced to verify that the correct clone was spotted. The amplified PCR fragments were purified using the Millipore Multi-screen 96 system (Millipore, UK) to a concentration of 500 μg/ml. Approximately 15 ng of each cDNA was contact-printed onto the membrane using a BioRobotics MicroGrid robot (BioRobotics Ltd, UK) with a 96-pin tool with 0.4 mm diameter solid pins to create 2112 individual DNA spots, representing known genes, expressed sequence tags (ESTs) unknown genes and calibration spikes. After spotting, the filters were denatured and neutralized and the DNA was cross-linked using a UV Stratalinker, model 1800 (Stratagene, USA) at 70 000 μJ/cm^2. The listing of all the cDNA on the array can be found at http://www.path.cam.ac.uk/~angio/.

Array hybridization

Radiolabelled cDNA probes were produced by labelling 5 μg of total RNA from five endometrial samples with [^{33}P]dCTP using the EndoFree RT Kit (Ambion, USA). Unincorporated [^{33}P]dCTP was removed using NICK columns (Amersham, Pharmacia Biotech). The filters were pre-hybridized at 65°C for 3 h using ExpressHyb buffer (Clontech, USA) containing 1 μg/ml Human Cot-1 DNA (Life Technologies), 1 μg/ml Poly dA (Amersham, Pharmacia Biotech) and 5 μg/ml Salmon sperm DNA (Sigma). cDNA probes were denatured then added to the hybridization buffer at 1×10^6 cpm/ml and hybridized at 65°C for 16 h. The filters were washed twice in 2×standard saline citrate (SSC), 0.5% sodium dodecyl sulphate (SDS) and twice in 0.1× SSC, 0.1% SDS for 30 min each at 60°C, then dried for 30 min at 60°C. The filters were exposed to low energy storage phosphor screens (Molecular Dynamics, USA) for 48 h and scanned at 50 μm resolution using a STORM 860 Scanner (Molecular Dynamics).

Array analysis

Hybridization signals were quantified using ImaGene v5.0 (BioDiscovery Inc., USA). The mean signal for each spot on the array was determined. The data from each pair of treated and untreated samples from the same patient were then normalized to overcome minor differences in labelling and hybridization efficiency. Normalization was performed by applying intensity-dependent scaling using the 'loess' function of the R-statistical software system, in a similar fashion to that used by the SNOMAD protocol (Colantuoni *et al*., 2002). The normalized transcript abundance data was then compared using a paired *t*-test to identify transcripts that showed a statistically significant change in expression following exposure to RU486 across all five samples. Statistical significance was defined as $P < 0.05$. The fold change values for each endometrial biopsy were calculated by taking the background subtracted mean signal for each cDNA spot and dividing the value obtained from the RU486-treated portion of the biopsy by the value of the corresponding spot from the control sample.

Real time RT–PCR

The relative expression of two genes, *JAK1* and *JNK1*, was compared between RU486 and control tissues by real time RT–PCR using an ABI PRISM 7700 sequence detection system (TaqMan) according to the manufacturer's

instructions. Primers and probes were designed using the Primer Express v5.0 software (Applied Biosystems, UK) and were designed within the same region of the cDNA clone as was spotted on the array. Areas in the cDNA that are known to be involved in alternate splicing were avoided. Details of the primers and probes used are detailed below. The probes were labelled with 5′FAM and 3′TAMRA and were purified by high-performance liquid chromatography. JAK1 primers and probes were: 5′-CATGAGAACATTGTGAAGTACAAAGGA-3′ (forward primer), 5′-CCCGAAGGCAGAAATTCCAT-3′ (reverse primer), 5′-GCTTAATACCATTTCCTCCGTCTTCTGTGCAG-3′ (probe); JNK1 primers: 5′-TCAATGGCTCTCAGCATCCA-3′ (forward primer), 5′-GCCAAAGTCGGATCTGTTGAC-3′ (reverse primer), 5′-CATCGTCGTCTGTCAATGATGTGTCTTCAA-3′ (probe). In addition, the endogenous control 18S ribosomal RNA was assayed using primers and probe from Applied Biosystems. Probe and primer optimization and real time PCR were performed using the manufacturer's recommended conditions. Standard curves were generated by serial dilution of a standard preparation of total RNA isolated from luteal phase endometrium. Data are expressed in arbitrary units relative to the level of the same gene in this standard RNA. cDNA was produced from each endometrial sample by reverse transcription using 5 µg of total RNA with 200 IU Superscript RT (Invitrogen, UK) according to the manufacturer's instructions. The expression values obtained were normalized against those from the control ribosomal 18S to account for differing amounts of starting material.

Immunohistochemistry

Biopsies for immunohistochemistry were fixed in neutral buffered 10% formalin for 6 h at room temperature and paraffin wax-embedded. Serial sections of 5–7 µm were cut from the paraffin blocks and mounted on APES-coated slides, de-waxed in xylene and rehydrated in graded alcohol. Slides were pressure-cooked at full pressure for 2 min in 10 mmol/l sodium citrate, pH 6.0. After cooling for 5 min, slides were washed in phosphate-buffered saline (PBS), endogenous peroxidase was quenched for 10 min in 0.3% hydrogen peroxide in methanol and blocked in 20% goat serum, 1% bovine serum albumin (BSA) for 30 min. Sections were incubated with rabbit anti-JAK1 (Santa Cruz, Biotechnology, USA) at 4°C for 16 h at a dilution of 1:300 for proliferative phase sections and 1:600 for secretory phase sections in PBS, 5% goat serum, 1% BSA. To confirm specificity of the JAK1 immunoreactivity, we preincubated the anti-JAK1 antibody with a 10-fold excess of the antigenic JAK1 peptide against which the antibody was raised. Slides were then reacted with biotin-labelled goat anti-rabbit IgG and incubated with preformed avidin–biotin–peroxidase complex (ABC kit; Vector Laboratories, USA). Diaminobenzidine (Sigma) was used as a substrate. Sections were counter-stained with haematoxylin, dehydrated and mounted.

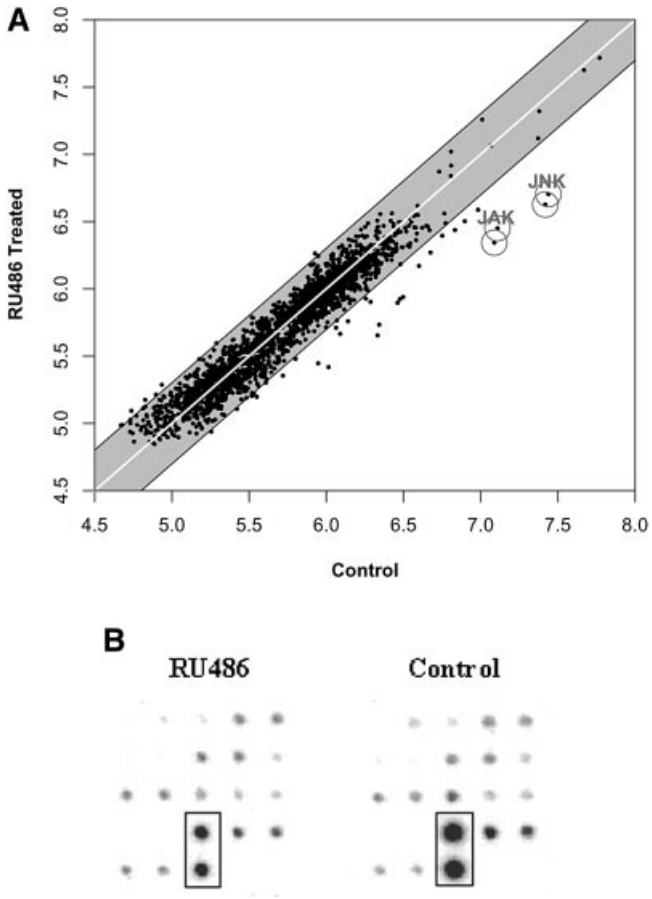

Figure 1. (**A**) Scatter plot comparing hybridization signals obtained for each cDNA after hybridization of arrays to control and RU486-treated secretory endometrial explants from the same patient. The graph shows the comparison of the relative expression of each of the ~1000 genes spotted in duplicate in the RU486-treated RNA (*y*-axis) versus control RNA (*x*-axis) from a representative analysis. Values have been normalized and logged ($\log_{10}$). The grey band denotes a 2-fold change in signal intensity between arrays (paired analysis). JNK1 and JAK1 are highlighted and show significant down-regulation in the treated group. (**B**) Part of a representative array showing the signal from duplicate JNK1 cDNA spots following hybridization to control or RU486-treated endometrium from the same patient.

Results

cDNA array analysis

Endometrium was collected from seven fertile women in the mid-secretory phase of the cycle. Each sample was divided into two equal pieces and cultured for 12 h in estradiol and progesterone with or without the antiprogestin RU486. Total RNA was extracted from each culture and used to probe a custom-made human cDNA array of ~1000 sequence-verified clones. Representative genes were chosen to include those important in molecular pathways involved in angiogenesis, apoptosis, cell cycle control, ECM remodelling and cell signalling. We also included markers for specific cell types in endometrium, including cytokeratin (epithelium), vimentin (stroma) and CD45 (leukocytes). These markers provide a means to assess the relative content of each cell type in the paired biopsies from each patient. Total RNA from five pairs of control and RU486-treated endometrial explants was hybridized on individual arrays and then normalized. Typical results of this analysis are shown by a representative scatter plot comparing the signals obtained for each cDNA clone on the array after hybridization to control and RU486-treated endometrium from the same patient (Figure 1A). The hybridization signal values obtained from control and treated tissue samples from five women were normalized in pairs and cDNA with significant changes determined by paired *t*-test. A total of 12 genes (~1.2%) displayed statistically significant changes in expression following RU486 treatment; six cDNA decreased (Table I) and six increased (Table II). These cDNA fulfil the following criteria: both duplicate spots on the array changed significantly, and the signal intensity was at least twice that of the backgound. An example of the change seen for the cDNA JNK1 on the cDNA array is shown in Figure 1B. The identity of the 12 genes identified as regulated by RU486, was confirmed by sequencing the actual PCR product spotted on the array corresponding to each regulated cDNA spot.

TaqMan verification of gene expression determined by array analyses

Real time RT–PCR was used to verify the changes in RNA expression levels indicated by the cDNA analysis. Two genes *JAK1* and *JNK1*, which both apparently decreased >2-fold following RU486 and which were highly expressed, were chosen for verification. cDNA was synthesized from the same five total RNA samples used for the array

Table IA. Genes down-regulated by RU486

Gene ID	Patient no.					Fold change		*P*–value
	1	2	3	4	5	Mean	± SD	
vav2/1	–2.00	–2.23	–1.57	–4.14	–4.01	–2.79	0.17	0.008
vav2/2	–2.06	–2.39	–1.47	–4.06	–4.30	–2.86	0.18	0.009
JAK1/1	–4.30	–2.24	–2.34	–2.72	–1.60	–2.64	0.14	0.005
JAK1/2	–2.22	–2.42	–2.55	–2.97	–1.73	–2.38	0.09	0.001
EST31/1	–3.02	–1.66	–2.81	–1.12	–2.87	–2.30	0.24	0.018
EST31/2	–3.34	–2.01	–2.67	–1.70	–3.34	–2.61	0.13	0.002
JNK1/1	–1.36	–1.93	–2.21	–2.33	–1.55	–1.88	0.13	0.004
JNK1/2	–1.29	–1.83	–2.11	–2.22	–1.58	–1.81	0.13	0.004
TNR/1	–1.94	–1.78	–1.27	–1.98	–1.24	–1.64	0.15	0.010
TNR/2	–2.00	1.67	–1.21	–2.48	–1.18	–1.71	0.20	0.026
CTSL/1	–1.10	–1.16	–1.15	–1.64	–1.60	–1.33	0.15	0.037
CTSL/2	–1.30	–1.67	–1.15	–1.41	–1.89	–1.48	0.13	0.013

The fold change shown by each duplicate (/1, /2) cDNA spotted on the array after treatment is given, together with the mean fold change derived from all five experiments.
The *P*-values are derived from a paired *t*-test.

Table IB. Identity of each Image cDNA clone spotted, the gene name and Unigene cluster

Gene ID	Image clone	Unigene	Identity
Vav2	2386937	Hs. 352272	Oncogene, involved in formation of lameliapodia and cell spreading
JAK1	177471	Hs. 50651	Janus kinase 1, protein-tyrosine kinases, cytokine receptor signalling
EST31	Mis-assigned	Not assigned	Ribosomal protein similar to regions found in 45s, 28s, 60s and L4E family
JNK1	119133	Hs. 267445	Mitogen-activated protein kinase
TNR	175767	Hs. 54433	Tenascin R, extracellular matrix protein
CTSL	130796	Hs. 78056	Cathepsin L, lysosomal cysteine proteinase

Table IIA. Genes up-regulated by RU486

Gene ID	Patient no.					Fold change		*P*-value
	1	2	3	4	5	Mean	± SD	
cPLA2/1	2.33	1.22	1.17	1.44	1.63	1.56	0.47	0.029
cPLA2/2	1.70	1.26	1.13	1.30	1.64	1.41	0.25	0.014
GST P1/1	1.10	1.18	1.23	1.17	1.31	1.20	0.08	0.003
GST P1/2	1.87	1.30	1.20	1.25	1.24	1.37	0.28	0.021
CD94/1	1.17	1.20	1.19	1.47	1.16	1.24	0.13	0.010
CD94/2	1.23	1.18	1.18	1.80	1.41	1.36	0.26	0.022
Bak/1	1.42	1.37	1.78	1.15	1.00	1.34	0.30	0.048
Bak/2	1.58	1.27	1.25	1.22	1.18	1.30	0.16	0.008
NIK/1	1.10	1.27	1.20	1.51	1.22	1.26	0.15	0.012
NIK/2	1.36	1.39	1.20	1.34	1.19	1.29	0.09	0.001
WISP1/1	1.10	1.45	1.31	1.20	1.26	1.26	0.13	0.008
WISP1/2	1.27	1.46	1.30	0.98	1.34	1.27	0.18	0.025

The fold change shown by each duplicate (/1, /2) cDNA spotted on the array after treatment is given, together with the mean fold change derived from all five experiments.
The *P*-values are derived from a paired *t*-test.

Table IIB. Identity of each Image cDNA clone spotted, the gene name and Unigene cluster

Gene ID	Image clone	Unigene	Function
cPLA2α	1676293	Hs. 211587	Cytosolic phospholipase A2α, signaling responses to extracellular ligands
GST P1	2224433	Hs. 226795	Glutathione *S*-transferase, PI, enzyme has important role in detoxification
CD94	1901363	Hs. 41682	Killer cell lectin-like receptor, regulation of NK cell function
Bak	235938	Hs. 93213	BCL2 antagonist/killer 1, suppressor of apoptosis
NIK	342349	Hs. 47007	Serine/threonine protein kinase, lymphotoxin-beta receptor signaling
WISP1	2125289	Hs. 194684	WNT1 inducible signalling pathway protein 1

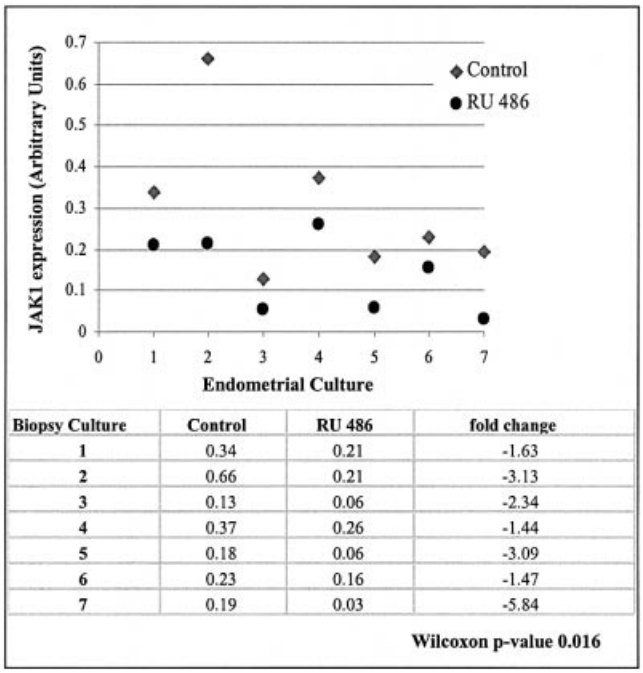

Biopsy Culture	Control	RU 486	fold change
1	0.34	0.21	-1.63
2	0.66	0.21	-3.13
3	0.13	0.06	-2.34
4	0.37	0.26	-1.44
5	0.18	0.06	-3.09
6	0.23	0.16	-1.47
7	0.19	0.03	-5.84

Wilcoxon p-value 0.016

Figure 2. JAK1 expression levels in control and RU486-treated endometrial explants determined by TaqMan PCR. Endometrial explants for biopsies 6 and 7 were not included from the array analysis as these biopsies were too small to extract enough total RNA. Values are normalized to ribosomal 18S for each culture and fold change in JAK1 expression for each experiment is indicated.

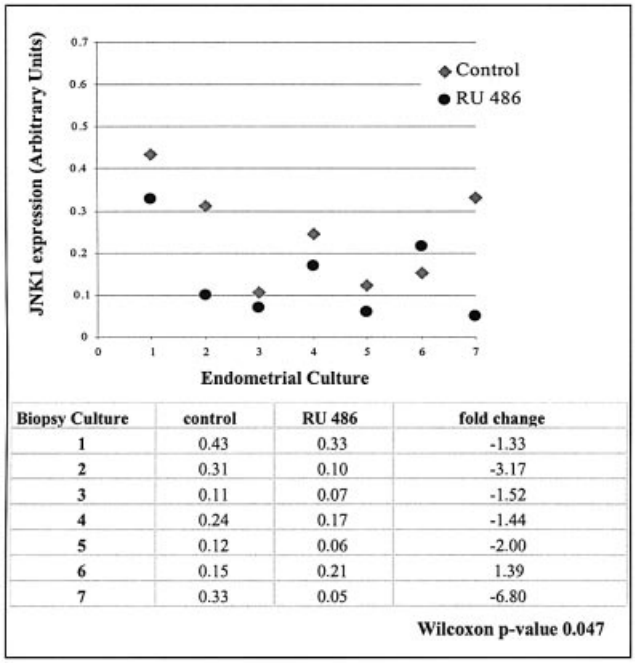

Biopsy Culture	control	RU 486	fold change
1	0.43	0.33	-1.33
2	0.31	0.10	-3.17
3	0.11	0.07	-1.52
4	0.24	0.17	-1.44
5	0.12	0.06	-2.00
6	0.15	0.21	1.39
7	0.33	0.05	-6.80

Wilcoxon p-value 0.047

Figure 3. JNK1 expression levels in control and RU486-treated endometrial explants determined by TaqMan PCR. Endometrial explants for biopsies 6 and 7 were not included from the array analysis as these biopsies were too small to extract enough total RNA. Values are normalized to ribosomal 18S for each culture, and fold change in JNK1 expression for each experiment is indicated.

analysis as well as two additional patient samples. Levels of JAK1 and JNK1 were measured by TaqMan analysis for each cDNA sample relative to a reference RNA and the values were corrected for differences in loading relative to the 18S ribosomal RNA. JAK1 expression decreased by a mean of 2.7-fold and JNK1 expression decreased by a mean of 2.1-fold in the seven RU486-treated samples (Figures 2 and 3). The decrease in both genes was statistically significant (JAK1, $P < 0.016$ and JNK1, $P < 0.047$). Therefore the gene list generated by the cDNA array analysis reflects reliable changes in gene expression following RU486 treatment of secretory phase endometrium.

Immunolocalization of JAK1 in endometrium

JAK1 immunostaining was predominantly in the glands in proliferative endometrium with only faint staining in the stroma (Figure 4A). The intensity of the immunostaining increased considerably in secretory endometrium and staining was seen within the stroma as well as in the glandular and luminal epithelium (Figure 4C). Immunostaining was present throughout the stroma in secretory phase endometrium but was clearly absent from lymphoid aggregates (Figure 4E). Therefore JAK1 immunoreactivity appears to be present within the glands throughout the menstrual cycle, but increases dramatically within the stroma and luminal epithelium at the mid-secretory phase. Staining of sections with JAK1 antibody preincubated with the JAK1 antigenic peptide abolished JAK1 immunoreactivity, indicating that the staining obtained was specific for JAK1 (Figure 4B, D and F).

Discussion

The genes and biochemical pathways believed to be involved in achieving a receptive uterus have been largely derived from animal models (Giudice, 1999; Lessey *et al*., 2000; Sharkey and Smith, 2003). Other than the progesterone receptor, no genes have yet been formally shown to be essential for implantation in humans. Recently, gene profiling using microarray analysis has been used to identify global expression patterns in endometrium during the menstrual cycle (Kao *et al*., 2002; Borthwick *et al*., 2003), the receptive phase (Carson *et al*., 2002) and in-vitro decidualization (Popovici *et al*., 2000). Changes in expression of hundreds of cDNA coincides with the transition from the non-receptive to the receptive state, but it is not known which of these molecules are critical for successful human implantation. The current study utilized the antiprogestin RU486 on cultured human secretory endometrium to identify steroid-regulated genes and molecular pathways, which, when disrupted, lead to implantation failure. Custom-made cDNA arrays which included genes known to be important in angiogenesis, apoptosis, cell signalling, ECM remodelling and cell cycle regulation, were used to identify genes which are altered by the action of RU486 on endometrial explants.

The arrays identified 12 genes whose expression was significantly altered after 12 h of treatment with RU486. The gene list represents 1.2% of the genes on the array and three show mean fold changes of $\geqslant 2$. Since the response to steroids alters over time, this 12 h time-point represents the early responses of the endometrium to RU486. Previous array studies on endometrial tissues and cell lines have revealed a similar number (1.3–5.8%) of genes with a significant change in gene expression (Popovici *et al*., 2000; Carson *et al*., 2002; Kao *et al*., 2002). A fold change of >2 is a frequently adopted cut-off for array profile analysis (Claverie *et al*., 1999). However, subtle alterations in transcript levels of genes below the 2-fold level should be considered if they are repeatable over a large number of biologically independent replicated experiments, because these smaller gene expression changes may be due to a robust response in a few cells in a complex tissue (Hamadeh *et al*., 2002). The results of the real time PCR for the

two genes *JAK1* and *JNK1* were in good agreement with the array results and confirm that the array analysis is reliable.

This study employed endometrial explants rather than isolated primary cells. This retains normal epithelial–stromal interactions and

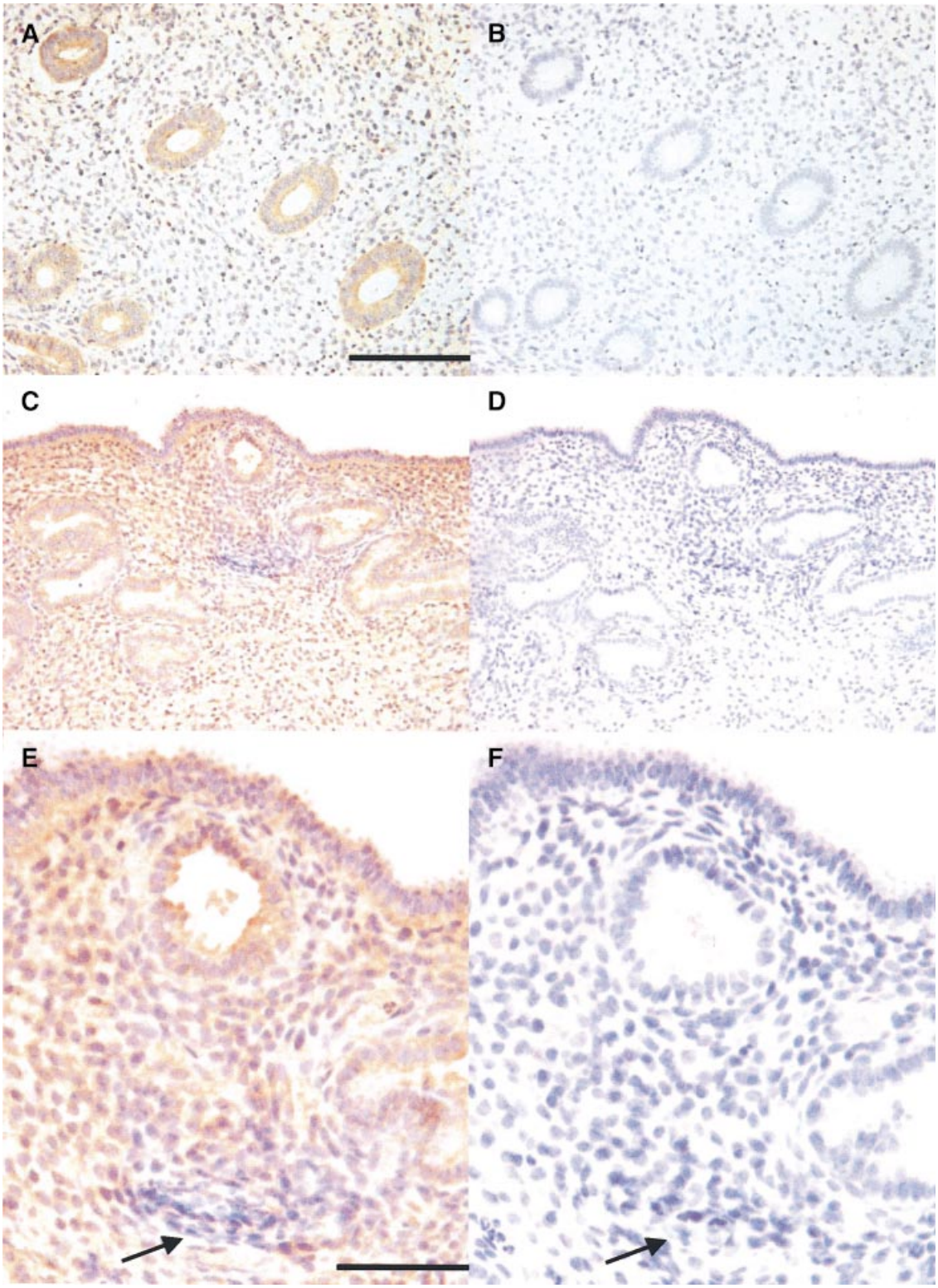

Figure 4. Immunolocalization of JAK1 protein in human endometrium during the proliferative and secretory phases of the menstrual cycle. JAK1 immunostaining (antibody dilution 1:300) is observed in the endometrial glands and faintly in the stroma during the proliferative phase (**A**). During the secretory phase JAK1 immunostaining (antibody dilution 1:600) was increased and was also observed in the stroma and luminal epithelium as well as the glandular epithelium (**C**). The lymphoid aggregates within the stroma of the secretory endometrium were devoid of staining (**E**). Arrows indicate lymphoid aggregate (**E**, **F**). Negative controls **B**, **D** and **F** are sections stained with JAK1 antibody which had been preincubated with an excess of JAK1 blocking peptide. Scale bar = 100 μm (**A**, **B**, **C**, **D**), 30 μm (**E**, **F**).

such explants have been shown to exhibit normal steroid responsiveness for up to 72 h (Koshiba *et al*., 2001). Recent reconstitution studies using endometrial tissue from mice deficient for the estrogen or progesterone receptor genes have shown that maintaining epithelial–stromal cell interactions is essential if normal responses to steroids are to occur (DeMayo *et al*., 2002). The use of explants retains these interactions and also demonstrates the extent of normal patient-to-patient variation in the expression level of individual genes. An example of this is seen in the TaqMan data for JAK1 (Figure 2), where the control samples vary up to 5-fold in the level of JAK1 expression. This variability has several sources including the fact that biopsies from different women vary in their cellular content. Secondly there is considerable variation in gene expression between different women even with fresh endometrial biopsies taken at LH+7 in the cycle (R.D.Catalano and A.M.Sharkey, unpublished data). The only way to overcome this variation is to perform multiple replicates, as we have done in this experiment in order to obtain reliable data.

The 12 genes identified represent genes involved in apoptosis, transcription, stress response, ECM, but predominantly those involved in cell signalling pathways. One of these, cPLA2, has been reported previously to be up-regulated by RU486 (Kol *et al*., 1998). Others have previously been reported to be expressed in the endometrium, including BAK (Tao *et al*., 1998), CD94 (Semino *et al*., 1995), cathepsin L (Jokimaa *et al*., 2001), GST Pi (Barnette *et al*., 1999) and NIK (King *et al*., 2001). To our knowledge there are no previous reports of steroid regulation of the expression of tenascin R, JNK1, JAK1, VAV2 and WISP1 in endometrium.

The gene list and real time RT–PCR data indicate that the components of two major intracellular signalling pathways, the JAK/STAT signalling pathway, and the JNK signalling pathway, are down-regulated by the action of RU486. Janus kinases (JAK) are cytoplasmic protein tyrosine kinases that are activated by binding of cytokines to their receptors. They phosphorylate cellular substrates including the transcription factor family named signal transducers and activators of transcription (STAT) (Schindler *et al*., 1995; Ihle *et al*., 1996). JAK1 is recruited by three major cytokine receptor subfamilies, class II cytokine receptors [receptors for interferon (INF)α/β, INFγ and interleukin (IL)-10], cytokine receptors that utilize the γc receptor subunit (receptors for IL-2, IL-4, IL-7, IL-9 and IL-15) and receptors that utilize the gp130 subunit (receptors for IL-6, IL-11, leukemia inhibitory factor (LIF), oncostatin M (OSM), cilary neurotrophic factor (CNTF) and cardiotrophin-1 (CT-1)). The results of this study indicate that signal transduction through all these receptors would be altered by the action of RU486.

Immunohistochemical analysis showed that JAK1 immunoreactivity is seen in the glands and only weakly in the stroma in proliferative endometrium. In mid-secretory endometrium the immunostaining increased, especially in the stroma and luminal epithelium. This staining was abolished by preincubation of the antibody with the JAK1 peptide. The data clearly indicate that JAK1 immunoreactivity is elevated in the stroma, endometrial glands and luminal epithelium in the receptive endometrium. Confirmation that JAK1 protein expression is down-regulated in explants or in vivo by RU486 will require accurate quantification by Western blot analysis. JAK2 expression has been shown to be negligible in the proliferative phase, but is elevated in the glands during the secretory phase with little JAK2 expression in the stroma (Jabbour *et al*., 1998). Therefore JAK1 appears to have a distinct role compared with JAK2 in the stroma and luminal epithelium in endometrium from the receptive phase.

The JNK family comprises three protein kinases, defined by their phosphorylation of the N-terminal region of c-jun (Pulverer *et al*., 1991; Kallunki *et al*., 1996). JNK also phosphorylates the transcription factor ATF2 (Gupta *et al*., 1995) and the Ets-domain transcription factor Elk-1 (Whitmarsh *et al*., 1995). The JNK signalling pathways are activated primarily by pro-inflammatory cytokines and stress stimuli. Depending upon the stimulus, JNK activation may be involved in mitogenesis, oncogenic transformation, differentiation, or induction of apoptosis (Minden and Karin, 1997). Prolactin induces activation of both JNK1 and JNK2 and inhibition of JNK1 activation prevents cellular proliferation and induces apoptosis (Schwertfeger *et al*., 2000). JNK1 was specifically down-regulated in our study and therefore only pathways specifically activated by JNK1 should be affected. Functional differences between JNK1 and JNK2 remain unclear as they share many of the same substrates and are activated by the same kinases. However, the recent development of *JNK1* and *JNK2* knockout mice shows that they have distinct and specific roles in modulating cell function. JNK1 is known to alter the expression of >30 genes including insulin-like growth factor binding protein 3 (IGFBP-3), vimentin, cytokeratin 18 and junD (Chen *et al*., 2002). Many of these genes are differentially regulated during the menstrual cycle. JNK1-deficient mice also show defective T-cell differentiation and enhanced Th2 cytokine production (Dong *et al*., 1998). This effect is seen even in *JNK1*+/–, *JNK2*+/– double heterozygotes, indicating that relatively small changes in the levels of JNK gene expression can have significant phenotypic effects (Sabapathy *et al*., 2001). There are four known isoforms of JNK1 which arise by differential splicing, and whose specificity of binding interaction differs between isoforms. The cDNA probe and TaqMan primers used in this study hybridize to the 3′ region common to all isoforms. We have not determined whether expression of all these isoforms is regulated simultaneously.

The action of RU486 on secretory phase endometrium rapidly renders this tissue non-receptive to the implanting embryo (Critchley *et al*., 1999). This is accompanied by changes in expression of genes such as integrins and leukaemia inhibitory factor, whose expression normally coincides with the receptive state (Ghosh *et al*., 1998). We have used endometrial explants treated with RU486 to identify genes whose expression is likely to differ between receptive and non-receptive endometrium. cDNA arrays and real time RT–PCR have confirmed that JNK1 and JAK1 are down-regulated in endometrium by RU486 within 12 h. These molecules act in the signal transduction pathways used by cytokines, growth factors and other physiological stimuli to control cell function. These two signalling pathways, together with the other genes we have identified in this study, identify new genes potentially involved in endometrial receptivity, and may provide new targets for the development of novel contraceptive agents.

Acknowledgements

The authors would like to thank the staff and patients at the Rosie Maternity Hospital, Cambridge for their assistance, without which this study would not have been possible. We would like to thank Tom Freeman and Tony Corps for their helpful advice on array analysis. This study was supported by the World Health Organization, and A.S. was supported by The Meres Research Studentship from St John's College, Cambridge.

References

Barnette, K.G., Sarkar, M.A., Glover, D.D., Li, P., Boyd, C. and Lalka, D. (1999) Glutathione *S*-transferase in human endometrium: quantitation and interindividual variability in isoform content. *Gynecol. Obstet. Invest.*, **47**, 114–119.

Beck, C.A., Estes, P.A., Bona, B.J., Muro-Cacho, C.A., Nordeen, S.K. and Edwards, D.P. (1993) The steroid antagonist RU486 exerts different effects on the glucocorticoid and progesterone receptors. *Endocrinology*, **133**, 728–740.

Borthwick, J.M., Charnock-Jones, D.S., Tom, B.D., Hull, M.L., Teirney, R., Phillips, S.C. and Smith, S.K. (2003) Determination of the transcript profile of human endometrium. *Mol. Hum. Reprod.*, **9**, 19–33.

ChabbertBuffet, N., Djakoure, S., Christin Maitre, S. and Bouchard, P. (1998) Regulation of the human menstrual cycle. *Front. Neuroendocrinol.*, **19**, 151–186.

Carson, D.D., Lagow, E., Thathiah, A., Al-Shami, R., Farach-Carson, M.C., Vernon, M., Yuan, L., Fritz, M.A. and Lessey, B. (2002) Changes in gene expression during the early to mid-luteal (receptive phase) transition in human endometrium detected by high-density microarray screening. *Mol. Hum. Reprod.*, **8**, 871–879.

Chen, N., She, Q.B., Bode, A.M. and Dong, Z. (2002) Differential gene expression profiles of Jnk1- and Jnk2-deficient murine fibroblast cells. *Cancer Res.*, **62**, 1300–1304.

Claverie, J.-M. (1999) Computational methods for the identification of differential and coordinated gene expression. *Hum. Mol. Genet.*, **8**, 1821–1833.

Colantuoni, C., Henry, G., Zeger, S. and Pevsner, J. (2002) Local mean normalization of microarray element signal intensities across an array surface: quality control and correction of spatially systematic artifacts. *Biotechniques*, **32**, 1316–1320.

Critchley, H.O., Kelly, R.W., Lea, R.G., Drudy, T.A., Jones, R.L. and Baird, D.T. (1996) Sex steroid regulation of leukocyte traffic in human decidua. *Hum. Reprod.*, **11**, 2257–2262.

Critchley, H.O., Tong, S., Cameron, S.T., Drudy, T.A., Kelly, R.W. and Baird, D.T. (1999) Regulation of bcl-2 gene family members in human endometrium by antiprogestin administration in vivo. *J. Reprod. Fertil.*, **115**, 389–395.

Danielsson, K.G., Swahn, M.L. and Bygdeman, M. (1997) The effect of various doses of mifepristone on endometrial leukaemia inhibitory factor expression in the midluteal phase—an immunohistochemical study. *Hum. Reprod.*, **12**, 1293–1297.

DeMayo, F.J., Zhao, B., Takamoto, N. and Tsai, S.Y. (2002) Mechanisms of action of estrogen and progesterone. *Ann. NY Acad. Sci.*, **955**, 48–59.

Dong, C., Yang, D.D., Wysk, M., Whitmarsh, A.J., Davis, R.J. and Flavell, R.A. (1998) Defective T cell differentiation in the absence of Jnk1. *Science*, **282**, 2092–2095.

Dudley, D.J., Hatasaka, H.H., Branch, D.W., Hammond, E. and Mitchell, M.D. (1992) A human endometrial explant system: validation and potential applications. *Am. J. Obstet. Gynecol.*, **167**, 1774–1780.

Elger, W., Bartley, J., Schneider, B., Kaufmann, G., Schubert, G. and Chwalisz, K. (2000) Endocrine pharmacological characterisation of progesterone antagonists and progesterone receptor modulators with respect to PR-agonistic and antagonistic activity. *Steroids*, **65**, 713–723.

Gemzell-Danielsson, K., Swahn, M.L., Svalander, P. and Bygdeman, M. (1993) Early luteal phase treatment with mifepristone (RU486) for fertility regulation. *Hum. Reprod.*, **8**, 870–873.

Ghosh, D., Kumar, P.G. and Sengupta, J. (1998) Effect of early luteal phase administration of mifepristone (RU486) on leukaemia inhibitory factor, transforming growth factor beta and vascular endothelial growth factor in the implantation stage endometrium of the rhesus monkey. *J. Endocrinol.*, **157**, 115–125.

Giudice, L.C. (1999) Potential biochemical markers of uterine receptivity. *Hum. Reprod.*, **14** (Suppl. 2), 3–16.

Gruidl, M., Buyuksal, A., Babaknia, A., Fazleabas, A.T., Sivarajah, S., Satyaswaroop, P.G. and Tabibzadeh, S. (1997) The progressive rise in the expression of alpha crystallin B chain in human endometrium is initiated during the implantation window: modulation of gene expression by steroid hormones. *Mol. Hum. Reprod.*, **3**, 337–342.

Gupta, S., Campbell, D., Derijard, B. and Davis, R.J. (1995) Transcription factor ATF2 regulation by the JNK signal transduction pathway. *Science*, **267**, 389–393.

Hamadeh, H.K. Bushel, P., Tucker, C.J., Martin, K., Paules, R. and Afshari, C.A. (2002) Detection of diluted gene expression alterations using cDNA microarrays. *Biotechniques*, **32**, 322–329.

Hackenberg, R., Hannig, K., Beck, S., Schmidt-Rhode, P. and Scholz, K.D. (1996) Androgen-like and anti-androgen-like effects of antiprogestins in human mammary cancer cells. *Eur. J. Cancer*, **32A**, 696–701.

Hegele-Hartung, C., Mootz, U. and Beier, H.M. (1992) Luteal control of endometrial receptivity and its modification by progesterone antagonists. *Endocrinology*, **131**, 2446–2460.

Hey, N.A., Graham, R.A., Seif, M.W. and Aplin, J.D. (1994) The polymorphic epithelial mucin MUC1 in human endometrium is regulated with maximal expression in the implantation phase. *J. Clin. Endocrinol. Metab.*, **78**, 337–342.

Ihle, J.N. (1996) STATs: signal transducers and activators of transcription. *Cell*, **84**, 331–334.

Ilouz, S., Boubli, L., Lavant, M.N., Allasia, C. and Charpin, C. (2000) Endometrial response to sexual steroids as assessed by prostaglandin F (2alpha) output in explant culture and hormone receptor expression. *Gynecol. Obstet. Invest.*, **50**, 43–49.

Jabbour, H.N., Critchley, H.O.D. and Boddy, S.C. (1998) Expression of functional prolactin receptors in nonpregnant human endometrium: janus kinase-2, signal transducer and activator of transcription-1 (STAT1), and STAT5 proteins are phosphorylated after stimulation with prolactin. *J. Clin. Endocrinol. Metab.*, **83**, 2545–2553.

Jackson, T.A., Richer, J.K., Bain, D.L., Takimoto, G.S., Tung, L. and Horwitz, K.B. (1997) The partial agonist activity of antagonist-occupied steroid receptors is controlled by a novel hinge domain-binding coactivator L7/SPA and the corepressors N-CoR or SMRT. *Mol. Endocrinol.*, **11**, 693–705.

Jokimaa, V., Oksjoki, S., Kujari, H., Vuorio, E. and Anttila, L. (2001) Expression patterns of cathepsins B, H, K, L and S in the human endometrium. *Mol. Hum. Reprod.*, **7**, 73–78.

Julkunen, M., Koistinen, R., Sjoberg, J., Rutanen, E.M., Wahlstrom, T. and Seppala, M. (1986) Secretory endometrium synthesizes placental protein 14. *Endocrinology*, **118**, 1782–1786.

Kallunki, T., Deng, T., Hibi, M. and Karin, M. (1996) c-Jun can recruit JNK to phosphorylate dimerization partners via specific docking interactions. *Cell*, **87**, 929–939.

Kao, L.C., Tulac, S., Lobo, S., Imani, B., Yang, J.P., Germeyer, A., Osteen, K., Taylor, R.N., Lessey, B.A. and Giudice, L.C. (2002) Global gene profiling in human endometrium during the window of implantation. *Endocrinology*, **143**, 2119–2138.

King, A.E., Critchley, H.O., Kelly, R.W. (2001) The NF-kappaB pathway in human endometrium and first trimester decidua. *Mol. Hum. Reprod.*, **7**, 175–183.

Kol, S., Ben-Shlomo, I., Payne, D.W., Ando, M., Rohan, R.M. and Adashi, E.Y. (1998) Glucocorticoids suppress basal (but not interleukin-1-supported) ovarian phospholipase A2 activity: evidence for glucocorticoid receptor-mediated regulation. *Mol. Cell. Endocrinol.*, **137**, 117–125.

Koshiba, H., Kitawaki, J., Ishihara, H., Kado, N., Kusuki, I., Tsukamoto, K. and Honjo, H. (2001) Progesterone inhibition of functional leptin receptor mRNA expression in human endometrium. *Mol. Hum. Reprod.*, **7**, 567–572.

Kumar, S., Zhu, L.J., Polihronis, M., Cameron, S.T., Baird, D.T., Schatz, F., Dua, A., Ying, Y.K., Bagchi, M.K. and Bagchi, I.C. (1998) Progesterone induces calcitonin gene expression in human endometrium within the putative window of implantation. *J. Clin. Endocrinol. Metab.*, **83**, 4443–4450.

Lessey, B.A. (2000) The role of the endometrium during embryo implantation. *Hum. Reprod.*, **15**, 39–50.

Lessey, B.A., Damjanovich, L., Coutifaris, C., Castelbaum, A., Albelda, S.M. and Buck, C.A. (1992) Integrin adhesion molecules in the human endometrium. Correlation with the normal and abnormal menstrual cycle. *J. Clin. Invest.*, **90**, 188–195.

Marions, L., Danielsson, K.G., Swahn, M.L. and Bygdeman, M. (1998) Contraceptive efficacy of low doses of mifepristone. *Fertil. Steril.*, **70**, 813–816.

Maslar, I.A. and Riddick, D.H. (1979) Prolactin production by human endometrium during the normal menstrual cycle. *Am. J. Obstet. Gynecol.*, **135**, 751–754.

McDonnell, D.P. and Goldman, M.E. (1994) RU486 exerts antiestrogenic activites through a novel progesterone receptor A form-mediated mechanism. *J. Biol. Chem.*, **269**, 11945–11949.

Minden, A. and Karin, M. (1997) Regulation and function of the JNK subgroup of MAP kinases. *Biochim. Biophys. Acta*, **1333**, F85–104.

Noyes, R.W., Hertig, A.T. and Rock, J. (1950) Dating the endometrial biopsy. *Fertil. Steril.*, **1**, 3–25.

Okulicz, W.C. and Ace, C.I. (1999) Progesterone-regulated gene expression in the primate endometrium. *Semin. Reprod. Endocrinol.*, **17**, 241–255.

Papp, C., Schatz, F., Krikun, G., Hausknecht, V. and Lockwood, C.J. (2000) Biological mechanism underlying the clinical effects of mifepristone (RU486) on the endometrium. *Early Pregnancy*, **4**, 230–239.

Popovici, R.M., Kao, L.C. and Giudice, L.C. (2000) Discovery of new inducible genes in in vitro decidualized human endometrial stromal cells using microarray technology. *Endocrinology*, **141**, 3510–3513.

Pulverer, B.J., Kyriakis, J.M., Avruch, J., Nikolakaki, E. and Woodgett, J.R. (1991) Phosphorylation of c-jun mediated by MAP kinases. *Nature*, **353**, 670–674.

Rutanen, E.M., Koistinen, R., Sjoberg, J., Julkunen, M., Wahlstrom, T., Bohn, H. and Seppala, M. (1986) Synthesis of placental protein 12 by human endometrium. *Endocrinology*, **118**, 1067–1071.

Sabapathy, K., Kallunki, T., David, J.P., Graef, I., Karin, M. and Wagner, E.F. (2001) c-Jun NH2-terminal kinase (JNK)1 and JNK2 have similar and stage-dependent roles in regulating T cell apoptosis and proliferation. *J. Exp. Med.*, **193**, 317–328.

Salamonsen, L.A., Nie, G., Dimitriadis, E., Robb, L. and Findlay, J.K. (2001) Genes involved in implantation. *Reprod. Fertil. Dev.*, **13**, 41–49.

Sarkar, N.N. (2002) Mifepristone: bioavailabilty, pharmacokinetics and use-effectiveness. *Eur. J. Obstet. Gynecol. Reprod. Biol.*, **101**, 113–120.

Schatz, F., Papp, C., Aigner, S., Krikun G., Hausknecht, V. and Lockwood, C.J. (1997) Biological mechanisms underlying the clinical effects of RU 486: modulation of cultured endometrial stromal cell stromelysin-1 and prolactin expression. *J. Clin. Endocrinol. Metab.*, **82**, 188–193.

Schindler, C. and Darnell, J.E. Jr (1995) Transcriptional responses to polypeptide ligands: the JAK-STAT pathway. *Annu. Rev. Biochem.*, **64**, 621–651.

Schwertfeger, K.L., Hunter, S., Heasley, L.E., Levresse, V., Leon, R.P., DeGregori, J. and Anderson, S.M. (2000) Prolactin stimulates activation of c-jun N-terminal kinase (JNK). *Mol. Endocrinol.*, **14**, 1592–1602.

Semino, C., Semino, A., Pietra, G., Mingari, M.C., Barocci, S., Venturini, P.L., Ragni, N. and Melioli, G. (1995) Role of major histocompatibility complex class I expression and natural killer-like T cells in the genetic control of endometriosis. *Fertil. Steril.*, **64**, 909–16.

Sharkey, A. and Smith, S.K. (2003) The endometrium as a cause of implantation failure. *Baillières Best Pract. Res. Clin. Obstet. Gynecol.*, **17**, 289–307.

Swahn, M.L., Bygdeman, M., Cekan, S., Xing, S., Masironi, B. and Johannisson, E. (1990) The effect of RU 486 administered during the early luteal phase on bleeding pattern, hormonal parameters and endometrium. *Hum. Reprod.*, **5**, 402–408.

Tabibzadeh, S. and Babaknia, A. (1995) The signals and molecular pathways involved in implantation, a symbiotic interaction between blastocyst and endometrium involving adhesion and tissue invasion. *Mol. Hum. Reprod.*, **10**, 1579–1602.

Tabibzadeh, S., Kong, Q.F., Babaknia, A. and May, L.T. (1995) Progressive rise in the expression of interleukin-6 in human endometrium during menstrual cycle is initiated during the implantation window. *Hum. Reprod.*, **10**, 2793–2799.

Tao, X.J., Sayegh, R.A., Tilly, J.L. and Isaacson, K.B. (1998) Elevated expression of the proapoptotic BCL-2 family member, BAK, in the human endometrium coincident with apoptosis during the secretory phase of the cycle. *Fertil. Steril.*, **70**, 338–343.

Taylor, R.N., Savouret, J.-F., Vaisse, C., Vigne, J.-L., Ryan, I., Hornung, D., Seppala, M. and Milgrom, E. (1998) Promegestone (R5020) and mifepristone (RU486) both function as progestational agonists of human glycodelin gene expression in isolated human epithelial cells. *J. Clin. Endocrinol. Metab.*, **83**, 4006–4012.

Wang, H.S., Kanzaki, H., Yoshida, M., Sato, S., Tokushige, M. and Mori, T. (1987) Suppression of lymphocyte reactivity *in vitro* by supernatants of explants of human endometrium. *Am. J. Obstet. Gynecol.*, **157**, 956–963.

Whitmarsh, A.J., Shore, P., Sharrocks, A.D. and Davis, R.J. (1995) Integration of MAP kinase signal transduction pathways at the serum response element. *Science*, **269**, 403–407.

Wilcox, A.J., Baird, D.D. and Weinberg, C.R. (1999) Time of implantation of the conceptus and loss of pregnancy. *N. Engl. J. Med.*, **340**, 1796–1799.

Submitted on March 3, 2003; accepted on April 3, 2003

PUBLICATION 4

Holland, C. M., Saidi, S. A., **Evans, A. L.,** Sharkey, A. S., Latimer, J. A., Crawford, R. A., Charnock-Jones, D. S., Print, C. G., and Smith, S. K. 2004. Transcriptome analysis of endometrial cancer identifies peroxisome proliferator-activated receptors as potential therapeutic targets *Mol. Cancer Therapeutics* 3, 993-1001.

Cited by 20, Impact factor 5.226

Print ISSN: 1535-7163, **Online ISSN:** 1538-8514

Journal Type

Molecular Cancer Therapeutics is published once a month by the American Association for Cancer Research (AACR). The journal publishes is the categories of Therapeutic Discovery, Preclinical Development, and Molecular Medicine in Practice. It also publishes mini reviews on molecular aspects of cancer. This paper was published as an original article.

Personal Contribution

My contribution to this paper was microarray production as described (Evans et al., 2003)[*1] and hybridisation experiments. The reporter studies in Ishikawa cells and *in-situ* hybridisation were performed by Catherine Holland, as a part of her PhD project.

Transcriptome analysis of endometrial cancer identifies peroxisome proliferator-activated receptors as potential therapeutic targets

Cathrine M. Holland,[1,2] Samir A. Saidi,[2] Amanda L. Evans,[1] Andrew M. Sharkey,[1] John A. Latimer,[2] Robin A.F. Crawford,[2] D. Stephen Charnock-Jones,[2] Cristin G. Print,[1] and Stephen K. Smith[1,2]

Departments of [1]Pathology and [2]Obstetrics and Gynaecology, University of Cambridge, The Rosie Hospital, Cambridge, United Kingdom

Abstract

Endometrial cancer is the most common gynecologic malignancy, frequently arising in association with obesity and diabetes mellitus. To identify gene pathways contributing to endometrial cancer development, we studied the transcriptome of 20 endometrial cancers and 11 benign endometrial tissues using cDNA microarrays. Among the transcript changes identified in endometrial cancer were up-regulation of the nuclear hormone receptors peroxisome proliferator-activated receptors (PPAR) α and γ, whereas retinoid X receptor β was down-regulated. To clarify the contribution of PPARα to endometrial carcinogenesis, we did experiments on cultured endometrial carcinoma cells expressing this transcript. Treatment with fenofibrate, an activating ligand for PPARα, significantly reduced proliferation and increased cell death, suggesting that altered expression of nuclear hormone receptors involved with fatty acid metabolism leads to deregulated cellular proliferation and apoptosis. These results support further investigation of members of the PPAR/retinoid X receptor pathway as novel therapeutic targets in endometrial cancer. [Mol Cancer Ther 2004;3(8):993–1001]

Introduction

Endometrial carcinoma is the most common gynecologic malignancy and comprises 97% of all uterine cancers (1). There is a peak incidence between ages 55 and 65 years, with <5% of endometrial cancers occurring below age 40 years (2). The majority are of an endometrioid histologic subtype and display an association with obesity and diabetes mellitus (2). There is a pressing need to better understand the molecular basis for this disease, as 25% of women present with extrauterine disease with 5-year survival rates of ~31% and 10% for Federation Internationale des Gynaecologistes et Obstetristes stages 3 and 4 disease, respectively (2). An improved understanding of events at a molecular level is essential in the development of targeted therapy, with a view to improving survival and cure rates.

There are increasing efforts to gain a more global view of the multiple, interrelated molecular changes that occur during tumorigenesis (3–6). The gene microarray is a high-throughput technology able to interrogate multiple genetic changes within tissues and cells (7–9). Consequently, there has been a marked increase in the use of microarrays to interrogate cancers at the genomic level. In addition to screening for candidate genes, microarrays may provide molecular diagnoses, thus avoiding some of the weaknesses of conventional diagnostic techniques (4, 10).

Despite the increasing use of microarray technology in cancer research, there have been difficulties obtaining meaningful biological information. The cost of genome-wide, commercially available arrays may prohibit large experimental samples, and there are multiple sources of variation in experimental results complicating data analysis and interpretation (11). Large-scale gene expression analyses of endometrial cancer have mostly been confined to small sample sets and cell lines (12, 13) and have employed genome-wide, commercially available microarray systems (12). Previous microarray studies in endometrial cancer have highlighted differences in the abundance of individual genes between benign and malignant tissues (12, 13), although there has been little advance in the understanding of pathway-specific alterations that may contribute to endometrial tumorigenesis. Independent component analysis (ICA) is a sophisticated statistical method that aims to identify patterns of coregulated genes rather than individual transcript changes (14). We previously have applied high-density cDNA microarrays to determine gene transcript abundance in epithelial ovarian cancer (14).

Materials and Methods

Tumor Samples and RNA Preparation

Twenty frozen endometrial carcinoma tissues, three atypical complex hyperplasias, and eight postmenopausal benign endometrial control tissues (four atrophic and four

Received 3/30/04; revised 5/4/04; accepted 5/14/04.

Grant support: Medical Research Council Clinical Training Fellowship G84/5733 (C.M. Holland), Medical Research Council Program grant G9623012 (S.K. Smith and D.S. Charnock-Jones), and Raymond and Beverly Sackler Award (C.M. Holland).

The costs of publication of this article were defrayed in part by the payment of page charges. This article must therefore be hereby marked advertisement in accordance with 18 U.S.C. Section 1734 solely to indicate this fact.

Requests for reprints: Cathrine M. Holland, Department of Obstetrics and Gynaecology, University of Cambridge, The Rosie Hospital, Box 223, Level 2, Robinson Way, Cambridge CB2 2SW, United Kingdom. Phone: 44-1223-336874; Fax: 44-1223-215327. E-mail: cath.holland@obgyn.cam.ac.uk

benign polyps) were obtained from the Department of Obstetrics and Gynecology, Addenbrooke's Hospital NHS Trust (Cambridge, United Kingdom) with ethical approval. Samples were frozen immediately in liquid nitrogen after surgery and stored at −70°C. Total RNA was extracted from the frozen tissues using an acid-guanidium thiocyanate-phenol-chloroform method (15). Clinical information and histopathologic reports were obtained for all frozen tissues.

Hybridization to cDNA Microarrays

Tailored nylon microarrays comprising 1,056 cDNA clones and including 37 expressed sequence tags were used for transcriptome analysis. These were manufactured in the Departments of Obstetrics and Gynecology and Pathology, University of Cambridge (Cambridge, United Kingdom) and designed for the study of endometrial function and vascular biology (16) The entire gene list can be seen at http://www.obgyn.cam.ac.uk/genearray. Labeled cDNA was produced from total RNA preparations as described previously (16). ULTRArray hybridization buffer (Ambion, Austin, TX) was used, and hybridization was carried out in 15 × 4 cm roller bottles as described previously (16). Microarrays were subjected to high stringency washes in SSC and SDS, dried at 60°C, and exposed to low-energy storage phosphor screens (Molecular Dynamics, Sunnyvale, CA) for 64 hours. Arrays were scanned at high resolution using a Storm 860 Phosphor-Imager (Molecular Dynamics).

Data Analysis

Images were imported into Imagene 4.0 software (Biodiscovery Inc., Marina del Ray, CA) for calculation of signal intensity. Total signal for each spot was squared to correct for the square root transformation applied by the scanning software (17). Data were processed using a normalization algorithm method similar to that used in the Web-based SNOMAD program (18). Normalized data were analyzed by two complementary methods, the Web-based Cyber-T and ICA. Cyber-T uses a Bayesian version of the *t* test, which is suitable for the large-throughput analysis required for microarray data (19). A Bayesian P value < 0.05 was considered significant. ICA reduces the data to a set of *components* that explain the data. Analysis of those components that correlate closely with a factor(s) of interest allows extraction of gene expression changes contributing most strongly to that factor. The method of ICA used is an ensemble learning method that allows identification of components constituting the data while at the same time providing an estimate of the inherent ''noise'' (20). The ICA model also allows refinement or filtering of the data (20).

Quantitative, Real-time PCR (TaqMan)

Total RNA (2 μg) was incubated with oligo(dT) primers (1 μg) at 68°C and reverse transcribed at 42°C using Super Reverse Transcriptase (HT Biotechnology Ltd., Cambridge, United Kingdom). Total RNA samples used were those used in the microarray experiments described earlier.

cDNA (1 μL each) was amplified using PCR Master Mix (Applied Biosystems, Warrington, United Kingdom). All quantitative, real-time PCR experiments were done in the ABI PRISM 7700 Sequence Detector (Applied Biosystems) according to the manufacturer's instructions and were done in triplicate. The resultant data were averaged for each sample. No-template controls were included in each experiment. Specific oligonucleotide primers and probes were used. These were designed for each of five genes [cyclooxygenase-2 (*COX-2*), vascular endothelial growth factor-B (*VEGF-B*), *PPARα*, *PPARγ*, and retinoid X receptor β (*RXRβ*)] using Primer Express 1.5 software (Applied Biosystems). Sequences are given below:

(a) *COX-2*
5′-TGATCCCCAGGGCTCAAA-3′ (forward primer),
5′-ATCTGTCTTGAAAAACTGATGCGT-3′ (reverse primer),
5′-6FAM-TGATGTTTGCATTCTTTGCCCAGCACT-TAMRA-3′ (probe);

(b) *VEGF-B*
5′-AGCACCAAGTCCGGATG-3′ (forward primer),
5′-GTCTGGCTTCACAGCACTG-3′ (reverse primer),
5′-6FAM-AGATCCTCATGATCCGGTACCCGT-TAMRA-3′ (probe);

(c) *PPARα*
5′-GACGTGCTTCCTGCTTCATAGA-3′ (forward primer),
5′-CACCATCGCGACCAGATG-3′ (reverse primer),
5′-6FAM-TGGAGCTCGGCGCACAACCA-TAMRA-3′ (probe);

(d) *PPARγ*
5′-CAGAGCAAAGAGGTGGCCAT-3′ (forward primer),
5′-GCTTTTGGCATACTCTGTGATCTC-3′ (reverse primer),
5′-6FAM-CATCTTTCAGGGCTGCCAGTTTCGC-TAMRA-3′ (probe);

(e) *RXRβ*
5′-CCATCCGCAAAGACCTTACATAC-3′ (forward primer),
5′-GTTCCGCTGGCGCTTG-3′ (reverse primer),
5-6FAM-TGCCGGGACAACAAAGACTGCACA-TAMRA-3′ (probe).

Results for gene abundance in each sample were normalized to abundance of an endogenous control gene. 18S rRNA was used as an endogenous control for all genes, with the exception of VEGF-B for which β-actin was used. Preliminary experiments to determine that each endogenous control sequence was amplified at the same rate as the target gene sequence identified that β-actin, but not 18S rRNA, was a suitable endogenous control for VEGF-B. Normalized log-transformed transcript levels were compared across samples using one-way ANOVA and unpaired Student's *t* tests. Mean target gene abundance for each tissue type was compared with the data obtained from microarray experiments.

Immunohistochemistry

Immunohistochemistry for PPARα protein was done on 6 μmol/L formalin-fixed, paraffin-embedded endometrial tissue sections identified from histopathologic archives. Six endometrioid cancers and four samples of benign endometrium were examined. Sections were dewaxed in xylene and rehydrated in graduated alcohols and antigens were retrieved with 0.1% trypsin for 15 minutes at 37°C. Nonspecific immunostaining was blocked with normal goat serum and sections were incubated with 4 μg/mL rabbit polyclonal anti-PPARα antibody (Santa Cruz Biotechnology, Santa Cruz, CA) overnight at 4°C. Rabbit IgG (4 μg/mL) provided a negative control. A biotinylated goat anti-rabbit secondary antibody (1:100 dilution) was used for 30 minutes at room temperature. Detection of the antibody reaction was carried out with the Vectastain Elite ABC reagent (Vector Laboratories, Burlingame, CA) combined with 3,3-diaminobenzidine color development (Sigma Chemical Co., MI). Endogenous peroxidases were blocked with 0.3% hydrogen peroxide in methanol. Results were analyzed using the two-tailed Fisher's exact probability test. Statistical significance was accepted as $P < 0.05$.

Cell Culture Assays

Ishikawa cells in the logarithmic growth phase were cultured in DMEM (Sigma Chemical) supplemented with glucose, L-glutamine, and FCS in 96-well plates. Cells were cultured for 24 hours at 37°C and 5% CO_2 with varying doses of the PPARα agonist fenofibrate (Sigma-Aldrich Co. Ltd., Dorset, United Kingdom) dissolved in DMSO (Sigma-Aldrich). Control cells were treated with vehicle only. A minimum of five replicates was done at each dose. Total RNA was extracted from untreated Ishikawa cells, and quantitative, real-time PCR was done for PPARα (as above). In addition, cell proliferation in fenofibrate-treated and DMSO-treated cells was assessed by the uptake of 5-bromo-2′-deoxyuridine (BrdUrd) using the BrdUrd Labeling and Detection Kit III (Roche Diagnostic, East Sussex, United Kingdom) according to the manufacturer's instructions. Absorbance values for each well were measured on a microtiter plate reader (Anthos Labtech Instruments, Salzburg, Austria).

Apoptosis was measured using two different methods. Cells were grown in 96-well plates as above. At 24 hours, the medium was replaced with fresh complete culture medium and fenofibrate (10–100 μmol/L). Six replicates were done for each drug dose, and control cells were treated with vehicle (DMSO) only. Apoptosis was quantified using the APOPercentage Apoptosis Assay dye (Biocolor Ltd., Northern Ireland, United Kingdom) according to the manufacturer's instructions. Dye absorbance values were measured as above. In a second assay, the medium was exchanged after 24 hours for fresh medium containing 75 μmol/L fenofibrate or DMSO only. After further incubation at 37°C for 1 hour, cells were fixed and stained with Hoechst bisbenzamide HB 3258 (Calbiochem, La Jolla, CA) and viewed by fluorescent microscopy. Seven separate optical fields were counted for each well, and both total numbers of cells and number of apoptotic cells were counted. An apoptotic index was calculated using the following formula: apoptotic index = [(number of apoptotic cells) / (total cell count)] × 100.

Data were analyzed using the InStat 2.1 statistical program. For the BrdUrd and APOPercentage assays, differences between median values across multiple treatment groups were analyzed using the Kruskal-Wallis nonparametric ANOVA method. Comparison between median values from each treatment group and negative control group was made using the Mann-Whitney U test. Ratio data arising from the Hoechst nuclear staining assay were log transformed and analyzed by Student's t test. Statistical significance was accepted at $P < 0.05$ throughout.

Reporter Studies

Ishikawa cells cultured in six-well plates were transfected with 3 μg luciferase reporter plasmid using 4 μg LipofectAMINE 2000 (Invitrogen, Paisley, United Kingdom). The reporter plasmid comprised a triple repeat of the peroxisome proliferator response element in direct orientation with a basal TK-luc reporter construct (21). Cells were grown and treated, before confluence was reached, with varying doses of fenofibrate and the specific PPARα antagonist GW496471. At 24 hours, cells were harvested and luciferase activity was measured using the Ascent Fluoroscan luminometer. Normalization was done against total protein using the BCA protein assay (catalogue no. 23227, Pierce Chemical Co. Rockford, IL). A control plasmid, pRL-CMV (catalogue no. E2261, Promega, Southampton, United Kingdom), was initially used as a transfection control but was found to respond to PPAR agonists and subsequently noted to contain a putative peroxisome proliferator response element within the cytomegalovirus promoter region (data not shown). The reporter plasmid and PPARα antagonist were kind donations from Dr. E. Shoenmakers and Prof. K. Chatterjee (Cambridge Institute for Medical Research, Cambridge, United Kingdom).

Results

Gene Microarrays Identify Differentially Expressed Transcripts in Endometrial Carcinoma

Transcript abundance, measured by mean signal intensity, was compared between benign and malignant tissues. The expression of 204 genes was altered in the cancers compared with the benign endometrium ($P < 0.05$) when the data were analyzed using Cyber-T. Of these 204 genes, 182 were up-regulated and 22 were down-regulated in the cancers compared with benign endometrium. The genes that were identified by the Cyber-T analysis were assigned to functional categories (Table 1). The ''housekeeping genes'' included on the arrays (e.g., *actin* and *glyceraldehyde 3-phosphate dehydrogenase*) were not significantly altered between the different tissue classes. Among the changes seen were significant alterations in angiogenesis-related genes. The VEGF-A splice variant (VEGF189) and angiopoietin-2 were up-regulated by 5.7- and 4.9-fold, respectively ($P < 0.05$). In addition, the VEGF-C and VEGF-D

Table 1. Selected examples of differentially expressed genes in endometrial carcinoma

Genbank Accession No.	Gene Name	*P**	Fold Change in Tumors†
Transcription factors and nuclear receptors			
U32849	N-*myc* (STAT) interactor (*NMI*)	0.006	8.2
L40904	*PPARγ*	0.039	6.1
U22431	Hypoxia-inducible factor 1α (*HIF1α*)	0.004	5.4
X06562	Growth hormone receptor (*GHR*)	0.030	5.1
Y07619	*PPARα*	0.026	4.3
V00568	v-*myc* myelocytomatosis viral oncogene homologue (*MYC*)	0.048	2.8
X07282	Retinoic acid receptor β (*RARβ*)	0.028	4.3
M84820	*RXRβ*	0.001	−1.4
Cell cycle and growth regulators			
X76132	Deleted in colorectal carcinoma (*DCC*)	0.018	6.2
M74091	Cyclin C	0.009	4.5
X05908	Annexin A1 (*ANXA1*)	0.012	4.8
L27560	Insulin-like growth factor binding protein 5 (*IGFBP5*)	0.025	2.2
Angiogenic factors, receptors, and mediators			
AB012911	VEGF189	0.013	5.7
AB009865	Angiopoetin-2 (*ANGPT2*)	0.020	4.9
U43143	Fms-related tyrosine kinase 4 (*FLT4*)	0.033	5.4
U48801	*VEGF-B*	1.48e−05	−1.9
Cell adhesion, recognition, and cytoskeleton			
Z13009	E-cadherin	0.014	4.2
J03209	Matrix metalloproteinase-3 (*MMP-3*)	0.015	4.4
M14083	Plasminogen activator inhibitor type 1 (*PAI-1*)	0.046	2.2
M13509	Matrix metalloproteinase 1 (interstitial collagenase; *MMP-1*)	0.025	3.9
Growth factors, cytokines, hormones, and receptors			
J02958	HGF receptor (*MET*)	0.009	3.0
M31172	Transforming growth factor-α (*TGFα*)	0.045	4.8
X06374	Platelet-derived growth factor receptor α (*PDGFα*)	0.045	4.5
X00588	Epidermal growth factor receptor (c-erbB; *EGFR*)	0.026	5.1
X04434	Insulin-like growth factor receptor 1 (*IGFR1*)	0.001	−1.9
Intracellular signaling			
X95282	Ras homologue gene family, member E (*RhoE*)	0.028	4.6
AB012911	Frizzled homologue 6 (*Drosophila*) (*FZD6*)	0.011	3.4
Enzymes/cellular metabolism			
U04636	*COX-2*, prostaglandin-endoperoxide synthase 2	0.038	5.6
M14777	Glutathione *S*-transferase A1 (*GSTA1*)	0.014	4.2
M61900	Prostaglandin D2 synthase (*PTGDS*)	2.45e−05	−2.1

NOTE: Selected examples of genes found to be differentially regulated in endometrial cancer. Microarray data from 20 endometrial cancers (17 endometrioid type and 3 papillary serous type) and 11 benign endometria were compared using Cyber-T. Fold change in the cancers compared with the benign tissues is shown with a minus sign indicating down-regulation. The *P* value for each transcript change is indicated. The genes are listed in potential functional categories with Genbank accession numbers.
*Tumor versus normal as assessed by Cyber-T.
† Fold changes <1.5 not included.

receptor tyrosine kinase, Fms-related tyrosine kinase 4 (VEGF receptor-3), was 5.4-fold more abundant in the endometrial cancers compared with benign postmenopausal endometrium. In contrast, the VEGF-related growth factor, VEGF-B and platelet-derived growth factor receptor β, were almost 2-fold down-regulated in the cancers ($P < 0.001$).

Only one independent component (the ''cancer'' component), resulting from ICA, showed statistical significance using the Mann-Whitney *U* test ($P < 0.001$) and was subjected to further analysis. Data for the 5% of genes contributing most highly to this component are represented in Fig. 1. Genes concerned with lipid metabolism were found to be significantly overrepresented in the ICA analysis (20). Of these, novel changes were identified in members of the nuclear hormone receptor superfamily. Genes encoding both PPARα ($P < 0.05$) and PPARγ ($P < 0.05$) were significantly up-regulated in the cancers compared with benign endometrium (4.3- and 6.1-fold, respectively). Conversely, the gene encoding a heterodimerization partner for these two nuclear receptors, *RXRβ*, was down-regulated 1.4-fold ($P < 0.01$).

Five genes were chosen to confirm the microarray results using quantitative, real-time PCR. Four of these genes are

components of the prostaglandin and fatty acid pathways (*COX-2*, *PPARα*, *PPARγ*, and *RXRβ*), whereas the fifth gene, *VEGF-B*, is an angiogenic growth factor. In addition to their biological interest, these genes were chosen based on their significant Bayesian *P* value (using Cyber-T) and high loading value within the ICA ''cancer'' component. The mean relative expression of these genes in cancers compared with benign tissues was calculated from normalized transcript abundance levels from real-time PCR and compared with the mean ratio of expression levels in cancer obtained from microarray experiments (Fig. 1B). Data from microarray experiments analyzed using Cyber-T indicated that transcripts for COX-2 ($P < 0.01$), PPARα ($P < 0.01$), and PPARγ ($P < 0.05$) were significantly up-regulated in the endometrial cancers examined compared with the benign endometrial samples (Table 1). Conversely, transcripts for VEGF-B ($P < 0.01$) and RXRβ ($P < 0.01$) were significantly down-regulated in the cancers compared with the benign tissues (Table 1). The up-regulation of COX-2, PPARα, and PPARγ and down-regulation of VEGF-B and RXRβ were confirmed using quantitative PCR (Fig. 1B). The direction and magnitude of fold changes was similar (Fig. 1B).

PPARα Protein Is Localized to Endometrial Carcinoma Cells but not to Stromal Cells

Paraffin-embedded tissue sections were used to confirm the expression of PPARα protein in endometrial cancers compared with benign (atrophic) endometrium. These specimens were unrelated to those used in the microarray experiments, thus providing independent confirmation. Specific immunostaining for PPARα protein was seen in five of six sections of endometrial cancer (Fig. 2) but in zero of four of the benign endometrial sections ($P < 0.05$). Negative controls did not show specific immunostaining (Fig. 2A). Immunostaining for PPAR protein was localized to the epithelial tumor cells and was cytoplasmic rather than nuclear (Fig. 2C). The intensity of staining was heterogeneous with some tumor cells demonstrating intense staining, whereas staining was weaker in others (Fig. 2B).

PPARα Agonists Inhibit the Growth of Endometrial Cancer Cells

Ishikawa cells were shown to have levels of PPARα mRNA comparable with those seen in the cancer samples (Fig. 3). These were cultured with the PPARα agonist

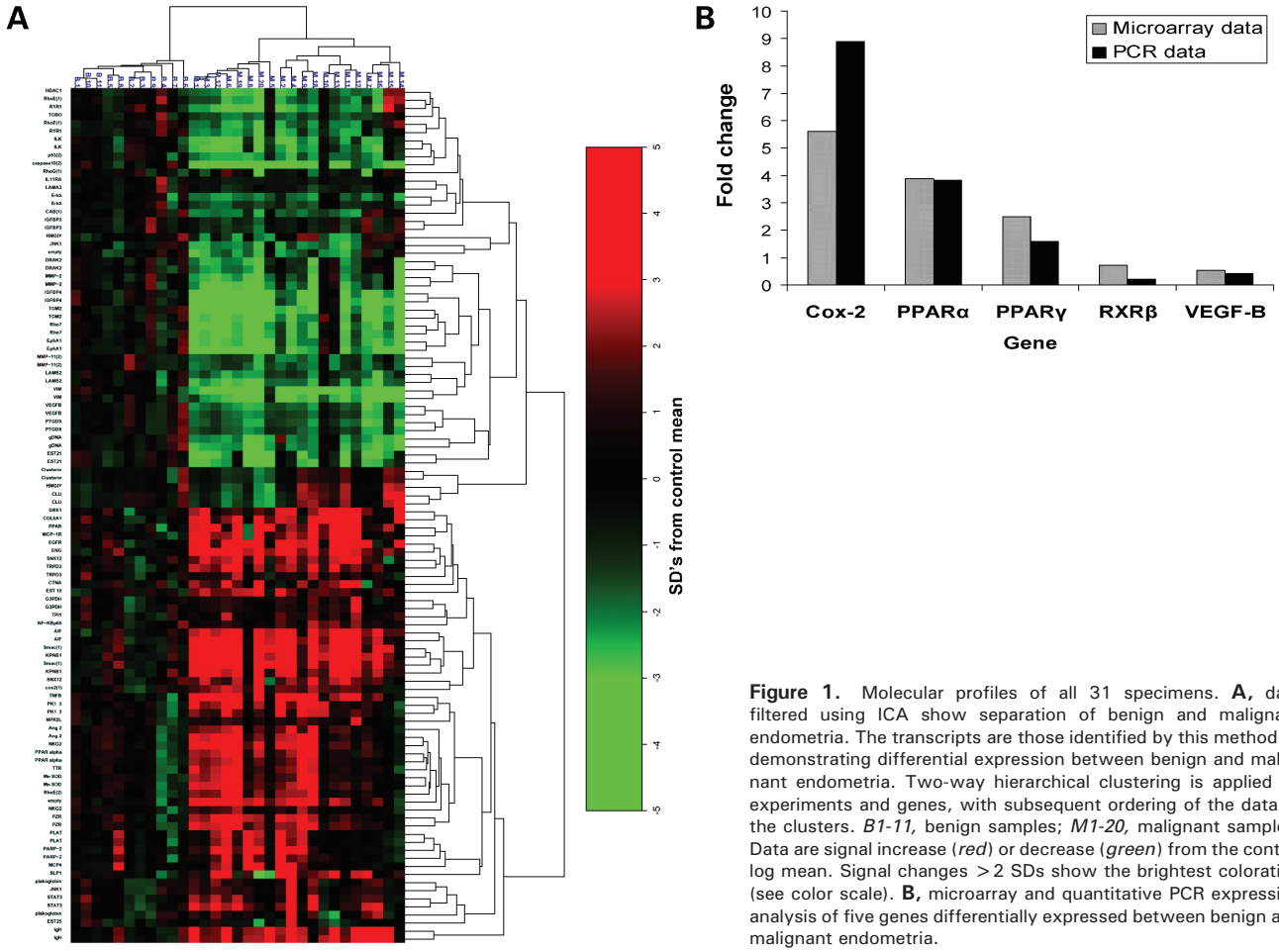

Figure 1. Molecular profiles of all 31 specimens. **A,** data filtered using ICA show separation of benign and malignant endometria. The transcripts are those identified by this method as demonstrating differential expression between benign and malignant endometria. Two-way hierarchical clustering is applied by experiments and genes, with subsequent ordering of the data to the clusters. *B1-11,* benign samples; *M1-20,* malignant samples. Data are signal increase (*red*) or decrease (*green*) from the control log mean. Signal changes >2 SDs show the brightest coloration (see color scale). **B,** microarray and quantitative PCR expression analysis of five genes differentially expressed between benign and malignant endometria.

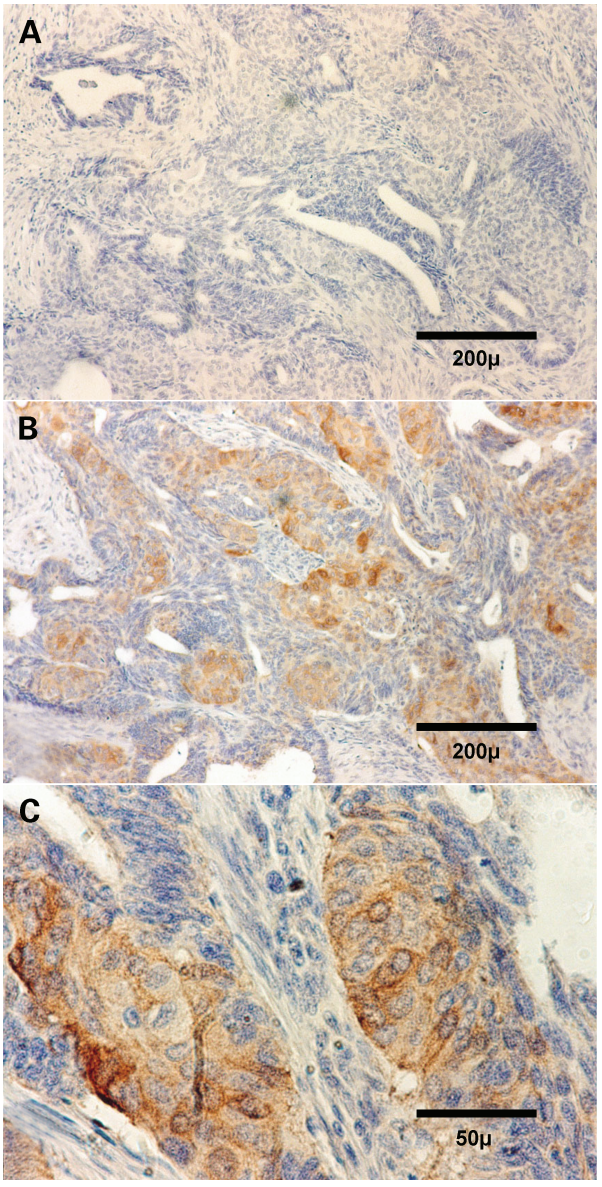

Figure 2. PPARα protein is localized to the cytoplasm of endometrial carcinoma cells. Paraffin-embedded sections of benign endometrium and endometrial cancer were subjected to immunohistochemistry for PPARα. A biotinylated secondary antibody was used for detection. **A,** a Federation Internationale des Gynaecologistes et Obstetristes grade 2 endometrial carcinoma incubated with IgG (negative control) showing no specific immunostaining (magnification ×100). **B,** a Federation Internationale des Gynaecologistes et Obstetristes grade 2 endometrioid endometrial adenocarcinoma showing positive heterogeneous immunostaining for PPARα (magnification ×100). **C,** a Federation Internationale des Gynaecologistes et Obstetristes grade 2 endometrioid endometrial adenocarcinoma at high power showing cytoplasmic epithelial tumor cell staining but no staining of stromal cells (magnification ×400).

fenofibrate and showed a decrease in DNA synthesis in a dose-dependent manner after 24 hours of incubation (Fig. 4A). The difference in BrdUrd incorporation across the range of drug doses used was highly statistically significant ($P < 0.001$) when analyzed using the Kruskal-Wallis nonparametric ANOVA. Low doses of fenofibrate had no significant effect on DNA synthesis (Fig. 4A). However, a reduction in BrdUrd uptake (as measured by dye absorbance) was seen at doses of 50 μmol/L ($P = 0.01$, 95% confidence interval 0.20–0.26) and 75 μmol/L ($P = 0.01$, 95% confidence interval 0.20–0.26).

Cells were treated with fenofibrate for 1 hour at 37°C, and uptake of a labeling dye for fragmented DNA was measured in a microplate reader after lysing the cells. There was a significant and dose-dependent increase of cells undergoing apoptosis among those treated with fenofibrate compared with cells treated with vehicle (DMSO) alone ($P < 0.0001$; Fig. 4B). This effect was maximal at 75 μmol/L fenofibrate. In the second assay, cells were treated with either 75 μmol/L fenofibrate or vehicle only. Nuclear fragmentation and apoptotic bodies were frequently seen in the treated cells but infrequently seen in the control cells (Fig. 5A and B). However, mitotic figures were seen in control cells consistent with increased proliferation. The apoptotic index was ~5 fold higher in treated compared with untreated cells ($P < 0.05$; Fig. 5C), confirming the results obtained from the BrdUrd proliferation assay.

Using a peroxisome proliferator response element containing a luciferase reporter construct, we showed functional activity of endogenous PPARα in Ishikawa cells. Transfected cells treated with fenofibrate showed a significant increase in luciferase activity compared with untreated control cells (Fig. 4C). However, addition of the highly specific PPARα antagonist GW496471 (3 μmol/L) significantly reduced the increased luciferase activity induced by equimolar fenofibrate.

Discussion

The use of ICA complemented Cyber-T analysis, enabling the identification of transcript patterns differentiating benign from malignant endometrium (20). Within these patterns, we showed up-regulation of two ligand-activated

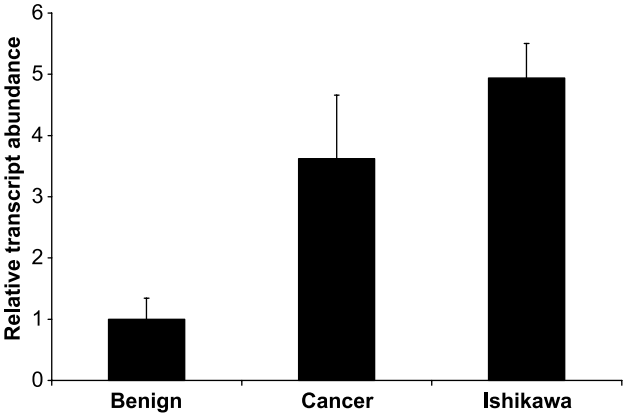

Figure 3. Ishikawa cells express PPARα mRNA. Quantitative PCR for PPARα was done on RNA extracted from Ishikawa cells and compared with mean transcript abundance in benign ($n = 8$) and malignant ($n = 17$) endometria. *Columns,* mean PPARα transcript abundance relative to levels of 18S rRNA; *bars,* SE. All experiments were done in triplicate.

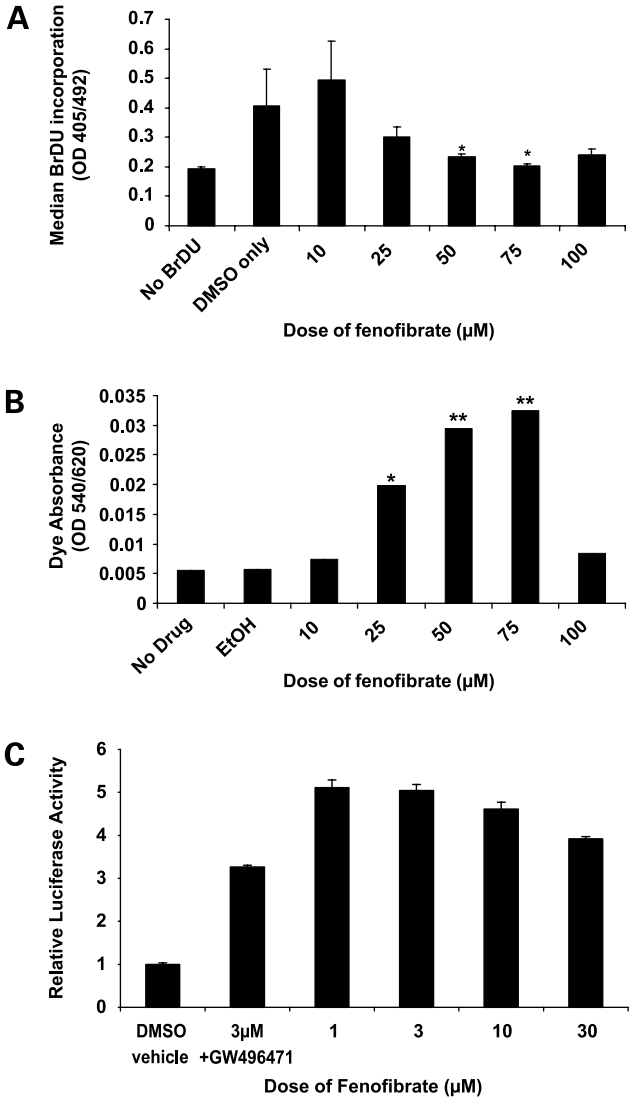

Figure 4. The PPARα agonist fenofibrate reduces proliferation and increases apoptosis in Ishikawa cells. **A,** PPARα-expressing Ishikawa cells in culture were treated with the PPARα agonist fenofibrate. After 24 hours, proliferation was assessed by BrdUrd uptake. Increasing doses of fenofibrate led to reduced proliferation compared with vehicle only. **B,** cultured Ishikawa cells were treated for 1 hour with fenofibrate, and uptake of dye into apoptotic cells was measured by dye absorbance. Apoptosis was increased in a dose-dependent manner by the addition of fenofibrate. **C,** in a reporter assay, cells were treated with DMSO or fenofibrate and 9-*cis*-retinoic acid (3 μmol/L) ± the PPARα antagonist GW496471 (3 μmol/L). *Columns,* luciferase activity (relative light units) relative to that seen in DMSO-treated cells in duplicate assays across two independent experiments; *bars,* SE.

transcription factors belonging to the nuclear hormone receptor superfamily, PPARα and PPARγ. These receptors form heterodimeric complexes with RXRβ that bind to specific response elements within the promoter region of target genes (22). We have further shown that RXRβ is significantly down-regulated in endometrial cancer.

The PPARs exist as three isoforms, PPARα, PPARβ/δ, and PPARγ. Genes induced by PPARα are primarily concerned with β-oxidation in normal cells (22), whereas PPARγ regulates adipocyte differentiation and macrophage function and is linked with glucose homeostasis (23). PPARβ/δ shows widespread tissue expression and is particularly abundant during development (24), although its functions are not fully known. Endogenous ligands for PPARβ are

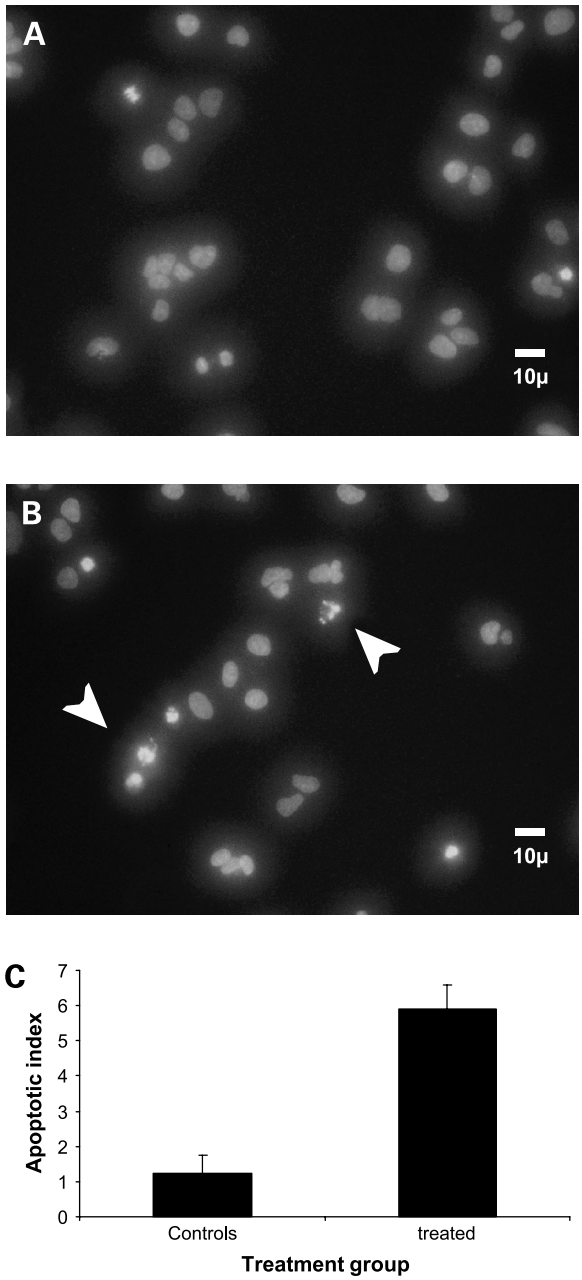

Figure 5. The PPARα agonist fenofibrate is proapoptotic for endometrial cancer cells. Cultured Ishikawa cells were treated with fenofibrate (75 μmol/L) or vehicle only for 1 hour, and apoptotic cells were counted after nuclear staining with Hoechst bisbenzamide. **A,** control cells show mitotic figures and few apoptotic cells. **B,** treated cells display nuclear fragmentation and apoptotic bodies (*arrows*). **C,** apoptosis is markedly increased in the presence of fenofibrate. *Columns,* mean of three replicates; *bars,* SD.

prostaglandins and leukotrienes. In addition to these, ligands for PPARα include fatty acids (25). Ligands for the PPARs also regulate COX-2, which is critically involved in lipid metabolism, inflammation, and tumor promotion (26).

Our findings suggest involvement of the lipid metabolic and prostaglandin pathways in endometrial cancer development. The prostaglandin pathway has been implicated previously in carcinogenesis, with overexpression of COX-2 being described in several cancers including endometrium (27, 28), malignant mesothelioma (29), cervix (30), breast (31), and colon (32–34). In addition, there is epidemiologic evidence of a protective effect of nonsteroidal anti-inflammatory drugs against colon cancer (35). In the colon cancer model, it is suggested that prostanoids may promote tumor development via the PPAR receptors, although the data are not conclusive (36).

PPARα is highly expressed in the cancer cells of other malignancies [e.g., prostate (37) and bladder (38)]. Localization of PPARα protein to malignant endometrial cells suggests that up-regulation of the *PPAR*α gene is also significant in endometrial carcinoma. Whereas PPARβ/δ is up-regulated in some endometrial cancers (27), neither PPARα nor PPARγ have been implicated previously in the development of this disease.

Although PPARα is up-regulated in endometrial carcinoma, proliferation was reduced by the addition of a PPARα-activating ligand. Conversely, apoptosis was markedly increased by a PPARα-activating ligand. We confirmed in reporter assays that addition of the same PPARα agonist was associated with an increase in PPARα activity. Therefore, increased apoptosis and reduction in DNA synthesis with fenofibrate administration are associated with an increase in PPARα activity. The downstream effectors that mediate these changes have not been identified. However, potential mechanisms include the generation of reactive oxygen species as a by-product of β-oxidation of fatty acids. PPARα regulates key enzymes within this metabolic pathway (25). We conclude therefore that aberrant function of the PPARα/RXR pathway occurs in endometrial carcinogenesis. Furthermore, we suggest that this pathway could potentially be targeted for therapeutic benefit. The underlying mechanism for the paradoxical effect of the PPARα agonist on cell growth is uncertain and warrants further investigation.

Endometrioid endometrial cancer is associated with obesity and metabolic abnormalities characterized by insulin resistance (2). Epidemiologic data suggest an association of dietary fat with increased endometrial cancer risk that may be independent of the association between increased fat intake and obesity (39). Earlier studies also revealed higher levels of sex hormone binding globulin in women eating a vegetarian diet (40), which could reduce the levels of free circulating estrogens. This raises the intriguing possibility of a link between fatty acid metabolism and the action of estrogens in endometrial cancer. There has been significant interest in the role of PPARs in metabolic disorders, although data on PPARs and lipid metabolism in endometrial cancer are scant. The data presented here suggest lipid metabolism and PPAR and RXR receptors as subjects for further study in endometrial cancer. PPARα activators are currently used for the treatment of hyperlipidemic disorders. The beneficial effects of a PPARα activator on the growth of endometrial cancer cells indicate that these drugs warrant further investigation as novel therapeutic options for the management of endometrial malignancy.

References

1. Rose PG. Endometrial carcinoma. N Engl J Med 1996;335:640–9.
2. Blake P, Lambert H, Crawford RAF. Molecular biology of gynecological cancer. In: Blake P, Lambert H, Crawford RAF, editors. Gynecological oncology. A guide to clinical management. Oxford: Oxford University Press; 1998. p. 137–52.
3. Golub TR, Slonim DK, Tamayo P, et al. Molecular classification of cancer: class discovery and class prediction by gene expression monitoring. Science 1999;286:531–7.
4. Khan J, Saal LH, Bittner ML, Chen Y, Trent JM, Meltzer PS. Expression profiling in cancer using cDNA microarrays. Electrophoresis 1999;20:223–9.
5. Dhanasekaran SM, Barrette TR, Ghosh D, et al. Delineation of prognostic biomarkers in prostate cancer. Nature 2001;412:822–6.
6. Beer DG, Kardia SL, Huang CC, et al. Gene-expression profiles predict survival of patients with lung adenocarcinoma. Nat Med 2002;8:816–24.
7. Duggan DJ, Bittner M, Chen Y, Meltzer P, Trent JM. Expression profiling using cDNA microarrays. Nat Genet 1999;21:10–4.
8. Brown PO, Botstein D. Exploring the new world of the genome with DNA microarrays. Nat Genet 1999;21:33–7.
9. Burgess JK. Gene expression studies using microarrays. Clin Exp Pharmacol Physiol 2001;28:321–8.
10. Bittner M, Meltzer P, Chen Y, et al. Molecular classification of cutaneous malignant melanoma by gene expression profiling. Nature 2000;406:536–40.
11. Nadon R, Shoemaker J. Statistical issues with microarrays: processing and analysis. Trends Genet 2002;18:265–71.
12. Smid-Koopman E, Blok LJ, Chadha-Ajwani S, Helmerhorst TJ, Brinkmann AO, Huikeshoven FJ. Gene expression profiles of human endometrial cancer samples using a cDNA-expression array technique: assessment of an analysis method. Br J Cancer 2000;83:246–51.
13. Matsushima-Nishiu M, Unoki M, Ono K, et al. Growth and gene expression profile analyses of endometrial cancer cells expressing exogenous PTEN. Cancer Res 2001;61:3741–9.
14. Martoglio AM, Tom BD, Starkey M, Corps AN, Charnock-Jones DS, Smith SK. Changes in tumorigenesis- and angiogenesis-related gene transcript abundance profiles in ovarian cancer detected by tailored high density cDNA arrays. Mol Med 2000;6:750–65.
15. Chomczynski P, Sacchi N. Single-step method of RNA isolation by acid guanidinium thiocyanate-phenol-chloroform extraction. Anal Biochem 1987;162:156–9.
16. Evans AL, Sharkey AS, Saidi SA, et al. Generation and use of a tailored gene array to investigate vascular biology. Angiogenesis 2003;6:93–104.
17. Ramdas L, Coombes KR, Baggerly K, et al. Sources of nonlinearity in cDNA microarray expression measurements. Genome Biol 2001;2:0047.1.
18. Colantuoni C, Henry G, Zeger S, Pevsner J. Local mean normalization of microarray element signal intensities across an array surface: quality control and correction of spatially systematic artifacts. Biotechniques 2002;32:1316–20.
19. Baldi P, Long AD. A Bayesian framework for the analysis of microarray expression data: regularized *t*-test and statistical inferences of gene changes. Bioinformatics 2001;17:509–19.
20. Saidi SA, Holland CM, Kreil DP, et al. Independent component analysis of microarray data in the study of endometrial cancer. Oncogene. In press 2004.
21. Kliewer SA, Umesono K, Noonan DJ, Heyman RA, Evans RM.

Convergence of 9-*cis* retinoic acid and peroxisome proliferator signaling pathways through heterodimer formation of their receptors. Nature 1992; 358:771 – 4.

22. Berger J, Moller DE. The mechanisms of action of PPARs. Annu Rev Med 2002;53:409 – 35.

23. Escher P, Wahli W. Peroxisome proliferator-activated receptors: insight into multiple cellular functions. Mutat Res 2000;448:121 – 38.

24. Braissant O, Wahli W. Differential expression of peroxisome proliferator-activated receptor-α, -β, and -γ during rat embryonic development. Endocrinology 1998;139:2748 – 54.

25. Corton JC, Anderson SP, Stauber A. Central role of peroxisome proliferator-activated receptors in the actions of peroxisome proliferators. Annu Rev Pharmacol Toxicol 2000;40:491 – 518.

26. Ledwith BJ, Pauley CJ, Wagner LK, Rokos CL, Alberts DW, Manam S. Induction of cyclooxygenase-2 expression by peroxisome proliferators and non-tetradecanoylphorbol 12,13-myristate-type tumor promoters in immortalized mouse liver cells. J Biol Chem 1997;272:3707 – 14.

27. Tong BJ, Tan J, Tajeda L, et al. Heightened expression of cyclooxygenase-2 and peroxisome proliferator-activated receptor-δ in human endometrial adenocarcinoma. Neoplasia 2000;2:483 – 90.

28. Fujiwaki R, Iida K, Kanasaki H, Ozaki T, Hata K, Miyazaki K. Cyclooxygenase-2 expression in endometrial cancer: correlation with microvessel count and expression of vascular endothelial growth factor and thymidine phosphorylase. Hum Pathol 2002;33:213 – 9.

29. Edwards JG, Faux SP, Plummer SM, et al. Cyclooxygenase-2 expression is a novel prognostic factor in malignant mesothelioma. Clin Cancer Res 2002;8:1857 – 62.

30. Ferrandina G, Lauriola L, Distefano MG, et al. Increased cyclooxygenase-2 expression is associated with chemotherapy resistance and poor survival in cervical cancer patients. J Clin Oncol 2002;20: 973 – 81.

31. Costa C, Soares R, Reis-Filho JS, Leitao D, Amendoeira I, Schmitt FC. Cyclo-oxygenase 2 expression is associated with angiogenesis and lymph node metastasis in human breast cancer. J Clin Pathol 2002;55: 429 – 34.

32. Eberhart CE, Coffey RJ, Radhika A, Giardiello FM, Ferrenbach S, DuBois RN. Up-regulation of cyclooxygenase 2 gene expression in human colorectal adenomas and adenocarcinomas. Gastroenterology 1994;107: 1183 – 8.

33. Sano H, Kawahito Y, Wilder RL, et al. Expression of cyclooxygenase-1 and -2 in human colorectal cancer. Cancer Res 1995;55:3785 – 9.

34. Kargman SL, O'Neill GP, Vickers PJ, Evans JF, Mancini JA, Jothy S. Expression of prostaglandin G/H synthase-1 and -2 protein in human colon cancer. Cancer Res 1995;55:2556 – 9.

35. Smalley WE, DuBois RN. Colorectal cancer and nonsteroidal anti-inflammatory drugs. Adv Pharmacol 1997;39:1 – 20.

36. Ota S, Bamba H, Kato A, Kawamoto C, Yoshida Y, Fujiwara K. Review article: COX-2, prostanoids and colon cancer. Aliment Pharmacol Ther 2002;16 Suppl 2:102 – 6.

37. Collett GP, Betts AM, Johnson MI, et al. Peroxisome proliferator-activated receptor α is an androgen-responsive gene in human prostate and is highly expressed in prostatic adenocarcinoma. Clin Cancer Res 2000;6:3241 – 8.

38. Fauconnet S, Lascombe I, Chabannes E, et al. Differential regulation of vascular endothelial growth factor expression by peroxisome proliferator-activated receptors in bladder cancer cells. J Biol Chem 2002;277: 23534 – 43.

39. Littman AJ, Beresford SAA, White E. The association of dietary fat and plant foods with endometrial cancer (United States). Cancer Causes & Control 2001;12:691 – 702.

40. Armstrong BK, Brown JB, Clarke HT, et al. J Natl Cancer Inst 1981; 67:761 – 7.

PUBLICATION 5

Schoenfeld, J., Lessan, K., Johnson, N., Charnock-Jones, D. S., **Evans, A. L**., Vourvouhaki, E., Scott, L., Stephens, R., Freeman, T., Saidi, S. A.*, et al.* 2004. Bioinformatic analysis of primary endothelial cell gene array data illustrated by the analysis of transcriptome changes in endothelial cells exposed to VEGF-A and PlGF. *Angiogenesis 7*, 143-156.

Cited by 20, Impact Factor 6.063

ISSN: 0969-6970

Journal Type

Angiogenesis is an international peer-reviewed journal devoted to the publication of original articles and reviews on the cellular and molecular mechanisms that regulate angiogenesis in physiological and pathological conditions. This journal publishes innovative experimental studies using molecular, in vitro, animal model systems and clinical investigations of angiogenic diseases. Angiogenesis also reports on novel therapeutic approaches for promoting or inhibiting angiogenesis as well as new markers and techniques for disease diagnosis and prognosis.

Personal Contribution

For this publication I performed Serial Analysis of Gene Expression SAGE as described in 2.1 of this work including sequencing and analysis of ditags.

Angiogenesis **7:** 143–156, 2004.

Bioinformatic analysis of primary endothelial cell gene array data illustrated by the analysis of transcriptome changes in endothelial cells exposed to VEGF-A and PlGF

Jonathan Schoenfeld[1], Khashayar Lessan[1], Nicola A. Johnson[1], D. Stephen Charnock-Jones[1], Amanda Evans [1], Ekaterini Vourvouhaki[1], Laurie Scott[2], Richard Stephens[2], Tom C. Freeman[2], Samir A. Saidi[1], Brian Tom[3], Gareth C. Weston[4], Peter Rogers[4], Stephen K. Smith[1] & Cristin G. Print[1]
[1]*Department of Pathology, Cambridge University, Cambridge, UK;* [2]*UK MRC Hinxton Genome Mapping Project Resource Centre, Hinxton. Cambridge, UK;* [3]*Medical Research Council Biostatistics Unit, Cambridge, UK;* [4]*Centre for Women's Health Research, Monash University, Department of Obstetrics and Gynaecology, Monash Medical Centre, Clayton, Victoria, Australia*

Received 19 March 2004; accepted in revised form 1 June 2004

Key words: bioinformatics, endothelial, gene array, PlGF, VEGF-A

Abstract

We recently published a review in this journal describing the design, hybridisation and basic data processing required to use gene arrays to investigate vascular biology (Evans et al. Angiogenesis 2003; 6: 93–104). Here, we build on this review by describing a set of powerful and robust methods for the analysis and interpretation of gene array data derived from primary vascular cell cultures. First, we describe the evaluation of transcriptome heterogeneity between primary cultures derived from different individuals, and estimation of the false discovery rate introduced by this heterogeneity and by experimental noise. Then, we discuss the appropriate use of Bayesian *t*-tests, clustering and independent component analysis to mine the data. We illustrate these principles by analysis of a previously unpublished set of gene array data in which human umbilical vein endothelial cells (HUVEC) cultured in either rich or low-serum media were exposed to vascular endothelial growth factor (VEGF)-A_{165} or placental growth factor (PlGF)-1_{131}. We have used Aymetrix U95A gene arrays to map the eects of these factors on the HUVEC transcriptome. These experiments followed a paired design and were biologically replicated three times. In addition, one experiment was repeated using serial analysis of gene expression (SAGE). In contrast to some previous studies, we found that VEGF-A and PlGF consistently regulated only small, non-overlapping and culture media-dependant sets of HUVEC transcripts, despite causing significant cell biological changes.

Abbreviations: ANOVA – analysis of variance; EC – endothelial cell(s); GEO – gene expression omnibus; HUVEC – human umbilical vein EC; ICA – independent component analysis; PlGF – placental growth factor; SAGE – serial analysis of gene expression; SAM – significance analysis of microarrays; VEGF – vascular endothelial growth factor

Introduction

The use of gene arrays has provided valuable information about the networks of molecular signals that regulate the biology and pathology of blood vessel walls. However, these studies often require the use of primary cultures of vessel wall cells derived from multiple individuals, with the associated problems of transcriptome heterogeneity and the idiosyncratic transcriptome response of each individual culture to treatment. Due to these problems, unless analysis is performed carefully, it is easy to be mislead by seemingly statistically 'significant' results that later cannot be repeated. While previous papers have addressed general issues in gene array design and data analysis [1, 2] none have addressed the specific issues that face investigators, such as vascular biologists, who need to use primary cell cultures. These issues include: (i) the need for biological replication using multiple cell cultures derived from different individuals; (ii) the need to evaluate transcriptome and phenotypic heterogeneity between the primary cultures used (iii) the need to judge gene array results against an estimate of the false discovery rate introduced by this heterogeneity and by experimental noise; and (iv) the correct use of techniques such as Bayesian *t*-tests, clustering and independent component analysis to extract meaningful data from biologically

Correspondence to: Dr Cristin Print, Department of Pathology, University of Cambridge, Tennis Court Rd, Cambridge CB2 1QP, UK. Tel: +44-1223-337733; Fax: +44-1223-333346; E-mail: cgp22@cam.ac.uk

replicated experiments. In this article, we attempt to illustrate these issues by taking the reader through the analysis of a previously unpublished set of Affymetrix gene array data. The background to this study and its design are described below.

Vascular endothelial growth factor (VEGF)-A is an EC growth and survival factor. It inhibits EC apoptosis and promotes proliferation *in vitro*, and it regulates vasculogenesis, angiogenesis, vascular remodeling and vascular permeability *in vivo*. The inactivation of a single copy of the mouse *VEGF-A* gene causes embryonic lethality [3, 4]. Therapy designed to alter the activity of the VEGF-A system is now used to treat several diseases including cancer [5, 6], coronary artery disease [7] and peripheral vascular disease [8]. VEGF-A activates intricate signaling networks in EC by binding to VEGFR-2 (Flk-1/KDR) and VEGFR-1 (Flt-1). VEGF-A signaling appears to be complex, since there is cross-talk [9] and heterodimerization [10] between VEGFR-1 and VEGFR-2. Placenta growth factor (PlGF) is a relative of VEGF-A that signals through VEGFR1 but not through VEGFR2 [11]. PlGF promotes angiogenesis and modulates VEGF-A signaling [10]. However, PlGF knock-out mice, unlike VEGF-A knock-out mice, survive with only a minor vascular phenotype that becomes more apparent under pathological conditions [9]. Several previous gene array studies have identified EC transcripts regulated by VEGF-A [12–18], receptor-specific *VEGF-A* mutants [10, 16] and PlGF [10]. These studies have each identified lists of VEGF- or PlGF-regulated transcripts. However, these lists only marginally overlap with one another. This lack of concordance presents difficulties – for example, it is not easy to hypothesise from these disparate results a set of candidate VEGF-regulated transcripts that warrant further biological and clinical investigation. The lack of concordance between these previous studies may in part reflect the different EC types and culture conditions used. However, the lack of concordance may also in some cases reflect inaccurate data generated by sub-optimal experimental design and analysis, since some of these studies used an unpaired design and contained very small numbers of biological replicates.

To illustrate robust methods for the analysis of gene array data from primary cell cultures, and to determine as definitively as possible whether VEGF-A and PlGF regulate large sets of transcripts in HUVEC, we have performed a three-fold biologically replicated paired-design Affymetrix gene array analysis of the effects of VEGF-A_{165} and PlGF-1_{131} on the transcriptome of human umbilical vein EC (HUVEC) cultured in either rich or low-serum media. We repeated one experiment in this study using a small-scale serial analysis of gene expression (SAGE), and confirmed a subset of our data using quantitative PCR. Our results showed that VEGF-A and PlGF consistently regulated only small, non-overlapping, and culture media-dependant sets of HUVEC transcripts, despite causing significant cell biological changes. This set of gene array data, in which only a few transcripts appear to be authentically regulated, is ideal to illustrate methods for analysing gene arrays derived from primary cells, and to illustrate the critical importance of biological replication and false discovery rate estimation.

Materials and methods

Cell culture and RNA collection

HUVEC were isolated from umbilical cords by collagenase digestion as described [19] and cultured to passage 5 using a rich medium which contained a proprietary mixture of heparin, hydrocortisone, epidermal growth factor, fibroblast growth factor and 2% foetal calf serum (large vessel EC medium; TCS, Buckingham, UK). In some cultures HUVEC were partially deprived of serum and growth factors using a low serum medium (basal EC medium {TCS} supplemented by 2% charcoal-stripped FCS only; Gibco/BRL, Maryland). Cells were cultured in these media in the presence or absence of 10 ng/ml human VEGF-A_{165} or 10 ng/ml carrier-free human PlGF-1_{131} (R&D Systems, Abingdon, UK). The collection of umbilical cords for HUVEC isolation was approved by the local ethical committee, and maternal consent was obtained in every case.

Assessment of cell biology

Total and apoptotic adherent HUVEC were enumerated in eight replicate wells in 48-well plates using an inverted epifluorescent relief-phase contrast microscope (Olympus OM40, marker; London, UK). Apoptotic cells were defined as those which excluded trypan blue (0.2%; Sigma, Gillingham, UK) and propidium iodine (20 μg/ml; Sigma), but which labeled with AnnexinV (Annexin V-Fluos staining kit used according to the manufacturer's instructions; Roche, UK) and also showed morphological characteristics of apoptosis (loss of adherence to substrate, shrinkage, membrane blebbing and nuclear condensation). In addition, relative viable cell numbers were estimated using a tetrazolium compound (MTS) assay (CellTiter 96 Aqueous Non-Radioactive Cell Proliferation Assay; Promega, Southampton, UK) used according to manufacturer's instructions.

Gene arrays

Total RNA was prepared using Trizol (Gibco/BRL) according to the manufacturer's instructions followed by passage through an RNeasy column (Qiagen, Crawley, UK). Biotin-labeled cRNA complex probes were prepared and hybridized to Affymetrix Human U95A gene-chips according to Affymetrix protocols (Affymetrix, London, UK). The quality of the expression data from the chips was assessed using Affymetrix Microarray Suite (version 5.0) and dChip software. Data from chips that failed these quality control tests was discarded. Transcript abundance data from all chips were globally and locally scaled [20]

using the 'Loess' function of the 'R' programming environment (http://rweb.stat.umn.edu/R/doc/html/index.html). Expression profiles were then compared using the CyberT algorithm (version 8.0; sliding window = 301; Bayes confidence estimate = 5 [21]). To assess false discovery rates Significance Analysis of Microarrays (SAM) software was used [22]. Independent component analysis was performed as described [23] using Matlab software. Mixed effects ANOVA analysis and clustering (by Ward's method to minimise the sum of squares using the 'Agnes' algorithm) was performed using the 'R' programming environment. Further graphical analysis was performed using GeneSpring Expression Analysis Software (Silicon Genetics, Redwood City, California). All data has been deposited in the NCBI Gene Expression Omnibus (GEO accession numbers GSM12894-GSM12926 as detailed in Table 2; http://www.ncbi.nlm.nih.gov/geo/).

Small-scale serial analysis of gene expression (SAGE) analysis

HUVEC were cultured as above under partial serum deprivation conditions with and without 10 ng/ml VEGF for 4 h. SAGE libraries were generated from 5 μg polyA + RNA following the SAGE protocol previously described [24]. Briefly, biotinylated Dynal bead-captured cDNAs were ligated to linkers that contained a recognition site for the tagging enzyme BsmF1 (NEB). SAGE tags were then released with BsmF1, blunt ended, and ligated head to head to form ditags. Ditags were released from linkers by Nla III digestion, concatenated and cloned into de-phosphorylated Sph I cut pGEM-3Zf+ (Promega Life Sciences), sequenced using the Applied Biosystems Prism Dye Terminator reaction kit and run on an ABI 373 automated sequencer (Applied Biosystems, Foster City, California). A total of 6698 di-tags were sequenced from untreated control cells and 5380 from VEGF-treated cells.

Quantitative PCR

The ABI PRISM 7700 Sequence Detection System (TaqMan) was used to perform real-time polymerase chain reactions according to the manufacturer's protocols. For all RNAs used in the Affymetrix study, the Ct values for each transcript were compared to those for *cyclophilin A*, which according to Affymetrix results remained relatively constant in abundance following serum deprivation and growth factor treatment. Primers and probe sets used to confirm transcripts regulated by VEGF-A were:

Tubby:

FORWARD	5′-CCCCCCAGGGTATCACCA-3′
REVERSE	5′-CCCCGGTCCATCCCTTT-3′
PROBE	FAM-5′-AAATGCCGCATCACTCGGGA-CAAT-3′-TAMRA;

PTP-1B:

FORWARD	5′-TGATCCAGACACAGCCGACCA-3′
REVERSE	5′-CCCATGATGAATTTGGCACC-3'
PROBE	FAM-5′-AAATGCCGCATCACTCGGGA-CAAT-3′-TAMRA;

RGS-3:

FORWARD	5′-GGCTGCTTCGACCTGGC-3′
REVERSE	5′-AAGCGAGGGTACGAGTCCTTT-3′
PROBE	FAM-5′-AGAAGCGCATCTTCGGGCTCA TGGT-3′-TAMRA;

CD34:

FORWARD	5′-CTGGATCAAAGTAGGCAGGAC C-3′
REVERSE	5′-TTTTTCGGAAGAGTACAGGTGA-GA-3′
PROBE	FAM-5′-TGGGACCAGGTCTTGGAGCT-GAGC-3′-TAMRA;

Thrombomodulin:

FORWARD	5′-CAGAGAGGCCTTTTGGAATGTG-3′
REVERSE	5′-TTCTAACCAGCTCCCATGGG-3′
PROBE	FAM-5′-CCCTGAACAAGAA-TTGGAAGC TGCCC-3′-TAMRA

Primers and probes used to confirm the PlGF-regulated transcripts *Musashi* (Probe Set 31396_r_at) and *Ephrin A2* (Probe Set 33090_at) were proprietary oligonucleotides obtained from Applied Biosystems 'Assays-on-Demand' and used a 5′ FAM reporter and 3′ non-fluorescent minor groove binder (MGB).

Results

The HUVEC transcriptome

To allow interpretation of the effects of VEGF-A and PlGF on the HUVEC transcriptome, we first determined the consensus transcriptome of untreated HUVEC cultures. To do this, RNA was extracted from passage five HUVEC cultures that were originally isolated from six different individuals and used to prepare complex cRNA probes, which were hybridized to 12,600-element (8900 unique transcript) Affymetrix gene arrays (U95A). The raw gene array data was normalized as described in the methods and in our previous review [20]. The most abundant 0.5% of HUVEC transcripts were clustered by function and are listed in Table 1.

We then assessed the heterogeneity of transcript abundance profiles in HUVEC cultures derived from the six different individuals, using simple arithmetic in Microsoft Excel. Substantial heterogeneity was found – between 25 and 30% of the 12,600 transcripts interrogated by the arrays differed in abundance between any 2 individuals by more than 36%, and between 2.6 and 4.7% of the 12,600 transcripts differed in abundance between any two individuals by more than 75%. To statistically quantify this heterogeneity we used analysis of variance (ANOVA) which confirmed that the overall transcriptomes of HUVEC from the different individuals varied significantly ($F = 3.4$;

Table 1. The 0.5% most abundant endothelial transcripts. *Signal* refers to normalized transcript abundance. *Probe set* denotes the Affymetrix probe set corresponding to each transcript.

Transcript	Signal	Probe set
G-PROTEIN SIGNALLING		
G-PROTEIN ALPHA SUBUNIT S	85.8	37449_i_at
RACK1	122.6	34608_at
CARBOHYDRATE METABOLISM		
ALDOLASE A	91.8	32336_at
PHOSPHOGLYCERATE MUTASE 1	87.2	41221_at
GAPDH	138.3	M33197_3_at
CYTOSKELETON		
BETA-TUBULIN	107.4	151_s_at
THYMOSIN BETA-4	119.7	31557_at
MYOSIN LIGHT CHAIN	87.8	33994_g_at
VIMENTIN	132.4	34091_s_at
GAMMA ACTIN 1	117.5	34160_at
BETA-ACTIN	164.6	X00351_M_at
RIBOSOMAL PROTEINS		
RIBOSOMAL PROTEIN S3A	83.8	1653_at
RIBOSOMAL PROTEIN L10	118.8	2016_s_at
RIBOSOMAL PROTEIN S19	93.5	31330_at
RIBOSOMAL PROTEIN L28	100.9	31385_at
RIBOSOMAL PROTEIN L8	99.9	31505_at
RIBOSOMAL PROTEIN S2	125.2	31527_at
RIBOSOMAL PROTEIN S18	97.3	31545_at
RIBOSOMAL PROTEIN S10	83.6	31568_at
RIBOSOMAL PROTEIN L3	93.6	31722_at
RIBOSOMAL PHOSPHOPROTEIN P1	90.3	31956_f_at
RIBOSOMAL PHOSPHOPROTEIN P1	111.1	31957_r_at
RIBOSOMAL PROTEIN L37A	125.8	31962_at
RIBOSOMAL PROTEIN L32	81.7	32276_at
RIBOSOMAL PROTEIN S11	87.7	32330_at
RIBOSOMAL PROTEIN S14	93.4	32412_at
RIBOSOMAL PROTEIN S5	87.2	32437_at
RIBOSOMAL PROTEIN S20	121.4	32438_at
RIBOSOMAL PROTEIN L41	121.9	32466_at
RIBOSOMAL PROTEIN S21	84.6	32744_at
RIBOSOMAL PROTEIN S12	99.6	33116_f_at
RIBOSOMAL PROTEIN L38	98.3	34085_at
RIBOSOMAL PROTEIN S17	109.0	34592_at
RIBOSOMAL PROTEIN S17	104.0	34593_g_at
RIBOSOMAL PROTEIN S4	90.2	34643_at
RIBOSOMAL PROTEIN S3	108.0	34645_at
RIBOSOMAL PROTEIN S28	99.0	347_s_at
RIBOSOMAL PROTEIN L13A	84.9	35119_at
MISCELLANEOUS		
LAMININ RECEPTOR (NON-INTEGRIN)	128.6	256_s_at
ANNEXIN A2 (LIPOCORT. II)	171.8	769_s_at
MIF	90.2	895_at
PLASMINOGEN ACTIVATOR INHIBITOR I	111.4	38125_at
ELONGATION FACTOR 1-ALPHA	148.6	1288_s_at
UBIQUITIN C	91.5	1367_f_at
ENOLASE 1	93.6	2035_s_at
POLYUBIQUITIN UBC	97.9	32334_f_at
BENZODIAZEPINE RECEPTOR	88.2	32806_at
CYCLOPHILIN A	97.0	33667_at
ELONGATION FACTOR 1-ALPHA	144.0	40887_g_at
ESTS		
EST AI535946	114.5	33412_at
EST AI541542	113.8	35278_at
EST U34995	172.4	35905_s_at

$F > 2.8$ implies $P < 0.05$). ANOVA tests are easily accessible within most commercial statistical software packages, and in the free 'R' statistical programming environment (http://rweb.stat.umn.edu/R/doc/html/index.html), which was used here.

Transcriptome heterogeneity data was then used to estimate the number of biological replicates (i.e., the number of repeated experiments using HUVEC from different individuals) that would be required for a robust transcriptome analysis of the effects of VEGF-A and PlGF on these cells. When any 2 of the 6 individual HUVEC cultures were compared using Microsoft Excel, we found that between 2.6 and 4.7% of the 12,600 transcripts differed by greater than 75% in abundance, as shown in Figure 1. However, when the *mean of any two* HUVEC cultures was compared to *the mean of any other two* HUVEC cultures only 0.9–1.6% of transcripts differed by greater than 75% in abundance. When *the mean of any three* HUVEC cultures was compared to *the mean of any other three* HUVEC cultures, only 0.1–0.4% of transcripts differed by greater than 75% in abundance. This analysis suggested to us that mean expression data obtained by biologically replicating each experiment three times would be much more useful than data from an un-replicate study. In addition, the non-linear nature of the curve that could be fitted to these results (Figure 1) suggested that additional biological replicates would provide diminishing returns.

Effect of VEGF-A and PlGF on EC biology

To confirm that VEGF-A and PlGF were active on HUVEC in the concentrations and culture conditions used in this study, and to catalogue the degree of heterogeneity in the response of biological replicates to VEGF-A and PlGF, we examined the effects of these factors on viable cell number and apoptosis incidence in HUVEC cultured in either rich or low serum media. While the incidence of apoptosis in HUVEC cultured in rich medium is low (1 to 2%), it is significantly elevated when these cells are cultured in low serum medium for 24 h (9 to 15%; [25]). Neither this serum deprivation-induced apoptosis nor total cell number was significantly altered by the addition to low serum media of 10 ng/ml VEGF-A_{165} for 4 h (ANOVA $P > 0.05$; data not shown). However, the addition to low serum media of either 10 ng/ml VEGF-A_{165} or 10 ng/ml PlGF-1_{131} for 24 h significantly reduced the incidence of apoptosis (ANOVA $P < 0.05$; Figures 2a and b) and significantly increased cell number (ANOVA $P < 0.05$; data not shown), indicating that 24 h incubation with either VEGF-A or PlGF can partially rescue serum-deprived HUVEC cultures from apoptosis. In HUVEC cultured in rich media, the addition to the media of 10 ng/ml VEGF-A_{165} for 24 h significantly reduced the already low incidence of apoptosis (ANOVA $P<0.05$; Figure 2C) and increased cell number (ANOVA $P < 0.05$; data not shown). Addition of 10 ng/ml PlGF-1_{131} to HUVEC cultured in rich media slightly reduced the apoptotic index (Figure 2d) and increased cell number, but these results were not statistically significant (ANOVA $P > 0.05$). Each experiment was conducted three times, each time using HUVEC isolated from a different individual. In an additional experiment, we found that the addition of either VEGF-A_{165} or PlGF-1_{131} to culture media were able to reduce the incidence of cell death in over-confluent HUVEC monolayers in a dose-dependant manner (Figure 2e–g). Taken together, these experiments confirmed that 10 ng/ml was a biologically eective concentration of both VEGF-A and PlGF in this culture system.

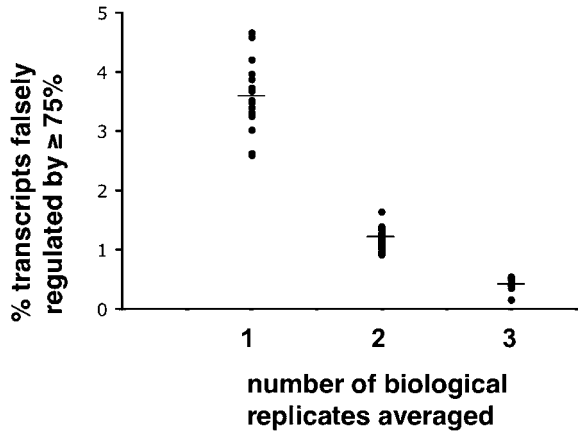

Figure 1. Biological replication. (A) The % of transcripts that appear to vary in abundance by >75% are shown when; the transcriptomes of single HUVEC cultures were compared to one another (*x*-axis = 1), when mean transcriptomes from any two biologically independent HUVEC cultures were compared to one another (*x*-axis = 2), or when mean transcriptomes from any three biologically independent HUVEC cultures were compared to one another (*x*-axis = 3).

Overall effects of VEGF-A and PlGF on the HUVEC transcriptome

Affymetrix U95A gene arrays were then used to catalogue transcript abundance changes in HUVEC in response to the following treatments (Table 2): (i) 10 ng/mL VEGF-A for 4 h in low serum medium; (ii) 10 ng/ml VEGF-A for 24 h in low serum medium, (iii) 10 ng/ml VEGF-A for 24 h in rich medium, (iv) 10 ng/ml PlGF for 24 h in low serum medium; and (v) 10 ng/ml PlGF for 24 h in rich medium. Each of these experiments was biologically replicated three times, each time using HUVEC isolated from a different individual. To minimise the confounding effects of the transcriptome heterogeneity between cultures described above, a paired design was used – i.e., for each biological replicate a passage 4 HUVEC culture was split into 2 flasks, the relevant growth factor was added to one flask and no treatment applied to the other.

Since each gene array experiment simultaneously investigates many thousands of transcripts, it is likely that some transcripts may falsely appear to have been regulated by growth factor treatment due to chance alone. Therefore, we assessed this 'false discovery rate' by applying *t*-tests to Affymetrix data derived from three randomly selected pairs of HUVEC cultures to which no experimental treatment had been given (i.e., a negative control experiment). As would be expected statistically, we found that approximately 1% of the 12,600 transcripts were, by chance, associated with *P*-values ≤ 0.01 (shown as 'negative control' in Figure 3).

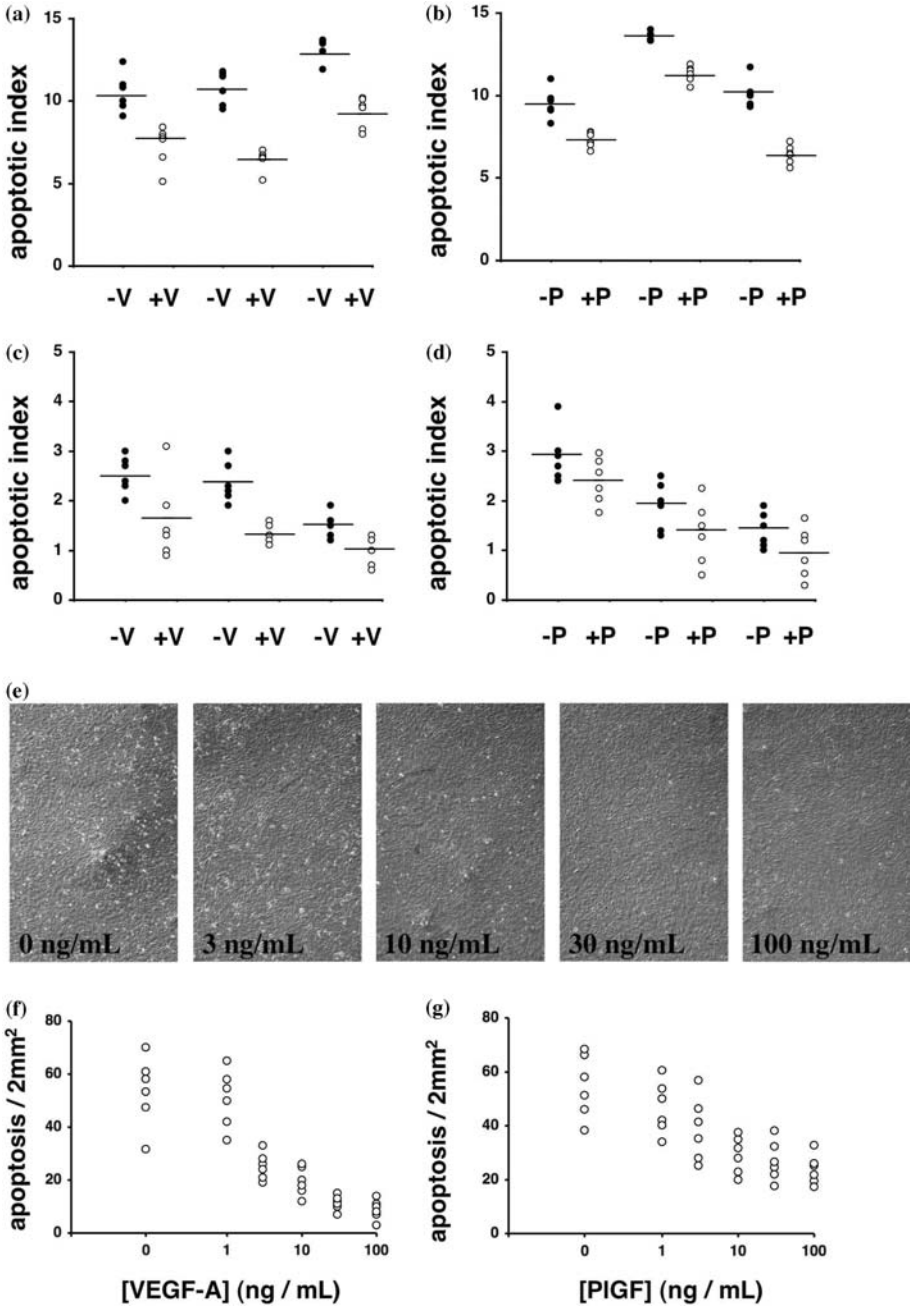

Figure 2. The cell biological effects of VEGF-A and PlGF-1. Three isolates of HUVEC were cultured in low serum media (a and b) or in rich media (c and d) for 24 h and then cultured for a further 24 h with; no additional treatment (solid circles), 10 ng/ml VEGF-A (a and c, hollow circles) or 10 ng/ml PlGF (b and d, hollow circles). Horizontal bars represent mean apoptotic index. (E) When HUVEC cultured in rich medium were allowed to become over-confluent for 24 h, cells with an apoptotic morphology became visible on the surface of the monolayer. Incubation with VEGF-A for 24 h reduced the number of these dying cells in a dose-dependant manner. The number of apoptotic cells adhering to the surface of the confluent monolayers following VEGF-A or PlGF (1, 3, 10, 30 or 100 ng/ml) incubation for 24 h is shown in panels (f) and (g).

The *t*-tests were performed through the web using the freely available the CyberT algorithm. This is a modified *t*-test optimised to generate accurate *t*-statistics for gene array data (in which there are usually many independent observations but relatively few replicates) by the incorporation of a Baysian prior based on the variance of transcripts with related expression levels (CyberT; http://visitor.ics.uci.edu/genex/cybert/) [21].

Next, we examined the effect of 4 hr incubation with 10 ng/ml VEGF-A_{165} on the transcriptome of HUVEC cultured in low serum medium. We analysed RNAs from this experiment using both Aymetrix arrays and SAGE. The Aymetrix analaysis showed that the number of transcripts associated with *P*-values ≤ 0.01 was approximately equal to the number obtained in the negative control experiment presented above and to the number expected by chance (1%), suggesting that only very small numbers of transcripts were authentically regulated in this experiment. SAGE analysis has recently been correlated with gene array analysis to detect differences between the transcriptomes

Table 2. Summary of experimental design. The design of the five experiments analysed in this report is described in this table. Data for each experiment can be retrieved from the GEO database (http://www.ncbi.nlm.nih.gov/geo/) using the accession numbers shown.

Experiment	HUVEC culture media	Treatment	Duration of treatment	GEO accession numbers for normalised array results
A	Rich medium	10 ng/ml VEGF-A	24 h	GSM12894-vs-GSM12895 GSM12896-vs-GSM12897 GSM12898-vs-GSM12899
B	Low serum medium	10 ng/ml VEGF-A	4 h	GSM12900-vs-GSM12901 GSM12902-vs-GSM12903 GSM12904-vs-GSM12905
C	Low serum medium	10 ng/ml VEGF-A	24 h	GSM12906-vs-GSM12907 GSM12908-vs-GSM12909 GSM12910-vs-GSM12911
D	Rich medium	10 ng/ml PlGF-1	24 h	GSM12912-vs-GSM12913 GSM12914-vs-GSM12915 GSM12916-vs-GSM12917
E	Low serum medium	10 ng/ml PlGF-1	24 h	GSM12918-vs-GSM12926 GSM12919-vs-GSM12920 GSM12921-vs-GSM12922

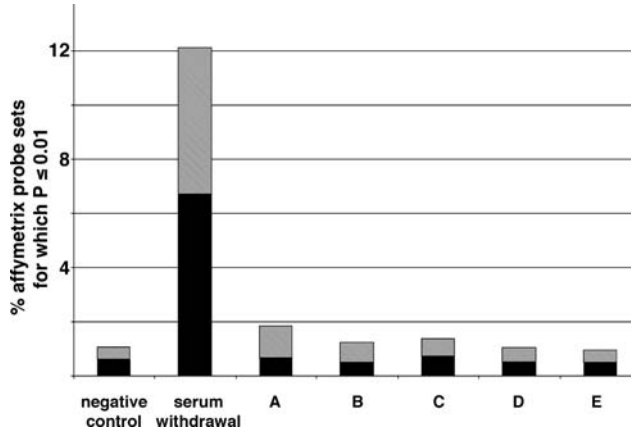

Figure 3. Percentage of total Affymetrix probe sets for which Baysian *t*-test $P < 0.01$. 'Negative control' represents the comparison between two groups, each containing data from three un-treated rich media HUVEC cultures derived from different individuals. 'Serum withdrawal' (a positive control) represents the comparison of three HUVEC cultures grown in rich media with three HUVEC cultures isolated from the same individuals but grown in low serum media. Treatments are; A, 24 h 10 ng/ml VEGF-A in rich medium; (B) 4 h 10 ng/ml VEGF-A in low serum medium; (C) 24 h 10 ng/ml VEGF-A in low serum medium; (D) 24 h 10 ng/ml PlGF-1 in rich medium; (E) 24 h 10 ng/ml PlGF-1 in low serum medium. Hatched bars represent transcript up-regulation by treatment, solid bars down-regulation.

of EC derived from different vascular sources [26]. We performed a small-scale (approximately 5400 paired di-tags) SAGE analysis on HUVEC cultured in low serum medium with and without incubation with 10 ng/ml VEGF-A for 4 h. Many of the most abundant 0.5% of transcripts identified by our SAGE analysis of untreated HUVEC were also identified in this previous study [26], and were among the most abundant 1% of transcripts identified by our corresponding Affymetrix analysis (Figure 4). However, SAGE indicated that none of these abundant transcripts was regulated by 4 h VEGF-A incubation (Figure 4). Due to the labour intensive nature of SAGE, additional biological replicates could not be performed.

We then examined the effect of 24 h incubation with 10 ng/ml VEGF-A_{165} on the transcriptome of HUVEC cultured in low serum medium. Again, the gene array analaysis showed that the number of transcripts associated with *P*-values ≤ 0.01 was approximately equal to the number expected by chance alone (1%). However, when we examined the effect of 24 h incubation with 10 ng/ml VEGF-A_{165} on the transcriptome of HUVEC cultured in rich medium, approximately 2% of the 12,600 transcripts

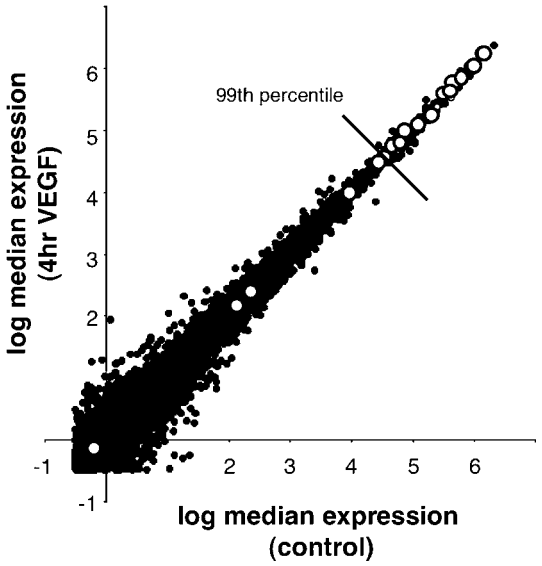

Figure 4. SAGE identifies the same abundant endothelial cell transcripts as Aymetrix analysis. A scatterplot is shown of $\log_2$ transcript abundance in HUVEC cultured in low serum media with (*y*-axis) or without (*x*-axis) 10 ng/ml VEGF-A for 4 h. Overlaid white circles show the position in the Affymetrix dataset of the most abundant 0.5% of transcripts detected by SAGE. The diagonal line marks the 99th percentile of the Affymetrix experiments.

were associated with P-values ≤ 0.01 (Figure 3) – i.e., approximately twice as many transcripts appeared to be regulated than would be expected by chance. When we investigated the effect of 24 h incubation with 10 ng/ml PlGF-1_{131} on the transcriptome of HUVEC cultured in either rich or low serum medium, no more transcripts were associated with P-values ≤ 0.01 than would be expected by chance alone (1%), suggesting that PlGF regulated few if any transcripts in either culture condition. To put these numbers into context, when the transcriptomes of three cultures of HUVEC in rich media were compared to the transcriptomes of three cultures of HUVEC in low serum media derived from the same individuals, the proportion of transcripts associated with P-values ≤ 0.01 was over 12% (Figure 3). This implies that the extent of transcript abundance regulation induced by VEGF-A or PlGF in the conditions used in this study is much less than that induced by transfer of these cells from rich to low serum media.

We then used the freely available SAM software [22] (http://www-stat.stanford.edu/~tibs/SAM/) as an alternative estimate of the false discovery rate for each experiment in our study. SAM is used as an 'add-in' package for Microsoft Excel. The results of this method concurred closely with the t-test results described above. SAM indicated that we should expect a false discovery rate of 4.5 transcripts for every 10 that appeared to be regulated by 24 h VEGF-A treatment of HUVEC cultured in rich medium. In contrast, SAM indicated that we should expect incubation of HUVEC cultured in low serum media with VEGF-A for 24 h, or incubation of HUVEC cultured in either rich or low serum media with PlGF for 24 h to produce a false discovery rate of 8 to 10 transcripts for every 10 that appeared to be regulated. To put these results in perspective, SAM indicated that we should expect a false discovery rate of only 0.9 transcripts for every 10 that appeared to be regulated by the transfer of HUVEC from rich to low serum media.

Multi-way ANOVA was performed using the 'R' statistical environment. It also concurred with the results described above. It showed that 24 h incubation with 10 ng/ml VEGF-A caused a small but significant alteration to the overall pattern of transcript abundance in HUVEC cultured in rich media ($F = 5.3$; $F > 3.9$ implies $P < 0.05$). However, incubation of HUVEC cultured in low serum media with VEGF-A for 4 or 24 h, or incubation of HUVEC cultured in either rich or low serum media with PlGF for 24 h, did not have any significant overall effect on the HUVEC transcriptome ($F < 3.9$ in each case).

In a further attempt to detect subtle HUVEC transcriptome changes associated with VEGF-A and PlGF treatment, independent component analysis (ICA) was used. ICA is a neural network (ensemble learning)-based method useful for analysis of noisy gene array data that can remove the effects of noise and identify sets of linearly co-regulated transcripts (which are referred to as 'components') [23]. We have previously found that ICA readily detected components in HUVEC associated with survival factor deprivation [23], anti-apoptotic transgene expression and treatment with cocktails of cytokines and growth factors (our unpublished data). However, when ICA was applied to the un-normalised data from the experiments performed here, no components associated with VEGF-A or PlGF treatment were detected. However a component related to the culture of the cells in rich media vs. low serum media was readily detected (component 8, Figure 5a). The transcripts that contributed most strongly to this component were those that we have previously described as being regulated in HUVEC by the transfer of HUVEC from rich to low serum media [25]. The detection of a component associated with the transfer of HUVEC from rich to low serum media, but not of components associated with exposure to VEGF-A or PlGF is not surprising, given the large number of transcripts regulated by the transfer of HUVEC from rich to low serum media (12%) compared to the small number regulated by either VEGF-A or PlGF (1 to 2%), as described above. Additional meaningful components were inferred by ICA. These associated with normalisation artifacts (component 4) and experiments performed by a particular investigator (KL) (component 27). We have found that ICA is more powerful than other techniques such as principal component Analysis (PCA) [23]. Since current versions of ICA require programming skills to use, this technique is not readily available to all laboratories. However, we hope that an easy-to-use version of ICA may be freely available soon, and ICA is currently available by collaboration with our laboratory and others.

Cluster analysis (the grouping of arrays into similar clusters) is another useful method to search for patterns hidden within gene array data. Cluster analysis is available in most commercial gene array analysis packages such as GeneSpring (Silicon Genetics), in addition to statistical programming environments such as 'R'. Here we have used 'R' to perform Ward's method clustering (an agglomerative clustering method that seeks to minimise the sum of squares between clustered arrays). As with ICA, Ward's clustering failed to detect any transcript clusters specific to VEGF-A or PlGF treatment. However, it readily clustered the arrays from HUVEC cultured in low serum and rich media into two distinct groups (Figure 5b).

Effects of VEGF-A and PlGF treatment on individual HUVEC transcripts

It is important to identify the most significantly regulated individual transcripts for further analysis. Here we have done this by using Microsoft Excel to apply a set of four criteria to all 12,600 transcripts investigated in each experiment: (i) Bayesian t-test (cyberT) comparing abundance of the transcript in the three control and treated cultures indicated $P < 0.01$; (ii) the transcript showed a greater than two-fold average regulation between the control and treated cultures; (iii) the direction of regulation between the control and treated cultures was the same in

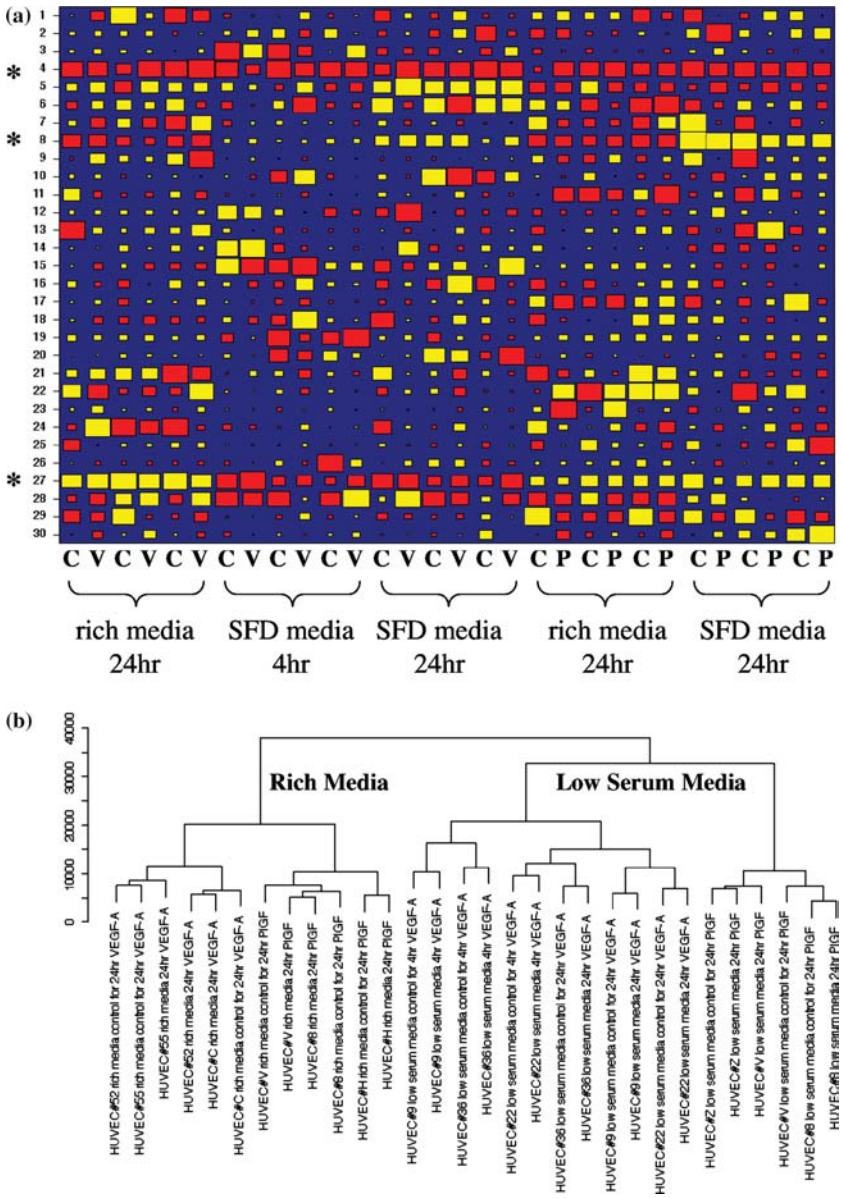

Figure 5. (a) Hinton plot. Independent component analysis (ICA) identified several biologically or experimentally meaningful components (*). These were associated with; survival factor-deprivation (component 8), normalisation effects (component 4), and experiments performed by a particular investigator (KL) (component 27). The area of each square is proportional to the magnitude of the contribution of each genechip to each component. Positive values are shown in yellow; negative values, in red. (b) Clustering. Ward's method clustering grouped the arrays into those representing HUVEC cultured in rich or low serum media. However, no consistent clustering was obtained that corresponded to the effects of VEGF-A or PlGF. The scale on the left of the dendrogram represents the degree of similarity of the clusters.

each of the three replicate cultures; (iv) the Affymetrix analysis software (MAS 5.0) indicated that the transcript was expressed above the noise in at least one cultures from each control and treated pair. Transcripts identified by this approach in HUVEC cultured in rich medium treated with VEGF-A for 24 h are listed in Table 3 and are discussed below. Our results suggested that the remaining experimental treatments regulated no more transcripts that would be expected by chance alone. This suggests that the chances of false discovery in these experiments are very high indeed, however, it does not of course rule out the authentic up- or down-regulation of a very small number of individual transcripts in each of these experiments. Indeed, this appears to be the case. Quantitative RT-PCR (TaqMan) was used to verify the regulation of a small number of individual transcripts for each experiment. These transcripts including; the transcription factor '*tubby*', *protein tyrosine phosphatase-1B* (*PTP1B*), *regulator of G-protein signaling-3 (RGPB3)*, *Thrombomodulin*, *CD34*, *Musashi* and *EphrinA2*. For these transcripts, VEGF-A and PlGF-induced changes in transcript abundance were consistent in direction between the Affymetrix arrays and quantitative RT-PCR, except for *Musashi*, which showed concordant regulation in only one out of the three PlGF-treated HUVEC cultured in rich media replicates (Figure 6).

Table 3. Transcripts regulated in HUVEC cultured in rich medium by 24 h incubation with 10 ng/ml VEGF-A. FC denotes average fold change.

Transcripts regulated in HUVEC cultured in rich medium by incubation with VEGF-A for 24 h			
Probe set	Transcript	FC	CyberT *P*-value
	Receptors		
33803_at	Thrombomodulin	3.6	5.88E-07
38747_at	CD34	2.2	3.23E-05
34235_at	G-protein coupled receptor-116	2.3	4.89E-05
1608_at	HGF receptor	5.3	7.97E-05
32114_s_at	Adenosine-A2 receptor	2.2	4.43E-03
836_at	Patched	3.1	4.88E-03
	Secreted factors		
37013_at	Angiotensin Converting Enzyme-1	2.1	8.08E-05
1003_s_at	B cell-attracting chemokine-1	−3.1	8.09E-03
33534_at	Endothelial cell-specific molecule-1	2.6	1.12E-04
209_at	Neuregulin-1	−4.0	1.50E-04
41354_at	Stanniocalcin-1	3.3	7.46E-04
	Signaling molecules		
37785_at	RHO-6	2.2	5.99E-04
39318_at	T-cell lymphoma-1	3.0	2.01E-03
32979_at	Grb2-associated-1	2.5	4.43E-03
36008_at	Phosphatase IVA-3	2.2	3.63E-04
	Adhesion & Cytoskeleton		
356_at	Kinesin-22	−3.2	5.05E-04
753_at	Osteonidogen	2.5	3.09E-04
39504_at	Connexin-46	2.9	1.50E-03
	Transcription factors		
37710_at	MADS box enhancer factor-2	2.6	5.61E-04
33484_at	Ring finger protein 2	2.1	6.86E-04
40448_at	Zinc finger protein-36	2.2	6.96E-04
40483_at	*Transcriptional activator of the c-fos promoter*	4.8	3.01E-04
204_at	HOX-A4	−2.7	3.85E-03
39909_g_at	PCAF associated factor-65a	−2.4	5.58E-03
31698_at	Forkhead-14	−2.1	7.61E-03
	Miscellaneous		
41767_r_at	Golgin-67	2.5	1.25E-03
33902_at	L-glycerol-3-phosphate-NAD oxidoreductase	−2.6	8.90E-03
	ETSs		
41494_at	EST X99802	2.4	8.27E-03
	Retinoic acid-inducible retroviral		
1090_f_at	DNA	−3.3	2.49E-03
	Down syndrome critical region gene		
32076_at	1-like-1	2.6	9.12E-04
37178_at	EST BC017169	2.7	7.27E-04
36727_at	EST M64936	−2.1	1.28E-03
39501_f_at	EST W28566	−2.7	2.92E-03

The transcriptome response of HUVEC to low serum media was partially reversed when the cultures were rescued from apoptosis by 24 h incubation with VEGF-A

It seemed possible that the transcriptome changes induced by transferring HUVEC from rich media into low serum media may be partly reversed when VEGF-A or PlGF was used to rescue the low serum media cultures from apoptosis. To test this hypothesis, we used GeneSpring software to display (Figure 7) linked scatterplots that showed; (column A) the effect of transferring HUVEC from rich media into low serum media and (column B) the effect of exposing HUVEC cultures in low serum media to VEGF-A for 24 h. Transcripts highlighted in the plots in column A are also highlighted automatically in the corresponding plots in column B. This simple analysis showed that transcripts that were not up- or down-regulated > two-fold when HUVEC were transferred form rich to low serum media did not appear to be regulated in any particular manner when HUVEC cultured in low serum media were incubated with VEGF-A for 24 h. However, transcripts that were up- or down-regulated > two-fold when HUVEC were transferred from rich to low serum media appeared on average to be regulated a small amount in the opposite direction when HUVEC cultured in low serum media were incubated with VEGF-A for 24 h. While most of these reciprocal changes were small, they may nevertheless together represent a biologically important partial reversal of the transcriptome changes induced by transferring HUVEC from rich media into low serum media. These results are shown graphically in histograms of fold change in Figure 7C (left panel). Incubation with VEGF-A for only 4 h was unable to induce the same reciprocal changes in transcript abundance (Figure 7C, right panel).

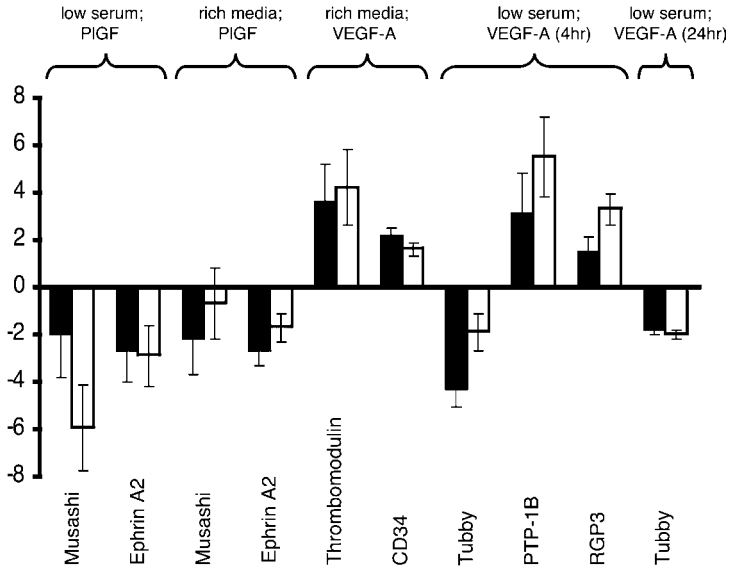

Figure 6. Quantitative PCR (TaqMAN) confirms the regulation of subset of transcripts. Black bars represent mean fold changes ($n = 3$ biological replicates) indicated by Affymetrix arrays, and open bars mean fold changes indicated by TaqMAN quantitative RT-PCR. Error bars denote standard deviations. The experimental conditions are shown above the graph. PTP-1B denotes protein tyrosine phosphatase–1B, RGP3 denotes regulator of G-protein signaling-3.

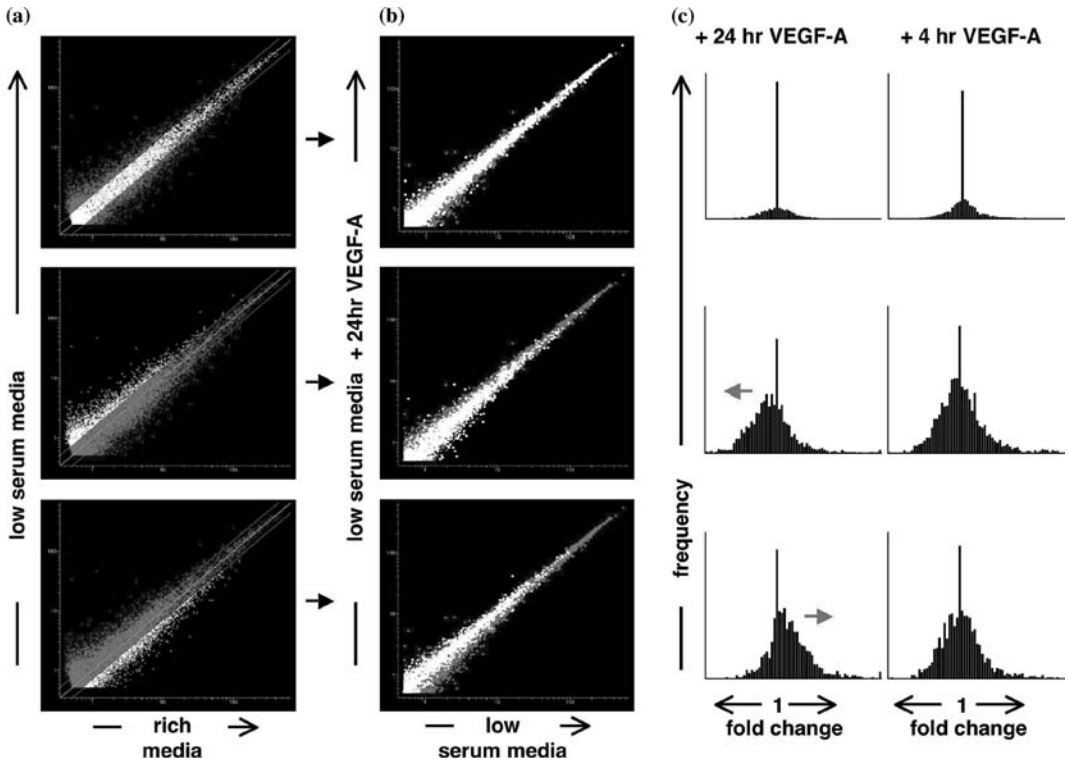

Figure 7. The transcriptome effects of transferring HUVEC from rich to low serum media are partially reversed by 24 h incubation with VEGF-A. The scatterplots in column A compare HUVEC cultured in rich media (horizontal axis) with HUVEC cultured in low serum media (vertical axis). The scatterplots in column B compare HUVEC cultured in low serum media (horizontal axis) with HUVEC cultured in low serum media with the addition of 10 ng/ml VEGF-A for 24 h (vertical axis). Transcripts highlighted in the plots in column A are automatically highlighted in the corresponding plots in column B. The top scatter-plots show those transcripts which were not up- or down-regulated > 2-fold when HUVEC were transferred from rich to low serum media. The middle and bottom scatter-plots show transcripts that were up- or down-regulated > 2-fold, respectively, when HUVEC were transferred from rich to low serum media. These transcripts are on average reciprocally regulated by a small amount when HUVEC cultured in low serum media are incubated with VEGF-A for 24 h. This is evident by the small shift up or down of groups of white highlighted transcripts in column B. Histograms of fold change (the left hand panel of column C) show these effects clearly. However, when HUVEC cultured in low serum media are incubated with 10 ng/ml VEGF-A for only 4hrs, no shift in the histograms is observed (the right hand panel of column C).

HUVEC derived from different individuals mount heterogeneous transcriptional responses to VEGF-A

As discussed above, the resting transcriptomes of HUVEC derived from different individuals differed substantially. To assess whether the *response* of HUVEC derived from different individuals to VEGF-A was heterogeneous, we used ANOVA. We found that the statistical 'interaction' between the effect of VEGF-A treatment and the effect of the individuals from whom the HUVEC were isolated was significant ($F = 4.4$ for HUVEC cultured in rich media and $F = 4.9$ for HUVEC cultured in low serum media; $F > 2.4$ implies $P < 0.05$), implying that HUVEC isolated from the different individuals respond differently to VEGF-A. These heterogeneous responses to VEGF-A may be due to differences dictated by the individuals from whom the HUVEC were isolated, and/or to random experimental factors. To assess the importance of differences dictated by the individuals from whom the HUVEC were isolated, we tested whether two duplicate HUVEC cultures isolated from the same individual (and cultured at different times from duplicate frozen vials) varied between one another in their transcriptional responses to VEGF-A to the same degree as any two HUVEC cultures derived from different individuals. Between any two unrelated cultures, 25 to 39% (average 29%) of transcripts exhibited > 1.5-fold variability in response to VEGF-A. However, between the two HUVEC cultures isolated from the same individual, only 15% of transcripts exhibited > 1.5-fold variability in response to VEGF-A. This suggested that the individuals from whom HUVEC were derived directly influenced VEGF-induced transcriptional responses.

Discussion

Technical aspects of data analysis

In this report we have used a previously unpublished set of experiments in HUVEC to illustrate the process of analysing gene array data derived from primary cultured cells. We found that, as we have previously reported [25], the transition from rich to low serum media induced repeatable and substantial transcriptome change in HUVEC. The number of transcripts regulated represented approximately 10 times the expected false discovery rate (determined either by comparing experimental *t*-test results to the *t*-test results of a negative control experiment and by SAM software). The effect of transition from rich to low serum media on the overall pattern of transcript abundance was also readily detected by ANOVA, Ward's method clustering and ICA.

In contrast, the effect of exposure to VEGF-A for 24 h on HUVEC cultured in rich media was more subtle, regulating only twice the number of transcripts that we expected by regulated due to chance alone (twice the false discovery rate). Although these transcriptome changes were detected by ANOVA, they were too subtle to be detected by Ward's method clustering or ICA.

The effect of VEGF-A on HUVEC cultured in low serum media, or of PlGF on HUVEC cultured in either rich or low serum media, was even more subtle, since the number of transcripts that appeared to be regulated in these experiments was no greater than the number we expected to appear to be regulated due to chance alone. These experiments carried a high risk of false discovery, and therefore must be treated with caution until validated by other means such as the quantitative RT-PCR shown in Figure 6.

If biological replication and false discovery rate analysis had not been performed, we would not have become aware of the high chance of false discovery in the experiments described above. The importance of biological replication is further supported by the statistically significant differences in the transcriptome responses to VEGF-A of HUVEC isolated from different patients. For example, ANOVA indicated that the transcriptome responses of HUVEC to VEGF-A differed between individuals. This result was confirmed by analyzing the effect of VEGF-A on the transcriptomes of duplicate batches of HUVEC derived from the same individual. This data suggests that paired design experiments (in which each biological replicate culture is split into two flasks and a treatment applied to one flask but not the other) may be much more sensitive than unpaired design experiments. The subtle effects of VEGF-A on HUVEC cultured in rich media may not have been detected if a paired design had not been used. While a set of 'single colour' array experiments have been use to illustrate these principles, they apply equally to 'two-colour' experiments, especially when one 'colour' is always used for a pooled common control.

The cohorts of VEGF-regulated EC transcripts identified by previous studies [12–18] only marginally overlap with one another. Only a few of these previously identified transcripts appeared to be regulated by VEGF-A in HUVEC cultured in rich medium in our study (e.g., *Thrombomodulin* [16], *Ademosine A2 receptor* [16], *Phosphatase IVA3* [16], and *Osteonidogen* [15]). This inconsistency may be largely explained by the different culture conditions (e.g., rich or low serum media), EC types, timing and gene array platforms used in each study. However, it is possible that in addition, some of these previous studies have overestimated the number of VEGF-regulated transcripts due to their sub-optimal biological replication, lack of false discovery rate analysis and/or unpaired designs. This would account for both the large numbers of 'regulated' transcripts and their apparent inconsistency.

Previous studies using *non-gene array* techniques have also identified a number of VEGF-regulated EC transcripts including; *tissue factor* (*thromboplastin* [27]), *intercellular adhesion molecule* (ICAM)-1 [28], plasminogen activators (*uPA* and *tPA*) and *plasminogen activator-inhibitor-1* [29], *interstitial collagenase* [30], *Bcl-2* and *A1* [31]. In general, these results are not reproduced in the published gene array studies of VEGF-mediated transcriptome regulation [12–18] or by our own study. The different experimental conditions used in these various studies may in part explain this inconsistency. However, the relative insensitivity of gene array techniques may also play a role. For example, *Bcl-2*,

ICAM-1 and *tissue factor* were expressed below the threshold for reliable comparisons in our data. Interestingly, the expression of *tissue factor*, which is widely recognised as a VEGF-responsive transcript, was in fact up-regulated 5.7-fold (gene ID *36543_at*) in HUVEC cultured in rich media following 24 h incubation with 10 ng/mlVEGF-A. However, since its expression level, even after up-regulation, was is the lowest 2% of the transcripts interrogated by the arrays and was on a par with the level of noise, it would be unwise to over-interpret this result.

Biological insights provided by these experiments

We catalogued the most abundantly expressed transcripts in HUVEC. These encoded cytoskeletal elements and their regulators, ribosomal proteins, enzymes involved in carbohydrate metabolism, members of the ubiquitin system, and proteins involved in various forms of signaling (Table 1), and overlap substantially with abundant HUVEC transcripts identified previously [26]. Many of these abundant transcripts encode proteins that perform essential functions in diverse cell types and are not EC-specific. Presumably, the synergistic combination of transcripts expressed at lower levels in EC, rather than the most abundant EC transcripts, specifies unique EC structure and function.

Our study then assessed the cell biological changes induced in HUVEC by VEGF-A and PlGF. This showed that both factors were biologically active in the concentrations and conditions used in this study. The cell biological effects of VEGF-A were more pronounced in HUVEC cultured in low serum media than in HUVEC cultured in rich media – perhaps due to VEGF-A's inability to further alter the already low incidence of apoptosis and the already high incidence proliferation of optimally-cultured cells. PlGF also had measurable effects on HUVEC biology, although the magnitude of these effects on HUVEC cultured in low serum media was not as great as the effect of VEGF-A.

We then related these cell-biological responses to transcriptome responses. We found that the most significant VEGF-induced transcriptome changes were in HUVEC cultured in rich media. These are likely to contribute to VEGF-induced proliferation and survival. They include (listed in Table 3): (i) membrane proteins; *patched* (↑3.1x, a receptor for the pro-angiogenic factor sonic hedgehog); *thrombomodulin* (↑3.6x, an EC surface glycoprotein involved in thrombin activation); *CD34* (↑2.2x, a sialomucin that appears to be involved in stem cell activity); *G-protein-coupled receptor-116* (↑2.3x) and the *hepatocyte growth factor receptor* (↑5.2x, pro-angiogenic); (ii) miscellaneous proteins and enzymes; *angiotensin converting enzyme-1* (↑2.1x, involved in the regulation of blood-pressure); *EC-specific molecule-1* (↑2.6x, a cytokine induced endothelial protein of unknown function) and *stanniocalcin-1* (↑3.3x); (iii) adhesion and cytoskeletal-associated molecules; *Nidogen-2* (↑2.5x, a basement membrane component), *Catenin* α 2 (↓4.0x) and *Connexin-46* (↑2.9x, a gap junction protein). (iv) cytoplasmic signaling molecules; *Tyrosine Phosphatase IVA-3* (↑2.2x, regulates AT II-mediated calcium signaling and promotes proliferation in other cell types), *TCL-1* (↑3.0x, an activator of AKT and therefore a potential promoter of cell survival) and *FK506 binding protein-1B* (↓3.2x). DNA-binding proteins/transcription factors; *Zinc finger protein-36* (↑2.2x, a component of a negative feedback loop that interferes with TNF-α production by destabilizing its mRNA); *HOX-14* (↓2.7x) and *CROC-4* (↑4.8x); (v) Several EST.

The relative lack of transcriptome responses to VEGF-A and PlGF, despite significant cell-biological responses, suggests that post-transcriptional mechanisms, rather than regulation of transcript abundance, may be largely responsible for the effects of these factors on HUVEC cultured as they were here. The different transcriptome responses to VEGF-A of HUVEC cultured in rich and low serum media is especially intriguing. Our gene array data suggests that altered abundance in cells cultured in low serum media of RNAs encoding transcription factors may in-part underlie this result. For example, in HUVEC cultured in low serum media NF-κB function appears to be reduced, in part due to the up-regulation of transcripts encoding the NF-κB inhibitors IκBα, IκBα, IκBε, RelB and p100 [25]. Previous studies have suggested that NF-κB plays an important role in the transcriptome responses of EC to VEGF-A [32, 33]. Several other transcription factors are also up- or down-regulated more than two-fold when HUVEC are transferred from rich to low serum media [25], including; hnRNP-U (↓9.8x, involved in pre-mRNA processing), Gu (also ↓9.8x, a helicase involved in several aspects of RNA editing and folding), DEK (↓2.9x, involved in pre-MRNA splicing), JunD (↑2.1x), HSF4 (↑2.0x, suppresses heat shock protein translation) and a further 26 transcription factors.

In conclusion, we have used a set of previously unpublished Affymetrix gene array experiments to lead the reader through the analysis of gene array data derived from primary cells. We have demonstrated the critical importance of biological replication and false discovery rate estimation and the value of a paired experimental design. We have demonstrated the use of ANOVA, false discovery rate analysis software, Baysian *t*-tests, clustering and independent component analysis to extract robust and meaningful conclusions from the raw data. The experiments we have analysed have shown that while the transfer of HUVEC from rich to low serum media regulates a substantial number of transcripts, VEGF-A and PlGF regulated only small numbers of transcripts. The regulation of transcripts by VEGF-A appeared to depend upon the media in which the cells were cultured – we suggest one explanation for this phenomenon based on the culture media-dependent abundance of transcripts encoding transcription factors. We also suggest that some previous gene array studies that have not been optimally designed and analysed may have overestimated the number of transcripts regulated by VEGF-A.

Acknowledgements

We wish to thank Dr Andrew Sharkey for advice about gene array analysis, Dr Paul Weston for statistical advice with

SAGE, as well as Kate Day and Isabelle Perault for technical assistance. J.S. was funded by a Gates studentship, N.J by a BBSRC studentship, and C.P. by a Wellcome Trust Fellowship. This work was part-funded by a project grant from Welbeing, UK.

References

1. Yang YH, Speed T. Design issues for cDNA microarray experiments. Nat Rev Genet 2002; 3: 579–88.
2. Jovanovic BD, Bergan RC, Kibbe WA. Some aspects of analysis of gene array data. Cancer Treat Res 2002; 113: 71–89.
3. Carmeliet P, Ferreira V, Breier G et al. Abnormal blood vessel development and lethality in embryos lacking a single VEGF allele. Nature 1996; 380: 435–9.
4. Ferrara N, Carver-Moore K, Chen H et al. Heterozygous embryonic lethality induced by targeted inactivation of the VEGF gene. Nature 1996; 380: 439–42.
5. Ferrara N. VEGF and the quest for tumour angiogenesis factors. Nat Rev Cancer 2002; 2: 795–803.
6. Willett CG, Boucher Y, Di Tomaso E et al. Direct evidence that the VEGF-specific antibody bevacizumab has antivascular effects in human rectal cancer. Nat Med 2004; 10: 145–7.
7. Symes JF, Losordo DW, Vale PR et al. Gene therapy with vascular endothelial growth factor for inoperable coronary artery disease. Ann Thorac Surg 1999; 68: 830–6; discussion 836–7.
8. Simovic D, Isner JM, Ropper AH et al. Improvement in chronic ischemic neuropathy after intramuscular phVEGF165 gene transfer in patients with critical limb ischemia. Arch Neurol 2001; 58: 761–8.
9. Carmeliet P, Moons L, Luttun A et al. Synergism between vascular endothelial growth factor and placental growth factor contributes to angiogenesis and plasma extravasation in pathological conditions. Nat Med 2001; 7: 575–83.
10. Autiero M, Waltenberger J, Communi D et al. Role of PlGF in the intra- and intermolecular cross talk between the VEGF receptors Flt1 and Flk1. Nat Med 2003; 9: 936–43.
11. Bussolati B, Dunk C, Grohman M et al. Vascular endothelial growth factor receptor-1 modulates vascular endothelial growth factor-mediated angiogenesis via nitric oxide. Am J Pathol 2001; 159: 993–1008.
12. Abe M, Sato Y. cDNA microarray analysis of the gene expression profile of VEGF-activated human umbilical vein endothelial cells. Angiogenesis 2001; 4: 289–98.
13. Vasile E, Tomita Y, Brown LF et al. Differential expression of thymosin {beta}-10 by early passage and senescent vascular endothelium is modulated by VPF/VEGF: Evidence for senescent endothelial cells in vivo at sites of atherosclerosis. FASEB J 2001; 15: 458–66.
14. Jih YJ, Lien WH, Tsai WC et al. Distinct regulation of genes by bFGF and VEGF-A in endothelial cells. Angiogenesis 2001; 4: 313–21.
15. Weston GC, Haviv I, Rogers PA. Microarray analysis of VEGF-responsive genes in myometrial endothelial cells. Mol Hum Reprod 2002; 8: 855–63.
16. Yang S, Toy K, Ingle G et al. Vascular endothelial growth factor-induced genes in human umbilical vein endothelial cells: relative roles of KDR and Flt-1 receptors. Arterioscler Thromb Vasc Biol 2002; 22: 1797–803.
17. Zhang H-T, Gorn M, Smith KA et al. Transcriptional profiling of human microvascular endothelial cells in the proliferating and quiescent state using cDNA arrays. Angiogenesis 1999; 3: 211–9.
18. Liu D, Jia H, Holmes DI et al. Vascular endothelial growth factor-regulated gene expression in endothelial cells: KDR-mediated induction of Egr3 and the related nuclear receptors Nur77, Nurr1, and Nor1. Arterioscler Thromb Vasc Biol 2003; 23: 2002–7.
19. Jaffe EA, Nachman RL, Becker CG, Minick CR. Culture of human endothelial cells derived from umbilical veins. Identification by morphologic and immunologic criteria. J Clin Invest 1973; 52: 2745–56.
20. Evans AL, Sharkey AS, Saidi S et al. Generation and use of a tailored gene array to investigate vascular biology. Angiogenesis 2003; 6: 93–104.
21. Long AD, Mangalam HJ, Chan BY et al. Improved statistical inference from DNA microarray data using analysis of variance and a Bayesian statistical framework. Analysis of global gene expression in *Escherichia coli* K12. J Biol Chem 2001; 276: 19937–44.
22. Tusher VG, Tibshirani R, Chu G. Significance analysis of microarrays applied to the ionizing radiation response. Proc Natl Acad Sci USA 2001; 98: 5116–21.
23. Saidi SA, Holland CM, Kreil DP et al. Independent Component Analysis is a valid model for microarray analysis in endometrial cancer. Oncogene 2004; in press.
24. Velculescu VE, Zhang L, Vogelstein B, Kinzler KW. Serial analysis of gene expression. Science 1995; 270: 484–7.
25. Johnson N, Sengupta S, Lessan K et al. Endothelial Cells preparing to die by apoptosis initiate a program of transcriptome and glycome regulation. FASEB J. 2003; 18: 188–190.
26. Ho M, Yang E, Matcuk G et al. Identification of endothelial cell genes by combined database mining and microarray analysis. Physiol Genomics 2003; 13: 249–62.
27. Clauss M, Gerlach M, Gerlach H et al. Vascular permeability factor: A tumor-derived polypeptide that induces endothelial cell and monocyte procoagulant activity, and promotes monocyte migration. J Exp Med 1990; 172: 1535–45.
28. Lu M, Perez VL, Ma N et al. VEGF increases retinal vascular ICAM-1 expression *in vivo*. Invest Ophthalmol Vis Sci 1999; 40: 1808–12.
29. Pepper MS, Ferrara N, Orci L, Montesano R. Vascular endothelial growth factor (VEGF) induces plasminogen activators and plasminogen activator inhibitor-1 in microvascular endothelial cells. Biochem Biophys Res Commun 1991; 181: 902–6.
30. Unemori EN, Ferrara N, Bauer EA, Amento EP. Vascular endothelial growth factor induces interstitial collagenase expression in human endothelial cells. J Cell Physiol 1992; 153: 557–62.
31. Gerber HP, Dixit V, Ferrara N. Vascular endothelial growth factor induces expression of the antiapoptotic proteins Bcl-2 and A1 in vascular endothelial cells. J Biol Chem 1998; 273: 13313–6.
32. Marumo T, Schini-Kerth VB, Busse R. Vascular endothelial growth factor activates nuclear factor-kappaB and induces monocyte chemoattractant protein-1 in bovine retinal endothelial cells. Diabetes 1999; 48: 1131–7.
33. Kim I, Moon SO, Kim SH, et al. Vascular endothelial growth factor expression of intercellular adhesion molecule 1 (ICAM-1), vascular cell adhesion molecule 1 (VCAM-1), and E-selectin through nuclear factor-kappa B activation in endothelial cells. J Biol Chem 2001; 276: 7614–20.

PUBLICATION 6

Print, C., R. Valtola, **A. Evans**, K. Lessan, S. Malik, and S. Smith. 2004. Soluble Factors from Human Endometrium Promote Angiogenesis and Regulate the Endothelial Cell Transcriptome. *Hum Reprod* 19, (10), 2356-66.

Cited by 5, Impact factor 4.475

ISSN: 0268-1161

Journal Type

Human Reproduction publishes full-length, peer-reviewed papers reporting original research, clinical case histories, as well as opinions and debates on topical issues. The scope of reproductive topics is wide. Papers published cover the scientific and medical aspects of reproductive physiology and pathology, endocrinology, andrology, gonad function, gametogenesis, fertilization, embryo development, implantation, pregnancy, genetics, genetic diagnosis, oncology, infectious disease, surgery, contraception, infertility treatment, psychology, ethics and social issues.

Personal Contribution

My contribution to this publication was the microarray production, hybridisation and primary data anaylsis as described in (Evans et al., 2003)[*1] . I also performed the experiments using endometrial tissue but was not involved in the menstrual effluent experiments.

Human Reproduction Vol.19, No.10 pp. 2356–2366, 2004
Advance Access publication July 8, 2004
DOI: 10.1093/humrep/deh411

Soluble factors from human endometrium promote angiogenesis and regulate the endothelial cell transcriptome

Cristin Print[1,3,*], Reija Valtola[1*], Amanda Evans[1], Khashayar Lessan[1], Shazia Malik[2] and Stephen Smith[2]

[1]Department of Pathology, Cambridge University, Tennis Court Road, Cambridge, CB2 1QP and [2]Department of Obstetrics and Gynaecology, The Rosie Hospital, Robinson Way, Cambridge CB2 2SW, UK

[3]To whom correspondence should be addressed at: Department of Pathology, Cambridge University, Tennis Court Road, Cambridge, CB2 1QP, UK. E-mail: cgp22@cam.ac.uk

BACKGROUND: Angiogenesis and vascular remodeling play critical roles in the cyclical growth and regression of endometrium. They also appear to play roles in the pathogenesis of endometriosis. METHODS and RESULTS: Supernatants were collected from cultured endometrium isolated from women with and without endometriosis. These supernatants induced endothelial cell proliferation and angiogenesis *in vitro*. They contained vascular endothelial growth factor (VEGF)-A, and their proliferative effects on endothelial cells were partially abrogated by a blocking anti-VEGF-A antibody. Gene array analysis showed that culture supernatants from proliferative phase endometrium, and to a lesser extent secretory phase endometrium, induced significant changes in the transcriptome of endothelial cells. We could not detect any association between endometriosis and the ability of endometrial-derived soluble factors to promote angiogenesis or to regulate the endothelial transcriptome. In addition, we could not detect any association between endometriosis and the concentration of VEGF-A in supernatants from cultured endometrium or in menstrual effluent. CONCLUSIONS: We have shown that endometrium cultured *in vitro* produced soluble factors, including VEGF-A, that promoted angiogenesis. Proliferative phase endometrium promoted significant endothelial cell transcriptome changes that appear overall to be pro-angiogenic. These transcriptome changes provide insight into the dynamic control of vessel structure on which both eutopic endometrium and endometriotic lesions depend.

Key words: endometrious/gene array/VEGF-A/transcriptome

Introduction

Angiogenesis and vascular remodeling play critical roles in the cyclical growth and regression of the endometrium (reviewed by Gargett *et al.*, 2001). In the proliferative phase of the menstrual cycle, angiogenesis occurs in the stratum functionalis as the endometrium approximately quadruples in thickness. In the secretory phase of the cycle, spiral arterioles lengthen and become more coiled and the sub-epithelial capillary plexus matures. In the post-menstrual phase, angiogenesis is involved in the repair of the superficial layer of the remaining stratum basalis. Endometrial angiogenesis is tightly coordinated with recruitment of vascular smooth muscle cells to the nascent vessels (Kohnen *et al.*, 2000). Endometrial angiogenesis may be directly controlled by reproductive steroids (Iruela-Arispe *et al.*, 1999; Hague *et al.*, 2002) and indirectly controlled by angiogenic regulators expressed by the diverse cell lineages present in the endometrium. Potential regulators of endometrial angiogenesis include: nitric oxide (Cameron *et al.*, 1998), vascular endothelial growth factor (VEGF)-A (Charnock-Jones *et al.*, 1993; Donnez *et al.*, 1998), VEGF-B and -C (Mints *et al.*, 2002; Moller *et al.*, 2002), relaxin (Unemori *et al.*, 1999), fibroblast growth factors (FGF) (Ferriani *et al.*, 1993), matrix metalloproteinases (MMPs) (Freitas *et al.*, 1999), thymidine phosphorylase (Fujiwaki *et al.*, 1999), angiopoietin-2 (Krikun *et al.*, 2000), erythropoietin (Yasuda *et al.*, 1998), adrenomedullin (Nikitenko *et al.*, 2000) and epidermal growth factor (EGF) (Sandberg *et al.*, 2001). Leukocyte-derived factors may play a particularly important role. Angiopoietin-2, VEGF-C and placental growth factor (PlGF) expressed by endometrial NK leucocytes (Li *et al.*, 2001) may drive spiral arteriole and sub-epithelial capillary plexus changes during the secretory phase of the cycle (Sandberg *et al.*, 2001), while VEGF-A expressed by intra-vascular neutrophils may promote angiogenesis in the stratum functionalis during the proliferative phase of the cycle (Gargett *et al.*, 2001).

Endometriosis, the growth of ectopic endometrial fragments in the peritoneum, is a debilitating disease that causes

*These authors contributed equally to this work

pain with menstruation, pain with intercourse and other symptoms. In addition, endometriosis also causes infertility (Haney, 1990). Despite a significant recent increase of the disease coincident with the introduction of widespread fertility regulation, the cause of the problem remains unknown. Tissues that grow to greater than $\sim 1\,mm^3$ need to establish a blood supply to prevent necrosis (Folkman, 2002). Therefore, for endometriotic lesions to survive they must recruit a vasculature from the surrounding tissues (reviewed by Smith, 1997). However, the processes that promote this angiogenesis are as yet uncertain. They may involve both endometrial and peritoneal factors—several examples of each have been proposed. Potential pro-endometriotic endometrial factors include increased proliferation capacity of endometrial endothelial cells (EC) (Wingfield *et al.*, 1995) and elevated expression of several molecules including: the pro-angiogenic integrin αvβ3 (Hii *et al.*, 1998), hepatocyte growth factor and its c-Met receptor (Khan *et al.*, 2003), endoglin (Kim *et al.*, 2001), nitric oxide synthases (Wu *et al.*, 2003), urokinase receptor (Sillem *et al.*, 1998) and tissue inhibitor of metalloproteinases-2 (TIMP-2) (Sillem *et al.*, 1998). Potential peritoneal factors include: macrophage migration inhibitory factor (MIF) in peritoneal fluid of endometriotic women (Kats *et al.*, 2002), steroidally-regulated VEGF-A production by peritoneal macrophages (McLaren *et al.*, 1996), elevated tumour necrosis factor (TNF)-α production from peritoneal macrophages (Noda *et al.*, 2003; Richter *et al.*, 2004) and elevation of soluble TNF receptor (Steff *et al.*, 2004), angiogenin (Steff *et al.*, 2004) and PlGF (Suzumori *et al.*, 2003).

Previously, the programmed variation of the transcriptome of whole endometrium through the menstrual cycle has been characterized (Borthwick *et al.*, 2003; Kao *et al.*, 2003). However, the effects of soluble factors produced by cells within the endometrium on endothelial gene expression, cell biology and angiogenesis have not been fully investigated. In this study, we have assessed the ability of the soluble factors secreted by endometrium collected from non-endometriotic and endometriotic women in the proliferative and secretory phases of the menstrual cycle to promote EC proliferation and angiogenesis and to modulate the EC transcriptome. Given the important role played by VEGF-A in angiogenesis, we have also assessed the concentration of VEGF-A in endometrial culture supernatants and in menstrual effluent from women with and without endometriosis.

Materials and methods

Collection and culture of endometrium

This study was approved by the local ethical review committee and patient consent was obtained for the collection of all human tissues used in this study. Since anti-inflammatory medications or medications related to reproductive steroids alter the cellular composition of endometrium and are therefore likely to alter the pro-angiogenic properties of endometrium, women currently on these medications as well as women who had received courses of these drugs in the previous 3 months were excluded. Women were also excluded who had irregular menstrual cycles or who were using an intrauterine device. In all women in the endometriotic group of this study the clinical diagnosis of endometriosis was confirmed laparoscopically. Women in the non-endometriotic group had no symptoms of endometriosis and in addition, 6 out of the 10 women in this group had the absence of endometriosis confirmed by laparoscopy. Only three of the women in the study were smokers (two non-endometriotic proliferative phase donors and one endometriotic secretory phase donor). Endometrium was collected by Pipelle biopsy, and the approximate stage of the menstrual cycle confirmed by histology. Adhering blood clot and included myometrial tissue were removed by washing and dissection. The endometrium was then disaggregated by incubation with agitation in phosphate-buffered saline (PBS) containing 100 mg/ml collagenase (Sigma, UK) and 100 mg/ml DNase (Sigma, UK). The disaggregated endometrial cells were then washed twice in PBS and plated at 70% confluence in tissue culture dishes in a fully humidified atmosphere of 5% CO_2 in a proprietary culture medium (LVEC, large vessel endothelial cell medium; TCS, Botolph, UK) supplemented with a mixture of heparin, hydrocortisone, epidermal growth factor, fibroblast growth factor, 2% fetal calf serum (FCS), gentamycin and amphotericin. This culture medium maintained both EC (for which it was designed) and endometrium, since the appearance of disaggregated endometrium after 4 days in this culture medium was equivalent to that of endometrium cultured in DMEM/Hams F12 (50:50 mix) supplemented with 10% FCS (data not shown). No reproductive steroids were added to the culture medium since reproductive steroids (Morales *et al.*, 1995; Alvarez *et al.*, 1997) and their metabolites (Yue *et al.*, 1997) have been show to affect EC. Disaggregated monolayer cultures were chosen in preference to explant cultures to maintain optimal oxygenation and nutrition for all cells, and to allow visible assessment of endometrial cell viability. After 24 h in culture the endometrial monolayers were washed twice in medium in order to completely remove dead cells and erythrocytes. After a further 24 h in the LVEC medium, culture supernatants were collected, centrifuged and stored at −70°C. To assess the cellular composition of the endometrial cultures, proliferative and secretory phase endometrium were disaggregated as described above, cultured on chamber slides for 24 h, fixed at −20°C with 50:50 acetone:ethanol, immunostained with an anti-pan cytokeratin antibody cocktail (DAKO N1589) and a fluorescein isothiocyanate (FITC)-conjugated secondary antibody and detected using an epifluorescence microscope.

EC proliferation and angiogenesis assays

Human umbilical vein EC(s) (HUVEC) were isolated by collagenase digestion as described (Jaffe *et al.*, 1973) and cultured to passage 5 in LVEC medium. Once at passage 5, HUVEC were plated into 24-well plates at 70% confluence and supernatants from endometrial cultures added (20% V/V) for 24 h. Viable HUVEC numbers were then counted using a haemocytometer after trypan blue staining (0.2% Sigma, UK). Four wells were used for each experimental condition. The 20% V/V dilution of the endometrial cell culture supernatants was chosen empirically since it on average induced maximal HUVEC responses without inducing signs of stress in these cells (data not shown). To prevent confounding, medium of identical composition (LVEC medium described above) was used for culture of all endometrial explants and all HUVEC in this study. Since we have shown that quiescing HUEVC by transfer to low serum medium reduces the ability of these cells to mount transcriptional responses to growth factors (Johnson *et al.*, 2003), the HUVEC were not quiesced before incubation with the endometrial culture supernatants. In additional experiments, a blocking anti-VEGF-A monoclonal antibody (clone 26503, R&D Systems, UK) was added

to HUVEC cultured as above, and relative cell numbers estimated using a tetrazolium compound (MTS) assay (CellTiter 96 Aqueous Non-Radioactive Cell Proliferation Assay; Promega) used according to the manufacturer's instructions.

In vitro angiogenesis assays consisted of co-cultures of HUVEC and human dermal fibroblasts (Bishop *et al.*, 1999). They were purchased pre-plated in 24-well tissue culture plates from TCS Cellworks (ZHA-1000; Botolph, UK) and cultured in the LVEC medium for 11 days with or without the addition of endometrial culture supernatants (20% V/V, replaced every 4 days). After 11 days cells were fixed in 2% paraformaldehyde for 20 min at 4°C, permeablized in 0.1% Triton X-100 and 0.1% Tween-20 for 30 min at room temperature, stained with Ulex–FITC (Sigma L9006, UK) at a concentration of 10 μg/ml and Hoescht Bisbenzimide 33342 (Calbiochem 382061, UK) at a concentration of 1 μg/ml. For each experimental condition, the number of branches and total length of capillary-like structures was measured by imaging 21 randomly chosen 1 mm^2 fields using a confocal microscope (Lieca, Germany). Images were processed to quantify angiogenesis using the TCS Angiogenesis assessment software (TCS, Botolph, UK).

Gene array analysis

RNA was prepared from HUVEC using Trizol reagent (Gibco/BRL, UK) followed by clean up through an RNeasy spin column (Qiagen, UK) and ethanol precipitation. RNA integrity was assessed using an Agilent 2100 bioanalyser (Agilent, UK). ^{33}P-labelled complex cDNA probes were prepared from the RNAs and hybridized to an array of ~1000 cDNAs immobilized onto nylon filters as described (Evans *et al.*, 2003). Hybridization was quantified using a phosphoimager (Molecular Dynamics Inc., CA) and IMAGENE software (Bio-Discovery, CA). After global and local normalization (Evans *et al.*, 2003), transcript abundance data were compared using the CyberT algorithm (version 7.03; sliding window = 301, Bayes estimate = 10). This algorithm is an unpaired *t*-test, modified by the inclusion of a Bayesian prior based on the variance of other transcripts in the data set (Long *et al.*, 2001). For further statistical analysis, the 'R' statistical software system and GeneSpring Expression Analysis Software (Silicon Genetics, Redwood City, CA) were used.

Quantitative polymerase chain reaction analysis

The ABI PRISM 7700 Sequence Detection System (TaqMan) was used to perform real-time polymerase chain reactions according to the manufacturer's protocols. 'Ct' values for each transcript were compared to those for cyclophilin A, which according to the gene array results remained relatively constant in abundance. Primers and probes for GSTP-1, VE-cadherin, IL1RL-1 and vimentin were proprietary oligonucleotides obtained from Applied Biosystems (ABI, UK) 'Assays-on-Demand' and used a 5′ FAM reporter and 3′ non-fluorescent minor groove binder.

ELISA for VEGF-A

To quantify VEGF-A in endometrial culture supernatants an ELISA assay was used (R&D systems, UK) according to the manufacturer's instructions, and the VEGF-A concentration determined by measuring absorbance at 490 nm by comparison with a standard curve. For each measurement six replicates were performed.

Collection of menstrual effluent

Menstrual effluent was collected by volunteers by vaginal insertion of a menstrual cup ('The Keeper'™, Eco Logique Inc., Canada) in the second 24 h of bleeding. The cup was left in situ for 4 h, the fluid sample collected and the volume measured. Menstrual cup samples were washed with an equal volume of PBS and centrifuged at 200 g for 10 min at 4°C. The supernatant was stored at −70°C for ELISA which was performed as described above.

Statistical analysis

All experimental data except those generated from gene arrays were analysed using the 'R' statistical software package (http://rweb.stat.umn.edu/R/doc/html/index.html). Before comparisons were made, data were tested for normality using Chi squared tests and then for equal variance between groups using Bartlett's method. Based on these results, we were able to use multi-way analysis of variance (ANOVA). In all cases where ANOVA suggested a statistically significant effect, post hoc Tukey's Multiple Comparison Tests were used to assess the source of the effect.

Results

Supernatants from cultured endometrium promote endothelial cell proliferation and angiogenesis in vitro

To assess the effects of soluble factors derived from endometrium on endothelial cell biology, endometrium was collected from five women without endometriosis in each of the mid-proliferative (days 6–10) and mid-secretory (days 16–21) phases of the menstrual cycle using Pipelle biopsy. Endometrial cells were disaggregated, cultured (see Methods) and culture supernatants collected over a 24 h period. These proliferative and secretory phase endometrial culture supernatants were applied to HUVEC (20% V/V). After 24 h exposure to these supernatants or to medium alone (control) or 10 ng/ml VEGF-A, cell numbers were counted. Relative to cultures supplemented with 10 ng/ml VEGF-A (standardized as 100%), cultures supplemented with medium alone contained 40 ± 3.5% cells, while cultures supplemented with the proliferative and secretory phase endometrial supernatants contained 88 ± 19% and 84 ± 10% cell numbers, respectively (expressed as mean ± 2 × standard error). ANOVA ($P \leq 0.05$) followed by Tukey's post hoc tests indicated that the differences in cell number between the control cultures and the cultures supplemented with either proliferative or secretory phase endometrial supernatants were significant. However, the effects of the supernatants from proliferative and secretory phase endometrial cultures were not significantly different from one another.

To assess whether soluble factors derived from endometrium could promote angiogenesis in addition to promoting endothelial proliferation, endometrial culture supernatants were added (20% V/V) to co-cultures of HUVEC and human dermal fibroblasts for an 11 day period. These co-cultures spontaneously formed capillary-like structures (*in vitro* angiogenesis; Bishop *et al.*, 1999). We found that endometrial culture supernatants promoted the acquisition of capillary length and branching (estimated by counting junction number) more effectively than medium alone. Medium alone ($n = 3$) induced vessels with a mean length of 4.0 ± 0.1 mm/mm^2 and a mean branching of 12 ± 1.5/mm^2, respectively (mean ± SEM). However, proliferative phase supernatants ($n = 4$) induced vessels with a mean length of 6.5 ± 0.1 mm/mm^2 and a mean branching of 26.3 ± 0.9/mm^2 (mean ± SEM) and secretory phase supernatants ($n = 2$) induced vessels with a

mean length of 5.8 and 6.0 mm/mm^2 and a mean branching of 19 and 21/mm^2 (Figure 1). Due to the small number of secretory phase endometrial supernatants, for statistical purposes the results for the two secretory phase and four proliferative phase endometrial supernatant groups were combined, and a Student's *t*-test indicated that both length and branching were significantly elevated when compared to the three control cultures ($P \leq 0.05$). The promotion of EC proliferation and *in vitro* angiogenesis appears to be specific to endometrium, since supernatants from HUVEC themselves, primary vascular smooth muscle cells, Jurkat T lymphocytes and primary human macrophages cultured in identical conditions to the endometrium had no significant effect on HUVEC cell biology or *in vitro* angiogenesis (data not shown). To assess the possibility that differences in the cellular composition of the endometrial cultures were responsible for these effects, we analysed the cellular composition of disaggregated endometrium derived from three patients in the mid-proliferative and two in the mid-secretory phases of the menstrual cycle after culture for 24 h. These cultures contained variable proportions (7–11%) of cytokeratin$^{+\ ve}$ epithelial cells. The cellular proportions were not significantly different (ANOVA; $P > 0.05$) in the cultures derived from either proliferative or secretory phase endometrium.

Supernatants from cultured endometrium regulate the endothelial cell transcriptome

The pattern of EC transcript abundance (transcriptome) contributes to the unique physical characteristics and functions of EC, and the response of EC to extracellular signals is in part mediated through transcriptome alteration. To assess the transcriptome changes that were associated with (and may have driven) endometrial supernatant-induced EC proliferation and angiogenesis, we collected RNA from HUVEC that were exposed to proliferative and secretory phase endometrial culture supernatants (20% V/V) for a 24 h period. Radio-labeled complex cDNA probes generated from these RNAs were hybridized to nylon filter gene arrays that

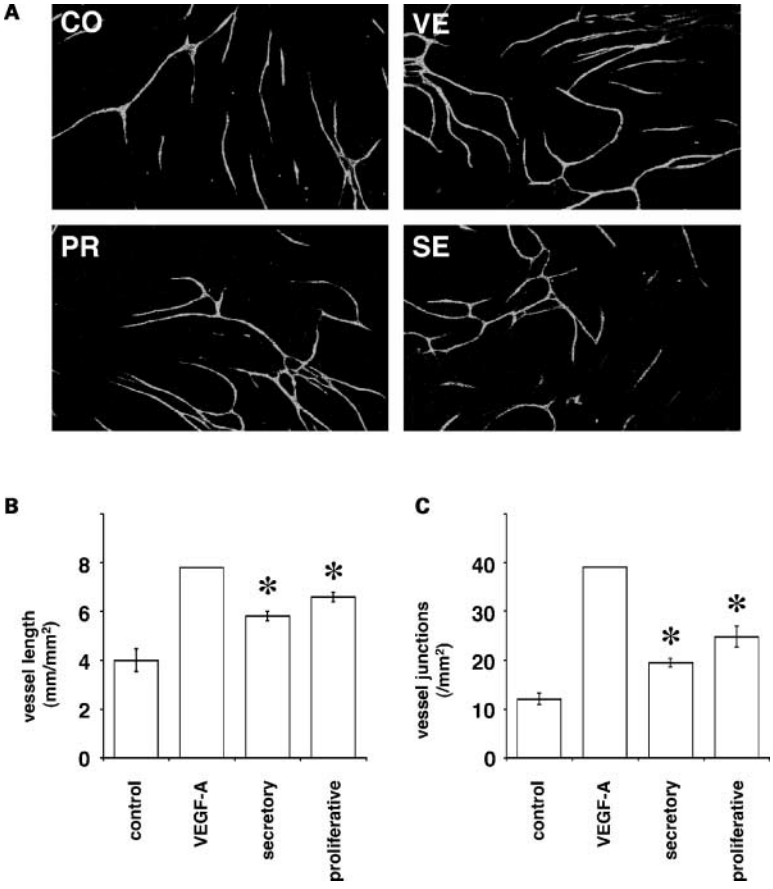

Figure 1. (**A**) Supernatants from cultured endometrium promoted *in vitro* angiogenesis. Endothelial cells co-cultured with dermal fibroblasts were detected with Ulex-FITC (Sigma, UK). Representative images of 320 μm × 1 mm fields are shown for: CO (untreated control), VE (10 ng/ml VEGF-A^{165}), PR and SE (supernatant from cultured proliferative- and secretory-phase endometrium, respectively). (**B** and **C**) The length of vessels and number of inter-vessel junctions (a measure of branching) per mm^2 were established for 21 randomly chosen 1 mm^2 fields for each of the following conditions: three untreated cultures (control), one culture treated with 10 ng/ml VEGF-A, two cultures each treated with secretory phase endometrial supernatants derived from different patients and four cultures each treated with proliferative phase endometrial supernatants derived from different patients. Bars represents group means ± SE. The mean length and number of inter-vessel junctions of HUVEC exposed to the endometrial supernatants ($n = 6$, composed of HUVEC exposed to two secretory phase and four proliferative phase endometrial supernatants) was significantly greater than the mean length and number of inter-vessel junctions of untreated HUVEC (Student's *t*-test; $P \leq 0.05$).

contained ~1000 genes related to endothelial cell biology (Evans *et al.*, 2003). Secretory phase endometrial supernatants induced few large-scale changes in HUVEC transcript abundance (Figure 2A). In contrast, proliferative phase endometrial supernatants induced numerous large-scale changes in HUVEC transcript abundance (Figure 2B). Transcript abundance in HUVEC treated with proliferative-phase and secretory-phase endometrial supernatants is compared in Figure 2C. The gene array results for four transcripts differentially regulated by proliferative- and secretory-phase endometrial supernatants were compared with results from TaqMan quantitative PCR and found to be concordant (Figure 2D). For all four transcripts, *t*-tests on the TaqMan data indicated a significant difference in expression between HUVEC exposed to supernatants from proliferative and secretory phase endometrium ($P \leq 0.01$).

To select those genes most significantly regulated in HUVEC by cultured endometrial supernatants relative to control medium-treated HUVEC, transcripts were selected where the 'fold change' was $\geqq$ 2-fold up or down and Baysian *t*-test *P*-value was ≤ 0.05. When untreated HUVEC ($n = 3$) were compared to HUVEC cultured in the presence of proliferative-phase endometrial supernatants ($n = 5$) 26 transcripts met these criteria—these are shown in Table I. However, when untreated HUVEC ($n = 3$) were compared to HUVEC cultured in the presence of secretory phase endometrial supernatants ($n = 5$) only two transcripts met these criteria (ADP ribosylation factor-like 2, $\uparrow$2.1; and CD36, $\downarrow$2.1). However, several transcripts regulated by proliferative-phase endometrial supernatants were in fact also regulated by secretory-phase endometrial supernatants, but to a lesser degree. For example, 50% of transcripts regulated $\geqq$ 2-fold

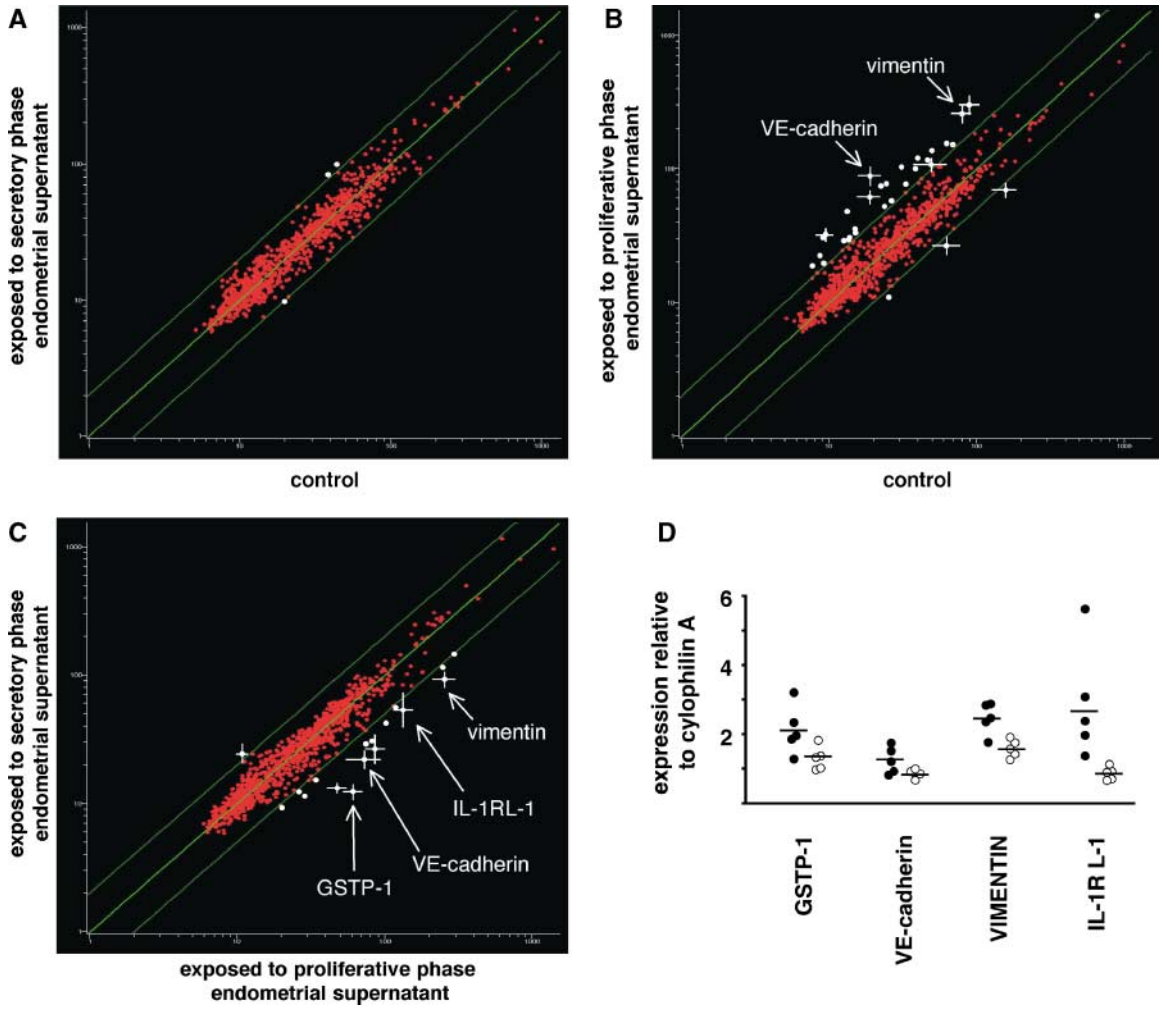

Figure 2. Gene array analysis of the response of HUVEC to endometrial culture supernatants is presented as a set of scatter-plots. White spots denote transcripts regulated up or down, on average, by $\geqq$ 2-fold. Error bars denote SE. (**A**) Untreated HUVEC ($n = 3$) compared to HUVEC cultured in the presence of secretory phase endometrial supernatants ($n = 5$). (**B**) Untreated HUVEC ($n = 3$) compared to HUVEC cultured in the presence of proliferative phase endometrial supernatants ($n = 5$). (**C**) HUVEC cultured in the presence of proliferative phase endometrial supernatants ($n = 5$) compared with HUVEC cultured in the presence of secretory phase endometrial supernatants ($n = 5$). (**D**) TaqMan quantitative PCR confirmed the regulated abundance of four transcripts in five replicate experiments. Transcript abundance is presented relative to the housekeeping transcript cyclophilin-A. Black and white dots represent transcript abundance in HUVEC incubated with proliferative and secretory phase endometrium, respectively. Horizontal lines denote means. For all four transcripts, *t*-tests (with Bonferroni correction to allow for four simultaneous comparisons) indicated a significant difference between expression levels in HUVEC exposed to supernatants from proliferative vs secretory phase endometrium ($P \leq 0.01$).

Table I. Transcripts differentially regulated in HUVEC cells by incubation with supernatants from cultured proliferative phase endometrium

Name	By *P*-value	Fold change
ADP ribosylation factor-like 2	0.000168	+2.61*
Angiopoetin 1	5.60E-06	−2.39*
c-Jun N-terminal kinase 3	0.000704	−2.02*
Collagen IV alpha 6	4.13E-05	+3.28*
CXC-receptor-4	0.001395	+2.18
Cystatin C	0.000768	+2.10*
EST DKFZP56600424	0.000291	+2.25
Endoglin	0.004326	+2.40
Fibronectin-1	0.000247	+4.49
Glutathione S transferase p1	0.000212	+3.55*
Glyceraldehyde-3-phosphate dehydrogenase	5.00E-13	+2.11*
Insulin-like growth factor binding protein-2	0.000591	+3.33
Interferon gamma receptor-2	0.000271	+2.14
Interleukin 1 receptor like-1	7.53E-07	+3.26
Mitogen-activated protein kinase-12	0.002262	+2.69*
Matrix metalloproteinase-2	0.000444	+2.15*
Matrix metalloproteinase-3	0.000164	+2.24
Myosin light chain regulator-B	0.001236	+2.28
Plasminogen activator inhibitor-1	8.47E-06	+3.09*
PECAM-1 (CD31)	2.13E-05	+2.19
Rho 7	0.003470965	+2.14*
Ryanodine receptor-1	1.89E-06	−2.29*
SIVA	0.000277083	+2.40
Tissue factor inhibitor-2	0.006458425	+3.32*
VE-Cadherin	6.43E-05	+3.20
Vimentin	4.93E-05	+3.19

Transcripts that were significantly regulated in HUVEC by incubation with proliferative phase endometrium are listed. In all cases mean transcript abundance regulation ('fold change') relative to control medium-treated HUVEC was ≧ 2-fold up (+) or down (−), and Baysian *t*-test *P*-value (By *P*-value) was ≤0.05. Asterisks denote those transcripts that were also up- or down-regulated in abundance ≧ 1.6-fold by exposure to supernatants from secretory phase endometrium.

up or down by proliferative-phase endometrial supernatants were also regulated, in the same direction, ≧ 1.6-fold up or down by secretory phase endometrial supernatants (asterisked in Table I).

Supernatants from cultured endometrium contain active VEGF-A

VEGF-A is an important regulator of endothelial cell survival, proliferation and angiogenesis, and appears to play a particular role in regulating angiogenesis in the endometrium. Therefore, we wished to determine whether VEGF-A may mediate, in part, the effects of cultured endometrial supernatants on EC. Using an ELISA, we confirmed that five proliferative and five secretory phase endometrial culture supernatants contained VEGF-A at a mean concentration of 5.2 ± 0.9 ng/ml and 5.0 ± 1.2 ng/ml, respectively (group mean ± SEM). These VEGF-A concentrations were significantly greater (ANOVA; $P \leq 0.01$ and Tukey's test) than those contained in medium alone (0.36 ± 0.2 ng/ml) or in medium conditioned by HUVEC themselves (0.43 ± 0.1 ng/ml). The concentration of VEGF-A secreted by proliferative and secretory phase endometrial cultures was not significantly different (ANOVA; $P > 0.05$). We then assessed the effects of saturating quantities (80 ng/ml) of an anti-VEGF-A monoclonal blocking antibody (clone 26503) on the ability of endometrial supernatants to promote HUVEC culture expansion. We found that

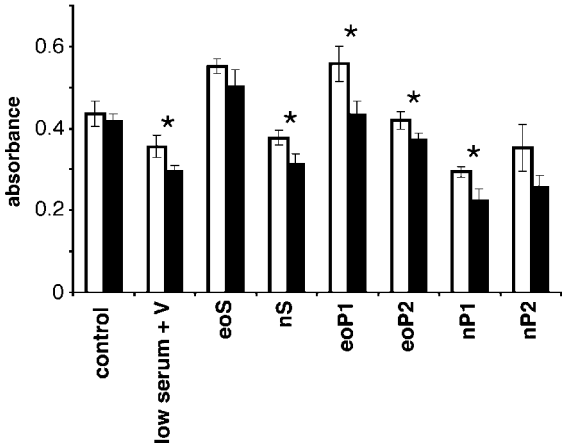

Figure 3. The effects of a blocking anti-VEGF-A antibody. Data represent HUVEC number ± 2 × SD (MTS assay) after 24 h culture with endometrial supernatants (20% V/V) in presence (black bars) or absence (white bars) of a blocking anti-VEGF-A antibody. Control denotes medium alone, low serum + V denotes low serum medium (2% FCS but no other growth factors) supplemented with 10 ng/ml VEGF-A^{165}, eoP and eoS denote culture supernatants of endometrium collected from women with endometriosis in the proliferative and secretory phases of their menstrual cycles, respectively. nP and nS denote culture supernatants of endometrium collected from women without endometriosis in the proliferative and secretory phases of their menstrual cycles, respectively. Asterisks denote a significant difference in cell number attributable to the effect of the anti-VEGF-A antibody on VEGF-A secretion by cultured endometrium (ANOVA; $P \leq 0.05$). The means of four measurements are shown, with error bars denoting 2 × SD.

the blocking antibody significantly (but not completely) inhibited the responses of the HUVEC to four out of the six endometrial supernatants tested. While the blocking antibody had no significant effect on HUVEC cultured in their optimal medium, it did significantly reduce the expansion of serum-starved HUVEC, presumably by reducing the VEGF-A-derived survival signals available to these stressed cells (Figure 3).

Endometriosis did not detectably alter the ability of endometrium to secrete soluble factors that influence endothelial cells

Angiogenesis is strongly implicated in the pathogenesis of endometriosis. Therefore, we wished to assess whether soluble factors produced by endometrium from women with endometriosis have a greater effect on EC than soluble factors produced by endometrium from women without the disease. Endometrial biopsies were collected from endometriotic patients and their secretion in culture of factors that promoted angiogenesis and EC transcriptome change assessed as above. Firstly, we assessed the effects on HUVEC proliferation of proliferative ($n = 3$) and secretory ($n = 3$) phase endometrial culture supernatants derived from eutopic endometrium of endometriotic women. These effects were not significantly different (ANOVA; $P \geqq 0.05$; Figure 4A) from the effects of cultured endometrial supernatants from women without the disease. Secondly, we assessed the effects of

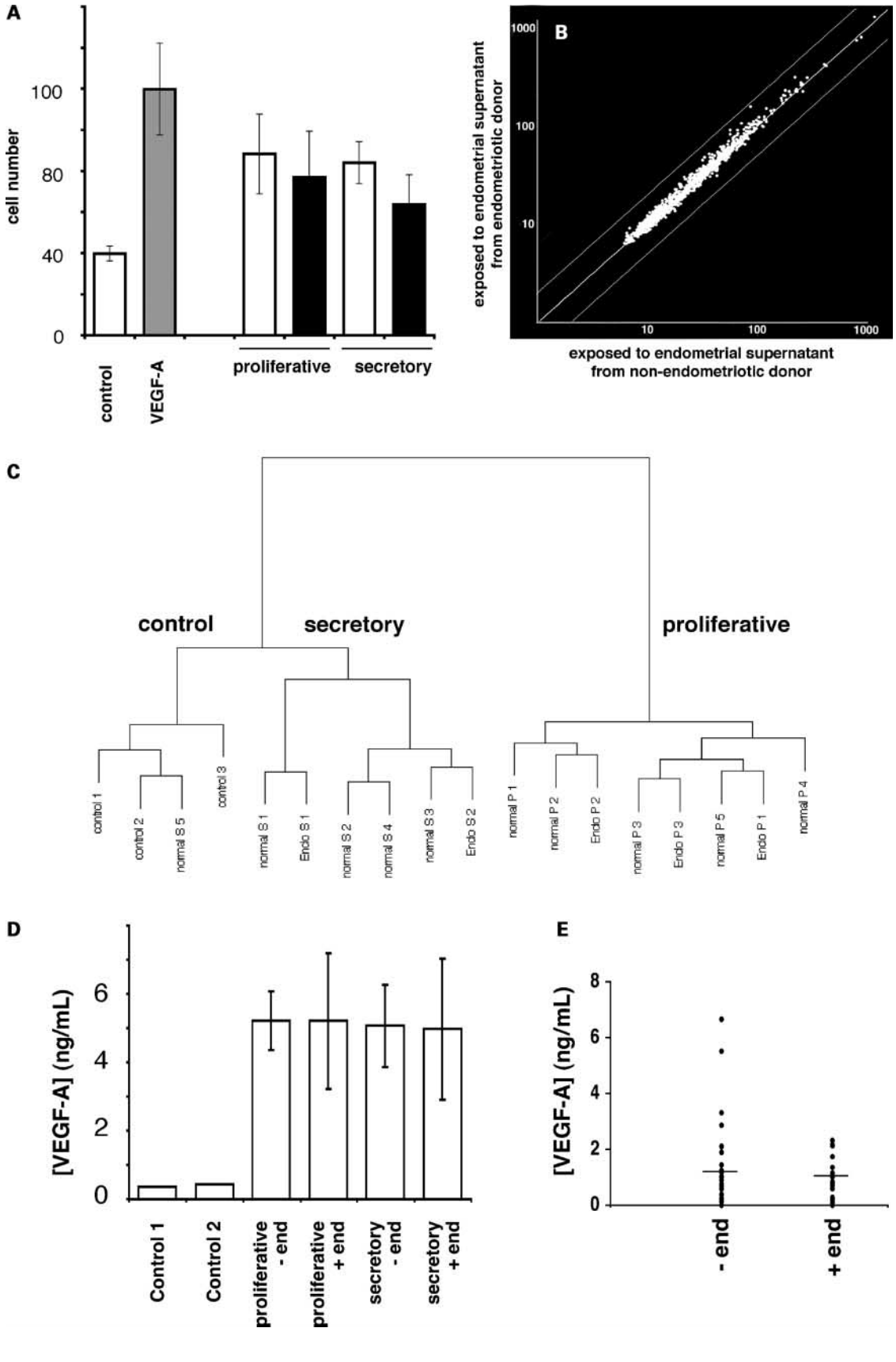

cultured endometrial supernatants from women with endometriosis on the HUVEC transcriptome. The effects of proliferative phase endometrial culture supernatants derived from women with and without endometriosis on HUVEC transcript abundance were indistinguishable (Figure 4B). Clustering of the array results separated HUVEC exposed to supernatants from proliferative vs secretory phase endometrial cultures, but could not separate HUVEC exposed to supernatants from endometrial cultures derived from endometriotic vs non-endometriotic women (Figure 4C). In addition, we could detect no differences between the concentrations of VEGF-A in endometrial supernatants derived from women with and without the disease (ANOVA; $P \geqq 0.05$; Figure 4D). Since retrograde menstruation is thought to be associated with endometriosis, and since VEGF-A within menstrual debris may promote angiogenesis when endometriotic lesions first implant in the peritoneum, we compared the concentration (Figure 4E) and total mass (data not shown) of VEGF-A in menstrual effluent from women with ($n = 16$) and without ($n = 24$) endometriosis using ELISA. No significant differences were detected (ANOVA; $P > 0.05$).

Discussion

We have shown that soluble factors derived from cultured endometrium promote HUVEC proliferation, angiogenesis and transcriptome change. One factor responsible for these effects appears to be VEGF-A, since we detected VEGF-A by ELISA in endometrial supernatants, and since a blocking anti-VEGF-A antibody partially inhibited EC proliferation in response to endometrial supernatants. In the small number of patients in our study, we were unable to correlate VEGF-A production with the stage of the menstrual cycle at which the endometrium was collected. This is not surprising, given that steroidal regulation of endometrial VEGF-A levels is limited (Sharkey *et al.*, 2000) and that regulation of VEGF-A production in endometrium may occur on a local (e.g. in intravascular neutrophils; Gargett *et al.*, 2001) rather than tissue-wide scale. Other endometrial factors may also promote EC proliferation, angiogenesis and transcriptome change. Previously published gene array studies of endometrium (Borthwick *et al.*, 2003; Kao *et al.*, 2003) provide clues to these. For example, the pro-angiogenic enzyme MMP-3 is within the most abundant 2% of endometrial transcripts (Borthwick *et al.*, 2003). SPARC is equally abundant in endometrium, and proteolysis of SPARC by MMP-3 produces potently pro-angiogenic peptides (Sage *et al.*, 2003). We could detect no difference between the pro-angiogenic abilities of proliferative and secretory phase endometrial supernatants, although this may have been due to the low sample number (secretory $n = 2$ and proliferative $n = 4$) examined. This concurs with the previous observation that endometrial EC proliferation indices *in vivo* do not correlate with the menstrual cycle (Rogers *et al.*, 1998). However, when we used gene arrays as a more sensitive indicator of EC responses to endometrial supernatants, we found that soluble factors secreted by proliferative phase endometrial cultures were more effective than those secreted by secretory phase endometrial cultures in promoting EC transcriptome change. This suggests that, even when disaggregated and removed from their specific endocrine environments, cultured cells isolated from proliferative and secretory phase endometrium retain their subtly different pro-angiogenic properties. A possible explanation is suggested by a previous study (Borthwick *et al.*, 2003), which found that the potent pro-angiogenic factors Intestinal Trefoil Factor (Rodrigues *et al.*, 2003) and MMP-11 (Nishizuka *et al.*, 2001) were many times more abundant in proliferative than in secretory phase endometrium. Although it is possible that cultures derived from proliferative and secretory phase endometrium contain different ratios of epithelial to stromal cells, and therefore secrete different amounts of factors such as VEGF-A (Gargett *et al.*, 1999), we suggest that this is unlikely to completely explain our results. Immunohistochemistry could not detect significant differences in the proportions of epithelial and stromal cells between cultures derived from mid-proliferative and mid-secretory phase endometrium. In addition, the concentrations of VEGF-A did not differ significantly when supernatants from cultures derived from mid-proliferative and mid-secretory phase endometrium were compared.

The transcriptome changes induced in EC by endometrium-derived factors may partly underlie the angiogenesis

Figure 4. Endometriosis did not detectably alter the ability of endometrium to secrete soluble factors that influence endothelial cells. (**A**) HUVEC were cultured with supernatants (20% V/V) taken from cultured secretory ($n = 3$) or proliferative ($n = 3$) phase endometrium, and mean viable HUVEC number (± SE, relative to VEGF-A-treated cultures) was measured after 24 h. Control represents medium alone and VEGF-A represents medium + 10 ng/ml VEGF-A^{165}. Black and white bars represent endometrium collected from patients with laparoscopically diagnosed endometriosis and patients without the disease, respectively. (**B**) Scatter-plot shows gene array analysis of the response of HUVEC to endometrial culture supernatants. HUVEC cultured in the presence of supernatants from proliferative phase endometrium collected from women with endometriosis ($n = 3$) were compared to HUVEC cultured in the presence of supernatants from proliferative phase endometrium collected from women without the disease ($n = 5$). (**C**) Ward's method clustering grouped the arrays into those representing HUVEC exposed to control, secretory and proliferative phase endometrial supernatants. However, the clustering could not identify whether the endometrium from which the supernatants were collected were derived from women with or without endometriosis. (**D**) ELISA for VEGF-A in cultured endometrial supernatants. Control 1 represents fresh medium alone; control 2, medium conditioned by confluent HUVEC for 24 h. 'Proliferative' and 'secretory' represent supernatants from endometrial cultures collected from women in the proliferative and secretory phases of the cycle, respectively. '+ end' and '− end' represent supernatants from endometrium collected from women with and without endometriosis, respectively. Error bars denote 2 × SEM. There were no significant differences between these groups (ANOVA; $P > 0.05$). (**E**) ELISA for VEGF-A in menstrual effluent. '+ end' denotes patients with endometriosis ($n = 16$) and '− end' denotes patients without the disease ($n = 24$). Horizontal lines represent means. There were no significant differences between these groups (*t*-test; $P > 0.05$).

that is also induced by these factors, since many of the regulated EC transcripts encode promoters of angiogenesis (Table I). These include transcripts previously found to be up-regulated during *in vitro* angiogenesis (Kahn *et al.*, 2000) such as CXC receptor-4, collagen IVα6 and tissue factor-inhibitor-2. Given that VEGF-A was secreted by the cultured endometrium, it is interesting that transcripts previously found to be up-regulated in EC by VEGF-A (Weston *et al.*, 2002; Yang *et al.*, 2002) were also up-regulated by endometrial supernatants, such as CXC receptor-4, MMP-2 tissue factor-inhibitor-2 and VE-cadherin. Several other transcripts regulated by the endometrial supernatants have clear associations with EC survival and proliferation. For example, angiopoietin-1 was down-regulated. Angiopoietin-1 usually functions to stabilize vessels, but is functionally inhibited by angiopoietin-2 during angiogenesis. Endoglin (up-regulated) is a component of the transforming growth factor beta receptor complex that is essential for vessel development (Zhang *et al.*, 2002). PECAM-1 and VE-cadherin (both up-regulated) are EC adhesion molecules that promote EC survival through protein kinase B (AKT) signaling. Other regulated signaling molecules include; ADP ribosylation factor-like-2, interleukin-1 receptor-like-1, interferon γ receptor-2, MAP kinase-12, Rho-7 and SIVA. Several transcripts associated with the extracellular matrix were regulated in EC by endometrial supernatants. These may contribute to cyclical remodeling of both vessels and other elements of endometrium. For example, Plasminogen activator-inhibitor-1 and fibronectin-1 were up-regulated. MMP-2 and MMP-3 were also up-regulated and have previously been associated with cyclical endometrial remodelling (Ueda *et al.*, 2002) and endometriosis (Cox *et al.*, 2001).

Previous studies (summarized in the Introduction) have suggested that both endometrial and peritoneal factors promote the angiogenesis that underlies endometriosis. Our study investigated the role played by endometrial factors. We found that endometriosis had no effect on the capacity of endometrial culture supernatants to induce angiogenesis or gene expression changes in EC. In addition, we found no relationship between endometriosis and VEGF-A production by cultured endometrium or VEGF-A concentration or mass in menstrual effluent. This suggests that differences between the soluble pro-angiogenic factors secreted by the endometrium of endometriotic and non-endometriotic women may not be a major determinant of this disease. It is possible that the small size of our study (dictated by our stringent patient selection criteria and the relative rarity of unmedicated endometriotic patients) has caused us to miss a subtle role played by soluble endometrial factors. However, it is also possible that confounding and the lack of stringent patient selection may have caused some previous investigators to overestimate the role played by endometrial factors in this disease. The importance of stringent patient selection criteria and measures to reduce confounding has been highlighted in a recent study published in this journal of soluble ICAM-1 in endometriotic patients (Steff *et al.*, 2004). Models of endometriosis in which human endometrium is transplanted into immunocompromized mice (Hull *et al.*, 2003) will provide powerful tools to dissect the relative roles of endometrial and peritoneal factors.

In conclusion, we have shown that endometrium cultured *in vitro* produces soluble factors, including VEGF-A, that promote angiogenesis. Endometrium, especially from the proliferative phase of the menstrual cycle, also promotes significant pro-angiogenic changes to the EC transcriptome. However, we were unable to detect any association between endometriosis and the effects of soluble endometrial factors on EC biology or gene expression. We believe that the endometrial factor-induced EC transcriptome changes identified here provide insight into the dynamic control of vessel structure on which both the eutopic endometrium and endometriotic lesions depend. They also provide potential therapeutic targets for the modulation of endometrial angiogenesis.

Acknowledgements

We wish to acknowledge Kate Day and Isabelle Perault for technical assistance and Andrew Sharkey and Stephen Charnock-Jones for advice on endometrial culture and gene array analysis, as well as Mr Andrew Prentice and the staff of the Rosie Hospital, Cambridge, for assistance with tissue collection. This study was funded by a Wellbeing project grant. C.P. was funded by a Wellcome Trust fellowship.

References

Alvarez RJ, Gips SJ, Moldovan N, Wilhide CC, Milliken EE, Hoang AT, Hruban RH, Silverman HS, Dang CV and Goldschmidt-Clermont PJ (1997) 17beta-estradiol inhibits apoptosis of endothelial cells. Biochem Biophys Res Commun 237,372–381.

Bishop ET, Bell GT, Bloor S, Broom IJ, Hendry NFK and Wheatley DN (1999) An in vitro model of angiogenesis: Basic features. Angiogenesis 3,335–344.

Borthwick JM, Charnock-Jones DS, Tom BD, Hull ML, Teirney R, Phillips SC and Smith SK (2003) Determination of the transcript profile of human endometrium. Mol Hum Reprod 9,19–33.

Cameron IT and Campbell S (1998) Nitric oxide in the endometrium. Hum Reprod Update 4,565–569.

Charnock-Jones DS, Sharkey AM, Rajput-Williams J, Burch D, Schofield JP, Fountain SA, Boocock CA and Smith SK (1993) Identification and localization of alternately spliced mRNAs for vascular endothelial growth factor in human uterus and estrogen regulation in endometrial carcinoma cell lines. Biol Reprod 48,1120–1128.

Cox KE, Piva M and Sharpe-Timms KL (2001) Differential regulation of matrix metalloproteinase-3 gene expression in endometriotic lesions compared with endometrium. Biol Reprod 65,1297–1303.

Donnez J, Smoes P, Gillerot S, Casanas-Roux F and Nisolle M (1998) Vascular endothelial growth factor (VEGF) in endometriosis. Hum Reprod 13,1686–1690.

Evans AL, Sharkey AS, Saidi S, Print CG, Catalano R, Smith SK and Charnock-Jones DS (2003) Generation and Use of a Tailored Gene Array to Investigate Vascular Biology. Angiogenesis 6,93–104.

Ferriani RA, Charnock-Jones DS, Prentice A, Thomas EJ and Smith SK (1993) Immunohistochemical localization of acidic and basic fibroblast growth factors in normal human endometrium and endometriosis and the detection of their mRNA by polymerase chain reaction. Hum Reprod 8,11–16.

Folkman J (2002) Role of angiogenesis in tumor growth and metastasis. Semin Oncol 29,15–18.

Freitas S, Meduri G, Le Nestour E, Bausero P and Perrot-Applanat M (1999) Expression of metalloproteinases and their inhibitors in blood vessels in human endometrium. Biol Reprod 61,1070–1082.

Fujiwaki R, Hata K, Iida K, Maede Y, Watanabe Y, Koike M and Miyazaki K (1999) Co-expression of vascular endothelial growth factor

and thymidine phosphorylase in endometrial cancer. Acta Obstet Gynecol Scand 78,728–734.

Gargett CE, Lederman F, Heryanto B, Gambino LS and Rogers PA (2001) Focal vascular endothelial growth factor correlates with angiogenesis in human endometrium; role of intravascular neutrophils. Hum Reprod 16, 1065–1075.

Gargett CE, Lederman FL, Lau TM, Taylor NH and Rogers PA (1999) Lack of correlation between vascular endothelial growth factor production and endothelial cell proliferation in the human endometrium. Hum Reprod 14, 2080–2088.

Gargett CE and Rogers PA (2001) Human endometrial angiogenesis. Reproduction 121,181–186.

Hague S, MacKenzie IZ, Bicknell R and Rees MC (2002) In-vivo angiogenesis and progestogens. Hum Reprod 17,786–793.

Haney AF (1990) Etiology and histogenesis of endometriosis. Prog Clin Biol Res 323,1–14.

Hii LL and Rogers PA (1998) Endometrial vascular and glandular expression of integrin alpha(v)beta3 in women with and without endometriosis. Hum Reprod 13,1030–1035.

Hull ML, Charnock-Jones DS, Chan CL, Bruner-Tran KL, Osteen KG, Tom BD, Fan TP and Smith SK (2003) Antiangiogenic agents are effective inhibitors of endometriosis. J Clin Endocrinol Metab 88,2889–2899.

Iruela-Arispe ML, Rodriguez-Manzaneque JC and Abu-Jawdeh G (1999) Endometrial endothelial cells express estrogen and progesterone receptors and exhibit a tissue specific response to angiogenic growth factors. Microcirculation 6,127–140.

Jaffe EA, Nachman RL, Becker CG and Minick CR (1973) Culture of human endothelial cells derived from umbilical veins; identification by morphologic and immunologic criteria. J Clin Invest 52,2745–2756.

Johnson N, Sengupta S, Lessan K, Charnock-Jones DS, Saidi S, Scott L, Stephens R, Freeman T, Tom B, Harris M et al. (2003) Endothelial Cells preparing to die by apoptosis initiate a program of transcriptome and glycome regulation. FASEB J 18,188–190.

Kahn J, Mehraban F, Ingle G, Xin X, Bryant JE, Vehar G, Schoenfeld J, Grimaldi CJ, Peale F, Draksharapu A et al. (2000) Gene expression profiling in an in vitro model of angiogenesis. Am J Pathol 156,1887–1900.

Kao LC, Germeyer A, Tulac S, Lobo S, Yang JP, Taylor RN, Osteen K, Lessey BA and Giudice LC (2003) Expression profiling of endometrium from women with endometriosis reveals candidate genes for disease-based implantation failure and infertility. Endocrinology 144,2870–2881.

Kats R, Collette T, Metz CN and Akoum A (2002) Marked elevation of macrophage migration inhibitory factor in the peritoneal fluid of women with endometriosis. Fertil Steril 78,69–76.

Khan KN, Masuzaki H, Fujishita A, Kitajima M, Sekine I and Ishimaru T (2003) Immunoexpression of hepatocyte growth factor and c-Met receptor in the eutopic endometrium predicts the activity of ectopic endometrium. Fertil Steril 79,173–181.

Kim SH, Choi YM, Chae HD, Kim KR, Kim CH and Kang BM (2001) Increased expression of endoglin in the eutopic endometrium of women with endometriosis. Fertil Steril 76,918–922.

Kohnen G, Campbell S, Jeffers MD and Cameron IT (2000) Spatially regulated differentiation of endometrial vascular smooth muscle cells. Hum Reprod 15,284–292.

Krikun G, Schatz F, Finlay T, Kadner S, Mesia A, Gerrets R and Lockwood CJ (2000) Expression of angiopoietin-2 by human endometrial endothelial cells: regulation by hypoxia and inflammation. Biochem Biophys Res Commun 275,159–163.

Li XF, Charnock-Jones DS, Zhang E, Hiby S, Malik S, Day K, Licence D, Bowen JM, Gardner L, King A et al. (2001) Angiogenic growth factor messenger ribonucleic acids in uterine natural killer cells. J Clin Endocrinol Metab 86,1823–1834.

Long AD, Mangalam HJ, Chan BY, Tolleri L, Hatfield GW and Baldi P (2001) Improved statistical inference from DNA microarray data using analysis of variance and a Bayesian statistical framework Analysis of global gene expression in Escherichia coli K12. J Biol Chem 276, 19937–19944.

McLaren J, Prentice A, Charnock-Jones DS, Millican SA, Muller KH, Sharkey AM and Smith SK (1996) Vascular endothelial growth factor is produced by peritoneal fluid macrophages in endometriosis and is regulated by ovarian steroids. J Clin Invest 98,482–489.

Mints M, Blomgren B, Falconer C and Palmblad J (2002) Expression of the vascular endothelial growth factor (VEGF) family in human endometrial blood vessels. Scand J Clin Lab Invest 62,167–175.

Moller B, Lindblom B and Olovsson M (2002) Expression of the vascular endothelial growth factors B and C their receptors in human endometrium during the menstrual cycleC. Acta Obstet Gynecol Scand 81,817–824.

Morales DE, McGowan KA, Grant DS, Maheshwari S, Bhartiya D, Cid MC, Kleinman HK and Schnaper HW (1995) Estrogen promotes angiogenic activity in human umbilical vein endothelial cells in vitro and in a murine model. Circulation 91,755–763.

Nikitenko LL, MacKenzie IZ, Rees MC and Bicknell R (2000) Adrenomedullin is an autocrine regulator of endothelial growth in human endometrium. Mol Hum Reprod 6,811–819.

Nishizuka I, Ichikawa Y, Ishikawa T, Kamiyama M, Hasegawa S, Momiyama N, Miyazaki K and Shimada H (2001) Matrilysin stimulates DNA synthesis of cultured vascular endothelial cells and induces angiogenesis in vivo. Cancer Lett 173,175–182.

Noda T, Murakami T, Terada Y, Yaegashi N and Okamura K (2003) Increased production of tumor necrosis factor-alpha by peritoneal fluid mononuclear cells induced by 60 kDa heat shock protein in women with minimal to mild endometriosis. Am J Reprod Immunol 50,427–432.

Richter ON, Dorn C, Rosing B and Ulrich U (2004) Tumour necrosis factor alpha secretion by peritoneal macrophages in patients with endometriosis. Arch Gynecol Obstet. In press.

Rodrigues S, Van Aken E, Van Bocxlaer S, Attoub S, Nguyen QD, Bruyneel E, Westley BR, May FE, Thim L, Mareel M et al. (2003) Trefoil peptides as proangiogenic factors in vivo and in vitro: implication of cyclooxygenase-2 and EGF receptor signalling. FASEB J 17,7–16.

Rogers PA, Lederman F and Taylor N (1998) Endometrial microvascular growth in normal and dysfunctional states. Hum Reprod Update 4, 503–508.

Sage EH, Reed M, Funk SE, Truong T, Steadele M, Puolakkainen P, Maurice DH and Bassuk JA (2003) Cleavage of the matricellular protein SPARC by matrix metalloproteinase 3 produces polypeptides that influence angiogenesis. J Biol Chem 278,7849–7857.

Sandberg T, Ehinger A and Casslen B (2001) Paracrine stimulation of capillary endothelial cell migration by endometrial tissue involves epidermal growth factor and is mediated via up-regulation of the urokinase plasminogen activator receptor. J Clin Endocrinol Metab 86,1724–3170.

Sharkey AM, Day K, McPherson A, Malik S, Licence D, Smith SK and Charnock-Jones DS (2000) Vascular endothelial growth factor expression in human endometrium is regulated by hypoxia. J Clin Endocrinol Metab 85,402–409.

Sillem M, Prifti S, Neher M and Runnebaum B (1998) Extracellular matrix remodelling in the endometrium and its possible relevance to the pathogenesis of endometriosis. Hum Reprod Update 4,730–735.

Smith SK (1997) Angiogenesis. Semin Reprod Endocrinol 15,221–227.

Steff AM, Gagne D, Page M, Hugo P and Gosselin D (2004) Concentration of soluble intercellular adhesion molecule-1 in serum samples from patients with endometriosis collected during the luteal phase of the menstrual cycle. Hum Reprod 19,172–178.

Steff AM, Gagne D, Page M, Rioux A, Hugo P and Gosselin D (2004) Serum concentrations of insulin-like growth factor-1, soluble tumor necrosis factor receptor-1 and angiogenin in endometriosis patients. Am J Reprod Immunol 51,166–173.

Suzumori N, Sugiura-Ogasawara M, Katano K and Suzumori K (2003) Women with endometriosis have increased levels of placental growth factor in the peritoneal fluid compared with women with cystadenomas. Hum Reprod 18,2595–2598.

Ueda M, Yamashita Y, Takehara M, Terai Y, Kumagai K, Ueki K, Kanda K, Yamaguchi H, Akise D, Hung YC et al. (2002) Survivin gene expression in endometriosis. J Clin Endocrinol Metab 87,3452–3459.

Unemori EN, Erikson ME, Rocco SE, Sutherland KM, Parsell DA, Mak J and Grove BH (1999) Relaxin stimulates expression of vascular endothelial growth factor in normal human endometrial cells in vitro and is associated with menometrorrhagia in women. Hum Reprod 14,800–806.

Weston GC, Haviv I and Rogers PA (2002) Microarray analysis of VEGF-responsive genes in myometrial endothelial cells. Mol Hum Reprod 8, 855–863.

Wingfield M, Macpherson A, Healy DL and Rogers PA (1995) Cell proliferation is increased in the endometrium of women with endometriosis. Fertil Steril 64,340–346.

Wu MY, Chao KH, Yang JH, Lee TH, Yang YS and Ho HN (2003) Nitric oxide synthesis is increased in the endometrial tissue of women with endometriosis. Hum Reprod 18,2668–2671.

Yang S, Toy K, Ingle G, Zlot C, Williams PM, Fuh G, Li B, de Vos A and Gerritsen ME (2002) Vascular endothelial growth factor-induced genes in

human umbilical vein endothelial cells: relative roles of KDR and Flt-1 receptors. Arterioscler Thromb Vasc Biol 22,1797–1803.

Yasuda Y, Masuda S, Chikuma M, Inoue K, Nagao M and Sasaki R (1998) Estrogen-dependent production of erythropoietin in uterus and its implication in uterine angiogenesis. J Biol Chem 273,25381–25387.

Yue TL, Wang X, Louden CS, Gupta S, Pillarisetti K, Gu JL, Hart TK, Lysko PG and Feuerstein GZ (1997) 2-Methoxyestradiol, an endogenous estrogen metabolite, induces apoptosis in endothelial cells and inhibits angiogenesis: possible role for stress-activated protein kinase signaling pathway and Fas expression. Mol Pharmacol 51,951–962.

Zhang EG, Smith SK and Charnock-Jones DS (2002) Expression of CD105 (endoglin) in arteriolar endothelial cells of human endometrium throughout the menstrual cycle. Reproduction 124,703–711.

Submitted on November 5, 2003; resubmitted on May 18, 2004; accepted on June 16, 2004

PUBLICATION 7

Xu, F., T. M. Hazzard, **A. Evans,** S. Charnock-Jones, S. Smith, and R. L. Stouffer. 2005. Intraovarian Actions of Anti-Angiogenic Agents Disrupt Periovulatory Events During the Menstrual Cycle in Monkeys. *Contraception* 71, (4), 239-48

Cited by 29, Impact factor 2.724

ISSN: 0010-7824

Journal Type

The journal Contraception covers all aspects of contraception from cost effectiveness, safety and failure rates to original research such as this article on prevention of implantation. Manuscripts are accepted from both clinicians and researchers.

Personal Contribution

For this project my role was to take a secondary hybridoma producing monoclonal anti human VEGF-A and from it create a tertiary clone. The line (4E3) was produced from a cross between B cells and NSO, a mouse myeloma non - IgG producing cell. Alongside this, another hybridoma line (NQ10) producing mouse anti human IgG_1 as an isotype control was produced. Antibody was then produced on a large scale in bioreactors, quantified by developing an in-house ELISA assay, and finally purified by FPLC (ÄKTAprime™, GE Healthcare) for *in vivo* injections.

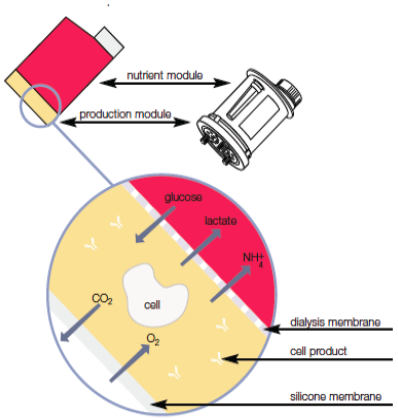

miniPERM Bioreactor
(VIVASCIENCE, Sartorius ,UK).
The semi-permeable membrane allows the nutrient module to provide nutrients and a high buffering capacity, waste products diffuse out to be diluted in the nutrient module, rotation speeds are optimised for maximum production

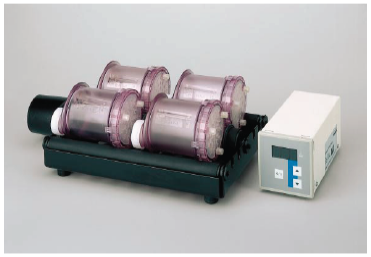

Available online at www.sciencedirect.com

SCIENCE DIRECT

Contraception 71 (2005) 239–248

Contraception

Review article

Intraovarian actions of anti-angiogenic agents disrupt periovulatory events during the menstrual cycle in monkeys

Fuhua Xu[a], Timothy M. Hazzard[a], Amanda Evans[b], Stephen Charnock-Jones[b], Stephen Smith[c], Richard L. Stouffer[a,*]

[a]*Division of Reproductive Sciences, Oregon National Primate Research Center, Oregon Health and Science University, Beaverton, OR 97006-3499, USA*
[b]*Department of Obstetrics and Gynecology, the Rosie Maternity Hospital, University of Cambridge, Cambridge CB2 2SW, UK*
[c]*Faculty of Medicine, Imperial College, London SW7 2AZ, UK*

Received 28 October 2004; accepted 2 December 2004

Abstract

To determine if anti-angiogenic agents disrupt primate ovarian function, vehicle or a general angiostatic compound (TNP-470), specific antagonists of vascular endothelial growth factor (soluble VEGF receptor-1, sVEGFR-1; anti-VEGF monoclonal antibody, VEGF Ab) and/or an angiopoietin antagonist (Ang-2) were administered to rhesus monkeys: (1) locally via injection into the preovulatory follicle at midcycle or the developing corpus luteum at the midluteal phase; or (2) systemically via subcutaneous injection in the early follicular phase or at midcycle during the natural menstrual cycle. Compared to controls, intrafollicular injection of TNP-470 or sVEGFR-1 decreased circulating progesterone (P) levels in the subsequent luteal phase. Treatment with sVEGFR-1, but not TNP-470, also decreased the incidence of ovulation. Intrafollicular injection of Ang-2 also prevented ovulation, as well as any functional luteal phase. In the absence of elevated P, serum estradiol levels rose to peak levels 11–12 days post-Ang-2 treatment, at which time another large antral follicle was observed on the contralateral (noninjected) ovary. Intraluteal and systemic injection of VEGF antagonists alone or with Ang-2 had minimal effects. Thus, anti-angiogenic factors can act locally in the primate follicle to disrupt the gametogenic (oocyte release) and endocrine (steroid) functions of the ovary. However, further studies are needed to optimize delivery of angiogenic agents before they can be meaningfully evaluated as possible contraceptive agents.

Keywords: Vascular endothelial growth factor; VEGF; Angiopoietin-2; Ovulation; Corpus luteum function; Rhesus monkeys; Ovarian disruption

1. Introduction

Aside from pathologic and trauma conditions, blood vessel development in healthy adults is primarily limited to the ovary and reproductive tract, that is, tissues that undergo sequential growth and regression during the ovarian cycle. In recent years, investigators have attempted to elucidate the factors and processes controlling vessel development, that is, angiogenesis, during follicle growth and subsequent development of the corpus luteum from the post-ovulatory follicle [1,2]. Considerable progress occurred with the realization that two classes of factors with a high degree of specificity of action on endothelial/peri-endothelial cells in the vasculature, namely, the vascular endothelial growth factors (VEGF) and angiopoietins (Ang), are present in ovarian follicles and corpora lutea (see reviews, [3–5]).

Members of the VEGF family (A-F), as well as isoforms of individual VEGFs (e.g., the 165-amino-acid form of VEGF-A), are found in many tissues during embryonic development and are believed to play critical roles in vasculogenesis [6]. However, their expression is more limited in adults, with most interest in VEGF pertaining to its production and actions in the vascular bed of diseased tissues (e.g., cancers). Attention to date in the ovary has focused on VEGF-A, and it is now evident that its lower molecular weight, secreted forms (VEGF-121 and -165) [7,8], its two receptors (VEGFR-1 and -2) [9,10] and possibly two coreceptors (neuropilin-1 and -2) [11] are expressed in ovarian tissues, including the primate ovary. Although mounting evidence, especially from the past 5 years, suggests that VEGF-A is important for vessel

* Corresponding author.
E-mail address: stouffri@ohsu.edu (R.L. Stouffer).

0010-7824/$ – see front matter © 2005 Elsevier Inc. All rights reserved.
doi:10.1016/j.contraception.2004.12.017

development in ovarian compartments [3–5], an emerging model (Fig. 1) proposes that the angiopoietins combine with VEGF to control vessel maturation, function and stability [12]. Notably, an endogenous Ang agonist, Ang-1, may act to promote vessel maturation, whereas the endogenous Ang antagonist, Ang-2, may cause vessel destruction [12]. There are few reports on Ang receptor (Tie-2) expression or action in the ovary [13–15], but there are observations that Ang-1 (not Ang-2) expression is elevated in luteinizing cells of the ovulatory follicle [16], whereas Ang-2 expression is associated with follicle atresia [17] and corpus luteum regression [13].

The importance of increased vascularity for follicle growth and subsequent corpus luteum development has been implied for years [1–3]. If true, it could be hypothesized that treatment with anti-angiogenic agent would disrupt vessel development and function (and perhaps cause vessel degeneration; Fig. 1), thereby preventing the gametogenic (oocyte) and endocrine (steroid hormone) functions of the ovary. From an applied perspective, anti-angiogenic agents could have contraceptive potential due to the limited sites of angiogenesis in the adult female, and potential actions on both the ovary and reproductive tract [18,19] as a dual approach to blocking pregnancy initiation. Therefore, studies were designed to examine the effects of three classes of anti-angiogenic agents: (1) a general angiostatic compound; (2) a specific VEGF-A antagonist; and (3) an Ang antagonist — on ovarian function when either delivered directly into the dominant structure (dominant follicle or corpus luteum) of the ovary or systemically during the menstrual cycle in a nonhuman primate model, the rhesus monkey. The former approach offers the advantage of examining the direct effects of agents in the ovary, whereas the latter approach was considered a prelude to future studies testing the contraceptive efficiency of antiangiogenic agents in monkeys. Due to the limited availability of other agents, systemic delivery was only possible using the anti-VEGF antibody.

The effects of intrafollicular delivery of general angiostatic compounds [20] and lower doses of a VEGF antagonist [21] on ovarian function were published previously. The Results section will summarize these findings and then describe in detail the data from studies involving intrafollicular injection of high-dose anti-VEGF or Ang antagonist, plus the results from studies of their local injection into the corpus luteum or systemic delivery.

2. Materials and methods

2.1. Animals

The general care and housing of rhesus monkeys was provided by the Division of Animal Resources at the Oregon National Primate Research Center (ONPRC) [22]. Animal protocols and experiments were approved by the ONPRC Animal Care and Use Committee, and studies were conducted in accordance with the *Guide for the Care and Use of Laboratory Animals* [23].

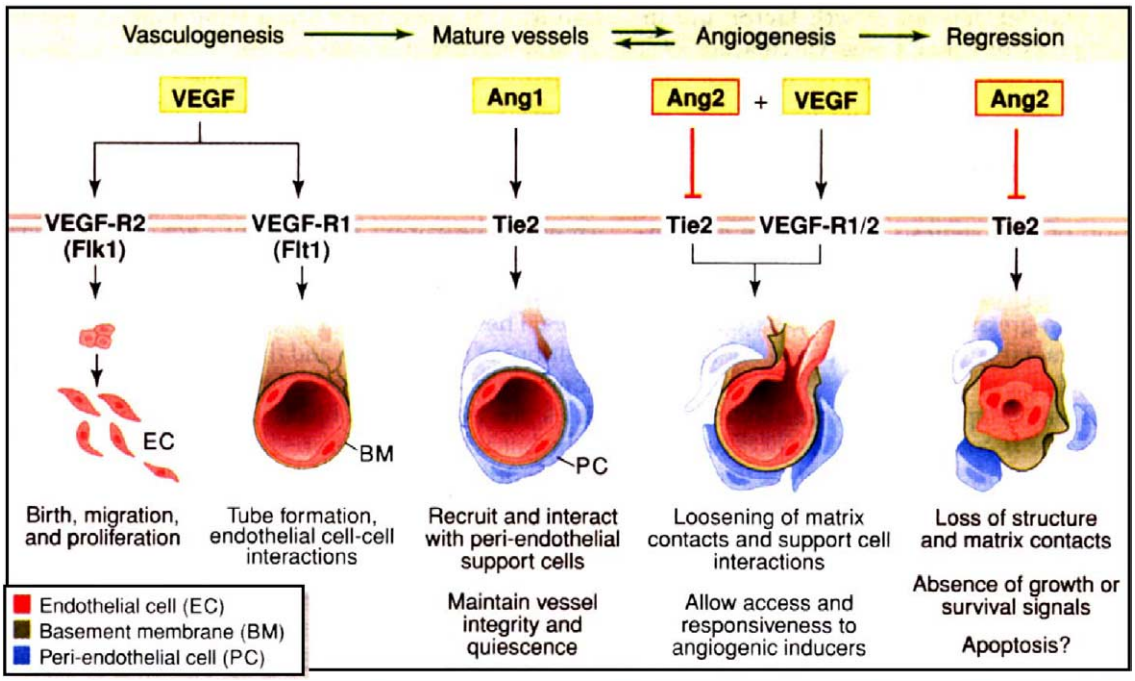

Fig. 1. A model for regulation of blood vessel development, maintenance, remodeling and degeneration, by VEGF and the endogenous angiopoietin agonist (Ang-1) and antagonist (Ang-2), via their receptor tyrosine kinases VEGFR-1 (Flt-1) or -2 (Flk-1) and Tie-2, respectively. Although originally proposed by Hanahan in 1997 (reprinted with permission from Ref. [12]. Illustration by K. Sutliff, © 1997 AAAS), this model can be applied to the cycle of vessel development and regression associated with follicle growth vs. atresia, and corpus luteum development vs. luteolysis during the ovarian cycle. Thus, blockade of vessel development or function, via specific VEGF or Ang antagonist, could disrupt normal gametogenic and endocrine function of the ovary and hence impair fertility.

Adult, female rhesus monkeys exhibiting normal menstrual cycles of approximately 28 days were bled daily by saphenous venipuncture beginning 6–8 days after the onset of menses. Serum concentrations of estradiol (E) and progesterone (P) were measured by RIAs validated for nonhuman primates in phase I [24,25]. In phase II, the serum E and P levels were determined by specific electrochemoluminescent assay using a Roche Elecsys 2010 Analyzer (Roche, Indianapolis, IN) in the Endocrine Services Laboratory of the ONPRC [26]. The interassay variation was 6.1% for E and 5.4% for P, and the limit of sensitivity was 5 pg/mL for E and 0.03 ng/mL for P. Estradiol values were used to estimate the day of the midcycle gonadotropin surge and time of ovulation as previously established in our laboratory [27]. Day 1 of the luteal phase is designated as the day when preovulatory serum E levels (range, 250–600 pg/mL) decline to less than 100 pg/mL [27].

2.2. Intrafollicular injection

Intrafollicular injection was performed as previously described [20,21] on anesthetized animals during surgery to expose the ovary bearing the dominant follicle on the day before (day −1) or the day of (day 0) the midcycle LH surge. The needle on an insulin syringe containing 50 μL of the test solution was inserted through the stroma of the ovary before penetrating the follicular wall. Then 50 μL of follicular fluid was aspirated into the syringe, diluting the syringe contents by half, before injecting 50 μL of this mixed solution into the follicle. Upon removal of the needle, the follicle was observed to make sure that deflation did not occur. Ovaries were viewed and photographed by laparoscopy at 3 days postinjection for evidence of follicle rupture and luteinization. Blood samples were collected on a daily basis until the first day of menses and analyzed for serum P levels. The day of the LH surge was confirmed, using a mouse Leydig cell bioassay for LH [28], and verified that all animals were injected on the day before (day −1) or the day of (day 0) the midcycle gonadotropin surge.

A sequential experimental design was typically employed whereby animals received an intrafollicular injection of vehicle (0.1% BSA in PBS, $n=14$ per drug), and then either a general angiostatic compound (TNP-470, also known as AGM-1470; Takeda Abbot Pharmaceuticals, Lake Forest, IL [29]), a specific VEGF antagonist (recombinant human soluble VEGFR-1/Fc chimera, sVEGFR-1; R&D Systems, Minneapolis, MN) or the endogenous Ang antagonist (recombinant human angiopoietin-2, Ang-2; R&D Systems) in subsequent treatment cycles. Although the general protocol typically does not alter ovarian function [28], the sequential approach beginning with vehicle injection permits identification of the rare animal that may be stressed and/or exhibits an aberrant ovarian cycle, enabling such animals to be removed from the treatment protocols. TNP-470 was selected for study based on evidence that treatment resulted in fewer and smaller corpora lutea in mice [29]. The final delivery doses of TNP-470 were 80 pg ($n=4$) and 400 ng ($n=5$); the former dose achieved an initial concentration in the dominant follicle (~200 μL antral fluid volume) that approximated the reported IC_{50} for endothelial cell proliferation [30]. A soluble VEGF receptor-1 (sVEGFR-1) compound was used to bind and neutralize angiogenic VEGF moieties (notably VEGF-A, but also VEGF-B), rather than sVEGFR-2 agents which also bind lymphangiogenic moieties (VEGF-C, VEGF-D as well as VEGF-A) [6]. The final delivery doses of sVEGFR-1 were 1.5 μg ($n=4$), 7.5 μg ($n=4$) and 30 μg ($n=3$). The final delivery dose of Ang-2 was 20 μg ($n=5$). After menses in each protocol, animals were permitted to recover for at least one menstrual cycle before blood samples were taken to start the next protocol.

In further protocols, TNP-470- and sVEGFR1-treated animals again acted as their own controls but were assigned randomly to receive an intrafollicular injection of either vehicle or the compound on day −1 or day 0. Animals were laparotomized 3 days after the injection and the ovary bearing the injected follicle was removed and fixed in formaldehyde overnight before embedding in paraffin. The paraffin-embedded tissues were serially sectioned using an American Optical (Southbridge, MA) microtome and mounted on Superfrost Plus slides (Fisher, Santa Clara, CA). Slides were stained with hematoxylin and eosin and viewed to determine if the oocyte was released from the follicle or trapped within the luteinized tissue.

2.3. Intraluteal injection

Intraluteal injection was performed on anesthetized animals during surgery to expose the ovary bearing the corpus luteum on day 6 of the luteal phase [21]. The needle on an insulin syringe containing 30 μL of solution was inserted through the stroma of the ovary before penetrating the corpus luteum. After injecting 10 μL of solution, 30 s was allowed for the solution to disseminate in the corpus luteum. Upon removal of the needle, no leakage was observed from the injection site. Blood samples were collected on a daily basis until the first day of menses and analyzed for serum P levels.

Again, a sequential experimental design was typically employed with vehicle (0.1% BSA in PBS, $n=10$) serving as control in the first protocol. A dose of 1.1 μg sVEGFR-1 ($n=4$), 15 μg sVEGFR-1 ($n=3$) or 15 μg sVEGFR-1 plus 20 μg Ang-2 ($n=3$) was injected in subsequent treatment protocols.

2.4. Systemic injection

Systemic injection was performed at subcutaneous sites. Animals were injected with monkey IgG (10 mg, Sigma, St. Louis, MO) on the days noted below as a control in the first protocol. In the subsequent protocol, one group of animals ($n=4$) received 10 mg anti-VEGF antibody (supplied by Dr. Stephen Charnock-Jones, Department of Obstetrics and Gynaecology, University of Cambridge, UK) on days 1, 3

and 5 of the follicular phase in the menstrual cycle. Another group of animals ($n=4$) received the same dose of anti-VEGF antibody on the day before or the day of the midcycle LH surge, and 2 days later. Blood samples were collected on a daily basis until the first day of next menses and analyzed for serum E and P levels.

2.5. Statistics

E and P levels in serum were analyzed by ANOVA with repeated measures to identify differences between controls and each treatment group (SigmaStat statistical software version 2.0, Chicago, IL). Differences were considered significant at $p<.05$ and values are presented as mean±SEM.

3. Results

3.1. Phase I: intrafollicular delivery of the anti-angiogenic agent TNP-470 [20]

We reported previously [20] that intrafollicular injection of vehicle into the preovulatory follicle of rhesus monkeys during spontaneous menstrual cycles resulted in circulating patterns and levels of serum E and P that were typically comparable to those observed in untreated animals in our colony [31]. Only 1 of the 14 animals did not display the typical patterns and was eliminated from further treatment protocols. In contrast, when TNP-470 (80 pg) was injected, serum P levels increased normally until the midluteal (day 8) phase, but then declined prematurely by day 9 ($p<.05$, compared to vehicle control) and remained below control levels until menses. Early menstruation also occurred in three of four TNP-470-treated animals. Following a higher dose (400 ng) of TNP-470, serum P levels were somewhat diminished in the early luteal phase (days 3–5, $p<.05$), but again reached typical levels at the midluteal phase, only to decline prematurely by day 9 ($p<.05$).

Vehicle-injected ovaries displayed indices of follicle rupture (protruding stigmata) and luteinization (yellowish tissue with prominent vessels) by 3 days postinjection. TNP-470-treated ovaries exhibited signs of distension (torn surface epithelium/tunica albuginea) and luteinization, but well-formed stigmata were not observed. However, upon serial sectioning of the tissue, a "trapped" oocyte was not observed in the developing corpora lutea of TNP-470-treated, nor in the vehicle-treated animals. Nevertheless, the early corpus luteum in TNP-470-injected ovaries contained pockets of abundant blood cells that were not observed in controls.

3.2. Phase II: delivery of anti-VEGF antagonist

3.2.1. Intrafollicular injection of sVEGFR-1

We reported previously [21] the results of injecting either vehicle or two different doses of sVEGFR-1 into the preovulatory follicle of rhesus monkeys during natural menstrual cycles. As noted in phase I, vehicle injection did not result in any changes in ovarian function in 13 of 14 animals. After vehicle injection, P levels (Fig. 2A, shaded region) increased on day 0 and continued to rise until the midluteal phase (days 5–10) and then declined through the late luteal phase until menstruation. Likewise, injection of low dose sVEGFR-1 (1.5 μg) into the preovulatory follicle did not significantly alter P levels as a group ($n=4$) compared to controls. However, when treated animals were examined individually [21] (data not shown), low-dose sVEGFR-1 injection suppressed P concentrations during the early to midluteal phase in two of four animals. However, there was no change in the day of menstruation between the

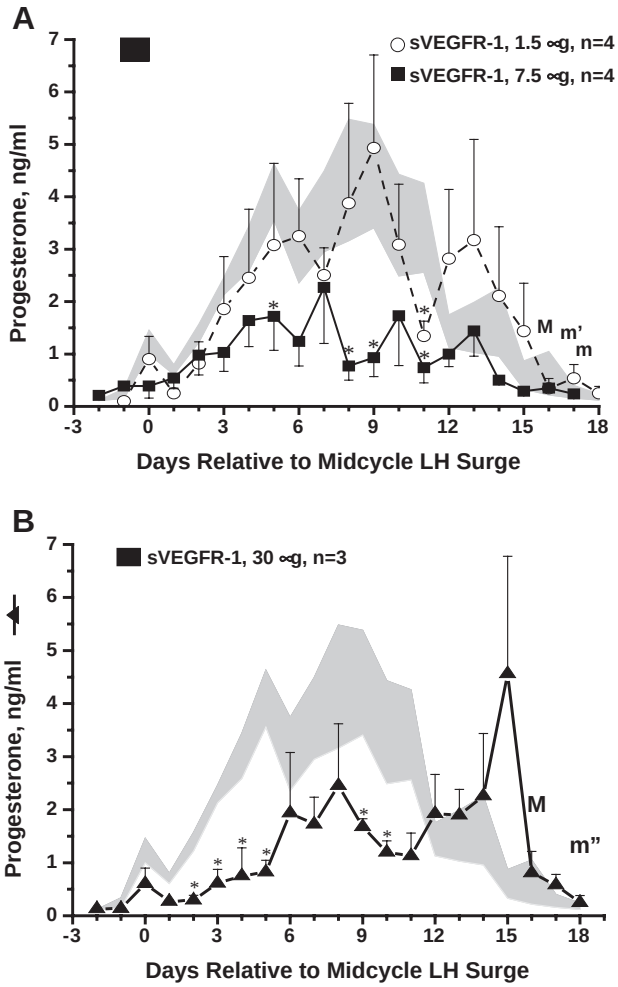

Fig. 2. Serum P levels in monkeys receiving an intrafollicular injection of a low, medium (panel A; adapted from Ref. [21]) or high (panel B; unpublished data) dose of sVEGFR-1 compared to vehicle-injected controls (shaded area=mean±SEM, $n=13$). Block rectangle depicts day of injection (day −1 to day 0 of LH surge) of the preovulatory follicle. Asterisks indicate significant ($p<.05$) differences in P concentrations on specific days. "M" denotes average days of onset of menstruation in controls, whereas an "m/m′/m″" depicts onset in low/medium/high dose of sVEGFR-1-treated animals. Although low-dose sVEGFR-1 treatment did not alter P levels as a group ($n=4$), levels were decreased in two of four animals (see Ref. [16]) until mid late luteal phase. The medium- and high-dose treatments significantly suppressed P levels until late luteal phase.

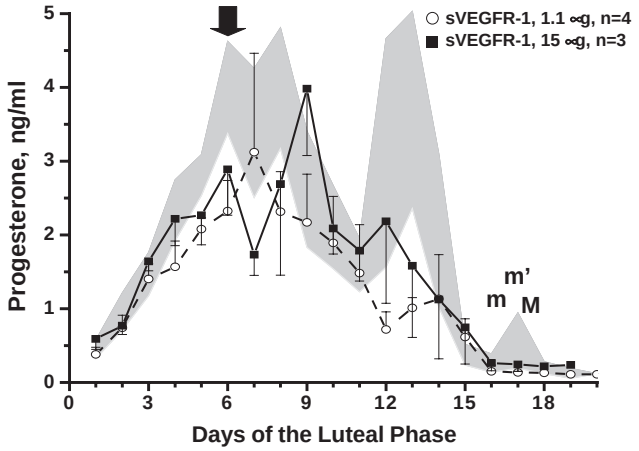

Fig. 3. Serum P levels in monkeys receiving an intraluteal injection of a low or high dose of sVEGFR-1 at midluteal phase compared to vehicle-injected controls (shaded area = mean ± SEM, $n = 7$). The arrow depicts the injection on day 6 of the luteal phase. "M" denotes average days of onset of menstruation in controls, "m" and "m′" depicts menses onset in low- and high-dose treatment groups. There were no significant effects of either treatment dose.

controls and low-dose sVEGFR-1-treated groups. Administration of higher dose of sVEGFR-1 (7.5 μg) resulted in a consistent hormonal profile (Fig. 2A). In all four animals, serum P concentrations were significantly reduced compared to controls ($p < .05$), with suppressed levels by the midluteal phase, which remained low until the late luteal phase. Again, however, there was no change in the day of onset of menstruation after sVEGFR-1 treatment. Following this initial report on the dose-response effects of sVEGFR-1 [21], an even greater dose (30 μg) was tested to determine if the luteal phase could be completely ablated. This highest dose of sVEGFR-1 (30 μg) significantly reduced serum P concentrations compared to controls ($p < .05$) from the early to the late luteal phase (Fig. 2B). But again, P levels rose above baseline during the luteal phase and there was no significant change in the day of menstruation between treatment and control groups.

Laparoscopic evaluation established that by 3 days after the intrafollicular injection all vehicle-injected follicles ($n = 13$) displayed indices of ovulation (protruding stigmata) and luteinization (yellowish tissue with prominent capillaries) [21]. Evaluation of serial sections of ovaries collected 3 days after the intrafollicular injection of vehicle revealed an ovulatory canal [21] that ran from within the luteinizing tissue to the surface of the ovary, as well as the absence of an oocyte. However, 5 of 11 follicles injected with VEGFR-1 did not exhibit any signs of follicular rupture; two of three follicles receiving the highest dose (30 μg sVEGFR-1) exhibited signs of distension with surface blood vessels but not follicle rupture. Serial sections from sVEGFR-1-injected follicles revealed that ovulation only occurred 50% of the time (three of six animals) [21] (data not shown). In three animals, ovulation was confirmed by the presence of an ovulatory canal as well as by the absence of an oocyte. In these sections, signs of luteinization (e.g., hypertrophy of granulosa cell layers) were apparent and similar to that observed in control tissues. However, these sVEGFR-1-treated tissues contained blood cells among the luteal tissue in a quantity beyond what was observed in the control tissues. In contrast, serial sections from 3 other animals were devoid of any ovulatory canal, and in two out of three animals an intact oocyte was found within the injected follicle [21] (data not shown). These follicles displayed few signs of luteinization, with small granulosa cells still lining the basement membrane, and occasionally found in the antral space. Blood cells were detectable within the antrum of two out of three of these unruptured follicles.

3.2.2. Intraluteal injection of sVEGFR-1

In contrast to intrafollicular injection, intraluteal administration of either a low (1.1 μg) or high (15 μg) dose of sVEGFR-1 at the midluteal phase (day 6) of the cycle did not alter significantly the pattern or level of serum P compared to vehicle-treated controls (Fig. 3). Also, there was no difference in the day of menstruation between controls and either low-dose or high-dose sVEGFR-1-treated animals.

3.2.3. Systemic injection of anti-VEGF antibody

Systemic injection of anti-VEGF antibody at the beginning of the menstrual cycle (days 1, 3, and 5) appeared to delay the midcycle peak in serum E (Fig. 4) and the LH surge (not shown) by 2–3 days, as well as the peak in serum P in the luteal phase (Fig. 4) by 3–4 days, but these intervals were not significantly different from controls. Also, peak hormone levels and length of the menstrual cycle did not vary between control and VEGF-Ab treatment groups.

Anti-VEGF antibody delivered at midcycle (day −1 to 0, and 3 days post-LH surge) appeared to modestly but not

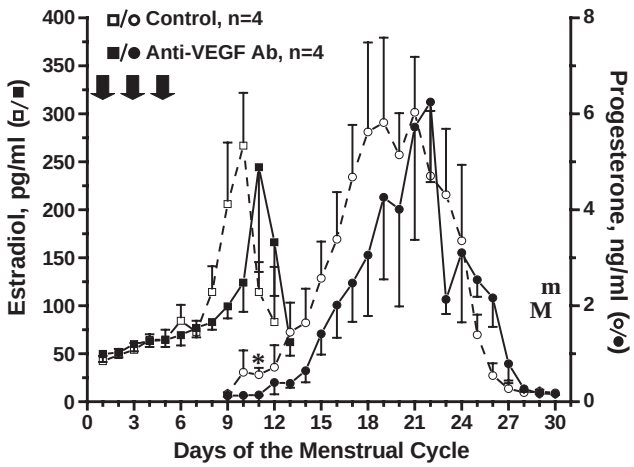

Fig. 4. Serum E and P levels in monkeys receiving vehicle (monkey IgG) or anti-VEGF antibody (10 mg) on days 1, 3 and 5 (arrows) of the menstrual cycle. "M" denotes average days of onset of menstruation in vehicle-treated controls, whereas an "m" depicts onset in VEGF Ab-treated animals. There were no significant differences between any parameters in control vs. treated cycles.

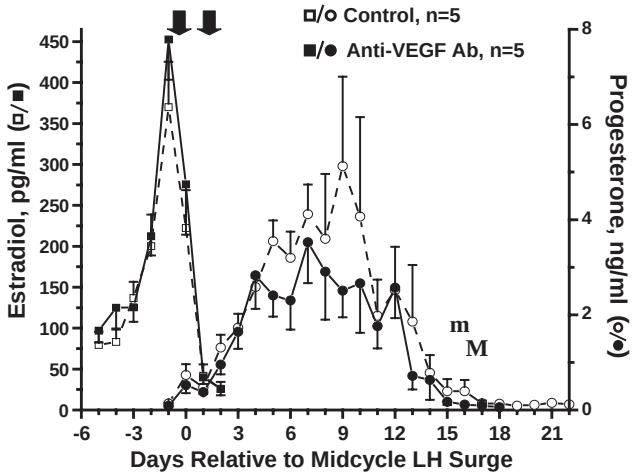

Fig. 5. Serum E and P levels in monkeys receiving vehicle (monkey IgG) or anti-VEGF antibody (10 mg) on the day before or the day of the midcycle LH surge and 2 days later (see legend of Fig. 3 for further details). Again, there were no significant differences between parameters in control vs. treated groups.

significantly decrease peak P levels (control 5.1 ng/mL; treatment 3.5 ng/mL) (Fig. 5). Again, however, the length of the luteal phase was no different between control and treatment cycles.

3.3. Phase III: delivery of Ang-2

3.3.1. Intrafollicular injection of Ang-2

Whereas vehicle injection resulted in the expected pattern and levels of serum P in the luteal phase, intrafollicular injection of Ang-2 (20 μg) resulted in P levels that never rose above baseline for 12–13 days (Fig. 6). However, only one of five Ang-2-treated animals exhibited menses

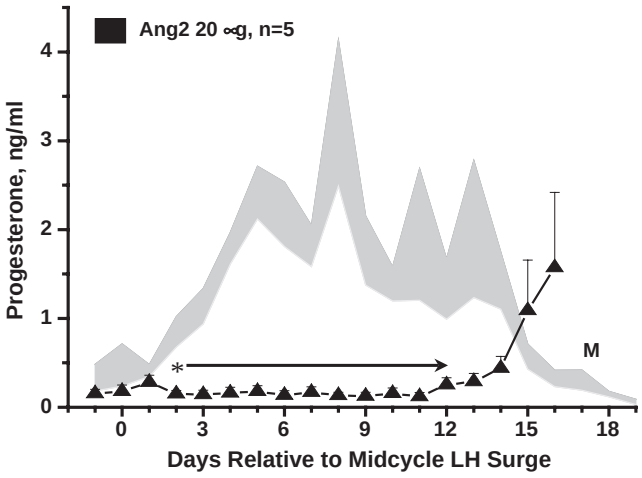

Fig. 6. Serum P levels in monkeys receiving an intrafollicular injection of Ang-2 (20 μg) at midcycle compared to vehicle-injected controls (shaded area=mean±SEM, $n=7$). An "M" denotes the average days of onset of menstruation in controls, whereas Ang-2-treated animals typically did not menstruate. An asterisk denotes the first day in the luteal phase when P levels were significantly different between groups. Ang-2-treated animals did not display a functional luteal phase for approximately 2 weeks.

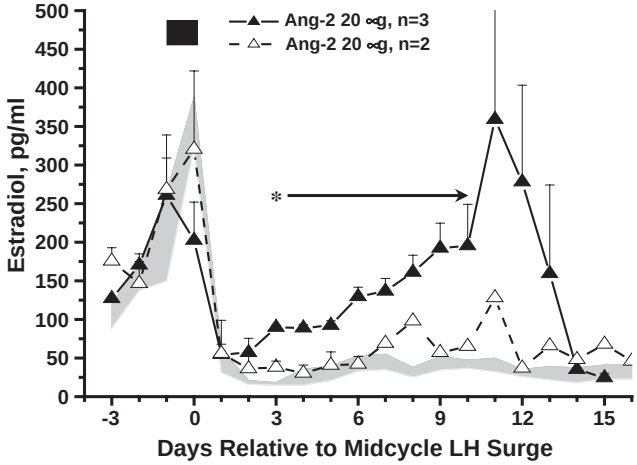

Fig. 7. Serum E levels in monkeys receiving an intrafollicular injection of Ang-2 (20 μg) at midcycle compared to vehicle-injected controls (shaded area=mean±SEM, $n=7$). An asterisk denotes the first day in the luteal phase when E levels in 3 treatment cycles (closed triangles) were significantly different from controls. Two other treatment cycles (open triangles) displayed lower peak levels at day 11 post-LH surge.

during this interval (day 7 post-LH surge). Thereafter, the rise in serum P in Ang-treated monkey coincided with its decline in control animals (days 15–16). After the preovulatory E rise at midcycle (Fig. 7), E levels declined following the LH surge and vehicle-treated animals exhibited the expected low levels during the luteal phase. In contrast, following the decline at midcycle, E levels in Ang-2-treated animals increased to reach peak levels 11–12 days after the LH surge. Three of five animals displayed peak E levels that were comparable to the prior preovulatory levels, whereas the other two animals exhibited lower peak

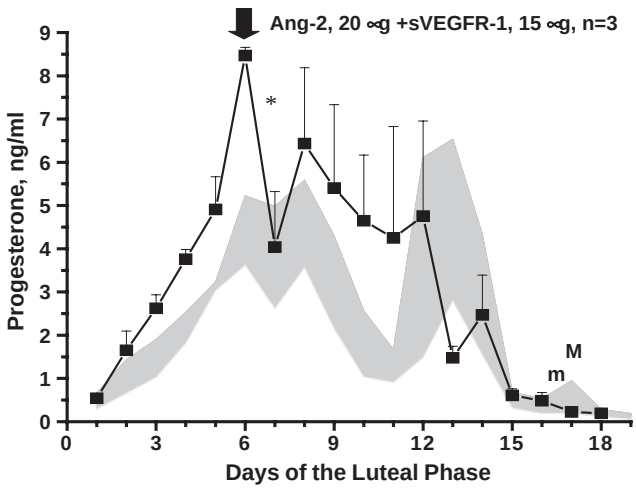

Fig. 8. Serum P levels in monkeys receiving an intraluteal injection of both Ang-2 (20 μg) and sVEGFR-1 (15 μg) at midluteal phase compared to vehicle-injected controls (shaded area=mean±SEM, $n=7$). P levels in treated cycles tended to be higher than controls both before (days 2–6) and after (days 8–11) treatment. However, P levels declined ($p<.05$, paired t test) for 1 day between days 6 and 7 (asterisk) in Ang-2+sVEGFR-1-treated animals. There was no difference between the onset of menstruation in control (M) vs. treated (m) animals.

levels. Notably, subsequent rises in serum P were noted in the former, but not the latter, animals.

Unlike in vehicle-injected controls ($n=7$), laparoscopy on day 3 did not detect any sign of ovulation in follicles injected with Ang-2 ($n=5$). However, a subsequent laparoscopy in one animal at 10 days post-Ang-2 injection detected a large follicle on the opposite (noninjected) ovary.

3.3.2. Intraluteal injection of Ang-2 plus sVEGFR-1

Injection of Ang-2 (20 μg) + sVEGFR-1 (15 μg) into the corpus luteum at the midluteal phase (day 6) did not suppress serum P levels or the length of the luteal phase compared to the control group (Fig. 8). However, serum P levels were reduced transiently (from 8.5 ± 0.2 to 4.0 ± 1.3 ng/mL; day 6 vs. 7, paired *t* test, $p<.05$) for one day following treatment.

4. Discussion

The data reported herein extend our previous published investigations demonstrating that acute local administration of a general anti-angiogenic agent TNP-470 (phase I) [20] or a specific VEGF-A antagonist (sVEGFR-1 chimera) (phase II) [21] into the preovulatory follicle can inhibit the subsequent development, function or life span of the corpus luteum, or ovulation. In our earlier report [21], we noted that intrafollicular injection of sVEGFR-1 resulted in a dose-dependent (0 vs. 1.5 vs. 7.5 μg) suppression of follicle rupture and reduced serum P levels in the subsequent luteal phase. Since ovulation and corpus luteum function was not totally abolished, a higher (30 μg) dose was tested. Although follicle rupture was not evident in two of three animals, and luteal P levels were suppressed, again ovulation and luteal function was not totally prevented. Whether experimental conditions, such as dose or treatment interval, could be improved to further optimize the anti-ovulatory and anti-luteal effects of a VEGF antagonist in the preovulatory follicle is unclear. Alternatively, it is possible that other angiogenic pathways, for example, via EG-VEGF [32] or Ang-1 [12], complement the actions of VEGF in the preovulatory follicle, and as such may continue critical ovarian functions despite suboptimal VEGF action at midcycle in primates. Nevertheless, our histologic evidence from ovaries of animals treated with sVEGFR-1 and vehicle, removed 3 and 6 days post-follicle injection [21], confirmed suppression of ovulation and luteal development/structure, as judged by trapped oocytes in nonruptured, poorly luteinized follicles and abnormal extracellular spaces (due either to lack of cell hypertrophy or cell shrinkage) in the corpus luteum. These data, plus evidence from studies by Fraser et al. [33] and Wulff et al. [34] that VEGF antagonist treatment during the early to midluteal phase reduces endothelial cell proliferation and the number of small capillaries in the nonhuman primate corpus luteum, strongly support an important role for the angiogenic, and perhaps vascular permeability, actions of VEGF-A in the preovulatory follicle and developing corpus luteum during the menstrual cycle.

It is noteworthy that unlike the current results, intrafollicular injection of a general anti-angiogenic compound, TNP-470, did not cause a decline in circulating P levels until the midluteal phase [20]. These compounds have different actions; VEGF reportedly is expressed in greater abundance in the developing vs. fully formed corpus luteum [13,35], which may explain the immediate action of sVEGFR-1 injection to suppress luteal function in the early luteal phase. In any case, sVEGFR-1 is not merely delaying normal luteal function because the duration of the luteal phase and the time of menstruation were not affected despite suppressed steroidogenic function.

In contrast to injection into the preovulatory follicle, acute, local administration of sVEGFR-1 into the developed corpus luteum at the midluteal (day 6) phase of the menstrual cycle had no apparent effect. Neither the function, as judged by P levels, or life span of the corpus luteum was altered. We hypothesized that if VEGF-A is required for the maintenance of the luteal vasculature, as well as its development, then VEGF antagonism would be detrimental to corpus luteum structure and function at the midluteal phase. The role of VEGF-A in maintaining the microvasculature in some tissues in becoming recognized [6,12], and the continued expression of VEGF-A and its receptors in the developed corpus luteum of several species [13,14,36–39] supports this premise. The negative findings of our study could result from limitations in dose, delivery or treatment interval. Unlike the preovulatory follicle, which provides an avascular antrum as a reservoir for injected substances, the highly vascularized corpus luteum may rapidly lose such substances into the circulation. Recently, Dickson et al. [40] reported that systemic administration of a VEGF antagonist to monkeys at the midluteal phase reduced circulating P levels by 50%, while suppressing proliferation and increasing apoptosis of endothelial cells in the corpus luteum. Their findings support a role for VEGF-A in maintaining the structure and function of the corpus luteum and its microvasulature in primates. Further studies attempting local delivery of anti-angiogenic agents into the corpus luteum may consider methods for continual infusion [41,42] or establishing a local reservoir [43] to sustain local, high levels. Alternatively, a role for other angiogenic factors, such as EG-VEGF [32], in the corpus luteum should be evaluated.

Also, subcutaneous administration of a neutralizing anti-VEGF monoclonal antibody (VEGF Ab) either in the early follicular phase or at midcycle had little effect on ovarian function, as judged from circulating hormone patterns, during the menstrual cycle. The VEGF Ab was utilized rather than sVEGFR-1 because of the large quantities required for systemic studies. Investigators using VEGF Abs to suppress primate reproduction in vivo report variable success from complete blockade of cyclic ovarian function [44], to significant but partial inhibition of circulating P levels during the luteal phase [40], to no

significant effect on steroid hormone levels or patterns (current data). Again, differences could be related to antibody binding affinity, dose and treatment regimens. However, recent studies suggest that antagonists that are VEGFR-1-IgG and/or VEGFR-2-IgG chimeras, rather than immunoneutralizing antibodies, are better at inhibiting angiogenesis [45] and disrupting mature, preexisting vessels [46]. The authors speculate that this is due to higher affinity of the VEGFR moieties, compared to VEGF Abs, for endogenous VEGF. However, the possibility that VEGFR antagonists have a greater effect due to blockade of other factors, for example, PlGF, VEGF-B that may act in the ovary [47], awaits investigation.

Further testing will be required to determine if anti-VEGF agents offer promise as contraceptive agents. Initial reports using an anti-VEGF Ab in marmosets [48] and a DNA vaccine against VEGFR in mice [49] reported no antifertility effects. In the former, VEGF immunoneutralization suppressed P levels, but the pregnancy rate was not reduced. In the latter, treatment provided protection from cancer challenges and delayed wound healing, but did not prevent fertility.

To our knowledge, this report also describes the first in vivo study on the effects of exogenous Ang-2 in the ovary. Recent studies indicate that the Ang receptor (Ang–Tie-2) system plays an important role in blood vessel formation and function, with the endogenous agonist Ang-1 promoting vessel maturation and stability and the endogenous antagonist Ang-2 blocking Ang-1–Tie-2 interaction to cause vessel instability. Current models propose that Ang-2 action may be important during angiogenesis to destabilize existing vessels and allow further growth [12]; however, there is also evidence that Ang-2 in the relative absence of angiogenic factors (e.g., VEGF) can cause vessel degeneration. To date, there are few reports on the expression [13–16], regulation [14,16] or action of Ang agonists/antagonists in the ovary. However, Maisonpierre et al. [17] noted that atretic antral follicles and regressing corpora lutea in the rat ovary contained minimal amounts of VEGF-A mRNA, but large amounts of Ang-2 mRNA. Therefore, we tested the hypothesis that local administration of the antagonist Ang-2 into the preovulatory follicle in monkeys would disrupt the balance between angiogenic (VEGF-A, Ang-1) and angiolytic (Ang-2) factors, thereby preventing periovulatory events and corpus luteum development.

Our data indicate that intrafollicular injection of 20 μg Ang-2 prevented follicle rupture and the timely rise in circulating P expected in the subsequent 2-week luteal phase. Since the latter P rise did not occur until after another peak in circulating E, which in three of five animals was reminiscent of a preovulatory E surge, we speculated that Ang-2 treatment severely impaired or destroyed the initial preovulatory follicle — such that it took 12–14 days to recover or to be replaced by another follicle at this stage. A laparoscopic evaluation of one animal 10 days post-Ang-2 injection detected a large antral follicle, not on the injected ovary, but on the noninjected, contralateral ovary. This finding suggests that Ang-2 treatment caused the destruction or atresia of the preovulatory follicle, and the subsequent selection and growth of another dominant follicle destined to ovulate and luteinize approximately 2 weeks later. Our observation is consistent with evidence from monkeys [50] and women [51] that ablation of the dominant structure on the ovary, that is, the follicle selected to ovulate or the corpus luteum, will reset the ovarian cycle with maturation of the next preovulatory follicle occurring 12—14 days later.

Further studies are ongoing to establish the dose dependency and specificity of Ang antagonist action to suppress the preovulatory follicle during the menstrual cycle in monkeys [52] (unpublished results). Likewise, experiments are warranted to examine the effects of Ang agonists (Ang-1) and antagonists (Ang-2) on follicle health and vascularity, including granulosa, theca and endothelial cell death. Finally, despite the caveats of acute injections into the corpus luteum (discussed earlier), it is noteworthy that intraluteal administration of Ang-2+VEGF antagonist (but not VEGF antagonist alone) caused a transient decline in circulating P levels for 24 h. Therefore, additional studies are needed to consider Ang-1/Ang-2 actions in the corpus luteum, as well as in the follicle.

In conclusion, our investigations establish the ability of specific VEGF-A (sVEGFR-1 chimera) and Ang (Ang-2) antagonists, and to a lesser extent the general angiostatic agent TNP-470, to disrupt periovulatory events and subsequent luteal structure and function when administered directly into the dominant follicle during the menstrual cycle in rhesus monkeys. Of the three mechanisms tested, blockade of Ang action appeared most effective in disrupting the gametogenic (ovulation) and steroidogenic (P production) functions of the mature follicle. However, since acute blockage of Ang action only temporarily blocked ovarian function, allowing rapid recovery of ovarian cyclicity, further studies are needed to consider whether acute or chronic treatment with Ang antagonists offers a potential as either an emergency (postcoital) or regular contraceptive. Limited success following intraluteal or systemic administration indicates the need for further studies to optimize delivery of angiogenic agents for contraceptive trials. It is possible that combinations of anti-angiogenic factors will be needed to optimally suppress luteal, and perhaps uterine, function to prevent pregnancy. Nevertheless, consideration of such treatment regimens as contraceptives, except perhaps as acute treatments for postcoital contraception, will be needed to evaluate potential deleterious effects in other vascular beds (e.g., the kidney) [53,54] or in wound healing [42,49].

Acknowledgments

The authors appreciate the services provided by the surgical group and animal care staff in the Division of

Animal Resources, the technical assistance of members of the Endocrine Services Laboratory and the Imaging & Morphology Core Laboratory, and the managerial skills and technical support provided by Dr. Ted Molskness and Ms. Jessica Vance in Dr. Stouffer's laboratory at the Oregon National Primate Research Center.

This research was supported by grant RF 96020 from the Rockefeller Foundation under the World Health Organization Initiative on Implantation Research and by an NIH Primate Centers grant RR00163. The project did not involve any collaborations with industry, except for the contribution of TNP-470 by Takeda Abbot Pharmaceuticals, Lake Forest, IL.

References

[1] Koos RD. Ovarian angiogenesis. In: Adashi EY, Leung PCK, editors. The Ovary. New York: Raven Press; 1993. p. 433–53.
[2] Reynolds LP, Redmer DA. Expression of the angiogenic factors, basic fibroblast growth factor and vascular endothelial growth factor, in the ovary. J Anim Sci 1998;76:1671–81.
[3] Hazzard TM, Stouffer RL. Angiogenesis in ovarian follicular and luteal development. Baillieres Best Pract Res Clin Obstet Gynaecol 2000;14:883–900.
[4] Fraser HM, Wulff C. Angiogenesis in the primate ovary. Reprod Fertil Dev 2001;13:557–66.
[5] Fraser HM, Wulff C. Angiogenesis in the corpus luteum. Reprod Biol Endocrinol 2003;1:88.
[6] Ferrara N, Gerber HP, LeCouter J. The biology of VEGF and its receptors. Nat Med 2003;9:669–76.
[7] Koos RD. Increased expression of vascular endothelial growth/permeability factor in the rat ovary following an ovulatory gonadotropin stimulus: Potential roles in follicle rupture. Biol Reprod 1995; 52:1426–35.
[8] Laitinen M, Ristimaki A, Honkasalo M, Narko K, Paavonen K, Ritvos O. Differential hormonal regulation of vascular endothelial growth factors VEGF, VEGF-B, and VEGF-C messenger ribonucleic acid levels in cultured human granulosa-luteal cells. Endocrinology 1997; 138:4748–56.
[9] Endo T, Kitajima Y, Nishikawa A, Manase K, Shibuya M, Kudo R. Cyclic changes in expression of mRNA of vascular endothelial growth factor, its receptors Flt-1 and KDR/Flk-1, and Ets-1 in human corpora lutea. Fertil Steril 2001;76:762–8.
[10] Hazzard TM, Nayak NR, Brenner RM, Stouffer RL. Dynamic expression of receptors for vascular endothelial growth factor (VEGFR1, VEGFR2) and angiopoietins (Tie-2) in the primate corpus luteum (CL) during the menstrual cycle. Biol Reprod 2000; 62(Suppl 1):271.
[11] Xu F, Hazzard TM, Scheffler LJ, Stouffer RL. Neuropilin-1 and -2 expression in the monkey corpus luteum during the menstrual cycle. Biol Reprod 2002;66(Suppl 1):181–2.
[12] Hanahan D. Signaling vascular morphogenesis and maintenance. Science 1997;277:48–50.
[13] Hazzard TM, Christenson LK, Stouffer RL. Changes in expression of vascular endothelial growth factor and angiopoietin-1 and -2 in the macaque corpus luteum during the menstrual cycle. Mol Hum Reprod 2000;6:993–8.
[14] Wulff C, Wilson H, Largue P, Duncan WC, Armstrong DG, Fraser HM. Angiogenesis in the human corpus luteum: Localization and changes in angiopoietins, tie-2, and vascular endothelial growth factor messenger ribonucleic acid. J Clin Endocrinol Metab 2000;85: 4302–9.
[15] Hata K, Udagawa J, Fujiwaki R, Nakayama K, Otani H, Miyazaki K. Expression of angiopoietin-1, angiopoietin-2, and Tie2 genes in normal ovary with corpus luteum and in ovarian cancer. Oncology 2002;62:340–8.
[16] Hazzard TM, Molskness TA, Chaffin CL, Stouffer RL. Vascular endothelial growth factor (VEGF) and angiopoietin regulation by gonadotrophin and steroids in macaque granulosa cells during the peri-ovulatory interval. Mol Hum Reprod 1999;5:1115–21.
[17] Maisonpierre PC, Suri C, Jones PF, et al. Angiopoietin-2, a natural antagonist for Tie2 that disrupts in vivo angiogenesis. Science 1997; 277:55–60.
[18] Klauber N, Rohan RM, Flynn E, D'Amato RJ. Critical components of the female reproductive pathway are suppressed by the angiogenesis inhibitor AGM-1470. Nat Med 1997;3:443–6.
[19] Ferrara N, Chen H, Davis-Smyth T, et al. Vascular endothelial growth factor is essential for corpus luteum angiogenesis. Nat Med 1998;4: 336–40.
[20] Hazzard TM, Rohan RM, Molskness TA, Fanton JW, D'Amato RJ, Stouffer RL. Injection of antiangiogenic agents into the macaque preovulatory follicle. Endocrine 2002;17:199–206.
[21] Hazzard TM, Xu F, Stouffer RL. Injection of soluble vascular endothelial growth factor receptor 1 into the preovulatory follicle disrupts ovulation and subsequent luteal function in rhesus monkeys. Biol Reprod 2002;67:1305–12.
[22] Wolf DP, Thomson JA, Zelinski-Wooten MB, Stouffer RL. In vitro fertilization-embryo transfer in nonhuman primates: The technique and applications. Mol Reprod Dev 1990;27:261–80.
[23] National Academy of Sciences. Guide for the care and use of laboratory animals. Washington (DC): National Academy Press; 1996.
[24] Resko JA, Ploem JG, Stadelman HL. Estrogens in fetal and maternal plasma of the rhesus monkey. Endocrinology 1975;97:425–30.
[25] Hess DL, Spies HG, Hendrickx AG. Diurnal steroid patterns during gestation in the rhesus macaque: Onset, daily variation, and the effects of dexamethasone treatment. Biol Reprod 1981;24: 609–16.
[26] Young KA, Stouffer RL. Gonadotropin and steroid regulation of matrix metalloproteinases and their endogenous tissue inhibitors in the developed corpus luteum of the rhesus monkey during the menstrual cycle. Biol Reprod 2004;70:244–52.
[27] Stouffer RL, Dahl KD, Hess DL, Woodruff TK, Mather JP, Molskness TA. Systemic and intraluteal infusion of inhibin A or activin A in rhesus monkeys during the luteal phase of the menstrual cycle. Biol Reprod 1994;50:888–95.
[28] Ellinwood WE, Norman RL, Spies HG. Changing frequency of pulsatile luteinizing hormone and progesterone secretion during the luteal phase of the menstrual cycle of rhesus monkeys. Biol Reprod 1984;31:714–22.
[29] Klauber N, Rohan RM, Flynn E, D'Amato RJ. Critical components of the female reproductive pathway are suppressed by the angiogenesis inhibitor AGM-1470. Nat Med 1997;3:443–6.
[30] Kusaka M, Sudo K, Matsutani E, et al. Cytostatic inhibition of endothelial cell growth by the angiogenesis inhibitor TNP-470 (AGM-1470). Br J Cancer 1994;69:212–6.
[31] Zelinski-Wooten MB, Slayden OD, Chwalisz K, Hess DL, Brenner RM, Stouffer RL. Chronic treatment of female rhesus monkeys with low doses of the antiprogestin ZK 137 316: Establishment of a regimen that permits normal menstrual cyclicity. Hum Reprod 1998;13: 259–67.
[32] LeCouter J, Kowalski J, Foster J, et al. Identification of an angiogenic mitogen selective for endocrine gland endothelium. Nature 2001;412: 877–84.
[33] Fraser HM, Dickson SE, Lunn SF, et al. Suppression of luteal angiogenesis in the primate after neutralization of vascular endothelial growth factor. Endocrinology 2000;141:995–1000.
[34] Wulff C, Wilson H, Rudge JS, Wiegand SJ, Lunn SF, Fraser HM. Luteal angiogenesis: Prevention and intervention by treatment with vascular endothelial growth factor trap (A40). J Clin Endocrinol Metab 2001;86:3377–86.

[35] Ravindranath N, Little-Ihrig L, Phillips HS, Ferrara N, Zeleznik AJ. Vascular endothelial growth factor messenger ribonucleic acid expression in the primate ovary. Endocrinology 1992;131:254–60.
[36] Berisha B, Schams D, Kosmann M, Amselgruber W, Einspanier R. Expression and tissue concentration of vascular endothelial growth factor, its receptors, and localization in the bovine corpus luteum during estrous cycle and pregnancy. Biol Reprod 2000;63:1106–14.
[37] Kawate N, Tsuji M, Tamada H, Inaba T, Sawada T. Changes of messenger RNAs encoding vascular endothelial growth factor and its receptors during the development and maintenance of caprine corpora lutea. Mol Reprod Dev 2003;64:166–71.
[38] Al-zi'abi MO, Watson ED, Fraser HM. Angiogenesis and vascular endothelial growth factor expression in the equine corpus luteum. Reproduction 2003;125:259–70.
[39] Boonyaprakob U, Gadsby JE, Hedgpeth V, Routh P, Almond GW. Expression and localization of vascular endothelial growth factor and its receptors in pig corpora lutea during the oestrous cycle. Reproduction 2003;126:393–405.
[40] Dickson SE, Bicknell R, Fraser HM. Mid-luteal angiogenesis and function in the primate is dependent on VEGF. J Endocrinol 2001;168: 409–16.
[41] Stouffer RL, Dahl KD, Hess DL, Woodruff TK, Mather JP, Molskness TA. Systemic and intraluteal infusion of inhibin A or activin A in rhesus monkeys during the luteal phase of the menstrual cycle. Biol Reprod 1994;50:888–95.
[42] Howdieshell TR, Callaway D, Webb WL, et al. Antibody neutralization of vascular endothelial growth factor inhibits wound granulation tissue formation. J Surg Res 2001;96:173–82.
[43] Wheeler YY, Kute TE, Willingham MC, Chen SY, Sane DC. Intrabody-based strategies for inhibition of vascular endothelial growth factor receptor-2: Effects on apoptosis, cell growth, and angiogenesis. FASEB J 2003;17:1733–5.
[44] Ryan AM, Eppler DB, Hagler KE. Preclinical safety evaluation of rhuMAbVEGF, an antiangiogenic humanized monoclonal antibody. Toxicol Pathol 1999;27:78–86.
[45] Kim ES, Serur A, Huang J, et al. Potent VEGF blockade causes regression of coopted vessels in a model of neuroblastoma. Proc Natl Acad Sci U S A 2002;99:11399–404.
[46] Huang J, Frischer JS, Serur A, et al. Regression of established tumors and metastases by potent vascular endothelial growth factor blockade. Proc Natl Acad Sci U S A 2003;100:7785–90.
[47] Sowter HM, Corps AN, Evans AL, Clark DE, Charnock-Jones DS, Smith SK. Expression and localization of the vascular endothelial growth factor family in ovarian epithelial tumors. Lab Invest 1997;77: 607–14.
[48] Rowe AJ, Morris KD, Bicknell R, Fraser HM. Angiogenesis in the corpus luteum of early pregnancy in the marmoset and the effects of vascular endothelial growth factor immunoneutralization on establishment of pregnancy. Biol Reprod 2002;67: 1180–8.
[49] Niethammer AG, Xiang R, Becker JC, et al. A DNA vaccine against VEGF receptor 2 prevents effective angiogenesis and inhibits tumor growth. Nat Med 2002;8:1369–75.
[50] Goodman AL, Koering MJ, Nixon WE, Williams RF, Hodgen GD. Follicle dominance and ovarian asymmetry after luteectomy in rhesus monkeys. Am J Physiol 1982;243:E325–31.
[51] Araki S, Chikazawa K, Akabori A, Ijima K, Tamada T. Hormonal profile after removal of the dominant follicle and corpus luteum in women. Endocrinol Jpn 1983;30:55–70.
[52] Xu F, Stouffer RL. Local delivery of angiopoietin-2 into the preovulatory follicle terminates the menstrual cycle in rhesus monkeys. Biol Reprod 2004;71(Suppl):97.
[53] Sugimoto H, Hamano Y, Charytan D. Neutralization of circulating vascular endothelial growth factor (VEGF) by anti-VEGF antibodies and soluble VEGF receptor 1 (sFlt-1) induces proteinuria. J Biol Chem 2003;278:12605–8.
[54] Mysliwski A, Kubasik-Juraniec J, Koszalka P, Szmit E. The effect of angiogenesis inhibitor TNP-470 on the blood vessels of the lungs, kidneys and livers of treated hamsters. Folia Morphol (Warsz) 2004; 63:5–9.

PUBLICATION 8

Sharkey, A. M., R. Catalano, **A. Evans**, D. S. Charnock-Jones, and S. K. Smith. 2005. Novel Antiangiogenic Agents for Use in Contraception. *Contraception* 71, (4), 263-71.

Cited by 25, Impact factor 2.724

ISSN: 0010-7824

Journal Type

The journal Contraception covers all aspects of contraception from cost effectiveness, safety and failure rates to original research such as this article on prevention of implantation. Manuscripts are accepted from both clinicians and researchers.

Personal Contribution

As in publication 3 I collected and processed endometrial samples from theatre. This included culture of explants followed by extraction of RNA and microarrays as described in (Evans et al., 2003)[*1], and included the verification of results by quantitative PCR. Although the anti-VEGF was originally produced in a small company (see acknowledgements in this publication to Sally Humphries) this required re-cloning and growing up as described for publication 8.

Available online at www.sciencedirect.com

SCIENCE DIRECT®

Contraception

Contraception 71 (2005) 263–271

Original research article

Novel antiangiogenic agents for use in contraception

Andrew M. Sharkey[a,*], Rob Catalano[a], Amanda Evans[a], D. Stephen Charnock-Jones[b], Stephen K. Smith[b]

[a]*Department of Pathology, University of Cambridge, CB2 1QP Cambridge, UK*
[b]*Department of Obstetrics and Gynaecology, Rosie Maternity Hospital, CB2 2SW Cambridge, UK*

Received 16 December 2004; accepted 20 December 2004

Abstract

Angiogenesis and vascular development are fundamental to the development of a receptive endometrium that permits implantation. The underlying hypothesis of this project is that implantation in primates and in humans is dependent on vascular remodeling in the endometrium and that the identification of agents that can disrupt this process prior to embryo attachment will lead to the development of new post coital contraceptives. To identify suitable targets for postcoital contraception, we studied the expression in endometrium of the vascular endothelial growth factor (VEGF) and angiopoietin families of angiogenic regulators. We produced a neutralizing antibody to VEGF-A, and this was shown to inhibit implantation in rhesus monkeys, apparently through direct antagonism of the action of VEGF-A in the endometrium. This demonstrated 'proof of principle' that agents antagonizing molecules that regulate angiogenesis can be developed as contraceptive agents. A second objective was to identify new contraceptive targets. We have developed microarrays to compare receptive endometrium with endometrium-rendered nonreceptive by a number of experimental strategies. We have identified over 100 RNA transcripts that are acutely regulated by administration of the antiprogestin RU486 to women, and 20 transcripts altered by antagonizing the action of VEGF-A in endometrium. These transcripts represent new potential targets for development of novel postcoital contraceptives.

Keywords: Angiogenesis; Endometrium; Contraception; Microarray

1. Introduction

In primates, successful implantation requires the development of a hatched blastocyst capable of implantation and an endometrium that is receptive to the embryo. Following menstruation, the endometrium undergoes a complex series of developmental changes under the influence of the ovarian steroids, estrogen and progesterone. This results in repair of the endometrium, proliferation and growth of epithelium and stroma, followed by differentiation in response to increasing levels of progesterone after ovulation. This culminates in a tissue that becomes receptive to signals from the implanting embryo for a limited period. In humans, embryo transfer experiments suggest that this receptive phase extends from approximately days 5 to 10 after the luteinizing hormone (LH) surge [1].

Extensive angiogenesis is an integral part of the development of the receptive endometrium. In the ovary, the source of the steroids that drive endometrial development changes in vascular permeability, and angiogenesis accompanies the maturation of the ovarian follicle and the processes of ovulation and luteinization. In the endometrium, arteriogenesis produces the characteristic spiral arterioles, supplying an extensive capillary network that develops just beneath the luminal epithelium and around the endometrial glands. At the same time, there is a large-scale influx of leucocytes consisting mainly of uterine natural killer (NK) cells and macrophages [2]. Many of these cells enter the endometrium from the blood stream by extravasation via endometrial capillaries. These cells play vital roles in the processes of implantation and decidualization if pregnancy occurs, or in the induction of menstruation and repair in a nonpregnant cycle [3]. Following attachment of the blastocyst, implantation and placental development are critically dependent on increased local vascular permeability and successful remodeling of spiral arteries by the invading trophoblast [4,5].

* Corresponding author. Tel.: +44 1223 333729; fax: +44 1223 333346.
E-mail address: as168@cam.ac.uk (A.M. Sharkey).

0010-7824/$ – see front matter © 2005 Elsevier Inc. All rights reserved.
doi:10.1016/j.contraception.2004.12.018

It is therefore clear that normal endometrial function and implantation are totally dependent upon carefully controlled angiogenesis in the endometrium and ovary. The female reproductive tract is unusual in that it is one of the few sites in adults where physiological angiogenesis occurs [6]. It is therefore an attractive target for new contraceptive strategies that target active angiogenesis. Inhibition of angiogenesis has the potential to affect either the endometrium directly or the ovary during ovulation and development of the corpus luteum. Direct evidence for the importance of angiogenesis in reproduction comes from experiments in which nonpregnant cycling mice were chronically treated with the nonspecific angiogenesis inhibitor AGM-1470 [7]. Inhibition of both endometrial maturation and corpus luteum maturation was observed, although the endometrial effects could have been in part due to the alteration in progesterone production by the corpus luteum. Administration of AGM-1470 to pregnant mice resulted in implantation failure due to impaired decidualization and vascular development in the placenta and embryo. Blocking the action of the specific angiogenic growth factor vascular endothelial growth factor (VEGF)-A in the early corpus luteum causes a failure of progesterone production in both rats and marmosets [8,9].

1.1. Control of angiogenesis by local growth factors

Angiogenesis is believed to result from the balance between stimulating and inhibitory factors leading to endothelial growth or loss. Functional experiments in mice involving gene knockouts have identified two families of genes, the VEGF family and the angiopoietins (Ang-1 and Ang-2), as important local regulators of angiogenesis [10]. Four different receptors are known for the VEGF family: VEGF-R1 (flt-1), VEGF-R2 (KDR), VEGF-R3 (flt-4) and neuropilin, and tie-2 is the receptor for Ang-1 and Ang-2 [11–15]. The VEGF family consists of five members, VEGF-A, B, C, D and placental growth factor PlGF, and some family members exhibit splice variants with altered bioactivity (Fig. 1) [16].

The generation of new blood vessels from preexisting blood vessels can occur by several different processes including sprouting, intussusception and intercalation [17–19]. The steps required for sprouting angiogenesis to take place have become considerably clearer in recent years, and many of the key factors involved in these steps have been elucidated. Because this is the best understood form, it is frequently assumed to be the principle mechanism in most circumstances. In the reproductive tract, this is not the case and there is little evidence that it occurs in the human endometrium. Goodger and Rogers [20,21] found no correlation with endothelial proliferation and the increase in capillary number, and determined that endometrial capillaries grow by elongation rather than sprouting.

In almost all situations examined to date, it seems that the level of VEGF-A is critical in determining whether the vessel tree grows or is pruned. For example, in tumor models, the local decrease in VEGF-A leads to capillary loss

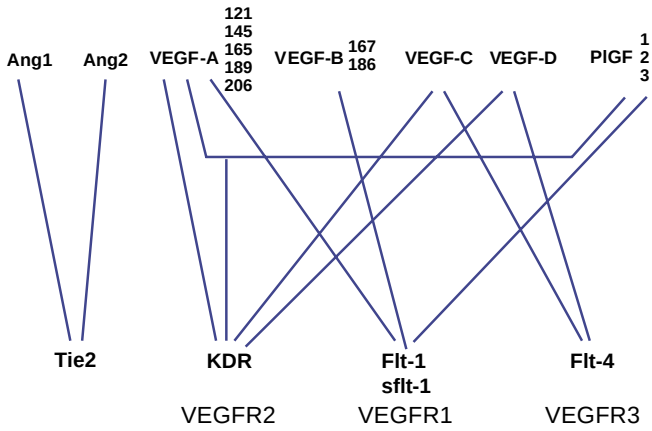

Fig. 1. The VEGF and angiopoietin gene families and their cognate receptors. VEGF-A, B and PlGF have alternatively spliced RNAs, which generate isoforms of different sizes. Figures show the number of amino acids in each isoform.

and tumor cell death [22]. The level of VEGF mRNA and protein is regulated at numerous levels suggesting that this factor is at a point of convergence of many regulatory signaling pathways. VEGF-A mRNA is up-regulated by transcriptional activation under conditions of reduced oxygen. These conditions also increase the stability of the VEGF-A transcript. In addition, VEGF-A mRNA level can be regulated by steroids, glucose and notch signaling [23,24]. VEGF-A is encoded by several differentially spliced transcripts, and the resulting polypeptides have different bioavailabilities due to variable binding to heparin sulfate proteoglycans. The relative amounts of the mRNAs encoding these variants change throughout the menstrual cycle [25]. These differences are important as the heparin binding forms can be released from the extracellular matrix reservoir by proteolytic cleavage by plasmin [26]. This is particularly pertinent in the endometrium, since following menstruation and activation of the clotting cascade, the damaged vessels need to be repaired.

However, VEGF-A is by no means the sole determinant of endothelial fate. These cells respond to antiapoptotic signals from other angiogenic factors such as Ang-1 and integrin-mediated stimuli from the extracellular matrix. Antiproliferative signals are also delivered by the matrix. In an attempt to determine the importance of individual factors in such a complex process, reductionist models have been employed. For example, the keratin 14 promotor cassette has been used to overexpress cDNAs encoding angiogenic growth factors in the skin of transgenic mice. These studies have shown that overexpression of VEGF-A, Ang-1 and placental growth factor all lead to an increase in vessel number, and in the case of VEGF-A and PlGF, an increase in vascular permeability [27–29]. Overexpression of VEGF-C or VEGF-D leads not to an increase in vascular structures but to an increase in lymphatic structures [30]. Studies on mice that overexpress both Ang-1 and VEGF-A in the skin have revealed that these two factors are able to

interact leading to an increase in vessel number (as was seen with VEGF-A or Ang-1 alone), but normal vascular permeability was restored [31]. In the case of the endometrium, many angiogenic and antiangiogenic factors are present, but the ways in which they interact and what the molecular consequences for such interactions are remain unclear. One of the major aims of this project has been to define more clearly the spatial and temporal patterns of expression of known angiogenic growth factors in endometrium through the cycle and during early pregnancy. There are clear changes in the cellular sites of production of these factors during the menstrual cycle, and the endothelial cells have differing characteristics in different vessel populations in the endometrium [32]. In light of this, it could be proposed that regional specialization of vessels in the endometrium has important functional consequences.

1.2. Role of vasculature in regulating endometrial function

Previously, it had been presumed that the vasculature is merely 'plumbing' to supply nutrients and remove waste products from a tissue. However, it is now clear that the endothelial cells actually play an active part in defining tissue structure, architecture and function [33]. Both tissue maintenance and its responses to physiological or pathological stimuli are dependent on an appropriate vascular supply. In the endometrium, several of the factors required for the growth and maintenance of this vascular supply are directly regulated by ovarian steroids. The most prominent of these is VEGF-A, and thus, we hypothesized that blocking the action of this factor in the postovulatory endometrium would be sufficient to prevent the tissue's physiological response to the embryo and to steroids and thereby prevent the establishment of pregnancy. We have also investigated the effect of perturbing endothelial function on the behavior of endometrial epithelium in response to estradiol [34].

1.3. Identification of other therapeutic targets involved in angiogenesis

Although the VEGF and angiopoietin families have been most intensively studied with regard to angiogenesis in endometrium, little is known in detail about their mechanisms of action at different stages of the menstrual cycle. The primary determinant of whether angiogenesis or vascular homeostasis occurs is the balance between the VEGF and Ang genes. However, angiogenesis is a complex process involving many other gene products. It is clear that these two gene families are not the sole targets for therapeutic intervention targeted at angiogenesis. The identification of other molecules that play important roles either as controllers of angiogenesis or as downstream mediators of angiogenesis initiated by the VEGF and Ang systems would provide additional targets for therapies aimed at disrupting normal endometrial development so as to prevent implantation.

Although several hundred molecules are known, which participate in angiogenesis, there has been no systematic attempt to study their expression in endometrium. cDNA microarrays are a novel methodology that permits the relative levels of thousands of RNA species to be determined simultaneously. We, therefore, sought to use this technique to examine patterns of expression of known angiogenic mediators at different stages of the menstrual cycle. The aim was to correlate gene expression patterns with known physiological angiogenesis, and to determine the effect on gene expression patterns of agents that disrupt normal angiogenesis. The purpose was to identify novel targets for antiangiogenic therapy in primate and human endometrium.

2. Rationale and objectives of the study

The prime objective of the study was to develop new contraceptives that prevent implantation. It is clear from rodent studies that disruption of angiogenesis in the endometrium or the ovary can achieve this by preventing development of a receptive endometrium. However, angiogenesis is also essential after implantation for normal placentation and decidualization. We aimed to target the angiogenic events leading to a receptive endometrium rather than postimplantation events to avoid any approach that interfered directly with the embryo. The project encompassed three specific research aims:

1. To define in detail the expression pattern of the VEGF and Ang families in human endometrium.
2. To determine whether implantation can be prevented in the rhesus monkey by use of a neutralizing antibody against the principle angiogenic regulator VEGF-A. The hypothesis to be tested here is whether a VEGF-A antagonist can modify endometrial function by a direct effect on the tissue rather than through effects on the corpus luteum.
3. To identify novel targets for antiangiogenic therapies by use of microarrays to examine expression of angiogenic genes in normal endometrium. The response of endometrium to drugs that disrupt angiogenesis will also be determined.

An essential aspect of the project was the collaboration with colleagues in the All India Institute of Medical Sciences (AIIMS) in New Delhi, India, whose results in the *rhesus macaque* are described in full elsewhere in this volume.

3. Work completed under the study

3.1. Defining the expression of the VEGF and Ang families in human endometrium

The VEGF and Ang families of growth factors act together as the principle effectors controlling endothelial fate in many tissues. Specifically, the ratio of Ang-1 and

Table 1
Localization of VEGFs and angiopoietins in endometrium and in early pregnancy

Factor/receptor	Preimplantation	Early pregnancy	Ref.
VEFG-A	Glands and stroma	Troph +Macs	[40,41]
VEGF-C	NK cells	NK cells	[42]
PlGF	NK cells	Trophoblast	[42,43]
Ang-2	NK cells	Trophoblast	[42,44]
VEGF-R1	Endothelial cells	Endothelial cells	[45]
sVEGF-R1	Endothelial cells	Trophoblast	[46]
VEGF-R2	Endothelial cells and superficial stroma	Endothelial cells	[47]
VEGF-R3	?	Trophoblast	unpublished
Tie-2	Endothelial cells	Endothelial cells	[44]

Ang-2 seems to determine whether the endothelial cells will be responsive to changes in the level of mitogenic growth factors such as VEGF-A [35]. We have therefore investigated the sites of production and regulation of these factors. In endometrium, VEGF-A mRNA expression has been shown to be maximal in the secretory phase with an abrupt increase in menstrual tissue [36–38].

Immunohistochemical studies indicate that VEGF-A is widely distributed in the human endometrium with the strongest staining apparent in the glandular epithelium. However, a subset of stromal cells also produce VEGF. Strong perivascular staining, probably in pericytes, is also apparent. However, because several of the spliced forms of VEGF-A are strongly heparin binding, we have used in situ hybridization to determine the sites of production. This analysis confirms the pattern seen by immunohistochemistry, with the epithelium as the major source of VEGF-A.

Although steroids regulate VEGF-A in the endometrium, it is known that local hypoxia can also regulate VEGF expression levels. At menstruation, blood vessels constrict creating hypoxia in the superficial endometrium. We have shown that both epithelial and stromal cells from endometrium strongly up-regulate VEGF-A expression in response to hypoxia [36]. It is therefore clear that VEGF-A expression and bioavailability are regulated in several ways at different stages of the menstrual cycle, and these include steroids as well as local factors such as hypoxia.

We have used immunohistochemistry and in situ hybridization studies to examine the expression of the VEGF and Ang genes and their receptors in endometrium. These show that VEGF-A, PlGF and VEGF-C are present in endometrium and are regulated during the menstrual cycle. We were unable to detect VEGF-B mRNA in normal endometrium and VEGF-D mRNA was only found in endometrial carcinoma specimens [39]. These results, together with published data from other studies on the localization of the VEGF and Ang genes and their receptors, are summarized in Table 1 [40–47].

3.2. Can neutralization of VEGF-A prevent implantation?

Gene ablation studies in mice indicate that of the many angiogenic proteins, VEGF-A acts as a key regulator of the process [16]. Even small changes in the level of expression of VEGF-A in tissue may be very significant, since disruption of a single allele of VEGF in mice results in abnormal blood vessel formation [48,49]. The expression studies in endometrium suggest that VEGF-A does play an important role during the menstrual cycle. Systemic treatment of rats with a soluble flt-1 receptor that inhibits VEGF-A bioactivity has previously been shown to suppress angiogenesis in the corpus luteum and inhibit progesterone release. This soluble flt-1 receptor competes with VEGF receptors on endothelial cells for binding to VEGF-A and inhibits the effects of VEGF-A. Failure of maturation of the endometrium was also observed, which is likely to be a result of lower progesterone secretion by the ovary [8]. There is no evidence that inhibitors of VEGF-A can affect endometrial maturation by directly affecting angiogenesis in the endometrium. We therefore tested whether inhibiting the actions of VEGF-A with soluble flt-1 (sflt-1) could have a direct effect on endometrial function in the absence of an ovarian effect [34]. Ovariectomized mice respond to a single injection of 17β-estradiol (E2) by edema due to increased vascular permeability as well as DNA and RNA synthesis and proliferation of the uterine epithelium. Mice injected with sflt-1 (4.0 mg/kg) at the same time as E2 showed reduced edema and a greatly decreased mitotic index of the luminal epithelial cells (Fig. 2). Thus, anti-VEGF agents such as sflt-1 are able to substantially modify the responses of the endometrium to steroids through a direct effect on the endometrium independent of the corpus luteum. There is no evidence for VEGF receptors on the epithelial cells, so this effect is likely to be due to alterations in endothelial cell function. Endothelial cells are known to release factors such as fibroblast growth factor and platelet-derived growth factor that control epithelial cell proliferation. Normally, E2 induces VEGF release from epithelial and stromal cells, which may regulate release of these epithelial mitogens

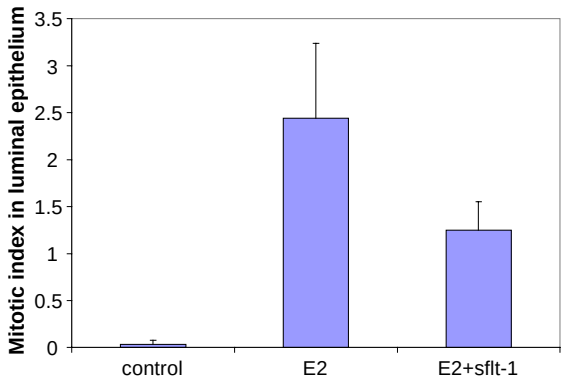

Fig. 2. Direct effect of sflt-1 on the mitotic index of luminal epithelium in response to E2. Ovariectomized BALB/c mice were treated with 10 μg/kg estradiol (E2) with or without sflt-1 in PBS (4.0 mg/kg). Twenty-four hours later, the uterine horns were excised, fixed and paraffin embedded and the mitotic index counted in luminal epithelial cells (percentage of mitotic figures). Epithelial proliferation was increased by treatment with E2 and this increase was inhibited by 4.0 mg/kg sflt-1 ($p < .01$, Fisher's Exact Test).

from endothelial cells. The action of sflt-1 may be to block this paracrine loop.

This experiment provided proof in principle that antagonizing the actions on VEGF-A could directly prevent the normal response to E2 in the endometrium. We therefore tested whether an anti-VEGF agent could prevent implantation in cycling rhesus monkeys. This study was performed in collaboration with the AIIMS. Neutralizing antibodies provide a potent means to inhibit the bioactivity of secreted growth factors such as VEGF-A. They have been widely used in studies of tumor growth, and recently, the anti-VEGF-A neutralizing antibody Avastin has been approved for treatment of metastatic colorectal cancer [16]. For this study, a suitable neutralizing monoclonal antibody directed against VEGF-A was produced in Cambridge by immunization of mice with recombinant VEGF-A_{165} conjugated to keyhole limpet hemocyanin. Spleens of these mice were collected and the B-cells fused with NSO cells. Stable cell lines that secreted immunoglobulins that bound to immobilized VEGF-A were identified. After additional rounds of cloning and screening against other possible cross-reacting antigens, one clone (4E3) was selected for large-scale growth. An isotype-matched (IgG1 κ) control antibody was also prepared in a similar manner. Both cell lines were grown in Heraeus miniperm bioreactors that produce immunoglobulin at high concentration to facilitate purification. The anti-VEGF-A antibody and control immunoglobulin were purified by binding to protein G sepharose, desalting (Centricon ultrafiltration) and lyophilized in 10 mg lots. The neutralizing activity of the antibody was demonstrated using a bioassay in which iodinated VEGF binds to its receptors on endothelial cells. Addition of the anti-VEGF antibody abolished ^{125}I-VEGF binding to the cell surface. The antibody 4E3 showed similar blocking activity in this assay as a commercially available neutralizing polyclonal anti-VEGF antibody raised in goats (Fig. 3).

Following production of the antibody, the effect of the antibody on implantation in rhesus monkeys was examined. Two specific questions were addressed:

1. Can anti-VEGF-A antibody prevent implantation in cycling rhesus monkeys?
2. Does anti-VEGF-A antibody prevent development of a receptive endometrium by directly inhibiting the action of VEGF-A on endometrium?

The studies to assess the effect of the antibody in vivo were carried out by our collaborators in AIIMS and are fully described elsewhere in this journal. The anti-VEGF-A antibody was administered by bolus subcutaneous injection in several dose regimens at different times after the LH surge and the effect on implantation rates monitored. Control animals received the same dose of an isotype-matched antibody. Two injections of 10 mg each on day 5 (LH+5) and day 10 (LH+10) following the LH surge were found to significantly reduce implantation rates. Monitoring of serum progesterone levels showed no significant reduction in levels

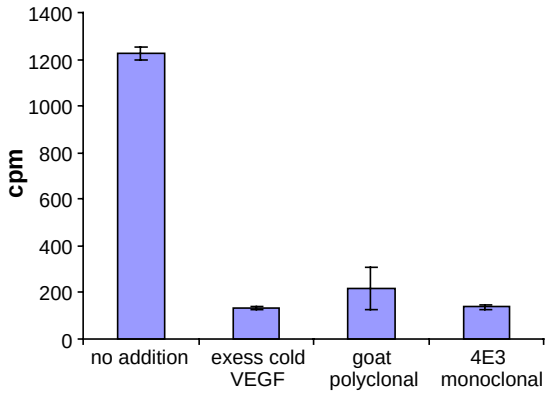

Fig. 3. Inhibition of VEGF binding to endothelial cells by the anti-VEGF antibody 4E3. Endothelial cells were grown in culture, and VEGF-A labeled with ^{125}I was added to the medium in the presence or absence of the anti-VEGF-A antibody. Binding of iodinated VEGF to the endothelial cells was measured by scintillation counting. VEGF-A binding to endothelial cells was specifically inhibited by excess cold VEGF, as well as by a commercially available goat anti-VEGF polyclonal antibody and also by the anti-VEGF-A monoclonal antibody 4E3. Reprinted with permission from Oxford University Press [54].

of this hormone following antibody treatment. This finding is extremely important since the effect on implantation cannot be attributed to decreased production of progesterone by the corpus luteum, which could lead to early pregnancy loss.

3.3. What effect does anti-VEGF antibody have on the endometrium?

In order to determine whether the anti-VEGF-A antibody had a direct effect on monkey endometrium, animals were first ovariectomized then allowed to recover. An artificial hormone cycle was initiated consisting of 3 weeks of estrogen administration followed by 1 week of progesterone. This regimen has previously been shown to faithfully reproduce normal endometrial development in this species [50]. Animals were treated during this cycle with anti-VEGF ($n=6$) or control antibody ($n=7$) by bolus injection on day 5 after initiation of progesterone treatment. This is the same treatment as used to successfully prevent implantation. RNA was isolated from endometrial biopsies taken on day 8 of progesterone treatment. Although endometrial histology of the biopsies from control and anti-VEGF-treated animals appeared normal, we used cDNA microarrays to identify possible mechanisms by which the anti-VEGF-A antibody could alter endometrial receptivity. This microarray was developed especially to study angiogenesis and receptivity in the endometrium. It consists of some 15,000 human cDNA sequences. One thousand one hundred of these were selected for inclusion specifically because they represent cDNAs known to be involved in angiogenesis or receptivity. The array includes genes involved in endothelial and smooth muscle proliferation, cell adhesion, cell signaling, apoptosis and extracellular matrix remodeling [51]. This array offers the advantage of selected angiogenesis content as well as

broader coverage of the transcriptome. cDNA labeled with Cy3 dye was synthesized from a reference RNA made by pooling endometrial samples from each of the seven control monkeys. cDNA labeled with Cy5 dye was synthesized from each of the control and VEGF-treated samples and was hybridized separately to microarrays in the presence of the Cy3 reference. Approximately 20 genes were identified as being significantly up- or down-regulated in endometrial samples from monkeys treated with the VEGF neutralizing antibody. Several of the genes have previously been described in the literature as being involved in angiogenesis; none has been shown before to be regulated by VEGF. These genes are implicated in the response of endometrium to VEGF-A withdrawal and may allow us to identify novel pathways controlling angiogenesis and endometrial receptivity. We are currently verifying these changes by real-time reverse transcriptase polymerase chain reaction (RT-PCR), and localization studies will be performed on selected genes in collaboration with Dr. Sengupta (AIIMS) to identify those that are promising mediators of local angiogenesis in the endometrium in response to VEGF-A. These may provide targets for future antiangiogenic therapies in the endometrium.

3.4. Identification of genes regulated by RU486 in the endometrium

In order to identify further targets for antiangiogenic strategies, we examined the response of the endometrium to the antiprogestin RU486. Administration of RU486 in vivo during the receptive phase rapidly renders the endometrium nonreceptive to the implanting embryo [52]. This drug also alters the integrity and stability of the spiral arterioles in the endometrium, and in many women, uterine bleeding is induced within 48 h of RU486 administration during the midsecretory phase [53]. In an initial pilot study, we used cDNA nylon arrays to monitor gene expression changes in short-term endometrial explants in response to RU486 [54]. Endometrial biopsies taken at midsecretory phase from five normal fertile women were divided and cultured in estradiol and progesterone with or without RU486 for 12 h. cDNA probes from the paired endometrial samples were hybridized to the arrays and hybridization signals were quantified. A total of 12 genes displayed significant changes in expression; six were up-regulated and six down-regulated following RU486 treatment. For five of these genes, this is the first report suggesting they are regulated by steroids in the endometrium. JAK1 and JNK1 were two of the genes shown by the arrays to be down-regulated in RU486-treated endometrial explants (Fig. 4). This was confirmed by using real-time RT-PCR [54]. These results show that components of two important signaling pathways in endometrium, the JAK/STAT pathway and the JNK pathway, are altered by RU486. Genes whose expression is controlled by these pathways are likely to be involved in the mechanism by which progesterone renders the endometrium receptive to the implanting embryo. Based on this work, we have successfully targeted components of the JAK/STAT pathway in endometrium. Preliminary studies suggest that this approach can prevent implantation in mice.

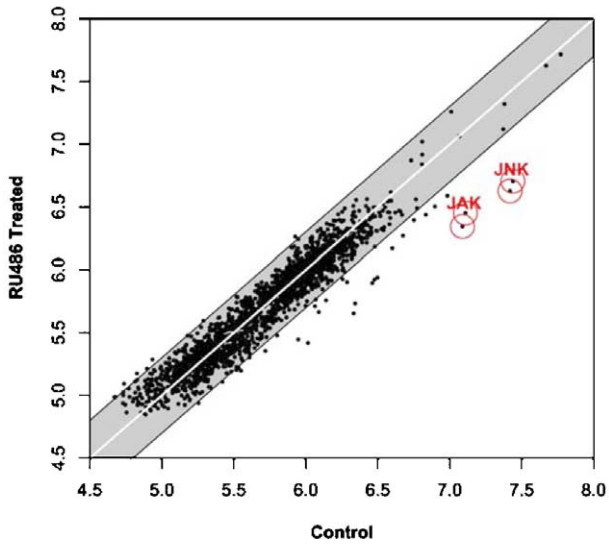

Fig. 4. Effect of RU486 on endometrial gene expression in vitro. The graph shows a scatterplot comparing the hybridization signal obtained for each spotted cDNA after hybridization of nylon custom arrays to labeled cDNA from endometrial explants treated with or without RU486 for 12 h in vitro. Each explant was taken in the secretory phase, divided into two and treated with RU486 or vehicle for 12 h in vitro. The data compare the relative expression of each of the 1000 genes spotted on the array in duplicate in the RU486-treated RNA versus control RNA from a representative sample. Values have been normalized and logged ($\log_{10}$). The gray band denotes a twofold change in intensity. Duplicate spots corresponding to JNK1 and JAK1 are highlighted, showing that these genes are reproducibly down-regulated by RU486; this was verified by real-time RT-PCR.

We have also initiated a full-scale study using our glass microarray system of 15,000 human cDNAs to study pipelle biopsies from the endometrium of women treated with a single dose of 200 mg RU486 on LH+7 of the secretory phase of their cycles. The aim being to identify progesterone-regulated genes that may be involved in receptivity or the maintenance of vascular integrity in women. RNA from three groups was compared: normal fertile women sampled at LH+7 ($n=7$), endometrial biopsies taken 6 h after administration of RU486 at LH+7 ($n=5$) and endometrial biopsies taken 24 h after administration of RU486 at LH+7 ($n=4$). Six hours after RU486 administration, some 100 genes with altered expression were identified, and over 200 genes showed altered gene expression at 24 h. Although RU486 can affect both glucocorticoid and androgen receptor function, the majority of these genes are likely to be directly regulated by progesterone. Studies are currently underway to localize expression of genes that may be involved in vascular integrity or in the luminal epithelium where embryo attachment occurs. These early response genes are likely to represent mediators of the rapid effects of RU486 action on endometrial receptivity and vascular integrity. A similar study of the effects of RU486 in the

mouse has led to the identification of several new genes that have been shown by functional studies to be essential for implantation [55,56]. No involvement for these genes in implantation had previously been suspected.

4. Conclusions and future work

We have sought to determine the expression pattern in endometrium of the principal factors known to control angiogenesis: the VEGF and Ang gene families. The site and levels of expression throughout the cycle have been determined for VEGF-A, B, C, D, PlGF, Ang-1 and Ang-2 with the objective of determining which of these factors had potential as a target for antiangiogenic strategies to disrupt implantation. These studies have shown that VEGF-B and VEGF-D are not expressed significantly in normal endometrium. Ang-1 was expressed at low levels that did not change throughout the cycle. VEGF-C, PlGF and Ang-2 are expressed in the mid and late secretory phase in uterine NK cells. VEGF-C is believed to control lymphatic endothelial cell function, whereas PlGF and Ang-2 in NK cells are probably involved in regulating vascular changes during decidualization and menstruation. In contrast, VEGF-A expression is widespread in both glands and stroma during the midsecretory phase and exhibits clear steroidal regulation. In view of this and its known functions, VEGF-A clearly represented the most promising target for antiangiogenic therapies to disrupt implantation.

In collaboration with colleagues at AIIMS, we have demonstrated 'proof of principle' that antagonizing the function of VEGF-A in endometrium can prevent implantation in rhesus monkeys. Preliminary experiments in mice using sflt-1 showed that antagonizing the actions of VEGF-A could modify the response of endometrium to steroids. A mouse monoclonal antibody specific to VEGF-A was produced, which was shown to neutralize the action of VEGF-A in vitro. Administration of this antibody after ovulation was shown to significantly reduce implantation in rhesus monkeys. This effect appeared to be due to a direct effect on VEGF-A action in endometrium, since there was no significant effect on ovarian progesterone production. The mechanism by which anti-VEGF-A antibody alters endometrial function was investigated by microarray analysis using endometrium from ovariectomized monkeys. These animals were treated with estradiol and progesterone to simulate a normal cycle, and treated with anti-VEGF-A antibody using the same regimen that had inhibited pregnancy. Over 20 transcripts were identified, which were up- or down-regulated by anti-VEGF-A antibody. These transcripts are implicated in the response of the endometrium to VEGF-A withdrawal and may allow us to identify novel pathways controlling angiogenesis and endometrial receptivity. These changes are currently being verified by RT-PCR and localization studies will be performed on selected genes in collaboration with Professor Sengupta at AIIMS to identify promising targets for future development.

In addition to using microarrays to identify novel antiangiogenic targets, we used this approach to find other targets for postcoital contraception. We have used microarrays to monitor the response of the endometrium to a single dose of RU486 administered as emergency contraception during the receptive phase. Some 100 genes were identified whose expression is altered within 6 h. Based on the known actions of RU486, these are likely to represent progesterone-regulated genes involved directly in receptivity or the maintenance of vascular integrity in women. Localization studies and verification of these changes by real-time RT-PCR are currently underway. We are particularly concerned with identifying which of these genes are expressed in the luminal epithelium, since such genes may be directly involved in transition of the endometrium to a nonreceptive state, in which the process of embryo attachment does not occur. The RU486 and anti-VEGF microarray studies have provided a number of potential targets for development of novel postcoital contraceptives. Future work will require functional studies in model systems to determine which of these targets play an important role in implantation, and to develop suitable therapeutic interventions.

Acknowledgment

This study was supported by the World Health Organization initiative on implantation research with funding from the Rockefeller Foundation and the Medical Research Council, UK (program grant G9623012). Much of the work was carried out in collaboration with Professor Jayasree Sengupta and Dr. Debabrata Ghosh of the All India Institute of Medical Sciences, New Delhi, India. AMS was supported by a research training fellowship from the Wellcome Trust and by the Meres Research studentship from St. John's College, Cambridge. We thank Professor Hilary Critchley, Edinburgh University, and Dr. Oskari Heikineimo, University of Helsinki, for their collaboration in the RU486 study in women. Sally Humphries produced the anti-VEGF-A antibody. We also thank the staff and patients of Addenbrookes Hospital, Cambridge, for their participation in providing human tissue samples.

References

[1] Bergh PA, Navot D. The impact of embryonic development and endometrial maturity on the timing of implantation. Fertil Steril 1992;58:537–42.
[2] Jones RK, Bulmer JN, Searle RF. Immunohistochemical characterization of stromal leukocytes in ovarian endometriosis: Comparison of eutopic and ectopic endometrium with normal endometrium. Fertil Steril 1996;66:81–9.
[3] Trundley A, Moffett A. Human uterine leukocytes and pregnancy. Tissue Antigens 2004;63:1–12.
[4] Goodger AM, Rogers PA. Blood vessel growth and endothelial cell density in rat endometrium. J Reprod Fertil 1995;105:259–61.
[5] Charnock-Jones DS, Kaufmann P, Mayhew TM. Aspects of human fetoplacental vasculogenesis and angiogenesis. I. Molecular regulation. Placenta 2004;25:103–13.

[6] Folkman J. Angiogenesis in cancer, vascular, rheumatoid and other disease. Nat Med 1995;1:27–31.
[7] Klauber N, Rohan RM, Flynn E, D'Amato RJ. Critical components of the female reproductive pathway are suppressed by the angiogenesis inhibitor AGM-1470. Nat Med 1997;3:443–6.
[8] Ferrara N, Chen H, Davis-Smyth T, et al. Vascular endothelial growth factor is essential for corpus luteum angiogenesis. Nat Med 1998; 4:336–40.
[9] Rowe AJ, Morris KD, Bicknell R, Fraser HM. Angiogenesis in the corpus luteum of early pregnancy in the marmoset and the effects of vascular endothelial growth factor immunoneutralization on establishment of pregnancy. Biol Reprod 2002;67:1180–8.
[10] Hanahan D. Signaling vascular morphogenesis and maintenance. Science 1997;277:48–50.
[11] Shibuya M, Yamaguchi S, Yamane A, et al. Nucleotide sequence and expression of a novel human receptor-type tyrosine kinase gene (flt) closely related to the fms family. Oncogene 1990;5:519–24.
[12] Matthews W, Jordan CT, Gavin M, Jenkins NA, Copeland NG, Lemischka IR. A receptor tyrosine kinase cDNA isolated from a population of enriched primitive hematopoietic cells and exhibiting close genetic linkage to c-kit. Proc Natl Acad Sci U S A 1991; 88:9026–30.
[13] Terman BI, Carrion ME, Kovacs E, Rasmussen BA, Eddy RL, Shows TB. Identification of a new endothelial cell growth factor receptor tyrosine kinase. Oncogene 1991;6:1677–83.
[14] Pajusola K, Aprelikova O, Korhonen J, et al. FLT4 receptor tyrosine kinase contains seven immunoglobulin-like loops and is expressed in multiple human tissues and cell lines. Cancer Res 1992;52:5738–43 [erratum in: Cancer Res. 53;1993:3845].
[15] Dumont DJ, Gradwohl GJ, Fong GH, Auerbach R, Breitman ML. The endothelial-specific receptor tyrosine kinase, tek, is a member of a new subfamily of receptors. Oncogene 1993;8:1293–301.
[16] Ferrara N. Related vascular endothelial growth factor: Basic science and clinical progress. Endocr Rev 2004;25:581–611.
[17] Ausprunk DH, Knighton DR, Folkman J. Differentiation of vascular endothelium in the chick chorioallantois: A structural and autoradiographic study. Dev Biol 1974;38:237–48.
[18] Djonov V, Schmid M, Tschanz SA, Burri PH. Intussusceptive angiogenesis: Its role in embryonic vascular network formation. Circ Res 2000;86:286–92.
[19] Asahara T, Masuda H, Takahashi T, et al. Bone marrow origin of endothelial progenitor cells responsible for postnatal vasculogenesis in physiological and pathological neovascularization. Circ Res 1999;85: 221–8.
[20] Goodger AM, Rogers PAW. Endometrial endothelial cell proliferation during the menstrual cycle. Hum Reprod 1994;9:399–405.
[21] Gambino LS, Wreford NG, Bertram JF, Dockery P, Lederman F, Rogers PAW. Angiogenesis occurs by vessel elongation in proliferative phase human endometrium. Hum Reprod 2002;17:1199–206.
[22] Benjamin LE, Golijanin D, Itin A, Pode D, Keshet E. Selective ablation of immature blood vessels in established human tumors follows vascular endothelial growth factor withdrawal. J Clin Invest 1999;103:159–65.
[23] Mueller MD, Vigne JL, Minchenko A, Lebovic DI, Leitman DC, Taylor RN. Regulation of vascular endothelial growth factor (VEGF) gene transcription by estrogen receptors alpha and beta. Proc Natl Acad Sci U S A 2000;97:10972–7.
[24] Hyder SM, Stancel GM, Chiappetta C, Murthy L, Boettger-Tong HL, Makela S. Uterine expression of vascular endothelial growth factor is increased by estradiol and tamoxifen. Cancer Res 1996;56:3954–60.
[25] Ancelin M, Buteau-Lozano H, Meduri G, et al. A dynamic shift of VEGF isoforms with a transient and selective progesterone-induced expression of VEGF189 regulates angiogenesis and vascular permeability in human uterus. Proc Natl Acad Sci U S A 2002;99:6023–8.
[26] Houck KA, Leung DW, Rowland AM, Winer J, Ferrara N. Dual regulation of vascular endothelial growth factor bioavailability by genetic and proteolytic mechanisms. J Biol Chem 1992;267:26031–7.
[27] Detmar M, Brown LF, Schon MP, et al. Increased microvascular density and enhanced leukocyte rolling and adhesion in the skin of VEGF transgenic mice. J Invest Dermatol 1998;111:1–6.
[28] Suri C, McClain J, Thurston G, et al. Increased vascularization in mice overexpressing angiopoietin-1. Science 1998;282:468–71.
[29] Odorisio T, Schietroma C, Zaccaria ML, et al. Mice overexpressing placenta growth factor exhibit increased vascularization and vessel permeability. J Cell Sci 2002;115:2559–67.
[30] Veikkola T, Jussila L, Makinen T, et al. Signalling via vascular endothelial growth factor receptor-3 is sufficient for lymphangiogenesis in transgenic mice. EMBO J 2001;20:1223–31.
[31] Thurston G, Suri C, Smith K, et al. Leakage-resistant blood vessels in mice transgenically overexpressing angiopoietin-1. Science 1999; 286:2511–4.
[32] Zhang EG, Smith SK, Charnock-Jones DS. Expression of CD105 (endoglin) in arteriolar endothelial cells of human endometrium throughout the menstrual cycle. Reproduction 2002;124:703–11.
[33] Cleaver O, Melton DA. Endothelial signalling during development. Nat Med 2003;9:661–8.
[34] Hastings JM, Licence DR, Burton GJ, Charnock-Jones DS, Smith SK. Soluble vascular endothelial growth factor receptor 1 inhibits edema and epithelial proliferation induced by 17beta-estradiol in the mouse uterus. Endocrinology 2003;144:326–34.
[35] Maisonpierre PC, Suri C, Jones PF, et al. Angiopoietin-2, a natural antagonist for tie2 that disrupts in vivo angiogenesis. Science 1997;277:55–60.
[36] Sharkey AM, Day K, McPherson A, et al. Vascular endothelial growth factor expression in human endometrium is regulated by hypoxia. J Clin Endocrinol Metab 2000;85:402–9.
[37] Torry DS, Holt VJ, Keenan JA, Harris G, Caudle MR, Torry RJ. Vascular endothelial growth factor expression in cycling human endometrium. Fertil Steril 1996;66:72–80.
[38] Shifren JL, Tseng JF, Zaloudek CJ, et al. Ovarian steroid regulation of vascular endothelial growth factor in the human endometrium: Implications for angiogenesis during the menstrual cycle and in the pathogenesis of endometriosis. J Clin Endocrinol Metab 1996; 81:3112–8.
[39] Yokoyama Y, Charnock-Jones DS, Licence D, et al. Expression of vascular endothelial growth factor (VEGF)-D and its receptor, VEGF receptor 3, as a prognostic factor in endometrial carcinoma. Clin Cancer Res 2003;9:1361–9.
[40] Charnock-Jones DS, Sharkey AM, Rajput-Williams J, et al. Identification and localization of alternately spliced mRNAs for vascular endothelial growth factor in human uterus and estrogen regulation in endometrial carcinoma cell lines. Biol Reprod 1993;48:1120–8.
[41] Sharkey AM, Charnock-Jones DS, Boocock CA, Brown KD, Smith SK. Expression of mRNA for vascular endothelial growth factor in human placenta. J Reprod Fertil 1993;99:609–15.
[42] Li XF, Charnock-Jones DS, Zhang E, et al. Angiogenic growth factor messenger ribonucleic acids in uterine natural killer cells. J Clin Endocrinol Metab 2001;86:1823–34.
[43] Clark DE, Smith SK, Sharkey AM, Charnock-Jones DS. Localization of VEGF and expression of its receptors flt and KDR in human placenta throughout pregnancy. Hum Reprod 1996;11:1090–8.
[44] Zhang EG, Smith SK, Baker PN, Charnock-Jones DS. The regulation and localization of angiopoietin-1, -2, and their receptor tie2 in normal and pathological human placentae. Mol Med 2001;7:624–35.
[45] Fong GH, Rossant J, Gertsenstein M, Breitman ML. Role of the Flt-1 receptor tyrosine kinase in regulating the assembly of vascular endothelium. Nature 1995;376:66–70.
[46] Clark DE, Smith SK, He Y, Day KA, et al. A vascular endothelial growth factor antagonist is produced by the human placenta and released into the maternal circulation. Biol Reprod 1998;59:1540–8.
[47] Nayak NR, Critchley HO, Slayden OD, et al. Progesterone withdrawal up-regulates vascular endothelial growth factor receptor type 2 in the superficial zone stroma of the human and macaque endometrium:

Potential relevance to menstruation. J Clin Endocrinol Metab 2000;85:3442–52.

[48] Carmeliet P, Ferreira V, Breier G, et al. Abnormal blood vessel development and lethality in embryos lacking a single VEGF allele. Nature 1996;380:435–9.

[49] Ferrara N, Carver-Moore K, Chen H, et al. Heterozygous embryonic lethality induced by targeted inactivation of the VEGF gene. Nature 1996;380:439–42.

[50] Ghosh D, De P, Sengupta J. Luteal phase ovarian oestrogen is not essential for implantation and maintenance of pregnancy from surrogate embryo transfer in the rhesus monkey. Hum Reprod 1994;9:629–37.

[51] Evans AL, Sharkey AS, Saidi SA, et al. Generation and use of a tailored gene array to investigate vascular biology. Angiogenesis 2003;6:93–104.

[52] Danielsson KG, Marions L, Bygdeman M. Effects of mifepristone on endometrial receptivity. Steroids 2003;68:1069–75.

[53] Hapangama DK, Critchley HO, Henderson TA, Baird DT. Mifepristone-induced vaginal bleeding is associated with increased immunostaining for cyclooxygenase-2 and decrease in prostaglandin dehydrogenase in luteal phase endometrium. J Clin Endocrinol Metab 2002;87:5229–34.

[54] Catalano RD, Yanaihara A, Evans AL, et al. The effect of RU486 on the gene expression profile in an endometrial explant model. Mol Hum Reprod 2003;9:465–73.

[55] Cheon Y-P, Xu X, Bagchi MK, Bagchi IC. Irg1 is a novel target of progesterone receptor and plays a critical role during implantation in the mouse. Endocrinology 2003;144:5623–30.

[56] Li Q, Cheon YP, Kannan A, Shanker S, Bagchi IC, Bagchi MK. A novel pathway involving progesterone receptor, 12/15-lipoxygenase-derived eicosanoids, and peroxisome proliferator-activated receptor gamma regulates implantation in mice. J Biol Chem 2004;279:11570–81.

PUBLICATION 9

Evans, A.L., Bryant, J., Skepper, J., Smith, S. K., Print, C. G., and Charnock-Jones, D. S. 2007. Vascular development in embryoid bodies: quantification of transgenic intervention and antiangiogenic treatment. Angiogenesis *10*, 217-226.

Cited by 7, Impact Factor 6.063

ISSN: 0969-6970

Journal Type

Angiogenesis is an international peer-reviewed journal devoted to the publication of original articles and reviews on the cellular and molecular mechanisms that regulate angiogenesis in physiological and pathological conditions. This journal publishes innovative experimental studies using molecular, in vitro, animal model systems and clinical investigations of angiogenic diseases. Angiogenesis also reports on novel therapeutic approaches for promoting or inhibiting angiogenesis as well as new markers and techniques for disease diagnosis and prognosis.

Personal Contribution

Author contributions: ALE: design, collection and assembly of data, data analysis and interpretation, manuscript writing; JB: Started the project but left the university; JS: Confocal training and supervision; SKS: Financial support and review of manuscript: CP & DSCJ: conception and design, interpretation, manuscript writing.
As is the way in research this paper was completed after my contract had ended and I was already working for Jim Smith then at the Gurdon Institute in Tennis Court Road, Cambridge. Cris Print was back in Auckland therefore acknowledgements should also go to skype (Skype Technologies Microsoft, 2003 available at www.Skype.com/).

Angiogenesis (2007) 10:217–226
DOI 10.1007/s10456-007-9076-y

ORIGINAL PAPER

Vascular development in embryoid bodies: quantification of transgenic intervention and antiangiogenic treatment

Amanda Lisabeth Evans · James Bryant · Jeremy Skepper · Stephen K. Smith · Cristin G. Print · D. Stephen Charnock-Jones

Received: 27 November 2006 / Accepted: 26 April 2007 / Published online: 19 June 2007

Abstract It has become increasingly clear that the investigation of vascular development is best considered in the context of a whole tissue environment since in vivo endothelial cells interact closely with other cell types. Murine embryoid bodies have been used as a model for the early development of a vascular network and are amenable to genetic manipulation and treatment with soluble modulators. However, quantifying morphological changes in these complex three-dimensional structures is challenging. In this paper we describe protocols to culture embryoid bodies on a large scale to study vascular development together with methods to quantify changes seen when antiangiogenic agents or endothelial cell-specific transgenes are introduced.

Cristin G. Print and D. Stephen Charnock-Jones are joint senior authors.

A. L. Evans · J. Bryant · S. K. Smith · C. G. Print
Department of Pathology, University of Cambridge, Tennis Court Rd, Cambridge CB2 1QP, UK

J. Skepper
Multi - imaging Centre, Department of Anatomy, Cambridge University, Cambridge CB2 3DY, UK

D. S. Charnock-Jones (✉)
Department of Obstetrics and Gynaecology, The Rosie Hospital, Robinson Way, Cambridge CB2 2SW, UK
e-mail: dscj1@cam.ac.uk

C. G. Print
Department of Molecular Medicine and Pathology, School of Medical Science, University of Auckland, Park Road, Grafton, Auckland, New Zealand

Keywords Embryoid body · Embryonic stem cells · Endothelial cells · Platelet endothelial cell adhesion molecule · Vessel-like structures

Introduction

Embryoid body development

Embryonic stem (ES) cell lines are derived from the inner cell mass (ICM) of early mouse embryos [1, 2]. Embryoid bodies (EBs) form as ES cells differentiate when cultured without feeder cells or Leukaemia Inhibitory Factor (LIF) [3, 4]. EBs consist of three-dimensional embryo-like structures containing cells derived from all three definitive embryonic germ layers–endoderm, mesoderm and ectoderm [5]. EBs recapitulate many features of embryonic development, although embryonic patterning is incomplete [6, 7], as reviewed by [8]. Murine EBs are particularly amenable to mesoderm induction and subsequent blood and vascular development [9, 10], which is thought to occur via a common precursor, the hemangioblast [11, 12] (Fig. 1A). Therefore, EBs model much of the complexity of vascular and haemopoietic development that occurs in vivo [13–15].

Like the many in vivo methods to study vasculogenesis [16] and angiogenesis [17] in common use (reviewed by [18, 19]) the EB system has the advantage that blood vessels develop in the context of whole tissues, with the inherent paracrine and contact-mediated signalling between cells of different lineages. However, unlike in vivo methods, the EB system does not require the use of sentient experimental animals. Like the commonly used in vitro methods in which extra-cellular matrices (ECM) are used to induce vascular morphogenesis of ECs, [19, 20] the EB

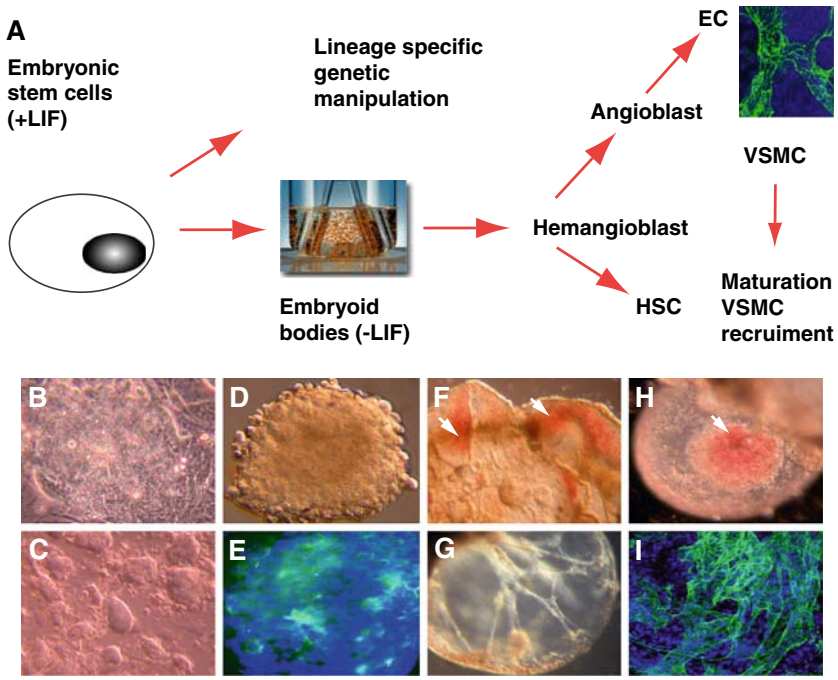

Fig. 1 (**A**) Investigating vascular development in the context of a whole tissue environment. Schematic showing EC development via mesoderm precursors. (HSC hematopoietic stem cells, VSMC vascular smooth muscle cell, EC endothelial cells. (**B**) An undifferentiated ES cell colony grown on STO feeders. (image 450 μm × 350 μm).(**C**) ES colonies grown without STO feeders for 24 h have more defined edges and show signs of differentiation (image 450 μm × 350 μm). (**D**) A single EB after 3 days in spinner culture. (image 4500 μm × 3500 μm (**E**). Whole mount day 3 EB in which endothelial precursors and nuclei were detected using an anti-CD31 antibody (green) and Hoechst 33528 (blue), respectively (image 4500 μm × 3500 μm). Note the increase in volume between B, C and D, E. (**F**) Part of a day 10 EB, arrows highlight blood islands. (**G**). Part of a cystic day 10 EB where the cavity is septate. (**H**). Part of a day 13 cystic EB with distinct central blood islands. (**I**) Maximum projection confocal image from a day 13 EB, stained as E. (images F-I 4500 μm × 3500 μm) B, C, D, F, G, H were captured using a Nikon Coolpix 995, E using a Zeiss Axiovert S100TV microscope with appropriate filters and I using a Leica TCS Laser Scanning Confocal Microscope

system allow well defined and easy to manipulate experiments to be performed. However, the EB system also has the disadvantage that vascular development that occurs in the absence of blood flow, which may modulate EC survival and differentiation [21]. Therefore, the EB system fall somewhere between the in vivo and in vitro methods of studying vascular development, and captures many of the advantages of both.

We chose the spinner flask approach to culture EBs since this method of culture consistently produces large numbers of EBs with a high degree of differentiation and synchronism of vascular development [22, 23]. Spinner culture allows continuous support for the delicate cystic structures and constant motion of the nutrients that maintains consistent exposure to nutrients and oxygen throughout the EB population and also prevents the aggregation of EBs often seen in suspension cultures in dishes. The system is also the best recapitulation of mouse embryogenesis resembling the zygote in the fluid-like environment of the oviduct.

One of the biggest challenges of studying vessel differentiation in these near-in vivo conditions is to adequately quantify the resulting complexity building upon purely visual descriptions.

To identify vascular structures a monoclonal anti-CD31 antibody (recognizing PECAM-1, Platelet Endothelial Cell Adhesion Molecule-1), which is widely expressed in the vascular compartment, was used [24–26]. We have quantified CD31-stained structures using what may at first appear to be complex stereology. However it is relatively simple to perform, and permits rigorous systematic quantification of vascular structures. This makes the EB system suitable as a tool for early developmental and vascular research.

In this article we demonstrate the utility of the EB system to quantify the effects of both transgene expression and soluble compounds on vascular development. For an example of transgene expression, regulatory regions from the mouse *tie2* gene [27] were used to drive endothelial-specific expression of wild type (wt) and mutant human *Bcl-2*. For an example of a soluble compound, the anti-angiogenic agent berberine [28, 29], a plant isoquinoline alkaloid with a long history of use in Ayurvedic and Chinese medicine, was used.

Methods

Establishment of STO feeder lines

All cell culture was conducted in a 37°C incubator with a humidified atmosphere of 10% CO_2 in air. The mouse embryo fibroblast line STO [30] was mitotically inactivated by 70 Gray X-irradiation. Inactivated STO cells were seeded into 60 mm^2 culture dishes coated with 0.1% gelatin (Sigma-Aldrich, Poole, Dorset, UK) in 5 ml of media at a concentration of 2–4 $\times$ 10^5 cells/ml. The seeding density required for a confluent STO monolayer was determined during pilot experiments. This may differ between different batches of frozen STO cells and is important to optimize by trial experiments, since sub-confluent or over-confluent STO monolayers provide poor substrates for ES cell culture. The medium for STO culture consisted of DMEM (Sigma-Aldrich) supplemented with 0.1 mM β Mercaptoethanol (Sigma), Non-Essential Amino Acids (Gibco Invitrogen Cell Culture, UK, 100× stock), 2 mM Glutamate (Gibco Invitrogen Cell Culture) and 10% foetal bovine serum (FBS) (Gibco Invitrogen Cell Culture). The FBS had previously been batch tested for optimal ES cell proliferation. Batch testing was an essential part of the preparation before growing EB. STO cells were seeded at least 24 h prior to thawing the ES cells to allow the production of sufficient LIF to prevent ES differentiation (Fig. 1B, C).

Propagation of undifferentiated ES cells

STO monolayers were washed with phosphate buffered saline (PBS). ES cell media was prepared identically to the STO media, with the exception that the concentration of FBS was increased to 15%. Passage 13 R1-strain mouse ES cells [31] were suspended at a concentration of 4 $\times$ 10^5 cells/ml in this medium. Medium was aspirated from the STO cells, and 5 ml of the ES cell suspension gently layered onto the washed STO feeder monolayer. The media was replaced daily and not allowed to become yellow. To prevent differentiation, the ES cells required passaging every 2–3 days. Differentiation was most easily recognised by the appearance of flat cells around colonies and the distinct appearance of the individual cells within the colonies. The avoidance of ES cell differentiation is essential since differentiation at this stage may alter the capacity of ES cells to subsequently differentiate into EC, and it may also reduce the usefulness of the transgenic ES cells for the generation of transgenic mice, should this be desired at a later time. The ES cells were fed with fresh media 4 hours prior to passaging. For passaging 0.05% Trypsin/EDTA was supplemented with 1% chicken serum, providing a cyto-protective protein mixture that was not a trypsin substrate. Care was taken to fully dissociate all of the trypsinised ES cells to a single-cell suspension by repeatedly passing through a 10 ml plastic pipette with a p200 tip attached.

Differentiation of ES cells into EBs in spinner flasks

Spinner medium was prepared identically to the STO media, but the concentration of FBS further increased to 20%. At day 0, adherent log phase ES cell colonies were dissociated as described above and resuspended in 10 ml of spinner media. A large proportion of the inactivated STO feeder cells contained in the ES cell suspension were removed through differential sedimentation by transferring the ES cell suspension to a 100 mm^2 gelatin coated plate at 37°C for 20 min. The gelatin coating ensures maximum adherence of the sedimenting STO feeders compared to undifferentiated ES cells, most of which remain in suspension. Minimising the STO cell contamination reduces potential anti-differentiation effect of STO cells, which are likely to alter vascular EB differentiation. The Cellspin culture system (Integra Biosciences, Letchworth, Hertfordshire, UK) was used, with the Cellspin control unit preset at a spin rate of 25 rpm and spin angle 720° (such that it reverses direction each two revolutions). Media (45 ml) was pre-equilibrated in 100 ml siliconised (Sigmacote, Sigma-Aldrich) spinner flasks (Integra Biosciences). ES cells were recovered from the gelatin coated differential sedimentation plates, and centrifuged at 800 g for 5 min. Cells were fully dissociated as described to ensure the cultures were initiated from single cells. To inoculate each spinner flask 1.0 $\times$ 10^7 cells in 5 ml spinner media were added to the 45 ml of pre-equilibrated media in each flask.

After 24 h (i.e. on day 1) a further 50 ml of spinner media was added to each flask. Each subsequent day, flasks were transferred to a sterile cell culture cabinet, where EB were allowed to settle for 1 min, and 50 ml of spinner media was aspirated and replaced with fresh pre-warmed spinner media. For treatment with the soluble anti-angiogenic agent berberine (berberine hemisulphate, Sigma-Aldrich) was dissolved in sterile water to 10 mM and filtered. EB were allowed to differentiate in spinners without treatment for 3 days and then treated with 10 μm berberine hemisulphate thereafter. EB were sampled on day 10 and 15 and then processed as described below.

Plasmid vectors for genetic modification of EB

For EC specific expression of transgenes in EBs, ES cells were transfected with vectors containing promoter/enhancer regions of the mouse *tie 2* gene generated from the plasmid *pTie2SV40* by removing the *pBSKII*$^+$ backbone and replacing it with the pBK-CMV backbone (Stratagene Europe, Amsterdam, The Netherlands) containing an

aminoglycoside phosphotransferase (*neo*) cassette. Thus cells containing this vector, *pTie2neo* could be selected with the neomycin analogue G418 sulphate (Geneticin Gibco Invitrogen Cell Culture, for ES and EB) or Kanamycin (for *E.coli*, Sigma-Aldrich). *pTie2neo* was used as a universal vector to produce further constructs in a single cloning step by insertion of coding sequences of interest into the unique *Not* I restriction site (Fig. 2A). Both human wt *Bcl-2* and the mutant *Bcl-2* G145E cDNAs were cloned in this way. Fragments were generated by PCR using a proof reading Taq polymerase (True Fidelity DNA polymerase, Continental Lab Products, San Diego, CA, USA). Clones were verified by restriction enzyme digestion and sequencing. Plasmid DNA for ES transfection was prepared using the Qiagen Endofree plasmid preparation kit (Qiagen Ltd., West Sussex, UK) and resuspended in sterile deionised water.

Transfection of STO feeders and ES cells

Passage 2 STO cells were made stably G418-resistant by transfection using Lipofectamine™Fig. 2). PCR conditions were [95°C for 15 min] × 1 cycle, then [95°C for 30 s denaturation, 58°C for 30 s annealing, 72°C for 30 s extension] × 35 cycles for all plasmids containing inserts of less than 1 kb in size. The extension time was increased

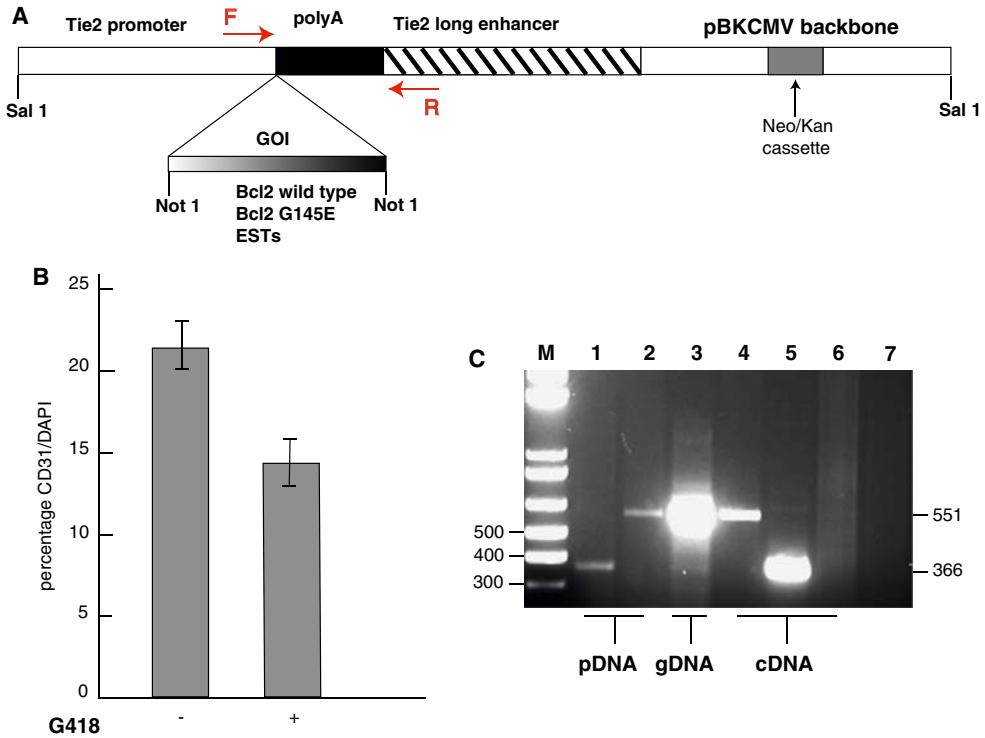

Fig. 2 (**A**) *pTie2neo* endothelial specific expression vector. The gene of interest (GOI) e.g. *Bcl-2* can be inserted into a unique *Not*I restriction endonuclease site between the *Tie2 promoter* and the *polyA cassette*. Arrows labelled F and R indicate PCR primers used for genotyping and RT-PCR in the 3′ transcribed region of the *Tie2* promoter and the 5′ transcribed region of the *Tie2* enhancer, respectively. (**B**) The effects of the selection antibiotic G418 on vessel development in EB. EB generated from a *pTie2neo* ES cell clone were differentiated in spinner flasks for 13 days in the presence or absence of G418 (500 μg/ml) and cryosectioned. The fraction of cellular EB volume occupied by CD31-stained structures after 13 days of differentiation was quantified as described in methods from 50 images without G418 (–G418) and 30 images with G418 (+G418). This was expressed as a percentage. Error bars represent standard error of the mean. The fraction of cellular EB volume occupied by ECs differed significantly between EB cultured with and without G418 ($P \leq 0.01$, *t*-test). (**C**) EB derived from ES cells retained and expressed transgenes after differentiation for at least 10 days in the absence of G418. 1.2% agarose gel showing PCR and RT-PCR products. Oligonucleotide primers used were F and R. Lanes are; M: 1 kb plus DNA ladder (New England Biolabs), (1) positive control (PCR using *pTie2neo* plasmid DNA), (2) positive control (PCR using *pTIE2neo* + *insert* plasmid DNA), (3): PCR using 5 ng EB genomic DNA, derived from ES cells transfected with the same construct as lane 2, grown without G418 for 10 days of differentiation, (4) RT-PCR using 100 ng of RNA prepared from EB containing the same construct as lanes 2 and 3, grown without G418 for 10 days of differentiation (no RT control not shown was negative), (5) RT-PCR using 100 ng of RNA prepared from EB containing *pTie2neo* (as lane 1) grown without G418 for 13 days of differentiation, (6) RT-PCR using 100 ng of RNA prepared from EB spontaneously differentiated from wild type ES cells, lane (7) PCR negative control using a water template

to 5 min for products > 2 kb. When the parent *pTie2neo* plasmid was used as a positive control for PCR, a 366 bp product was amplified (Fig. 2C, lane 1).

RT-PCR of differentiating EB

RNA was isolated from differentiated EB using Tri-Reagent LS (Sigma-Aldrich), digested with 2 units of DNase enzyme (DNA-*free*, Ambion Europe Ltd, Cambridgeshire, UK) per 50 µl for 30 min at 37°C and re-purified using the RNeasy Mini Kit (Qiagen Ltd.). RNA was then checked for integrity and purity using an Agilent Technologies 2100 Bioanalyser (Agilent Technologies UK Limited, Cheshire, UK). cDNA was generated using Superscript III Reverse Transcriptase (Invitrogen, Life Technologies) from 1 µg of RNA according to the manufacturers instructions. All samples were checked for genomic DNA contamination by amplification without prior reverse transcription (data not shown).

Immunofluorescent and immunohistochemical staining

Samples (1 ml) were taken via the side arms of the spinner flasks and collected in glass vials, EB allowed to settle, washed two times with PBS, then either frozen in optimal cutting temperature compound (OCT, Tissue Tek, Sakura Inc., Torrance, CA., USA) while stirring with a glass rod to maintain a uniform distribution, or fixed whole in acetone/methanol (3:7) at –20°C for 20 min. Cryosections of 10 µm were cut from EB that had been frozen in OCT and transferred to uncoated glass slides, then fixed for 10 min at room temperature in acetone. Sections were washed in wash buffer (PBS plus 0.01% Triton- × -100, Sigma) then blocked for 1 h at room temperature in a humidified chamber using PBS plus 10% goat serum (Sigma-Aldrich) and 0.2% bovine serum albumin (fraction V, Sigma-Aldrich). Sections were then washed and incubated overnight at 4°C with primary antibody; a monoclonal rat anti-mouse antibody directed against CD31 (clone MEC13.3, BD PharMingen, Oxford, UK) at 1:100, or polyclonal rabbit anti-human Bcl-2 (Oncogene Research, CA., USA) at 1:500 followed by three washes for 10 min at room temperature in wash buffer. As secondary antibodies either Alexa Fluor 488 goat anti-rat IgG (H + L) or Alexa Fluor 568 goat anti-rabbit IgG (H + L) (Molecular Probes Europe, Leiden, The Netherlands) were used at 1:200. Sections were mounted using Vectashield mounting medium containing DAPI (Vector Laboratories Ltd., Peterborough, UK) and the coverslips sealed with nail varnish.

Whole fixed EB, washed in PBS, can be stored at 4°C for up to 6 months. For whole-mount staining they were first incubated with 1 µg/ml Hoechst 33528 (Bis-benzimide trihydrochloride) nucleic acid-binding dye (Calbiochem Merck Biosciences Ltd, Nottingham, UK) in PBS plus 0.01% Triton- × -100 (PBST) overnight at 4°C, then washed overnight at 4°C in PBST. Thereafter they were stained as for immunofluorescent frozen sections but wash times increased from 10 min to 20 minutes and Vectashield mounting medium without DAPI was used. Whole EB were mounted on single cavity microscope slides (Superior, West Germany).

Due to the inherent fluorescence of berberine (Ex. 420 nm, Em. 520 nm) in these experiments biotinylated Anti-Rat IgG (H + L) (Vector Laboratories) was used at 1:200, followed by Vectastain Elite ABC kit (Vector Laboratories) with DAB chromagen (DakoCytomation Ltd, UK). Slides were counterstained with Carazzi's heamatoxylin, then dehydrated and mounted using DPX (Fisher Scientific Ltd, Leicestershire, UK).

Imaging and stereology

Digital images were captured with a Nikon Coolpix 995 camera attached to a Zeiss Axiovert S100TV microscope. A Leica TCS Laser Scanning Confocal Microscope was used for higher-resolution images and for three-dimensional reconstructions of whole mount EB (LCS Leica Microsystems, Heidelberg, GmBH). Digital 1024 × 1024 or 1300 × 1300 pixel images of fluorescently or chromogenically stained cryosections of EB were captured, each covering an area of 1000 µm × 1000 µm or 2000 µm × 2000 µm respectively. Quantification of endothelial differentiation was carried out after importing the images into Computer-Aided Stereological Toolbox (CAST) software (Olympus, Denmark). The principles of isotropic, uniform and random (IUR) sampling were followed as far as practically possible. Specifically, EB were stirred during embedding in OCT to maintain a uniform distribution of orientations, and images for quantification were selected by systematic random sampling from each slide. Volume fractions were determined by point counting using a quadratic lattice and overlaying 100 intersections over each image with a minimum of five randomly selected images per slide and five systematically randomly selected slides per clone. A pilot study was analysed using the cumulative mean technique to verify that this was adequate to ensure that sufficient images were counted. Running means and standard deviations were plotted to ensure mean stabilisation and standard deviation reduction to determine the number of fields to be scored. Results of volume fraction analysis were expressed as percentage of CD31/DAPI or CD31/haematoxylin staining. This provided an estimate of the proportion of the cellular regions of EB that were occupied by endothelial marker-stained structures

Stained sections were also scored, where relevant, for additional features relating to EB differentiation including the number of CD31 positive cells appearing as part of vessel like structures (VLS). It would be useful to convert these proportional values of VLS into absolute volumes of VLS per EB, thus avoiding the sterological 'reference trap' [33]. However, we could not do this reliably, since the irregular shape and cavitation prevented reliable assessment of EB volume. For statistical analysis, log transformation of data was required to bring it to a near-Gaussian distribution in order to allow the use of parametric statistical tests such as ANOVA.

Results and discussion

Vascular development in EBs

In spinner culture ES cells aggregate to form early morula-like structures clearly visible as solid balls of cells (Fig. 1D) the surface of which later smoothens to resemble a compact morula. We know that in addition to vascular expression CD31 is also expressed in the pluripotent cells of the mouse inner cell mass [34] and CD31 staining in Fig. 1E suggests progenitors that give rise to vasculature do develop from mesodermal cells located throughout the early embryo. This is supported by evidence in *Xenopus Laevis* using EC fate maps [35] and by other studies such as those in the chick-quail system [36], and the mouse [37]. Expression of the early mesoderm marker brachyury peaks at day 4 under these conditions (data not shown) and ECs appeared by day 4–5 of differentiation (approximating to day 7.5 of mouse embryonic development) and coalesced into a rudimentary network of angioblasts [11, 38]. After 10 days EBs had increased in size by more than twenty times (from Fig. 1D–F) and all had become cavitated, usually with a central septate cavity (Fig. 1G), surrounded by an endodermal coat, as shown at the top edge of the EB in Fig. 1F. This outer layer has been shown to express the transcription factor GATA-4, which first appears in visceral and parietal endoderm in mouse embryogenesis [39]. Cavitation of the EBs is a critical part of the differentiation process [40], and in parallel with this process vascularisation may improve oxygen supply to the depth of the EB [41]. By 10–13 days of differentiation blood island-like structures (Fig. 1F, H) containing cells filled with haemoglobin are seen near the centre of cavitated areas (Fig. 1H).

The development of vascular networks within EB is thought to be in-part promoted by vascular endothelial growth factor (VEGF)-A produced within the EB [42] as well as VEGF and basic fibroblast growth factor supplied by the serum [43]. VEGF-A further promotes survival by the upregulation of *Bcl-2* in ECs and the migration and patterning of endothelial progenitors and cells in the embryo [44].

After 13 days of differentiation angioblasts had developed into networks of CD31 positive VLS around the edges of the central cavities (Fig. 1I) in all EBs sampled from a synchronised culture. Confocal microscopy showed that these CD31 staining VLS were complex, multi-cellular and interconnected, resembling those found in the early vertebrate yolk sac (Fig. 3). Many VLS did not appear to have continuous lumen while others had large lumens lined by relatively thin $CD31^{+ve}$ endothelial walls reminiscent of venous sinuses (Fig. 3 B–F). Frequently networks of varying size and shape with both sinusoid capillaries up to 150 μm diameter (Fig. 3E) and narrow capillaries seen in the same EB. None of the vessels observed in this study were filled with blood cells as described using quail derived EBs [45].

During embryonic vessel development ECs and blood cells are the first to develop while supporting pericytes and smooth muscle cells appear later. Immunostaining for smooth muscle actin together with CD31 did not reveal pericyte investment of VLS during the time course of this study (data not shown). Murine EBs may therefore be a useful model for immature vessels at the plasticity window [46] when the existence of a pericyte free endothelial plexus makes ECs sensitive to VEGF withdrawal and anti-angiogenic therapy [47].

Quantification of vascular-targeted transgene expression in EBs

Having established the pattern and timing of vessel development as described above we were then able to genetically manipulate the system to examine and quantify the role of apoptosis in new vessel formation. Following vasculogenesis, de novo vessel formation from mesoderm-derived angioblasts, angiogenic remodelling of the primary plexus involves a subtle balance between cell growth and apoptosis [11, 17]. Inhibition of apoptosis has been shown to alter vascular development both in vitro [48] and in vivo [49], although the mechanism is incompletely understood. To test the hypothesis that apoptosis contributes to vascular development in EBs, independent ES cell clones were generated carrying either a *wt Bcl-2* transgene (which inhibits apoptosis, and in a small number of studies also inhibits proliferation) or *G145E* mutant *Bcl-2* transgene, which contains a single base pair substitution that abrogates the anti-apoptotic but not the proliferation-restraining activity of *Bcl-2* [50, 51]. These ES cell clones were then differentiated into EBs as separate populations in spinner culture. Double immunofluoresence for CD31 and human *Bcl-2* revealed an overlaping pattern of EC and transgene staining (Fig. 4A). The anti-Bcl-2 antibody was capable of

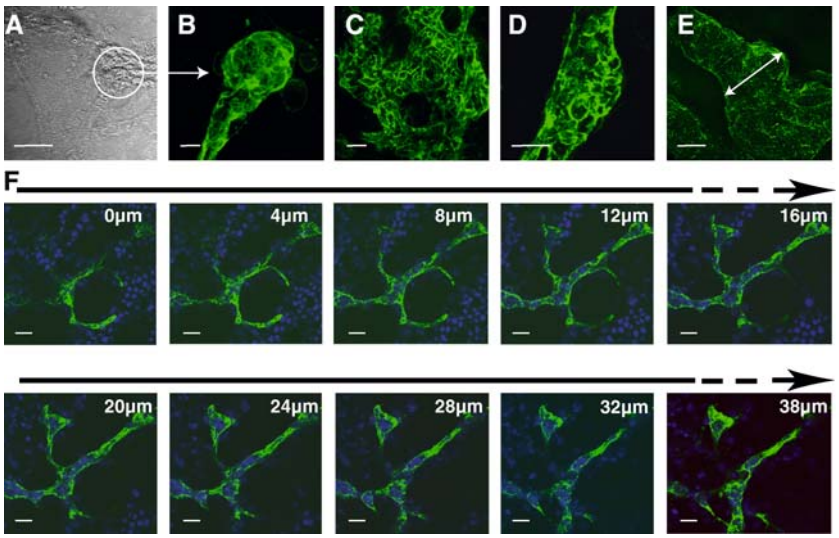

Fig. 3 Confocal microscopy detected CD31-stained vascular structures within whole mount EB. (**A**) Pseudo-phase contrast image of a region within an EB after 11 days of differentiation. (**B**) The structure circled in panel A was revealed as a developing 'vessel' within the EB by anti-CD31 staining (green, maximum projection image combining twenty-five 1 μm confocal Z-series sections). (**C**–**E**) Developing vessels within EB after 11 days of differentiation revealed by anti-CD31 staining (maximum projection images). (**F**) A Z-series fly-through (38 μm total depth) of branched, interconnected multicellular vascular structures within an EB after 11 days of differentiation. Endothelial cells and nuclei were detected using an anti-CD31 antibody (green) and Hoechst 33528 (blue), respectively. Scale bars in A–E are 100 μm

detecting endogenous mouse Bcl-2, but none was detected in this study. Endogenous mouse Bcl-2 levels are likely to be low during early stages of EB differentiation relative to transgene-derived Bcl-2.

Volume fraction stereology suggested that the expression of *wt Bcl-2* reduced the percentage of cellular EB volume occupied by VLS (Fig. 4B) compared to the expression of the non-functional mutant *Bcl-2 G145E*. Medians for all mutant non-functional *Bcl-2* clones where higher than those for the *wt Bcl-2* clones and ANOVA of log-transformed data further supported the suggestion that significant differences were attributable to the effect of wild type versus *G145E* mutant *Bcl-2* transgene expression ($P \leq 0.05$). Along with the previous studies referred to above, this experiment suggests that vascular development may utilise apoptosis though an as-yet undefined mechanism. The EB system will be useful to elucidate this mechanism in future studies. We noted some variability between the transfected clones (Fig. 4B). This inter-clone variation in vascular development may be due to a combination of transgene integration site and copy number differences as well as a degree of stochastic patterning and developmental noise. Single clone experiments may therefore produce misleading results and several independent transgenic ES cell clones provide a more robust analysis of EB vascular development. Replication using independent transgenic EB cultures has an additional advantage in controlling for technical variation between flasks.

In addition we noticed that EBs that are grown in the presence of 500 μg/ml G418 contained fewer VLS than EBs grown without antibiotic. To quantify this observation we identified cellular regions of EBs with DAPI and stained the VLS within these cellular regions using anti-CD31 immunohistochemistry. We found that the percentage of the volume of cellular regions occupied by CD31 positive cells was significantly lower (Student's *t*-test $P \leq 0.01$) in EBs cultured in the presence of 500 μg/ml G418 than in EBs cultured without antibiotic (Fig. 2B). As a result G418 selection was withdrawn after ES cells were transferred to spinner flasks and we showed that, in EB cultures examined, this approach does not result in the loss of transgene presence (Fig. 2C lanes 3 and 5) or expression (lane 4).

The progress of vascular differentiation in EBs may be subtly altered by the addition of soluble factors

To illustrate the use of the EB system to study the effects of soluble factors on vessel development, the isoquinoline alkaloid berberine was used. Berberine altered the progression of EB development (Fig. 5B). However, if scored simply on the basis of percentage of anti-CD31 compared to nuclear staining (Fig. 5A) this was not apparent. Control EBs became increasingly cystic between day 10 and day 15 of spinner culture, accompanied by an increase in total (Fig. 5A) and peripheral (Fig. 5C) VLS and a corresponding decrease in central CD31 staining (Fig. 5D). In contrast, berberine treated EBs did not become cystic

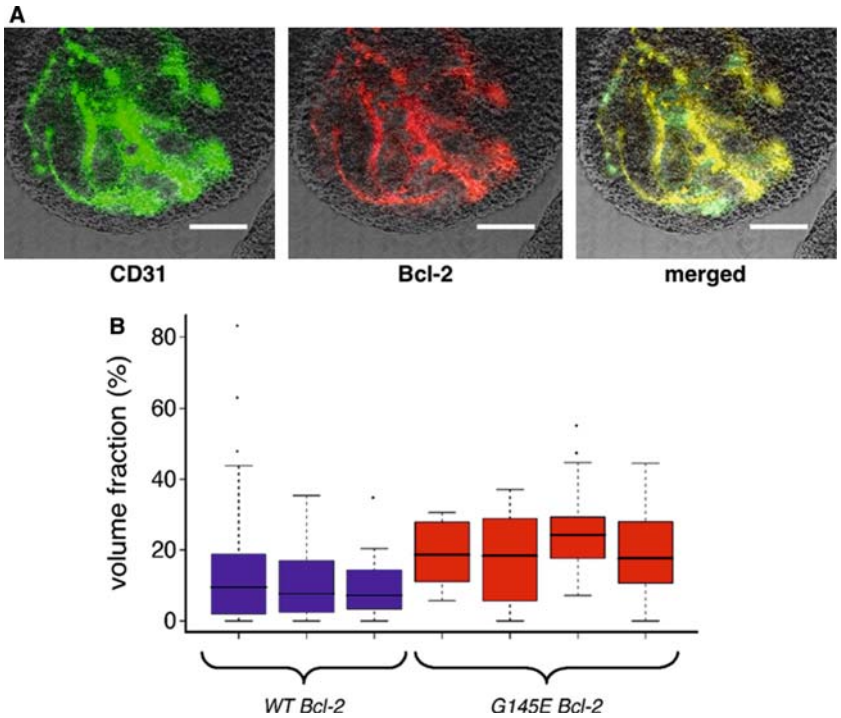

Fig. 4 The effect of endothelial specific transgene expression on EB vascular development. (**A**) EBs derived from *pTie2Bcl2G145E*-transfected ES cells were differentiated for 8 days in spinner culture and whole mounts immunostained for CD31 (green) and Bcl-2 (red). Scale bars are 200 μm. A representative image showing co-expression of Bcl-2 and CD31. (**B**) Three clones of ES cells transfected with *pTie2Bcl2WT*, and four clones transfected with *pTie2Bcl2G145E* were differentiated into EB for 8 days in spinner cultures and cryosectioned. EC were detected using an anti-CD31 antibody, and cellular regions of EBs assessed by staining nuclei with DAPI. To estimate the fraction of cellular EB volume occupied by CD31-stained structures, the volume fraction of CD31-stained structures was calculated for the EB derived from each clone as described and expressed as a percentage. In the box-and-whisker plot the central blocks represents volume fractions from the lower to upper quartile (blue boxes are wild type and red are mutant clones) and the solid middle line the median, the vertical dashed lines extend to the farthest data points within 3/2 times the interquartile ranges for each clone excluding outliers displayed as separate points

between day 10 and day 15 of spinner culture and did not develop peripheral VLS (Fig. 5C). Anti-CD31 staining was present in the centre of the berberine treated EBs (Fig. 5D) although VLS were not formed (Fig. 5B). This suggests angioblast precursors of the vascular network were present much like the staining seen in early day 3–4 EBs. Berberine is known to inhibit the hypoxia responsive transcription factor HIF1α and subsequently the VEGF autocrine loop [29], which results in inhibition of vessel formation. Therefore, it is possible that berberine may have prevented the normal hypoxic response in the centre of the immature uncavitated EBs resulting in reduced angiogenesis. Since the microenvironment of solid tumours is often hypoxic [52], murine EBs may provide a further model for early tumour neovascularisation.

Conclusion

The EB recapitulates many of the developmental processes that occur in an embryo, including vasculogenesis and angiogenesis. In EBs vascular development occurs in the context of a whole tissue including both paracrine growth factor and contact-mediated signals between cells of several lineages. Therefore, the EB system provides a method to study vascular development in a near-in vivo environment while retaining the practical and ethical advantages of in vitro experiments.

We have shown that EBs can be used to quantify the effects of both transgene expression and pharmacological agents on vascular development. This method can be used on a relatively small scale as described, but could easily be scaled up to assess anti-angiogenic agents in a medium throughput screen.

We hope that the methods described here will contribute to the expanded use of the EB system in vascular biology research as an alternative or adjunct to studies involving experimental animals.

Acknowledgements This work was supported by a British Heart Foundation project grant and the University of Cambridge, Department of Pathology, Cambridge, UK. We wish to acknowledge: Professor T. Sato for the gift of mouse *tie2* gene sequences, Professor A. Nagy (Samuel Lunenfeld Research Institute, Ontario, Canada) for the gift of R1 embryonic stem cells, Dr G. J. Burton (University of

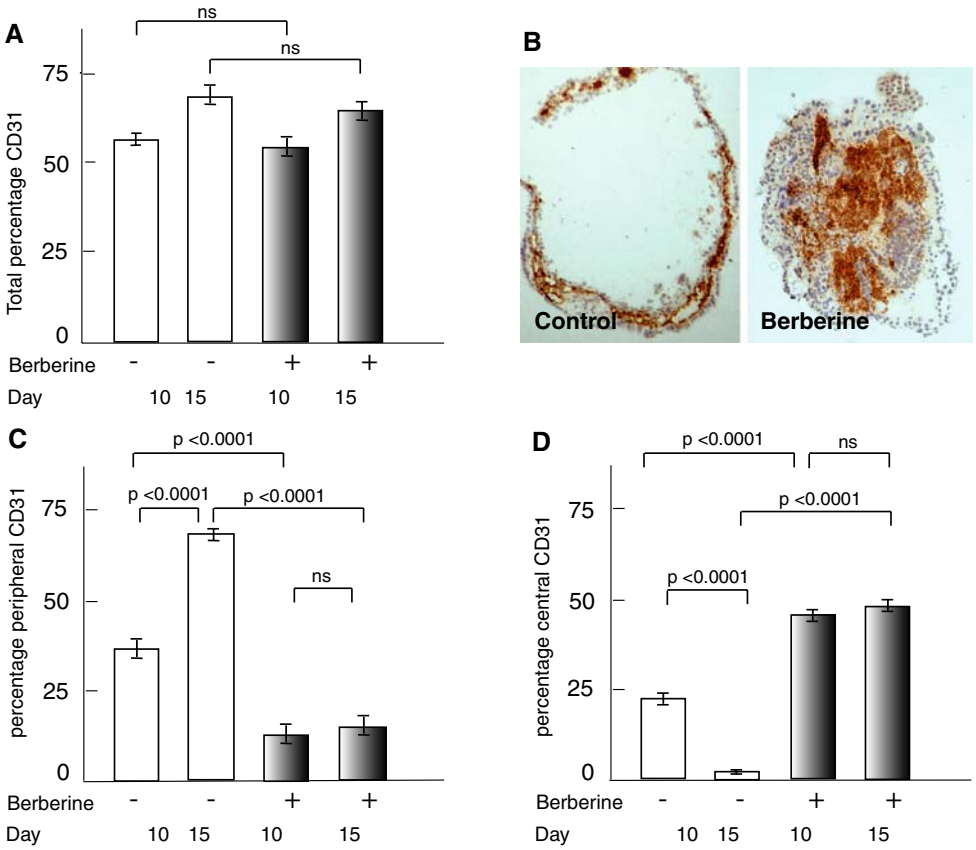

Fig. 5 The plant alkaloid berberine has a significant effect on the distribution of CD31 staining, but not on the total fraction of EB cellular volume occupied by CD31-stained structures. Wild type ES cells were differentiated into EB in the presence (white bars) or absence (grey bars) of 10 μm berberine. EB were harvested after either 10 days or 15 days of spinner culture, cryosectioned and immunostained with anti-CD31 antibody, which was detected with the chromogenic substrate DAB. Cellular regions of EB were detected with a haematoxylin counterstain. (**A**) The percentage of anti-CD31 stained EC within the total EB was quantified as described in the methods. (**B**) Example images of control or berberine treated day15 EBs Images 2mm × 2 mm. The percentage of the cellular volumes of the peripheral and central regions of EB occupied by anti-CD31 stained ECs are shown in (**C**) and (**D**), respectively. Central regions are defined as regions more than 3 cell-widths from the EB edge. Data for A, C and D were each based on the means of 38 images for each treatment group and error bars show the standard error of the mean. Students *t*-tests were performed, ns indicates no significant difference, $P \leq 0.0001$ for all other values

Cambridge, Department of Anatomy, Cambridge, UK) for assistance with stereology, Dr H. Duval (Department of Pathology, Cambridge University) for *pTie2SV40*.

References

1. Evans MJ, Kaufman MH (1981) Establishment in culture of pluripotential cells from mouse embryos. Nature 292:154–156
2. Martin GR (1981) Isolation of a pluripotent cell line from early mouse embryos cultured in medium conditioned by teratocarcinoma stem cells. Proc Natl Acad Sci USA 78:7634–7638
3. Zandstra PW, Le HV, Daley GQ et al. (2000) Leukemia inhibitory factor (LIF) concentration modulates embryonic stem cell self-renewal and differentiation independently of proliferation. Biotechnol Bioeng 69:607–617
4. Williams RL, Hilton DJ, Pease S et al. (1988) Myeloid leukaemia inhibitory factor maintains the developmental potential of embryonic stem cells. Nature 336:684–687
5. Karbanova J, Mokry J (2002) Histological and histochemical analysis of embryoid bodies. Acta Histochem 104:361–365
6. Hopfl G, Gassmann M, Desbaillets I (2004) Differentiating embryonic stem cells into embryoid bodies. Methods Mol Biol 254:79–98
7. Desbaillets I, Ziegler U, Groscurth P et al. (2000) Embryoid bodies: an in vitro model of mouse embryogenesis. Exp Physiol 85:645–651
8. Weitzer G (2006) Embryonic stem cell-derived embryoid bodies: an in vitro model of eutherian pregastrulation development and early gastrulation, vol 174 Springer Berlin Heidleberg, Heidleberg
9. Boheler KR, Czyz J, Tweedie D et al. (2002) Differentiation of pluripotent embryonic stem cells into cardiomyocytes. Circ Res 91:189–201
10. Daley GQ (2003) From embryos to embryoid bodies: generating blood from embryonic stem cells. Ann N Y Acad Sci 996:122–131
11. Risau W, Sariola H, Zerwes HG et al. (1988) Vasculogenesis and angiogenesis in embryonic-stem-cell-derived embryoid bodies. Development 102:471–478

12. Risau W (1995) Differentiation of endothelium. Faseb J 9: 926–933
13. Dang SM, Kyba M, Perlingeiro R et al. (2002) Efficiency of embryoid body formation and hematopoietic development from embryonic stem cells in different culture systems. Biotechnol Bioeng 78:442–453
14. Vittet D, Prandini MH, Berthier R et al. (1996) Embryonic stem cells differentiate in vitro to endothelial cells through successive maturation steps. Blood 88:3424–3431
15. Feraud O, Vittet D (2003) Murine embryonic stem cell in vitro differentiation: applications to the study of vascular development. Histol Histopathol 18:191–199
16. Risau W, Flamme I (1995) Vasculogenesis. Annu Rev Cell Dev Biol 11:73–91
17. Risau W (1997) Mechanisms of angiogenesis. Nature 386: 671–674
18. Hasan J, Shnyder SD, Bibby M et al. (2004) Quantitative angiogenesis assays in vivo–a review. Angiogenesis 7:1–16
19. Robert A, Nasim A, Rachel LL et al. (2000) Angiogenesis assays: problems and pitfalls. Cancer Meta Rev V19:V167
20. Vailhe B, Vittet D, Feige JJ (2001) In vitro models of vasculogenesis and angiogenesis. Lab Invest 81:439–452
21. Chien S, Li S, Shyy YJ (1998) Effects of mechanical forces on signal transduction and gene expression in endothelial cells. Hypertension 31:162–169
22. Wartenberg M, Gunther J, Hescheler J et al. (1998) The embryoid body as a novel in vitro assay system for antiangiogenic agents. Lab Invest 78:1301–1314
23. Niimi M, Kim MY, Tao L et al. (2005) Single embryonic stem cell-derived embryoid bodies for gene screening. Biotechniques 38:349–50, 352
24. DeLisser HM, Newman PJ, Albelda SM (1994) Molecular and functional aspects of PECAM-1/CD31. Immunol Today 15: 490–495
25. DeLisser HM, Baldwin HS, Albelda SM (1997) Platelet endothelial cell adhesion molecule 1 (PECAM-1/CD31): a multifunctional vascular cell adhesion molecule. Trends Cardiovas Med 7:203
26. Vecchi A, Garlanda C, Lampugnani MG et al. (1994) Monoclonal antibodies specific for endothelial cells of mouse blood vessels. Their application in the identification of adult and embryonic endothelium. Eur J Cell Biol 63:247–254
27. Schlaeger TM, Bartunkova S, Lawitts JA et al. (1997) Uniform vascular-endothelial-cell-specific gene expression in both embryonic and adult transgenic mice. Proc Natl Acad Sci USA 94:3058–3063
28. Wartenberg M, Budde P, De Marees M et al. (2003) Inhibition of tumor-induced angiogenesis and matrix-metalloproteinase expression in confrontation cultures of embryoid bodies and tumor spheroids by plant ingredients used in traditional chinese medicine. Lab Invest 83:87–98
29. Lin S, Tsai SC, Lee CC et al. (2004) Berberine inhibits HIF-1alpha expression via enhanced proteolysis. Mol Pharmacol 66:612–619
30. Martin GR, Evans MJ (1975) Differentiation of clonal lines of teratocarcinoma cells: formation of embryoid bodies in vitro. Proc Natl Acad Sci USA 72:1441–1445
31. Nagy A, Rossant J, Nagy R et al. (1993) Derivation of completely cell culture-derived mice from early-passage embryonic stem cells. Proc Natl Acad Sci USA 90:8424–8428
32. Lakshmipathy U, Pelacho B, Sudo K et al. (2004) Efficient transfection of embryonic and adult stem cells. Stem Cells 22:531–543
33. Mayhew TM, Huppertz B, Kaufmann P et al. (2003) The 'reference trap' revisited: examples of the dangers in using ratios to describe fetoplacental angiogenesis and trophoblast turnover. Placenta 24:1–7
34. Robson P, Stein P, Zhou B et al. (2001) Inner cell mass-specific expression of a cell adhesion molecule (PECAM-1/CD31) in the mouse blastocyst. Dev Biol 234:317–329
35. Mills KR, Kruep D, Saha MS (1999) Elucidating the origins of the vascular system: a fate map of the vascular endothelial and red blood cell lineages in Xenopus laevis. Dev Biol 209:352–68
36. Noden DM (1990) Origins and assembly of avian embryonic blood vessels. Ann N Y Acad Sci 588:236–249
37. Choi K, Kennedy M, Kazarov A et al. (1998) A common precursor for hematopoietic and endothelial cells. Development 125:725–732
38. Wang R, Clark R, Bautch VL (1992) Embryonic stem cell-derived cystic embryoid bodies form vascular channels: an in vitro model of blood vessel development. Development 114:303–316
39. Soudais C, Bielinska M, Heikinheimo M et al. (1995) Targeted mutagenesis of the transcription factor GATA-4 gene in mouse embryonic stem cells disrupts visceral endoderm differentiation in vitro. Development 121:3877–3888
40. Coucouvanis E, Martin GR (1995) Signals for death and survival: a two-step mechanism for cavitation in the vertebrate embryo. Cell 83:279–287
41. Gassmann M, Fandrey J, Bichet S et al. (1996) Oxygen supply and oxygen-dependent gene expression in differentiating embryonic stem cells. Proc Natl Acad Sci USA 93:2867–72
42. Ng YS, Ramsauer M, Loureiro RM et al. (2004) Identification of genes involved in VEGF-mediated vascular morphogenesis using embryonic stem cell-derived cystic embryoid bodies. Lab Invest 84:1209–1218
43. Dixelius J, Jakobsson L, Genersch E et al. (2004) Laminin-1 promotes angiogenesis in synergy with fibroblast growth factor by distinct regulation of the gene and protein expression profile in endothelial cells. J Biol Chem 279:23766–23772
44. Ambler CA, Schmunk GM, Bautch VL (2003) Stem cell-derived endothelial cells/progenitors migrate and pattern in the embryo using the VEGF signaling pathway. Dev Biol 257:205–219
45. Krah K, Mironov V, Risau W et al. (1994) Induction of vasculogenesis in quail blastodisc-derived embryoid bodies. Dev Biol 164:123–132
46. Benjamin LE, Hemo I, Keshet E (1998) A plasticity window for blood vessel remodelling is defined by pericyte coverage of the preformed endothelial network and is regulated by PDGF- B and VEGF. Development 125:1591–1598
47. Benjamin LE, Golijanin D, Itin A et al. (1999) Selective ablation of immature blood vessels in established human tumors follows vascular endothelial growth factor withdrawal. J Clin Invest 103:159–165
48. Segura I, Serrano A, De Buitrago GG et al. (2002) Inhibition of programmed cell death impairs in vitro vascular-like structure formation and reduces in vivo angiogenesis. Faseb J 16:833–841
49. Duval H, Johnson N, Li J et al. (2007) Vascular development is disrupted by endothelial cell-specific expression of the anti-apoptotic protein Bcl-2. Angiogenesis 10:55
50. Huang DC, O'Reilly L A, Strasser A et al. (1997) The anti-apoptosis function of Bcl-2 can be genetically separated from its inhibitory effect on cell cycle entry. Embo J 16:4628–4638
51. Yin XM, Oltvai ZN, Korsmeyer SJ (1994) BH1 and BH2 domains of Bcl-2 are required for inhibition of apoptosis and heterodimerization with Bax. Nature 369:321–323
52. Tang N, Wang L, Esko J et al. (2004) Loss of HIF-1alpha in endothelial cells disrupts a hypoxia-driven VEGF autocrine loop necessary for tumorigenesis. Cancer Cell 6:485–495

PUBLICATION 10

Duval, H., N. Johnson, J. Li, **A. Evans**, S. Chen, D. Licence, J. Skepper, D. S. Charnock-Jones, S. Smith, and C. Print. 2007. Vascular Development is disrupted by Endothelial Cell-Specific Expression of the Anti-Apoptotic Protein Bcl-2. *Angiogenesis* 10, (1), 55-68.

Cited by 11, Impact Factor 6.063

ISSN: 0969-6970

Journal Type

Angiogenesis is an international peer-reviewed journal devoted to the publication of original articles and reviews on the cellular and molecular mechanisms that regulate angiogenesis in physiological and pathological conditions. This journal publishes innovative experimental studies using molecular, in vitro, animal model systems and clinical investigations of angiogenic diseases. Angiogenesis also reports on novel therapeutic approaches for promoting or inhibiting angiogenesis as well as new markers and techniques for disease diagnosis and prognosis.

Personal Contribution

My contribution to this work was HUVEC isolation and culture, and cloning of Tie 2 promoter and enhancer constructs.

Angiogenesis (2007) 10:55–68
DOI 10.1007/s10456-006-9057-6

ORIGINAL PAPER

Vascular development is disrupted by endothelial cell-specific expression of the anti-apoptotic protein Bcl-2

Hélène Duval · Nicola Johnson · Jia Li · Amanda Evans · Shuo Chen · Diana Licence · Jeremy Skepper · D. Stephen Charnock-Jones · Stephen Smith · Cristin Print

Received: 23 August 2006 / Accepted: 22 October 2006 / Published online: 6 December 2006

Abstract Endothelial cell (EC) apoptosis has been detected in remodelling blood vessels in vivo, and inhibition of EC apoptosis appears to alter vascular morphogenesis in vitro, suggesting that EC apoptosis may play a role in blood vessel remodelling. However, apoptotic EC are difficult to quantify in vivo, and studies of the incidence of EC apoptosis and the sites at which it occurs in vivo have produced contradictory results. Therefore, the specific biological roles played by EC apoptosis remain unclear. Here, we have used a transgenic approach to determine the biological function of EC apoptosis in vivo. Anti-apoptotic *Bcl-2* transgenes were expressed in mice under control of the EC-specific *tie2* promoter. These transgenic mice died during the second half of gestation. While the development and remodelling of large vessels including aortic arch arteries and great veins proceeded normally, abnormally dense and disorganised networks of small vessels were present in the skin and internal organs. In addition, vessel organisation and lumen formation were disrupted in the placental labyrinth. This study provides direct experimental evidence that endothelial cell apoptosis plays an essential role during embryogenesis. Our results suggest that EC apoptosis plays an important role in determining the structure of the microcirculation but may be dispensable for large vessel development.

Keywords Apoptosis · Endothelial · Angiogenesis · Vascular regression · Bcl-2 · Transgenic

Abbreviations

EC	Endothelial cell
HUVEC	Human umbilical vein EC
BAEC	Bovine aortic EC
TNF	Tumour necrosis factor
FCS	Foetal calf serum
PCR	Polymerase chain reaction
eGFP	Enhanced green fluorescent protein
IRES	Internal ribosome entry site

Introduction

Blood vessels in the developing embryo, yolk sac and placenta are continually remodelled to meet the changing requirements of the tissues they supply [1]. There is circumstantial evidence that apoptosis of cells within vessel walls, in particular endothelial cells (EC),

The authors Hélène Duval and Nicola Johnson contributed equally to this study.

H. Duval · N. Johnson · J. Li · A. Evans · S. Chen · D. Licence · C. Print
Department of Pathology, Cambridge University, Tennis Court Road, Cambridge CB2 1QP, UK

J. Skepper
Multi-imaging Centre, Department of Anatomy, Cambridge University, Cambridge CB2 3DY, UK

D. S. Charnock-Jones · S. Smith
Department of Obstetrics and Gynaecology, Cambridge University, Rosie Hospital, Robinson Way, Cambridge CB2 2SW, UK

C. Print (✉)
Department of Molecular Medicine and Pathology, School of Medical Sciences, University of Auckland, Park Road, Grafton, Auckland, New Zealand
e-mail: c.print@auckland.ac.nz

contributes to this remodelling. For example, apoptosis has been detected in embryonic blood vessels undergoing programmed developmental regression including: aortic arches [2], the abdominal aorta [3], umbilical vessels [4] and the ductus arteriosus [4]. In addition, EC apoptosis has been detected in the developing eye during regression of the tunica vasculosa lentis [5], pupillary membranes [6], and hyaloid vessels [7]. EC apoptosis has also been detected during blood vessel development and remodelling in the placenta [8]. EC apoptosis appears to be less frequent in adult animals than during embryogenesis. Nevertheless, EC apoptosis has been hypothesised to play a role in the cyclical remodelling of vessels within female reproductive tissues [9, 10] and in several pathologies including atherosclerosis [11] and cancer [12].

Further circumstantial evidence to support a role for EC apoptosis in blood vessel remodelling and regression comes from the dramatic vascular phenotypes produced when genes encoding regulators of EC apoptosis are inactivated. For example, inactivation of *VEGF-A* [13], *AKT* [14], *Ang-1*, *Tie-2* [15] or *VE-cadherin* [16] disrupted vascular development and caused embryonic death. In addition, cell culture studies have suggested that EC apoptosis occurs during angiogenesis [17, 18] and may contribute to lumen formation [19]. Inhibition of EC apoptosis by peptide caspase inhibitors or anti-apoptotic Bcl-2 over-expression can inhibit both vessel regression [20] and vascular morphogenesis [21, 22].

However, the role played by EC apoptosis in vessel development and remodelling remains controversial. Some studies have not supported the hypothesis that EC apoptosis contributes to blood vessel remodelling. For example, surprisingly few apoptotic EC were detected in studies of vessel regression within the ovarian corpus luteum [23] and developing rat retina [24]. The authors of the latter study suggested that vessel regression may in fact be mediated primarily by EC migration, and that EC apoptosis may only occur when the redeployment of EC is not possible [24]. Further, in *Xenopus* the expression of transgenes encoding anti-apoptotic XIAP or Bcl-xL proteins did not cause any detectable alteration to blood vessel structure or EC number [25]. In addition, apoptosis was not observed when vessels were disrupted in vitro by angiogenic inhibitors [26].

EC apoptosis appears to be controlled by a vast network of converging signals (reviewed in [18]). Members of the Bcl-2 family of apoptotic regulators [27] appear to provide especially important signals for determining EC fate. For example, over-expression of Bcl-2 or Bcl-x_L inhibited EC apoptosis induced in vitro by serum deprivation, staurosporine, ceramide and tumour necrosis factor (TNF)-α [28, 29]. Conversely, inhibition of pro-survival Bcl-xL expression using antisense oligonucleotides induced apoptosis in HUVEC [30], and *bcl-2* knockout mice had impaired retinal blood vessel development [31]. A proven approach to understand the biological role of apoptosis in specific cell lineages has been to express lineage-specific anti-apoptotic transgenes (including Bcl-2) in mice. This approach has revealed the function of apoptosis in diverse cell types ranging from lymphocytes [32] to male germ cells [33]. Here, we have used this approach to investigate the role played by EC apoptosis during mouse embryogenesis. Our results provide direct evidence that the apoptosis of EC plays a role in embryo development. Our results suggest that EC apoptosis is required for the normal development and remodelling of small vessels, but may be dispensable for large vessel development.

Materials and methods

Induction of EC apoptosis under flow conditions

Human umbilical vein EC (HUVEC) was isolated from umbilical cords of five individuals by collagenase digestion as described [34] and cultured to passage 5 in basal EC culture medium supplemented with a proprietary mixture of heparin, hydrocortisone, epidermal growth factor, fibroblast growth factor, 2% fetal calf serum (FCS), gentamycin, and amphotericin (large vessel EC medium; TCS, Botolph, UK). At passage 5, cells were plated at 100% confluence on microscope slides coated with matrigel (Becton Dickinson). The slides were inserted into a rectangular parallel flow chamber (Glycotech, Gaithersburg, Maryland, USA), and cultures were partially deprived of growth factors for 24 h by culturing in basal medium supplemented with only 2% charcoal-stripped FCS (Gibco/BRL), gentamycin, and amphotericin. Recirculating laminar flow of media over the cells was then established to achieve a constant wall shear stress of 0.1 Pa as previously described [35, 36]. Annexin V-FITC and Propidium Iodine (Annexin V-Fluos staining kit used according to the manufacturers instructions; Roche, Basel, Switzerland) were added to the media, and the process of apoptosis recorded using a fluorescence phase contrast microscope placed within a tissue culture incubator.

Transgene preparation

To generate a bicistronic transgene that would express both Bcl-2 and GFP specifically in EC the plasmid

pTie2Bcl-2IRESeGFP was constructed. The human *Bcl-2* coding region was excised from *pVav-Bcl2* [32] using the restriction enzyme *Eag*I and cloned into *pIRES2-eGFP* (Clontech). The resulting *Bcl2-IRES-eGFP* sequences were then inserted into *pSPTgT2FpAXK* [37] between the murine *Tie2* promoter (2 kb) and an SV40 polyA signal sequence. The resulting plasmid was digested with *Xho*I and *Sal*I to release a *Tie2-hBcl2-IRESGFP-pA* fragment that was cloned into pBSIIKS+. Finally, a murine *Tie2* genomic sequence containing a 10 kb enhancer fragment was excised from *pg50-2.11* [37] by *Nae*I-*Not*I digestion and inserted downstream of the *Tie2-hBcl2-GFP-pA* sequences to generate the *pTie2Bcl-2IRESeGFP* transgene plasmid. To generate the control transgene plasmid *pTie2eGFP*, proofreading polymerase chain reaction (PCR) was used to amplify all but the *Bcl-2IRESeGFP* sequences from *pTie2Bcl-2IRESeGFP* using the primers 5′-AAA-AgC-ggC-CgC-TAA-TAA-CCg-ggC-Agg-ggg-gA-3′ and 5′-AAA-AgC-ggC-GcG-gAC-CTg-Cag-gAA-TTC-gAT-ATC-AAg-3′. This generated the transgene vector *pTie2SV40* containing (from 5′ to 3′); the *pBSIIKS+* plasmid backbone, a *Tie2* promoter (2 kb), a unique *Not*I site into which any coding region could be cloned, an *SV40pA-splice* sequence and a *Tie2* enhancer (10 kb). An enhanced green fluorescent protein (*eGFP)* coding region was amplified from *pTie2Bcl-2IRESeGFP* using 5′-TTT-TgC-ggC-CgC-CAC-CAT-ggT-gAg-CAA-ggg-CgA-ggA-3′ and 5′-TTT-TgC-ggC-CgC-TTA-CTT-gTA-CAg-CTC-gTC-CAT-gC-3′ primers and sub-cloned into the unique *Not*I site of *pTie2SV40* to generate *pTie2eGFP*. Plasmid DNA was prepared with Qiagen Endofree Maxi kit (Qiagen, UK).

Transfection of BAEC

Passage 5 bovine aortic EC (BAEC) were cultured in M199 media supplemented with 10% FCS. Around 4 μg of plasmid DNA (1 mg/ml) was diluted in 150 μl with serum-free M199 medium. This was mixed with 36 μl of Superfect transfection reagent (Qiagen, UK) by gentle pipetting and incubated at room temperature for 10 min. Around 1.5 ml of M199 medium containing 10% FCS was then mixed with the DNA/Superfect mixture and added to 40% confluent BAEC that had been washed with PBS and aspirated to dryness. After 1hr incubation this media was removed and replaced with M199 media + 10% FCS. This transfection method delivered a control *pCMVeGFP* plasmid (Clontech, Palo Alto, CA, USA) to approximately 60% of the BAEC and induced apoptosis in approximately 15% of the cells—the apoptotic cells floated off and were removed when the cultures were washed and media was changed 24 h after transfection. Cultures were fixed in 2% paraformaldehyde for 20 min at 4°C, permeablised in 0.1% Triton X-100 and 0.1% Tween-20 for 30 min at room temperature, stained with Ulex-FITC (L9006, Sigma, Gillingham, UK) at a concentration of 10 μg/ml, anti-cleaved caspase 3 antibody (G7481, Promega, Southampton, UK) at 1:100 dilution, and Hoescht Bisbenzimide 33342 (382061, Calbiochem, Nottingham, UK) at a concentration of 1 μg/ml.

Generation of transgenic mice

Plasmid backbones were removed and linear DNAs for microinjection were generated from *pTie2Bcl-2IRES-eGFP* and *pTie2eGFP* by *Sal*I digestion followed by purification and electro-elution from a 0.6 % agarose gel. Further purification was performed using Elutip-D columns (Schleicher and Schuell, Germany) and the eluted DNA was microdialyzed against the injection buffer Tris HCl 10 mM pH 7.4/EDTA 0.1 mM. The 14.5 kb DNA derived from *pTie2Bcl-2IRESeGFP* and the 12.4 kb DNA derived from *pTie2eGFP* were microinjected into the pro-nucleus of fertilized mouse eggs (C57BL/6 × DBA/2), and embryos transferred to pseudo-pregnant recipients as described [38]. To identify transgenic embryos, genomic DNA was extracted from tail biopsies or limb buds after an overnight digestion with proteinase K (Sigma, UK) then precipitated with isopropanol and resuspended in TE buffer. *GFP* sequences within transgenes were amplified by PCR using the primers 5′-gCA-gAA-gAA-Cgg-CAT-CAA-ggT-3′ and 5′-gCg-gCg-gTC-Acg-Aac-TCC-A-3′ using Ready-to-Go PCR beads (Amersham, Little Chalfont, UK) and cycle parameters of; 94°C for 3 min, then 30 cycles of 30 s at 94°C, 30 s at 63°C and 45 s at 72°C followed by 7 min extension at 72°C. Amplified products were analyzed by electrophoresis through a 1% agarose gel. All mouse experiments were ethically approved in accordance with the UK Home Office regulations as prescribed in the UK Animals (Scientific Proceedures) Act 1980.

Histology and immunohistochemistry

Embryos and their corresponding placentae were dissected free of uterine decidua and separated from their yolk sacs, weighed and photographed. Tissues were then either snap frozen, fixed in Zinc fixative (BD Pharmingen, Oxford, UK) or Bouin's fixative for 6 h. About 10 μm sections were cut from either frozen tissue blocks or fixed paraffin-embedded tissue blocks, and transferred to uncoated glass slides. EC were

detected by overnight incubation at 4°C with a rat anti-mouse monoclonal antibody directed against CD31 (clone MEC13.3, BD Pharmingen) used at 1:100 dilution. Bcl-2-expressing cells were detected by incubation for 2 h at room temperature with a monoclonal mouse anti-human Bcl-2 antibody (clone Bcl-2-100, which does not cross-react with mouse Bcl-2, Sigma, UK) used at 1:400 dilution. Vascular smooth muscle cells and pericytes were detected using a rabbit anti-human anti-smooth muscle actin antibody (AB15267, AbCam, UK). Apoptotic cells were detected using a polyclonal rabbit anti-active Caspase 3 antibody (Promega, Southampton, UK) at 1:200 dilution. Rat and rabbit primary antibodies were detected with either FITC-conjugated, TRITC-conjugated or peroxidase-conjugated goat anti-rat and goat anti-rabbit IgG (Molecular Probes Europe, The Netherlands). Mouse primary antibodies were detected with the 'mouse on mouse' peroxidase system (Vector Laboratories, Burlington, CA) followed by incubation with streptavidin-conjugated horseradish peroxidase (Vector Laboratories) and 0.1% diaminobenzidine (DAB) with 0.1% hydrogen peroxidase. Sections for fluorescent/confocal microscopy were mounted using Vectashield mounting medium (Vector Laboratories, Burlington, CA). Sections for bright-field microscopy were counterstained with Carazzi's haematoxylin, then dehydrated and mounted using DPX (Fisher Scientific Ltd, Leicester, UK). For stereology to assess the volume fraction of cells immunostained by the anti-CD31 antibody, or the proportion of CD31-expressing cells that were also immunostained by the anti-cleaved caspase 3 antibody, at least thirty 750 × 750 μM fields were chosen by systematic random sampling [39] from at least six different sections. Volume fraction was calculated based on point counting as described [40]. Data were log-transformed before statistical tests were performed.

Results

A survey of embryonic EC apoptosis

Given the inconsistent observations of EC apoptosis described in the introduction, as a first step to further understanding this process, we wished to confirm that EC apoptosis did in fact occur within the developing mouse embryo. To do this we used double immunohistochemistry for CD31 (an EC marker) and active caspase 3 (an apoptosis marker) to survey the incidence of EC apoptosis in wild type mouse embryos at E8.5, E10.5, E12.5 and E14.5 of gestation. At each gestational age, between 6 and 13 separate immunostained sagittal sections from three complete embryos were examined. Few if any caspase 3^{+ve} apoptotic EC were detected in either large or small vessels at E8.5, E10.5 or E12.5 (<0.5% of the vessels we studied in cross-section in these embryos contained an apoptotic EC). In addition, at E14.5 few if any active caspase 3^{+ve} apoptotic EC were detected in any large trunk vessels (including aortic arches). In contrast, at E14.5 active caspase 3^{+ve} apoptotic EC were clearly detectable in small arterioles, capillaries and post-capillary venules found within the loose connective tissues of limb buds, the orbit and the gut. Up to 2% of the vessels we studied in cross-section in these tissues contained an apoptotic EC (Fig. 1). The nuclei of most of these active caspase 3^{+ve} EC had a pyknotic morphology consistent with apoptosis. In several cases we detected multiple apoptotic EC in a single vessel (Fig. 1). Due to background fluorescence it was difficult to assess EC apoptosis in the placenta. In summary, these results suggest that EC apoptosis does indeed occur within developing mouse embryos, and that apoptotic EC were most commonly detected in small vessels at the latest gestation examined (E14.5).

It is possible that when EC undergo apoptosis, they loose adhesion to their basement membrane and are rapidly deported by the flowing blood. This may make it difficult to estimate the true incidence of EC apoptosis. In support of this concept, we have previously shown by time-lapse video microscopy that EC undergoing apoptosis become separated from their basement membrane substrate early in the apoptotic process [41]. To explore the kinetics of EC apoptosis under flow, we cultured HUVEC on glass slides coated with basement membrane components (matrigel), and pumped media over the HUVEC monolayer under laminar flow conditions. We used a flow rate calculated to generate a shear stress on the EC of 0.1 Pa (1 dyne/cm^2). This represents the lower end of the range of shear stresses observed in human venules [36, 42]. We induced apoptosis in the HUVEC by partial serum deprivation, and observed the apoptotic process by fluorescence microscopy. AnnexinV-FITC and Propidium Iodine were added to the media to detect the membrane changes that accompany apoptosis and post-apoptotic necrosis, respectively. The apoptosis of 35 HUVEC was observed. We found that 24 (68%) of the apoptotic HUVEC lost adhesion to their basement membrane substrate and were deported in the flowing media *after* initiating apoptosis (as indicated by binding of AnnexinV-FITC and membrane blebbing) but *before* becoming permeable to Propidium Iodine (Fig. 2a). Half of these 24 cells were deported in the

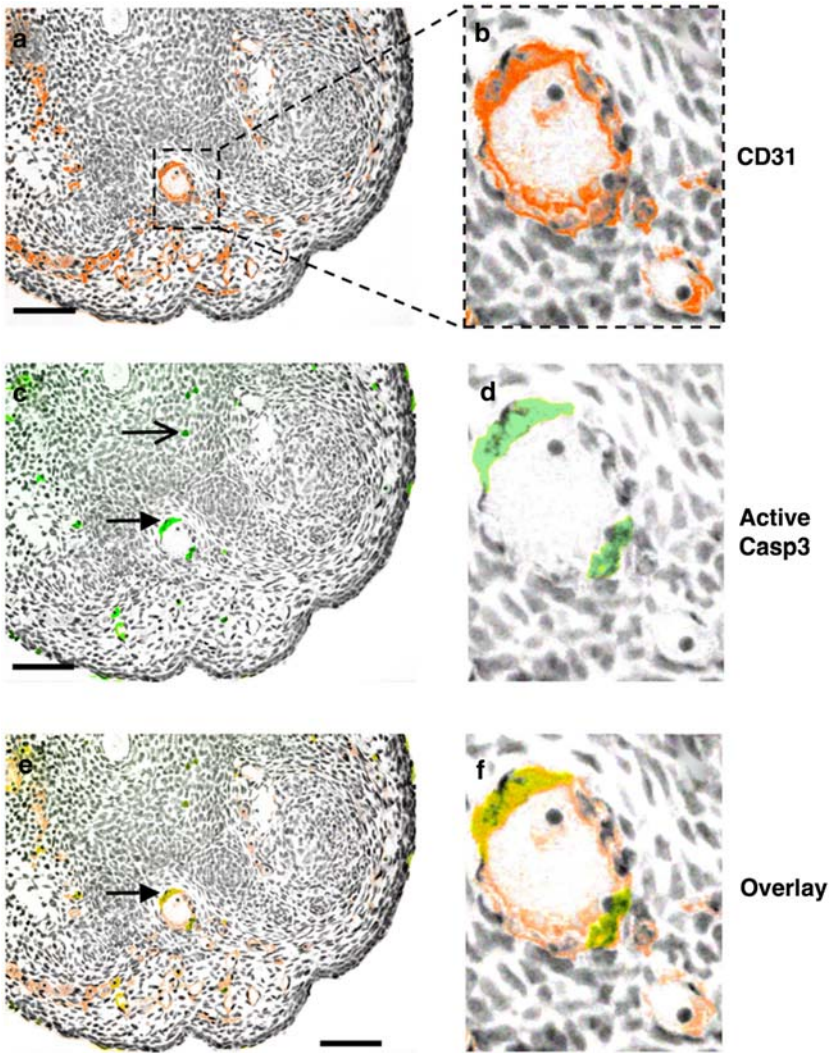

Fig. 1 Detection of EC apoptosis in a developing limb bud of a wild type E14.5 mouse embryo. Fluorescent double immunohistochemistry was used to detect CD31 (**a**, **b**; red) and active caspase 3 (**c**, **d**; green). In panels **c** and **d** examples of apoptosis in EC and non-endothelial cells are indicated by closed and open arrows, respectively. The images were generated by confocal microscopy, and were overlaid onto a grey scale pseudo-phase contrast image to show tissue structure. Scale bars are 125 μm. Panels **e** and **f** show overlaid anti-CD31 and anti-active caspase 3 images. Panels **b**, **c** and **f** are higher magnification representations of regions within panels **a**, **b**, and **c**

flowing media within 30 min of initiating membrane blebbing (Fig. 2b). This suggests that, due to loss of EC adhesion and deportation of apoptotic EC into the bloodstream, the incidence of EC apoptosis in vivo may be underestimated by simply enumerating apoptotic EC in situ in vessel walls.

Generation and verification of plasmids for the production of transgenic mice

After confirming that EC apoptosis can be detected during mouse embryogenesis, we wished to determine the role played by EC apoptosis in vivo. To do this, we expressed an anti-apoptotic human *Bcl-2* transgene specifically in mouse EC. We generated a transgene plasmid *pTie2Bcl-2IRESeGFP* that contained mouse *Tie-2* gene regulatory sequences (including an enhancer region that is required for widespread expression of the *tie2* gene postnatally [37]) and a human *Bcl-2* coding region. To facilitate the detection of cells in which the transgene was expressed, the *Bcl-2* coding region was linked to an eGFP coding region by an IRES (Fig. 3a). A control transgene plasmid *pTie2eGFP* that lacked the *Bcl-2* coding region was also generated (Fig. 3b). BAEC transfected with *pTie2Bcl-2IRESeGFP* were 1.8-fold more resistant to apoptosis induced by the combination of 10 ng/ml TNFα + 100 μg/ml cycloheximide, and 2.5-fold more resistant to apoptosis induced by 50 nM staurosporine, than BAEC transfected with the control plasmid *pTie2eGFP*(data not shown). We could detect no difference in incidence of mitosis between BAEC transfected with *pTie2Bcl-2IRESeGFP* and *pTie2eGFP* (data not shown).

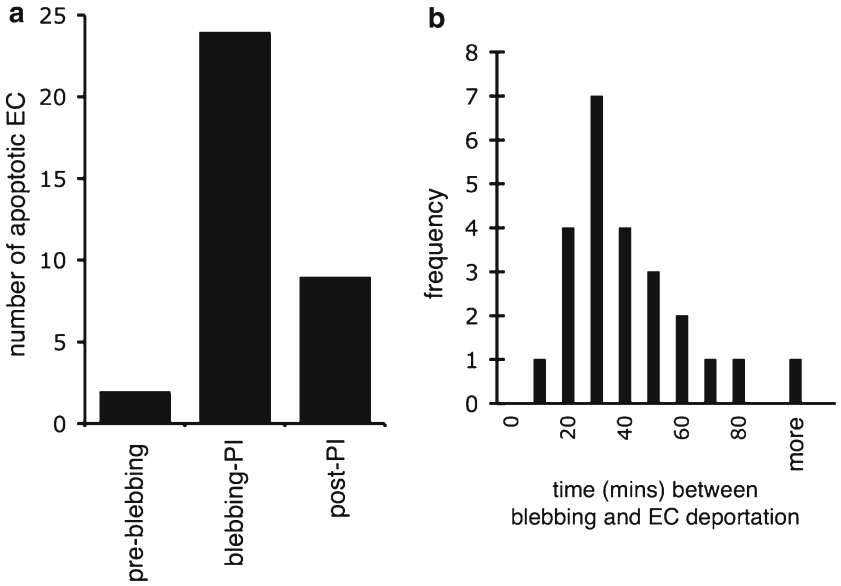

Fig. 2 (**a**) Time lapse fluorescent video microscopy was used to determine whether EC were deported into media flowing over their monolayer at a physiological flow rate during apoptosis. Serum deprivation-induced apoptosis of 35 HUVECs was observed. The timing of deportation of each cell into flowing media relative to the timing of apoptotic membrane blebbing was noted. *Pre-blebbing* indicates that apoptotic EC lost adhesion and was deported into the flowing media before EC displayed membrane blebbing or became Annexin V^{+ve}. *Blebbing-PI* indicates that apoptotic EC were deported into the flowing media after they displayed membrane blebbing but before they took up the PI dye.*Post-PI* indicates that apoptotic EC were deported into the flowing media after they took up the PI dye. (**b**) The kinetics of apoptosis for the 24 HUVEC that were deported into the flowing media after they displayed membrane blebbing but before they took up the PI dye was examined in more detail. The histogram shows the time interval in minutes between the first appearance of either membrane blebbing or Annexin V staining and cell deportation into the flowing media

Most pTie2Bcl-2IRESeGFP-transgenic mice die during embryogenesis

The plasmids *pTie2Bcl-2IRESeGFP* and *pTie2eGFP* were microinjected into the male pro-nuclei of fertilised eggs, and the resulting embryos transferred to pseudo-pregnant recipients. Transgene integration into the genome of embryos was detected by PCR using GFP-specific oligonucleotide primers (Fig. 3c). Around 20% of embryos injected with *pTie2eGFP* and collected at E12.5 carried this transgene in their genome. A similar proportion of *pTie2eGFP*-injected embryos still carried the transgene at E19.5, suggesting that carriage of the *pTie2eGFP* transgene had little effect on the survival of embryos during the second half of gestation. In contrast, while 22% of embryos injected with *pTie2Bcl-2IRESeGFP* carried the transgene at E12.5, only 15% of injected embryos carried the transgene at E14.5, and only 6% of injected embryos carried the transgene at E19.5 (Fig. 3d). This indicated that the presence of *pTie2Bcl-2IRESeGFP* may lead to embryo lethality during the second half of gestation.

Vascular abnormalities become apparent between E12.5 and E14.5

To determine the cause of *pTie2Bcl-2IRESeGFP*-induced embryonic lethality, at E12.5 we examined five *pTie2Bcl-2IRESeGFP*-transgenic embryos, five non-transgenic littermate control embryos and two *pTie2eGFP*-transgenic embryos. To identify transgene expression we examined these embryos for eGFP-derived fluorescence, however, while this was faintly detectable in EC it was not sufficiently intense for reliable quantification. Therefore, we used immunohistochemistry to identify human Bcl-2 immunoreactivity. This was detected only within EC lining both small and large vessels, but not in other cell types of all five *pTie2Bcl-2IRESeGFP*-transgenic embryos and not in any tissues of wild type or *pTie2eGFP*-transgenic animals (Fig. 3e). The embryos expressing human Bcl-2 had no obvious external abnormalities, and tissue sections stained with haematoxylin and eosin or an anti-CD31 antibody revealed normal blood vessel development and no detectable tissue abnormalities. Transgenic placentae and yolk sacs also appeared normal at E12.5 gestation.

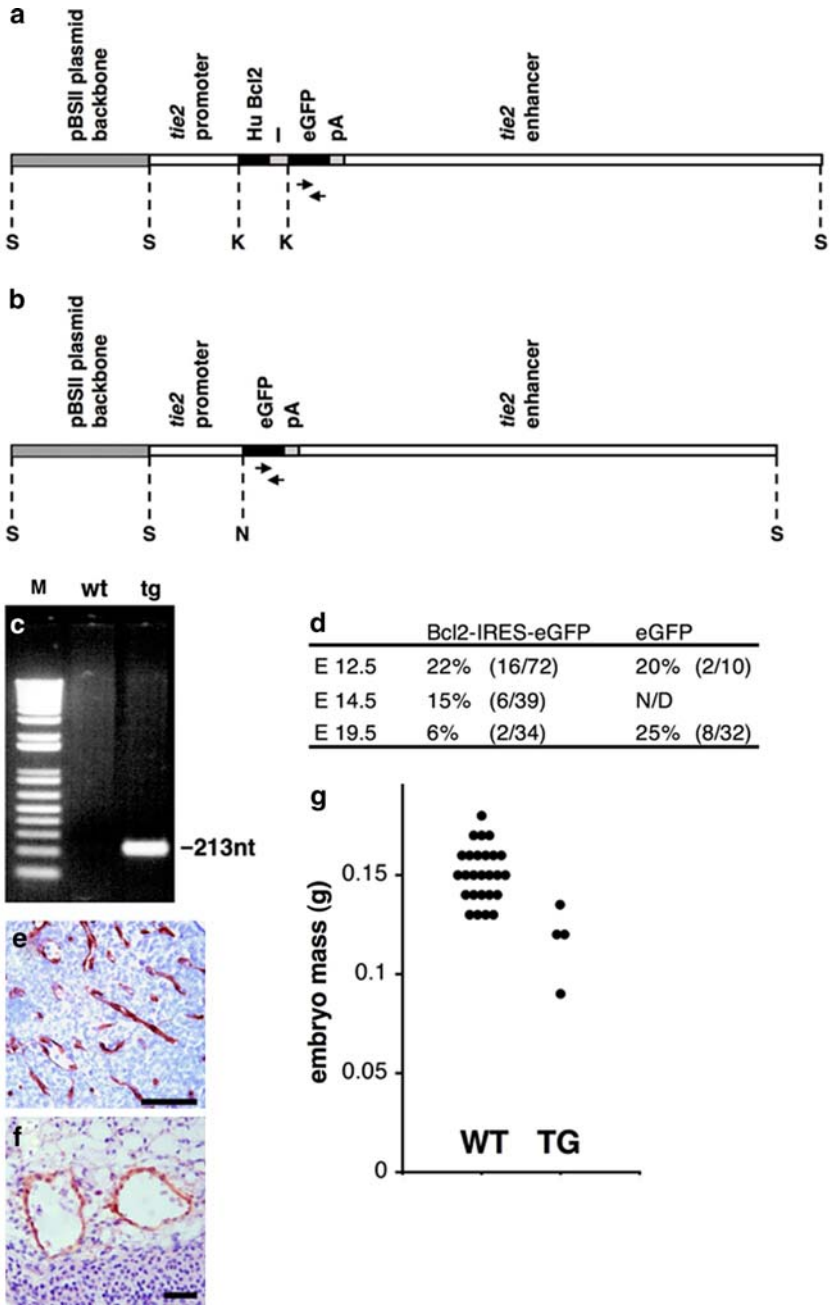

Fig. 3 (**a**) The transgene vector *pTie2Bcl-2IRESeGFP*. Open bars represent regulatory sequences derived from the murine *tie-2* gene, black bars wild type human *Bcl-2* and *eGFP*, respectively, grey bars an IRES and *SV40 pA* sequence, and hatched bars pBSII plasmid backbone sequences. S, K and N represent recognition sites for restrictions endonucleases *Sal*I, *Kpn*I and *Not*I, respectively. I denotes an IRES, and the arrows the PCR primers used for genotyping. (**b**) The transgene vector *pTie2eGFP* was similar to*pTie2Bcl-2IRESeGFP* except for the deletion of the Bcl-2 and IRES sequences. (**c**) PCR amplified a 340 bp transgene-specific product from genomic templates prepared from tail biopsies of a *pTie2Bcl-2IRESeGFP*-transgenic embryo but not from a wild type littermate. (**d**) Embryos carrying the *pTie2Bcl-2IRESeGFP* transgene die during the second half of embryogenesis, while embryos carrying a control *pTie2eGFP* transgene were unaffected. Figures represent the % of animals derived from embryos micro-injected with each transgene that still carry the transgenes at the given gestation. Numbers of transgenic animals/total numbers of animals assessed are shown in brackets. N/D denotes assay not done. Cells in E12.5 (**e**) and E14.5 (**f**) embryonic brain that expressed the *pTie2Bcl-2IRESeGFP* transgene were detected using an anti-human Bcl-2 antibody (red-brown). Scale bars are 80 μm. (**g**) E14.5 embryos expressing the *pTie2Bcl-2IRESeGFP* transgene (TG) and wild type littermate controls (WT) were blotted dry and weighed after dissection away from their yolk sacs and placentae

We then examined six *pTie2Bcl-2IRESeGFP*-transgenic embryos and six non-transgenic littermate control embryos at E14.5. One transgenic embryo had no heartbeat and poorly preserved tissues. Based on its degree of maturity it appeared to have died at approximately E13. Of the remaining five viable transgenic embryos, immunohistochemistry showed that four expressed Bcl-2 in EC (for example, Fig. 3f). The one transgenic embryo in which Bcl-2 expression was not detected, as well as the transgenic embryo that had died, were excluded from subsequent analysis. The mass of the remaining four *pTie2Bcl-2IRESeGFP*-transgenic embryos was on average less than the mass of four non-transgenic littermate controls (*t*-test $P \leq 0.05$, Fig. 3g), suggesting that *pTie2Bcl-2IRESeGFP* transgene expression retarded intra-uterine growth. A set of further abnormalities were observed in all four *pTie2Bcl-2IRESeGFP* embryos that expressed Bcl-2 in EC; (i) There were abnormally dense networks of vessels in the embryonic skin interspersed with patches of haemorrhage (Fig. 4A, B). Similar abnormally dense vascular networks were faintly visible in the skin of the dead transgenic embryo described above (data not shown). (ii) Inter-digital cleft formation appeared to be retarded relative to wild type littermates (arrow, Fig. 4A, B). (iii) Anti-CD31 immunohistochemistry revealed an increased density of capillaries, non-muscular venules and small arterioles in the dermis and subcutaneous tissues (Fig. 4C), consistent with the external appearance of these animals. (iv) Increased small vessel density was also seen in the developing lung and heart of two of the *pTie2Bcl-2IRESeGFP*-expressing embryos (Figs. 4D, 5a). Due to a technical difficulty, the thoracic regions of sections obtained from the remaining two *pTie2Bcl-2IRESeGFP*-expressing embryos were of insufficient quality for immunohistochemistry. (v) In connective tissues of the orbit small vessels were more extensive in *pTie2Bcl-2IRESeGFP*-expressing embryos than in non-transgenic controls (Fig. 4E). (vi) Increased density of small vessels was also consistently seen in the developing gut (Figs. 4F, 5b) of *pTie2Bcl-2IRESeGFP*-

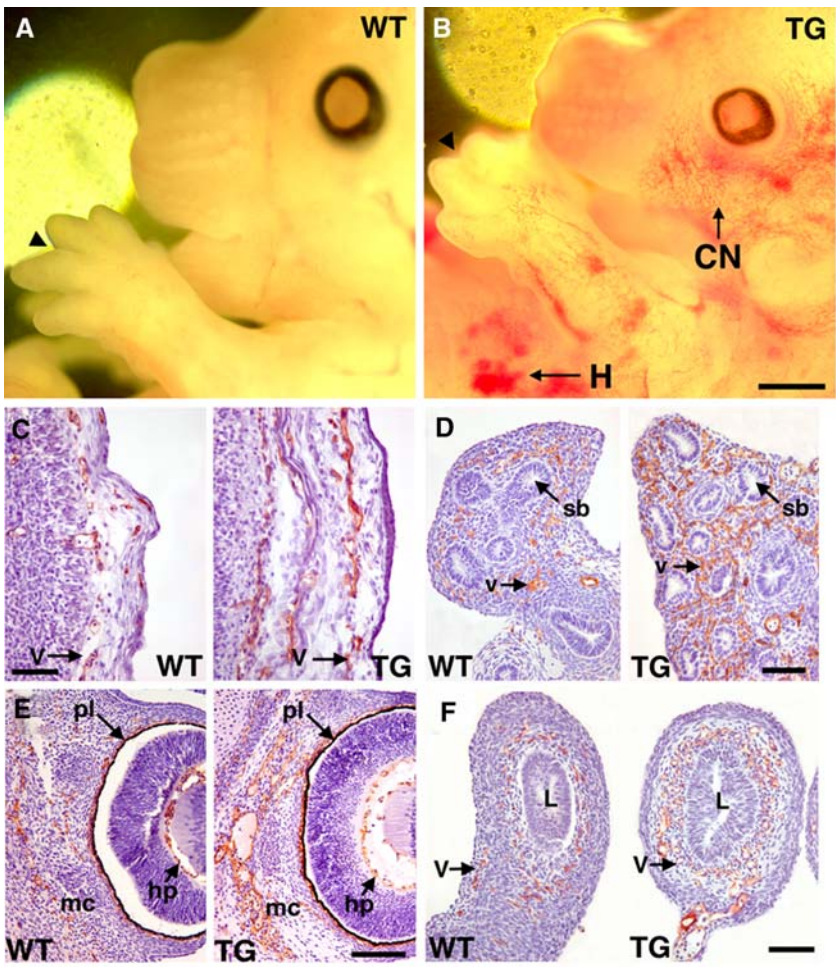

Fig. 4 Phenotype of *pTie2Bcl-2IRESeGFP*-transgenic mouse embryos. (**A**) The head region of an E14.5 wild type mouse embryo. (**B**) The head region of a *pTie2Bcl-2IRESeGFP*-transgenic mouse embryo. CN indicates capillary networks, H haemorrhage and arrows inter-digital clefts. Scale bar is 750 μm. (**C**–**F**) EC of E14.5 *pTie2Bcl-2IRESeGFP*-transgenic (TG) and wild type control (WT) mouse embryos were detected using an anti-CD31 antibody (brown). Panels show (**C**) facial skin, (**D**) lung, (**E**) eye and (**F**) gut. H indicates haemorrhage, hp the hyaloid plexus, l lumen, mc the mesodermal condensation, pl pigment layer, sb segmental bronchi, and v vessels. Scale bars are 100 μM

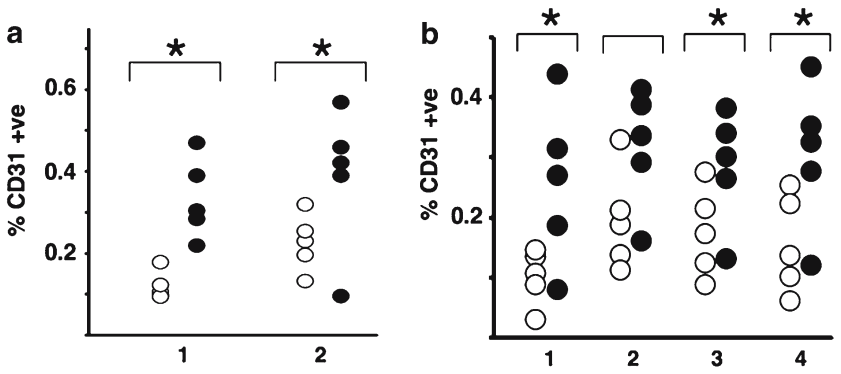

Fig. 5 Stereology of *pTie2Bcl-2IRESeGFP*-transgenic and wild type tissues at E14.5. EC of paired E14.5 TG (black points) and WT (hollow points) tissues were detected using an anti-CD31 antibody and the volume fraction occupied by $CD31^{+ve}$ cells was calculated. Each point represents the average volume fraction from seven 650×650 μM fields randomly chosen from one section—five sections were used from each animal. *Indicates $P \leq 0.05$ (*t*-test). Numbers indicate pairs of wild type and transgenic littermates (**a**) analysis of developing lung, (**b**) analysis of developing small bowel

expressing embryos. Interestingly, no obvious vascular abnormalities were seen in brain, kidney or liver of transgenic embryos. The structure of the heart, all branches of the aorta and the large veins and arteries of the neck, thorax and abdomen appeared to be normal. In addition, no obvious abnormalities were detected in the vessels of the yolk sac. To allow for immunohistochemistry, this analysis was conducted on paraffin-embedded rather than plastinated sections, which precluded a more detailed analysis of EC morphology, fenestrations and contact with pericytes. However, based on close examination of our paraffin-embedded sections no significant differences could be detected between the general morphology EC in both wild type and *pTie2Bcl-2IRESeGFP*-expressing embryos. Immunostaining for anti-active caspase 3 detected very few apoptotic EC in either large or small vessels of *pTie2Bcl-2IRESeGFP*-expressing embryos. Since the expression of Bcl-2 in HUVECs transplanted into immunodeficient mice promotes the recruitment of pericyte-like cells [29], the perictye/vascular smooth muscle cell investment of EC in the transgenic embryos and their placentae was examined, however, no alteration in the distribution of peri-vascular cells was detected in the paraffin-embedded sections of *pTie2Bcl-2IRESeGFP*-expressing embryos (data not shown).

Abnormalities in placental vasculature

The development of the placentae of all four *pTie2Bcl-2IRESeGFP*-expressing conceptuses at E14.5 was disrupted; (i) Transgenic placentae had an irregular nodular external appearance and had greater average diameter and mass than the placentae of non-transgenic controls (*t*-test $P \leq 0.01$, Fig. 6A). (ii) The umbilical arteries of all transgenic placentae appeared to be dilated (data not shown). (iii) Anti-CD31 immunohistochemistry revealed that the labyrinth layer of transgenic placentae was irregular and in some regions expanded into the maternal decidua (Fig. 6B, C). The usual labyrinthine structure consists of a regular array of trophoblast-lined maternal spaces and EC-lined foetal capillaries. In contrast, the labyrinth in the centre of *pTie2Bcl-2IRESeGFP*-transgenic placentae contained dense networks of foetal EC, many of which lacked an obvious lumen and contained few foetal erythrocytes. Maternal spaces appeared to have been partially lost and few maternal erythrocytes were present (iv) Areas of foetal vessel haemorrhage were also visible (Fig. 6D, E). (v) The labyrinth in the periphery of *pTie2Bcl-2IRESeGFP*-transgenic placentae was less severely affected, and usually both maternal spaces and foetal capillaries remained. Presumably these relatively less affected peripheral regions maintained sufficient gas and nutrient exchange to keep the embryos alive. Nevertheless, even in these peripheral regions there was evidence of haemorrhage from foetal vessels (data not shown). (vi) Stereological assessment of the overall labyrinth suggested that foetal EC density was increased but density of lumenised vessels was decreased in transgenic placentae relative to non-transgenic littermates (Fig. 6F, G). Since the labyrinth morphology of *pTie2Bcl-2IRESeGFP*-transgenic placentae were irregular (Fig. 6C), we were unable to reliably estimate labyrinth volume, and therefore were unable to infer from these vessel density measurements of absolute blood vessel or EC volume or number.

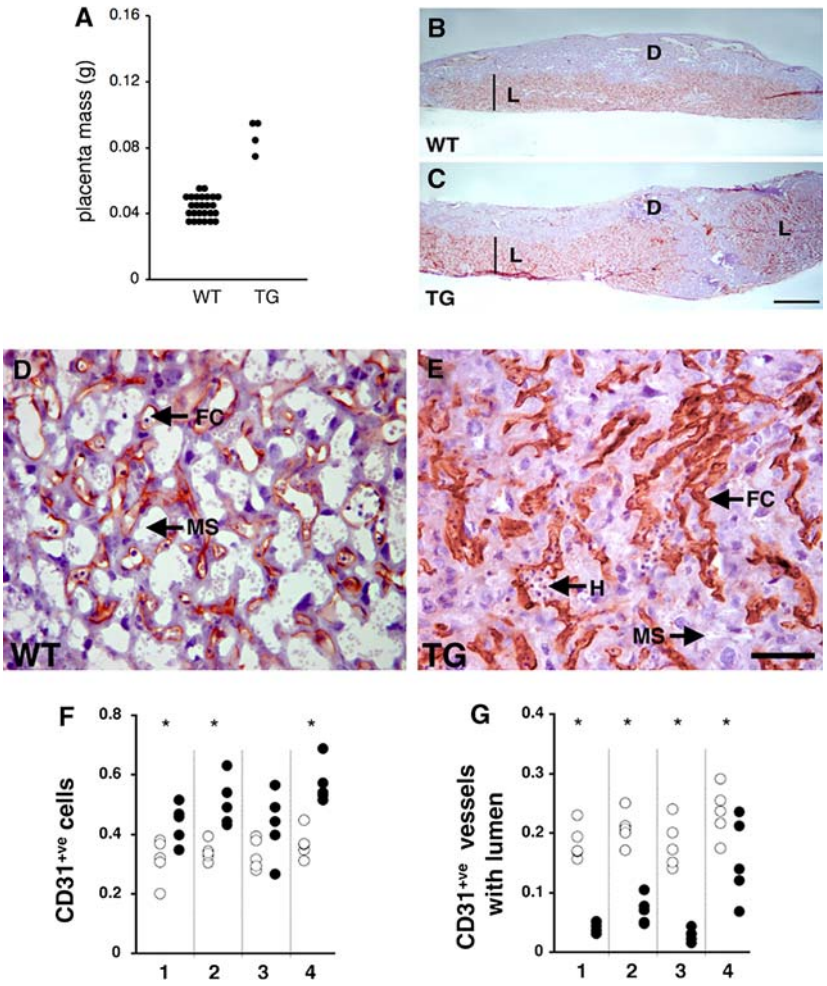

Fig. 6 Phenotype of *pTie2Bcl-2IRESeGFP*-transgenic placentae. (**A**) Placentae of E14.5 conceptuses expressing the *pTie2Bcl-2IRESeGFP* transgene (TG) and wild type littermate controls (WT) were weighed after dissection away from the embryos and foetal membranes. (**B**–**E**) EC of E14.5 TG and WT placentae were detected using an anti-CD31 antibody (brown). (**B**) and (**C**) show overall placental structure, L indicates labyrinth and *d* maternal decidua. Scale bar in C is 750 μm and in E is 100 μm. (**D**) and (**E**) show detail of the labyrinth. FC indicates foetal capillaries containing nucleated foetal erythrocytes, H haemorrhage, MS trophoblast-lined maternal spaces. (**F** and **G**) EC of paired E14.5 TG (black points) and WT (hollow points) placentae were detected using an anti-CD31 antibody and the mean volume fraction of labyrinth occupied by $CD31^{+ve}$ cells was calculated from five sections of each placenta. *Indicates $P \leq 0.05$ (*t*-test)

Discussion

EC apoptosis contributes to vessel development and regression

Several studies have detected EC apoptosis during embryo development. However, other studies have not detected EC apoptosis in regressing vessels where it would be expected to occur [23, 24, 26]. Therefore, the role played by EC apoptosis in vessel development and remodelling remains uncertain. As a first step to better understanding this process, we wished to confirm that EC apoptosis occurred within the developing mouse embryo. We detected caspase 3^{+ve} apoptotic EC in small vessels of E14.5 mouse embryos, however we found EC apoptosis difficult to detect in large vessels at this gestational age and in any vessels at the earlier stages of gestation we examined. These results suggest that EC apoptosis does indeed occur during mouse development in vivo, but is relatively rare. Interestingly, we observed multiple apoptotic EC in single vessels (Fig. 1). This concords with the hypothesis that microvascular segments regress *en masse* [6], possibly after flow has been blocked by the apoptosis of a single EC [43]. It is difficult to directly compare our results to previously published surveys of EC apoptosis during embryogenesis, since our study differs substantially from others in terms of species used, gestational age examined, tissues examined, and the techniques used to detect apoptosis.

We then showed that apoptotic EC can be rapidly deported into flowing media (Fig. 2). Several previous studies are consistent with this concept. Our laboratory previously showed that apoptotic EC lose adhesion from their substrate and neighbouring cells early in the apoptotic process [41]. This loss of adhesion may be promoted by proteolytic shedding of VE-cadherin [44] and caspase-mediated cleavage of focal adhesion kinase pp125 [45]. In addition, apoptotic EC [46] and apoptotic EC-derived microparticles [47] have been detected in blood. Therefore, due to potentially rapid deportation of apoptotic EC into blood, simple

enumeration of apoptotic EC in situ may underestimate the incidence and importance of this process.

To determine the role played by EC apoptosis in vivo, we then expressed EC-specific Bcl-2 transgenes in mice. This transgene expression caused embryonic lethality during the second half of gestation (Fig. 3d). All embryos that expressed Bcl-2 in EC had abnormally dense networks of small vessels in skin, some internal organs and placenta (Figs. 4–6). These data suggest that EC apoptosis performs important developmental functions in vivo. Transgene expression appeared to have the greatest effect on those vessels in which we had most readily observed EC apoptosis, such as vessels within connective tissue, developing limbs and gut. In contrast, transgene expression had no observable effect on vessels in which little EC apoptosis was observed, such as large thoracic vessels. Based on these results, we suggest that EC apoptosis may play an important role in the development and remodelling of small vessels in tissues such as limb buds, connective tissue, and gut. However we suggest that EC apoptosis may play a less important role in the development and remodelling of large vessels including the aortic arch arteries. The observation of relatively little EC apoptosis in large vessels, and the lack of any obvious effect of inhibiting EC apoptosis on large vessels, concords with the relative stability of large vessels and with the low rates of EC mitosis in these vessels [48]. Since EC apoptosis may cause thrombosis [49] and potentially damage downstream tissues through occlusion or thrombo-embolism, it would seem intuitive not to utilise EC apoptosis as a developmental strategy for the regression of large conductance vessels. In adult mice, the level of *tie2*-driven transgene expression has been shown to vary between arterioles and venules [50]. Although this may in theory lead to a stronger phenotype in arteries than in veins, we did not observe any systematic patterns of human Bcl-2 expression or phenotype within embryonic small vessels that were consistent with artery–vein differences. Tie2 is also expressed in some lymphatics. It is possible that aspects of the small vessel phenotype we observed were due to Bcl-2 transgene expression in lymphatic vessels, however we did not observe any clear lympahtic vessel phenotype.

The phenotype of our *tie2-Bcl2*-transgenic mice only became apparent after approximately E12.5. This was initially surprising, since endogenous *Tie2* is expressed as soon as the first EC arise and persist into adulthood. However, the phenotype of *pTie2Bcl-2IRESeGFP*-transgenic mice appeared to arise at approximately the stage when we were first able to readily detect EC apoptosis, which is presumably a stage at which EC apoptosis may play a major role. It is also interesting to note that embryonic lethality occurred at a developmental stage when small vessel growth and remodelling was especially rapid. For example, between E12 and E14 the total foetal capillary length in the mouse placental labyrinth increases by a factor of 3.8-fold [51].

In *Xenopus* the expression of transgenes encoding XIAP or Bcl-xL did not cause any detectable alteration to blood vessel structure or EC number [25]. This contrasts with our findings in mice, however these differences may be due to the different expression systems used as well as different mechanisms of vascular development in *Xenopus* and mice.

Mechanisms through which EC apoptosis may contribute to vascular development

There are several mechanisms through which EC apoptosis may contribute to the growth, organisation and regression of blood vessels in the embryo: (i) EC apoptosis may play an important role in blood vessel regression. The abnormally dense microvascular networks seen in a subset of *pTie2Bcl-2IRESeGFP*-transgenic tissues may reflect the persistence of vessels that were destined to regress, but were unable to do so due to the transgene-mediated inhibition of EC apoptosis. (ii) The formation of new capillary loops may involve the TGF-β/plasmin-induced apoptosis of specific EC in the walls of existing vessels [52]. (iii) Engulfment of apoptotic EC debris by viable neighbouring EC may cause the release of pro-angiogenic factors. Golpon et al. recently found that engulfment of apoptotic (but not necrotic) cell debris by non-professional phagocytes led to their release of pro-angiogenic factors including VEGF-A, which were able to promote in vitro angiogenesis [53]. (iv) The negatively charged membrane surface of apoptotic EC may promote angiogenic sprouting of adjacent vessels by causing localized plasma membrane hyperpolarisation [54]. (v) EC apoptosis may also promote lumen formation, which in turn provides the blood flow and shear stress that allows EC to survive and express growth factors that promote angiogenesis [43]. Although lumen formation in blood vessels appears to involve CDC42- and RhoA-mediated intracellular vacuole formation [55], the apoptosis of centrally placed EC may also play a role [19]. Indeed, several studies have detected apoptotic debris within newly formed lumen during in vitro angiogenesis [17, 18, 56]. In the current study we have shown that the placentae of *pTie2Bcl-2IRESeGFP*-transgenic mice contained reduced numbers of lumenised vessels and increased numbers of

poorly perfused vessels with a closed lumen (Fig. 6). Interestingly, a previous study detected EC apoptosis in the lumen of developing human placental capillaries [8]. A contribution of apoptosis to blood vessel lumenisation is not surprising, since apoptosis plays a role in lumen formation in diverse tissues [57]. For example, apoptosis is seen during the formation of lumen within cultured kidney epithelial cell cysts, and inhibition of this apoptosis by Bcl-2 expression inhibits formation of the cyst lumen [58]. Apoptosis of centrally placed cells is also seen during the development of mammary acini, and acinar lumen formation can be delayed by Bcl-2 expression [59]. We hope that in the future, inducible EC-specific *Bcl-2* transgenic mice will allow us to examine these mechanisms, and the role played by EC apoptosis, in later developmental stages and in adult diseases such as cancer and atherosclerosis.

Inhibition of EC apoptosis may secondarily disrupt the development of non-vascular tissues

We observed that inter-digital cleft formation was retarded in *tie2-Bcl2*-transgenic mice (Fig. 4a, b). This appearance was analogous to that of mice in which components of the apoptotic machinery such as APAF-1 have been inactivated in the germline [60]. Delayed inter-digital cleft formation in *tie2-Bcl2*-transgenic mice may reflect an overall slowing of intrauterine growth (IUGR). Alternatively, it is interesting to speculate whether EC apoptosis and vessel regression may be an obligate component of inter-digital tissue regression.

In the placentae of *tie2-Bcl2*-transgenic mice the structure of the trophoblast-lined maternal spaces was altered, even though the transgene was not expressed in trophoblasts. We are unsure of the mechanism for this abnormality. This may represent a purely mechanical effect where patent and correctly organized foetal vessels are physically required to support open maternal spaces. However, as with the inter-digital cleft formation, this phenotype may also reflect the disrupted cross-talk between EC populations and their neighbouring cells.

Effects of Bcl-2 expression unrelated to apoptosis

In addition to its anti-apoptotic role, Bcl-2 has been shown in some cell types to inhibit the cell cycle [61], promote the recruitment of peri-vascular cells [29] and to inhibit TNFα-induced and NFκB-dependant EC activation [62]. It is possible that subtle effects of the *pTie2Bcl-2IRESeGFP* transgene on these processes may contribute to the phenotype we observed. However, it seems unlikely that these processes are the dominant cause of the phenotype. We demonstrated that *pTie2Bcl-2IRESeGFP* expression in BAEC conferred resistance to apoptosis but had no detectable effect on EC proliferation in vitro, in agreement with previous publications [20, 28]. Further, we could detect no alteration in pericyte or vascular smooth muscle cell behaviour in *pTie2Bcl-2IRESeGFP*-transgenic mice. It is unlikely that the eGFP transgene significantly altered vascular development since the survival of embryos carrying the *pTie2eGFP* transgene was not altered and since GFP appeared to be expressed at very low levels, possibly due to our deliberate use of an inefficient IRES to drive its translation.

Conclusion

We have investigated the function of EC apoptosis during vascular development by expressing an anti-apoptotic *Bcl-2* transgene in mice under control of the EC-specific *tie2* promoter. This study provides direct experimental evidence that EC apoptosis plays an essential role during embryogenesis. Specifically, it appears to play a key role in determining the structure of the microcirculation in the placenta and in a subset of embryonic tissues, but may be dispensable for large vessel development.

Acknowledgements We wish to acknowledge the Transgenic Unit of Cambridge University Central Biomedical Services for assistance with the generation of transgenic mice. Dr Cecile Goujet (SEAT, Villejuif, France) provided training and assistance with transgenic mouse generation. Professor Thomas Sato (University of Texas Southwestern Medical Centre, USA) provided mouse *tie2* gene sequences. Dr Sarah Ogilvy (Cambridge University Department of Haematology) provided human Bcl-2 sequences. Dr Graham Burton and Professor Anne Ferguson-Smith (Department of Anatomy, Cambridge University) and Professor Jordan Pober (Yale University) provided advice on phenotype interpretation. Daniel Hurley and Anita Muthukaruppan provided advise on the manuscript. This project was funded by a Medical Research Council UK component grant. Jai Li and Shou Chen were supported by a St. Edmund's College Cambridge Scholarship donated by Dr Ming-Wei Wang of China.

References

1. Clarke M, Bennett M, Littlewood T (2006) Cell death in the cardiovascular system. Heart (in press)
2. Fisher SA, Langille BL, Srivastava D (2000) Apoptosis during cardiovascular development. Circ Res 87: 856–864
3. Cho A, Courtman DW, Langille BL (1995) Apoptosis (programmed cell death) in arteries of the neonatal lamb. Circ Res 76:168–175
4. Kim HS, Hwang KK, Seo JW, Kim SY, Oh BH, Lee MM, Park YB (2000) Apoptosis and regulation of Bax and Bcl-X

proteins during human neonatal vascular remodeling. Arterioscler Thromb Vasc Biol 20:957–963
5. Mitchell CA, Risau W, Drexler HC (1998) Regression of vessels in the tunica vasculosa lentis is initiated by coordinated endothelial apoptosis: a role for vascular endothelial growth factor as a survival factor for endothelium. Dev Dyn 213:322–333
6. Lang R, Lustig M, Francois F, Sellinger M, Plesken H (1994) Apoptosis during macrophage-dependent ocular tissue remodelling. Development 120:3395–3403
7. Lobov IB, Rao S, Carroll TJ, Vallance JE, Ito M, Ondr JK, Kurup S, Glass DA, Patel MS, Shu W, Morrisey EE, McMahon AP, Karsenty G, Lang RA (2005) WNT7b mediates macrophage-induced programmed cell death in patterning of the vasculature. Nature 437:417–421
8. Tertemiz F, Kayisli UA, Arici A, Demir R (2005) Apoptosis contributes to vascular lumen formation and vascular branching in human placental vasculogenesis. Biol Reprod 72:727–735
9. Modlich U, Kaup FJ Augustin HG (1996) Cyclic angiogenesis and blood vessel regression in the ovary: blood vessel regression during luteolysis involves endothelial cell detachment and vessel occlusion. Lab Invest 74:771–780
10. Dickson SE, Bicknell R, Fraser HM (2001) Mid-luteal angiogenesis and function in the primate is dependent on vascular endothelial growth factor. J Endocrinol 168:409–416
11. Norata GD, Tonti L, Roma P, Catapano AL (2002) Apoptosis and proliferation of endothelial cells in early atherosclerotic lesions: possible role of oxidised LDL. Nutr Metab Cardiovasc Dis 12:297–305
12. Garcia-Barros M, Paris F, Cordon-Cardo C, Lyden D, Rafii S, Haimovitz-Friedman A, Fuks Z, Kolesnick R (2003) Tumor response to radiotherapy regulated by endothelial cell apoptosis. Science 300:1155–1159
13. Gerber HP, Hillan KJ, Ryan AM, Kowalski J, Keller, GA, Rangell L, Wright BD, Radtke F, Aguet M, Ferrara N (1999) VEGF is required for growth and survival in neonatal mice. Development 126:1149–1159
14. Chen J, Somanath PR, Razorenova O, Chen WS, Hay N, Bornstein P, Byzova TV (2005) Akt1 regulates pathological angiogenesis, vascular maturation and permeability in vivo. Nat Med 11:1188–1196
15. Dumont DJ, Gradwohl G, Fong GH, Puri MC, Gertsenstein M, Auerbach A, Breitman ML (1994) Dominant-negative and targeted null mutations in the endothelial receptor tyrosine kinase, tek, reveal a critical role in vasculogenesis of the embryo. Genes Dev 8:1897–1909
16. Carmeliet P, Lampugnani MG, Moons L, Breviario F, Compernolle V, Bono F, Balconi G, Spagnuolo R, Oostuyse B, Dewerchin M, Zanetti A, Angellilo A, Mattot V, Nuyens D, Lutgens E, Clotman F, de Ruiter MC, Gittenberger-de Groot A, Poelmann R, Lupu F, Herbert JM, Collen D, Dejana E (1999) Targeted deficiency or cytosolic truncation of the VE-cadherin gene in mice impairs VEGF-mediated endothelial survival and angiogenesis. Cell 98:147–157
17. Bishop ET, Bell GT, Bloor S, Broom IJ, Hendry NFK, Wheatley DN (1999) An in vitro model of angiogenesis: basic features. Angiogenesis 3:335–344
18. Duval H, Harris M, Li J, Johnson N, Print C (2003) New insights into the function and regulation of endothelial cell apoptosis. Angiogenesis 6:171–183
19. Meyer GT, Matthias LJ, Noack L, Vadas MA, Gamble JR (1997) Lumen formation during angiogenesis in vitro involves phagocytic activity, formation and secretion of vacuoles, cell death, and capillary tube remodelling by different populations of endothelial cells. Anat Rec 249:327–340
20. Pollman MJ, Naumovski L, Gibbons GH (1999) Endothelial cell apoptosis in capillary network remodeling. J Cell Physiol 178:359–370
21. Satake S, Kuzuya M, Ramos MA, Kanda S, Iguchi A (1998) Angiogenic stimuli are essential for survival of vascular endothelial cells in three-dimensional collagen lattice. Biochem Biophys Res Commun 244:642–646
22. Segura I, Serrano A, De Buitrago GG, Gonzalez MA, Abad JL, Claveria C, Gomez L, Bernad A, Martinez AC, Riese HH (2002) Inhibition of programmed cell death impairs in vitro vascular-like structure formation and reduces in vivo angiogenesis. Faseb J 16: 833–841
23. Arfuso F, Meyer GT (2003) Apoptosis does not affect the vasculature of the corpus luteum of pregnancy in the rat. Apoptosis 8:665–671
24. Hughes S, Chang-Ling T (2000) Roles of endothelial cell migration and apoptosis in vascular remodeling during development of the central nervous system. Microcirculation 7:317–333
25. Du Pasquier D, Phung AC, Ymlahi-Ouazzani Q, Sinzelle L, Ballagny C, Bronchain O, Du Pasquier L, Mazabraud A (2006) Survivin increased vascular development during Xenopus ontogenesis. Differentiation 74:244–253
26. Friis T, Hansen AB, Houen G, Engel AM (2006) Influence of angiogenesis inhibitors on endothelial cell morphology in vitro. Apmis 114:211–224
27. Cory S, Huang DC, Adams JM (2003) The Bcl-2 family: roles in cell survival and oncogenesis. Oncogene 22:8590–8607
28. Zheng L, Dengler TJ, Kluger MS, Madge LA, Schechner JS, Maher SE, Pober JS, Bothwell AL (2000) Cytoprotection of human umbilical vein endothelial cells against apoptosis and CTL-mediated lysis provided by caspase-resistant Bcl-2 without alterations in growth or activation responses. J Immunol 164:4665–4671
29. Schechner JS, Nath AK, Zheng L, Kluger MS, Hughes CC, Sierra-Honigmann MR, Lorber MI, Tellides G, Kashgarian M, Bothwell AL, Pober JS (2000) In vivo formation of complex microvessels lined by human endothelial cells in an immunodeficient mouse. Proc Natl Acad Sci USA 97:9191–9196
30. Ackermann EJ, Taylor JK, Narayana R, Bennett CF (1999) The role of antiapoptotic Bcl-2 family members in endothelial apoptosis elucidated with antisense oligonucleotides. J Biol Chem 274:11245–11252
31. Wang S, Sorenson CM, Sheibani N (2005) Attenuation of retinal vascular development and neovascularization during oxygen-induced ischemic retinopathy in Bcl-2-/- mice. Dev Biol 279:205–219
32. Ogilvy S, Metcalf D, Print CG, Bath ML, Harris AW, Adams JM (1999) Constitutive Bcl-2 expression throughout the hematopoietic compartment affects multiple lineages and enhances progenitor cell survival. Proc Natl Acad Sci USA 96:14943–14948
33. Rodriguez I, Ody C, Araki K, Garcia I, Vassalli P (1997) An early and massive wave of germinal cell apoptosis is required for the development of functional spermatogenesis. Embo J 16:2262–2270
34. Jaffe EA, Nachman RL, Becker CG, Minick CR (1973) Culture of human endothelial cells derived from umbilical veins Identification by morphologic and immunologic criteria. J Clin Invest 52:2745–2756
35. Kirton CM, Nash GB (2000) Activated platelets adherent to an intact endothelial cell monolayer bind flowing neutrophils and enable them to transfer to the endothelial surface. J Lab Clin Med 136:303–313

36. Lawrence MB, Smith CW, Eskin SG, McIntire LV (1990) Effect of venous shear stress on CD18-mediated neutrophil adhesion to cultured endothelium. Blood 75:227–237
37. Schlaeger TM, Bartunkova S, Lawitts JA, Teichmann G, Risau W, Deutsch U, Sato TN (1997) Uniform vascular-endothelial-cell-specific gene expression in both embryonic and adult transgenic mice. Proc Natl Acad Sci USA 94:3058–3063
38. Hogan B, Beddington R, Constantini F, Lacy E (1994) Manipulating the mouse embryo. Cold Spring Harbor Laboratory, New York
39. Gundersen HJ, Jensen EB (1987) The efficiency of systematic sampling in stereology and its prediction. J Microsc 147(Pt3):229–263
40. Howard CV, Reed MG (1998) Three dimensional measurement in microscopy. Bios Scientific, Oxford
41. Johnson NA, Sengupta S, Saidi SA, Lessan, K, Charnock-Jones SD, Scott L, Stephens R, Freeman TC, Tom, BD, Harris M, Denyer G, Sundaram M, Sasisekharan R, Smith SK, Print CG (2004) Endothelial cells preparing to die by apoptosis initiate a program of transcriptome and glycome regulation. Faseb J 18:188–190
42. Schmid-Schonbein GW, Usami S, Skalak R, Chien S (1980) The interaction of leukocytes and erythrocytes in capillary and postcapillary vessels. Microvasc Res 19:45–70
43. Meeson A, Palmer M, Calfon M, Lang RA (1996) relationship between apoptosis and flow during programmed capillary regression is revealed by vital analysis. Development 122:3929–3938
44. Herren B, Levkau B, Raines EW, Ross R (1998) Cleavage of beta-catenin and plakoglobin and shedding of VE-cadherin during endothelial apoptosis: evidence for a role for caspases and metalloproteinases. Mol Biol Cell 9:1589–1601
45. Levkau B, Herren B, Koyama H, Ross R, Raines EW (1998) Caspase-mediated cleavage of focal adhesion kinase pp125FAK and disassembly of focal adhesions in human endothelial cell apoptosis. J Exp Med 187:579–586
46. Solovey A, Gui L, Ramakrishnan S, Steinberg MH, Hebbel RP (1999) Sickle cell anemia as a possible state of enhanced anti-apoptotic tone: survival effect of vascular endothelial growth factor on circulating and unanchored endothelial cells. Blood 93:3824–3830
47. Jimenez JJ, Jy W, Mauro LM, Soderland C, Horstman LL, Ahn YS (2003) Endothelial cells release phenotypically and quantitatively distinct microparticles in activation and apoptosis. Thromb Res 109:175–180
48. Wright HP (1968) Endothelial mitosis around aortic branches in normal guinea pigs. Nature 220:78–79
49. Durand E, Scoazec A, Lafont A, Boddaert J, Al Hajzen A, Addad F, Mirshahi M, Desnos M, Tedgui A, Mallat Z (2004) In vivo induction of endothelial apoptosis leads to vessel thrombosis and endothelial denudation: a clue to the understanding of the mechanisms of thrombotic plaque erosion. Circulation 109:2503–2506
50. Anghelina M, Moldovan L, Moldovan NI (2005) Preferential activity of Tie2 promoter in arteriolar endothelium. J Cell Mol Med 9:113–121
51. Coan PM, Ferguson-Smith AC, Burton GJ (2004) Developmental dynamics of the definitive mouse placenta assessed by stereology. Biol Reprod 70:1806–1813
52. Choi ME, Ballermann BJ (1995) Inhibition of capillary morphogenesis and associated apoptosis by dominant negative mutant transforming growth factor-beta receptors. J Biol Chem 270:21144–21150
53. Golpon HA, Fadok VA, Taraseviciene-Stewart L, Scerbavicius R, Sauer C, Welte T, Henson PM, Voelkel NF (2004) Life after corpse engulfment: phagocytosis of apoptotic cells leads to VEGF secretion and cell growth. Faseb J 18:1716–1718
54. Weihua Z, Tsan R, Schroit AJ, Fidler IJ (2005) Apoptotic cells initiate endothelial cell sprouting via electrostatic signaling. Cancer Res 65:11529–11535
55. Davis GE, Bayless KJ, Mavila A (2002) Molecular basis of endothelial cell morphogenesis in three-dimensional extracellular matrices. Anat Rec 268:252–275
56. Peters K, Troyer D, Kummer S, Kirkpatrick CJ, Rauterberg J (2002) Apoptosis causes lumen formation during angiogenesis in vitro. Microvasc Res 64:334–338
57. Lubarsky B, Krasnow MA (2003) Tube morphogenesis: making and shaping biological tubes. Cell 112:19–28
58. Lin HH, Yang TP, Jiang ST, Yang HY, Tang MJ (1999) Bcl-2 overexpression prevents apoptosis-induced Madin-Darby canine kidney simple epithelial cyst formation. Kidney Int 55:168–178
59. Debnath J, Mills KR, Collins NL, Reginato MJ, Muthuswamy SK, Brugge JS (2002) The role of apoptosis in creating and maintaining luminal space within normal and oncogene-expressing mammary acini. Cell 111:29–40
60. Cecconi F, Alvarez-Bolado G, Meyer BI, Roth KA, Gruss P (1998) Apaf1 (CED-4 homolog) regulates programmed cell death in mammalian development. Cell 94:727–737
61. Borner C (1996) Diminished cell proliferation associated with the death-protective activity of Bcl-2. J Biol Chem 271:12695–12698
62 Badrichani AZ, Stroka DM, Bilbao G, Curiel DT, Bach FH, Ferran C (1999) Bcl-2 and Bcl-XL serve an anti-inflammatory function in endothelial cells through inhibition of NF-kappaB. J Clin Invest 103:543–553

PUBLICATION 11

Sengupta, J., P. G. Lalitkumar, A. R. Najwa, D. S. Charnock-Jones, **A. L. Evans,** A. M. Sharkey, S. K. Smith, and D. Ghosh. 2007. Immunoneutralization of Vascular Endothelial Growth Factor Inhibits Pregnancy Establishment in the Rhesus Monkey (Macaca Mulatta). *Reproduction* 133, (6), 1199 -211.

Cited by 13, Impact factor: 3.090
ISSN: 1470-1626

Journal Type

Reproduction focuses on cellular and molecular reproductive biology and medicine. It was submitted as research article and includes work from all species including human. The remit is wide and now includes embryonic stem cells, epigenetic effects on reproduction and development as well as reproductive technology in model systems such as the rhesus monkey.

Personal Contribution

As described for publication 7 my role was to produce, purify and quantify all antibodies used in the study. Probably the most challenging part of this aside from re-cloning from a single cell (the only sample was a contaminated secondary hybridoma clone), was the need to find a functioning accessible freeze dryer in cambridge capable of dealing with milligrams of antibody. This is a story in itself involving the Department of Zoology elementary laboratory and a night with a tarantula in a post September 11 2001 world where India would not accept dry ice deliveries. To purchase at current prices of £470 per 100µg anti VEGFA antibody (Abcam, UK) each dose of 10mg per rhesus monkey would cost £47,000.

REPRODUCTION
RESEARCH

Immunoneutralization of vascular endothelial growth factor inhibits pregnancy establishment in the rhesus monkey (*Macaca mulatta*)

J Sengupta, P G L Lalitkumar, A R Najwa, D S Charnock-Jones[1], A L Evans[2], A M Sharkey[2], S K Smith[1] and D Ghosh

Department of Physiology, All India Institute of Medical Sciences, New Delhi 110029, India, [1]Department of Obstetrics and Gynecology, University of Cambridge, Cambridge CB2 2SW, UK and [2]Department of Pathology, University of Cambridge, Cambridge CB2 1QP, UK

Correspondence should be addressed to D Ghosh; Email: dghosh@aiims.ac.in

S K Smith is now at Faculty of Medicine, Imperial College London, London SW7 2 AZ, UK

Abstract

Maternal endometrial vascular endothelial growth factor (VEGF) is considered important in blastocyst implantation. However, there is no direct evidence to support this conjecture in the primate. In the present study, we have examined this hypothesis by testing whether immunoneutralization of VEGF during the peri-implantation stage of gestation affects embryo implantation in the rhesus monkey. Adult female animals ($n=36$) during mated ovulatory cycles were randomly assigned to one of the experimental groups treated subcutaneously with either isotype-matched mouse immunoglobulin (group 1: control, $n=8$) or monoclonal mouse antibody against VEGF-A (anti-VEGF Mab; group 2: 10 mg on day 5 after ovulation, $n=8$; group 3: 20 mg on day 5 after ovulation, $n=8$; group 4: 10 mg on day 10 after ovulation, $n=4$; group 5: 10 mg on days 5 and 10 after ovulation, $n=8$). Anti-VEGF Mab-treated animals in groups 2–4 did not show any marked inhibition in pregnancy establishment. On pooled analysis, however, anti-VEGF Mab administration in groups 2–5 ($n=28$) resulted in a significant ($P<0.04$) decline in the number of viable term pregnancy when compared with control animals. The observed difference was explained by the fact that 10 mg anti-VEGF Mab given to each animal on days 5 and 10 after ovulation in group 5 ($n=8$) inhibited pregnancy establishment significantly ($P<0.02$) when compared with control group 1. There was no significant change in serum concentrations of estradiol-17β, progesterone, and free VEGF among groups. Furthermore, animals treated with anti-VEGF Mab ($n=8$) as in group 5 revealed marked decrease in immunoreactive VEGF, *fms*-like tyrosine kinase-1, and kinase-insert domain region in trophoblast cells associated with shallow uterine invasion on day 13 of gestation when compared with samples from control group animals ($n=8$). Thus, VEGF action is required for successful blastocyst implantation in the rhesus monkey.

Reproduction (2007) **133** 1199–1211

Introduction

Blastocyst implantation in the rhesus monkey is initiated around days 7–9 after ovulation and fertilization. Local signaling between the pre-implantation stage embryo and the endometrium is likely to play a critical role ensuring synchronous growth and differentiation of embryonic and endometrial cells in a time- and stage-specific manner (Lopata 1996, Ghosh & Sengupta 1998). Of various factors, vascular endothelial growth factor-A (VEGF-A), a potent regulator of the integrity, permeability, and proliferation of blood vessels (Ferrara & Smith 1997), appears to be important in embryo–endometrium interaction at blastocyst implantation in rodents (Rabbani & Rogers 2001, Rockwell *et al.* 2002). In the human and the monkey, menstrual cycle-dependent changes in endometrial VEGF-A have been reported (Shifren *et al.* 1996, Nayak & Brenner 2002). Expression of $VEGF_{189}$ mRNA, an extracellular matrix-bound isoform, was found to be dependent on progesterone action in cynomolgus monkey (Greb *et al.* 1997) and in human uterus (Ancelin *et al.* 2002). The endometrial expression of both VEGF mRNA and protein reportedly occurs during the mid-secretory stage in the human (Charnock- Jones *et al.* 1993, Li *et al.* 1994). The *fms*-like tyrosine kinase-1 (FLT-1 and VEGFR1) and the kinase-insert domain region (KDR

ISSN 1470–1626 (paper) 1741–7899 (online)
DOI: 10.1530/rep.1.01228
Online version via www.reproduction-online.org

and VEGFR2) are high-affinity tyrosine kinase receptors for VEGF. They are co-expressed in capillaries during the mid-secretory period and this observation correlates well with the increased microvascular density and vascular permeability observed at this time (Krussel *et al.* 1999, Meduri *et al.* 2000). However, VEGF is secreted preferentially into lumina of endometrial glands in polarized human endometrial cell cultures, suggesting that apically secreted VEGF may also function as an endometrial signal for blastocyst development and/or implantation (Hornung *et al.* 1998). The expression of VEGF mRNA and its protein has been detected in trophoblast cells and in maternal glandular and vascular compartments of lacuna and early villous stages of implantation–placentation in the rhesus monkey (Ghosh *et al.* 2000). Failure of pregnancy in the rhesus monkey following early luteal phase, mifepristone treatment was reportedly associated with endometrial dysynchronization along with downregulation in expression and secretion of VEGF (Ghosh *et al.* 1998).

Taken together, this evidence suggests two potential roles for endometrial VEGF during implantation: a role in endometrial blood vessels and the establishment of receptivity and also a role in blastocyst implantation and trophoblast invasion. However, to date, there has been no direct evidence to show that VEGF is essential for successful implantation in the primate. In the present study, we have examined this hypothesis by testing whether immunoneutralization of VEGF-A during the receptive preparation of endometrium (day 5 after ovulation) and/or the implantation window (day 10 after ovulation) of gestational cycle affects embryo implantation in the rhesus monkey.

Materials and Methods

Animals and experimental procedures

Proven-fertile, adult female rhesus monkeys ($n=40$) showing two consecutive menstrual cycles of normal length (26–30 days) were placed for mating with male monkeys of proven fertility during cycle days 8–16. Peripheral blood samples were collected for hormone assays and vaginal smears were checked daily for the presence of spermatozoa. Ovulation was detected by rapid assay from the daily serum profiles of estradiol (E_2) and progesterone (P), as described in the following section. The assumed day of ovulation was taken 24 h after the day of peak rise of serum E_2 and had showed clearly detectable serum P level. The details have been given elsewhere (Ghosh & Sengupta 1993). Vaginal smears were immediately scored on a scale of 4: poor, good, very good, and excellent based on number, viability, and forward movement of spermatozoa. Four female monkeys were removed from this study when they had either failed to ovulate and/or sperm profiles were found to be consistently poor. Thus, female monkeys ($n=36$) showing positive ovulation and very good to excellent vaginal sperm profiles were randomly assigned to one of the experimental groups (groups 1–5), and received s.c. injection of either isotype-matched mouse immunoglobulin (IgG) or monoclonal mouse antibody against VEGF (anti-VEGF Mab). The doses and timings of the different treatment regimes are shown in Table 1. All injections were administered between 1000 and 1030 h on the assigned day. Sera were obtained from daily blood samples collected by venipuncture from experimental animals from cycle days 8 to 40, or the onset of next menstrual cycle and stored at −70 °C till their use in immunoassays to determine the peripheral concentrations of E_2, P, and monkey chorionic gonadotropin (mCG) as described below to monitor the pregnancy outcome for animals in groups 1–5. The pregnancy establishment was checked by per-rectum uterine palpation as described previously (Ghosh *et al.* 1997) and the pregnant animals were routinely monitored until they delivered. The normal length of gestation in monkeys of our colony is 170 ± 15 (mean $\pm$ S.D.) days.

An additional 16 ovulated and successfully mated females were classified into two groups, eight in each group, and they were treated with either control mouse isotype-matched IgG (like group 1 in Table 2), or anti-VEGF Mab (like group 5 in Table 1). They were laparotomized under ketamine anesthesia (12 mg/kg body weight; Parke Davis, Mumbai, India) on day 13 post-ovulation for performing hysterectomy under aseptic conditions to collect implantation sites and maternal endometrium (Sengupta *et al.* 2003). Tissues were fixed and processed for histology and immunohistochemistry to localize the site of expressions of VEGF and its receptors, KDR and FLT-1 in fetal and maternal compartments. Endothelial cells were stained for von Willebrand factor (vWF)-associated antigen and platelet–endothelial cell adhesion molecule (PECAM, CD31), and cytokeratin, neural cell adhesion molecule (NCAM, CD56), and PECAM were used for the immunolocalization of trophoblast cells as described previously (Sengupta & Ghosh 2002, Sengupta *et al.* 2003, Ghosh *et al.* 2004).

The Primate Research Facility of the All India Institute of Medical Sciences provided routine animal care and management. The present study was conducted with the approval of the Ethics Committee for the Use of Non-Human Primates in Biomedical Research of the All India Institute of Medical Sciences.

Anti-VEGF Mab and isotype-matched IgG

A neutralizing Mab directed against VEGF-A was produced by immunization of mice with recombinant human VEGF-A_{165} conjugated to keyhole limpet hemocyanin as described previously (Sharkey *et al.* 2005). Both anti-VEGF-A antibody and control IgG

Table 1 Effects subcutaneous administration of isotype matched mouse immunoglobulin (control IgG) or mouse monoclonal antibody against vascular endothelial growth factor (anti-VEGF Mab) during peri-implantation stage of mated ovulated cycles of rhesus monkeys on the pregnancy outcome.

Group (*n*)	Treatment s.c. (mg)	Day of treatment p.ov	Number of animals showing			Number of animals failed to be pregnant (length of menstrual cycle, days)
			Biochemical pregnancy[a]	Term pregnancy	Aborted pregnancy	
1 (8)	Control IgG (10, 10)	5 and 10	6	6	0	2 (27,31)
2 (8)	Anti-VEGF Mab (10)	5	3	3	0	5 (26,28,28,31,32)
3 (8)	Anti-VEGF Mab (20)	5	5	3	2[b]	3 (27,31,31)
4 (4)	Anti-VEGF Mab (10)	10	4	3	1[c]	0
5 (8)	Anti-VEGF Mab (10,10)	5 and 10	1	0**	1[d]	7* (27,29,29,29,30,32)

p.ov., after ovulation. $^{**}P<0.01$, $^{*}P<0.02$ as compared to group 1.
[a]Based on detectable mCG. [b]Days 18 and 133 of gestation, respectively. [c]Day 139 of gestation. [d]Day 135 of gestation.

(isotype-matched, IgG1κ) were purified by binding to protein G sepharose, desalting (Centricon ultrafiltration) and lyophilized in 10 mg lots. The neutralizing activity of the antibody was demonstrated using a bioassay in which iodinated VEGF binds to its receptors on endothelial cells as described previously (Sharkey *et al.* 2005).

Estimation of serum concentrations of E_2, P, mCG, VEGF, and mouse IgG

Serum concentrations of E_2 and P were measured by competitive ELISA using reagents and protocols provided by DRG International Inc. (NJ, USA). The results were analyzed using log–logit transformation of the data and the hormone values were log transformed for further analysis. The assay sensitivity was 4.6 pg/ml and 0.5 ng/ml for E_2 and P respectively; intra- and inter-assay coefficients of variations for E_2 assays were 6.3 and 7.8% respectively, and those for P assays were 4.8 and 6.5% respectively.

Serum concentration of mCG was measured by the sandwich enzyme-linked immunoabsorbent technique reported earlier (Ghosh *et al.* 1997). The Mab (Mab 518 B7) was generated against bovine luteinizing hormone (LH) and it was horse radish peroxidase (HRP) conjugated, and the polyclonal antiserum was raised in rabbits against human chorionic gonadotropin (hCG cr-121). Positive and negative controls were added to each plate and all the samples were assayed in one run. The assay sensitivity for mCG was 0.03 ng/ml.

Serum concentrations of free VEGF antigen in animals of the different groups were measured to discern if anti-VEGF Mab administration affected systemic VEGF levels. Serum levels of free VEGF were estimated using ELISA kit from R&D Systems (Minneapolis, MN, USA) according to manufacturer's instruction. A seven-point standard curve was plotted using twofold serial dilution to calculate the concentration of free VEGF in the sample. The assay sensitivity for VEGF was found to be 65 pg/ml; intra- and inter-assay coefficients of variations for VEGF antigen were 3.6 and 5.1% respectively.

Serum concentrations of immunoreactive mouse IgGs, the anti-VEGF mouse Mab (anti-VEGF Mab), and isotype-matched control mouse IgG, were estimated using a mouse IgG ELISA kit from Roche diagnostics GmbH (Manheim, Germany) according to manufacturer's instructions. Standards, antibodies, solutions, and reagents for this assay were supplied by the manufacturer. Serum samples collected from each animal before treatment with isotype-matched IgG or anti-VEGF Mab were used as internal negative baseline controls. The assay sensitivity for anti-mouse IgG was 10 ng IgG/ml; intra- and inter-assay coefficients of variations for mouse IgG were 2.7 and 5.9% respectively.

Serum profiles and clearance kinetics of serum mouse IgG

Data for mouse IgG concentration in serum versus time for rhesus monkeys injected subcutaneously with either control IgG or anti-VEGF Mab were analyzed using standard formulations for one compartment model (Shargel & Yu 1999). The clearance rate constant (k), time to reach maximal level of concentration (T_{max}), and the concentration of antibody at this level (C_{max}), area under curve (AUC) of antibody, and mean resident time (MRT) were subsequently estimated using standard methods (Shargel & Yu 1999).

Table 2 Characteristics of primary antibodies used for immunohistochemistry.

Antigen	Specification of antisera	Dilution (μg/ml)	Source
VEGF	Goat IgG	1.0	R&D Systems
FLT-1	Goat IgG	2.5	R&D Systems
KDR	Goat IgG	1.5	R&D Systems
Cytokeratin	Mouse IgG	1.8	DAKO
Vimentin	Mouse IgG	4.5	DAKO
vWF	Rabbit IgG	25.0	DAKO
NCAM (CD56)	Mouse IgG	1.0	NeoMarkers
PECAM (CD31)	Mouse IgG	2.5	NeoMarkers

R&D Systems, Minneapolis, MN, USA. DAKO, Glostrup, Denmark. NeoMarkers, Fremont, CA, USA.

Endometrial tissue/implantation stage morphology and immunohistochemistry

Sixteen females were successfully mated during days 8–16 of their ovulatory cycles and eight were treated with control mouse isotype-matched IgG (like group 1 in Table 1), and the other eight females were treated with anti-VEGF Mab (like group 5 in Table 1). On day 13 post-ovulation, endometrial tissue from the uterine corpus was removed by hysterectomy, washed in fresh ice-cold PBS (pH 7.2) to remove adhering blood, and immediately fixed in neutral phosphate-buffered paraformaldehyde (4%, w/v). The samples were embedded in paraffin wax and examined for normal histology as described previously (Sengupta *et al.* 2003, Ghosh *et al.* 2004). Paraffin sections (5 μm) were employed for hematoxylin staining and for immunohistochemical localization of VEGF, FLT-1, and KDR. Trophoblast cells and plaque–epithelial cells were identified by immunostaining with antibody against cytokeratin, invasive extravillous (interstitial) trophoblast cells were identified from immunolocalization of NCAM (CD56) and PECAM (CD31), and endothelial cells by immunostaining with antibody against PECAM and vWF as described elsewhere (Sengupta & Ghosh 2002, Sengupta *et al.* 2003, Ghosh *et al.* 2004). The sources of antibodies and dilutions of stock antibodies were optimized based on four to five points titration as shown in Table 2. Final visualization was achieved using the ABC peroxidase kits (Vector Laboratories, Burlingame, CA, USA) and freshly prepared diaminobenzidine hydrochloride with hydrogen peroxide (Sigma Chemical). Specificity of the antibodies was assessed by omitting primary antibodies, immunosorption of primary antibodies with target peptides, replacing primary antibodies with unrelated IgG from same species and other species, omitting secondary antibodies, and replacing secondary antibody with unrelated labeled IgGs from same species and other species. Labeled and unlabeled IgGs, non-immune sera, and other supplies were purchased from Vector Laboratories and Sigma Chemical.

The sections (5 μm) of primary implantation sites and endometrial tissue samples after hematoxylin staining and immunostaining were independently examined by three investigators and microphotographs were taken using a Leica DMRBE microscope attached with a Leitz DMRD microphotograph processor and a digital camera.

Statistical analysis

The pregnancy outcome in different groups was analyzed using the Fisher's exact probability test (Zar 1999). The AUCs for serum E_2, P, VEGF, and mouse IgG, and k, C_{max}, and T_{max} for mouse IgG in monkey serum samples, and body weights and crown–rump lengths of neonates in different groups were subjected to ANOVA followed by multiple comparison tests (Zar 1999). Statistical correlation between the circulatory concentrations of VEGF antigen and the Mab in animals of groups 2–5 was examined using standard SPSS v. 10.0.1 statistical analysis software.

Results

Pregnancy outcome

Table 1 provides a summary of the data obtained in the pregnancy outcome of monkeys in groups 1–5 following s.c. injection of isotype-matched mouse IgG and anti-VEGF Mab. Although there was an apparent decline in the number of mCG-positive pregnancy cycles in groups treated with anti-VEGF Mab in groups 2–4 (12 pregnancies from 20 animals) compared with control animals (six pregnancies from eight animals), this difference was statistically not significant ($P<0.4$). Similarly, there was statistically no significant ($P<0.2$) change in the number of successful term pregnancy in animals of groups 2–4 (9 out of 20 animals) compared with the control group. However, administration of anti-VEGF Mab to animals on days 5 and 10 after ovulation at 10 mg doses on each day as in group 5 resulted in significant inhibition of establishment of pregnancy as marked by mCG positivity ($P<0.02$) and term pregnancies ($P<0.01$) when compared with that found in the control group of animals injected with isotype-matched IgG at same dosage and schedule. Collectively, anti-VEGF Mab administration in groups 2–5 resulted in a significant ($P<0.04$) decline in the number of term pregnancies (9 out of 28 animals), however, with no significant ($P<0.2$) change in total number of mCG-positive pregnancy cycle when compared with control-treated animals (group 1).

As shown in Table 1, 4 out of 13 pregnant animals from anti-VEGF Mab-treated groups had pregnancy loss at different time points of pregnancy. However, the 30% abortion rate in anti-VEGF Mab-treated animals was statistically not significant ($P<0.4$) when compared with the cumulative abortion profile (22%) in our monkey colony. Three cases of abortion were observed between days 133 and 139 of gestation (Table 1) and these females exhibited failure to establish implantation stage rise in serum P levels as shown in Fig. 1J. As expected, the body weights (236.7 ± 28.9 g) and crown–rump (C–R) lengths (16.3 ± 1.5 cm) of aborted fetuses were significantly ($P<0.001$) lower than the body weights (435.6 ± 63.2 g) and C–R lengths (21.5 ± 1.7 cm) of neonates from all the groups, however, no gross physical abnormality was observed in the aborted fetuses.

The gestation lengths for live births in all the groups ranged between 157 and 182 days, and there was no

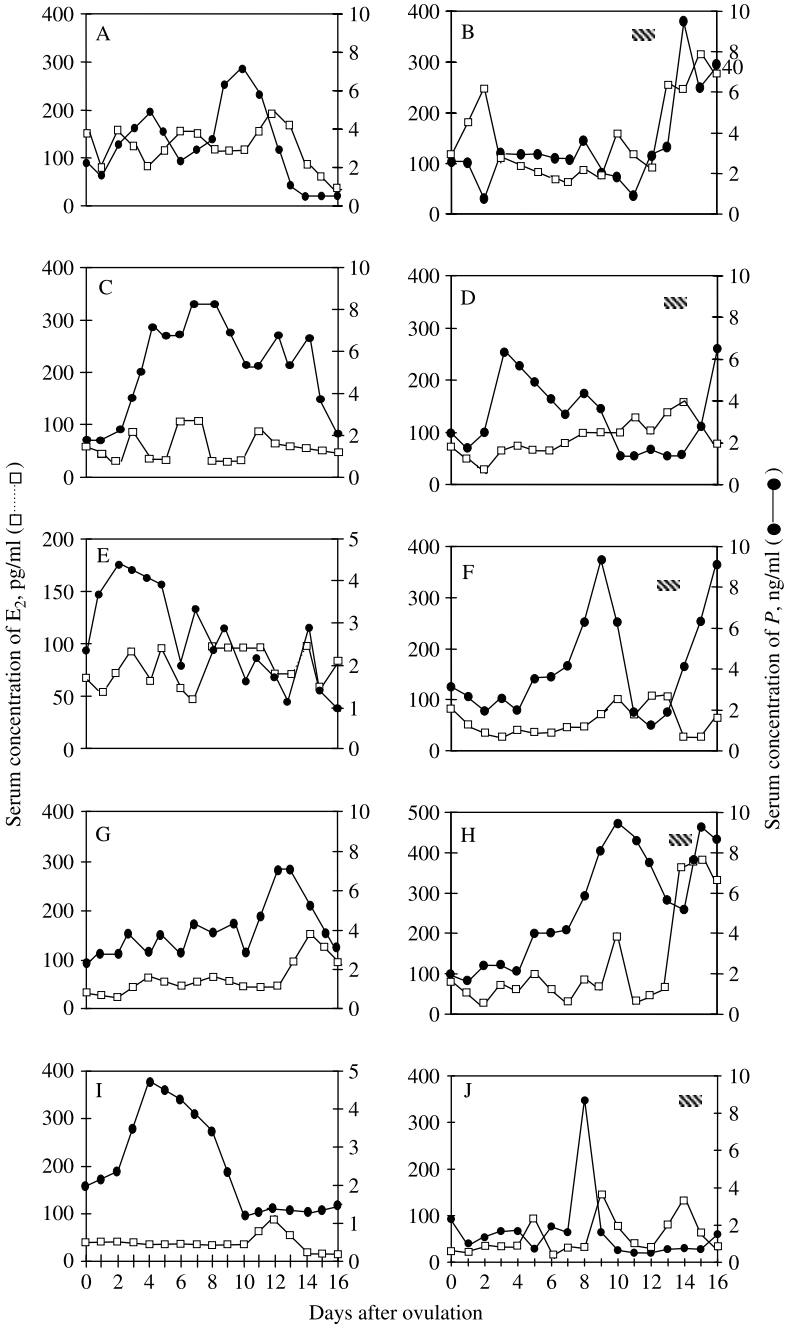

Figure 1 Serum profiles of estradiol-17β, E_2 (blank square) and progesterone, P (solid circle) in non-pregnant (A, C, E, G, and I) and pregnant (B, D, F, H, and J) animals from groups 1 (A and B), 2 (C and D), 3 (E and F), 4 (G and H), and 5 (I and J). The first day of mCG detection in the circulation (hatched bar) is shown. The details of different treatment groups are given in Table 1.

marked change in the gestation length between control- and anti-VEGF Mab-treated groups. Although neonates from anti-VEGF antibody-treated mothers showed a tendency of lower body weights (380–450 g) when compared with neonates from control-treated mothers (500–520 g), the difference was not significant.

Anti-VEGF Mab or control IgG exposure during the pre- and peri-implantation stages did not affect the length of the luteal phase (26–32 days) in monkeys that remained non-pregnant in the treatment cycles (Table 1).

Serum E_2, P, mCG, and VEGF

Figure 1 shows the representative serum profiles of E_2 and P, and the day of first mCG detection in the animals following antibody injection under the different treatment schedules detailed in Table 1. Despite differences in serum profiles for these hormones in individual animals, analyses of AUCs for E_2 and P during the luteal phase showed no difference among groups ($P<0.3$). Interestingly, three cases of abortion between days 135 and 139 showed failure in serum progesterone rise

during implantation (Table 1 and Fig. 1J). Evidently, the sample size ($n=3$) is too small to make any comment. Serum mCG was detected in all pregnant monkeys between days 12 and 18 after ovulation. An analysis of the data of AUCs for free VEGF antigen in serum samples of animals of groups 1–5 ($n=36$) revealed no significant change in AUCs for VEGF antigen between the pregnant animals from the control treatment (2177.2±229.7 pg/ml per day) group (group 1) and the non-pregnant animals from anti-VEGF Mab treatment (2039.6± 247.3 pg/ml per day) groups (groups 2–5). The concentrations of free VEGF were marginally higher ($P<0.05$) in serum samples of pregnant animals exposed to anti-VEGF Mab (3783.2±278.6 pg/ml per day) compared with the antigen concentration (2177.2±229.7 pg/ml per day) in pregnant animals exposed to isotype-matched IgG (group 1).

Serum profiles and clearance kinetics of mouse IgG

Table 3 shows serum profiles and clearance kinetics of mouse IgG respectively, in monkeys belonging to groups 2–5. As expected, there was a clear increase in serum mouse IgG after each injection. A single s.c. injection of anti-VEGF Mab irrespective of its dose resulted in maximum level of antibody being reached between 1.3 and 2.3 days in animals of groups 2–4. In animals of group 5 injected s.c. twice (10+10 mg) with anti-VEGF Mab on days 5 and 10 after ovulation, maximal levels in sera occurred a week after the first injection. The C_{max} varied from 2.3 to 4.6 μg/ml in monkeys exposed to 10 mg anti-VEGF Mab. The mean resident time (MRT) was 3.2–5.5 days. No significant difference was obtained between the clearance rates (k) among the different treatment groups. Analyses of AUCs for Mab concentration in sera of animals receiving 20 mg anti-VEGF Mab in group 3 showed significantly higher values when compared with the Mab concentration in animals in groups 2 and 4 ($P<0.01$) that had received 10 mg Mab, and with animals of group 5 ($P<0.02$) administered with 10+10 mg Mab against VEGF. Statistically no correlation was found between the circulatory concentrations of VEGF antigen and the Mab in animals of groups 2–5.

Histological characteristics of primary implantation sites and endometrial samples following exposure to mouse antibody

In order to examine the implantation sites and endometrial histology of animals treated with either isotype-matched mouse IgG or anti-VEGF Mab, additional number of animals were treated identically to groups 1 and 5 as shown in Table 1 and primary implantation sites and/or endometrial samples were collected on day 13 after ovulation. Of samples collected from eight mated animals exposed to control mouse IgG on days 5 and 10 after ovulation (like group 1, Table 1), seven samples showed typical primary implantation sites (Fig. 2A), and one sample revealed late secretory stage histology. Typical lacuna stage implantation sites exhibited embryonic disk with secondary yolk sac development typical of a stage in which cytokeratin-positive trophoblast cells blocked arterioles, extensive plaque acini (pl) flanked area enclosing embryonic disk, glands showed hypertrophied features, and dilated blood vessels were abundant at sites of implantation (Fig. 3A and E).

In endometrial samples collected on day 13 after ovulation from eight mated animals exposed to anti-VEGF Mab (10 mg each day) on days 5 and 10 after ovulation (like group 5 in Table 1), only one sample exhibited clear-cut blastocyst implantation (Fig. 2B), while one sample revealed typical late secretory stage histology (Fig. 2D). The primary implantation site of the implantation stage sample from the anti-VEGF Mab treatment group showed highly superficial embryo implantation, with small chorionic diameter (Fig. 2B). Based on serial sectioning of the primary implantation site, a small area of embryonic cells were located within the embryonic cavity without any distinctive organization in the formation of embryonic disk; lacunae showed extensive vascular congestion with disruption of lacunar septae (Fig. 2B); extensive cytokeratin-positive pl (Fig. 3B) and dilated blood vessels (Fig. 3F) were, however, seen at the site of implantation. Other six endometrial samples retrieved after VEGF Mab treatment showed epithelial plaque response (Fig. 2C) and scattered cytokeratin-positive trophoblast cells adjoining blood vessels (Fig. 3C and G).

Table 3 Serum profiles and clearance kinetics of monoclonal antibody following s.c. administration.

	Treatment (Group number)			
Parameter	10 mg Mab on day 5 p.ov. (Group 2)	20 mg Mab on day 5 p.ov. (Group 3)	10 mg Mab on day 10 p.ov. (Group 4)	10 mg Mab on days 5 and 10 p.ov (Group 5)
Clearance rate constant, k	0.2±0.1	0.3±0.2	0.3±0.2	0.4±0.3
Time to reach maximal concentration, T_{max} (days)	1.3±0.7	1.3±0.4	2.3±0.6	7.0±1.1
Concentration at maximal level, C_{max} (μg/ml)	4.3±1.8	11.9±7.2	2.3±0.9	4.6±1.4
Area under curve, AUC (μg/ml per day)	28.6±10.3†	58.4±10.3	21.6±5.1†	34.7±10.9*

p.ov., after ovulation. Results are shown as means±S.D. *$P<0.01$, †$P<0.02$ compared with Group 3.

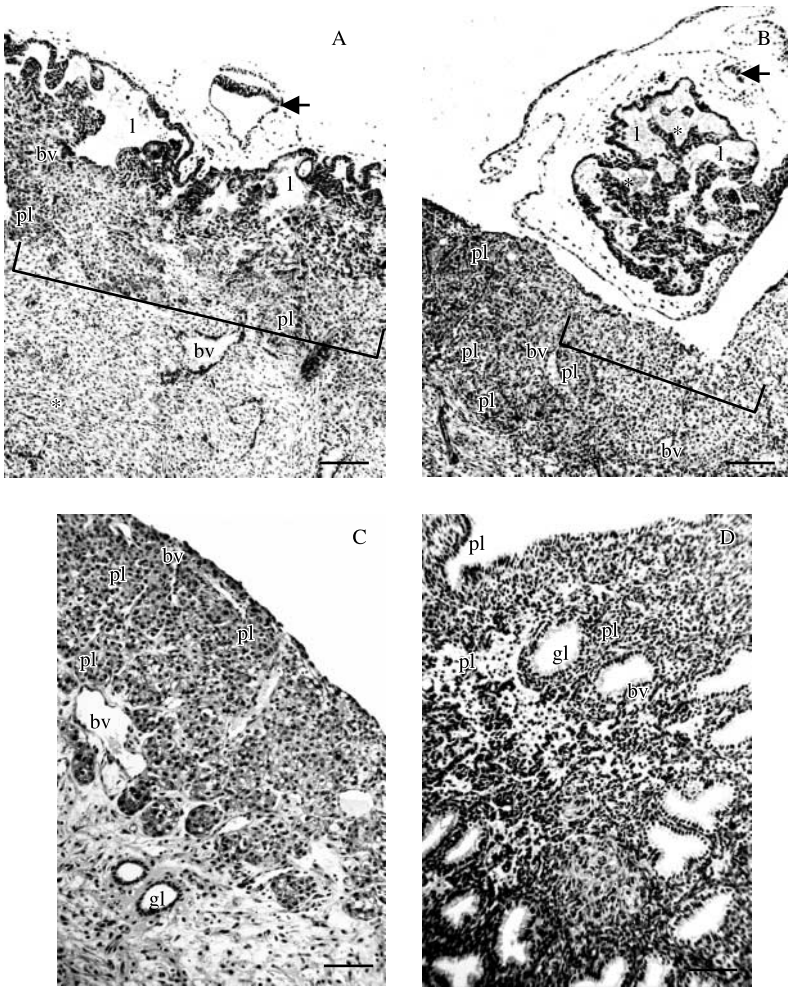

Figure 2 Histology of primary implantation sites collected on day 13 post-ovulation from rhesus monkeys treated with control IgG (A) or anti-VEGF Mab (B–D) on days 5 and 10 post-ovulation. In control IgG-treated sample (A), well-developed plaque acini (pl) flank the primary lacuna stage implantation site, cytotrophoblast cells enclose lacunae (l), extensive trophoblast plate region (bracket) below the embryonic disk (arrow). In anti-VEGF Mab-exposed sample (B), a superficially located primary implantation site shows plaque acini (pl) flanking dilated blood vessels (BV), highly scattered cytotrophoblast cells within a shallow trophoblast plate (bracket); chorion membrane enclosing cytotrophoblast cells with disrupted lacunar septae and extensive vascular congestion (asterisk) are seen; embryonic cells show clear lack of organization in forming putative embryonic disk (arrow). In anti-VEGF Mab-exposed samples (C and D), small glands (gl), typical plaque acini (pl), and scattered cytotrophoblast adjoining superficial dilated venules (BV) are found (C); late secretory stage histological features evident with effete glands (gl) within moderately edematous mucosal ground substance (D). Bars = 100 μm.

Immunolocalization of VEGF, FLT-1, KDR, PECAM, and NCAM

We examined the distribution of immunoreactive VEGF, FLT-1, and KDR in endometrial samples collected from animals that were treated with control IgG ($n=7$) and anti-VEGF Mab ($n=7$); as described above, these samples did not exhibit typical late secretory changes. VEGF immunoreactivity in cytotrophoblast cells lining lacunae and in cytotrophoblast cell columns was markedly lower in implantation stage tissue from anti-VEGF Mab-exposed animal (Fig. 4E and F) when compared with animals exposed to IgG (Fig. 4A and B). In control IgG-exposed animals, cells of embryonic disk, cytotrophoblast cells, cell columns, and syncytiotrophoblast cells were immunopositive for KDR (Fig. 4C), while FLT-1 expression was found primarily in syncytiotrophoblast cells (Fig. 4D). Following anti-VEGF Mab exposure, trophoblast cells showed very low immunostaining for KDR (Fig. 4G) and FLT-1 (Fig. 4H), however, these cells were immunopositive for both cytokeratin (Fig. 3B and C) and PECAM (Fig. 5E, F_1, F_2 and I). In the maternal compartment of anti-VEGF Mab-exposed animals, VEGF expression (Fig. 4E, F and I), expression for KDR (Fig. 4G and J), and FLT-1 (Fig. 4H and K) in pl, gland, and stromal cells were comparable with that found in primary implantation sites in IgG-exposed animals (Fig. 4A–D). Immunoreactivity for NCAM was predominantly present in syncytiotrophoblast cells, invasive extravillous (interstitial) trophoblast cells, endothelial, and endovascular trophoblast cells (Fig. 5C and D), and these cells were also immunopositive for PECAM (Fig. 5A and B). In lacuna stage samples obtained after control IgG treatment, cytotrophoblast cells, endometrial glands, and stromal cells were negative for NCAM, however, large endometrial granulocytes surrounding glands and spiral arterioles were immunopositive for NCAM (Fig. 5K). There was no distinctive staining for NCAM in trophoblast cells of the primary implantation site recovered from anti-VEGF Mab-exposed animal (Fig. 5G-H_2), except for a few trophoblast cells lining chorion (Fig. 5H_1). Large endometrial granulocytes adjoining pl of the same section and in samples in which only pl were obtained showed distinctive immunoreactivity for NCAM (Fig. 5J).

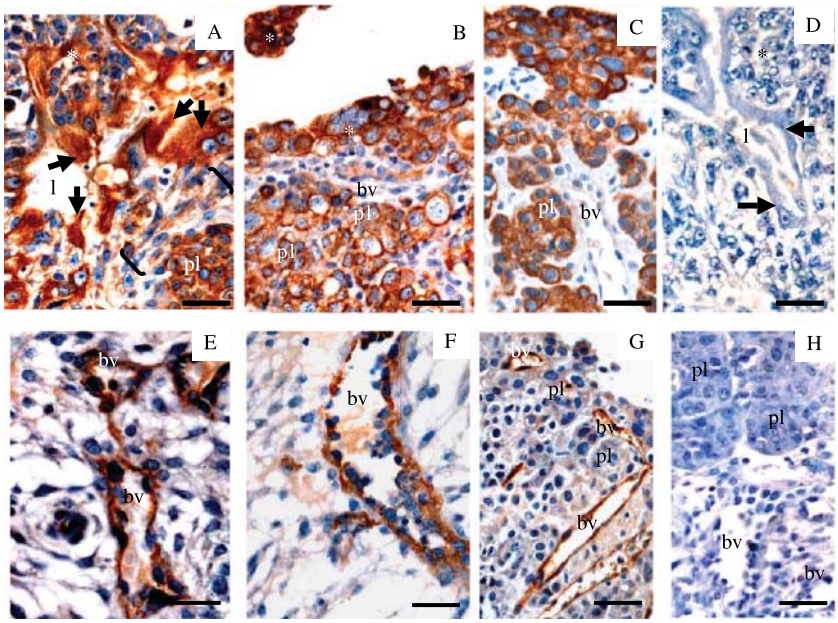

Figure 3 Immunohistochemical localization of cytokeratin (A–C), von Willebrand factor (vWF), (E–G) in primary implantation sites obtained on day 13 post-ovulation from animals treated with control IgG (A and E) or anti-VEGF Mab (B and F), and in endometrial samples collected on day 13 post-ovulation from anti-VEGF Mab-treated animals (C and G). Cytokeratin immunostaining detected in syncytiotrophoblast cells (arrows) lining lacunae (l), cytotrophoblast cells of cell columns (*), invasive cytotrophoblast cells (brackets) adjoining immunostained plaque acinar cells (pl) (A). Cytotrophoblast cells within chorion membrane (*), chorionic plate, and plaque cells showed immunopositive staining for cytokeratin (B). Strong immunostaining for vWF found in endothelial cells lining dilated venules (bv) (E and F). Cytokeratin-positive plaque cells (pl), (C) and vWF immunostaining of blood vessels (bv), (G) found in endometrial samples collected on day 13 post-ovulation from anti-VEGF Mab-treated animals. Control immunohistochemistry of primary implantation site samples showing trophoblast cell columns (*), syncytiotrophoblast (arrow) lining lacunae (l) following incubation in medium lacking primary antibody for cytokeratin (D), and following incubation in medium lacking primary antibody for vWF (H) showing plaque acinar cells (pl) adjoining dilated blood vessels. Bars=15 μm.

PECAM expression in the maternal endometrium was not discernibly affected by anti-VEGF Mab treatment (Fig. 5E, F_2 and I).

Discussion

In the present study, we have examined the hypothesis whether immunoneutralization of VEGF-A during the receptive preparation of endometrium (day 5 after ovulation) and/or the implantation window (day 10 after ovulation) of gestational cycle affects embryo implantation in the rhesus monkey. In addition, we have avoided applying multiple injections around the time of implantation based on the rationale that such treatment might markedly suppress ovarian function. Systemic injection of anti-VEGF mouse Mab during the receptive and implantation stages of gestation inhibited blastocyst implantation in the rhesus monkey. In addition, in animals treated with anti-VEGF Mab, the expression of both VEGF and its receptors, KDR and FLT-1, exhibited changes in expression in early conceptus tissue suggesting a complex involvement of VEGF in both blastocyst implantation and placental development (Ghosh *et al.* 2000, Demir *et al.* 2004). Thus, the results from the present study indicate that VEGF plays a critical physiological role in the process of implantation and placentation in primates. The observation of the present study corroborates well with our earlier pilot study (Ghosh & Sengupta 2005).

Contrary to our observations, Rowe *et al.* (2002) observed that anti-VEGF Mab administration via i.v. route on days 0–10 of luteal phase to marmosets did not affect the pregnancy rate, although plasma progesterone secretion was markedly suppressed compared with animals exposed to mouse γ-globulin during the same period. We believe that the observed differences in the results of pregnancy outcome after anti-VEGF Mab administration between marmosets and rhesus monkeys arise from the difference in the process of blastocyst implantation in these species. In the marmoset, there is a prolonged period of time when the implantation site expands in the plane of uterine epithelium (trophoblast plate stage) with fusion of syncytiotrophoblast with uterine epithelial cells, but even at day 31 after ovulation syncytiotrophoblast cells do not breach maternal blood vessels; uterine blood vessels are invaded only around days 45–60 of gestation by trophoblast cells expressing FLT-1 (Enders & Lopata 1999, Wulff *et al.* 2002, Rowe *et al.* 2003). In contrast, in the macaque and the baboon, soon after embryo attachment, there is invasion of maternal blood vessels around days 12 of gestation by trophoblast cells similar to the human (Enders & Schlafke

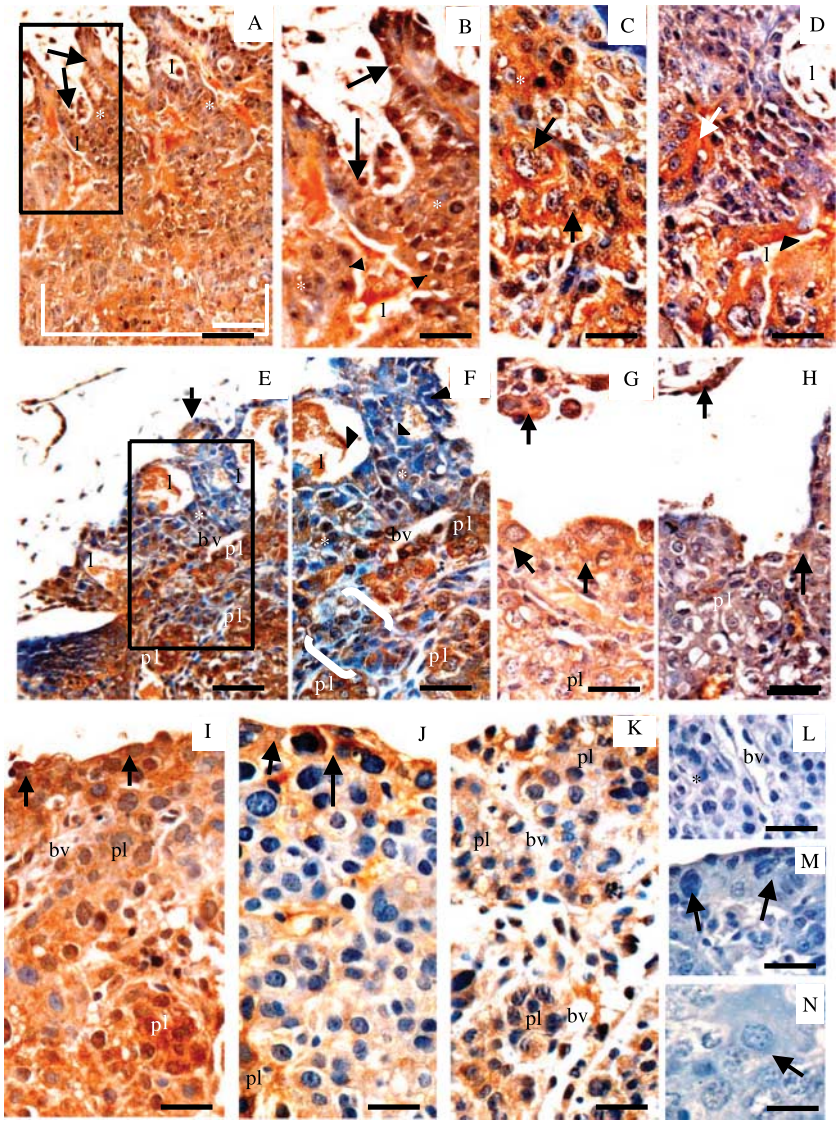

Figure 4 Immunohistochemical localization of VEGF (A, B, E, F, and I), KDR (C, G, and J), and FLT-1 (D, H, and K) in primary implantation sites obtained on day 13 post-ovulation from animals following treatment with control IgG (A–D) or anti-VEGF Mab (E–H) and in day 13 post-ovulation endometrial samples of anti-VEGF Mab treatment (I–K). Strong immunoprecipitation of VEGF protein found in trophoblast cells within the chorionic plate, in cell columns (*), in cells lining embryonic cavity (arrows), and lacunae (l) (A); inset in A is shown in B. On the other hand, there is absence of VEGF immunostaining in cytotrophoblast cells of cell columns (*), in syncytiotrophoblast lining lacunae (arrow-heads), in invasive trophoblast cells (brackets) (E and F). VEGF immunostaining is, however, detected in plaque acini (pl), endothelial cells lining dilated blood vessels (bv) (E); inset is shown in F. Immunopositivity for KDR (C) is seen in cytotrophoblast cells of cell columns (*) and in extravillous cytotrophoblast cells at base of column (arrows), while FLT-1 protein immunoprecipitation (D) is found in syncytiotrophoblast cells (*) lining lacunae in implantation sites from IgG-exposed animals. Generally low expression of KDR (G) and FLT-1 (H) in trophoblast cells (arrows) and in plaque acinar cells (pl) within trophoblast plate region of the primary implantation site from anti-VEGF Mab-treated animal. In endometrial samples from anti-VEGF Mab-treated animals, VEGF (I), KDR (J), and FLT-1 (K) immunostaining found in plaque acinar cells (pl) adjoining blood vessel (bv), stromal cells, and in few trophoblast cells (arrows) found in luminal border. Control immunochemistry of primary implantation site samples, trophoblast cell column (*) adjoining blood vessel (bv) incubated with immunoadsorbed primary antibody against VEGF-A protein with recombinant human antigen, $VEGF_{165}$ (L); trophoblast cells (arrows) of sample incubated in medium lacking primary antibody for KDR (M); syncytiotrophoblast (arrow) showing no immunoprecipitation for FLT-1 following incubation of sample in medium lacking primary antibody for FLT-1 (N). Bars = 15 μm (B–D and F–N), 50 μm (A), and 100 μm (E).

1986). Thus, it is possible that the timing of VEGF immunoneutralization in the marmoset in the luteal phase of mated cycle was inadequate to block VEGF-induced paracrine actions on trophoblast cell invasive functions necessary for pregnancy establishment. In fact, the results of the present study also indicate that the timing of anti-VEGF Mab administration is important in efficacious inhibition of pregnancy in rhesus monkeys. For example, in pregnancy outcome experiment, administration of 10 mg anti-VEGF Mab on days 5 and 10 after ovulation in eight animals yielded no viable pregnancy, although one animal exhibited mCG on day 18 after

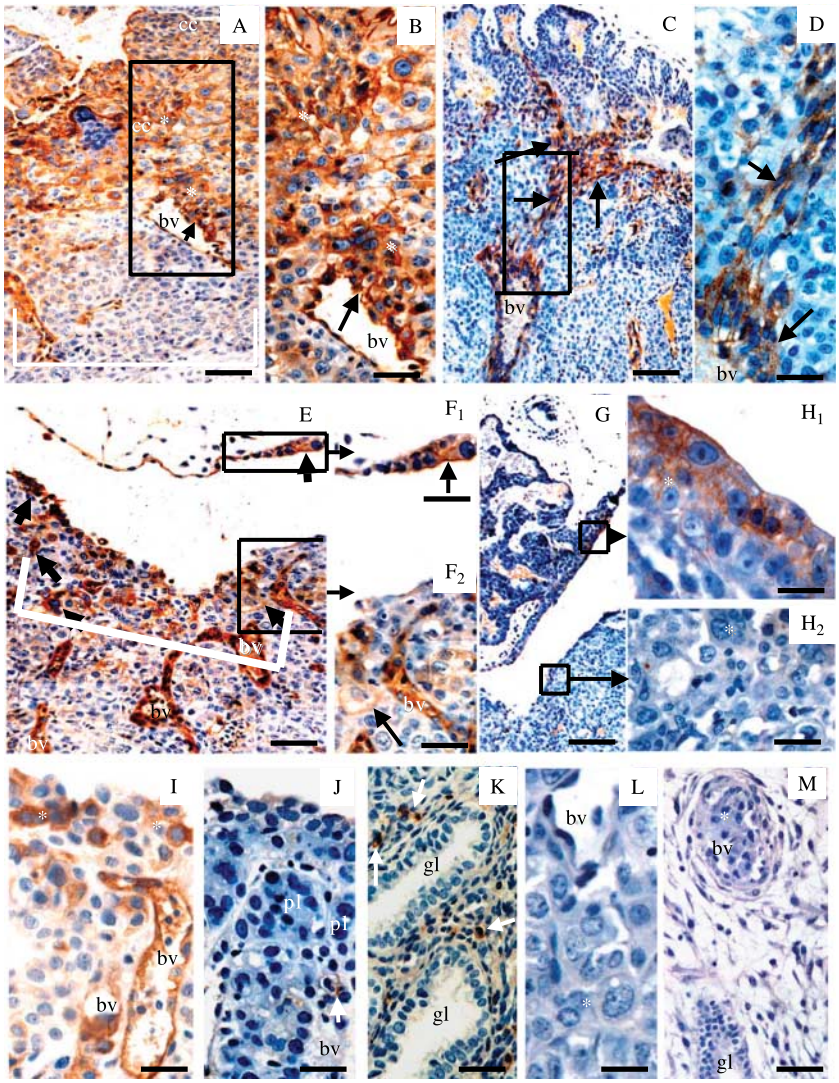

Figure 5 Immunohistochemical localization of PECAM (A, B, E, F_1, F_2, and I) and NCAM (C, D, G, H_1, H_2, J, and K) in primary implantation sites obtained on day 13 post-ovulation from animals following treatment with control IgG (A–D and K) or anti-VEGF MAb (E–H_2) and in day 13 post-ovulation endometrial samples after anti-VEGF Mab treatment (I and J). Strong immunoprecipitation of PECAM protein is seen in trophoblast cells of cell columns (cc), in invasive trophoblast cells (*) within the chorionic plate, and in endothelial cells (arrows) lining dilated blood vessel (bv); inset in A is shown in B. In implantation site from anti-VEGF Mab-treated animal, shallow trophoblast plate (bracket) shows immunopositive staining for PECAM in endothelial cells lining dilated blood vessels (bv) and in trophoblast cells (arrows) (E); insets in E are shown in F_1 and F_2. NCAM protein immunoprecipitation found in invasive trophoblast cells (arrows) at the feto-maternal border, in endovascular trophoblast cells lining dilated blood vessel (bv) of implantation site sample from an IgG-treated animal (C); inset in C is shown in D; NCAM immunostaining also found in large granulated lymphocytes (arrows) adjoining glands (gl), (K). In anti-VEGF Mab-exposed animal, NCAM immunostaining is not evident in trophoblast cells (G) except for few trophoblast cells lining chorion (H_1) or in maternal cells (H_2) of implantation stage sample. In endometrial samples from anti-VEGF Mab-treated animals, PECAM immunostaining clearly detected in trophoblast cells adjoining luminal border (*), in endothelial cells of dilated blood vessels (bv) (I); NCAM immunostaining seen in large endometrial granulated lymphocyte adjoining blood vessel (bv) (J). Control immunochemistry of primary implantation site samples of IgG-exposed animal showing absence of immunoprecipitation in endothelial cells of blood vessel (bv), in endovascular cytotrophoblast cells (*), in gland (gl) following incubation in medium lacking primary antibody for PECAM (L) and NCAM (M). Bars = 15 μm (B, D, F1, F2, H_1–J, and L), 50 μm (E and K), 100 μm (A, C, and G), and 250 μm (M).

ovulation; similar results were obtained in another set of eight animals that were treated with same regimen of anti-VEGF Mab followed by collection of uteri on day 13 after ovulation for histology and immunohistochemistry.

Previously, studies with rodent models have shown that VEGF action is critical for blastocyst implantation, since timed administration of antibody against VEGF resulted in reduced numbers of implantation sites and inhibition of uterine vascular permeability (Rabbani & Rogers 2001, Rockwell *et al.* 2002). However, there was a possibility that inhibition of VEGF action might have affected ovarian steroid synthesis in these studies (Kashida *et al.* 2001, Rockwell *et al.* 2002). In a pre-clinical safety study using cynomolgus monkeys, it has

been observed that administration of recombinant humanized Mab against VEGF for 4 or 13 weeks at twice weekly doses of 10 and 50 mg/kg resulted in defective corpora lutea formation (Ryan *et al.* 1999). In the present study, however, the systemic administration of anti-VEGF Mab in the rhesus monkey did not result in any apparent inadequacy in ovarian function. This is in contrast to the observed pregnancy inhibition following administration of antibody to VEGF-receptor 2 in mice that was associated with compromised ovarian function as marked by a significant fall in circulatory progesterone concentration and administration of progesterone protected the antibody-treated animals from pregnancy loss (Pauli *et al.* 2005). In the present study, there was no apparent difference in serum E_2 or P levels between pregnant animals following anti-VEGF Mab and those following control IgG injection. This is critical, since it indicates that the effects on pregnancy rates in this study might have resulted from local inhibition of VEGF action in the endometrium and/or developing conceptus. Other groups have observed in the rhesus monkey that systemic injection of anti-VEGF antibody on day 3 after ovulation did not result in significant change in serum progesterone levels (Xu *et al.* 2005) and such an antibody (AA98) preferentially binds to the newly formed blood vessels at the feto-maternal interface of the implantation site (Liu *et al.* 2005). It is possible that the sensitivity of blood vessels to VEGF withdrawal depends on their degree of vascular maturation (Otani *et al.* 1999). We speculate that if anti-VEGF Mab is given at the time of and immediately after ovulation, while vascularization of the corpus luteum is occurring as in the case of the cynomolgus experiment (Ryan *et al.* 1999), the vessels would be susceptible to disruption and ovarian steroid production would be affected (Zimmerman *et al.* 2001). On the other hand, if VEGF action is neutralized after the corpus luteum has vascularized as in the present study, no significant effect on ovarian steroid production may be seen due to the existence of a sufficient local cytokine network (Otani *et al.* 1999), while newly forming blood vessels at feto-maternal interface become more vulnerable (Liu *et al.* 2005). This possibility is also further substantiated by our observation that the serum concentrations of free VEGF were generally higher in pregnant animals exposed to anti-VEGF Mab compared with that in non-pregnant and control pregnant animals. Although the physiological basis and significance of higher serum VEGF in the antibody-treated pregnant monkeys is not known, it may be speculated that the animals that could mount rebound increase in antigen after antibody treatment are less vulnerable to pregnancy loss after antibody administration.

VEGF mRNA and protein expression are elevated in mid-secretory stage of endometrium with increased protein secretion in the primate (Charnock-Jones *et al.* 1993, Li *et al.* 1994). Pregnancy failure due to endometrial insufficiency, a block in pre-implantation embryo development and viability in the rhesus monkey after early luteal phase mifepristone exposure is associated with low VEGF expression and secretion (Ghosh *et al.* 1998). Furthermore, a dialogue between embryo and endometrium is considered essential for blastocyst implantation and may involve the synthesis and secretion of hCG and VEGF from embryonic and maternal sources respectively (Licht *et al.* 2001). Several reported studies earlier indicated a possible role of VEGF in the regulation of invasive and migratory capacities of early placental trophoblasts (Lash *et al.* 2003, Anteby *et al.* 2004). Thus, it appears that the observed high incidence of pregnancy failure following anti-VEGF Mab treatment might have been precipitated by inadequate trophoblast invasion and placental formation associated with their lower expression of VEGF, KDR, and FLT-1. However, it is not evident why conceptus tissues were primarily affected, while maternal endometrium did not show any clear-cut change in histology and in immunopositive profiles for proteins VEGF, KDR, and FLT-1 following anti-VEGF Mab treatment. It becomes yet more complex with the recognition of the fact that administered antibody to a pregnant animal tends to remain in the maternal compartment and generally does not reach to the embryonic tissue (Pauli *et al.* 2005). It would be interesting to investigate a comparative differential display in the protein–protein interactions using proteomics approach in the maternal endometrium between control and anti-VEGF Mab treatment, rather than the functional cluster of VEGF action associated proteins only (Graham *et al.* 2005).

Our data also support a role for NCAM or CD56 in trophoblast invasion (Blankenship & King 1996, Slukvin *et al.* 2000). NCAM is a multifunctional protein and considered as a receptor that responds to both homophilic and heterophilic cues as a mediator of cell adhesion and neural cell migration via two distinct domains for NCAM and heparan sulfate (Hinsby *et al.* 2004). Trophoblast cell invasion of spiral arterioles is likely to involve migratory and invasive behavior of NCAM-mediated cell-type segregation, involving changes in cadherin-mediated adhesion and cell polarity (Burrows *et al.* 1994, Blankenship & King 1996, Proll *et al.* 1999). In the present study, we observed a clear decline in expression of cell adhesion molecule NCAM and it was associated with shallow uterine invasion and failure to invade spiral arterioles in anti-VEGF Mab-exposed animals. In the present study, we also observed that extravillous trophoblast cells and vascular endothelium expressed immunopositive PECAM-1, and that its expression was not markedly modified in anti-VEGF Mab-treated samples. Although there is evidence in the literature to suggest that PECAM-1 expression in conceptus may play important role in embryo development, as well as in trophoblast cell invasion of the spiral arteries (Blankenship & Enders 1997, Robson *et al.*

2001), its actual physiological role has been debated (Lyall *et al.* 2001).

An important physiological consideration in the present study had been the timing of anti-VEGF Mab treatment for effective pregnancy inhibition. The best opportunity for therapeutic intervention was considered to be the point when pro-inflammatory responses are induced for supporting an evolutive pregnancy with heightened vascular permeability along with an influx at the site of blastocyst implantation of pro-inflammatory blood cells, vasotropic growth factors, such as VEGF and placenta growth factor (PlGF), and pro-inflammatory cytokines, such as leukemia inhibitory factor (LIF), IL-1α, IL-1β, and IL-6 (Ghosh *et al.* 2000, 2004, Sengupta *et al.* 2003).

Finally, we conclude that inadequate invasion by trophoblast cells following timed systemic mid-luteal phase administration of sufficient amount of murine VEGF Mab results in pregnancy failure. This provides the proof of concept that VEGF action is required for successful blastocyst implantation in the rhesus monkey.

Acknowledgements

This study was supported by a grant from the WHO–Rockefeller Foundation 'Initiative on Implantation Research'. AS was supported by a Meres Research Studentship from St John's College, Cambridge. The control hybridoma was obtained from Richard Pannell in Dr C Milstein's lab in the Laboratory of Molecular Biology, Cambridge. Both Mab (Mab 518 B7) generated against bovine luteinizing hormone (LH) and polyclonal antiserum against human chorionic gonadotropin (hCG cr-121) were kindly provided by Prof. Bill L Lasley (University of California, Davis, CA, USA). The authors declare that there is no conflict of interest that would prejudice the impartiality of this scientific work.

References

Ancelin M, Buteau-Lozano H, Meduri G, Osborne-Pellegrin M, Sordello S, Plouet H & Perrot-Applanat M 2002 A dynamic shift of VEGF isoforms with a transient and selective progesterone-induced expression of VEGF189 regulates angiogenesis and vascular permeability in human uterus. *PNAS* **99** 6023–6028.

Anteby EY, Greenfield C, Natanson-Yaron S, Goldman-Wohl D, Hamani Y, Khudyak V, Ariel I & Yagel S 2004 Vascular endothelial growth factor, epidermal growth factor and fibroblast growth factor-4 and -10 stimulate trophoblast plasminogen activator system and metalloproteinases-9. *Molecular Human Reproduction* **10** 229–235.

Blankenship TN & Enders AC 1997 Expression of platelet-endotheial cell adhesion molecule-1 (PECAM) by macaque trophoblast cells during invasion of the spiral arteries. *Anatomical Record* **247** 413–419.

Blankenship TN & King BF 1996 Macaque intra-arterial trophoblast and extravillous trophoblast of cell columns and cytotrophoblast shell express neural cell adhesion molecule (NCAM). *Anatomical Record* **245** 525–531.

Burrows TD, King A & Loke YW 1994 Expression of adhesion molecules by endovascular trophoblast and decidual endothelial cells: implications of vascular invasion during implantation. *Placenta* **15** 21–33.

Charnock-Jones DS, Sharkey AM, Rajput-Williams J, Burch D, Schofield JP, Fountain SA, Boocock CA & Smith SK 1993 Identification and localization of alternately spliced mRNAs for vascular endothelial growth factor in human uterus and estrogen regulation in endometrial carcinoma cell lines. *Biology of Reproduction* **48** 1120–1128.

Demir R, Kayisli UA, Seval Y, Celik-Ozenci C, Korgun ET, Demir-Weusten AY & Huppertz B 2004 Sequential expression of VEGF and its receptors in human placental villi during very early pregnancy: differences between placental vasculogenesis and angiogenesis. *Placenta* **25** 560–572.

Enders AC & Lopata A 1999 Implantation in the marmoset monkey: expansion of the early implantation site. *Anatomical Record* **256** 279–299.

Enders AC & Schlafke S 1986 Implantation in non-human primates and in the human. In *Reproduction and Development*, pp 291–310. Eds WR Dukelow & J Erwin. Indianapolis: John Wiley.

Ferrara N & Smith DT 1997 The biology of vascular endothelial growth factor. *Endocrine Reviews* **18** 4–25.

Ghosh D & Sengupta J 1993 Anti-nidatory effect of a single, early post-ovulation administration of mifepristone (RU 486) in the rhesus monkey. *Human Reproduction* **8** 352–358.

Ghosh D & Sengupta J 1998 Recent developments in the endocrinology and paracrinology of blastocyst implantation in the primate. *Human Reproduction Update* **4** 153–168.

Ghosh D & Sengupta J 2005 Target-oriented anti-implantation approaches for pregnancy interception: experiences in the rhesus monkey model. *Contraception* **71** 294–301.

Ghosh D, Stewart DR, Nayak N, Lasley B, Overstreet JW, Hendrickx AG & Sengupta J 1997 Serum concentrations of oestradiol-17β, progesterone, relaxin and chorionic gonadotrophin during blastocyst implantation in natural pregnancy cycle and in embryo transfer cycle in the rhesus monkey. *Human Reproduction* **12** 914–920.

Ghosh D, Lalitkumar PGL & Sengupta J 1998 Effects of early luteal phase administration of mifepristone (RU486) on leukemia inhibitory factor, transforming growth factor β and vascular endothelial growth factor in the preimplantation stage endometrium of the rhesus monkey. *Journal of Endocrinology* **157** 115–125.

Ghosh D, Sharkey AM, Charnock-Jones DS, Dhawan L, Dhara S, Smith SK & Sengupta J 2000 Expression of vascular endothelial growth factor (VEGF) and placental growth factor (PlGF) in conceptus and endometrium during implantation in the rhesus monkey. *Molecular Human Reproduction* **6** 935–941.

Ghosh D, Bell SC & Sengupta J 2004 Immunohistochemical localization of insulin-like growth factor binding protein-1 in primary implantation sites and trauma-induced deciduomal tissues of the rhesus monkey. *Placenta* **25** 197–207.

Graham DRM, Elliott ST & Van Eyk JE 2005 Broad-based proteomic strategies: a practical guide to proteomics and functional screening. *Journal of Physiology* **563** 1–9.

Greb RR, Heikinheimo O, Williams RF, Hodgen GD & Goodman AL 1997 Vascular endothelial growth factor in primate endometrium is regulated by oestrogen-receptor and progesterone-receptor ligands *in vivo*. *Human Reproduction* **12** 1280–1292.

Hinsby AM, Berezin V & Bock E 2004 Molecular mechanisms of NCAM function. *Frontiers in Bioscience* **9** 2227–2244.

Hornung D, Lebovic DI, Shifren JL, Vigne JL & Taylor RN 1998 Vectorial secretion of vascular endothelial growth factor by polarized human endometrial epithelial cells. *Fertility and Sterility* **69** 909–915.

Kashida S, Sugino N, Takiguchi S, Karube A, Takayama H, Yamagata Y, Nakamura Y & Kato H 2001 Regulation and role of vascular endothelial growth factor in the corpus luteum during mid-pregnancy in rats. *Biology of Reproduction* **64** 317–323.

Krussel JS, Casan EM, Raga F, Hirchenhain J, Wen Y, Huang H-Y, Bielfeld P & Polan ML 1999 Expression of mRNA for vascular endothelial growth factor transmembraneous receptors FLT-1 and KDR and the soluble receptor s-flt in cycling human endometrium. *Molecular Human Reproduction* **5** 452–458.

Lash GE, Warren AY, Underwood S & Baker PN 2003 Vascular endothelial growth factor is a chemoattractant for trophoblast cells. *Placenta* **24** 549–556.

Li XF, Gregory J & Ahmed A 1994 Immunolocalization of vascular endothelial growth factor in human endometrium. *Growth Factors* **11** 277–282.

Licht P, Russu V & Wildt L 2001 On the role of human chorionic gonadotropin (hCG) in the embryo-endometrial microenvironment: implications for differentiation and implantation. *Seminars in Reproductive Medicine* **19** 37–47.

Liu Y-X, Gao F, Wei P, Chen X-L, Gao H-J, Zou R-J, Siao L-J, Xu F-H, Feng Q, Liu K, *et al.* 2005 Involvement of molecules related to angiogenesis, proteolysis and apoptosis in implantation in rhesus monkey and mouse. *Contraception* **71** 249–262.

Lopata A 1996 Blastocyst-endometrial interaction: an appraisal of some old and new ideas. *Molecular Human Reproduction* **2** 519–525.

Lyall F, Bulmer JN, Duffie E, Cousins F, Theriault A & Robson SC 2001 Human trophoblast invasion and spiral artery transformation: the role of PECAM-1 in normal pregnancy, preeclampsia, and fetal growth restriction. *American Journal of Pathology* **158** 1713–1721.

Meduri G, Bausero P & Perrot-Applanat M 2000 Expression of vascular endothelial growth factor receptors in the human endometrium: modulation during the menstrual cycle. *Biology of Reproduction* **62** 439–447.

Nayak NR & Brenner RM 2002 Vascular proliferation and vascular endothelial growth factor expression in the rhesus macaque endometrium. *Journal of Clinical Endocrinology and Metabolism* **87** 1845–1856.

Otani N, Minami S, Yamoto M, Shikone T, Otani H, Nishiyama R, Otani T & Nakano R 1999 The vascular endothelial growth factor/fms-like tyrosine kinase system in human ovary during the menstrual cycle and early pregnancy. *Journal of Clinical Endocrinology and Metabolism* **84** 3845–3851.

Pauli SA, Tang H, Wang J, Bohlen P, Posser R, Hartman T, Sauer MV, Kitajewski J & Zimmerman RC 2005 The vascular endothelial growth factor (VEGF)/VEGF receptor 2 pathway is critical for blood vessel survival in corpora lutea of pregnancy in the rodent. *Endocrinology* **146** 1301–1311.

Proll J, Blaschitz A, Hartmann M, Thalhamer J & Dohr G 1999 Human first trimester placenta intra-arterial trophoblast express the neural cell adhesion molecule. *Early Pregnancy* **2** 271–275.

Rabbani ML & Rogers PA 2001 Role of vascular endothelial growth factor in endometrial vascular events before implantation in rats. *Reproduction* **122** 85–90.

Robson P, Stein P, Zhou B, Schultz RM & Baldwin HS 2001 Inner cell mass specific expression of a cell adhesion molecule (PECAM-1/CD31) in the mouse blastocyst. *Developmental Biology* **234** 317–329.

Rockwell LC, Pillai S, Olson CE & Koos RD 2002 Inhibition of vascular endothelial growth factor/vascular permeability factor action blocks estogen induced uterine edema and implantation in rodents. *Biology of Reproduction* **67** 1804–1810.

Rowe AJ, Morris KD, Bicknell R & Fraser HM 2002 Angiogenesis in the corpus luetum of early pregnancy in the marmoset and the effects of vascular endothelial growth factor immunoneutralization on establishment of pregnancy. *Biology of Reproduction* **67** 1180–1188.

Rowe AJ, Wulff C & Fraser H 2003 Localization of mRNA for vascular endothelial growth factor (VEGF), angiopoietins and their receptors during the peri-implantation period and early pregnancy in marmosets (*Callithrix jacchus*). *Reproduction* **126** 227–238.

Ryan AM, Eppler DB, Hagler KE, Bruner RH, Thomford PJ, Hall RL, Shopp GM & O'Neill CA 1999 Preclinical safety evaluation of rhuMabVEGF, an antiangiogenic humanized monoclonal antibody. *Toxicologic Pathology* **27** 78–86.

Sengupta J & Ghosh D 2002 Blastocyst-endometrium interaction at implantation in the rhesus monkey. *Journal of Reproductive Immunology* **53** 227–239.

Sengupta J, Dhawan L & Ghosh D 2003 Immunohistochemical localization of leukemia inhibitory factor, interleukins 1 and 6 at the primary implantation site in the rhesus monkey. *Cytokine* **24** 277–285.

Shargel L & Yu ABC 1999 *Applied Biopharmaceutics & Pharmacokinetics*, 4 New Jersey: Prentice-Hall, pp. 608–642.

Sharkey AM, Catalano R, Evans A, Charnock-Jones DS & Smith SK 2005 Novel antiangiogenic agents for use in contraception. *Contraception* **71** 263–271.

Shifren JL, Tseng JF, Zaloudek CJ, Ryan IP, Meng G, Ferrara N, Jaffe RB & Taylor RN 1996 Ovarian steroid regulation of vascular endothelial growth factor in the human endometrium: implications for angiogenesis during the menstrual cycle and in the pathogenesis of endometriosis. *Journal Clinical Endocrinology and Metabolism* **81** 3112–3118.

Slukvin II, Lunn DP, Watkins DI & Golos TG 2000 Placental expression of the nonclassical MHC class I molecule Mamu-AG at implantation in the rhesus monkey. *PNAS* **97** 9104–9109.

Wulff C, Wilson H, Dickson SE, Wiegand SJ & Fraser HM 2002 Hemochorial placentation in the primate: expression of vascular endothelial growth factor, angiopoietins and their receptors throughout pregnancy. *Biology of Reproduction* **66** 802–812.

Xu F, Hazzard TM, Evans A, Charnock-Jones S, Smith S & Stouffer RL 2005 Intraovarian actions of anti-angiogenic agents disrupts preiovulatory events during the menstrual cycle in monkeys. *Contraception* **71** 239–248.

Zar JH 1999 *Biostatistical Analysis*, 4 New Jersey: Prentice-Hall, pp. 177–254.

Zimmerman RC, Xiao E, Husami N, Sauer MV, Lobo R, Kitajewski J & Ferin M 2001 Short-term administration of antivascular endothelial growth factor antibody in the late follicular phase delays follicular development in the rhesus monkey. *Journal of Clinical Endocrinology and Metabolism* **86** 768–772.

Received 13 April 2006
First decision 17 May 2006
Revised manuscript received 24 November 2006
Accepted 22 December 2006

PUBLICATION 12

Evans, A. L., Faial, T., Gilchrist, M. J., Down, T., Vallier, L., Pedersen, R. L., Wardle F. C., and Smith J.C.et al. 2012. Genomic targets of *Brachyury* (T) in differentiating mouse embryonic stem cells. *PLoS One* [Online], 7, 3, e33346. Available:http://www.ncbi.nlm.nih.gov/entrez/query.fcgi?cmd=Retrieve&db=PubMed&dopt=Citation&list_uids=22479388.

Citied by 9, Impact factor 4.092

Total Article Views **4967** (between March 30 2012-Sept 2013)

ISSN: 1932-6203

Journal Type

PLoS One is an open access peer-reviewed journal and submissions are considered on the basis of scientific validity and technical quality rather than the perceived impact. The editorial board ensures the scientific integrity. The type of license ensures authors retain copyright but allows free access to download and print and papers are published daily after review so there is no editorial calendar.

Personal Contribution

Experiments were conceived and designed by myself, Roger Pederson, Ludovic Vallier, Fiona Wardle and Jim Smith for all the mouse data and Tiago Faial then joined with the human data. It was Tiago who helped out at the final stages when I was unable to work and he carried out the human ESC experiments to strengthen the data. Tiago contributed Figure 7, Supplementary Table S5 and part of Table S8 (human). All other Figures are my own. I did the majority of the writing and Jim's expertise as an editor brought it all together.

OPEN ACCESS Freely available online

PLoS one

Genomic Targets of Brachyury (T) in Differentiating Mouse Embryonic Stem Cells

Amanda L. Evans[1,4], Tiago Faial[2,3,4], Michael J. Gilchrist[1,4], Thomas Down[1], Ludovic Vallier[2], Roger A. Pedersen[2], Fiona C. Wardle[5], James C. Smith[1,3,4]*

1 Wellcome Trust/Cancer Research UK Gurdon Institute, University of Cambridge, Cambridge, United Kingdom, **2** The Anne McLaren Laboratory for Regenerative Medicine, University of Cambridge, Cambridge, United Kingdom, **3** Department of Zoology, University of Cambridge, Cambridge, United Kingdom, **4** Medical Research Council, National Institute for Medical Research, London, United Kingdome, **5** Randall Division of Cell and Molecular Biophysics, King's College London, London, United Kingdom

Abstract

Background: The T-box transcription factor Brachyury (T) is essential for formation of the posterior mesoderm and the notochord in vertebrate embryos. Work in the frog and the zebrafish has identified some direct genomic targets of Brachyury, but little is known about Brachyury targets in the mouse.

Methodology/Principal Findings: Here we use chromatin immunoprecipitation and mouse promoter microarrays to identify targets of Brachyury in embryoid bodies formed from differentiating mouse ES cells. The targets we identify are enriched for sequence-specific DNA binding proteins and include components of signal transduction pathways that direct cell fate in the primitive streak and tailbud of the early embryo. Expression of some of these targets, such as *Axin2, Fgf8* and *Wnt3a,* is down regulated in *Brachyury* mutant embryos and we demonstrate that they are also Brachyury targets in the human. Surprisingly, we do not observe enrichment of the canonical T-domain DNA binding sequence 5′-TCACACCT-3′ in the vicinity of most Brachyury target genes. Rather, we have identified an $(AC)_n$ repeat sequence, which is conserved in the rat but not in human, zebrafish or *Xenopus*. We do not understand the significance of this sequence, but speculate that it enhances transcription factor binding in the regulatory regions of Brachyury target genes in rodents.

Conclusions/Significance: Our work identifies the genomic targets of a key regulator of mesoderm formation in the early mouse embryo, thereby providing insights into the Brachyury-driven genetic regulatory network and allowing us to compare the function of Brachyury in different species.

Citation: Evans AL, Faial T, Gilchrist MJ, Down T, Vallier L, et al. (2012) Genomic Targets of Brachyury (T) in Differentiating Mouse Embryonic Stem Cells. PLoS ONE 7(3): e33346. doi:10.1371/journal.pone.0033346

Editor: David S. Milstone, Brigham and Women's Hospital, United States of America

Received September 6, 2010; **Accepted** February 13, 2012; **Published** March 30, 2012

Funding: This work was supported by a Wellcome Trust Programme Grant to JCS (www.wellcome.ac.uk); MRC core support to JCS (www.nimr.mrc.ac.uk); a Fundação para a Ciência e a Tecnologia fellowship (www.fct.pt) to TF; an MRC Career Development Award (www.mrc.ac.uk) and a Lister Institute Research Prize (www.lister-institute.org.uk) to FCW; an MRC Programme grant (www.mrc.ac.uk) and an EU/PluriSys (plurisys.biotalentum.eu/) grant to RAP; a Diabetes/UK-MRC Career Development Fellowship to LV (diabetes.org.uk); and by the Cambridge NIHR Biomedical Research Centre (RAP and LV). The funders had no role in study design, data collection and analysis, decision to publish, or preparation of the manuscript.

Competing Interests: A proportion of the consumables funding for the RAP laboratory during the period in which the work was accomplished was provided by PluriSys. PluriSys is a non-commercial, FP7 consortium grant funded by the European Commission. BioTalentum, a Hungarian limited company, coordinates the PluriSys consortium but does not take any commercial interest in the materials or results generated by the consortium. There are no patents, products in development or marketed products to declare. This does not alter the authors' adherence to all the PLoS ONE policies on sharing data and materials.

* E-mail: jim.smith@nimr.mrc.ac.uk

Introduction

Brachyury (*T*) is expressed in the primitive streak, tailbud and notochord of the early mouse embryo [1,2]. It plays a key role in early development: mouse embryos lacking functional Brachyury protein do not gastrulate properly, fail to form a differentiated notochord, lack structures posterior to somite seven, and have defects in left-right patterning [3,4,5]. The expression patterns of the *Xenopus* [6] and zebrafish [7,8] *Brachyury* orthologues resemble those of the mouse, and these genes play similar roles in early development [8,9,10,11], indicating that *Brachyury* function has been conserved throughout evolution.

In an effort to understand how Brachyury exerts its effects, we have searched for genomic targets of this transcription factor. In previous work using *Xenopus* embryos we have used differential screening approaches to isolate target genes such as *eFGF* [12], members of the *Bix* family [13,14] and *Wnt11* [15], while a chromatin immunoprecipitation-microarray (ChIP-chip) approach in the zebrafish embryo has allowed us to identify more than 200 potential targets of No-tail a (Ntla), the orthologue of Brachyury [16]. In this paper, we apply a ChIP-chip approach to identify targets of Brachyury during mouse embryonic stem (ES) cell differentiation. ES cells provide an abundant source of material as they differentiate towards embryoid bodies (EBs), and we predict that the identification of Brachyury targets in these cells will shed light on ES cell differentiation as well as help identify such targets in the early embryo. This work might also indicate the extent to which the biological function of Brachyury

has been conserved in vertebrates and provide information on how Brachyury binding motifs are disposed within target cis-regulatory regions.

Our results show that Brachyury targets in differentiating ES cells are enriched for sequence-specific DNA binding proteins and components of signal transduction pathways that direct cell fate in the primitive streak and tailbud of the early embryo. Interestingly, most binding peaks were not enriched for the canonical T-box binding site 5′-TCACACCT-3′ [17,18] but did contain a repeating AC motif. Amongst the signal transduction pathway components were regulators of the WNT and FGF pathways. These include *Axin2* (*Axil/Conductin*), which encodes a negative regulator of Wnt signalling, as well as *Wnt3a* and *Fgf8*. Significantly, expression of all three genes is down regulated in homozygous *Brachyury* mutant embryos and we show by ChIP-qPCR that these are also genomic targets of BRACHYURY in differentiating human ES cells. These results are consistent with work in the zebrafish emphasising the importance of Wnt and Fgf signal transduction pathway components as Brachyury targets [16]. In demonstrating that expression of *Axin2* in the early mouse embryo is regulated by Brachyury as well as by TCF/Lef proteins [19,20,21,22], our results emphasise the complex interplay between signalling pathways in the regulation of gene expression in the early embryo.

Results

ES cell culture

Preliminary experiments demonstrated that our ES cell culture regime yielded embryoid bodies of uniform size, similar to that of EBs grown on hydrophobic surfaces [23], and that expression of *Brachyury* usually peaked at day 4 of differentiation (Fig. 1). Immunohistochemical analysis indicated that approximately 15% of cells in our embryoid bodies express Brachyury (data not shown).

ChIP-chip and bioinformatic analysis

Binding sites of Brachyury were identified by ChIP-chip experiments and the closest gene was identified using version NBI35.1 of the annotated mouse genome (see Material and Methods). Following filtration, our analysis gave a list of 520 enriched probes representing 396 genes (Table S1). Genomic quantitative PCR on a selection of genes called as bound or unbound confirmed that our ChIP-chip approach identified genuine binding events (Fig. S1).

Brachyury is expressed at its highest levels in the primitive streak and haematopoietic progenitors at E7.5 to E8.5. Later expression is restricted to the tailbud and notochord (E12.5), and then to parts of the brain and tail [2]. Of the Brachyury targets identified in our embryoid body experiments whose expression patterns are known, most (63%) are activated during this period of 7.5 to 17.5 dpc of mouse development (Fig. 2A). And of these 250 genes, many are restricted to the primitive streak or its mesodermal derivatives, with 30% (75 transcripts) expressed exclusively in the mesoderm (Fig. 2A). In addition to *Axin2*, *Wnt3a* and *Fgf8*, which are discussed below, genes that have been reported to be co-expressed with *Brachyury* include *Msgn1*, whose expression is down regulated in *Brachyury* mutants [24], *Meis1* [25] *Trim 28* [26] and *Zic2* [27], which are expressed in the primitive streak during gastrulation, *Foxa2*, present in the node and notochord [28], and *Adam19* (*meltrin beta*), present in tailbud mesenchyme [29]. These and other transcripts (see below) are also co-expressed with *Brachyury* (or are activated shortly after *Brachyury*) in embryoid bodies, and typical profiles of *Msgn1*, *Meis1* and *Foxa2* expression are shown in Fig. 2B.

The targets we identify include components of the WNT, MAPK, JNK, TGF-β, Hedgehog, FGF and G-protein coupled signal transduction pathways (Table S2). Analysis of the targets yielded a set of gene ontology (GO) terms consistent with the function of *Brachyury* during gastrulation [30].

In particular, cellular component analysis highlights gene products involved in morphogenesis, cell adhesion and cell

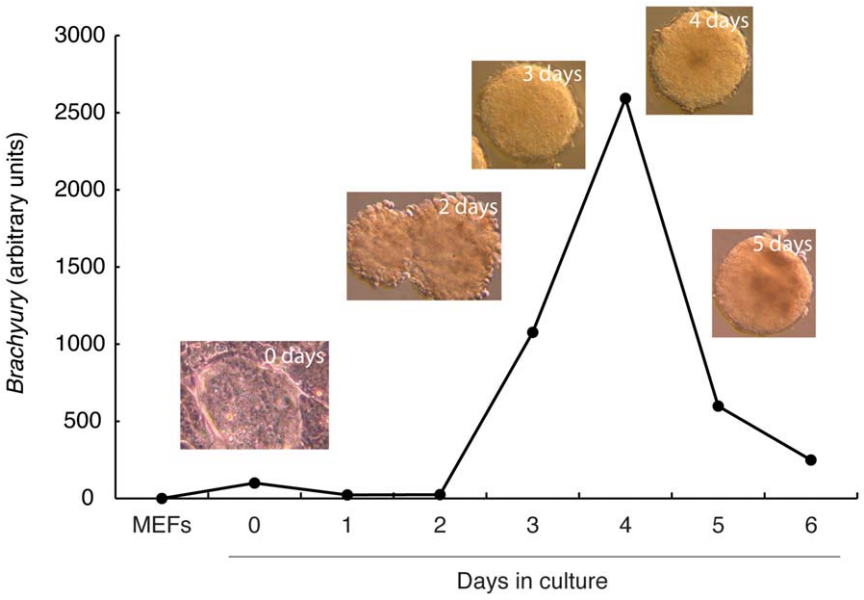

Figure 1. Temporal expression pattern of *Brachyury* during early ES cell differentiation. The graph shows a quantitative RT-PCR profile from an embryoid body spinner culture. *Brachyury* expression is calculated relative to *beta actin*. Images show undifferentiated R1 cells on mouse embryo fibroblast feeders at day 0, early blast colonies at day 2, and embryoid bodies at days 3, 4 (when they are cross-linked) and 5.
doi:10.1371/journal.pone.0033346.g001

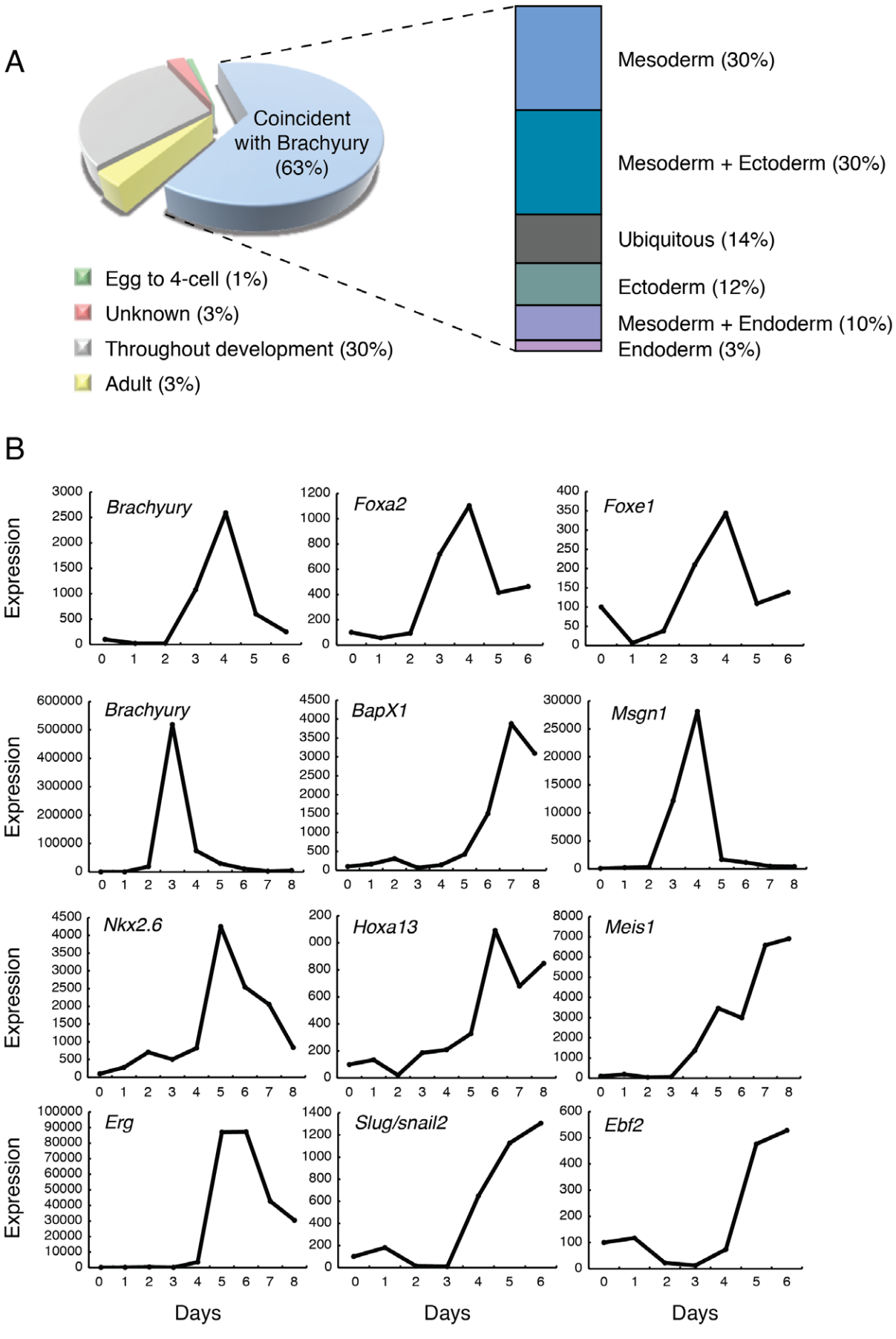
A
Coincident with Brachyury (63%)
Egg to 4-cell (1%)
Unknown (3%)
Throughout development (30%)
Adult (3%)
Mesoderm (30%)
Mesoderm + Ectoderm (30%)
Ubiquitous (14%)
Ectoderm (12%)
Mesoderm + Endoderm (10%)
Endoderm (3%)
B
Brachyury
Foxa2
Foxe1
Brachyury
BapX1
Msgn1
Nkx2.6
Hoxa13
Meis1
Erg
Slug/snail2
Ebf2
Expression
Days

Figure 2. Analysis of Brachyury targets. (A) Pie chart showing the times in development at which Brachyury target gene expression begins in the mouse embryo (as a percentage of total; n = 396). Most genes (63%) start to be expressed between E7.5, when *Brachyury* is expressed in the primitive streak, notochord and tailbud, and E17.5, when expression is restricted to trunk mesenchyme. Of targets showing this temporal expression pattern, 30% are restricted to mesodermal derivatives, as indicated in the bar chart to the right. Others are expressed in various combinations of ectoderm, mesoderm and endoderm. (B) Temporal expression of transcription factor targets of Brachyury during ES cell differentiation in spinner culture, obtained by RT-PCR. The three panels in the top row were taken from a batch of cells in which *Brachyury* expression peaked at day 4 of culture; the rest were taken from a batch in which *Brachyury* expression peaked at day 3. All show means of triplicate measurements and are normalised to levels of *beta actin*. *Foxa2* and *Foxe1* in the top row peak with *Brachyury* at day 4; genes in the lower panel peak later than *Brachyury*.
doi:10.1371/journal.pone.0033346.g002

polarity. Targets such as *Gdf5*, *Lmx1b* and *Dlx5* are involved in morphogenesis (Fig. S2A: GO:0048598; $P<10^{-6}$), *Gabra1*, *Gfra3* and *Cbln3* are involved in anchoring the plasma membrane to cytoskeletal proteins (Fig. S2B: GO:0030054; $P=1\times10^{-3}$) and others encode proteins involved in cell adhesion, such as the glycosyltransferases *B4galnt2* and *Cml4/Nat8*. This last observation is consistent with data showing that glycosyltransferases, and especially galactotransferases, are mis-expressed in T/T mutant mice [31], that the extracellular matrix is reduced in such embryos [32], and that cells have fewer cytoplasmic processes, especially in the somites and mesenchyme [32]. Significantly, over-expression of Cml4, or its *Xenopus* orthologue *Camello* (*Xcml*), inhibits gastrulation in *Xenopus* [33].

Interestingly, another group of targets is associated with germ cells (Table S3), including *Asap1* (*Ddef1*), which encodes an ADP-ribosylation factor GTPase-activating protein implicated in metastatic prostate cancer [34], and also the Wilms' tumour gene *WT1* [35].

Transcription factor targets

Of the 396 genes identified as potential targets of Brachyury, 53 (13.4%) are transcription factors (Table S4), and indeed gene ontology analysis demonstrates significant enrichment for sequence-specific DNA binding proteins (Fig. S2C GO:0043565, $p<10^{-5}$). Several families of transcription factors are represented, including the Ets, paired box, homeobox, winged helix/forkhead, bZip and zinc finger families. Under our ES cell culture conditions, expression of many of these transcription factors peaks either at the same time as *Brachyury* (*Foxa2*, *Foxe1*) or just afterwards (*BapX1*, *Ebf2*, *Erg*, *Hoxa13*, *Meis1*, *Msgn1*, *Nkx2.6* and *Slug*) (Fig. 2B). As we discuss below, our data provide a basis for deciphering the transcription factor genetic regulatory network underlying mesoderm formation in ES cells and in the embryo.

T-box protein binding motifs

Previous work indicates that Brachyury interacts with the sequence 5′-TCACACCT-3′ [16,36,37,38]. To our surprise, neither nested MICA nor RSAT identified this motif as significantly enriched in the DNA sequences selected in our experiments. Rather, both packages identified enrichment of the simple sequence repeat $(AC)_n$ (Fig. S3A). However, although it was not enriched, we did observe that several regulatory regions contain a sequence resembling a T-box site (in which 1 to 3 nucleotides differ from the consensus) close to an AC repeat. These genes include *Axin2*, *Ctnnb1/β-catenin*, *Erg*, *Etv1*, *Fgf8*, *Fev*, *Foxa2*, *Foxe1*, *Fyb*, *Id4*, *Meis1*, and *Hoxa3* where the T-box like sites may be positioned either 5′ or 3′ to the repeat sequence.

To assess the significance of these observations we first performed electrophoretic mobility shift assays (Fig. S3B). As expected, the T-domain of mouse Brachyury binds the canonical TCACACCT sequence, binding can be competed by unlabelled oligonucleotide, and the complex can be 'super-shifted' by a Brachyury antibody. The $(AC)_n$ repeat motif also forms a complex with Brachyury, but although the complex can also be 'supershifted', unlabelled oligonucleotide competes very poorly. Finally, when both motifs are present in the radiolabelled oligonucleotide, competition using an excess of cold oligonucleotide in which just the T-box site is mutated is poor, and so is competition in which just the $(AC)_n$ region is mutated. Together, these observations indicate that the $(AC)_n$ sequence interacts only weakly with Brachyury, if at all, and that its role may be restricted to stabilizing binding to an adjacent or even a distant T box site.

If true, such a role is likely to be restricted to rodent species. Our dataset contains 111 peaks with associated AC repeats longer than eight nucleotides (Table S5). Comparison with rat, human, zebrafish and *Xenopus* genomes shows that 38 of these AC-rich regions are unique to the mouse while 68 are also present in the rat. Sixteen of the AC repeats are present in the human genome, of which 11 are also present in rat. However, none of the repeats are conserved in zebrafish or *Xenopus* (Table S5).

Axin2 and *Wnt3a* as targets of Brachyury

Amongst the identified Brachyury targets are many genes encoding positive and negative regulators of the Wnt signalling pathway (Fig. 3A). Enrichment peaks in the promoter regions of *Dkk1*, *Ctnnb1/β-catenin*, *Dvl3*, and *γ-catenin/Jup* show Brachyury binding (Fig. 3B, C, D and E) and also reveal the presence of AC repeats (green bars) and imperfect T-binding sites (blue bars). Of these Wnt-related genes, *Wnt3a* and *Axin2* both show strong Brachyury binding peaks around their transcription start sites in our ChIP-chip analyses (Figs. 4A, 5A), and their temporal expression patterns both resemble that of *Brachyury* in our embryoid body system (Figs. 4B, 5B). For *Wnt3a*, a variant Brachyury site is positioned close to an AC repeat sequence in the first intron, and a canonical TCACACCT Brachyury site is upstream of the transcription start site (Fig. 4A). In the case of *Axin2*, a canonical Brachyury site is positioned close to a variant site and to an AC repeat (Fig. 5A).

To ask whether Brachyury is required for expression of *Wnt3a* and *Axin2*, we crossed mice that are heterozygous for a *Brachyury* mutation [39] and assessed expression of the two genes. In wild-type embryos at E7.5 the expression patterns of *Brachyury*, *Wnt3a* and *Axin2* overlap significantly (Fig. S4). Expression of W*nt3a* in *Brachyury* homozygous mutant embryos at this stage resembles that in heterozygous and wild type individuals, as has been reported previously [40], but by E8.5, when *Wnt3a* expression is restricted to the primitive streak, its expression is significantly down regulated in *Brachyury* mutant embryos (Fig. 4C,D).

Like *Wnt3a*, *Axin2* is expressed in *Brachyury* mutant embryos at 7.5 dpc, but this expression is more variable than that of *Wnt3a*, and is sometimes reduced or even absent (data not shown). By E8.5, when *Axin2* is expressed in the headfold, tailbud and primitive streak of wild type embryos, its expression in the posterior region of *Brachyury* mutant embryos is very weak or absent (Fig. 5C,D). Together, these data indicate that Brachyury is

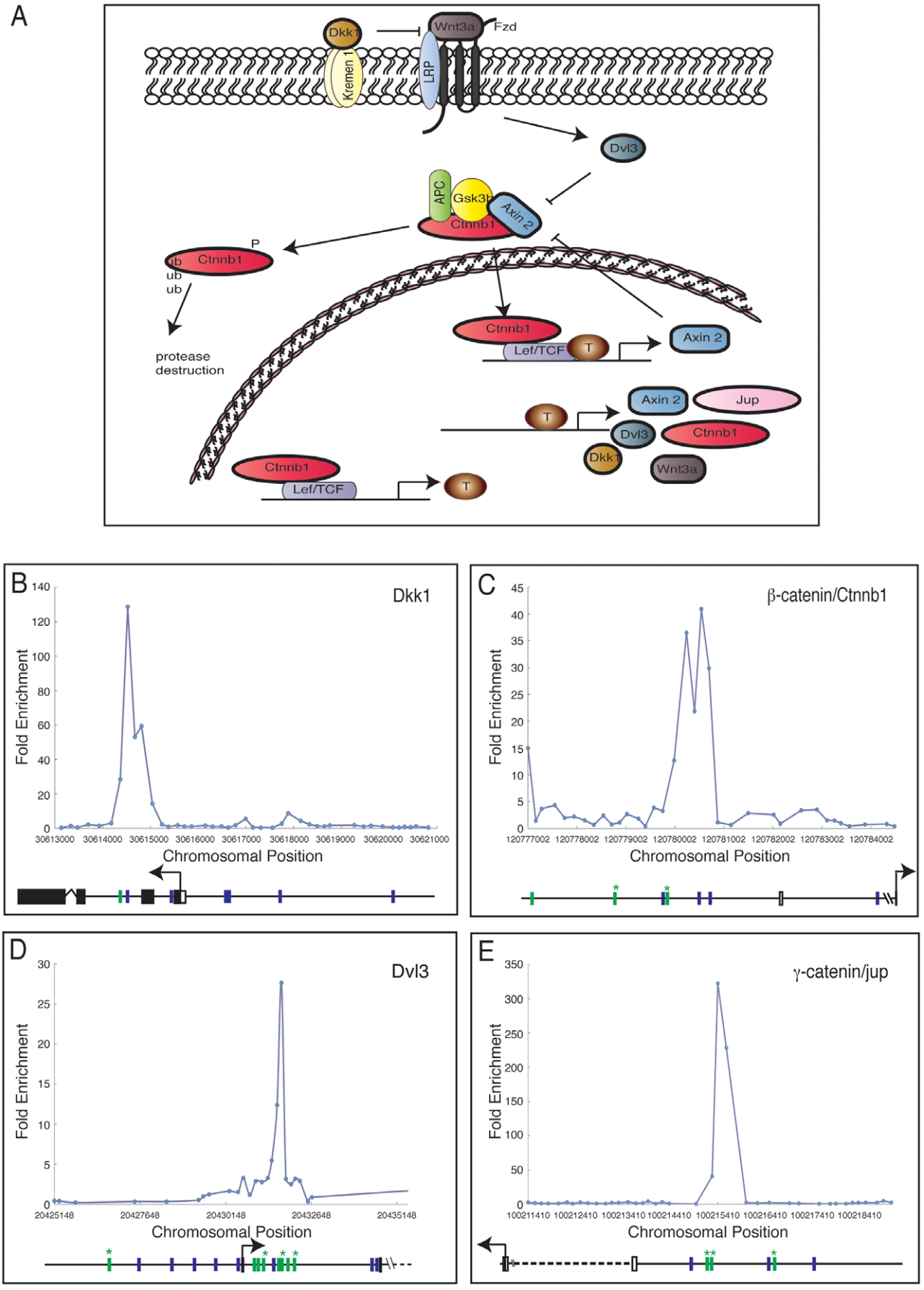
A
Dkk1
Wnt3a
Fzd
Kremen 1
LRP
Dvl3
APC
Gsk3b
Axin 2
Ctnnb1
P
ub
ub
ub
Ctnnb1
protease
destruction
Ctnnb1
Lef/TCF
T
Axin 2
Axin 2
Jup
T
Dvl3
Ctnnb1
Dkk1
Wnt3a
Ctnnb1
Lef/TCF
T
B
Dkk1
Fold Enrichment
Chromosomal Position
30613000 30614000 30615000 30616000 30617000 30618000 30619000 30620000 30621000
C
β-catenin/Ctnnb1
Fold Enrichment
Chromosomal Position
120777002 120778002 120779002 120780002 120781002 120782002 120783002 120784002
D
Dvl3
Fold Enrichment
Chromosomal Position
20425148 20427648 20430148 20432648 20435148
E
γ-catenin/jup
Fold Enrichment
Chromosomal Position
100211410 100212410 100213410 100214410 100215410 100216410 100217410 100218410

Figure 3. Components of the Wnt pathway as Brachyury targets. (A) The Wnt signalling pathway. Arrows indicate positive interactions and bars represent negative interactions. Targets identified in this study are outlined in **bold**. (B–E) Brachyury binding in genomic regions around *Dkk1* (B); *Ctnnb1/β-catenin* (C); *Dvl3* (D); and *γ-Catenin/jup/plakoglobin* (E). Each target shows fold enrichment against chromosomal position. Blue bars represent the T box-like site TSACANNT (N = any base, S = G/C) and green bars represent $(AC)_n$. Stars above bars represent sequence on the reverse strand. Plots are average of triplicate chip results, aligned to the mm8 Feb. 2006 assembly.
doi:10.1371/journal.pone.0033346.g003

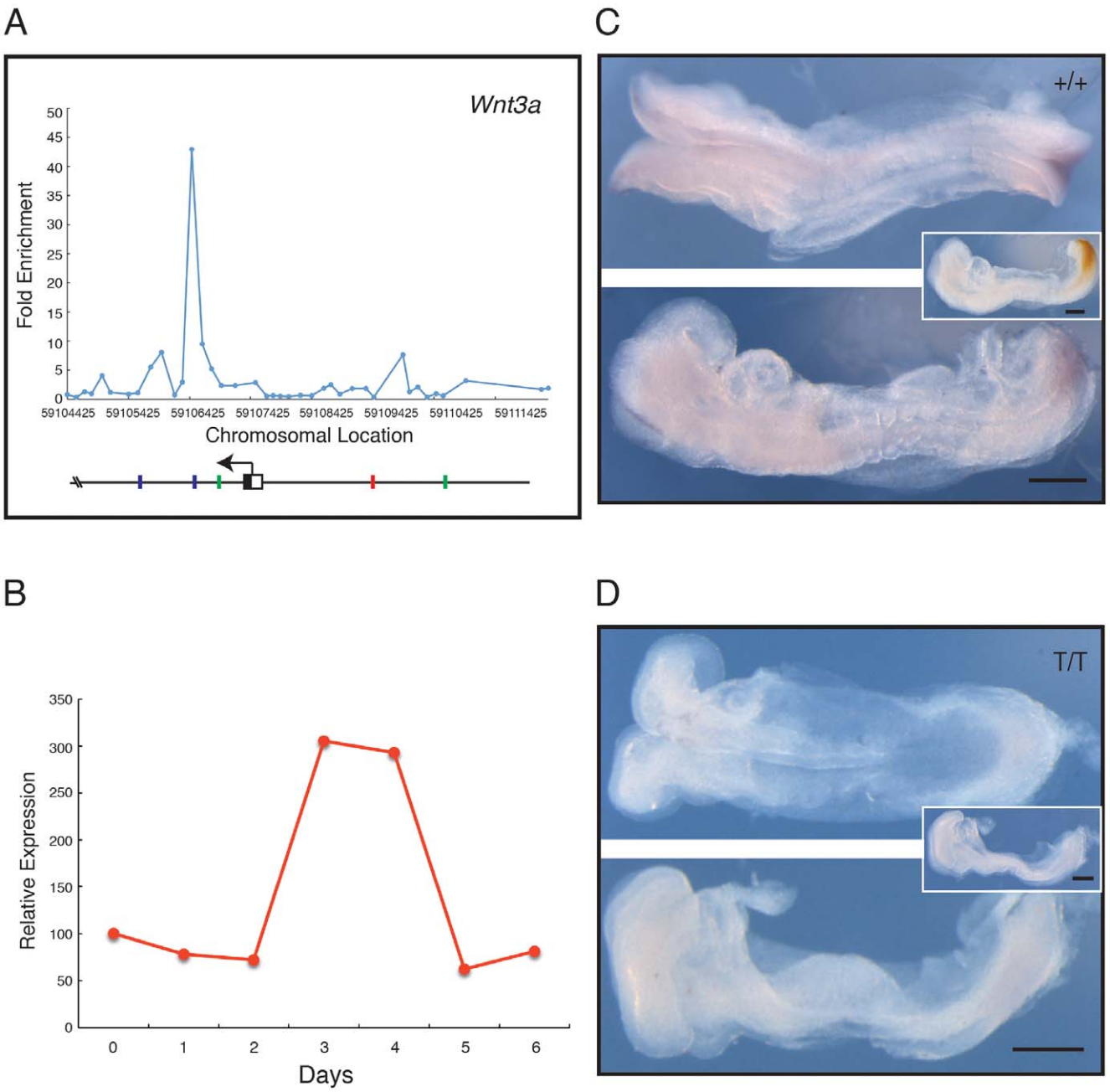

Figure 4. Analysis of *Wnt3a*, a positive regulator of the Wnt pathway. (A) Location analysis of *Wnt3a*. The figure (and Figs. 5, 6) shows fold enrichment against chromosomal position. Plot is the mean of triplicate chip results, aligned to the mm8 Feb. 2006 assembly. Blue bars represent the T box-like site TSACANNT (N = any base, S = G/C); green bars represent $(AC)_n$; red bars the consensus TCACACCT. Stars above bars represent sequence on reverse strand. (B) Quantitative RT-PCR expression profile for *Wnt3a* during ES cell differentiation, expressed relative to *beta actin*. (C, D) Expression of *Wnt3a* studied by in situ hybridisation; in each, the top image shows a dorsal view, and the bottom image a lateral view. (C) Phenotypically wild type (+/+ or +/*T*) embryo at E8.5–8.75, and (D) a mutant (*T*/*T*) embryo from crosses of *Brachyury* heterozygous mutant mice. *Wnt3a* expression is detected with NBT/BCIP (purple) and the insets show a lateral view after double staining for *Brachyury* detected with INT/BCIP (orange brown). Note that in the wild type embryo *Wnt3a* is expressed in tailbud and paraxial mesoderm. In the mutant embryo expression of *Wnt3a* staining is absent or greatly reduced (n = 3). Scale bars indicate 250 μm.
doi:10.1371/journal.pone.0033346.g004

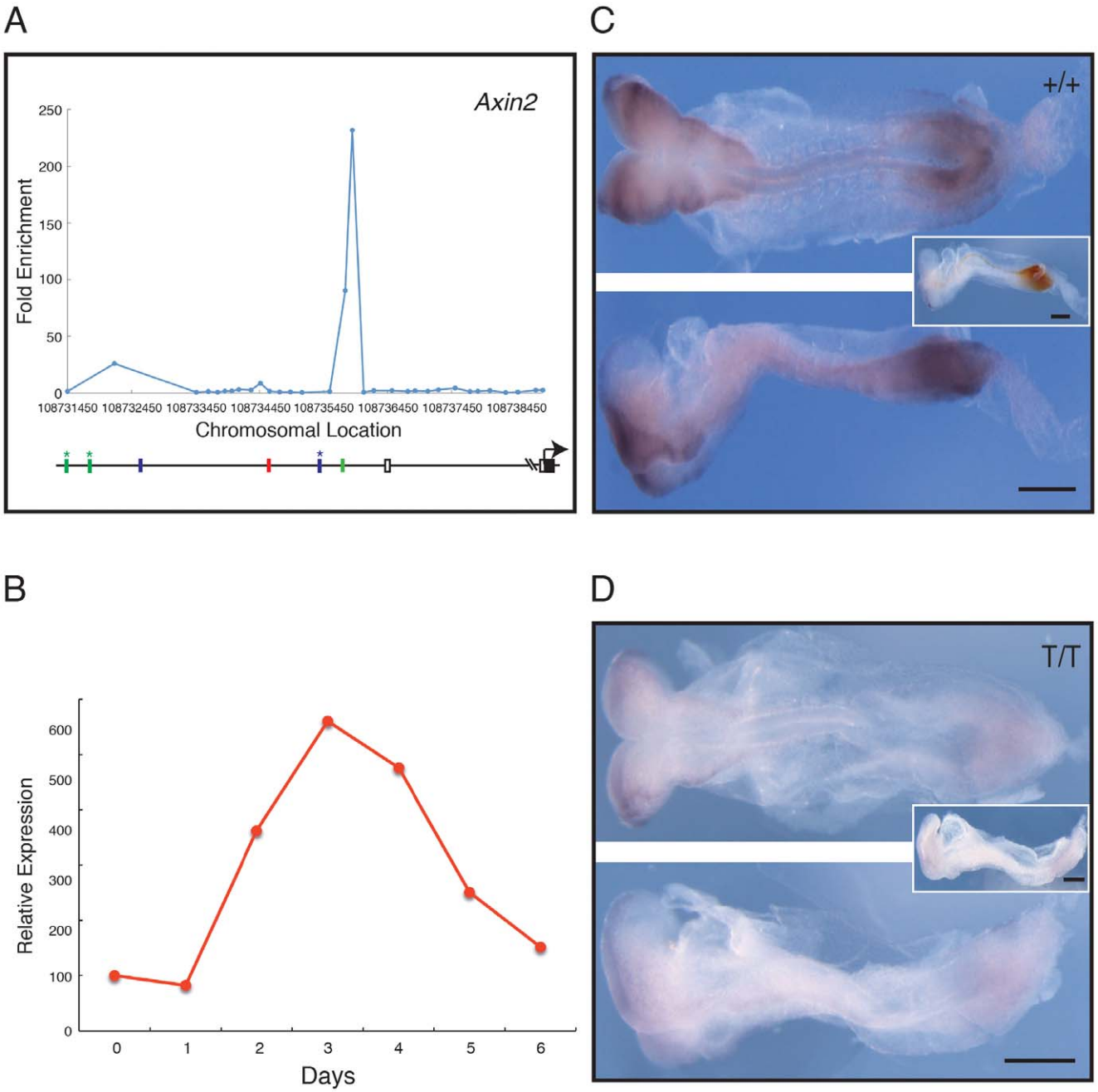

Figure 5. Analysis of *Axin2*, a negative regulator of the Wnt pathway. (A) Location analysis of *Axin2*. For details see legend to Fig. 4. (B) Quantitative RT-PCR expression profile for *Axin2* during ES cell differentiation, expressed relative to *beta actin*. (C, D) Expression of *Axin2* studied by in situ hybridisation; in each, the top image shows a dorsal view, and the bottom image a lateral view. (C) Phenotypically wild type (+/+ or +/*T*) embryo at E8.5–8.75 and (D) a mutant (*T/T*) embryo, both derived from crosses of *Brachyury* heterozygous mutant mice. *Axin2* expression is detected with NBT/BCIP (purple) and the insets show a lateral view after double staining for *Brachyury* detected with INT/BCIP (orange brown). Note that in the wild type embryo *Axin2* is expressed in tailbud, paraxial mesoderm and lateral margin of the neural folds. In the mutant embryo expression of *Axin2* is greatly reduced (n = 9). Scale bars are 250 μm.
doi:10.1371/journal.pone.0033346.g005

required for the proper expression of *Wnt3a* and *Axin2*, which encode key components of the WNT signalling pathway (see Discussion).

Fgf8 as a target of Brachyury

A strong Brachyury binding peak was also detected 5′ of the transcription start site of *Fgf8* (Fig. 6A), with a variant Brachyury site (5′-TCACAGAT-3′; underlined bases differ from consensus) positioned 63 nucleotides from an $(AC)_{19}$ repeat. The temporal expression profile of *Fgf8* resembles that of *Brachyury* during embryoid body differentiation (Fig. 6B), and the gene is co-expressed with *Brachyury* in the primitive streak of embryos at E7.5 and E8.0–E8.25 (Fig. S5; Fig. 6C). Expression of *Fgf8* in mutant *Brachyury* embryos at E8.0 is greatly reduced (Fig. 6C), indicating that Brachyury is required for expression of this gene as it is for *Wnt3a* and *Axin2*.

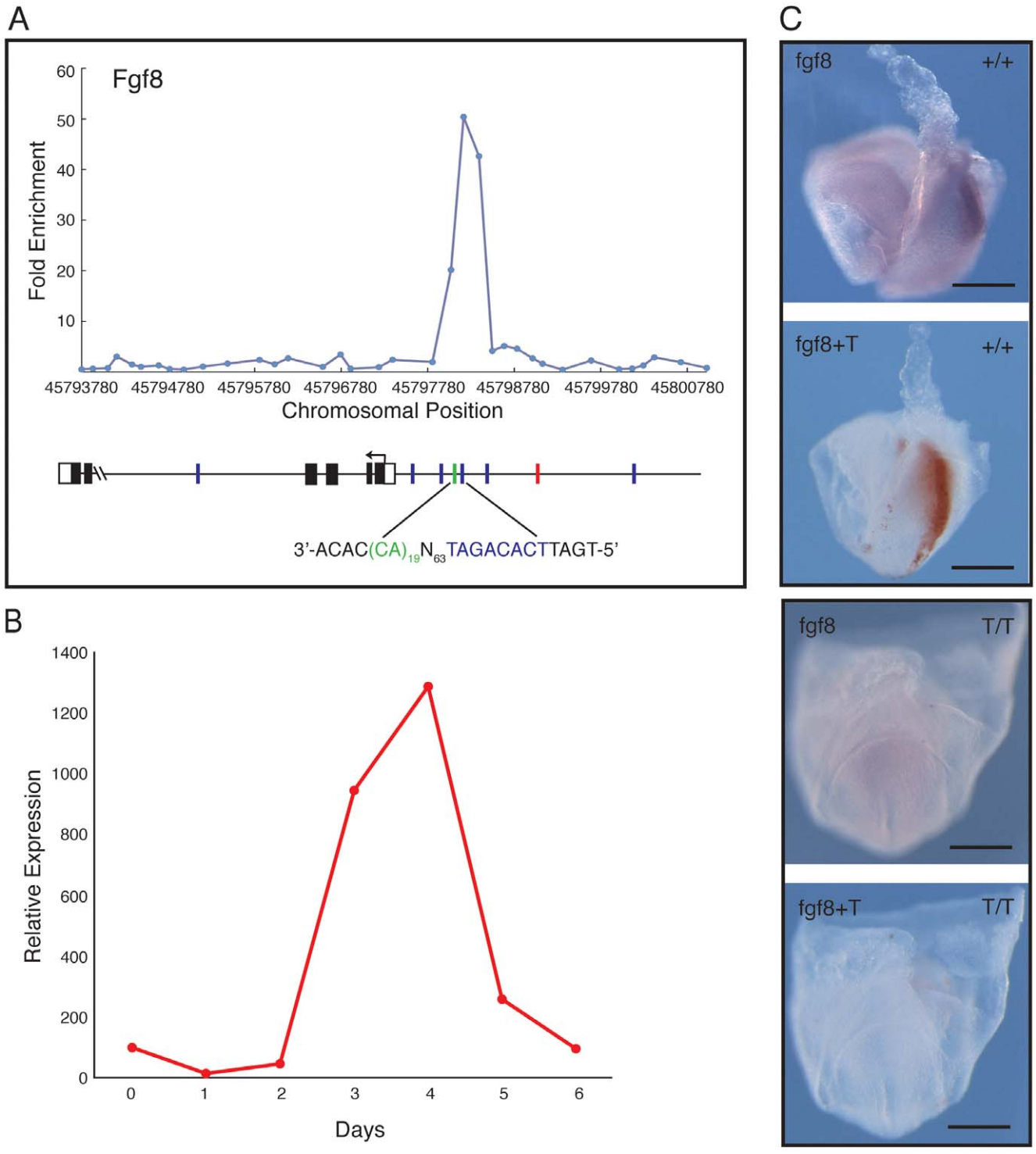

Figure 6. *Fgf8* as a target of Brachyury. (A) Location analysis of *Fgf8*. For details of methods see legend to Fig. 4. (B) Quantitative RT-PCR expression profile for *Fgf8* during ES cell differentiation, expressed relative to *beta actin*. (C) Expression of *Fgf8* studied by in situ hybridisation. The images show a phenotypically wild type (+/+ or +/*T*) embryo (top pair) and a mutant *T*/*T* (bottom pair) embryo derived from crosses of *Brachyury* heterozygous mutant mice. The wild type embryo is orientated with anterior to the left and posterior to the right; the mutant is viewed from the posterior. *Fgf8* expression is detected with NBT/BCIP (purple) and *Brachyury* with INT/BCIP (orange brown). In the wild type embryo *Fgf8* is expressed in the primitive streak and paraxial mesoderm; such expression is absent or greatly reduced in the mutant. Scale bars indicate 200 μm.
doi:10.1371/journal.pone.0033346.g006

AXIN2, JUP, FGF8 and WNT3A are conserved targets of BRACHYURY in the human

Because some of the Brachyury targets we discovered in the mouse were not previously identified in the frog or the zebrafish [16], we decided to investigate whether these are conserved in other species, in an attempt to further validate our results. For this purpose we decided to look for BRACHYURY binding in the human genome.

We have recently optimised culture conditions that cause human embryonic stem cells to differentiate into mesoderm-like cells [41]. These cell populations express BRACHYURY at high levels and, importantly, they also up regulate other mesoderm markers, including many of the Brachyury targets we have identified in the mouse, namely, *DKK1*, *HOXA13*, *ID4*, *JUP*, *KRT8*, *MEIS1*, *MSGN1*, *SNAI2*, and *WNT3A*.

We therefore made use of this newly developed *in vitro* differentiation system to ask if BRACHYURY binds the homologous human regulatory regions of some key mouse targets: *AXIN2*, *FGF8*, *JUP* and *WNT3A*. As in the mouse, these regions contain imperfect T-binding motifs (data not shown). Our experiments involving ChIP-qPCR with hESC-derived mesoderm cells indeed detected a strong enrichment for these sequences, thus indicating that BRACHYURY binds to the same genomic regions in the human (Fig. 7A).

Interestingly, these promoter sequences seem to be conserved between the mouse and human genomes, but not in the zebrafish or in other vertebrates (Fig. 7B) suggesting that these targets might be unique to mammals.

Discussion

We have identified genomic targets of Brachyury in differentiating mouse ES cells, demonstrating that embryoid bodies provide sufficient material for chromatin immunoprecipitation experiments and that they represent an effective model of early mouse development. Although they do not undergo proper morphogenesis, they do generate pattern, as illustrated by the formation of beating cardiomyocytes [42]. The embryoid bodies produced in our experiments form cardiomyocytes after eight to ten days in culture, close to the time at which the heart tube forms during normal development. As discussed below, at least three Brachyury targets (*Wnt3a*, *Axin2* and *Fgf8*) are expressed in the early mouse embryo during formation of the primitive streak, and their proper expression during development requires *Brachyury* function. We also note that several targets are expressed in primordial germ cells, perhaps the first differentiated population to emerge during early gastrulation [43,44,45]. These cells express *Brachyury* until E12.5, when the gene is down regulated in a non-migrating population [46,47]. Although *Brachyury* may not be involved directly in the specification of the germ cells [48,49] it may regulate their migration and their potency.

Classification of Brachyury targets and comparison with zebrafish and frog

Our work has identified 396 potential targets of Brachyury, and gene ontology analysis indicates that many of these encode sequence-specific DNA binding proteins and proteins involved in cell adhesion and embryonic morphogenesis. Analysis of the former category will help in the elucidation of the genetic regulatory network that underlies mesoderm formation (see below). The latter category includes cell junction proteins and glycosyltransferases [31], consistent with the finding that the extracellular matrix of homozygous mutant *Brachyury* mouse embryos is poorly developed [32] and that cells have fewer

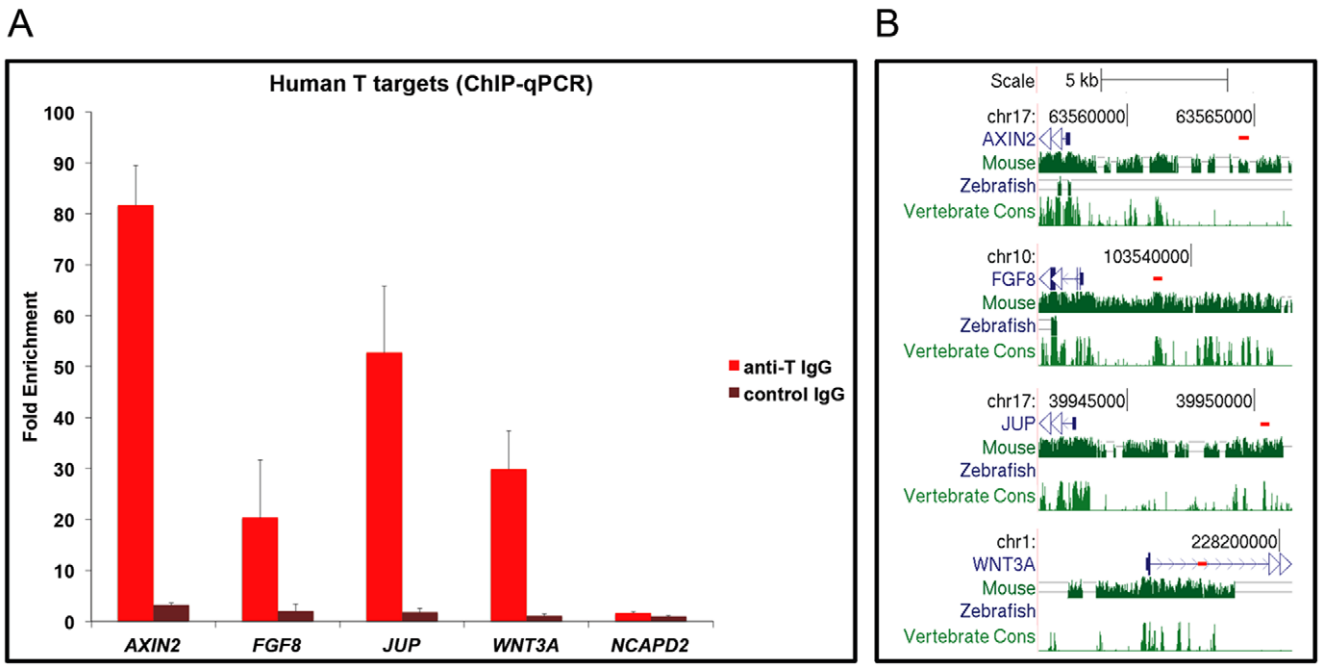

Figure 7. Conservation of BRACHYURY binding in the human genome. (A) ChIP-qPCR performed on samples from differentiated hECSs using a specific anti-BRACHYURY IgG and a non-specific control IgG. Graph shows enrichment for regulatory regions of Brachyury targets (*AXIN2*, *FGF8*, *JUP*, *WNT3A*) and a negative control region (*NCAPD2*). Results are expressed relative to input chromatin divided by the enrichment for the non-specific control antibody. (B) BRACHYURY binding in the human genome. The short red lines below the chromosomal coordinates (hg19) depict the position of the PCR amplicons relative to the beginning of the human genes (blue). The three bottom tracks show the genome sequence conservation between human and mouse, zebrafish and vertebrate genomes (Genome Browser, http://genome.ucsc.edu/).
doi:10.1371/journal.pone.0033346.g007

cytoplasmic processes, both of which may contribute to the failure of mutant cells to move out of the primitive streak and to the failure of elongation of the antero-posterior axis [30]. Amongst the other genes regulated by Brachyury are those encoding cytokines and components of signal transduction pathways, and in most of these respects our results are reminiscent of those obtained in similar experiments using the zebrafish embryo [16].

It is significant that embryoid bodies resemble developing embryos in this way, and it is also important to note the overlap between the Brachyury targets identified in this study and the Ntl targets identified in the zebrafish [16]. Both studies identified transcriptional regulators as being enriched, including members of the homeobox, winged helix, paired box, zinc finger and odd-paired families. There are also similarities in the functions of genes regulated by the two orthologues. These functions include gastrulation (where the zebrafish study identified *wnt11, snail1a* and *blf* and this analysis *Wnt3a*, *Snail2* and genes such as *Gdf5*, *Etv1*, *Krt5*, *Krt8*, *Lmx1b*, *Syk*, and *Gnaq*); muscle specification (where both studies identified *Msgn1* and *Pax3*); posterior identity (where the zebrafish study identified *fgfr4, fgfr2β, vent, vox*, and *notch3* and this analysis *Fgf8* [50]) and left-right patterning (zebrafish genes include *cx43.4* [51] and our mouse targets *Rttn* [52], *Fgf8* [53], and cytoplasmic dyneins *Dync1li1*, *Dync2li1* [54] and *Dpcd* [55]).

The fact that there are some differences between the mouse and zebrafish targets may derive from the presence of an additional *Brachyury* gene in the zebrafish genome [8] or from the 'sharing' of gene function between different T box family members. For example, the *Bix* genes were identified as targets of Brachyury and VegT in *Xenopus* [13,14], but their mouse ortholog *Mixl1* seems to be regulated mainly by Eomesodermin [56,57]. Furthermore, as illustrated in Fig. 7B, some regulatory sequences of mammalian genes (*Axin2*, *Fgf8*, *Jup* and *Wnt3a*) share little homology with those of their zebrafish orthologues. It is possible that Brachyury binds different locations in different genomes, which has been noted for other transcription factors [58], despite target conservation. It is also likely that Brachyury binds not only to promoters near the gene transcription start site but also to distant enhancers [59], which is indeed the case in the human genome (T. Faial *et al.*, in preparation). We note that both the mouse and zebrafish arrays were based on promoter regions, so that enhancer binding is not available in these datasets, perhaps explaining why some targets seem to be unique to each species.

Canonical and non-canonical T-box binding sites

Our previous work searching for targets of zebrafish Ntl showed that the canonical T-box site TCACACCT was enriched in the vicinity of Ntl target genes [16]. A significant enrichment of this motif was not observed in the present experiments for the majority of targets. Rather, we identified a novel $(AC)_n$ repeat sequence that recognised, albeit weakly, the Brachyury T domain in electrophoretic mobility shift experiments. We do not yet fully understand the significance of this observation. Mouse Brachyury binds to an imperfect T-box site palindrome in the *Nanog* promoter [60], but no other Brachyury target has been characterised in any detail in this species. It is possible that mouse Brachyury resembles *Drosophila* Brachyenteron, where modular variations on the T-box consensus binding sequence determine the degree of transcriptional activation [61]. A similar system controls notochord formation in *Ciona*, with regulatory motifs comprising Ci-Brachyury and Ci-foxA binding sites [62].

Moreover, many transcription factors bind directly to DNA in distal enhancer elements [59], and are then linked to the promoter region by chromatin looping, allowing interaction with other proteins involved in transcription regulation [59]. It is likely that in some mouse targets, canonical Brachyury binding motifs are not present in the promoter region but rather in upstream or downstream regulatory regions. Our results show that this does occur in the human genome (T. Faial *et al.*, in preparation).

It is also possible that the AC repeats cause the transient formation of left handed DNA helices and bends, changing the chromatin architecture and encouraging transcription factor binding [63]. Brachyury may be an example of a protein with a secondary recognition motif [64] and that the presence of both an AC repeat and a TCACACCT sequence allows stable binding that cannot be competed by an excess of just the TCACACCT sequence (Fig. S3B). Repetitive sequences may also function as pre-sites; that is, as regions of DNA that are predisposed to evolve into new regulatory sequences [65].

Brachyury modulation of Wnt and Fgf signalling

Several components of the Wnt signal transduction pathway were identified as Ntl targets in the zebrafish, and we find that the same is true for Brachyury in the mouse. In an effort to determine whether Brachyury regulates expression of these potential targets during normal mouse development we asked whether *Wnt3a* and *Axin2* are expressed normally in *Brachyury* homozygous mutant embryos, and found that although both genes are expressed at E7.5 (albeit rather variably in the case of *Axin2*), neither is expressed at E8.5 in mesodermal derivatives (Figs. 4, 5). This suggests that Brachyury is not required for the initial activation of *Wnt3a* or *Axin2*, but is needed for maintenance of their expression. Together with the observation that Wnt3a maintains *Brachyury* expression in the early mouse embryo via TCF/Lef signalling [20,21], and that *Axin2* is down regulated in *Wnt3a* mutants [66], our data indicate that Brachyury and Wnt signalling cooperate to create a regulatory network that specifies the formation of posterior mesoderm in the mouse embryo.

Part of this network may involve Fgf signalling. Brachyury and Fgf signalling form part of an autoregulatory loop in *Xenopus* and zebrafish embryos [67,68,69,70], and we note that *Fgf8* is a target of Brachyury in embryoid bodies, and that its expression is down regulated in *Brachyury* mutant embryos (Fig. 6).

Finally, our work reveals that the promoter regions of *AXIN2*, *FGF8* and *WNT3A* are also bound by BRACHYURY (Fig. 7A) in human ES cells as they differentiate into mesoderm-like cells [41]. These results further substantiate the identity of these genes as *bona fide* Brachyury targets and suggest that the regulation of these key signalling components is conserved during human development.

Making a genetic regulatory network for mesoderm

Attempts to understand the Brachyury genetic regulatory network are important not only because Brachyury is required for proper formation of mesoderm in the vertebrate embryo, but because it is sufficient for the formation of some mesodermal cell types, at least in *Xenopus* [71]. The identification of new Brachyury targets will enable the integration of Brachyury with other components of genetic regulatory networks that include it, such as the Ets family member Elk-1 and the caudal homologue, Cdx2 [72] and to ask to what extent such networks have been conserved during evolution.

Materials and Methods

Ethics statement

Animal procedures were performed under a UK Home Office project license within the conditions of the Animals (Scientific Procedures) Act 1986.

Mouse ESC culture

Embryonic stem (ES) cell culture was as described [73] except that mitotically inactivated primary mouse embryonic fibroblasts (MEFs) were used as feeders. Culture dishes were coated with 0.1% gelatin (Sigma-Aldrich). MEFs and ES cells were maintained in DMEM (Sigma-Aldrich) supplemented with 0.1 mM β-mercaptoethanol, non-essential amino acids (Gibco Invitrogen), 2 mM glutamate (Gibco Invitrogen), and batch-tested 10% (MEFs) or 15% (ES cells) foetal bovine serum (FBS) (Gibco Invitrogen). ES cell medium was also supplemented with Leukaemia Inhibitory Factor (LIF) (ESGRO®, Millipore) at 10^3 units/ml [74]. Early passage R1 mouse ES cells [75] were passaged every 2 days and medium was changed daily to prevent differentiation.

ES cells were differentiated in spinner flasks to produce large numbers of embryoid bodies (EBs) undergoing synchronized differentiation [76,77]. The Cellspin culture system (Integra Biosciences) was set at 25 rpm and spin angle 720° so as to avoid aggregation of EBs. Spinner medium was prepared as above, but with LIF omitted and FBS increased to 20%. On day 0, adherent log phase ES cell colonies were dissociated and resuspended in 10 ml spinner medium. Feeder cells were depleted by differential sedimentation at 37°C for 20 min.

Medium (45 ml) was pre-equilibrated in 100 ml silicon-coated (Sigmacote, Sigma-Aldrich) spinner flasks (Integra Biosciences). ES cells were recovered from the gelatin-coated differential sedimentation plates and centrifuged at 800 g for 5 min. Cells were fully dissociated to ensure that cultures were initiated from single cells, and each spinner flask was inoculated with 10^7 cells in 5 ml medium. After 24 h (day 1 of differentiation) a further 50 ml spinner medium was added to each flask. Each day thereafter EBs were allowed to sink and 50 ml medium was aspirated and replaced with 50 ml fresh pre-warmed spinner medium.

Human ESC culture

Human ESCs (H9 [WiCell, Madison, WI]) were maintained and differentiated as previously described [41]. Briefly, hESCs were induced to express BRACHYURY by culturing them in a chemically defined medium (CDM) supplemented with FGF2 (20 ng/ml), LY294002 (10 μM) and BMP4 (10 ng/ml) (termed FLyB medium). Cells were collected for ChIP after 36 h of culture in FLyB medium, when BRACHYURY expression peaked.

Quantitative RT-PCR

Gene expression was analysed by real-time RT-PCR. RNA was isolated from differentiated EBs using Tri-Reagent LS (Sigma-Aldrich), digested with DNA-free DNAse I (Ambion), and checked for integrity using an Agilent Technologies 2100 Bioanalyser. cDNA was generated from l μg RNA using Superscript III Reverse Transcriptase (Invitrogen, Life Technologies), and this was followed by real-time PCR using the LightCycler 480 SYBR Green I master kit (Roche). Mouse *beta actin* primers were used as an endogenous control to express relative expression levels (Table S6).

Antibodies

Several anti-Brachyury antibodies were tested for use in this work. Of these, the goat polyclonal C19 antibody (SC-17745, Santa Cruz Biotechnology), raised against a C-terminal sequence of human Brachyury, performed best in chromatin immunoprecipitation. This antibody, raised against a divergent region of Brachyury that does not include the T box, has been well characterised in previous studies [78,79,80]. It gave the expected pattern of staining in early mouse embryos (Fig. S6A,B) and recognised Brachyury protein (of the correct size) in immunoprecipitation experiments followed by western blots (Fig. S6C). Such experiments failed to detect Brachyury in ES cells in which Brachyury expression was inhibited by use of ShRNA constructs (Fig. S6D,E).

Whole-mount *in situ* hybridization

Wild type mouse embryos were collected from MF1 or 129 strains, and *Brachyury* mutant embryos from BTBR T^+tT/J×BTBR T^+tT/J heterozygote crosses [39]. Embryos were fixed overnight in 4% paraformaldehyde in phosphate-buffered saline (PBS), after which they were dehydrated and stored in 100% methanol at −20°C. The mouse Brachyury coding sequence was subcloned into pCS2+ and used to generate a probe. An *Axin2* probe was generated from IMAGE clone 1361800 (Geneservice), a *Wnt3a* probe from IMAGE clone pENTR223.1 100015989 after subcloning into pCS2+ (Table S7), and an *Fgf8* probe from IMAGE clone 6513131 (Geneservice) in pCMV-SPORT 6.1. Digoxigenin labelled or fluorescein labelled antisense RNA probes were generated using T7 RNA polymerase from linearised templates and whole mount in situ hybridisation was performed as described [81]. Alkaline phosphatase was detected using (i) BM purple; (ii) 2-[4-iodophenyl]-3-[4-nitrophenyl]-5- phenyltetrazolium chloride (250 μg/ml) plus magenta phosphate (250 μg/ml) (INT/Mag); or (iii) nitro blue tetrazolium (175 μg/ml) plus 5-bromo-4-chloro-3-indolyl phosphate (337.5 μg/ml) (NBT/BCIP) (Roche). These gave dark blue, orange brown or purple staining respectively. A final concentration of 5% polyvinyl alcohol (Sigma-Aldrich) was used in the staining reaction.

Whole-mount immunohistochemistry

Embryos were fixed as described above and rehydrated to PBS for staining. Free aldehyde groups were blocked using 1 M glycine, embryos were washed in PBS/0.1% Tween 20 (PBST), and endogenous peroxidases were blocked using 3% hydrogen peroxide in PBS. Embryos were incubated overnight at 4°C in 1:400 C19 antibody in PBST supplemented with 0.2% bovine serum albumin (BSA) and 10% heat inactivated FBS. They were then washed, incubated with 1:400 rabbit anti-goat biotinylated IgG (E0466, Dako), and stained using Vectastain Elite ABC substrate (Vector laboratories) with Sigma Fast Nickel Enhanced DAB chromagen (Sigma).

In vitro translation and western blotting

Brachyury mRNA was synthesized using the pCS2+ construct described above and the Ambion mMessage mMachine (Applied Biosystems/Ambion). mRNA was translated in a rabbit reticulocyte lysate (Promega). In vitro translation products and embryoid body extracts were subjected to polyacrylamide gel electrophoresis (PAGE) and western blots were performed using CAPS transfer buffer (10 mM CAPS pH 11, 10% Methanol). Membranes were blocked with 5% milk powder in PBST overnight, and antibodies were diluted in the same solution. Washes were in PBST. Primary antibodies were R&D Systems anti-T and SantaCruz anti-T (see above). Both were used at a dilution of 1:250. Secondary antibodies were HRP-linked SantaCruz D anti-goat IgG (1:20,000) and HRP-linked Amersham NA934V anti-rabbit IgG (1:100,000). All antibody incubations were 1 hour at room temperature. Both endogenous and *in vitro* translated T proteins were immunoprecipitated for western blotting using the Santacruz Exactacruz D anti-goat system (SC-45041, Santa Cruz) to avoid detection of heavy and light chains of the IP antibody. Detection used the Pierce Supersignal West Dura Extended Duration Substrate (Thermo Scientific).

Chromatin immunoprecipitation (mouse ESCs)

Chromatin immunoprecipitation/location analysis was based on the Agilent Mammalian ChIP-chip Protocol, incorporating the Whole Genome Amplification GenomePlex Kit (Sigma) [82]. Intact EBs (1.5×10^9 cells) were fixed in 1 M formaldehyde for 20 min when *Brachyury* expression was at its highest level (usually after 4 days of differentiation). This was followed by quenching and isolation of nuclei. Our protocol differs from a previously-published procedure [83] in that EBs are not disrupted before fixation. Nuclei were sonicated using a Misonix 3000 ultrasonicator to create fragments of 500 bp, and these were immunoprecipitated using polyclonal goat anti-Brachyury C-19 (Santa Cruz Biotechnology) or normal goat IgG (Santa Cruz Biotechnology) as an isotype control. Following washing and elution steps, cross-links were reversed overnight at 65°C. Samples were analysed by promoter-specific primers or amplified by GenomePlex whole genome amplification for microarray studies.

Chromatin immunoprecipitation (human ESCs)

ChIP was performed as previously described [83] with some modifications. Briefly, H9 hESCs (one confluent 10 cm dish) were collected after 36 hr of culture in FLyB medium [41], when BRACHYURY expression peaked. Cells were fixed as described [83], the nuclei were isolated and sonicated using a Misonix 4000 to obtain DNA fragments of around 1000 bp. Samples were incubated at 4°C overnight using 10 µg of an anti-BRACHYURY goat IgG (R&D systems) and with10 µg of a non-specific goat IgG as a control. The chromatin was immunoprecipitated by adding 100 µl of Protein G Dynabeads (Invitrogen), then incubating at 4°C 1 h, and collecting the beads using a magnetic rack. After washing the beads, the chromatin was eluted and the crosslinking was reversed at 65°C overnight. Samples were then treated with RNAse and Proteinase K and the DNA was extracted by phenol/chloroform, ethanol-precipitated and finally eluted in nuclease-free water. This experiment was repeated three times with similar results.

Verification of target enrichment was performed on a selection of targets using genomic quantitative PCR. DNA fragments were amplified using Fast SYBR® Green Master Mix (Applied Biosystems) according to manufacturers instructions on a 7500 Fast Real-Time PCR System (Applied Biosystems). Promoter specific primers (Table S8) were designed to amplify the homologous regions of mouse T-binding sites (AXIN2, FGF8, JUP and WNT3A). *NCAPD2* was used as a negative control gene.

Microarray hybridization, analysis and verification of binding targets

Agilent Technologies mouse promoter 244K (G4490A) 60-mer oligonucleotide arrays (''chips'') covering 17,000 mouse genes and extending 5.5 kb upstream and 2.5 kb downstream of transcriptional start sites were hybridized with 5 µg amplified chromatin per sample. Arrays were annotated to NBI35.1 of the mouse genome. Immunoprecipitated (or isotype control) and total input samples were labelled with Cy5 or Cy3 respectively. Hybridizations were performed and analysed in triplicate using independently differentiated cultures. The isotype control experiment was performed once to confirm no significant enrichment over input chromatin (data not shown).

Microarrays were scanned using an Agilent scanner to a resolution of 5 µm. Data were extracted using Agilent G2567AA Feature Extraction Software (v.9.1). The significance of binding events was determined using Agilent Chip Analytics 1.3 software. Initial analysis was done using Chip Analytics defaults settings and then further filtered using the parameters $P(x) < 0.01$ and $P(\overline{x}) < 0.005$. The confidence of binding calls is represented as a P-value: $P(x)$ defines the value for each probe, and $P(\overline{x})$ uses the intensities of neighbouring probes to assess peak shape, in an effort to eliminate false positives. Original raw data files can be accessed from GEO Gene Expression Omnibus http://www.ncbi.nlm.nih.gov/geo (accession GSM417692/GSM417704 for design 1 and 2 Brachyury data; GSM417714/GSM417756 for design 1 and 2 isotype control data).

Verification of enrichment was performed on a selection of targets using promoter specific genomic quantitative PCR. Promoter specific primers (Table S8) were designed so as to span bound peaks using mouse build mm8 promoter sequence retrieved from the UCSC genome browser (http://genome.ucsc.edu/). Negative control genes from the list not called as bound were included. Results were expressed relative to input chromatin divided by relative enrichment for the isotype control antibody.

Bioinformatic analyses and Motif Finding

The GOToolBox (http://burgundy.cmmt.ubc.ca/GOToolBox/) [84] was used to access Gene Ontology (GO) resources and to search for any functional bias in our dataset. The Benjamini and Hochberg multiple testing correction was applied to assess the significance of enrichment ratios. Target probes and surrounding promoter sequences were scanned for the published consensus *in vitro* T-box binding motif TCACACCT [17,18] using NestedMICA http://www.sanger.ac.uk/Software/analysis/nmica/index.shtml [85]. We also used Regulatory Sequence Analysis Tools (RSAT) http://rsat.ulb.ac.be/rsat/ [86], to scan each target gene over a region −5 kb to +1 kb relative to its ATG for over-represented cis-regulatory modules, applying background models and taking promoter sequences from 400 random mouse promoters as the control set. Sequences representing enriched motifs were then stacked into positional weight matrices and converted to sequence logos using WebLogo (http://weblogo.berkeley.edu/logo.cgi) [87].

Electrophoretic mobility shift assays

The T domain of mouse *Brachyury* was amplified by PCR (primer sequences in Table S7) and inserted in-frame into the glutathione-S-transferase (GST) fusion vector pGEX-6P-1. The fusion protein was expressed in *E. coli* by isopropyl-β-D-thiogalactoside induction and purified at 4°C using GSTrap FF columns and Pre-Scission Protease (GE Healthcare), leaving only a glycine and a proline residue attached to the protein. This was concentrated using Amicon Ultra 4 columns (Millipore), and the identity of the resulting protein was confirmed by SDS PAGE and mass spectrometry.

Double stranded oligomers containing (i) the core Brachyury consensus binding sequence TCACACCT, (ii) a simple AC repeat, or (iii) the core Brachyury sequence together with the AC repeat, and mutated versions of each, had identical BglII/BamH1 5′ overhangs (Table S7). These were PAGE purified, annealed, and end-labelled with [α-^{32}P] dCTP using Klenow fragment. Unincorporated nucleotides were removed using Sephadex G-50 columns (GE Healthcare). Binding reactions were incubated on ice for 40 minutes in 1× EMSA binding buffer (25 mM HEPES pH8.0, 100 mM KCl, 1 mM DTT, 0.1% NP-40, 5% glycerol, 10 mM EDTA), 0.5% milk powder and 50 ng/µl dI/dC using 30,000 cpm/µl and 8–10 fmol labelled oligomer. Competition reactions using 4 pmol cold oligomers were pre-incubated for 10 min on ice. In supershift experiments goat polyclonal anti-Brachyury N19 antibody (SC-17743, Santa Cruz) was added after binding and then incubated a further 20 min on ice.

Supporting Information

Figure S1 Validation of targets. Box plot showing genomic quantitative PCR of bound promoter regions for targets *Axin2*, *Foxe1*, *Mapre2*, *Nkx2.6*, *Pax3*, *Rttn*, *Van Gogh* and the published target *Nanog*, and unbound or negative promoter regions *Nanog 3′*, *1700010C24Rik* and *beta actin*. Boxes represent the interquartile range, the upper edge being the 75th percentile and lower edge the 25th percentile. The whiskers show the minimum and maximum values. Values above the line are enriched in chromatin immunoprecipitations. Data were obtained from five independent chromatin immunoprecipitations. Probes recognising *Nanog* were not present on Agilent 244K promoter arrays.
(TIF)

Figure S2 Functional analysis of target genes. Bar charts show Gene Ontology (GO) annotations for (A) biological process; (B) cellular component; and (C) molecular function using the GOToolBox. Horizontal bars represent enrichment ratio (observed frequency/expected frequency) and vertical axis gives the GO term followed by the GO identification number in brackets and hierarchy level. Colour bars indicate statistical significance. GO terms related to the function of Brachyury are highlighted in red boxes.
(TIF)

Figure S3 Interaction of the mouse Brachyury T domain with DNA. (A) Sequences surrounding bound probes are enriched for an $(AC)_n$ repeat relative to their genomic neighbours. The motif was generated using the NestedMICA position weight matrix. This may represent a secondary Brachyury recognition motif. (B) Electrophoretic mobility shift assays. Panel a: Binding reactions using ^{32}P-labelled TCACACCT. Lane 1, no protein; lane 2, control protein derived from empty vector; lanes 3–6, mouse T domain protein: lane 4 includes excess unlabelled probe; lane 5 includes excess unlabelled mutated probe; lane 6 is a 'supershift' using anti-T N-19 (SC-17743, Santa Cruz). Notice that the Brachyury T domain binds the T site oligonucleotide and that binding is competed by cold wild-type oligonucleotide but not by a mutated oligonucleotide. Panel b: Lanes 7–9 include ^{32}P-labelled TCACACCT; lane 10 uses the indicated mutated version of this oligonucleotide. Note that the Brachyury T domain does not bind the mutated oligonucleotide. Panel c: Binding reaction using a ^{32}P-labelled AC repeat oligonucleotide. Lanes 11–13 as panel a; lane 14 includes excess unlabelled probe; lane 15 includes excess of an unlabelled mutated probe; lane 16 is a 'supershift'. Notice that the Brachyury T domain binds the AC repeat oligonucleotide weakly but that binding does not seem to be competed by cold wild-type oligonucleotide. The complex however is 'supershifted' using the Brachyury antibody. Panel d: Binding reactions using a ^{32}P labelled motif that includes both the T site TCACACCT and an AC repeat. Lanes 17–20 show that Brachyury binds this oligonucleotide, and that binding is competed by cold wild-type oligonucleotide. Lanes 21 and 22 show that binding is not competed significantly by unlabelled oligonucleotides in which either motif is mutated. Lane 23 shows a 'supershift'. Experiments in (a–d) were performed under identical conditions and exposed for the same times.
(TIF)

Figure S4 The expression domains of *Brachyury*, *Wnt3a* and *Axin2* overlap in E7.75 mouse embryos. (A) Expression of *Axin2* analysed using a fluorescein labelled antisense probe detected with NBT/BCIP (purple). (B) The embryo in (A) analysed using a digoxigenin labelled antisense *Brachyury* probe detected with INT/Mg phosphate (brown). (C) Expression of *Wnt3a* analysed using a fluorescein labelled antisense probe detected with NBT/BCIP (purple). (D) The embryo in (C) analysed using a digoxigenin labelled antisense *Brachyury* probe detected with INT/Mg phosphate (brown). All embryos orientated as in (A). Scale bars are 200 μm.
(TIF)

Figure S5 The expression domains of *Brachyury* and Fgf8 overlap in the primitive streak of E7.75 mouse embryos. (A). Expression of *Fgf8* analysed using a fluorescein labelled antisense probe detected with NBT/BCIP (purple). (B). The embryo in (A) analysed using a digoxigenin labelled antisense *Brachyury* probe detected with INT/Mg phosphate (brown). Black bars are 200 μm.
(TIF)

Figure S6 Verification of anti Brachyury antibody. (A) Immunohistochemistry of E9.5 embryo using Santa Cruz anti-human T C19 with nickel enhanced DAB substrate. Staining is present in the notochord (arrowhead), pre-somitic mesoderm (arrow) and tailbud. Staining was absent in controls in which primary or secondary antibodies were omitted. (B) Expression of *Brachyury* RNA in an E9.5 embryo studied by in situ hybridisation. Note similarity to (A). Bars in (A) and (B) represent 250 μm. (C) Western blot testing antibody specificity. Size markers are shown to the left. Lane 1: Mouse Brachyury reticulocyte lysate translation product; lane 2: unprogrammed reticulocyte lysate translation product; lane 3: Immunoprecipitated material derived from Brachyury reticulocyte lysate translation product; lane 4: Supernatant of immunoprecipitated material in lane 3; lane 5: Immunoprecipitated material derived from day 4 embryoid bodies; lane 6: Supernatant of immunoprecipitated material in lane 5; lane 7: Immunoprecipitated material derived from day 4 embryoid bodies, having omitted first antibody; lane 8: Supernatant of immunoprecipitated material in lane 7. All immunoprecipitations used Santa Cruz anti-T C19. Western blots used R&D Systems anti-T as a primary antibody and SantaCruz D anti-goat IgG HRP linked secondary antibody. (D) Strategy to create ES cell clones lacking Brachyury. Clones were created using 65 bp ShRNA duplexes targeting the first exon of *Brachyury* (*T*). Sequences were inserted into the XhoI/HindIII site of the pSingle ShRNA vector (Clontech) which includes a tetracyclin-controlled transcriptional repressor that in turn regulates the expression of the ShRNA sequence. Selection of stable lines is achieved by culture in G418 and induction of ShRNA expression occurs through addition of 1 μg/ml doxycycline. (E) Western blot analysis of day 5 embryoid body extracts from clones containing ShRNA constructs targeted to *Brachyury* exon 1 (T1) or a scrambled version of this sequence (Ts), either treated with doxycycline (+) or left untreated (−). Samples were immunoprecipitated as in (C). Note loss of Brachyury band in lane 3.
(TIF)

Table S1 Full gene list.
(DOC)

Table S2 Targets involved in key signalling pathways.
(DOC)

Table S3 Genes associated with germ cell development.
(DOC)

Table S4 Targets identified as transcription factors.
(DOC)

Table S5 Conservation of AC repeats.
(DOC)

Table S6 Quantitative PCR primers.
(DOC)

Table S7 In situ hybridisation, T box, and electrophoretic mobility shift assay primers.
(DOC)

Table S8 Genomic quantitative PCR primers.
(DOC)

Acknowledgments

We thank Valerie Wilson (Centre for Regenerative Medicine, Edinburgh) for the mouse T plasmid. We are grateful to our colleagues for helpful discussions throughout the course of this work, and especially James Smith and Rick Livesey (Gurdon Institute) for their advice concerning ChIP-chip experiments.

Author Contributions

Conceived and designed the experiments: ALE TF RAP LV FCW JCS. Performed the experiments: ALE TF. Analyzed the data: ALE TF FCW MJG TD JCS. Contributed reagents/materials/analysis tools: LV RAP. Wrote the paper: ALE TF RAP FCW JCS.

References

1. Herrmann BG, Labeit S, Poustka A, King TR, Lehrach H (1990) Cloning of the T gene required in mesoderm formation in the mouse. Nature 343: 617–622.
2. Wilkinson DG, Bhatt S, Herrmann BG (1990) Expression pattern of the mouse T gene and its role in mesoderm formation. Nature 343: 657–659.
3. Dobrovolskaïa-Zavadskaïa N (1927) Sur la mortification spontanee de la queue chez la souris nouveau-nee et sur l'existence d'un caractere (facteur) hereditaire. C R Seances Soc Biol Fil 97: 114–116.
4. Naiche LA, Harrelson Z, Kelly RG, Papaioannou VE (2005) T-box genes in vertebrate development. Annu Rev Genet 39: 219–239.
5. Yanagisawa KO, Fujimoto H, Urushihara H (1981) Effects of the Brachyury (T) mutation on morphogenetic movement in the mouse embryo. Developmental Biology 87: 242.
6. Smith JC, Price BM, Green JB, Weigel D, Herrmann BG (1991) Expression of a Xenopus homolog of Brachyury (T) is an immediate-early response to mesoderm induction. Cell 67: 79–87.
7. Schulte-Merker S, Ho RK, Herrmann BG, Nusslein-Volhard C (1992) The protein product of the zebrafish homologue of the mouse T gene is expressed in nuclei of the germ ring and the notochord of the early embryo. Development 116: 1021–1032.
8. Martin BL, Kimelman D (2008) Regulation of Canonical Wnt Signaling by Brachyury Is Essential for Posterior Mesoderm Formation Developmental. Cell 15: 121–133.
9. Herrmann BG, Kispert A (1994) The T genes in embryogenesis. Trends in Genetics 10: 280–286.
10. Conlon FL, Sedgwick SG, Weston KM, Smith JC (1996) Inhibition of Xbra transcription activation causes defects in mesodermal patterning and reveals autoregulation of Xbra in dorsal mesoderm. Development 122: 2427–2435.
11. Schulte-Merker S, van Eeden FJ, Halpern ME, Kimmel CB, Nusslein-Volhard C (1994) no tail (ntl) is the zebrafish homologue of the mouse T (Brachyury) gene. Development 120: 1009–1015.
12. Casey ES, O'Reilly MA, Conlon FL, Smith JC (1998) The T-box transcription factor Brachyury regulates expression of eFGF through binding to a non-palindromic response element. Development 125: 3887–3894.
13. Casey ES, Tada M, Fairclough L, Wylie CC, Heasman J, et al. (1999) Bix4 is activated directly by VegT and mediates endoderm formation in Xenopus development. Development 126: 4193–4200.
14. Tada M, Casey ES, Fairclough L, Smith JC (1998) Bix1, a direct target of Xenopus T-box genes, causes formation of ventral mesoderm and endoderm. Development 125: 3997–4006.
15. Tada M, Smith JC (2000) Xwnt11 is a target of Xenopus Brachyury: regulation of gastrulation movements via Dishevelled, but not through the canonical Wnt pathway. Development 127: 2227–2238.
16. Morley RH, Lachani K, Keefe D, Gilchrist MJ, Flicek P, et al. (2009) A gene regulatory network directed by zebrafish No tail accounts for its roles in mesoderm formation. Proceedings of the National Academy of Sciences 106: 3829–3834.
17. Kispert A, Hermann BG (1993) The Brachyury gene encodes a novel DNA binding protein. Embo J 12: 3211–3220.
18. Kispert A (1995) The Brachyury protein: A T-domain transcription factor. Seminars in Developmental Biology 6: 395–403.
19. Leung JY, Kolligs FT, Wu R, Zhai Y, Kuick R, et al. (2002) Activation of AXIN2 expression by beta-catenin-T cell factor. A feedback repressor pathway regulating Wnt signaling. J Biol Chem 277: 21657–21665.
20. Yamaguchi TP, Takada S, Yoshikawa Y, Wu N, McMahon AP (1999) T (Brachyury) is a direct target of Wnt3a during paraxial mesoderm specification. Genes Dev 13: 3185–3190.
21. Galceran J, Hsu S, Grosschedl R (2001) Rescue of a Wnt mutation by an activated form of LEF-1: Regulation of maintenance but not initiation of Brachyury expression. Proceedings of the National Academy of Sciences. 151258098 p.
22. Aulehla A, Wehrle C, Brand-Saberi B, Kemler R, Gossler A, et al. (2003) Wnt3a plays a major role in the segmentation clock controlling somitogenesis. Dev Cell 4: 395–406.
23. Valamehr B, Jonas SJ, Polleux J, Qiao R, Guo S, et al. (2008) Hydrophobic surfaces for enhanced differentiation of embryonic stem cell-derived embryoid bodies. Proc Natl Acad Sci U S A 105: 14459–14464.
24. Wittler L, Shin EH, Grote P, Kispert A, Beckers A, et al. (2007) Expression of Msgn1 in the presomitic mesoderm is controlled by synergism of WNT signalling and Tbx6. EMBO Rep 8: 784–789.
25. Tamplin O, Kinzel D, Cox B, Bell C, Rossant J, et al. (2008) Microarray analysis of Foxa2 mutant mouse embryos reveals novel gene expression and inductive roles for the gastrula organizer and its derivatives. BMC Genomics 9: 511.
26. Sousa-Nunes R, Rana AA, Kettleborough R, Brickman JM, Clements M, et al. (2003) Characterizing embryonic gene expression patterns in the mouse using nonredundant sequence-based selection. Genome Res 13: 2609–2620.
27. Elms P, Scurry A, Davies J, Willoughby C, Hacker T (2004) Overlapping and distinct expression domains of Zic2 and Zic3 during mouse gastrulation. Gene Expression Patterns.
28. Weinstein DC, Ruiz i Altaba A, Chen WS, Hoodless P, Prezioso VR, et al. (1994) The winged-helix transcription factor HNF-3 beta is required for notochord development in the mouse embryo. Cell 78: 575–588.
29. Kurisaki T, Masuda A, Osumi N, Nabeshima Y, Fujisawa-Sehara A (1998) Spatially- and temporally-restricted expression of meltrin alpha (ADAM12) and beta (ADAM19) in mouse embryo. Mech Dev 73: 211–215.
30. Wilson V, Manson L, Skarnes WC, Beddington RS (1995) The T gene is necessary for normal mesodermal morphogenetic cell movements during gastrulation. Development 121: 877–886.
31. Shur BD (1982) Cell surface glycosyltransferase activities during normal and mutant (T/T) mesenchyme migration. Dev Biol 91: 149–162.
32. Jacobs-Cohen RJ, Spiegelman M, Bennett D (1984) Abnormalities of cells and extracellular matrix of T/T embryos. Differentiation 25: 48–55.
33. Popsueva AE, Luchinskaya NN, Ludwig AV, Zinovjeva OY, Poteryaev DA, et al. (2001) Overexpression of camello, a member of a novel protein family, reduces blastomere adhesion and inhibits gastrulation in Xenopus laevis. Dev Biol 234: 483–496.
34. Lin D, Watahiki A, Bayani J, Zhang F, Liu L, et al. (2008) ASAP1, a Gene at 8q24, Is Associated with Prostate Cancer Metastasis. Cancer Res 68: 4352–4359.
35. Armstrong J, Pritchard-Jones K, Bickmore W, Hastie N, Bard J (1992) The Expression of the Wilms' tumour gene, Wt1, in the developing mammalian embryo. Mechanisms of Development 40: 85–97.
36. Garnett AT, Han TM, Gilchrist MJ, Smith JC, Eisen MB, et al. (2009) Identification of direct T-box target genes in the developing zebrafish mesoderm. Development 136: 749–760.
37. Conlon FL, Fairclough L, Price BMJ, Casey ES, Smith JC (2001) Determinants of T box protein specificity. Development 128: 3749–3758.
38. Kispert A, Koschorz B, Herrmann BG (1995) The T protein encoded by Brachyury is a tissue-specific transcription factor. Embo J 14: 4763–4772.
39. King T, Beddington RS, Brown NA (1998) The role of the brachyury gene in heart development and left-right specification in the mouse. Mech Dev 79: 29–37.
40. Rashbass P, Wilson V, Rosen B, Beddington RS (1994) Alterations in gene expression during mesoderm formation and axial patterning in Brachyury (T) embryos. Int J Dev Biol 38: 35–44.
41. Bernardo AS, Faial T, Gardner L, Niakan KK, Ortmann D, et al. (2011) BRACHYURY and CDX2 mediate BMP-induced differentiation of human and mouse pluripotent stem cells into embryonic and extraembryonic lineages. Cell stem cell 9: 144–155.
42. White SM, Claycomb WC (2005) Embryonic stem cells form an organized, functional cardiac conduction system in vitro. Am J Physiol Heart Circ Physiol 288: H670–679.
43. Anderson R, Copeland TK, Scholer H, Heasman J, Wylie C (2000) The onset of germ cell migration in the mouse embryo. Mech Dev 91: 61–68.
44. Ginsburg M, Snow MH, McLaren A (1990) Primordial germ cells in the mouse embryo during gastrulation. Development 110: 521–528.
45. Lawson KA, Hage WJ (1994) Clonal Analysis of the Origin of Primordial Germ Cells in the Mouse. In: Joan Marsh JG, ed. Ciba Foundation Symposium 182 - Germline Development. pp 68–91.

46. Clements D, Taylor HC, Herrmann BG, Stott D (1996) Distinct regulatory control of the Brachyury gene in axial and non-axial mesoderm suggests separation of mesoderm lineages early in mouse gastrulation. Mechanisms of Development 56: 139–149.
47. Saitou M, Barton SC, Surani MA (2002) A molecular programme for the specification of germ cell fate in mice. Nature 418: 293–300.
48. Lawson KA, Dunn NR, Roelen BA, Zeinstra LM, Davis AM, et al. (1999) Bmp4 is required for the generation of primordial germ cells in the mouse embryo. Genes Dev 13: 424–436.
49. Ohinata Y, Ohta H, Shigeta M, Yamanaka K, Wakayama T, et al. (2009) A signaling principle for the specification of the germ cell lineage in mice. Cell 137: 571–584.
50. Crossley PH, Martin GR (1995) The mouse Fgf8 gene encodes a family of polypeptides and is expressed in regions that direct outgrowth and patterning in the developing embryo. Development 121: 439–451.
51. Essner JJ, Laing JG, Beyer EC, Johnson RG, Hackett PB, Jr. (1996) Expression of zebrafish connexin43.4 in the notochord and tail bud of wild-type and mutant no tail embryos. Dev Biol 177: 449–462.
52. Faisst AM, Alvarez-Bolado G, Treichel D, Gruss P (2002) Rotatin is a novel gene required for axial rotation and left-right specification in mouse embryos. Mechanisms of Development 113: 15.
53. Tsang TE, Kinder SJ, Tam PP (1999) Experimental analysis of the emergence of left-right asymmetry of the body axis in early postimplantation mouse embryos. Cell Mol Biol (Noisy-le-grand) 45: 493–503.
54. Rana AA, Barbera JP, Rodriguez TA, Lynch D, Hirst E, et al. (2004) Targeted deletion of the novel cytoplasmic dynein mD2LIC disrupts the embryonic organiser, formation of the body axes and specification of ventral cell fates. Development 131: 4999–5007.
55. Zariwala M, O'Neal WK, Noone PG, Leigh MW, Knowles MR, et al. (2004) Investigation of the Possible Role of a Novel Gene, DPCD, in Primary Ciliary Dyskinesia. Am J Respir Cell Mol Biol 30: 428–434.
56. Pearce JJ, Evans MJ (1999) Mml, a mouse Mix-like gene expressed in the primitive streak. Mech Dev 87: 189–192.
57. Russ AP, Wattler S, Colledge WH, Aparicio SAJR, Carlton MBL, et al. (2000) Eomesodermin is required for mouse trophoblast development and mesoderm formation. Nature 404: 95–99.
58. Schmidt D, Wilson MD, Ballester B, Schwalie PC, Brown GD, et al. (2010) Five-vertebrate ChIP-seq reveals the evolutionary dynamics of transcription factor binding. Science 328: 1036–1040.
59. Farnham PJ (2009) Insights from genomic profiling of transcription factors. Nature reviews Genetics 10: 605–616.
60. Suzuki A, Raya A, Kawakami Y, Morita M, Matsui T, et al. (2006) Nanog binds to Smad1 and blocks bone morphogenetic protein-induced differentiation of embryonic stem cells. Proc Natl Acad Sci U S A 103: 10294–10299.
61. Kusch T, Storck T, Walldorf U, Reuter R (2002) Brachyury proteins regulate target genes through modular binding sites in a cooperative fashion. Genes Dev 16: 518–529.
62. Passamaneck YJ, Katikala L, Perrone L, Dunn MP, Oda-Ishii I, et al. (2009) Direct activation of a notochord cis-regulatory module by Brachyury and FoxA in the ascidian Ciona intestinalis. Development 136: 3679–3689.
63. Istrail S, Davidson EH (2005) Logic functions of the genomic cis-regulatory code. Proceedings of the National Academy of Sciences of the United States of America 102: 4954–4959.
64. Badis G, Berger MF, Philippakis AA, Talukder S, Gehrke AR, et al. (2009) Diversity and complexity in DNA recognition by transcription factors. Science 324: 1720–1723.
65. Wilson MD, Odom DT (2009) Evolution of transcriptional control in mammals. Curr Opin Genet Dev 19: 579–585.
66. Nakaya M, Biris K, Tsukiyama T, Jaime S, Rawls JA, et al. (2005) Wnt3a Links Left-Right Determination with Segmentation and Anterior-Posterior Axis Elongation. Development 132: 5425–5436.
67. Isaacs HV, Pownall ME, Slack JM (1994) eFGF regulates Xbra expression during Xenopus gastrulation. EMBO J 13: 4469–4481.
68. Schulte-Merker S, Smith JC (1995) Mesoderm formation in response to Brachyury requires FGF signalling. Curr Biol 5: 62–67.
69. Draper BW, Stock DW, Kimmel CB (2003) Zebrafish fgf24 functions with fgf8 to promote posterior mesodermal development. Development 130: 4639–4654.
70. Griffin KJ, Kimelman D (2003) Interplay between FGF, one-eyed pinhead, and T-box transcription factors during zebrafish posterior development. Dev Biol 264: 456–466.
71. Cunliffe V, Smith J (1992) Ectopic mesoderm formation in Xenopus embryos caused by widespread expression of a Brachyury homologue. Nature 358: 427–430.
72. Nentwich O, Dingwell KS, Nordheim A, Smith JC (2009) Downstream of FGF during mesoderm formation in Xenopus: the roles of Elk-1 and Egr-1. Dev Biol 336: 313–326.
73. Evans A, Bryant J, Skepper J, Smith S, Print CG, et al. (2007) Vascular development in embryoid bodies: quantification of transgenic intervention and antiangiogenic treatment. Angiogenesis 10: 217–226.
74. Williams RL, Hilton DJ, Pease S, Willson TA, Stewart CL, et al. (1988) Myeloid leukaemia inhibitory factor maintains the developmental potential of embryonic stem cells. Nature 336: 684–687.
75. Nagy A, Rossant J, Nagy R, Abramow-Newerly W, Roder JC (1993) Derivation of completely cell culture-derived mice from early-passage embryonic stem cells. Proc Natl Acad Sci U S A 90: 8424–8428.
76. Niimi M, Kim MY, Tao L, Liu H, Wu X, et al. (2005) Single embryonic stem cell-derived embryoid bodies for gene screening. Biotechniques 38: 349–350, 352.
77. Wartenberg M, Gunther J, Hescheler J, Sauer H (1998) The embryoid body as a novel in vitro assay system for antiangiogenic agents. Lab Invest 78: 1301–1314.
78. Thomson M, Liu SJ, Zou LN, Smith Z, Meissner A, et al. (2011) Pluripotency factors in embryonic stem cells regulate differentiation into germ layers. Cell 145: 875–889.
79. Van Eynde A, Nuytten M, Dewerchin M, Schoonjans L, Keppens S, et al. (2004) The nuclear scaffold protein NIPP1 is essential for early embryonic development and cell proliferation. Molecular and cellular biology 24: 5863–5874.
80. Bernemann C, Greber B, Ko K, Sterneckert J, Han DW, et al. (2011) Distinct developmental ground states of epiblast stem cell lines determine different pluripotency features. Stem cells 29: 1496–1503.
81. Wilkinson DG (1992) Whole mount in situ hybridization of vertebrate embryos In: Wilkinson DG, ed. In situ hybridization: A Practical Approach. Oxford: IRL Press. pp 75–83.
82. O'Geen H, Nicolet CM, Blahnik K, Green R, Farnham PJ (2006) Comparison of sample preparation methods for ChIP-chip assays. Biotechniques 41: 577–580.
83. Brown S, Teo A, Pauklin S, Hannan N, Cho CH, et al. (2011) Activin/Nodal signaling controls divergent transcriptional networks in human embryonic stem cells and in endoderm progenitors. Stem cells 29: 1176–1185.
84. Martin D, Brun C, Remy E, Mouren P, Thieffry D, et al. (2004) GOToolBox: functional analysis of gene datasets based on Gene Ontology. Genome Biol 5: R101.
85. Down TA, Hubbard TJP (2005) NestedMICA: sensitive inference of over-represented motifs in nucleic acid sequence. Nucl Acids Res 33: 1445–1453.
86. Thomas-Chollier M, Sand O, Turatsinze J, Janky R, Defrance M, et al. (2008) RSAT: regulatory sequence analysis tools. Nucleic acids research. 10 p.
87. Crooks GE, Hon G, Chandonia J-M, Brenner SE (2004) WebLogo: A Sequence Logo Generator. Genome Res 14: 1188–1190.

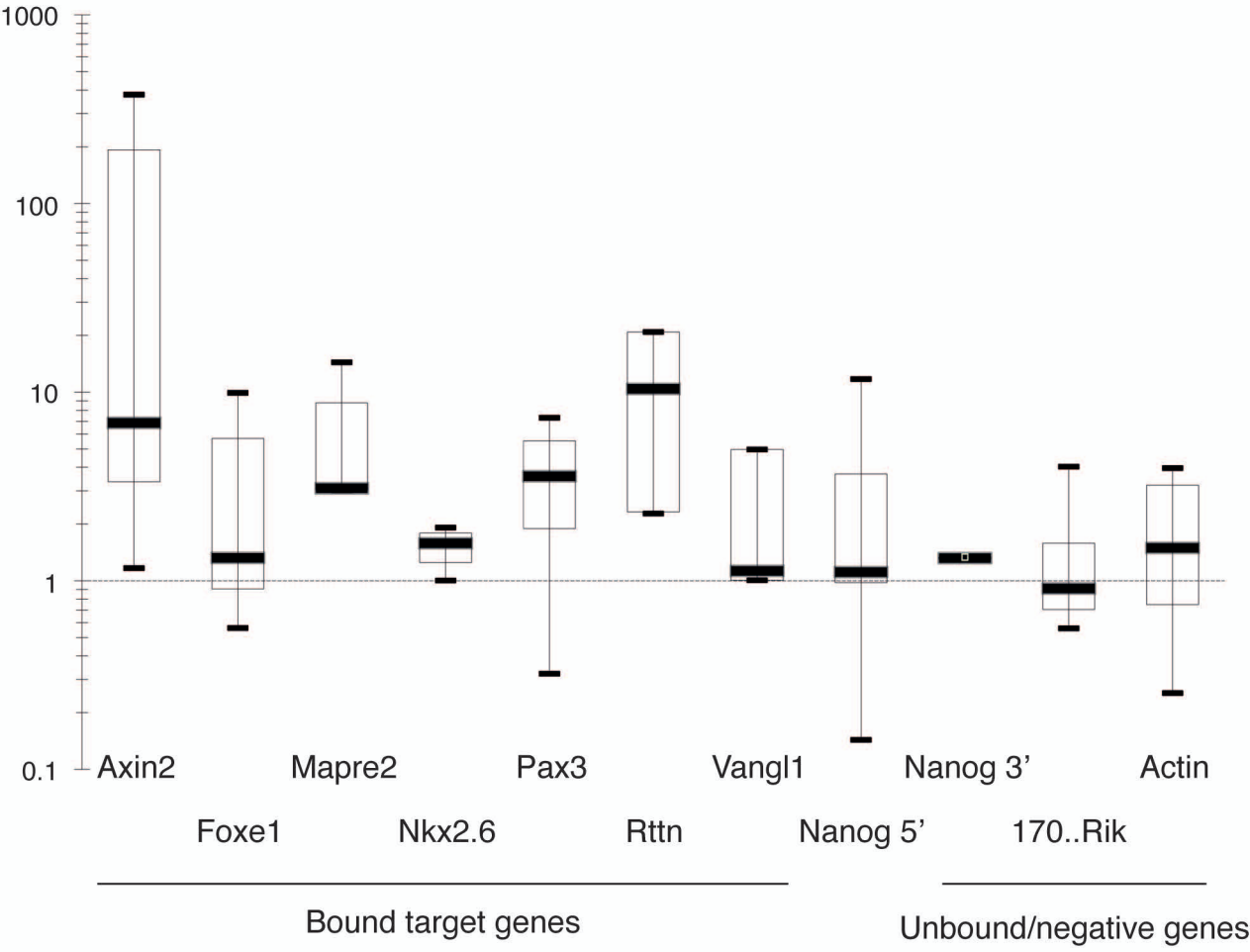
1000
100
10
1
0.1
Axin2
Foxe1
Mapre2
Nkx2.6
Pax3
Rttn
Vangl1
Nanog 5'
Nanog 3'
170..Rik
Actin
Bound target genes
Unbound/negative genes

Figure S1

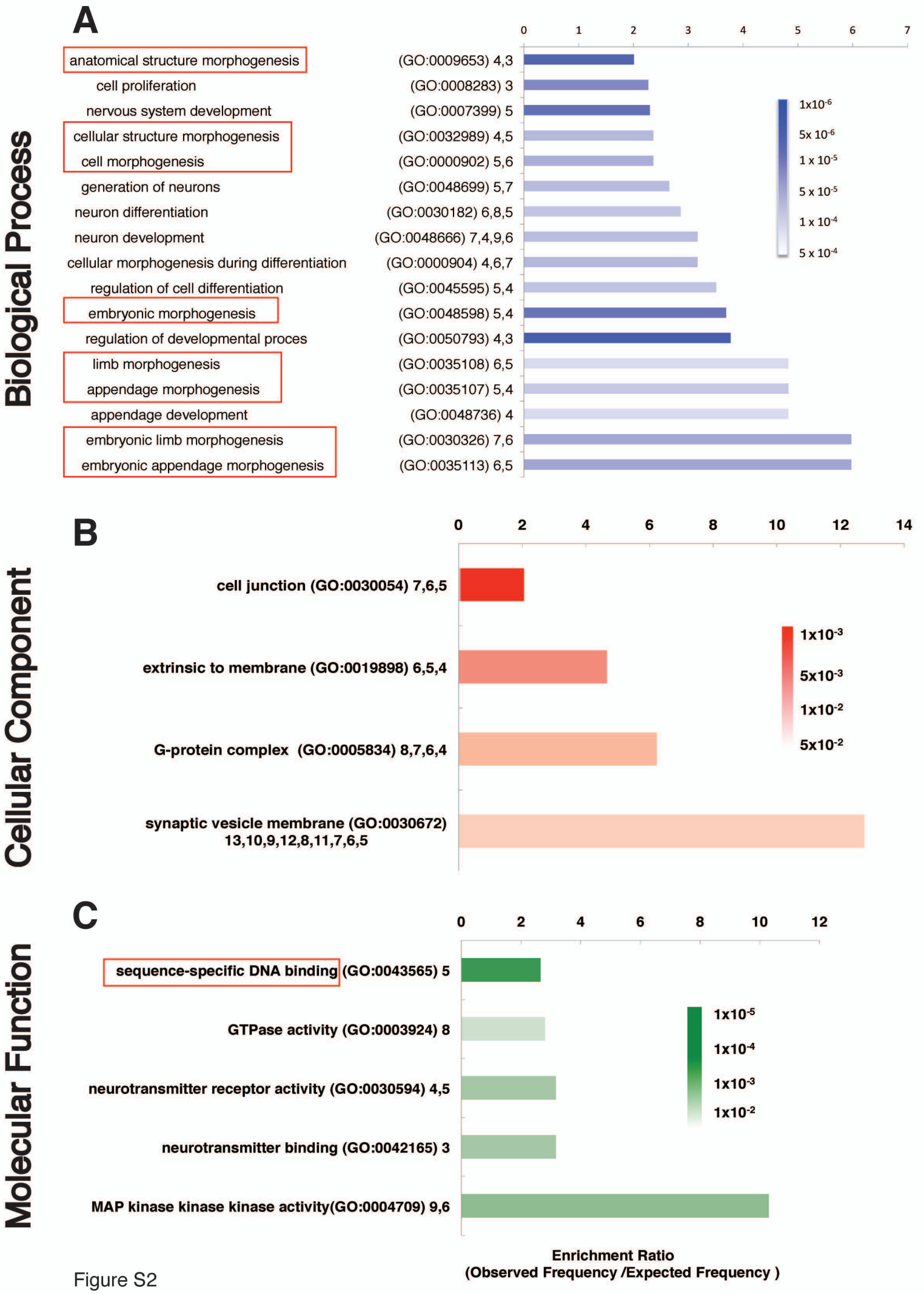
A
Biological Process
anatomical structure morphogenesis
cell proliferation
nervous system development
cellular structure morphogenesis
cell morphogenesis
generation of neurons
neuron differentiation
neuron development
cellular morphogenesis during differentiation
regulation of cell differentiation
embryonic morphogenesis
regulation of developmental proces
limb morphogenesis
appendage morphogenesis
appendage development
embryonic limb morphogenesis
embryonic appendage morphogenesis
(GO:0009653) 4,3
(GO:0008283) 3
(GO:0007399) 5
(GO:0032989) 4,5
(GO:0000902) 5,6
(GO:0048699) 5,7
(GO:0030182) 6,8,5
(GO:0048666) 7,4,9,6
(GO:0000904) 4,6,7
(GO:0045595) 5,4
(GO:0048598) 5,4
(GO:0050793) 4,3
(GO:0035108) 6,5
(GO:0035107) 5,4
(GO:0048736) 4
(GO:0030326) 7,6
(GO:0035113) 6,5
0 1 2 3 4 5 6 7
1x10-6
5x 10-6
1 x 10-5
5 x 10-5
1 x 10-4
5 x 10-4
B
Cellular Component
cell junction (GO:0030054) 7,6,5
extrinsic to membrane (GO:0019898) 6,5,4
G-protein complex (GO:0005834) 8,7,6,4
synaptic vesicle membrane (GO:0030672) 13,10,9,12,8,11,7,6,5
0 2 4 6 8 10 12 14
1x10-3
5x10-3
1x10-2
5x10-2
C
Molecular Function
sequence-specific DNA binding (GO:0043565) 5
GTPase activity (GO:0003924) 8
neurotransmitter receptor activity (GO:0030594) 4,5
neurotransmitter binding (GO:0042165) 3
MAP kinase kinase kinase activity(GO:0004709) 9,6
0 2 4 6 8 10 12
1x10-5
1x10-4
1x10-3
1x10-2
Enrichment Ratio
(Observed Frequency /Expected Frequency)

Figure S2

A

B

TCACACCT				+																		
GCACGCTT					+																	
ACACACACAC														+								
ACTCGCACTC															+							
TCACACCT-ACACACACAC																			+			
GCACGCTT-ACACACACAC																				+		
TCACACCT-ACTCGCACTC																					+	
T box protein			+	+	+	+			+	+			+	+	+	+			+	+	+	+	+
Control		+						+				+						+					
Supershift						+										+							+

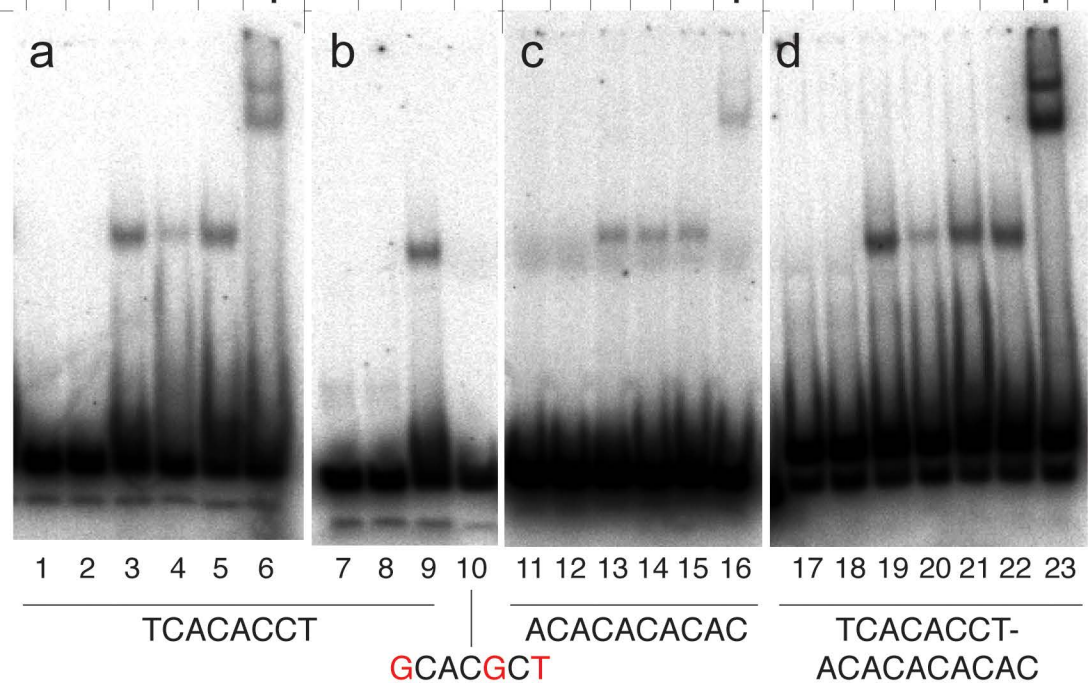

Figure 3

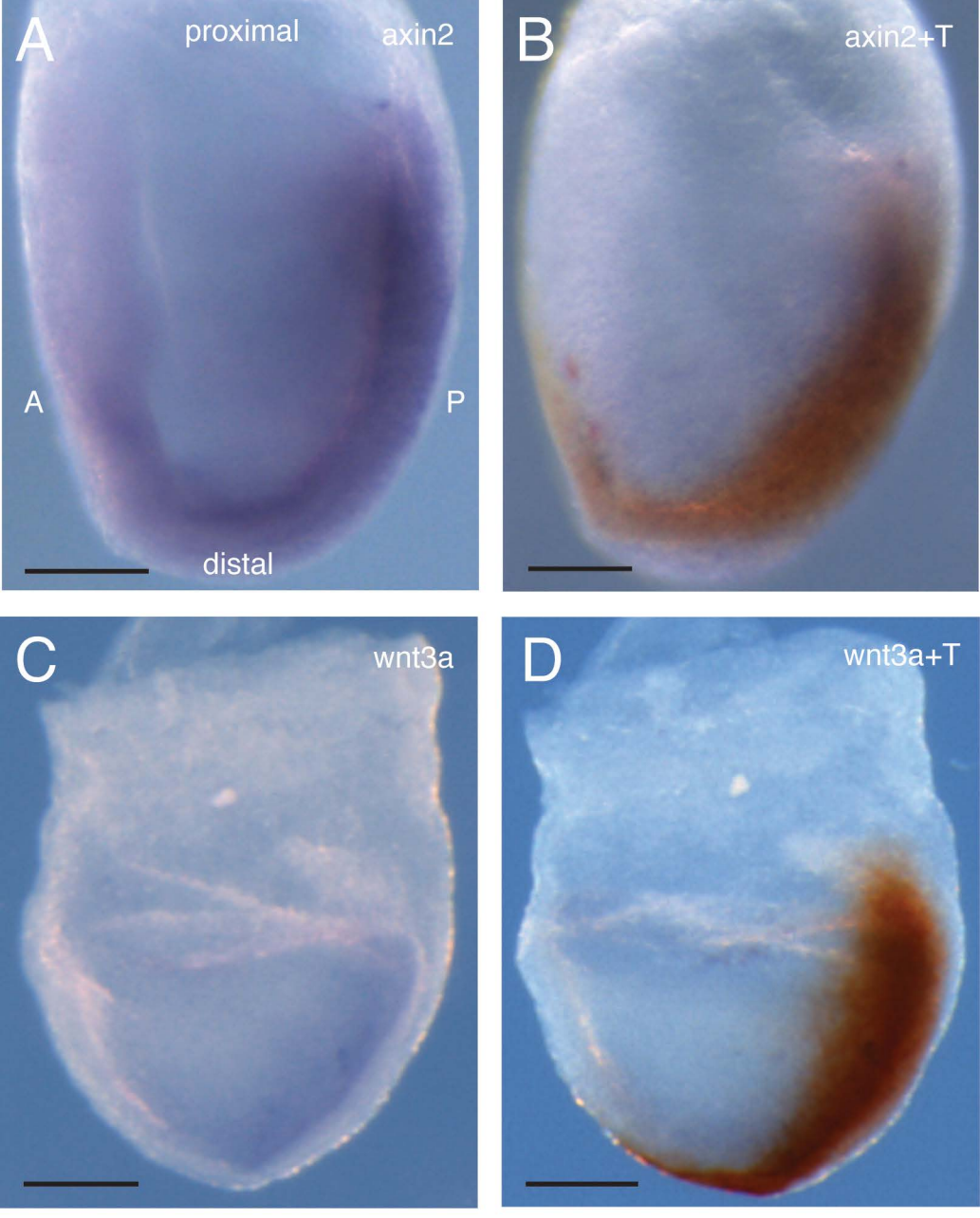

Figure S3

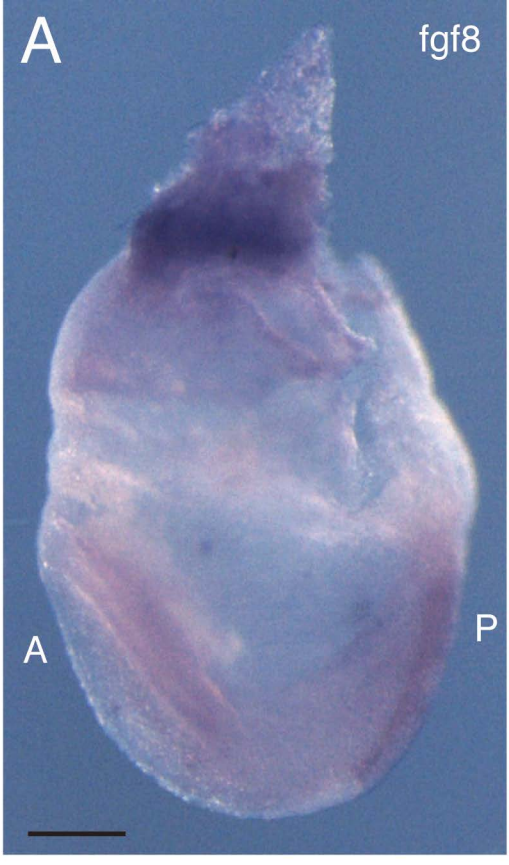

Figure S4

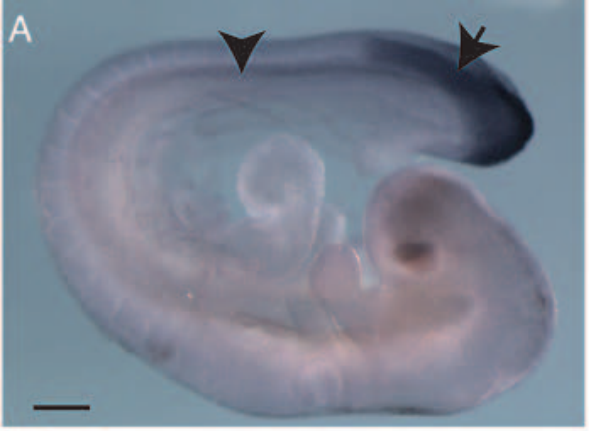
A

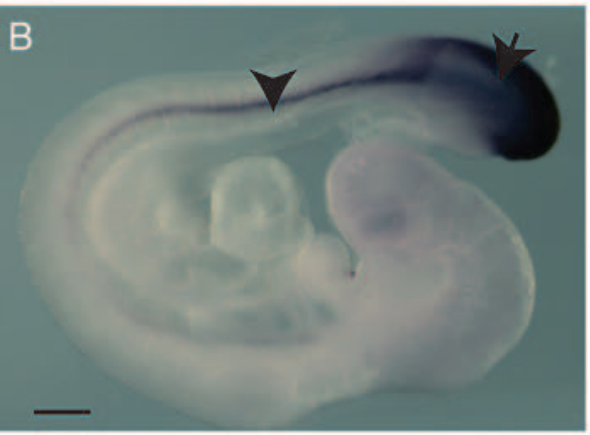
B

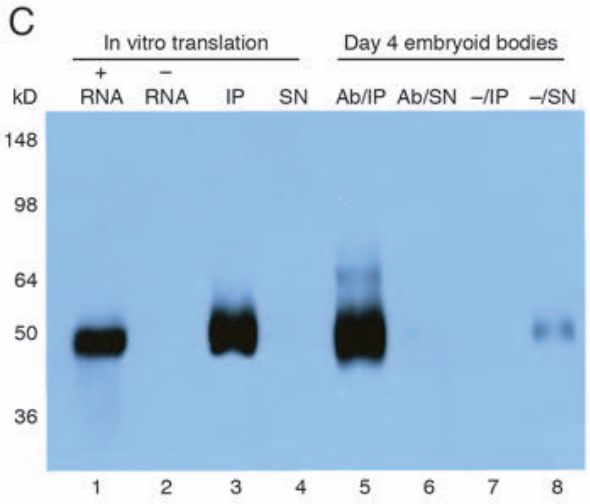
C
In vitro translation
Day 4 embryoid bodies
+ RNA
− RNA
IP
SN
Ab/IP
Ab/SN
−/IP
−/SN
kD
148
98
64
50
36
1
2
3
4
5
6
7
8

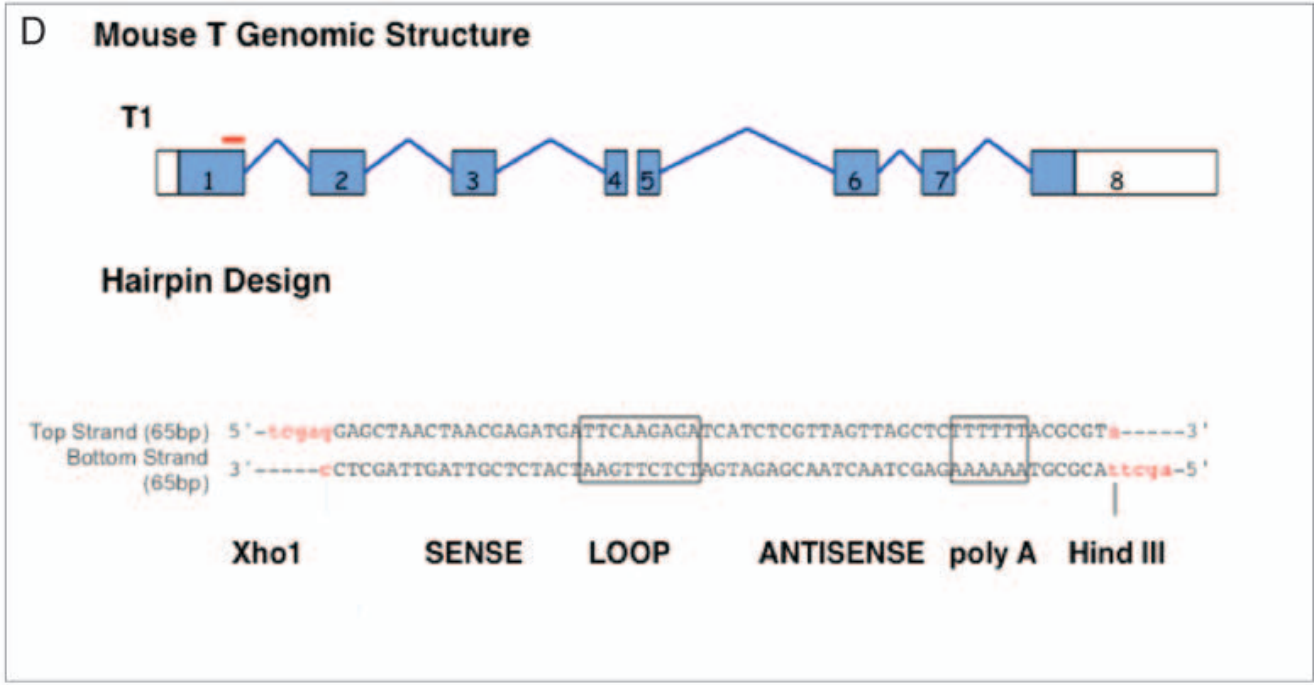
D
Mouse T Genomic Structure
T1
1
2
3
4
5
6
7
8
Hairpin Design
Top Strand (65bp)
Bottom Strand (65bp)
Xho1
SENSE
LOOP
ANTISENSE
poly A
Hind III

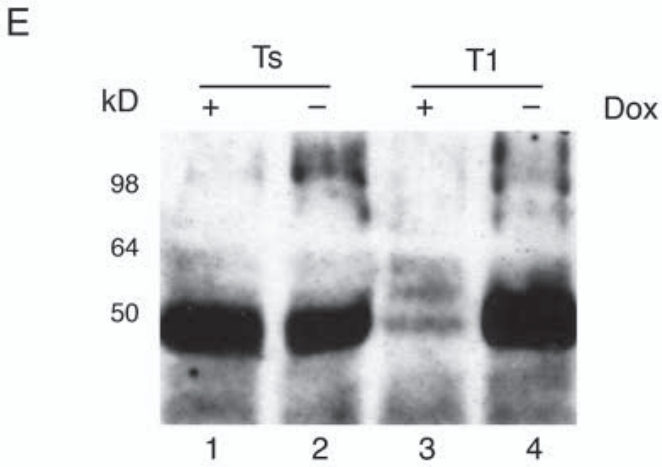
E
Ts
T1
kD
+
−
+
−
Dox
98
64
50
1
2
3
4

Supplementary Table S1

Full Gene List

Gene	Common Name	Chromosome	Peak Position
0610040J01Rik	unknown	chr5	promoter
1110004B13Rik	Tmem107	chr11	promoter
1110014K08Rik	D030012E24Rik	chr11	promoter
1110032A13Rik	RNA binding protein	chr18	divergent
1110059G10Rik	unknown	chr9	inside
1190002N15Rik	C3orf58	chr9	inside
1200009I06Rik	1600013K19Rik/sec6	chr12	inside
1300014I06Rik	unknown	chr13	promoter
1700012A16Rik	unknown	chr1	promoter
1700029I08Rik	unknown	chr17	promoter
2310079F23Rik	unknown	chr5	promoter
2410146L05Rik	Ooep, oocyte expressed protein homolog (dog)	chr9	promoter
2610207I05Rik	5430435M13Rik, C130002K18Rik, mKIAA0421, smg1	chr7	inside
4732495E13Rik	transmembrane protein 184b	chr15	inside
4930404H21Rik	unknown/C16orf65 homolog	chr7	inside
4930408O21Rik	hypothetical PDZ domain containing protein Uqcrc2	chr7	promoter
4930412F15Rik	unknown	chr4	promoter
4930441O14Rik	unknown	chr13	inside
4930504O13Rik	unknown	chr11	promoter
4930546H06Rik	B230206P06Rik	chr17	inside
4930556P03Rik	Bcdin3d BCDIN3 domain containing	chr15	promoter
4930578I06Rik	unknown	chr14	inside
5330431N19Rik	Dpcd, deleted in primary ciliary dyskinesia	chr19	inside
6330514A18Rik	polo-like kinase 5	chr10	inside
6430573F11Rik	unknown	chr8	inside
9030425E11Rik	ACAM; ASP5; CLMP; AW557819	chr9	promoter
9530068E07Rik	Keratinocytes-associated transmembrane protein 2	chr11	inside
A230056P14Rik	unknown	chr7	inside

A630055G03Rik	LOC381034	chr16	promoter
A730017C20Rik	unknown function	chr18	promoter
AA407270	unknown	chr9	promoter
Abcc2	ATP-binding cassette, sub-family C (CFTR/MRP), member 2 C, Mrp2, multidrug resistance protein 2	chr19	promoter
Abhd1	Abhydrolase domain containing 1,LABH-1, LABH1	chr5	promoter
Acly	ATP citrate lyase A730098H14Rik	chr11	inside
Adam19	A Disintegrin and metallopeptidase domain 19 (meltrin beta)	chr11	inside
Adam24	A Disintegrin and metallopeptidase domain 24 (testase 1) Dtgn5	chr8	promoter
Adam5	A Disintegrin and metallopeptidase domain 5 tMDCII	chr8	promoter
Adamts10	ADAM metallopeptidase with thrombospondin type 1 motif 10, kuz, kuzbanian	chr17	inside
Adar	adenosine deaminase, RNA-specific, ADAR1, mZaADAR	chr3	inside
Aipl1	aryl hydrocarbon receptor-interacting protein-like 1	chr11	divergent
Akap10	A kinase (PRKA) anchor protein 10	chr11	promoter
Aldoc	aldolase 3, C isoform Aldo3, Aldolase C, Scrg2, zebrin II	chr11	inside
Ankrd13d	ankyrin repeat domain 13 family, member D	chr19	inside
Anxa7	annexin A7 Anx7, synexin	chr14	inside
Apoa2	apolipoprotein A-II,Alp-2, Apoa-2, ApoA-II, Hdl-1	chr1	inside
Appbp1	amyloid beta precursor protein binding protein1, Nae1, NEDD8 activating enzyme E1	chr8	divergent
Aqp11	aquaporin 11	chr7	promoter
Aqp4	aquaporin 4	chr18	promoter
Arhgef4	rho/rac guanine nucleotide exchange factor (GEF) 4	chr1	promoter
Arid1a	AT rich interactive domain 1A (Swi1 like) BAF250a	chr4	promoter
Atcay	ataxia, cerebellar, Cayman type homolog (human), BNIP-H, ji	chr10	inside
Athl1	ATH1, acid trehalase-like 1 (yeast)	chr7	downstream
Atoh7	atonal homolog 7 (Drosophila), Math5	chr10	promoter
Atp1a3	ATPase, Na+/K+ transporting, alpha 3 polypeptide, Atpa-2	chr7	promoter
Atp6v1d	ATPase H+ transporting lysosomal V1 subunit D, lysosomal 34kDa, VATD, Vma8	chr12	inside
AU041783	Afap1l2, actin filament associated protein 1-like 2	chr19	inside
AW544981	Mouse E7.5 Extraembryonic cDNA Library	chr15	promoter
Axin2	Axin2/axil/conductin	chr11	promoter
B230218O03	maybe related Homo sapiens neuroplastoma apoptosis-related RNA-binding protein (CUGBP2)	chr2	promoter
B4galnt2	beta-1,4-N-acetyl-galactosaminyl transferase 2 Dlb-1, Dlb1, Galgt2	chr11	inside

Bapx1	NK3 homeobox 2 Bapx1, Nkx-3.2, Nkx3-2	chr5	promoter
BC002017	phospholipid scramblase 1Plscr1 MmTRA1a, MmTRA1b, MuPLSCR2, NOR1, Tras1/2	chr9	Unknown
BC017647	unknown	chr11	inside
BC019143	1300010F03Rik	chr14	Unknown
BC035295	Csnrp2 cysteine-serine-rich nuclear protein 2	chr15	promoter
BC048651	LOC330277, NYD-SP18	chr6	promoter
BC052496	Grap2,GRB2-related adaptor protein 2, Gads, GRAP-2, Grb2-related adaptor downstream of Sch, GRB2L, GrbX, Grf40, GRID, GrpL, Mona, P38	chr15	Unknown
BC054059	SMAF1likely orthologue of H. sapiens small adipocyte factor 1 (SMAF1)	chr2	inside
BC072639	2010300C02Rik	chr1	unknown
BC100404	Cpm, carboxypeptidase M	chr10	unknown
Bcl6	B-cell leukemia/lymphoma 6 Bcl5	chr16	promoter
Blr1	burkitt lymphoma receptor 1 Blr1, CXCR-5, Gpcr6	chr9	promoter
Bmp1	bone morphogenetic protein 1	chr14	inside
Boc	biregional cell adhesion molecule-related/down-regulated by oncogenes (Cdon) binding protein	chr16	inside
C030030A07Rik	transmembrane protein 72	chr6	inside
C1qtnf6	C1q and tumor necrosis factor related protein 6, CTRP6	chr15	inside
C230095G01Rik	unknown	chr6	promoter
C78339	unknown	chr13	promoter
C79407	DNA binding protein	chr12	promoter
Cables2	Cdk5 and Abl enzyme substrate 2 ik3-2	chr2	promoter
Camk2a	calcium/calmodulin-dependent protein kinase II alpha alpha-CaMKI	chr18	inside
Cant1	C calcium activated nucleotidase 1, SCAN-1, Shapy, Apy1h	chr11	promoter
Capns1	calpain, small subunit 1, Capa4, Capn4	chr7	promoter
Car10	CA-RP X	chr11	inside
Carhsp1	calcium regulated heat stable protein 1	chr16	promoter
Cbln3	cerebellin 3 precursor protein	chr14	inside
Ccdc52	coiled-coil domain containing 52	chr16	inside
Ccdc85a	coiled-coil domain containing 85A	chr11	promoter
Ccl1	chemokine (C-C motif) ligand 1, Scya1, Tca-3	chr11	inside
Cd300e	CD300e antigen Cd300le, Clm2, Trem5	chr11	promoter
Cdc42ep5	CDC42 effector protein (Rho GTPase binding) 5, Borg3, CEP5	chr7	promoter
Cdk9	cyclin-dependent kinase 9 (CDC2-related kinase) PITALRE	chr2	inside

Cebpa	CCAAT/enhancer binding protein (C/EBP), alpha	chr7	promoter
Ces6	carboxylesterase 6 9130231C15Rik	chr8	promoter
Chn2	chimerin (chimaerin) 2, Rho GTPase-activating protein 3	chr6	promoter
Chrm2	cholinergic receptor, muscarinic 2, cardiac AChR M2, M2	chr6	promoter
Chrnb1	cholinergic receptor, nicotinic, beta polypeptide 1 (muscle) Achr-2, Acrb	chr11	inside
Chst8	carbohydrate (N-acetylgalactosamine 4-0) sulfotransferase 8 GalNAc4ST-1	chr7	promoter
Cit	Citron, Cit-k, citron kinase, citron-N, CRIK, CRIK-SK	chr5	inside
Clnk	cytokine-dependent hematopoietic cell l linker MIST D5Dmo5	chr5	inside
Cml4	camello-like 4, Nat8 N-acetyltransferase 8 (GCN5-related, putative)	chr6	promoter
Cmtm2b	CKLF-like MARVEL transmembrane domain containing 2B	chr8	inside
Cnga3	cyclic nucleotide gated channel alpha 3 CNG3	chr1	promoter
Cnn1	calponin 1 calponin h1, CN, CnnI	chr9	promoter
Coq10b	coenzyme Q10 homolog B (S. cerevisiae)	chr1	promoter
Coq2	coenzyme Q2 homolog, prenyltransferase (yeast)	chr5	promoter
Cryba2	crystallin beta A2	chr1	inside
Crygn	crystalline gamma N	chr5	inside
Ctla4	cytotoxic T-lymphocyte-associated protein 4, Cd152, Ctla-4, Ly-56	chr1	promoter
Ctnnb1	catenin (cadherin associated protein), beta 1 Catnb, Mesc	chr9	promoter
Ctrc	chymotrypsin C (caldecrin) ELA4, Elastase iv	chr4	inside
Cugbp2	CUG triplet repeat, RNA binding protein 2, ETR-3, Napor-2	chr2	promoter
Cygb	cytoglobin, Staap	chr11	promoter
D030011O10Rik	Dennd5b, DENN/MADD domain containing 5B	chr6	promoter
D130058I21Rik	Smtnl2 smoothelin-like 2	chr11	promoter
D630039A03Rik	unknown	chr4	inside
Ddef1	development and differentiation enhancing Asap1	chr15	inside
Defb27	beta defensin 27,similar to beta defensin 123 predicted gene	chr2	inside
Dhrs3	dehydrogenase/reductase (SDR family) member 3	chr4	inside
Diras2	DIRAS family, GTP-binding RAS-like 2	chr13	promoter
Dkk1	dickkopf homolog 1 (Xenopus laevis)	chr19	inside
Dlx5	distal-less homeobox 5	chr6	inside
Dnase1l3	deoxyribonuclease 1-like 3	chr14	divergent
Dpp4	dipeptidylpeptidase 4, CD26, THAM	chr2	promoter
Dscr1l1	regulator of calcineurin 2,Csp2, Dscr1l1, MCIP2, ZAKI-4, new symbol Rcan2	chr17	promoter

Dvl3	dishevelled 3, dsh homolog (Drosophila)	chr16	inside
Dync1li1	dynein cytoplasmic 1 light intermediate chain 1, Dnclic1, LIC-1	chr9	inside
Dync2li1	dynein cytoplasmic 2 light intermediate chain 1, D2lic, LIC3, mD2LIC	chr17	promoter
E130309D14Rik	unknown	chr11	downstream
E430004N04Rik	Themis, thymocyte selection associated, Gasp, Tsepa	chr10	promoter
Ebf1	early B-cell factor 1 O/E-1, Olf-1, Olf1	chr11	inside
Ebf2	early B-cell factor 2 D14Ggc1e, Mmot1, O/E-3	chr14	promoter
EG574403	predicted gene, conserved	chr11	promoter
Elavl4	ELAV (embryonic lethal, abnormal vision, Drosophila)-like 4 (Hu antigen D)	chr4	promoter
Elmod1	ELMO domain containing 1	chr9	promoter
Epb4.1l4a	erythrocyte protein band 4.1-like 4a /NBL4	chr18	inside
Epb4.9	dematin, erythrocyte protein band 4.9	chr14	promoter
Ephx1	epoxide hydrolase 1, microsomal Eph-1, Eph1	chr1	promoter
Erg	avian erythroblastosis virus E-26 (v-ets) oncogene related	chr16	promoter
Etv1	ets variant gene 1, ER81, Etsrp81	chr12	promoter
Eva1	Mpzl2 myelin protein zero-like 2	chr9	inside
Fabp1	fatty acid binding protein 1, liver Fabpl, L-FABP, MGC:13855	chr6	promoter
Farp1	FERM, RhoGEF (Arhgef) and pleckstrin domain protein 1 (chondrocyte-derived) Cdep	chr14	inside
Fbxl10	F-box and leucine-rich repeat protein 10 Cxxc2, Jhdm1b, KDM2B, JEMMA (Jumonji domain, EMSY-interactor, methyltransferase motif)	chr5	inside
Fev	FEV (ETS oncogene family) mPet-1, Pet1 Fifth Ewing Variant	chr1	promoter
Fgf8	Fibroblast growth factor 8, Aigf	chr19	promoter
Foxa2	Forkhead box A2 Hnf-3b, HNF3-beta, Hnf3b, HNF3beta, Tcf-3b, Tcf3b	chr2	promoter
Foxe1	Forkhead box E1 (thyroid transcription factor 2), Titf2	chr4	promoter
Foxi2	Forkhead box I2	chr7	promoter
Foxn1	Forkhead box N1, Hfh11, whn	chr11	promoter
Fut8	fucosyltransferase 8, alpha (1,6) fucosyltransferase	chr12	promoter
Fxyd6	FXYD domain-containing ion transport regulator 6, Php	chr9	promoter
Fyb	FYN binding protein, ADAP, FYB-120/130	chr15	promoter
Gabra1	gamma-aminobutyric acid (GABA-A) receptor, subunit alpha 1	chr11	promoter
Gabra2	gamma-aminobutyric acid (GABA) A receptor, alpha 2	chr5	inside
Gabrb2	gamma-aminobutyric acid (GABA) A receptor, beta 2	chr11	promoter
Gcnt2	glucosaminyl (N-acetyl) transferase 2, I-branching enzyme, IGnTA, IGnTB, IGnTC	chr13	promoter

Gdf5	growth differentiation factor 5 (cartilage-derived morphogenetic protein-1), CDMP-1	chr2	inside
Gdpd4	glycerophosphodiester phosphodiesterase domain containing 4	chr7	promoter
Gfra3	glial cell line derived neurotrophic factor family receptor alpha 3	chr18	promoter
Glt8d1	glycosyltransferase 8 domain containing 1	chr14	inside
Glt8d3	glycosyltransferase 8 domain containing 3	chr15	promoter
Gm879	gene model 879	chr11	promoter
Gnaq	guanine nucleotide binding protein, alpha q polypeptide Dsk1, Dsk10, G alpha q, Gq	chr19	promoter
Gnaz	guanine nucleotide binding protein, alpha z subunit Gz	chr10	inside
Gnb2l1	RACK1 receptor for activated kinase C1	chr11	promoter
Gsg1	germ cell-specific gene 1	chr6	promoter
Gstm7	glutathione S-transferase, mu 7, Cd203c, GSTm2 muscle	chr3	inside
H2afy2	H2A histone family, member Y2 macroH2A2	chr10	promoter
Hcrtr1	hypocretin (orexin) receptor 1OX1R	chr4	promoter
Hdgfrp2	hepatoma-derived growth factor, related protein 2 HRP-2	chr17	INSIDE
Hnrpl	Hnrnpl heterogeneous nuclear ribonucleoprotein L, Hnrpl	chr7	promoter
Hnrpul1	heterogeneous nuclear ribonucleoprotein U-like 1, E1B-AP5	chr7	inside
Hoxa13	homeo box A13 Hox-1.10	chr6	promoter
Hoxa3	homeo box A3	chr6	divergent
Hsd17b3	hydroxysteroid (17-beta) dehydrogenase 3 17(beta)HSD type 3	chr13	inside
I830134H01Rik	unknown	chr19	inside
Ica1	islet cell autoantigen 169kDa, ICA69	chr6	inside
Id4	inhibitor of DNA binding 4 Idb4	chr13	promoter
Igsf11	immunoglobulin superfamily, member 11	chr16	promoter
Il1r1	interleukin 1 receptor, type i	chr1	inside
Il21	Interleukin-21	chr3	promoter
Il6	interleukin 6	chr5	promoter
Irx6	Iroquois related homeobox 6 (Drosophila)	chr8	inside
Junb	Jun-B oncogene/AP-1 activator protein 1	chr8	divergent
Jup	junction plakoglobin, gamma-catenin, PG, plakoglobin	chr11	promoter
Kcnd3	potassium voltage-gated channel, member 3 potassium channel Kv4.3L	chr3	inside
Kcnn4	potassium intermediate/small conductance calcium-activated channel, subfamily N, member 4 IK1, mIKCa1, SK4	chr7	promoter
Kctd13	potassium channel tetramerisation domain containing 13, Poldip1	chr7	promoter

Kif23	kinesin family member 23, C87313, CHO1, Knsl5, MKLP-1, MKLP1	chr9	inside
Krt16	keratin 16, K16, Krt1-16	chr11	promoter
Krt5	keratin 5, K5, Krt2-5, Tfip8	chr15	promoter
Krt8	Card2, cytokeratin 8, EndoA, K8, Krt-2.8, Krt2-8	chr15	promoter
Lama4	laminin, alpha 4	chr10	promoter
Lancl1	LanC (bacterial lantibiotic synthetase component C)-like 1, LanC-like protein 1, p40	chr1	promoter
Laptm5/E3	lysosomal-associated protein transmembrane 5 Retinoic acid-inducible E3 protein	chr4	promoter
Large	like-glycosyltransferase BPFD#36, enr, fg, froggy	chr8	promoter
Lctl	lactase-like, KLPH, klotho gamma,Klotho/lactase-phlorizin hydrolase- related protein	chr9	promoter
Leprotl1	leptin receptor overlapping transcript-like 1	chr8	divergent
Lhfpl2	lipoma HMGIC fusion partner-like 2	chr13	promoter
Lhx5/Lim2	LIM homeobox protein 5	chr5	inside
Lif	leukemia inhibitory factor	chr11	promoter
Lifr	leukemia inhibitory factor receptor, soluble differentiation-stimulating factor receptor	chr15	promoter
Lmx1b	LIM homeobox transcription factor 1 beta LMX1.2	chr2	inside
Lphn3	latrophilin 3, LEC3, lectomedin 3	chr5	promoter
Lrig1	leucine-rich repeats and immunoglobulin-like domains 1 Img, LIG-1	chr6	promoter
Lrrc4c	leucine rich repeat containing 4C, netrin g1 ligand	chr2	promoter
Map2k5	mitogen activated protein kinase kinase 5 MAPK/ERK kinase 5, Mapkk5, MEK5	chr9	promoter
Map3k11	mitogen activated protein kinase kinase kinase 11 2610017K16Rik, Mlk3, PTK1	chr19	inside
Map3k2	mitogen activated protein kinase kinase kinase 2, MEK kinase 2, Mekk2	chr18	promoter
Map3k3	mitogen activated protein kinase kinase kinase 3 MAPKKK3, Mekk3	chr11	promoter
Mapre2/EB1/EB2	microtubule-associated protein, RP/EB family, member 2 C820009F03Rik, EB2, RP1	chr18	promoter
Marcks	myristoylated alanine rich protein kinase C substrate Macs	chr10	inside
Marcksl1	MARCKS-like 1, F52, MacMARCKS, Macs-2, Macs-3, Macs2, Macs3, Mlp, Mrp	chr4	promoter
Mbp	myelin basic protein golli-mbp, Hmbpr	chr18	inside
Med4	mediator of RNA polymerase II transcription, subunit 4 homolog (yeast), DRIP36, HSPC126, p36 TRAP/SMCC/PC2 subunit, TRAP36, Vdrip	chr14	inside
Meis1	Meis homeobox 1	chr11	promoter
MGC117608	possible psuedogene similar to mitochondrial protein L32	chr6	inside
Mical1	microtubule associated monoxygenase, calponin and LIM domain containing, Nical	chr10	promoter
Morn2	MORN repeat containing 2 Mopt	chr17	promoter
Mov10	Moloney leukemia virus 10	chr3	promoter

Mrpl14	mitochondrial ribosomal protein L14, MRP-L32, Rpml32	chr17	inside
Mrps23	mitochondrial ribosomal protein S23, Rpms23	chr11	promoter
Msgn1	mesogenin 1	chr12	downstream
Msi2	Musashi homolog 2 (Drosophila) msi2h, Musashi 2	chr11	promoter
Mttp	microsomal triglyceride transfer protein	chr3	inside
Nat3	N-acetyltransferase 3	chr8	promoter
Ndn	necdin Peg6	chr7	promoter
Nedd4l	neural precursor cell expressed, developmentally down-regulated gene 4-like 1, Nedd4b	chr18	inside
Neu3	neuraminidase 3 ganglioside sialidase, membrane sialidase	chr7	inside
Ngb	neuroglobin	chr12	inside
Nhlrc1	NHL repeat containing 1, EPM2B, Malin	chr13	promoter
Nhp2l1	NHP2 non-histone chromosome protein 2-like 1(S. cerevisiae), FA-1, Fertilization antigen-1, Fta1, Ssfa1	chr15	promoter
Nkx2-6	NK2 transcription factor related, locus 6 tinman, Tix	chr14	inside
Nlrp4b	NLR family, pyrin domain containing 4B	chr7	promoter
Npffr2	neuropeptide FF receptor 2 Gpr74, NPFF2	chr5	promoter
Nsl1	NSL1, MIND kinetochore complex component, homolog (S. cerevisiae)	chr1	promoter
Nudt16	nudix (nucleoside diphosphate linked moiety X)-type motif 16	chr9	promoter
Oas1f	2'-5' oligoadenylate synthetase 1F	chr5	inside
Olfr1026	olfactory receptor 1026 GA_x6K02T2Q125-47402610-47403533, MOR196-4	chr2	promoter
Olfr1388	olfactory receptor 1388 GA_x6K02T2QP88-5991012-5990077, MOR256-28	chr11	promoter
Olfr209	olfactory receptor 209 GA_x54KRFPKG5P-55590495-55589578, MOR182-6	chr16	promoter
Olfr473	olfactory receptor 473 GA_x6K02T2PBJ9-10262759-10263691, MOR204-4	chr7	promoter
Olfr702	olfactory receptor 702 GA_x6K02T2PBJ9-9202245-9201289, MOR260-4	chr7	promoter
Olfr71	olfactory receptor 71 GA_x6K02T2N78B-16230286-16231224, mOR17, MOR262-4	chr4	promoter
Olfr907	olfactory receptor 907 GA_x6K02T2PVTD-32204729-32205661, MOR165-5	chr9	promoter
Olfr934	olfactory receptor 934 GA_x6K02T2PVTD-32678895-32677963, MOR224-6	chr9	promoter
Olfr95	olfactory receptor 95 GA_x6K02T2PSCP-1651760-1650822, MOR263-6	chr17	downstream
Otop2	otopetrin 2	chr11	inside
Ovgp1	oviductal glycoprotein 1, 120kDa, Chit5, MOGP, muc 9, OGP, Ovgp1, oviductin	chr3	promoter
Oxr1	oxidation resistance, C7, C7B	chr15	promoter
Pabpn1	poly(A) binding protein, nuclear 1PAB2, Pabp3, poly(A) binding protein II	chr14	promoter
Palmd	palmdelphin, PALML	chr3	inside

Park7	Parkinson disease (autosomal recessive, early onset) 7, DJ-1, Dj1	chr4	divergent
Parvg	parvin, gamma	chr15	promoter
Pax2	paired box gene 2	chr19	promoter
Pax3	paired box gene 3	chr1	inside
Pax5	paired box gene 5, B cell-specific activator protein EBB-1 BSAP	chr4	inside
Pcdha7	protocadherin alpha 7 Crnr4	chr18	promoter
Pck2	phosphoenolpyruvate carboxykinase 2 (mitochondrial)	chr14	promoter
Pcolce2	procollagen C-endopeptidase enhancer 2, Pcpe2	chr9	promoter
Pde2a	phosphodiesterase 2A, cGMP-stimulated	chr7	promoter
Pde7b	phosphodiesterase 7B	chr10	inside
Pdpk1	3-phosphoinositide dependent protein kinase-1 Pdk1, Pkb kinase	chr17	inside
Pdss1	prenyl (solanesyl) diphosphate synthase, subunit 1, mSPS1, Tprt	chr2	promoter
Pdx1	pancreatic and duodenal homeobox 1,IDX-1, IPF-1, Ipf1, Mody4, pdx-1, STF-1	chr5	promoter
Pelp1	proline, glutamic acid and leucine rich protein 1	chr11	promoter
Pfn4	profilin family, member 4	chr12	inside
Pigc	phosphatidylinositol glycan anchor biosynthesis, class C	chr1	promoter
Pigk	phosphatidylinositol glycan anchor biosynthesis, class K	chr3	promoter
Pitpnc1	phosphatidylinositol transfer protein, cytoplasmic 1, RDGB-BETA, RDGBB1	chr11	divergent
Pogk	pogo transposable element with KRAB domain, BASS2	chr1	promoter
Pold3	polymerase (DNA-directed), delta 3, accessory subunit, C85233, GC12, P66, P68	chr7	promoter
Ppargc1a	peroxisome proliferative activated receptor, gamma, coactivator 1 alpha, Pgc-1alpha, Pgc-1alphaa, Pgc1, Pgco1, PPAR Gamma Coactivator-1	chr5	promoter
Ppargc1b	peroxisome proliferative activated receptor, gamma coactivator 1 beta, Perc, PGC-1beta/ERRL1	chr18	inside
Ppm1m	protein phosphatase 1M	chr9	divergent
Ppp2r2b	protein phosphatase 2 (formerly 2A) regulatory subunit B (PR 52), beta isoform PP2A-PR55B, PR55-BETA, SCA12	chr18	promoter
Pqlc3	PQ loop repeat containing	chr12	promoter
Prcp	prolylcarboxypeptidase (angiotensinase C)	chr7	promoter
Prkag3	protein kinase, AMP-activated, gamma 3 non-catatlytic subunit, AMPKg3L, AMPKg3S	chr1	promoter
Prlpa	prolactin family 4, subfamily a, member 1 PLP-A, Prlpa	chr13	promoter
Prune	prune homolog (Drosophila) Prune-M1	chr3	inside
Psap	prosaposin SGP-1	chr10	inside
Psmd2	proteasome (prosome, macropain) 26S subunit, non-ATPase, TEG-190, Tex190	chr16	promoter

Ptgir	prostaglandin i receptor (ip) IP, prostacyclin receptor	chr7	promoter
Ptk2b	PTK2 protein tyrosine kinase 2 beta, CAKbeta, calcium-dependent tyrosine kinase, cellular adhesion kinase beta, proline-rich tyrosine kinase 2, PYK2, Raftk, related adhesion focal tyrosine kinase	chr14	inside
Ptn	Pleiotrophin, Osf1, heparin-binding growth factor 8, HBGF-8, HB-GAM, heparin-binding growth-associated molecule	chr6	inside
Pyy	peptide YY	chr11	promoter
Qpct	glutaminyl-peptide cyclotransferase (glutaminyl cyclase)	chr17	promoter
R74862	expressed sequence R74862	chr7	promoter
Rab11fip4	RAB11 family interacting protein 4 (class II), RAB11-FIP4	chr11	inside
Rab15	RAB15, member RAS oncogene family	chr12	inside
Rab17	RAB17, member RAS oncogene family	chr1	promoter
Rab5b	RAB5B, member RAS oncogene family	chr10	promoter
Rab6b	RAB6B, member RAS oncogene family	chr9	promoter
Ralgps2	Ral GEF with PH domain and SH3 binding motif	chr1	inside
Rbed1	RNA binding motif and ELMO domain 1, ELMOD3, RBM29	chr6	inside
Rbp1	retinol binding protein 1, cellular, Crbp, CRBPI	chr9	promoter
Rgs2	regulator of G-protein signaling 2 GOS8	chr1	inside
Rhou	Ras homolog gene family, member U, Arhu, CDC42L1, mG28K, WRCH1	chr8	promoter
Ripk5	receptor interacting protein kinase 5 dusty protein kinase	chr1	inside
Rnf207	ring finger protein 207	chr4	divergent
Rnf26	ring finger protein 26	chr9	promoter
Robo4	roundabout homolog 4 (Drosophila), Magic roundabout	chr9	first intron
Rpl36	ribosomal protein L36	chr17	inside
Rsl1	regulator of sex limited protein 1 rslcan-9	chr13	promoter
Rttn	rotatin (no turning)	chr18	promoter
Rufy3	RUN and FYVE domain containing 3, mKIAA0871, Rpipx	chr5	inside
Sart2	dermatan sulfate epimerase new symbol Dse	chr10	promoter
Schip1	schwannomin interacting protein 1 merlin	chr3	promoter
Scml4	sex comb on midleg-like 4 (Drosophila)	chr10	promoter
Scrg1	scrapie responsive gene 1	chr8	inside
Sec22a	SEC22 vesicle trafficking protein-like A (S. cerevisiae), Sec22l2	chr16	promoter
Sema4a	sema domain, immunoglobulin domain (Ig), transmembrane domain (TM) and short cytoplasmic domain, (semaphorin) 4A, Semab, SemB	chr3	promoter

Serpinb1c	serine (or cysteine) peptidase inhibitor, clade B, member 1c EIC, ovalbumin	chr13	promoter
Serpinb6c	serine (or cysteine) peptidase inhibitor, clade B, member 6c ovalbumin, Spi3C, SPIC	chr13	promoter
Sertad2	SERTA domain containing 2, SEI-2, Sei2, Trip-Br2	chr11	promoter
Sh3px3	SH3 and PX domain containing 3 sorting nexin	chr9	divergent
Slc16a6	solute carrier family 16 (monocarboxylic acid transporters), member 6	chr11	promoter
Slc17a5	solute carrier family 17 (anion/sugar transporter), member 5	chr9	promoter
Slc25a29	solute carrier family 25 (mitochondrial carrier, palmitoylcarnitine transporter) 29	chr12	promoter
Slc25a37	solute carrier family 25, member 37, Frascati, Mfrn, mitoferrin, Mscp	chr14	promoter
Slc30a7	solute carrier family 30 (zinc transporter), member 7, ZnT-7, ZnT7	chr3	inside
Slc37a2	solute carrier family 37 (glycerol-3-phosphate transporter), member cI-2, G3PP, Slc37a1	chr9	inside
Slc41a3	solute carrier family 41, member 3, SLC41A1-L2	chr6	promoter
Slc5a3	solute carrier family 5 (inositol transporters), member 3 Smit1	chr16	promoter
Slc5a6	solute carrier family 5 (sodium-dependent vitamin transporter), member 6	chr5	inside
Slc5a8	solute carrier family 5 (iodide transporter), member 8 MGC:19357, SMCT	chr10	promoter
Slu7	SLU7 splicing factor homolog (S. cerevisiae)	chr11	inside
Smarca2	SWI/SNF related, matrix associated, actin dependent regulator of chromatin, subfamily a, member 2 brm, Snf2l2	chr19	promoter
Snai2	snail homolog 2 (Drosophila), Slug, Slugh, Snail2	chr16	inside
Snx26	sorting nexin 26 Tcgap	chr7	promoter
Sppl3	signal peptide peptidase 3, Usmg3	chr5	promoter
Srrp	serine-arginine repressor protein	chr4	promoter
Sstr3	somatostatin receptor 3, Smstr3, sst3	chr15	inside
St6galnac1	ST6 (alpha-N-acetyl-neuraminyl-2,3-beta-galactosyl-1,3)-N-acetylgalactosaminide alpha-2,6-sialyltransferase 1, Siat7a, ST6GalNAc I	chr11	promoter
St8sia3	ST8 alpha-N-acetyl-neuraminide alpha-2, 8-sialyltransferase 3 Siat8c, ST8SiaIII	chr18	inside
Stk38	serine/threonine kinase 38, Ndr1	chr17	promoter
Stmn1	stathmin 1, Lag, Lap18, leukemia associated phosphoprotein p18, metablastin, oncoprotein 18, op18, p18, p19, pig, PP17, PP18, PR22, prosolin, SMN	chr4	inside
Stra13	stimulated by retinoic acid 13	chr11	downstream
Stra6	stimulated by retinoic acid gene 6	chr9	promoter
Stxbp1	syntaxin binding protein 1, Munc-18a, N-sec1, Rb-sec1, Sxtbp1, Unc18h	chr2	inside
Sumo2	SMT3 suppressor of mif two 3 homolog 2 (yeast), Smt3b, Smt3h2, SUMO-2	chr11	inside
Syk	spleen tyrosine kinase	chr13	promoter

Synpr	synaptoporin	chr14	inside
Syt1	synaptotagmin I	chr10	inside
Tbc1d21	TBC1 domain family, member 21	chr9	promoter
Tbc1d9b	TBC1 domain family, member 9B	chr11	inside
Tbl1xr1	transducin (beta)-like 1X-linked receptor 1, C21, DC42, Ira1, TBLR1	chr3	promoter
Tcf19	transcription factor 19	chr17	inside
Tcl1b2	T-cell leukemia/lymphoma 1B, 2	chr12	inside
Tfg	Trk-fused gene	chr16	promoter
Tgfa	Transforming growth factor alpha	chr6	promoter
Tiprl	TIP41, TOR signalling pathway regulator-like (S. cerevisiae)	chr1	promoter
Tmbim4	transmembrane BAX inhibitor motif containing 4	chr10	inside
Tmcc2	transmembrane and coiled-coil domains 2	chr1	inside
Tmem10	transmembrane protein10, Opalin, oligodendrocytic myelin paranodal inner loop protein	chr19	promoter
Tmprss11e	transmembrane protease, serine 11e DESC1	chr5	inside
Tnfrsf19	RELT tumor necrosis factor receptor	chr7	inside
Tnni2	troponin I, skeletal, fast 2	chr7	promoter
Toe1	target of EGR1, member 1 (nuclear)	chr4	divergent
Tox	thymus high mobility group box protein	chr4	inside
Trim28	tripartite motif protein 28, KAP-1, KRIP-1, Tif1b	chr7	promoter
Trpd52l3	tumor protein D52-like 3	chr19	promoter
Trpm6	transient receptor potential cation channel, subfamily M, member 6 CHAK2	chr19	promoter
Tspan11	tetraspanin 11	chr6	promoter
Tspan31	tetraspanin 31, Sas, Tspan31	chr10	divergent
Ttll12	tubulin tyrosine ligase-like family, member 12	chr15	promoter
Ttll6	tubulin tyrosine ligase-like family, member 6	chr11	promoter
Ubxd3	UBX domain containing 3	chr4	promoter
Uqcrh	ubiquinol-cytochrome c reductase hinge protein	chr4	inside
Usp18	ubiquitin specific peptidase 18 UBP43	chr6	promoter
Usp25	ubiquitin specific peptidase 25	chr16	promoter
Utp18	UTP18, small subunit (SSU) processome component, homolog (yeast), Wdr50	chr11	inside
V1rd6	vomeronasal 1 receptor, D6 V3R6	chr7	promoter
Vangl1	vang-like 1(van gogh, Drosophila), KITENIN, Lpp2, mStbm, stbm 2	chr3	inside
Vax1	ventral anterior homeobox 1	chr19	promoter

Veph1	ventricular zone expressed PH domain homolog 1 (zebrafish), Veph	chr3	promoter
Vil2	villin 2 cytovillin, ezrin, p81 NB ezrin is new symbol	chr17	promoter
Vps25	vacuolar protein sorting 25 (yeast)	chr11	promoter
Wasf1	WASP family 1,Scar, WAVE, WAVE-1	chr10	promoter
Wdr33	WD repeat domain 33	chr18	promoter
Wnt3a	wingless-related MMTV integration site 3A	chr11	inside
Wt1	wilms tumor (Nephroblastoma) homolog	chr2	promoter
Xlkd1	lymphatic vessel endothelial hyaluronan receptor 1, lymphatic vessel endothelial HA receptor-1, Lyve-1	chr7	inside
Xpo6	exportin 6, Ranbp20	chr7	inside
Zap70	zeta-chain (TCR) associated protein kinase Srk, TZK, ZAP-70	chr1	promoter
Zbtb41	zinc finger and BTB domain containing 41 homolog	chr1	promoter
Zdhhc17	zinc finger, DHHC domain containing 17, Hip14	chr10	inside
Zfp206	zinc finger and SCAN domain containing 10 Zfp206, Zscan10	chr17	inside
Zfp27	zinc finger protein 27 mkr-4 mszf76	chr7	promoter
Zfp276	zinc finger protein (C2H2 type) 276	chr8	promoter
Zic2	Zic finger protein of the cerebellum 2, GENA 29, Ku, odd-paired homolog	chr14	inside
Zic5	zinc finger protein of the cerebellum 5, odd-paired related, Opr	chr14	divergent
Zw10	ZW10 homolog (Drosophila), centromere/kinetochore protein MmZw10	chr9	promoter
Hoxc8	Homeo box C8	chr15	promoter
Lef1	Lymphoid Enhancer Binding Factor 1	chr3	inside
Sall1	Spalt-like transcription factor 1 Msal-3	chr8	promoter
Sox1	SRY-box containing gene 1	chr8	promoter

Supplementary Table S2

Members of Key Signaling Pathways

Target Gene	Key pathway	Role	Non-canonical & additional pathways
Axin2/conductin	Wnt signaling pathway	Inhibitor of wnt signaling, associates APC/βcatenin/GSKβ3/DVL	Crosstalk TGFβ pathway (Smad 3) Crosstalk MEKK1 SAPK stress pathway
Ctnnb1/β catenin	Wnt signaling pathway	LEF/TCF dependent transcriptional activation	A Component of adherens junctions
Dkk1/dickkopf homolog 1	Wnt signaling pathway	Antagonist wnt signaling, anterior side embryo	
Dvl3/dishevelled 3	Wnt signaling pathway	Dvl1/3 <<< Dvl2 pool Signaling canonical pathway sensitive to Dvl3 levels	JNK signaling PCP pathway Nodal pathway
Jup/Ctnng plakoglobin/γ-catenin	Wnt signaling pathway	Associates APC and axin Possible TCF/LEF transcriptional activity	A Component of adherens junctions and desmosomal plaques
Ppp2r2b	Wnt signaling pathway	Modulation of PP2A activity	Tight junctions
Wnt3a	Wnt signaling pathway	AP elongation, somite, tailbud formation	JNK signaling PCP pathway
Map2k5/MEK5	MapK signaling pathway	*In vivo* activator of ERK5	
Map3k11/PTK1/MLK3	MapK signaling pathway	Positive regulator JNK signaling	NF-κβ signaling JNK pathway TNF signaling
Map3k2/MEKK2	MapK signaling pathway	Activates MEK5 Required for T cell signaling	GnRH signaling pathway
Map3k3/MEKK3	MapK signaling pathway	Activates MEK5 cardiovascular development	GnRH signaling pathway
Cdc42ep5/CEP5	c-Jun N-Terminal Kinase (JNK) pathway	Regulation of cell shape	Rho GTPase
Junb	JNK pathway	Regulates erythroid cell survival, proliferation, and differentiation	Smad interacting protein
Syk	JNK pathway	Cell-cell adhesion via E cadherin & α catenin	NF-κβ signaling B cell Receptor Signaling T cell Receptor Signaling Ras/MAPK signaling
BMP1	TGFβ signaling pathway	Tolloid related	
Fut 8	TGFβ signaling pathway	Required for VEGFR2 expression	N-glycan biosynthesis Keratin sulphate biosynthesis Integrin mediated signaling
GDF5	TGFβ signaling	Embryonic limb morphogenesis	Cytokine-cytokine

	pathway		receptor interaction
BOC	Hedgehog Signaling pathway	Robo related, sonic hedgehog receptor Required myogenesis	
ERG	Fgf signaling	Regulation angiogenesis	Receptor signaling B cell receptor signaling
FGF8	Fgf signaling	L-R determinant, competence to respond to nodal signals	actin cytoskeleton signaling
Adam 19	Integrin signaling	Heart development & dendritic cell marker	
Adam 24 Testase 1	Integrin signaling	Protease implicated in sperm function during epididymal maturation or fertilization	
Rhou / WRCH1	Integrin signaling	Wnt-1 responsive Cdc42 hom stimulates cells to reenter the cell cycle	
Akap10 (D-AKAP2)	G-protein Coupled Receptor signaling	Localisation camp dep PKA , implicated heart rhythm regulation	AMP mediated signaling
Arhgef4	G-protein Coupled Receptor signaling	cell migration & cell-cell adhesion	Rho guanine nucleotide exchange factor
Camk2a	G-protein Coupled Receptor signaling		B cell receptor signaling
Gnaq	G-protein Coupled Receptor signaling	Vascular smooth muscle contraction cell morphogenesis	GnRH signaling pathway Wnt pathway
Gnaz	G-protein Coupled Receptor signaling		
Gnb2l1/Rack1	G-protein Coupled Receptor signaling	Localized to proliferating endothelial cells	
Ptk2b, Pyk2, Raftk	G-protein Coupled Receptor signaling	Cell adhesion Activation EGFR	GnRH signaling pathway Calcium signaling pathway
Lphn3/LEC3	G-protein Coupled Receptor signaling	Ca^{2+}independent receptor	neuropeptide signaling pathway
Rgs2	G-protein Coupled Receptor signaling	Negative regulator of G coupled receptor signalling	
Sstr3	G-protein Coupled Receptor signaling	May activate G-proteins at tight junctions	Neuroactive ligand-receptor interaction
Bcl6	B cell Receptor signaling	Repressor of transcription, memory B cell development	
Chn2	T cell Receptor signaling	Proliferation & migration SMC	Rac-specific GTPase activating proteins
Dpp4/CD26	T cell Receptor signaling		
Zap70	T cell Receptor signaling	Like syk non receptor PK. Associates TCR zeta chain	NK-κβ signaling
IL6	Cytokine/Jak/STAT pathway	First cytokine developing circulation osteoblasts to osteoclasts	
Lif	Cytokine/Jak/STAT pathway	Down regulated on differentiation cell morphogenesis	Gastrulation is inhibited in mouse embryos overexpressing LIF

Lifr	Cytokine/Jak/STAT pathway	Down regulated on differentiation	
Acly	Insulin Receptor signaling	Synthesis Acetyl CoA May have additional tissue specific function development	TCA cycle CO_2 fixation
TGFα	ErbB/HER signaling	Angiogenesis, cell proliferation	
Pck2/PEPCK	PPAR signaling pathway		Adipocytokine signaling pathway
Gcnt2	Sphingolipid Metabolism & N-Glycan Metabolism	Branching enzyme responsible conversion fetal to adult blood antigens	
Neu3	Sphingolipid Metabolism & N-Glycan Metabolism	skeletal muscle differentiation Suppression of apoptosis Mobilises membrane ruffles	
St8sia3	Sphingolipid Metabolism & N-Glycan Metabolism	Fetal blood formation & neuronal development	
Hsd17b3	Androgen & Estrogen Metabolism	Lipid biosynthesis	
St6galnac1	O-glycan Biosysnthesis	Decreases cell adhesion & increases cell migration	
Pde2aPdpk1	Purine Metabolism	Phosphodiesterase activity Cell communication	
Pde7b	Purine Metabolism	Phosphodiesterase activity	
Pold3	Purine & Pyrimidine Metabolism	DNA replication & repair subunit DNA polδ	
Prune	Purine Metabolism	Pyrophosphatase activity	
Nedd4l	Protein Ubiquitination pathway	ubiquitin protein-ligase activity	
Sumo2	Protein Ubiquitination pathway	Protein modification	NK-κβ signaling
Usp18	Protein Ubiquitination pathway	Deubiquitinating enzyme	
Usp25	Protein Ubiquitination pathway	Deubiquitinating enzyme	
Appbp1	NEDD8 conjugation pathway	Neddylation	Apoptosis and cell cycle progression
Ephx1	NFR2 Mediated Oxidative Stress Response	Protective enzyme	
Gstm7	NFR2 Mediated Oxidative Stress Response		Glutathione metabolism
Rab5b	Clathrin & Calveolar Mediated Endocytosis	Establishment of localization	small GTPase mediated signal transduction
Abcc2Mrp2	RXR Activation	Membrane transport multidrug resistance	ABC Transport
Robo4	Src Family Kinase Activation	Vascular -specific inhibits endothelial migration	Slit-Robo signaling
Cit	Protein serine/threonine kinase activity	Tissue specific neural tube regulator of cytokinesis	Rho interacting kinase
Dscr1l1 Rcan2	Calcium mediated signaling	Regulation of calcineurin	calcineurin-NFAT pathway.

Supplementary Table S3

Germ Cell Associated Targets

Gene	Alt. Symbol	Name
1700012A16Rik	MGI1919086	
1700029I08Rik	AV259599, Actl9	Actin-like 9
Ooep	2410146L05Rik, Floped, Moep19	Ooep, oocyte expressed protein homolog (dog)
4930412F15Rik	MGI2441678	
4930441O14Rik		
4930504O13Rik		
4930578I06Rik	AI429111	
Adam5	tMDCII	A Disintegrin and metallopeptidase domain 5
Adam19	Mltnb	A Disintegrin and metallopeptidase domain 19 (meltrin beta)
Adam24	Dtgn5	A Disintegrin and metallopeptidase domain 24 (testase 1)
Asap1	Ddef1	Development and differentiation enhancing Asap1 ArfGAP with SH domain, ankyrin repeat and PH domain 1
Cmtm2b	Cklfsf2b 1700013O04Rik	CKLF-like MARVEL transmembrane domain containing 2B homolog of human CKLFSF2
Fam196b	Gm6041 EG574403	Predicted gene, conserved Family with sequence similarity 196, member B
Gsg1		Germ cell-specific gene 1, germ cell associated 1
Hsd17b3	17(beta) HSD type 3	Hydroxysteroid (17-beta) dehydrogenase 3
Id4	Idb4	Inhibitor of DNA binding 4, bHLHb27
Morn2	Mopt	MORN repeat containing 2 Mopt
Pfn4	2900024P18Rik	Profilin family, member 4 testis specific
Ttll6	633044416Rik	tubulin tyrosine ligase-like family, member 6
Wdr33	WDC146	WD repeat domain 33, 1110001N06Rik, 2310011G05Rik, 2810021O11Rik, 8430413N20Rik
Wt1	D630046I16Rik	Wilms tumor (Nephroblastoma) homolog
Zfp206	Zscan10	zinc finger and SCAN domain containing 10

Supplementary Table S4

Transcription Factors Bound

Gene	Alt. Symbol	Name
Anxa7	Anx7	Annexin A7, synexin
Arid1a	BAF250a	AT rich interactive domain 1A (Swi1 like)
Atoh7	Math5	Atonal homolog 7 (*Drosophila*)
Bapx1	Nkx-3.2	NK3 homeobox 2
Bcl6	Bcl5	B-cell leukemia/lymphoma 6
C79407		DNA binding protein
Cdk9	PITALRE	Cyclin-dependent kinase 9 (CDC2-related kinase)
Cebpa		CCAAT/enhancer binding protein (C/EBP), alpha
Ctnnb1	Catnb; Mesc	Catenin (cadherin associated protein), beta 1
Ddef1	Asap1	Development and differentiation enhancing
Dlx5		Distal-less homeobox 5
Ebf1	O/E-1, Olf1	Early B-cell factor 1
Ebf2	D14Ggc1e, Mmot1, O/E-3	Early B-cell factor 2
Erg		Avian erythroblastosis virus E-26 (v-ets) oncogene related
Etv1	ER81, Etsrp81	Ets variant gene 1
Fbxl10	Jhdm1b, JEMMA	F-box and leucine-rich repeat protein 10, Jumonji domain, EMSY-interactor, methyltransferase motif
Fev	mPet-1, Pet1	FEV (ETS oncogene family), Fifth Ewing Variant
Foxa2	HNF3beta, Tcf3b	Forkhead box A2
Foxe1	Titf2	Forkhead box E1 (thyroid transcription factor 2)
Foxi2	B130055A05Rik	Forkhead box I2
Foxn1	Hfh11, whn	Forkhead box N1
Hoxa13	Hox-1.10	Homeo box A13
Hoxa3**		Homeo box A3
Irx6		Iroquois related homeobox 6 (*Drosophila*)
Jun B	AP-1	Jun-B oncogene/AP-1 activator protein 1
Lhx5	Lim2	LIM homeobox protein 5
Lmx1b	LMX1.2	LIM homeobox transcription factor 1 beta
Meis1	C530044H18Rik	Meis homeobox 1
Msgn1		Mesogenin 1
Nkx2-6	Tix	NK2 transcription factor related, locus 6 Tinman
Pax 2		Paired box gene 2
Pax 3		Paired box gene 3
Pax 5	EBB-1	Paired box gene 5, B cell-specific activator protein
Pdx1	IDX-1, Ipf1, Mody4, STF-1	Pancreatic and duodenal homeobox 1
Ppargc1a	Pgc-1alpha, Pgc1, Pgco1	Peroxisome proliferative activated receptor, gamma, coactivator 1 alpha
Ppargc1b	ERRL1, PGC1 beta	Peroxisome proliferative activated receptor, gamma, coactivator 1 beta
Snai2	Slug, Snail2	Snail homolog 2 (*Drosophila*)
Snx26	Tcgap	Sorting nexin 26
Stra13		Stimulated by retinoic acid 13
Stra6		Stimulated by retinoic acid gene 6
Tcf19	5730403J10Rik	Transcription factor 19
Tfg	Trk-fused gene	Trk-fused gene

Tox	1700007F02Rik	Thymus high mobility group box protein
Trim28	KAP-1, KRIP-1	Tripartite motif protein 28
Usp18	UBP43	Ubiquitin specific peptidase 18
Usp25		Ubiquitin specific peptidase 25
Vax1		Ventral anterior homeobox 1
Wt1	D630046I19Rik	Wilms tumor (Nephroblastoma) homolog
Zbt41	8430415N23Rik 9830132G07Rik	Zinc finger and BTB domain containing 41 homolog
Zfp206	Zscan10	Zinc finger and SCAN domain containing 10 Zfp206
Zfp27	mkr-4 mszf76	Zinc finger protein 27
Zfp276	D8Ertd370e, D8Ertd377e	Zinc finger protein (C2H2 type) 276
zic2	GENA 29, Ku	Zinc finger protein of the cerebellum 2 odd-paired homolog
zic5	Opr	Zinc finger protein of the cerebellum 5 odd-paired related

** Agilent software miss-called HoxA2 as target, binding peak in 5'UTR HoxA3

Supplementary Table S5

List of genes with AC repeats (with at least 8 nucleotides), their peak coordinates and sequence conservation analysis (presence of at least 8 nucleotides) in other species

Gene	Peak Coordinates	Conservation
1700029I08Rik	chr17:33034104-33034403	R
1700029I08Rik	chr17:33034240-33034539	R
4732495E13Rik	chr15:79229514-79229813	R
4930404H21Rik	chr7:133438288-133438587	R
4930556P03Rik	chr15:99303073-99303372	-
AA407270	chr9:71391930-71392229	H
AA407270	chr9:71391930-71392229	H
Abcc2	chr19:43832060-43833309	R
Adar	chr3:89817795-89818142	R
Ankrd13d	chr19:4271423-4271722	-
Aqp11	chr7:97614984-97615283	-
Atp6v1d	chr12:79779006-79779305	R
BC035295	chr15:100324504-100324803	R
BC048651	chr6:29268348-29268647	R
BC052496	chr15:80395457-80395824	-
Bcl6	chr16:23906124-23906653	R
Boc	chr16:44476590-44477179	R, H
Car10	chr11:92916538-92916837	R, H
Carhsp1	chr16:8591255-8591554	-
Ccdc85a	chr11:28484974-28485273	-
Cebpa	chr7:34824106-34824552	R
Chn2	chr6:54197731-54198030	R
Chrnb1	chr11:69610020-69610319	-
Cit	chr5:116227765-116228064	-
Cit	chr5:116227898-116228197	-
Cml4	chr6:85798316-85798615	-
Cnga3	chr1:37158481-37158780	R
Cnn1	chr9:21847791-21848090	R
Coq2	chr5:100918565-100918864	-
Crygn	chr5:24265622-24265921	-
D130058I21Rik	chr11:72232485-72232784	R
Dkk1	chr19:30614182-30615042	-
Dpp4	chr2:62213205-62213504	R
Dvl3	chr16:20431495-20431777	R
Ebf2	chr14:66183281-66183930	R
Etv1	chr12:39287680-39288047	R
Fabp1	chr6:71128736-71129035	-
Fev	chr1:74824484-74824783	R, H
Fgf8	chr19:45798051-45798373	R
Foxa2	chr2:147741739-147742038	-

Foxe1	chr4:46361799-46362327	R
Fyb	chr15:6524500-6524799	R
Gdf5	chr2:155634454-155634753	H
Hcrtr1	chr4:129642547-129643326	R, H
Hnrpul1	chr7:25461007-25461306	-
Hoxa13	chr6:52190959-52191258	R
Hoxa2	chr6:52102665-52103432	R, H
Id4	chr13:48270971-48271270	-
Junb	chr8:87873059-87873358	R, H
Kcnn4	chr7:24077403-24077702	R
Lama4	chr10:38656104-38656934	R
Lhfpl2	chr13:95155518-95155817	-
Lhx5/Lim2	chr5:120694575-120694874	R
Map2k5	chr9:63180895-63181194	R
Mapre2	chr18:23942472-23942710	-
Mbp	chr18:82610668-82610967	R
Meis1	chr11:18922898-18923197	H
MGC117608	chr6:12058209-12058508	-
Morn2	chr17:80196589-80196888	-
Mov10	chr3:104946714-104947013	-
Mrpl14	chr17:45150894-45151193	R
Mttp	chr3:138067297-138067596	R
Nat3	chr8:70450322-70450621	R
Nlrp4b	chr7:9561454-9561753	R
Npffr2	chr5:90600955-90601254	R
Oas1f	chr5:121109912-121110211	R
Olfr473	chr7:107719324-107719623	R
Olfr71	chr4:43729710-43730009	-
Olfr934	chr9:38735851-38736150	R
Otop2	chr11:115124749-115125048	R
Pax3	chr1:78077797-78077993	R
Pdzd9	chr7:120469324-120469623	R
Pelp1	chr11:70227398-70228397	R
Pigk	chr3:152650934-152651233	R
Pitpnc1	chr11:107287768-107288067	R
Pogk	chr1:168247826-168248125	H
Pold3	chr7:99997329-99997628	-
Ppm1m	chr9:106060544-106060843	-
Pqlc3	chr12:17027118-17027417	R
Prune	chr3:95366332-95366631	R
Psmd2	chr16:20560174-20560473	-
Ptn	chr6:36738757-36739401	R, H
Rab17	chr1:92802585-92802884	-
Rab6b	chr9:102969066-102969365	-
Rsl1	chr13:67669189-67669488	R

Rttn	chr18:89104706-89105203	R
Rufy3	chr5:89658618-89658917	R, H
Sart2	chr10:33899902-33900432	R
Sart2	chr10:33897285-33897822	R, H
Schip1	chr3:68658542-68658841	R
Serpinb1c	chr13:32905891-32906190	-
Sertad2	chr11:20439814-20440113	-
Slc41a3	chr6:90566229-90566838	-
Smarca2	chr19:26669021-26669320	-
St6galnac1	chr11:116594420-116594719	R
Syk	chr13:52604075-52604374	R, H
Tcl1b2	chr12:105548348-105548647	R
Tiprl	chr1:167074926-167075225	-
Tnfrsf19	chr7:100736389-100736688	R
Tnni2	chr7:142250655-142250954	-
Tox	chr4:6916154-6916453	R
Trim28	chr7:11923729-11924028	-
Tspan31	chr10:126478722-126478891	-
Ttll6	chr11:95947178-95947477	R, H
Ubxd3	chr4:138009399-138009698	-
V1rd6	chr7:5615400-5615699	R
V1rg3	chr7:11100370-11100974	-
Vil2 / ezrin	chr17:6635815-6636274	R
Wasf1	chr10:40567697-40567996	R
Zfp27	chr7:29617531-29617830	R
Zic2	chr14:121611987-121612286	R

Key	**Species**
-	Mouse
R	Rat
H	Human

Supplementary Table S6

PCR primers used for quantitative RT-PCR analysis

Primer	Type	Sequence 5' → 3'	Amplicon bp
βactinF	Endogenous control	AGGTCATCACTATTGGCAACGA	117
βactinR	Endogenous control	CACTTCATGATGGAATTGAATGTAG	
BrachyuryF	Primitive streak	GCTTCAAGGAGCTAACTAACGAG	117
BrachyuryR	Primitive streak	CCAGCAAGAAAGAGTACATGGC	
Axin2F	Wnt Target gene	TGACTCTCCTTCCAGATCCCA	105
Axin2R	Wnt Target gene	TGCCCACACTAGGCTGACA	
Ctnnb1F	Wnt Target gene	ATGGAGCCGGACAGAAAAGC	108
Ctnnb1R	Wnt Target gene	CTTGCCACTCAGGGAAGGA	
Dkk1F	Wnt Target gene	CTCATCAATTCCAACGCGATCA	105
Dkk1R	Wnt Target gene	GCCCTCATAGAGAACTCCCG	
Dvl3F	Wnt Target gene	GTCACCTTGGCGGACTTTAAG	128
Dvl3R	Wnt Target gene	AAGCAGGGTAGCTTGGCATTG	
JupF	Wnt Target gene	TGGCAACAGACATACACCTACG	135
JupR	Wnt Target gene	GGTGGTAGTCTTCTTGAGTGTG	
Wnt3a F	Wnt Target gene	CTCCTCTCGGATACCTCTTAGTG	186
Wnt3a R	Wnt Target gene	GCATGATCTCCACGTAGTTCCTG	
Bapx1F	Target gene	TCCAGGCGATCCTCAACAAGA	248
Bapx1R	Target gene	GGCTGAGTCTGAGTCCCAAC	
ERGF	Target gene	ACCTCACCCCTCAGTCCAAA	105
ERGR	Target gene	TGGTCGGTCCCAGGATCTG	
FevF	Target gene	ACGCCTACCGCTTTGACTTC	186
FevR	Target gene	AAGCTGCCATCAAGTTGAGTT	
Foxa2F	Target gene	TAG CGG AGG CAA GAA GAC C	150
Foxa2R	Target gene	CTT AGG CCA CCT CGC TTG T	
Foxe1F	Target gene	ATCGCGCTCATCGCTATGG	108
Foxe1R	Target gene	GGGGTTGTCGCGGTAGAAC	
Hoxa2F	Target gene	TACGAATTTGAGCGAGAGATTGG	116
Hoxa2R	Target gene	GTCGAGGTCTTGATTGATGAACT	
Hoxa3F	Target gene	TCAGCGATCTACGGTGGCTA	250
Hoxa3R	Target gene	GAGGCAAAGGTGGTTCACCC	
Meis1F	Target gene	GCAAAGTATGCCAGGGGAGTA	235
Meis1R	Target gene	TCCTGTGTTAAGAACCGAGGG	
Msgn1F	Target gene	CTTCTGACACCGCTGGTCTG	188
Msgn1R	Target gene	GTGACTGCCGTAGCCATCG	
Pax3F	Target gene	GGGCAGAATTACCCACGCA	177
Pax3R	Target gene	CTGGCGAGAAATGACGCAA	
Nkx2.6F	Target gene	GCATTCCTGGTCCCTACAAA	78
Nkx2.6R	Target gene	AGCTAGCGTCGTAGGGAGTG	
snai2F/Slug	Target gene	TGGTCAAGAAACATTTCAACGCC	131
snai2R/Slug	Target gene	GGTGAGGATCTCTGGTTTTGGTA	

Supplementary Table S7

Mouse *in situ*, T-box and EMSA primers

Primer	Sequence 5' → 3'
Wnt3a Bam F	AGGGATCCATGGCTCCTCTCGGATAC
Wnt3a Xba R	CGTCTAGACTACTTGCAGGTGTGCA
T BamH1 F	AGGGATCCATGAGCTCGCCGGGCACAGAGA
T Box Xho1 R	ACCGCTCGAGGGTGCCAGCACCAGGA
Sequencing Primer pGEX 5' F	GGGCTGGCAAGCCACGTTTGGTG
Sequencing Primer pGEX 3' R	CCGGGAGCTGCATGTGTCAGAGG
Motif 1 F BamH1 end	AGATCTCGGTTT**TCACACCT**ATAGACCG**GATCC**
Motif 1 R Bgl II end	GGATCCGGTCTAT**AGGTGTGA**AAACCGA**GATCT**
Mutated Motif 1F	AGATCTCGGTTT**GCACGCTT**ATAGACCG**GATCC**
Mutated Motif 1R	GGATCCGGTCTAT**AAGCGTGC**AAACCGA**GATCT**
Motif 2 F BamH1 end	AGATCTCAA**ACACACACACCT**AGA**GATCC**
Motif 2 R Bgl II end	GGATCTCTAG**GTGTGTGTGT**TTGA**GATCT**
Mutated Motif 2F	AGATCTCAA**ACTCGCACTCCT**AGAGATCC
Mutated Motif 2R	GGATCTCTAG**GAGTGCGAGT**TTGAGATCT
Motif 3 F Bgl II	AGATCTCGGTT**TCACACCT**ATAGACCT**ACACACACACCT**AGA**GATCC**
Motif 3 R BamH1	GGATCTCT**AGGTGTGTGTGT**AGGTCTAT**AGGTGTGA**AACCGA**GATCT**
Mutated 3 F T site intact $(AC)_n$ altered	AGATCTCGGTT**TCACACCT**ATAGACCT**ACTCGCACTCCT**AGAGATCC
Mutated 3 R T site intact $(AC)_n$ altered	GGATCTCT**AGGAGTGCGAGT**AGGTCTAT**AGGTGTGA**AACCGAGATCT
Mutated 3 F T site altered $(AC)_n$ intact	AGATCTCGGTT**GCACGCTT**ATAGACCT**ACACACACACCT**AGAGATCC
Mutated 3 R T site altered $(AC)_n$ intact	GGATCTCT**AGGTGTGTGTGT**AGGTCTAT**AAGCGTGC**AACCGAGATCT

The motifs investigated in EMSA experiments are highlighted in **bold**. Nucleotides in **blue bold** indicate mutated versions of these motifs. Nucleotides in **red bold** were included in oligonucleotides designed for unlabelled competition experiments and were absent from oligonucleotides intended for end labelling.

Supplementary Table S8

PCR primers used for genomic quantitative PCR

MOUSE

Primer	Sequence 5' → 3'	Amplicon
Bound genes		
Axin2 F	TGGAAAGGAATTCGAAGGTG	176
Axin2 R	CTTCCTTGCACACTCATGGA	
Foxe1 F	CACCCAGTGCTCACTGAAGA	144
Foxe1 R	CACGGTGAAGCCAGTACCTT	
Mapre2 F	GCCACTGTGCACTCTGCTTA	176
Mapre2 R	CAGTTTCTTGCCCATCAGGT	
Nkx2.6 F	AGAAGGGGCAAACAAGGAAT	184
Nkx2.6 R	GGCTGGTTGTGCCAAACTAT	
Pax3 F	AATCTCCCTCCCTTGCAAAT	199
Pax3 R	CACTCCCTAGCCAGCAGAAC	
Rttn F	GCTGGAGGTTGGGAAAAGAT	158
Rttn R	CTTCAAAAACAGGGCTGCAT	
Vangogh F	TATGGTTGGGGCTTTGATGT	148
Vangogh R	GCAACTGCATCCCTGAAAAT	
Published Target		
Nanog 5'F	GCTTGAACCAGCCAGTTCTC	200
Nanog 5'R	TTCCTCTCCCTCAGCTACCA	
Negative Regions/Genes		
Nanog 3' F	CACCCACCCATGCTAGTCTT	150
Nanog 3' R	ACCCTCAAACTCCTGGTCCT	
1700010C24Rik F	GCTTTGCCACAGCAGACATA	128
1700010C24Rik R	AGCCAACAAGGTGGACATTC	
β Actin F	GGGAATACTCTGGGCTCTCC	132
β Actin R	CCCTGGCCTTGTATTTCTCA	

HUMAN

Primer	Sequence 5' → 3'	Amplicon
Bound genes		
AXIN2 F	AGCCCTAACCCCTGACCCCC	105
AXIN2 R	TGTGCAGCCGGGGAGGATCT	
FGF8 F	AGCGATCAGTGGCATCGCGG	128
FGF8 R	TGGCAGGAGGAGCGGGAGAC	
JUP F	CCCCTAAGCCGACCAGCGGA	108
JUP R	GGGAAGCAGAGAGGGCCGGA	
WNT3A F	TTGGCCACACAGGGAAGCGG	82
WNT3A R	GTGGGGATGGGGGAGGGGTC	
Negative Region/Gene		
NCAPD2 F	GAGCCTTTCCACACCATCAT	109
NCAPD2 R	GCCGAGGTGGAATTCAAATA	

Bibliography

Abe, K., Rossman, K. L., Liu, B., Ritola, K. D., Chiang, D., Campbell, S. L., Burridge, K. & Der, C. J. 2000. Vav2 is an activator of Cdc42, Rac1, and RhoA. *The Journal of Biological Chemistry,* 275**,** 10141-9.

Abulafia, O. & Sherer, D. M. 1999. Angiogenesis of the endometrium. *Obstet Gynecol,* 94**,** 148-53.

Acevedo, L. M., Weis, S. M. & Cheresh, D. A. 2008. Robo4 counteracts VEGF signaling. *Nature Methods,* 14**,** 372-3.

Achen, M. G., Jeltsch, M., Kukk, E., Makinen, T., Vitali, A., Wilks, A. F., Alitalo, K. & Stacker, S. A. 1998. Vascular endothelial growth factor D (VEGF-D) is a ligand for the tyrosine kinases VEGF receptor 2 (Flk1) and VEGF receptor 3 (Flt4). *Proc Natl Acad Sci U S A,* 95**,** 548-53.

Albers, C. A., Cvejic, A., Favier, R., Bouwmans, E. E., Alessi, M. C., Bertone, P., Jordan, G., Kettleborough, R. N., Kiddle, G., Kostadima, M., Read, R. J., Sipos, B., Sivapalaratnam, S., Smethurst, P. A., Stephens, J., Voss, K., Nurden, A., Rendon, A., Nurden, P. & Ouwehand, W. H. 2011. Exome sequencing identifies NBEAL2 as the causative gene for gray platelet syndrome. *Nature Genetics,* 43**,** 735-7.

Albers, C. A., Paul, D. S., Schulze, H., Freson, K., Stephens, J. C., Smethurst, P. A., Jolley, J. D., Cvejic, A., Kostadima, M., Bertone, P., Breuning, M. H., Debili, N., Deloukas, P., Favier, R., Fiedler, J., Hobbs, C. M., Huang, N., Hurles, M. E., Kiddle, G., Krapels, I., Nurden, P., Ruivenkamp, C. A., Sambrook, J. G., Smith, K., Stemple, D. L., Strauss, G., Thys, C., Van Geet, C., Newbury-Ecob, R., Ouwehand, W. H. & Ghevaert, C. 2012. Compound inheritance of a low-frequency regulatory SNP and a rare null mutation in exon-junction complex subunit RBM8A causes TAR syndrome. *Nature Genetics,* 44**,** 435-9, S1-2.

Anastas, J. N., Biechele, T. L., Robitaille, M., Muster, J., Allison, K. H., Angers, S. & Moon, R. T. 2012. A protein complex of SCRIB, NOS1AP and VANGL1 regulates cell polarity and migration, and is associated with breast cancer progression. *Oncogene,* 31**,** 3696-708.

Ang, S. L. & Rossant, J. 1994. HNF-3 beta is essential for node and notochord formation in mouse development. *Cell,* 78**,** 561-74.

Argiropoulos, B., Yung, E. & Humphries, R. K. 2007. Unraveling the crucial roles of Meis1 in leukemogenesis and normal hematopoiesis. *Genes & Development,* 21**,** 2845-9.

Arici, A., Engin, O., Attar, E. & Olive, D. L. 1995. Modulation of leukemia inhibitory factor gene expression and protein biosynthesis in human endometrium. *J Clin Endocrinol Metab,* 80**,** 1908-15.

Armulik, A., Abramsson, A. & Betsholtz, C. 2005. Endothelial/pericyte interactions. *Circ Res,* 97**,** 512-23.

Asimaki, A., Syrris, P., Wichter, T., Matthias, P., Saffitz, J. E. & Mckenna, W. J. 2007. A novel dominant mutation in plakoglobin causes arrhythmogenic right ventricular cardiomyopathy. *American Journal of Human Genetics,* 81**,** 964-73.

Auerbach, R., Lewis, R., Shinners, B., Kubai, L. & Akhtar, N. 2003. Angiogenesis assays: a critical overview. *Clinical Chemistry,* 49**,** 32-40.

Azcoitia, V., Aracil, M., Martinez, A. C. & Torres, M. 2005. The homeodomain protein Meis1 is essential for definitive hematopoiesis and vascular patterning in the mouse embryo. *Developmental Biology,* 280**,** 307-20.

Baldi, P. & Long, A. D. 2001. A Bayesian framework for the analysis of microarray expression data: regularized t -test and statistical inferences of gene changes. *Bioinformatics,* 17**,** 509-19.

Bando, H., Weich, H. A., Brokelmann, M., Horiguchi, S., Funata, N., Ogawa, T. & Toi, M. 2005. Association between intratumoral free and total VEGF, soluble VEGFR-1, VEGFR-2 and prognosis in breast cancer. *Br J Cancer,* 92**,** 553-61.

Barnes, T. C., Anderson, M. E. & Moots, R. J. 2011. The many faces of interleukin-6: the role of IL-6 in inflammation, vasculopathy, and fibrosis in systemic sclerosis. *Int J Rheumatol,* 2011**,** 721608.

Barski, A., Cuddapah, S., Cui, K., Roh, T. Y., Schones, D. E., Wang, Z., Wei, G., Chepelev, I. & Zhao, K. 2007. High-resolution profiling of histone methylations in the human genome. *Cell,* 129**,** 823-37.

Bedford, F. K., Ashworth, A., Enver, T. & Wiedemann, L. M. 1993. HEX: a novel homeobox gene expressed during haematopoiesis and conserved between mouse and human. *Nucleic Acids Res,* 21**,** 1245-9.

Benjamin, L. E., Golijanin, D., Itin, A., Pode, D. & Keshet, E. 1999. Selective ablation of immature blood vessels in established human tumors follows vascular endothelial growth factor withdrawal. *J Clin Invest,* 103**,** 159-65.

Bergers, G. & Song, S. 2005. The role of pericytes in blood-vessel formation and maintenance. *Neuro Oncol,* 7**,** 452-64.

Bernardo, A. S., Faial, T., Gardner, L., Niakan, K. K., Ortmann, D., Senner, C. E., Callery, E. M., Trotter, M. W., Hemberger, M., Smith, J. C., Bardwell, L., Moffett, A. & Pedersen, R. A. 2011. BRACHYURY and CDX2 mediate BMP-induced differentiation of human and mouse pluripotent stem cells into embryonic and extraembryonic lineages. *Cell Stem Cell,* 9**,** 144-55.

Berns, H., Humar, R., Hengerer, B., Kiefer, F. N. & Battegay, E. J. 2000. RACK1 is up-regulated in angiogenesis and human carcinomas. *FASEB J,* 14**,** 2549-58.

Bettenhausen, B., Hrabe De Angelis, M., Simon, D., Guenet, J. L. & Gossler, A. 1995. Transient and restricted expression during mouse embryogenesis of Dll1, a murine gene closely related to Drosophila Delta. *Development,* 121**,** 2407-18.

Bigas, A., Robert-Moreno, A. & Espinosa, L. 2010. The Notch pathway in the developing hematopoietic system. *The International Journal of Developmental Biology,* 54**,** 1175-88.

Bland, J. M. & Altman.D.G 1999. Measuring agreement in method comparism studies. *Statistical Methods in Medical Research,* 8**,** 135-140.

Bolos, V., Peinado, H., Perez-Moreno, M. A., Fraga, M. F., Esteller, M. & Cano, A. 2003. The transcription factor Slug represses E-cadherin expression and induces

epithelial to mesenchymal transitions: a comparison with Snail and E47 repressors. *J Cell Sci,* 116**,** 499-511.

Bonon, A., Mangolini, A., Pinton, P., Del Senno, L. & Aguiari, G. 2013. Berberine slows cell growth in autosomal dominant polycystic kidney disease cells. *Biochem Biophys Res Commun,* 441**,** 668-74.

Bradley, A., Evans, M., Kaufman, M. H. & Robertson, E. 1984. Formation of germ-line chimaeras from embryo-derived teratocarcinoma cell lines. *Nature,* 309**,** 255-6.

Brckalo, T., Calzetti, F., Perez-Cabezas, B., Borras, F. E., Cassatella, M. A. & Lopez-Botet, M. 2010. Functional analysis of the CD300e receptor in human monocytes and myeloid dendritic cells. *European Journal of Immunology,* 40**,** 722-732.

Brook, F. A. & Gardner, R. L. 1997. The origin and efficient derivation of embryonic stem cells in the mouse. *Proc Natl Acad Sci U S A,* 94**,** 5709-12.

Brose, K., Bland, K. S., Wang, K. H., Arnott, D., Henzel, W., Goodman, C. S., Tessier-Lavigne, M. & Kidd, T. 1999. Slit proteins bind Robo receptors and have an evolutionarily conserved role in repulsive axon guidance. *Cell,* 96**,** 795-806.

Broxmeyer, H. E., Hoggatt, J., O'leary, H. A., Mantel, C., Chitteti, B. R., Cooper, S., Messina-Graham, S., Hangoc, G., Farag, S., Rohrabaugh, S. L., Ou, X., Speth, J., Pelus, L. M., Srour, E. F. & Campbell, T. B. 2012. Dipeptidylpeptidase 4 negatively regulates colony-stimulating factor activity and stress hematopoiesis. *Nature Methods,* 18**,** 1786-1796.

Busslinger, M. & Urbanek, P. 1995. The role of BSAP (Pax-5) in B-cell development. *Curr Opin Genet Dev,* 5**,** 595-601.

Cai, M., Langer, E. M., Gill, J. G., Satpathy, A. T., Albring, J. C., Kc, W., Murphy, T. L. & Murphy, K. M. 2012. Dual actions of Meis1 inhibit erythroid progenitor development and sustain general hematopoietic cell proliferation. *Blood,* 120**,** 335-46.

Cao, M. Y., Davidson, D., Yu, J., Latour, S. & Veillette, A. 1999. Clnk, a novel SLP-76-related adaptor molecule expressed in cytokine-stimulated hemopoietic cells. *Journal of Experimental Medicine,* 190**,** 1527-1534.

Carmeliet, P. 2003. Angiogenesis in health and disease. *Nat Med,* 9**,** 653-60.

Carmeliet, P. & Jain, R. K. 2000. Angiogenesis in cancer and other diseases. *Nature,* 407**,** 249-57.

Catalano, R. D., Yanaihara, A., Evans, A. L., Rocha, D., Prentice, A., Saidi, S., Print, C. G., Charnock-Jones, D. S., Sharkey, A. M. & Smith, S. K. 2003. The effect of RU486 on the gene expression profile in an endometrial explant model. *Mol Hum Reprod,* 9**,** 465-73.

Chakrabarti, R., Hwang, J., Andres Blanco, M., Wei, Y., Lukacisin, M., Romano, R. A., Smalley, K., Liu, S., Yang, Q., Ibrahim, T., Mercatali, L., Amadori, D., Haffty, B. G., Sinha, S. & Kang, Y. 2012. Elf5 inhibits the epithelial-mesenchymal transition in mammary gland development and breast cancer metastasis by transcriptionally repressing Snail2. *Nat Cell Biol,* 14**,** 1212-22.

Chang, A. N., Cantor, A. B., Fujiwara, Y., Lodish, M. B., Droho, S., Crispino, J. D. & Orkin, S. H. 2002. GATA-factor dependence of the multitype zinc-finger protein FOG-1 for its essential role in megakaryopoiesis. *Proc Natl Acad Sci U S A,* 99**,** 9237-42.

Chapman, D. L. & Papaioannou, V. E. 1998. Three neural tubes in mouse embryos with mutations in the T-box gene Tbx6. *Nature,* 391**,** 695-7.

Charnock-Jones, D. S., Sharkey, A. M., Fenwick, P. & Smith, S. K. 1994. Leukaemia inhibitory factor mRNA concentration peaks in human endometrium at the time of implantation and the blastocyst contains mRNA for the receptor at this time. *J Reprod Fertil,* 101**,** 421-6.

Chen, F. L., Yang, Z. H., Liu, Y., Li, L. X., Liang, W. C., Wang, X. C., Zhou, W. B., Yang, Y. H. & Hu, R. M. 2008. Berberine inhibits the expression of TNFalpha, MCP-1, and IL-6 in AcLDL-stimulated macrophages through PPARgamma pathway. *Endocrine,* 33**,** 331-7.

Chen, G., Gulbranson, D. R., Hou, Z., Bolin, J. M., Ruotti, V., Probasco, M. D., Smuga-Otto, K., Howden, S. E., Diol, N. R., Propson, N. E., Wagner, R., Lee, G. O., Antosiewicz-Bourget, J., Teng, J. M. & Thomson, J. A. 2011. Chemically defined conditions for human iPSC derivation and culture. *Nature Methods,* 8**,** 424-9.

Chen, H. C., Chu, R. Y., Hsu, P. N., Hsu, P. I., Lu, J. Y., Lai, K. H., Tseng, H. H., Chou, N. H., Huang, M. S., Tseng, C. J. & Hsiao, M. 2003. Loss of E-cadherin expression correlates with poor differentiation and invasion into adjacent organs in gastric adenocarcinomas. *Cancer Letters,* 201**,** 97-106.

Chen, P. P., Li, W. J., Wang, Y., Zhao, S., Li, D. Y., Feng, L. Y., Shi, X. L., Koeffler, H. P., Tong, X. J. & Xie, D. 2007. Expression of Cyr61, CTGF, and WISP-1 correlates with clinical features of lung cancer. *PLoS ONE,* 2**,** e534.

Chen, Y., Costa, R. M., Love, N. R., Soto, X., Roth, M., Paredes, R. & Amaya, E. 2009. C/EBPalpha initiates primitive myelopoiesis in pluripotent embryonic cells. *Blood,* 114**,** 40-8.

Chesley, P. 1935. Development of the short-tailed mutant in the house mouse. *Journal of Experimental Zoology,* 70**,** 429-459.

Chiang, C. K., Chowdhury, M. F., Iyer, R. K., Stanford, W. L. & Radisic, M. 2010. Engineering surfaces for site-specific vascular differentiation of mouse embryonic stem cells. *Acta Biomaterialia,* 6**,** 1904-1916.

Choi, K., Kennedy, M., Kazarov, A., Papadimitriou, J. C. & Keller, G. 1998. A common precursor for hematopoietic and endothelial cells. *Development,* 125**,** 725-32.

Clark, D. E., Smith, S. K., He, Y., Day, K. A., Licence, D. R., Corps, A. C., Lammoglia, R. & Charnock-Jones, D. S. 1998. A vascular endothelial growth factor antagonist is produced by the human placenta and released into the maternal circulation. *Biology of Reproduction,* 59**,** 1540-1548.

Clarke, C. L., Feil, P. D. & Satyaswaroop, P. G. 1987. Progesterone Receptor Regulation by 17β-Estradiol in Human Endometrial Carcinoma Grown in Nude Mice. *Endocrinology,* 121**,** 1642-1648.

Clemetson, K. J. 2012. Platelets and primary haemostasis. *Thrombosis Research,* 129**,** 220-4.

Conlon, F. L., Sedgwick, S. G., Weston, K. M. & Smith, J. C. 1996. Inhibition of Xbra transcription activation causes defects in mesodermal patterning and reveals autoregulation of Xbra in dorsal mesoderm. *Development,* 122**,** 2427-2435.

Costa, C., Soares, R., Reis-Filho, J. S., Leitao, D., Amendoeira, I. & Schmitt, F. C. 2002. Cyclo-oxygenase 2 expression is associated with angiogenesis and lymph node metastasis in human breast cancer. *J Clin Pathol,* 55**,** 429-34.

Cox, E. A., Bennin, D., Doan, A. T., O'toole, T. & Huttenlocher, A. 2003. RACK1 regulates integrin-mediated adhesion, protrusion, and chemotactic cell migration via its Src-binding site. *Mol Biol Cell,* 14**,** 658-69.

Cramer, E. M., Vainchenker, W., Vinci, G., Guichard, J. & Breton-Gorius, J. 1985. Gray platelet syndrome: immunoelectron microscopic localization of fibrinogen and von Willebrand factor in platelets and megakaryocytes. *Blood,* 66**,** 1309-16.

Crossley, P. H. & Martin, G. R. 1995. The mouse Fgf8 gene encodes a family of polypeptides and is expressed in regions that direct outgrowth and patterning in the developing embryo. *Development,* 121**,** 439-51.

Cui, G., Qin, X., Zhang, Y., Gong, Z., Ge, B. & Zang, Y. Q. 2009. Berberine differentially modulates the activities of ERK, p38 MAPK, and JNK to suppress Th17 and Th1 T cell differentiation in type 1 diabetic mice. *J Biol Chem,* 284**,** 28420-9.

Cunliffe, V. & Smith, J. C. 1992. Ectopic mesoderm formation in Xenopus embryos caused by widespread expression of a Brachyury homologue. *Nature,* 358**,** 427-30.

Czubayko, F., Liaudet-Coopman, E. D., Aigner, A., Tuveson, A. T., Berchem, G. J. & Wellstein, A. 1997. A secreted FGF-binding protein can serve as the angiogenic switch in human cancer. *Nature Methods,* 3**,** 1137-40.

Davies, S. R., Watkins, G., Mansel, R. E. & Jiang, W. G. 2007. Differential expression and prognostic implications of the CCN family members WISP-1, WISP-2, and WISP-3 in human breast cancer. *Annals of Surgical Oncology,* 14**,** 1909-18.

Dekker, J., Rippe, K., Dekker, M. & Kleckner, N. 2002. Capturing chromosome conformation. *Science,* 295**,** 1306-11.

Demir, R., Kaufmann, P., Castellucci, M., Erbengi, T. & Kotowski, A. 1989. Fetal vasculogenesis and angiogenesis in human placental villi. *Acta Anatomica(Basel),* 136**,** 190-203.

Deutsch, V. R. & Tomer, A. 2006. Megakaryocyte development and platelet production. *Br J Haematol,* 134**,** 453-66.

Dias, J., Gumenyuk, M., Kang, H., Vodyanik, M., Yu, J., Thomson, J. A. & Slukvin, Ii 2011. Generation of red blood cells from human induced pluripotent stem cells. *Stem cells and Development,* 20**,** 1639-47.

Dobrovolskaïa-Zavadskaïa, N. 1927. Sur la mortification spontanee de la queue chez la souris nouveau-nee et sur l'existence d'un caractere (facteur) hereditaire *Comptes Rendus des Séances et Mémoires de la Société de Biologieet des ses Filiales (Paris),* 97**,** 114-16.

Duval, H., Johnson, N., Li, J., Evans, A., Chen, S., Licence, D., Skepper, J., Charnock-Jones, D. S., Smith, S. & Print, C. 2007. Vascular development is disrupted by endothelial cell-specific expression of the anti-apoptotic protein Bcl-2. *Angiogenesis,* 10**,** 55-68.

Dzierzak, E. 2005. The emergence of definitive hematopoietic stem cells in the mammal. *Curr Opin Hematol,* 12**,** 197-202.

Eaker, E. Y. & Sninsky, C. A. 1989. Effect of berberine on myoelectric activity and transit of the small intestine in rats. *Gastroenterology,* 96**,** 1506-13.

Easterday, M. C., Dougherty, J. D., Jackson, R. L., Ou, J., Nakano, I., Paucar, A. A., Roobini, B., Dianati, M., Irvin, D. K., Weissman, I. L., Terskikh, A. V., Geschwind, D. H. & Kornblum, H. I. 2003. Neural progenitor genes. Germinal zone expression and analysis of genetic overlap in stem cell populations. *Developmental Biology,* 264**,** 309-22.

Eberhart, C. E., Coffey, R. J., Radhika, A., Giardiello, F. M., Ferrenbach, S. & Dubois, R. N. 1994. Up-regulation of cyclooxygenase 2 gene expression in human colorectal adenomas and adenocarcinomas. *Gastroenterology,* 107**,** 1183-8.

Eberle, I., Moslem, M., Henschler, R. & Cantz, T. 2012. Engineered MSCs from Patient-Specific iPS Cells. *Adv Biochem Eng Biotechnol*.

Eichmann, A., Corbel, C., Nataf, V., Vaigot, P., Breant, C. & Le Douarin, N. M. 1997. Ligand-dependent development of the endothelial and hemopoietic lineages from embryonic mesodermal cells expressing vascular endothelial growth factor receptor 2. *Proc Natl Acad Sci U S A,* 94**,** 5141-6.

Eilken, H. M., Nishikawa, S. & Schroeder, T. 2009. Continuous single-cell imaging of blood generation from haemogenic endothelium. *Nature,* 457**,** 896-900.

El Messaoudi-Aubert, S., Nicholls, J., Maertens, G. N., Brookes, S., Bernstein, E. & Peters, G. 2010. Role for the MOV10 RNA helicase in polycomb-mediated repression of the INK4a tumor suppressor. *Nature Structural & Molecular Biology,* 17**,** 862-8.

Evans, A., Bryant, J., Skepper, J., Smith, S., Print, C. G. & Charnock-Jones, D. S. 2007. Vascular development in embryoid bodies: quantification of transgenic intervention and antiangiogenic treatment. *Angiogenesis,* 10**,** 217-26.

Evans, A. L., Faial, T., Gilchrist, M. J., Down, T., Vallier, L., Pedersen, R. A., Wardle, F. C. & Smith, J. C. 2012. Genomic targets of brachyury (T) in differentiating mouse embryonic stem cells. *PLoS One* [Online], 7. Available: http://www.ncbi.nlm.nih.gov/entrez/query.fcgi?cmd=Retrieve&db=PubMed&dopt=Citation&list_uids=22479388 [Accessed 2012].

Evans, A. L., Sharkey, A. S., Saidi, S. A., Print, C. G., Catalano, R. D., Smith, S. K. & Charnock-Jones, D. S. 2003. Generation and use of a tailored gene array to investigate vascular biology. *Angiogenesis,* 6**,** 93-104.

Evans, M. J. & Kaufman, M. H. 1981. Establishment in culture of pluripotential cells from mouse embryos. *Nature,* 292**,** 154-6.

Fairfax, B. P., Vannberg, F. O., Radhakrishnan, J., Hakonarson, H., Keating, B. J., Hill, A. V. S. & Knight, J. C. 2010. An integrated expression phenotype mapping approach defines common variants in LEP, ALOX15 and CAPNS1 associated with induction of IL-6. *Human Molecular Genetics,* 19**,** 720-730.

Faisst, A. M., Alvarez-Bolado, G., Treichel, D. & Gruss, P. 2002. Rotatin is a novel gene required for axial rotation and left-right specification in mouse embryos. *Mech Dev,* 113**,** 15-28.

Faivre, E. J. & Lange, C. A. 2007. Progesterone receptors upregulate Wnt-1 to induce epidermal growth factor receptor transactivation and c-Src-dependent sustained activation of Erk1/2 mitogen-activated protein kinase in breast cancer cells. *Mol Cell Biol,* 27**,** 466-80.

Fernando, R. I., Litzinger, M., Trono, P., Hamilton, D. H., Schlom, J. & Palena, C. 2010. The T-box transcription factor Brachyury promotes epithelial-mesenchymal transition in human tumor cells. *J Clin Invest,* 120**,** 533-44.

Ferrara, N. & Davis-Smyth, T. 1997. The biology of vascular endothelial growth factor. *Endocrine Reviews,* 18**,** 4-25.

Fesus, L., Thomazy, V., Autuori, F., Ceru, M. P., Tarcsa, E. & Piacentini, M. 1989. Apoptotic hepatocytes become insoluble in detergents and chaotropic agents as a result of transglutaminase action. *FEBS Letters,* 245**,** 150-4.

Fitzgerald, S., Sheehan, K. M., O'grady, A., Kenny, D., O'kennedy, R., Kay, E. W. & Kijanka, G. S. 2013. Relationship between epithelial and stromal TRIM28 expression predicts survival in colorectal cancer patients. *J Gastroenterol Hepatol,* 28**,** 967-74.

Folkman, J. 1990. What is the evidence that tumors are angiogenesis dependent? *J Natl Cancer Inst,* 82**,** 4-6.

Fosslien, E. 2000. Molecular pathology of cyclooxygenase-2 in neoplasia. *Annals of Clinical and Laboratory Science,* 30**,** 3-21.

Fu, L., Chen, W., Guo, W., Wang, J., Tian, Y., Shi, D., Zhang, X., Qiu, H., Xiao, X., Kang, T., Huang, W., Wang, S. & Deng, W. 2013. Berberine Targets AP-2/hTERT, NF-kappaB/COX-2, HIF-1alpha/VEGF and Cytochrome-c/Caspase Signaling to Suppress Human Cancer Cell Growth. *PLoS ONE,* 8**,** e69240.

Fujiwaki, R., Iida, K., Kanasaki, H., Ozaki, T., Hata, K. & Miyazaki, K. 2002. Cyclooxygenase-2 expression in endometrial cancer: correlation with microvessel count

and expression of vascular endothelial growth factor and thymidine phosphorylase. *Human Pathology,* 33**,** 213-9.

Fukuda, K., Hibiya, Y., Mutoh, M., Koshiji, M., Akao, S. & Fujiwara, H. 1999. Inhibition by berberine of cyclooxygenase-2 transcriptional activity in human colon cancer cells. *J Ethnopharmacol,* 66**,** 227-33.

Furushima, K., Yamamoto, A., Nagano, T., Shibata, M., Miyachi, H., Abe, T., Ohshima, N., Kiyonari, H. & Aizawa, S. 2007. Mouse homologues of Shisa antagonistic to Wnt and Fgf signalings. *Developmental Biology,* 306**,** 480-92.

Gadue, P., Huber, T. L., Nostro, M. C., Kattman, S. & Keller, G. M. 2005. Germ layer induction from embryonic stem cells. *Experimental Hematology,* 33**,** 955-64.

Gao, J., Yan, X. L., Li, R., Liu, Y., He, W., Sun, S., Zhang, Y., Liu, B., Xiong, J. & Mao, N. 2010. Characterization of OP9 as authentic mesenchymal stem cell line. *J Genet Genomics,* 37**,** 475-82.

George, A. L., Bangalore-Prakash, P., Rajoria, S., Suriano, R., Shanmugam, A., Mittelman, A. & Tiwari, R. K. 2011. Endothelial progenitor cell biology in disease and tissue regeneration. *J Hematol Oncol,* 4**,** 24.

Gering, M., Rodaway, A. R., Gottgens, B., Patient, R. K. & Green, A. R. 1998. The SCL gene specifies haemangioblast development from early mesoderm. *EMBO J,* 17**,** 4029-45.

Geti, I., Ormiston, M. L., Rouhani, F., Toshner, M., Movassagh, M., Nichols, J., Mansfield, W., Southwood, M., Bradley, A., Rana, A. A., Vallier, L. & Morrell, N. W. 2012. A practical and efficient cellular substrate for the generation of induced pluripotent stem cells from adults: blood-derived endothelial progenitor cells. *Stem Cells Transl Med,* 1**,** 855-65.

Ghosh, D. & Sengupta, J. 2005. Target-oriented anti-implantation approaches for pregnancy interception: experiences in the rhesus monkey model. *Contraception,* 71**,** 294-301.

Giarratana, M. C., Kobari, L., Lapillonne, H., Chalmers, D., Kiger, L., Cynober, T., Marden, M. C., Wajcman, H. & Douay, L. 2005. Ex vivo generation of fully mature human red blood cells from hematopoietic stem cells. *Nat Biotechnol,* 23**,** 69-74.

Gitton, Y., Dahmane, N., Baik, S., Altaba, A. R. I., Neidhardt, L., Scholze, M., Herrmann, B. G., Kahlem, P., Benkahla, A., Schrinner, S., Yildirimman, R., Herwig, R., Lehrach, H., Yaspo, M. L. & Initiative, H. E. M. 2002. A gene expression map of human chromosome 21 orthologues in the mouse. *Nature,* 420**,** 586-590.

Gluecksohn-Schoenheimer, S. 1944. The Development of Normal and Homozygous Brachy (T/T) Mouse Embryos in the Extraembryonic Coelom of the Chick. *Proc Natl Acad Sci U S A,* 30**,** 134-140.

Gombert, M., Dieu-Nosjean, M.-C., Winterberg, F., Bünemann, E., Kubitza, R. C., Da Cunha, L., Haahtela, A., Lehtimäki, S., Müller, A., Rieker, J., Meller, S., Pivarcsi, A., Koreck, A., Fridman, W.-H., Zentgraf, H.-W., Pavenstädt, H., Amara, A., Caux, C., Kemeny, L., Alenius, H., Lauerma, A., Ruzicka, T., Zlotnik, A. & Homey, B. 2005. CCL1-CCR8 Interactions: An Axis Mediating the Recruitment of T Cells and Langerhans-Type Dendritic Cells to Sites of Atopic Skin Inflammation. *The Journal of Immunology,* 174**,** 5082-5091.

Gordon, J. D., Shifren, J. L., Foulk, R. A., Taylor, R. N. & Jaffe, R. B. 1995. Angiogenesis in the human female reproductive tract. *Obstet Gynecol Surv,* 50**,** 688-97.

Gore, A., Li, Z., Fung, H. L., Young, J. E., Agarwal, S., Antosiewicz-Bourget, J., Canto, I., Giorgetti, A., Israel, M. A., Kiskinis, E., Lee, J. H., Loh, Y. H., Manos, P. D., Montserrat, N., Panopoulos, A. D., Ruiz, S., Wilbert, M. L., Yu, J., Kirkness, E. F., Izpisua Belmonte, J. C., Rossi, D. J., Thomson, J. A., Eggan, K., Daley, G. Q., Goldstein, L. S. & Zhang, K. 2011. Somatic coding mutations in human induced pluripotent stem cells. *Nature,* 471**,** 63-7.

Gottgens, B., Nastos, A., Kinston, S., Piltz, S., Delabesse, E. C., Stanley, M., Sanchez, M. J., Ciau-Uitz, A., Patient, R. & Green, A. R. 2002. Establishing the transcriptional programme for blood: the SCL stem cell enhancer is regulated by a multiprotein complex containing Ets and GATA factors. *EMBO J,* 21**,** 3039-50.

Grossmann, V., Bacher, U., Kohlmann, A., Butschalowski, K., Roller, A., Jeromin, S., Dicker, F., Kern, W., Schnittger, S., Haferlach, T. & Haferlach, C. 2012. Expression of CEBPA is reduced in RUNX1-mutated acute myeloid leukemia. *Blood Cancer Journal,* 2**,** e86.

Hall, J. G., Levin, J., Kuhn, J. P., Ottenheimer, E. J., Van Berkum, K. A. & Mckusick, V. A. 1969. Thrombocytopenia with absent radius (TAR). *Medicine (Baltimore),* 48**,** 411-39.

Hamsa, T. P. & Kuttan, G. 2012. Antiangiogenic activity of berberine is mediated through the downregulation of hypoxia-inducible factor-1, VEGF, and proinflammatory mediators. *Drug Chem Toxicol,* 35**,** 57-70.

Harvey, S. A., Tumpel, S., Dubrulle, J., Schier, A. F. & Smith, J. C. 2010. no tail integrates two modes of mesoderm induction. *Development,* 137**,** 1127-35.

Hasan, J., Shnyder, S. D., Bibby, M., Double, J. A., Bicknel, R. & Jayson, G. C. 2004. Quantitative angiogenesis assays in vivo--a review. *Angiogenesis,* 7**,** 1-16.

Hashimoto, I., Kodama, J., Seki, N., Hongo, A., Miyagi, Y., Yoshinouchi, M. & Kudo, T. 2000. Macrophage infiltration and angiogenesis in endometrial cancer. *Anticancer Res,* 20**,** 4853-6.

Hawkins, E. D. & Lo Celso, C. 2013. Subdivision of bone marrow microenvironments: purpose built homes for haematopoietic stem cells. *EMBO J,* 32**,** 176-7.

Hayami, Y., Iida, S., Nakazawa, N., Hanamura, I., Kato, M., Komatsu, H., Miura, I., Dave, B. J., Sanger, W. G., Lim, B., Taniwaki, M. & Ueda, R. 2003. Inactivation of the E3/LAPTm5 gene by chromosomal rearrangement and DNA methylation in human multiple myeloma. *Leukemia,* 17**,** 1650-7.

Hecksher-Sorensen, J., Watson, R. P., Lettice, L. A., Serup, P., Eley, L., De Angelis, C., Ahlgren, U. & Hill, R. E. 2004. The splanchnic mesodermal plate directs spleen and pancreatic laterality, and is regulated by Bapx1/Nkx3.2. *Development,* 131**,** 4665-75.

Henderson, R. B., Grys, K., Vehlow, A., De Bettignies, C., Zachacz, A., Henley, T., Turner, M., Batista, F. & Tybulewicz, V. L. 2010. A novel Rac-dependent checkpoint in

B cell development controls entry into the splenic white pulp and cell survival. *J Exp Med,* 207**,** 837-53.

Herrmann, B. G., Labeit, S., Poustka, A., King, T. R. & Lehrach, H. 1990. Cloning of the T gene required in mesoderm formation in the mouse. *Nature,* 343**,** 617-22.

Hesslein, D. G., Fretz, J. A., Xi, Y., Nelson, T., Zhou, S., Lorenzo, J. A., Schatz, D. G. & Horowitz, M. C. 2009. Ebf1-dependent control of the osteoblast and adipocyte lineages. *Bone,* 44**,** 537-46.

Himburg, H. A., Muramoto, G. G., Daher, P., Meadows, S. K., Russell, J. L., Doan, P., Chi, J. T., Salter, A. B., Lento, W. E., Reya, T., Chao, N. J. & Chute, J. P. 2010. Pleiotrophin regulates the expansion and regeneration of hematopoietic stem cells. *Nature Methods,* 16**,** 475-82.

Hoeben, A., Landuyt, B., Highley, M. S., Wildiers, H., Van Oosterom, A. T. & De Bruijn, E. A. 2004. Vascular endothelial growth factor and angiogenesis. *Pharmacological Reviews,* 56**,** 549-80.

Holash, J., Maisonpierre, P. C., Compton, D., Boland, P., Alexander, C. R., Zagzag, D., Yancopoulos, G. D. & Wiegand, S. J. 1999. Vessel cooption, regression, and growth in tumors mediated by angiopoietins and VEGF. *Science,* 284**,** 1994-8.

Holland, C. M., Day, K., Evans, A. & Smith, S. K. 2003. Expression of the VEGF and angiopoietin genes in endometrial atypical hyperplasia and endometrial cancer. *Br J Cancer,* 89**,** 891-8.

Holland, C. M., Saidi, S. A., Evans, A. L., Sharkey, A. M., Latimer, J. A., Crawford, R. A., Charnock-Jones, D. S., Print, C. G. & Smith, S. K. 2004. Transcriptome analysis of endometrial cancer identifies peroxisome proliferator-activated receptors as potential therapeutic targets. *Mol Cancer Ther,* 3**,** 993-1001.

Hovanes, K., Li, T. W., Munguia, J. E., Truong, T., Milovanovic, T., Lawrence Marsh, J., Holcombe, R. F. & Waterman, M. L. 2001. Beta-catenin-sensitive isoforms of lymphoid enhancer factor-1 are selectively expressed in colon cancer. *Nature Genetics,* 28**,** 53-7.

Hua, H., Li, M., Luo, T., Yin, Y. & Jiang, Y. 2011. Matrix metalloproteinases in tumorigenesis: an evolving paradigm. *Cell Mol Life Sci,* 68**,** 3853-68.

Huang, H. & Cantor, A. B. 2009. Common features of megakaryocytes and hematopoietic stem cells: what's the connection? *J Cell Biochem,* 107**,** 857-64.

Huber, T. L., Kouskoff, V., Fehling, H. J., Palis, J. & Keller, G. 2004. Haemangioblast commitment is initiated in the primitive streak of the mouse embryo. *Nature,* 432**,** 625-30.

Huminiecki, L., Gorn, M., Suchting, S., Poulsom, R. & Bicknell, R. 2002. Magic roundabout is a new member of the roundabout receptor family that is endothelial specific and expressed at sites of active angiogenesis. *Genomics,* 79**,** 547-52.

Hunter, A. J., Ottoson, N., Boerth, N., Koretzky, G. A. & Shimizu, Y. 2000. Cutting edge: A novel function for the SLAP-130/FYB adapter protein in beta(1) integrin signaling and T lymphocyte migration. *Journal of Immunology,* 164**,** 1143-1147.

Hussein, S. M., Batada, N. N., Vuoristo, S., Ching, R. W., Autio, R., Narva, E., Ng, S., Sourour, M., Hamalainen, R., Olsson, C., Lundin, K., Mikkola, M., Trokovic, R., Peitz, M., Brustle, O., Bazett-Jones, D. P., Alitalo, K., Lahesmaa, R., Nagy, A. & Otonkoski, T. 2011. Copy number variation and selection during reprogramming to pluripotency. *Nature,* 471**,** 58-62.

Hwang, Y. S., Chung, B. G., Ortmann, D., Hattori, N., Moeller, H. C. & Khademhosseini, A. 2009. Microwell-mediated control of embryoid body size regulates embryonic stem cell fate via differential expression of WNT5a and WNT11. *Proc Natl Acad Sci U S A,* 106**,** 16978-83.

Inaba, N., Hiruma, T., Togayachi, A., Iwasaki, H., Wang, X. H., Furukawa, Y., Sumi, R., Kudo, T., Fujimura, K., Iwai, T., Gotoh, M., Nakamura, M. & Narimatsu, H. 2003. A novel I-branching beta-1,6-N-acetylglucosaminyltransferase involved in human blood group I antigen expression. *Blood,* 101**,** 2870-2876.

Ingersoll, R. G., Paznekas, W. A., Tran, A. K., Scott, A. F., Jiang, G. & Jabs, E. W. 2001. Fibroblast growth factor receptor 2 (FGFR2): genomic sequence and variations. *Cytogenetics and Cell Genetics,* 94**,** 121-6.

Ishiguro, H., Furukawa, Y., Daigo, Y., Miyoshi, Y., Nagasawa, Y., Nishiwaki, T., Kawasoe, T., Fujita, M., Satoh, S., Miwa, N., Fujii, Y. & Nakamura, Y. 2000. Isolation and characterization of human NBL4, a gene involved in the beta-catenin/Tcf signaling pathway. *Japanese Journal of Cancer Research,* 91**,** 597-603.

Jackson, M. R., Carney, E. W., Lye, S. J. & Ritchie, J. W. 1994. Localization of two angiogenic growth factors (PDECGF and VEGF) in human placentae throughout gestation. *Placenta,* 15**,** 341-53.

Jacobs-Cohen, R. J., Spiegelman, M. & Bennett, D. 1984. Abnormalities of cells and extracellular matrix of T/Tembryos. *Differentiation,* 25**,** 48-55.

Jaffe, E. A., Nachman, R. L., Becker, C. G. & Minick, C. R. 1973. Culture of human endothelial cells derived from umbilical veins. Identification by morphologic and immunologic criteria. *J Clin Invest,* 52**,** 2745-56.

Jaquemar, D., Kupriyanov, S., Wankell, M., Avis, J., Benirschke, K., Baribault, H. & Oshima, R. G. 2003. Keratin 8 protection of placental barrier function. *J Cell Biol,* 161**,** 749-56.

Johnson, K. R., Longo-Guess, C. M. & Gagnon, L. H. 2012. Mutations of the mouse ELMO domain containing 1 gene (Elmod1) link small GTPase signaling to actin cytoskeleton dynamics in hair cell stereocilia. *PLoS ONE,* 7**,** e36074.

Jones, C. A., London, N. R., Chen, H., Park, K. W., Sauvaget, D., Stockton, R. A., Wythe, J. D., Suh, W., Larrieu-Lahargue, F., Mukouyama, Y. S., Lindblom, P., Seth, P., Frias, A., Nishiya, N., Ginsberg, M. H., Gerhardt, H., Zhang, K. & Li, D. Y. 2008. Robo4 stabilizes the vascular network by inhibiting pathologic angiogenesis and endothelial hyperpermeability. *Nature Methods,* 14**,** 448-53.

Kahr, W. H., Hinckley, J., Li, L., Schwertz, H., Christensen, H., Rowley, J. W., Pluthero, F. G., Urban, D., Fabbro, S., Nixon, B., Gadzinski, R., Storck, M., Wang, K., Ryu, G. Y., Jobe, S. M., Schutte, B. C., Moseley, J., Loughran, N. B., Parkinson, J., Weyrich, A. S. & Di Paola, J. 2011. Mutations in NBEAL2, encoding a BEACH protein, cause gray platelet syndrome. *Nature Genetics,* 43**,** 738-40.

Kaku, T., Kamura, T., Kinukawa, N., Kobayashi, H., Sakai, K., Tsuruchi, N., Saito, T., Kawauchi, S., Tsuneyoshi, M. & Nakano, H. 1997. Angiogenesis in endometrial carcinoma. *Cancer,* 80**,** 741-7.

Kanatsu, M. & Nishikawa, S. I. 1996. In vitro analysis of epiblast tissue potency for hematopoietic cell differentiation. *Development,* 122**,** 823-30.

Kanteti, R., Nallasura, V., Loganathan, S., Tretiakova, M., Kroll, T., Krishnaswamy, S., Faoro, L., Cagle, P., Husain, A. N., Vokes, E. E., Lang, D. & Salgia, R. 2009. PAX5 is expressed in small-cell lung cancer and positively regulates c-Met transcription. *Lab Invest,* 89**,** 301-14.

Kardel, M. D. & Eaves, C. J. 2012. Modeling human hematopoietic cell development from pluripotent stem cells. *Experimental Hematology,* 40**,** 601-11.

Karst, A. M., Levanon, K., Duraisamy, S., Liu, J. F., Hirsch, M. S., Hecht, J. L. & Drapkin, R. 2011. Stathmin 1, a marker of PI3K pathway activation and regulator of microtubule dynamics, is expressed in early pelvic serous carcinomas. *Gynecologic Oncology,* 123**,** 5-12.

Kaufman, R. M., Airo, R., Pollack, S. & Crosby, W. H. 1965. Circulating megakaryocytes and platelet release in the lung. *Blood,* 26**,** 720-31.

Kaushansky, K. 2008. Historical review: megakaryopoiesis and thrombopoiesis. *Blood,* 111**,** 981-6.

Kawamata, N., Miki, T., Ohashi, K., Suzuki, K., Fukuda, T., Hirosawa, S. & Aoki, N. 1994. Recognition DNA sequence of a novel putative transcription factor, BCL6. *Biochem Biophys Res Commun,* 204**,** 366-74.

Keller, G., Kennedy, M., Papayannopoulou, T. & Wiles, M. V. 1993. Hematopoietic commitment during embryonic stem cell differentiation in culture. *Mol Cell Biol,* 13**,** 473-86.

Kennedy, M., Firpo, M., Choi, K., Wall, C., Robertson, S., Kabrun, N. & Keller, G. 1997. A common precursor for primitive erythropoiesis and definitive haematopoiesis. *Nature,* 386**,** 488-93.

Kerr, J. F., Wyllie, A. H. & Currie, A. R. 1972. Apoptosis: a basic biological phenomenon with wide-ranging implications in tissue kinetics. *Br J Cancer,* 26**,** 239-57.

Kibar, Z., Torban, E., Mcdearmid, J. R., Reynolds, A., Berghout, J., Mathieu, M., Kirillova, I., De Marco, P., Merello, E., Hayes, J. M., Wallingford, J. B., Drapeau, P., Capra, V. & Gros, P. 2007. Mutations in VANGL1 Associated with Neural-Tube Defects. *New England Journal of Medicine,* 356**,** 1432-1437.

Kilic, N., Feldhaus, S., Kilic, E., Tennstedt, P., Wicklein, D., Wasielewski, R., Viebahn, C., Kreipe, H. & Schumacher, U. 2011. Brachyury expression predicts poor prognosis at early stages of colorectal cancer. *European Journal of Cancer,* 47**,** 1080-5.

Kim, H. S., Hwang, K. K., Seo, J. W., Kim, S. Y., Oh, B. H., Lee, M. M. & Park, Y. B. 2000. Apoptosis and regulation of Bax and Bcl-X proteins during human neonatal vascular remodeling. *Arterioscler Thromb Vasc Biol,* 20**,** 957-63.

Kimmel, C. B., Ballard, W. W., Kimmel, S. R., Ullmann, B. & Schilling, T. F. 1995. Stages of embryonic development of the zebrafish. *Developmental Dynamics,* 203**,** 253-310.

King, A. E., Critchley, H. O. & Kelly, R. W. 2001. The NF-kappaB pathway in human endometrium and first trimester decidua. *Mol Hum Reprod,* 7**,** 175-83.

King, T., Beddington, R. S. & Brown, N. A. 1998. The role of the brachyury gene in heart development and left-right specification in the mouse. *Mech Dev,* 79**,** 29-37.

Kispert, A. & Hermann, B. G. 1993. The Brachyury gene encodes a novel DNA binding protein. *EMBO J,* 12**,** 3211-3220.

Knapp, P., Chabowski, A., Blachnio-Zabielska, A., Jarzabek, K. & Wolczynski, S. 2012. Altered peroxisome-proliferator activated receptors expression in human endometrial cancer. *PPAR Res,* 2012**,** 471524.

Kodama, H., Nose, M., Niida, S., Nishikawa, S. & Nishikawa, S. 1994. Involvement of the c-kit receptor in the adhesion of hematopoietic stem cells to stromal cells. *Experimental Hematology,* 22**,** 979-84.

Kol, S., Ben-Shlomo, I., Payne, D. W., Ando, M., Rohan, R. M. & Adashi, E. Y. 1998. Glucocorticoids suppress basal (but not interleukin-1-supported) ovarian phospholipase A2 activity: evidence for glucocorticoid receptor-mediated regulation. *Mol Cell Endocrinol,* 137**,** 117-25.

Kong, W., Wei, J., Abidi, P., Lin, M., Inaba, S., Li, C., Wang, Y., Wang, Z., Si, S., Pan, H., Wang, S., Wu, J., Li, Z., Liu, J. & Jiang, J. D. 2004. Berberine is a novel cholesterol-lowering drug working through a unique mechanism distinct from statins. *Nature Methods,* 10**,** 1344-51.

Korhonen, J., Polvi, A., Partanen, J. & Alitalo, K. 1994. The mouse tie receptor tyrosine kinase gene: expression during embryonic angiogenesis. *Oncogene,* 9**,** 395-403.

Kowalski, P. J., Rubin, M. A. & Kleer, C. G. 2003. E-cadherin expression in primary carcinomas of the breast and its distant metastases. *Breast Cancer Res,* 5**,** R217-22.

Krah, K., Mironov, V., Risau, W. & Flamme, I. 1994. Induction of vasculogenesis in quail blastodisc-derived embryoid bodies. *Dev Biol,* 164**,** 123-32.

Kruse, E. A., Loughran, S. J., Baldwin, T. M., Josefsson, E. C., Ellis, S., Watson, D. K., Nurden, P., Metcalf, D., Hilton, D. J., Alexander, W. S. & Kile, B. T. 2009. Dual requirement for the ETS transcription factors Fli-1 and Erg in hematopoietic stem cells and the megakaryocyte lineage. *Proc Natl Acad Sci U S A,* 106**,** 13814-9.

Kubo, H. & Alitalo, K. 2003. The bloody fate of endothelial stem cells. *Genes & Development,* 17**,** 322-9.

Kut, C., Mac Gabhann, F. & Popel, A. S. 2007. Where is VEGF in the body? A meta-analysis of VEGF distribution in cancer. *Br J Cancer,* 97**,** 978-85.

Laiosa, C. V., Stadtfeld, M. & Graf, T. 2006. Determinants of lymphoid-myeloid lineage diversification. *Annu Rev Immunol,* 24**,** 705-38.

Lambert, M. P., Sullivan, S. K., Fuentes, R., French, D. L. & Poncz, M. 2013. Challenges and promises for the development of donor-independent platelet transfusions. *Blood,* 121**,** 3319-24.

Lancrin, C., Sroczynska, P., Serrano, A. G., Gandillet, A., Ferreras, C., Kouskoff, V. & Lacaud, G. 2009. Blood cell generation from the hemangioblast. *J Mol Med (Berl),* 88**,** 167-72.

Lashkari, D. A., Derisi, J. L., Mccusker, J. H., Namath, A. F., Gentile, C., Hwang, S. Y., Brown, P. O. & Davis, R. W. 1997. Yeast microarrays for genome wide parallel genetic and gene expression analysis. *Proc Natl Acad Sci U S A,* 94**,** 13057-62.

Le Bouteiller, P., Pizzato, N., Barakonyi, A. & Solier, C. 2003. HLA-G, pre-eclampsia, immunity and vascular events. *J Reprod Immunol,* 59**,** 219-34.

Lee, T. I., Johnstone, S. E. & Young, R. A. 2006a. Chromatin immunoprecipitation and microarray-based analysis of protein location. *Nature Protocols,* 1**,** 729-48.

Lee, Y. S., Kim, W. S., Kim, K. H., Yoon, M. J., Cho, H. J., Shen, Y., Ye, J. M., Lee, C. H., Oh, W. K., Kim, C. T., Hohnen-Behrens, C., Gosby, A., Kraegen, E. W., James, D. E. & Kim, J. B. 2006b. Berberine, a natural plant product, activates AMP-activated protein kinase with beneficial metabolic effects in diabetic and insulin-resistant states. *Diabetes,* 55**,** 2256-64.

Leimeister, C., Dale, K., Fischer, A., Klamt, B., Hrabe De Angelis, M., Radtke, F., Mcgrew, M. J., Pourquie, O. & Gessler, M. 2000. Oscillating expression of c-Hey2 in the presomitic mesoderm suggests that the segmentation clock may use combinatorial signaling through multiple interacting bHLH factors. *Developmental Biology,* 227**,** 91-103.

Leonhardt, S. A., Boonyaratanakornkit, V. & Edwards, D. P. 2003. Progesterone receptor transcription and non-transcription signaling mechanisms. *Steroids,* 68**,** 761-770.

Leonhardt, S. A. & Edwards, D. P. 2002. Mechanism of action of progesterone antagonists. *Experimental Biological Medicine* 227**,** 969-80.

Li, P. T., Liao, C. J., Wu, W. G., Yu, L. C. & Chu, S. T. 2011. Progesterone-regulated B4galnt2 expression is a requirement for embryo implantation in mice. *Fertility and Sterility,* 95**,** 2404-9, 2409 e1-3.

Lin, S., Tsai, S. C., Lee, C. C., Wang, B. W., Liou, J. Y. & Shyu, K. G. 2004. Berberine inhibits HIF-1alpha expression via enhanced proteolysis. *Mol Pharmacol,* 66**,** 612-9.

Lister, R., Pelizzola, M., Kida, Y. S., Hawkins, R. D., Nery, J. R., Hon, G., Antosiewicz-Bourget, J., O'malley, R., Castanon, R., Klugman, S., Downes, M., Yu, R., Stewart, R., Ren, B., Thomson, J. A., Evans, R. M. & Ecker, J. R. 2011. Hotspots of aberrant epigenomic reprogramming in human induced pluripotent stem cells. *Nature,* 471**,** 68-73.

Littman, A. J., Beresford, S. A. & White, E. 2001. The association of dietary fat and plant foods with endometrial cancer (United States). *Cancer Causes Control,* 12**,** 691-702.

Liu, J. & Mayne, R. 1996. The complete cDNA coding sequence and tissue-specific expression of the mouse laminin alpha 4 chain. *Matrix Biol,* 15**,** 433-7.

Liu, J. C., Chan, P., Chen, Y. J., Tomlinson, B., Hong, S. H. & Cheng, J. T. 1999. The antihypertensive effect of the berberine derivative 6-protoberberine in spontaneously hypertensive rats. *Pharmacology,* 59**,** 283-9.

Loughran, S. J., Kruse, E. A., Hacking, D. F., De Graaf, C. A., Hyland, C. D., Willson, T. A., Henley, K. J., Ellis, S., Voss, A. K., Metcalf, D., Hilton, D. J., Alexander, W. S. & Kile, B. T. 2008. The transcription factor Erg is essential for definitive hematopoiesis and the function of adult hematopoietic stem cells. *Nat Immunol,* 9**,** 810-9.

Lu, S. J., Feng, Q., Caballero, S., Chen, Y., Moore, M. A., Grant, M. B. & Lanza, R. 2007. Generation of functional hemangioblasts from human embryonic stem cells. *Nature Methods,* 4**,** 501-9.

Machlus, K. R. & Italiano, J. E., Jr. 2013. The incredible journey: From megakaryocyte development to platelet formation. *J Cell Biol,* 201**,** 785-96.

Maekawa, M., Yamamoto, T., Tanoue, T., Yuasa, Y., Chisaka, O. & Nishida, E. 2005. Requirement of the MAP kinase signaling pathways for mouse preimplantation development. *Development,* 132**,** 1773-83.

Maines-Bandiera, S., Woo, M. M., Borugian, M., Molday, L. L., Hii, T., Gilks, B., Leung, P. C., Molday, R. S. & Auersperg, N. 2010. Oviductal glycoprotein (OVGP1, MUC9): a differentiation-based mucin present in serum of women with ovarian cancer. *International Journal of Gynecological Cancer,* 20**,** 16-22.

Maisonpierre, P. C., Suri, C., Jones, P. F., Bartunkova, S., Wiegand, S. J., Radziejewski, C., Compton, D., Mcclain, J., Aldrich, T. H., Papadopoulos, N., Daly, T. J., Davis, S., Sato, T. N. & Yancopoulos, G. D. 1997. Angiopoietin-2, a natural antagonist for Tie2 that disrupts in vivo angiogenesis. *Science,* 277**,** 55-60.

Maloney, M. A. & Patt, H. M. 1975. On the Origin of Hematopoietic Stem Cells after Local Marrow Extirpation. *Experimental Biology and Medicine,* 149**,** 94-97.

Mantena, S. K., Sharma, S. D. & Katiyar, S. K. 2006a. Berberine inhibits growth, induces G1 arrest and apoptosis in human epidermoid carcinoma A431 cells by regulating Cdki-Cdk-cyclin cascade, disruption of mitochondrial membrane potential and cleavage of caspase 3 and PARP. *Carcinogenesis,* 27**,** 2018-27.

Mantena, S. K., Sharma, S. D. & Katiyar, S. K. 2006b. Berberine, a natural product, induces G1-phase cell cycle arrest and caspase-3-dependent apoptosis in human prostate carcinoma cells. *Mol Cancer Ther,* 5**,** 296-308.

Mantovani, A., Sozzani, S., Locati, M., Allavena, P. & Sica, A. 2002. Macrophage polarization: tumor-associated macrophages as a paradigm for polarized M2 mononuclear phagocytes. *Trends Immunol,* 23**,** 549-55.

Marles, R. J. & Farnsworth, N. R. 1995. Antidiabetic plants and their active constituents. *Phytomedicine,* 2**,** 137-89.

Martin, B. L. & Kimelman, D. 2008. Regulation of Canonical Wnt Signaling by Brachyury Is Essential for Posterior Mesoderm Formation *Developmental Cell,* 15**,** 121-133.

Martin, G. R. & Evans, M. J. 1975. Differentiation of clonal lines of teratocarcinoma cells: formation of embryoid bodies in vitro. *Proc Natl Acad Sci U S A,* 72**,** 1441-5.

Masur, K., Schwartz, F., Entschladen, F., Niggemann, B. & Zaenker, K. S. 2006. DPPIV inhibitors extend GLP-2 mediated tumour promoting effects on intestinal cancer cells. *Regulatory Peptides,* 137**,** 147-55.

Mcconkey, D. J. & Orrenius, S. 1997. The role of calcium in the regulation of apoptosis. *Biochem Biophys Res Commun,* 239**,** 357-66.

Mcgrath, E., Ryan, E. J., Lynch, L., Golden-Mason, L., Mooney, E., Eogan, M., O'herlihy, C. & O'farrelly, C. 2009. Changes in endometrial natural killer cell expression of CD94, CD158a and CD158b are associated with infertility. *American Journal of Reproductive Immunology,* 61**,** 265-76.

Mcgrath, K. E. & Palis, J. 2005. Hematopoiesis in the yolk sac: more than meets the eye. *Experimental Hematology,* 33**,** 1021-8.

Mclaren, J. 2000. Vascular endothelial growth factor and endometriotic angiogenesis. *Human Reproduction Update,* 6**,** 45-55.

Mclaren, J., Prentice, A., Charnock-Jones, D. S., Millican, S. A., Muller, K. H., Sharkey, A. M. & Smith, S. K. 1996. Vascular endothelial growth factor is produced by peritoneal fluid macrophages in endometriosis and is regulated by ovarian steroids. *J Clin Invest,* 98**,** 482-9.

Mehta, P. B., Jenkins, B. L., Mccarthy, L., Thilak, L., Robson, C. N., Neal, D. E. & Leung, H. Y. 2003. MEK5 overexpression is associated with metastatic prostate cancer, and stimulates proliferation, MMP-9 expression and invasion. *Oncogene,* 22**,** 1381-9.

Meister, M. & Lagueux, M. 2003. Drosophila blood cells. *Cellular Microbiology,* 5**,** 573-80.

Messner, H. A. & Jamal, N. 1993. Cell culture assessment of hematopoietic progenitors in bone marrow transplantation. *J Hematother,* 2**,** 19-25.

Minot, C. S. 1883. Origin of the Mesoderm. *Science,* 2**,** 815-818.

Mochly-Rosen, D., Smith, B. L., Chen, C. H., Disatnik, M. H. & Ron, D. 1995. Interaction of protein kinase C with RACK1, a receptor for activated C-kinase: a role in beta protein kinase C mediated signal transduction. *Biochem Soc Trans,* 23**,** 596-600.

Mokhtar, N. M., Cheng, C.-W., Cook, E., Bielby, H., Smith, S. K. & Charnock-Jones, D. S. 2010. Progestin regulates chemokine (C-X-C motif) ligand 14 transcript level in human endometrium. *Mol Hum Reprod,* 16**,** 170-177.

Morgan, J. P., Delnero, P. F., Zheng, Y., Verbridge, S. S., Chen, J., Craven, M., Choi, N. W., Diaz-Santana, A., Kermani, P., Hempstead, B., Lopez, J. A., Corso, T. N., Fischbach, C. & Stroock, A. D. 2013. Formation of microvascular networks in vitro. *Nat Protoc,* 8**,** 1820-36.

Morley, R. H., Lachani, K., Keefe, D., Gilchrist, M. J., Flicek, P., Smith, J. C. & Wardle, F. C. 2009. A gene regulatory network directed by zebrafish No tail accounts for its roles in mesoderm formation. *Proc Natl Acad Sci* 106**,** 3829-3834.

Moskow, J. J., Bullrich, F., Huebner, K., Daar, I. O. & Buchberg, A. M. 1995. Meis1, a PBX1-related homeobox gene involved in myeloid leukemia in BXH-2 mice. *Mol Cell Biol,* 15**,** 5434-43.

Mudgett, J. S., Ding, J., Guh-Siesel, L., Chartrain, N. A., Yang, L., Gopal, S. & Shen, M. M. 2000. Essential role for p38alpha mitogen-activated protein kinase in placental angiogenesis. *Proc Natl Acad Sci U S A,* 97**,** 10454-9.

Mueller, M. D., Vigne, J. L., Minchenko, A., Lebovic, D. I., Leitman, D. C. & Taylor, R. N. 2000. Regulation of vascular endothelial growth factor (VEGF) gene transcription by estrogen receptors alpha and beta. *Proc Natl Acad Sci U S A,* 97**,** 10972-7.

Muller, A. M., Medvinsky, A., Strouboulis, J., Grosveld, F. & Dzierzak, E. 1994. Development of hematopoietic stem cell activity in the mouse embryo. *Immunity,* 1**,** 291-301.

Murray, P. D. F. 1932. The Development in vitro of the Blood of the Early Chick Embryo. *Proceedings of the Royal Society Biological Sciences,* 111**,** 497-521.

Murthy, K. N. C., Jayaprakasha, G. K. & Patil, B. S. 2012. The natural alkaloid berberine targets multiple pathways to induce cell death in cultured human colon cancer cells. *European Journal of Pharmacology,* 688**,** 14-21.

Nagata, D., Mogi, M. & Walsh, K. 2003. AMP-activated protein kinase (AMPK) signaling in endothelial cells is essential for angiogenesis in response to hypoxic stress. *J Biol Chem,* 278**,** 31000-6.

Nagy, A., Rossant, J., Nagy, R., Abramow-Newerly, W. & Roder, J. C. 1993. Derivation of completely cell culture-derived mice from early-passage embryonic stem cells. *Proc Natl Acad Sci U S A,* 90**,** 8424-8.

Naiche, L. A., Harrelson, Z., Kelly, R. G. & Papaioannou, V. E. 2005. T-box genes in vertebrate development. *Annu Rev Genet,* 39**,** 219-39.

Nakagawa, Y., Nakamura, S., Nakajima, M., Endo, H., Dohda, T., Takayama, N., Nakauchi, H., Arai, F., Fukuda, T. & Eto, K. 2013. Two differential flows in a bioreactor promoted platelet generation from human pluripotent stem cell-derived megakaryocytes. *Experimental Hematology*.

Narod, S. A., Seth, A. & Nam, R. 2008. Fusion in the ETS gene family and prostate cancer. *Br J Cancer,* 99**,** 847-51.

Nelson, A. C., Pillay, N., Henderson, S., Presneau, N., Tirabosco, R., Halai, D., Berisha, F., Flicek, P., Stemple, D. L., Stern, C. D., Wardle, F. C. & Flanagan, A. M. 2012. An integrated functional genomics approach identifies the regulatory network directed by brachyury (T) in chordoma. *J Pathol,* 228**,** 274-85.

Nelson, W. J. & Nusse, R. 2004. Convergence of Wnt, {beta}-Catenin, and Cadherin Pathways. *Science,* 303**,** 1483-1487.

Ng, A. P., Loughran, S. J., Metcalf, D., Hyland, C. D., De Graaf, C. A., Hu, Y., Smyth, G. K., Hilton, D. J., Kile, B. T. & Alexander, W. S. 2011. Erg is required for self-renewal of hematopoietic stem cells during stress hematopoiesis in mice. *Blood,* 118**,** 2454-61.

Ng, E. S., Davis, R. P., Azzola, L., Stanley, E. G. & Elefanty, A. G. 2005. Forced aggregation of defined numbers of human embryonic stem cells into embryoid bodies fosters robust, reproducible hematopoietic differentiation. *Blood,* 106**,** 1601-3.

Nhsbt 2011. NHSBT Platelet Strategy 2011-2014 "Delivering for patients and donors". *In:* Nhsbt (ed.). NHS.

Nichols, J., Zevnik, B., Anastassiadis, K., Niwa, H., Klewe-Nebenius, D., Chambers, I., Scholer, H. & Smith, A. 1998. Formation of pluripotent stem cells in the mammalian embryo depends on the POU transcription factor Oct4. *Cell,* 95**,** 379-91.

Nickkho-Amiry, M., Mcvey, R. & Holland, C. 2012. Peroxisome proliferator-activated receptors modulate proliferation and angiogenesis in human endometrial carcinoma. *Mol Cancer Res,* 10**,** 441-53.

Nishida, M., Kasahara, K., Kaneko, M., Iwasak, I. H. & Hayashi, K. 1985. [Establishment of a new human endometrial adenocarcinoma cell line, Ishikawa cells, containing estrogen and progesterone receptors]. *Nihon Sanka Fujinka Gakkai zasshi* 37**,** 1103-11.

Nishimura, K., Sano, M., Ohtaka, M., Furuta, B., Umemura, Y., Nakajima, Y., Ikehara, Y., Kobayashi, T., Segawa, H., Takayasu, S., Sato, H., Motomura, K., Uchida, E., Kanayasu-Toyoda, T., Asashima, M., Nakauchi, H., Yamaguchi, T. & Nakanishi, M. 2011. Development of defective and persistent Sendai virus vector: a unique gene delivery/expression system ideal for cell reprogramming. *J Biol Chem,* 286**,** 4760-71.

Nislow, C., Lombillo, V. A., Kuriyama, R. & Mcintosh, J. R. 1992. A plus-end-directed motor enzyme that moves antiparallel microtubules in vitro localizes to the interzone of mitotic spindles. *Nature,* 359**,** 543-7.

Niwa, A., Umeda, K., Chang, H., Saito, M., Okita, K., Takahashi, K., Nakagawa, M., Yamanaka, S., Nakahata, T. & Heike, T. 2009. Orderly hematopoietic development of induced pluripotent stem cells via Flk-1(+) hemoangiogenic progenitors. *J Cell Physiol,* 221**,** 367-77.

Ohno, S., Ohno, Y., Suzuki, N., Kamei, T., Koike, K., Inagawa, H., Kohchi, C., Soma, G. & Inoue, M. 2004. Correlation of histological localization of tumor-associated macrophages with clinicopathological features in endometrial cancer. *Anticancer Res,* 24**,** 3335-42.

Oshima, Y., Deering, T., Oshima, S., Nambu, H., Reddy, P. S., Kaleko, M., Connelly, S., Hackett, S. F. & Campochiaro, P. A. 2004. Angiopoietin-2 enhances retinal vessel sensitivity to vascular endothelial growth factor. *J Cell Physiol,* 199**,** 412-7.

Palena, C., Polev, D. E., Tsang, K. Y., Fernando, R. I., Litzinger, M., Krukovskaya, L. L., Baranova, A. V., Kozlov, A. P. & Schlom, J. 2007. The human T-box mesodermal transcription factor Brachyury is a candidate target for T-cell-mediated cancer immunotherapy. *Clinical Cancer Research,* 13**,** 2471-8.

Park, D. W., Ryu, H. S., Choi, D. S., Park, Y. H., Chang, K. H. & Min, C. K. 2001. Localization of matrix metalloproteinases on endometrial cancer cell invasion in vitro. *Gynecol Oncol,* 82**,** 442-9.

Patt, H. M. & Maloney, M. A. 1972. Bone Formation and Resorption as a Requirement for Marrow Development. *Experimental Biology and Medicine,* 140**,** 205-207.

Pecina-Slaus, N. 2003. Tumor suppressor gene E-cadherin and its role in normal and malignant cells. *Cancer Cell International,* 3**,** 17.

Petrascheck, M., Escher, D., Mahmoudi, T., Verrijzer, C. P., Schaffner, W. & Barberis, A. 2005. DNA looping induced by a transcriptional enhancer in vivo. *Nucleic Acids Res,* 33**,** 3743-50.

Pillay, N., Plagnol, V., Tarpey, P. S., Lobo, S. B., Presneau, N., Szuhai, K., Halai, D., Berisha, F., Cannon, S. R., Mead, S., Kasperaviciute, D., Palmen, J., Talmud, P. J., Kindblom, L. G., Amary, M. F., Tirabosco, R. & Flanagan, A. M. 2012. A common single-nucleotide variant in T is strongly associated with chordoma. *Nature Genetics,* 44**,** 1185-7.

Pimanda, J. E., Donaldson, I. J., De Bruijn, M. F., Kinston, S., Knezevic, K., Huckle, L., Piltz, S., Landry, J. R., Green, A. R., Tannahill, D. & Gottgens, B. 2007a. The SCL transcriptional network and BMP signaling pathway interact to regulate RUNX1 activity. *Proc Natl Acad Sci U S A,* 104**,** 840-5.

Pimanda, J. E. & Gottgens, B. 2010. Gene regulatory networks governing haematopoietic stem cell development and identity. *The International Journal of Developmental Biology,* 54**,** 1201-11.

Pimanda, J. E., Ottersbach, K., Knezevic, K., Kinston, S., Chan, W. Y., Wilson, N. K., Landry, J. R., Wood, A. D., Kolb-Kokocinski, A., Green, A. R., Tannahill, D., Lacaud, G., Kouskoff, V. & Gottgens, B. 2007b. Gata2, Fli1, and Scl form a recursively wired gene-regulatory circuit during early hematopoietic development. *Proc Natl Acad Sci U S A,* 104**,** 17692-7.

Plate, K. H., Breier, G., Weich, H. A. & Risau, W. 1992. Vascular endothelial growth factor is a potential tumour angiogenesis factor in human gliomas in vivo. *Nature,* 359**,** 845-8.

Polakis, P. 2000. Wnt signaling and cancer. *Genes & Development,* 14**,** 1837-51.

Popsueva, A. E., Luchinskaya, N. N., Ludwig, A. V., Zinovjeva, O. Y., Poteryaev, D. A., Feigelman, M. M., Ponomarev, M. B., Berekelya, L. & Belyavsky, A. V. 2001. Overexpression of camello, a member of a novel protein family, reduces blastomere adhesion and inhibits gastrulation in Xenopus laevis. *Developmental Biology,* 234**,** 483-96.

Porcher, C., Swat, W., Rockwell, K., Fujiwara, Y., Alt, F. W. & Orkin, S. H. 1996. The T cell leukemia oncoprotein SCL/tal-1 is essential for development of all hematopoietic lineages. *Cell,* 86**,** 47-57.

Print, C., Valtola, R., Evans, A., Lessan, K., Malik, S. & Smith, S. 2004. Soluble factors from human endometrium promote angiogenesis and regulate the endothelial cell transcriptome. *Human Reproductive,* 19**,** 2356-66.

Qian, H., Buza-Vidas, N., Hyland, C. D., Jensen, C. T., Antonchuk, J., Mansson, R., Thoren, L. A., Ekblom, M., Alexander, W. S. & Jacobsen, S. E. 2007. Critical role of thrombopoietin in maintaining adult quiescent hematopoietic stem cells. *Cell Stem Cell,* 1**,** 671-84.

Quinn, T. P., Peters, K. G., De Vries, C., Ferrara, N. & Williams, L. T. 1993. Fetal liver kinase 1 is a receptor for vascular endothelial growth factor and is selectively expressed in vascular endothelium. *Proc Natl Acad Sci U S A,* 90**,** 7533-7.

Rabot, M., Tabiasco, J., Polgar, B., Aguerre-Girr, M., Berrebi, A., Bensussan, A., Strbo, N., Rukavina, D. & Le Bouteiller, P. 2005. HLA class I/NK cell receptor interaction in

early human decidua basalis: possible functional consequences. *Chem Immunol Allergy,* 89**,** 72-83.

Rada-Iglesias, A., Bajpai, R., Swigut, T., Brugmann, S. A., Flynn, R. A. & Wysocka, J. 2011. A unique chromatin signature uncovers early developmental enhancers in humans. *Nature,* 470**,** 279-83.

Ragone, G., Bresin, A., Piermarini, F., Lazzeri, C., Picchio, M. C., Remotti, D., Kang, S. M., Cooper, M. D., Croce, C. M., Narducci, M. G. & Russo, G. 2009. The Tcl1 oncogene defines secondary hair germ cells differentiation at catagen-telogen transition and affects stem-cell marker CD34 expression. *Oncogene,* 28**,** 1329-38.

Rajakumari, S., Wu, J., Ishibashi, J., Lim, H. W., Giang, A. H., Won, K. J., Reed, R. R. & Seale, P. 2013. EBF2 determines and maintains brown adipocyte identity. *Cell Metabolism,* 17**,** 562-74.

Reddy, V. A., Iwama, A., Iotzova, G., Schulz, M., Elsasser, A., Vangala, R. K., Tenen, D. G., Hiddemann, W. & Behre, G. 2002. Granulocyte inducer C/EBPalpha inactivates the myeloid master regulator PU.1: possible role in lineage commitment decisions. *Blood,* 100**,** 483-90.

Rodriguez, F. J., Lewis-Tuffin, L. J. & Anastasiadis, P. Z. 2012. E-cadherin's dark side: possible role in tumor progression. *Biochim Biophys Acta,* 1826**,** 23-31.

Roselli, M., Fernando, R. I., Guadagni, F., Spila, A., Alessandroni, J., Palmirotta, R., Costarelli, L., Litzinger, M., Hamilton, D., Huang, B., Tucker, J., Tsang, K. Y., Schlom, J. & Palena, C. 2012. Brachyury, a driver of the epithelial-mesenchymal transition, is overexpressed in human lung tumors: an opportunity for novel interventions against lung cancer. *Clinical Cancer Research,* 18**,** 3868-79.

Rossi, M., Sharkey, A. M., Vigano, P., Fiore, G., Furlong, R., Florio, P., Ambrosini, G., Smith, S. K. & Petraglia, F. 2005. Identification of genes regulated by interleukin-1beta in human endometrial stromal cells. *Reproduction,* 130**,** 721-9.

Russ, A. P., Wattler, S., Colledge, W. H., Aparicio, S. a. J. R., Carlton, M. B. L., Pearce, J. J., Barton, S. C., Surani, M. A., Ryan, K., Nehls, M. C., Wilson, V. & Evans, M. J.

2000. Eomesodermin is required for mouse trophoblast development and mesoderm formation. *Nature,* 404**,** 95-99.

Sabin, F. R. 1917. Preliminary note on the differentiation of angioblasts and the method by which they produce blood-vessels, blood-plasma and red blood-cells as seen in the living chick. *Anatomical Record,* 13**,** 199-204.

Saidi, S. A., Holland, C. M., Kreil, D. P., Mackay, D. J., Charnock-Jones, D. S., Print, C. G. & Smith, S. K. 2004. Independent component analysis of microarray data in the study of endometrial cancer. *Oncogene,* 23**,** 6677-83.

Sampson, J. A. 1927. Peritoneal endometriosis due to dissemination of endometrial tissue into the peritoneal cavity. *American Journal of Obstetrics and Gynecology,* 14 422-469.

Samuel, R., Daheron, L., Liao, S., Vardam, T., Kamoun, W. S., Batista, A., Buecker, C., Schafer, R., Han, X., Au, P., Scadden, D. T., Duda, D. G., Fukumura, D. & Jain, R. K. 2013. Generation of functionally competent and durable engineered blood vessels from human induced pluripotent stem cells. *Proc Natl Acad Sci U S A,* 110**,** 12774-9.

Santaguida, M., Schepers, K., King, B., Sabnis, A. J., Forsberg, E. C., Attema, J. L., Braun, B. S. & Passegue, E. 2009. JunB protects against myeloid malignancies by limiting hematopoietic stem cell proliferation and differentiation without affecting self-renewal. *Cancer Cell,* 15**,** 341-52.

Sarkar, D., Shields, B., Davies, M., Muller, J. & Wakeman, J. A. 2012. BRACHYURY confers cancer stem cell characteristics on colorectal cancer cells. *International Journal of Cancer,* 130**,** 328-337.

Sarkar, N. N. 2002. Mifepristone: bioavailability, pharmacokinetics and use-effectiveness. *Eur J Obstet Gynecol Reprod Biol,* 101**,** 113-20.

Sauer, H., Gunther, J., Hescheler, J. & Wartenberg, M. 2000. Thalidomide inhibits angiogenesis in embryoid bodies by the generation of hydroxyl radicals. *The American Journal of Pathology,* 156**,** 151-8.

Schoenfeld, J., Lessan, K., Johnson, N., Charnock-Jones, D., Evans, A., Vourvouhaki, E., Scott, L., Stephens, R., Freeman, T., Saidi, S., Tom, B., Weston, G., Rogers, P., Smith, S. & Print, C. 2004. Bioinformatic analysis of primary endothelial cell gene array data illustrated by the analysis of transcriptome changes in endothelial cells exposed to VEGF-A and PlGF. *Angiogenesis,* 7**,** 143-156.

Schofield, R. 1978. The relationship between the spleen colony-forming cell and the haemopoietic stem cell. *Blood Cells,* 4**,** 7-25.

Schulte-Merker, S., Ho, R. K., Herrmann, B. G. & Nusslein-Volhard, C. 1992. The protein product of the zebrafish homologue of the mouse T gene is expressed in nuclei of the germ ring and the notochord of the early embryo. *Development,* 116**,** 1021-32.

Schulte-Merker, S., Van Eeden, F. J., Halpern, M. E., Kimmel, C. B. & Nusslein-Volhard, C. 1994. no tail (ntl) is the zebrafish homologue of the mouse T (Brachyury) gene. *Development,* 120**,** 1009-15.

Seimiya, M., J, O. W., Bahar, R., Kawamura, K., Wang, Y., Saisho, H. & Tagawa, M. 2003. Stage-specific expression of Clast6/E3/LAPTM5 during B cell differentiation: elevated expression in human B lymphomas. *International Journal of Oncology,* 22**,** 301-4.

Sengupta, J., Lalitkumar, P. G., Najwa, A. R., Charnock-Jones, D. S., Evans, A. L., Sharkey, A. M., Smith, S. K. & Ghosh, D. 2007. Immunoneutralization of vascular endothelial growth factor inhibits pregnancy establishment in the rhesus monkey (Macaca mulatta). *Reproduction,* 133**,** 1199-211.

Serafim, T. L., Oliveira, P. J., Sardao, V. A., Perkins, E., Parke, D. & Holy, J. 2008. Different concentrations of berberine result in distinct cellular localization patterns and cell cycle effects in a melanoma cell line. *Cancer Chemother Pharmacol,* 61**,** 1007-18.

Shaffer, A. L., Yu, X., He, Y., Boldrick, J., Chan, E. P. & Staudt, L. M. 2000. BCL-6 represses genes that function in lymphocyte differentiation, inflammation, and cell cycle control. *Immunity,* 13**,** 199-212.

Shalaby, F., Ho, J., Stanford, W. L., Fischer, K. D., Schuh, A. C., Schwartz, L., Bernstein, A. & Rossant, J. 1997. A requirement for Flk1 in primitive and definitive hematopoiesis and vasculogenesis. *Cell,* 89**,** 981-90.

Shalaby, F., Rossant, J., Yamaguchi, T. P., Gertsenstein, M., Wu, X. F., Breitman, M. L. & Schuh, A. C. 1995. Failure of blood-island formation and vasculogenesis in Flk-1-deficient mice. *Nature,* 376**,** 62-6.

Sharkey, A. M., Day, K., Mcpherson, A., Malik, S., Licence, D., Smith, S. K. & Charnock-Jones, D. S. 2000. Vascular endothelial growth factor expression in human endometrium is regulated by hypoxia. *J Clin Endocrinol Metab,* 85**,** 402-9.

Sharkey, A. M., King, A., Clark, D. E., Burrows, T. D., Jokhi, P. P., Charnock-Jones, D. S., Loke, Y. W. & Smith, S. K. 1999. Localisation of leukaemia inhibitory factor and its receptor in human placenta throughout pregnancy. *Biology of Reproduction,* 60**,** 355-364.

Silberstein, G. B., Dressler, G. R. & Van Horn, K. 2002. Expression of the PAX2 oncogene in human breast cancer and its role in progesterone-dependent mammary growth. *Oncogene,* 21**,** 1009-16.

Silver, L. & Palis, J. 1997. Initiation of Murine Embryonic Erythropoiesis: A Spatial Analysis. *Blood,* 89**,** 1154-1164.

Simeone, A., D'apice, M. R., Nigro, V., Casanova, J., Graziani, F., Acampora, D. & Avantaggiato, V. 1994. Orthopedia, a novel homeobox-containing gene expressed in the developing CNS of both mouse and Drosophila. *Neuron,* 13**,** 83-101.

Singh, A., Duggal, S., Kaur, N. & Singh, J. 2010. Berberine: Alkaloid with wide spectrum of pharmacological activities. *Journal of Natural Products,* 3**,** 64-75.

Singh, T., Vaid, M., Katiyar, N., Sharma, S. & Katiyar, S. K. 2011. Berberine, an isoquinoline alkaloid, inhibits melanoma cancer cell migration by reducing the expressions of cyclooxygenase-2, prostaglandin E(2) and prostaglandin E(2) receptors. *Carcinogenesis,* 32**,** 86-92.

Skloot, R. 2010. *The immortal life of Henrietta Lacks,* Pan Macmillan, UK, Macmillan.

Smith, J. C., Price, B. M., Green, J. B., Weigel, D. & Herrmann, B. G. 1991. Expression of a Xenopus homolog of Brachyury (T) is an immediate-early response to mesoderm induction. *Cell,* 67**,** 79-87.

Smith, S. 2001. Regulation of angiogenesis in the endometrium. *Trends Endocrinol Metab,* 12**,** 147-51.

Smith, S. K., Charnock-Jones, D. S. & Sharkey, A. M. 1998. The role of leukemia inhibitory factor and interleukin-6 in human reproduction. *Hum Reprod,* 13 Suppl 3**,** 237-43; discussion 244-6.

Smith-Berdan, S., Schepers, K., Ly, A., Passegue, E. & Forsberg, E. C. 2012. Dynamic expression of the Robo ligand Slit2 in bone marrow cell populations. *Cell Cycle,* 11**,** 675-82.

Soeda, S., Nakamura, N., Ozeki, T., Nishiyama, H., Hojo, H., Yamada, H., Abe, M. & Sato, A. 2008. Tumor-associated macrophages correlate with vascular space invasion and myometrial invasion in endometrial carcinoma. *Gynecol Oncol,* 109**,** 122-8.

Somers, A., Jean, J. C., Sommer, C. A., Omari, A., Ford, C. C., Mills, J. A., Ying, L., Sommer, A. G., Jean, J. M., Smith, B. W., Lafyatis, R., Demierre, M. F., Weiss, D. J., French, D. L., Gadue, P., Murphy, G. J., Mostoslavsky, G. & Kotton, D. N. 2010. Generation of transgene-free lung disease-specific human induced pluripotent stem cells using a single excisable lentiviral stem cell cassette. *Stem Cells,* 28**,** 1728-40.

Spyropoulos, D. D., Pharr, P. N., Lavenburg, K. R., Jackers, P., Papas, T. S., Ogawa, M. & Watson, D. K. 2000. Hemorrhage, impaired hematopoiesis, and lethality in mouse embryos carrying a targeted disruption of the Fli1 transcription factor. *Mol Cell Biol,* 20**,** 5643-52.

Stainier, D. Y., Weinstein, B. M., Detrich, H. W., 3rd, Zon, L. I. & Fishman, M. C. 1995. Cloche, an early acting zebrafish gene, is required by both the endothelial and hematopoietic lineages. *Development,* 121**,** 3141-50.

Staton, C. A., Reed, M. W. & Brown, N. J. 2009. A critical analysis of current in vitro and in vivo angiogenesis assays. *International Journal of Experimental Pathology,* 90**,** 195-221.

Su, J. L., Yang, P. C., Shih, J. Y., Yang, C. Y., Wei, L. H., Hsieh, C. Y., Chou, C. H., Jeng, Y. M., Wang, M. Y., Chang, K. J., Hung, M. C. & Kuo, M. L. 2006. The VEGF-C/Flt-4 axis promotes invasion and metastasis of cancer cells. *Cancer Cell,* 9**,** 209-23.

Sugiyama, T., Kohara, H., Noda, M. & Nagasawa, T. 2006. Maintenance of the hematopoietic stem cell pool by CXCL12-CXCR4 chemokine signaling in bone marrow stromal cell niches. *Immunity,* 25**,** 977-88.

Suzuki, N., Labosky, P. A., Furuta, Y., Hargett, L., Dunn, R., Fogo, A. B., Takahara, K., Peters, D. M. P., Greenspan, D. S. & Hogan, B. L. M. 1996. Failure of ventral body wall closure in mouse embryos lacking a procollagen C-proteinase encoded by Bmp1, a mammalian gene related to Drosophila tolloid. *Development,* 122**,** 3587-3595.

Takahashi, K., Tanabe, K., Ohnuki, M., Narita, M., Ichisaka, T., Tomoda, K. & Yamanaka, S. 2007. Induction of pluripotent stem cells from adult human fibroblasts by defined factors. *Cell,* 131**,** 861-72.

Takahashi, K. & Yamanaka, S. 2006. Induction of Pluripotent Stem Cells from Mouse Embryonic and Adult Fibroblast Cultures by Defined Factors. *Cell,* 126**,** 663-676.

Takayama, N., Nishikii, H., Usui, J., Tsukui, H., Sawaguchi, A., Hiroyama, T., Eto, K. & Nakauchi, H. 2008. Generation of functional platelets from human embryonic stem cells in vitro via ES-sacs, VEGF-promoted structures that concentrate hematopoietic progenitors. *Blood,* 111**,** 5298-5306.

Takayama, N., Nishimura, S., Nakamura, S., Shimizu, T., Ohnishi, R., Endo, H., Yamaguchi, T., Otsu, M., Nishimura, K., Nakanishi, M., Sawaguchi, A., Nagai, R., Takahashi, K., Yamanaka, S., Nakauchi, H. & Eto, K. 2010. Transient activation of c-MYC expression is critical for efficient platelet generation from human induced pluripotent stem cells. *J Exp Med,* 207**,** 2817-30.

Tamura, M., Sebastian, S., Yang, S., Gurates, B., Ferrer, K., Sasano, H., Okamura, K. & Bulun, S. E. 2002. Up-regulation of cyclooxygenase-2 expression and prostaglandin synthesis in endometrial stromal cells by malignant endometrial epithelial cells. A paracrine effect mediated by prostaglandin E2 and nuclear factor-kappa B. *J Biol Chem,* 277**,** 26208-16.

Tan, K., Tamura, K., Lai, M., Veerakumarasivam, A., Nakanishi, Y., Ogawa, M. & Sugiyama, D. 2013. Molecular Pathways Governing Development of Vascular Endothelial Cells from ES/iPS Cells. *Stem Cell Reviews and Reports***,** 1-13.

Tang, Q., Jiang, X., Li, H., Lin, Z., Zhou, X., Luo, X., Liu, L. & Chen, G. 2011. Expression and prognostic value of WISP-1 in patients with endometrial endometrioid adenocarcinoma. *The Journal of Obstetrics and Gynaecology Research,* 37**,** 606-12.

Taresa, E., Kedei, N., Thomazy, V. & Fesus, L. 1992. An involucrin-like protein in hepatocytes serves as a substrate for tissue transglutaminase during apoptosis. *J Biol Chem,* 267**,** 25648-51.

Tavian, M. & Peault, B. 2005. Embryonic development of the human hematopoietic system. *The International Journal of Developmental Biology,* 49**,** 243-50.

Taylor, P. M. 2007. Biological matrices and bionanotechnology. *Philos Trans R Soc Lond B Biol Sci,* 362**,** 1313-20.

Technau, U. & Scholz, C. B. 2003. Origin and evolution of endoderm and mesoderm. *The International Journal of Developmental Biology,* 47**,** 531-9.

Teng, C. B., Diao, H. L., Ma, X. H., Xu, L. B. & Yang, Z. M. 2004. Differential expression and activation of Stat3 during mouse embryo implantation and decidualization. *Mol Reprod Dev,* 69**,** 1-10.

Thermes, V., Grabher, C., Ristoratore, F., Bourrat, F., Choulika, A., Wittbrodt, J. & Joly, J. S. 2002. I-SceI meganuclease mediates highly efficient transgenesis in fish. *Mech Dev,* 118**,** 91-8.

Tirabosco, R., Mangham, D. C., Rosenberg, A. E., Vujovic, S., Bousdras, K., Pizzolitto, S., De Maglio, G., Den Bakker, M. A., Di Francesco, L., Kalil, R. K., Athanasou, N. A., O'donnell, P., Mccarthy, E. F. & Flanagan, A. M. 2008. Brachyury expression in extra-axial skeletal and soft tissue chordomas: a marker that distinguishes chordoma from mixed tumor/myoepithelioma/parachordoma in soft tissue. *The American Journal of Surgical Pathology,* 32**,** 572-80.

Tirino, V., Desiderio, V., Paino, F., De Rosa, A., Papaccio, F., La Noce, M., Laino, L., De Francesco, F. & Papaccio, G. 2013. Cancer stem cells in solid tumors: an overview and new approaches for their isolation and characterization. *FASEB J,* 27**,** 13-24.

Tirnauer, J. S., Canman, J. C., Salmon, E. D. & Mitchison, T. J. 2002. EB1 targets to kinetochores with attached, polymerizing microtubules. *Mol Biol Cell,* 13**,** 4308-16.

Tong, B. J., Tan, J., Tajeda, L., Das, S. K., Chapman, J. A., Dubois, R. N. & Dey, S. K. 2000. Heightened expression of cyclooxygenase-2 and peroxisome proliferator-activated receptor-delta in human endometrial adenocarcinoma. *Neoplasia,* 2**,** 483-90.

Torry, D. S. & Torry, R. J. 1997. Angiogenesis and the expression of vascular endothelial growth factor in endometrium and placenta. *Am J Reprod Immunol,* 37**,** 21-9.

Toyofuku, T., Yabuki, M., Kamei, J., Kamei, M., Makino, N., Kumanogoh, A. & Hori, M. 2007. Semaphorin-4A, an activator for T-cell-mediated immunity, suppresses angiogenesis via Plexin-D1. *EMBO J,* 26**,** 1373-84.

Tusher, V. G., Tibshirani, R. & Chu, G. 2001. Significance analysis of microarrays applied to the ionizing radiation response. *Proc Natl Acad Sci U S A,* 98**,** 5116-21.

Ungrin, M. D., Joshi, C., Nica, A., Bauwens, C. L. & Zandstra, P. W. 2008. Reproducible, Ultra High-Throughput Formation of Multicellular Organization from Single Cell Suspension-Derived Human Embryonic Stem Cell Aggregates. *PLoS ONE,* 3**,** e1565.

Vailhe, B., Vittet, D. & Feige, J.-J. 2001. In-vitro models of vasculogenesis and angiogenesis. *Laboratory investigation,* 81**,** 439-452.

Van Den Bogert, C., Van Kernebeek, G., De Leij, L. & Kroon, A. M. 1986. Inhibition of mitochondrial protein synthesis leads to proliferation arrest in the G1-phase of the cell cycle. *Cancer Lett,* 32**,** 41-51.

Vandenberg, L. N. & Levin, M. 2013. A unified model for left-right asymmetry? Comparison and synthesis of molecular models of embryonic laterality. *Developmental Biology*.

Vecchi, A., Garlanda, C., Lampugnani, M. G., Resnati, M., Matteucci, C., Stoppacciaro, A., Schnurch, H., Risau, W., Ruco, L., Mantovani, A. & Et Al. 1994. Monoclonal antibodies specific for endothelial cells of mouse blood vessels. Their application in the identification of adult and embryonic endothelium. *Eur J Cell Biol,* 63**,** 247-54.

Velculescu, V. E., Zhang, L., Vogelstein, B. & Kinzler, K. W. 1995. Serial analysis of gene expression. *Science,* 270**,** 484-7.

Waddington, C. H. 1957. *The Strategy of Genes. A discussion of some aspects of theoretical biology.With an appendix by H.Kascer*, George Allen & Unwin: London.

Waltenberger, J., Claesson-Welsh, L., Siegbahn, A., Shibuya, M. & Heldin, C. H. 1994. Different signal transduction properties of KDR and Flt1, two receptors for vascular endothelial growth factor. *J Biol Chem,* 269**,** 26988-95.

Wang, G. L. & Semenza, G. L. 1995. Purification and Characterization of Hypoxia-inducible Factor 1. *Journal of Biological Chemistry,* 270**,** 1230-1237.

Wang, H. X. & Ng, T. B. 1999. Natural products with hypoglycemic, hypotensive, hypocholesterolemic, antiatherosclerotic and antithrombotic activities. *Life Sci,* 65**,** 2663-77.

Wang, X., Fukuda, T., Li, W., Gao, C. X., Kondo, A., Matsumoto, A., Miyoshi, E., Taniguchi, N. & Gu, J. 2009. Requirement of Fut8 for the expression of vascular endothelial growth factor receptor-2: a new mechanism for the emphysema-like changes observed in Fut8-deficient mice. *Journal of Biochemistry,* 145**,** 643-51.

Warren, L., Manos, P. D., Ahfeldt, T., Loh, Y. H., Li, H., Lau, F., Ebina, W., Mandal, P. K., Smith, Z. D., Meissner, A., Daley, G. Q., Brack, A. S., Collins, J. J., Cowan, C., Schlaeger, T. M. & Rossi, D. J. 2010. Highly efficient reprogramming to pluripotency and directed differentiation of human cells with synthetic modified mRNA. *Cell Stem Cell,* 7**,** 618-30.

Watanabe, K., Ueno, M., Kamiya, D., Nishiyama, A., Matsumura, M., Wataya, T., Takahashi, J. B., Nishikawa, S., Nishikawa, S., Muguruma, K. & Sasai, Y. 2007. A ROCK inhibitor permits survival of dissociated human embryonic stem cells. *Nat Biotechnol,* 25**,** 681-6.

Watson, D. K., Smyth, F. E., Thompson, D. M., Cheng, J. Q., Testa, J. R., Papas, T. S. & Seth, A. 1992. The ERGB/Fli-1 gene: isolation and characterization of a new member of the family of human ETS transcription factors. *Cell Growth and Differentiation,* 3**,** 705-13.

Watt, F. M. & Huck, W. T. 2013. Role of the extracellular matrix in regulating stem cell fate. *Nat Rev Mol Cell Biol,* 14**,** 467-73.

Weibel, E. R. & Palade, G. E. 1964. New Cytoplasmic Components in Arterial Endothelia. *J Cell Biol,* 23**,** 101-12.

White, J. D., Hewett, P. W., Kosuge, D., Mcculloch, T., Enholm, B. C., Carmichael, J. & Murray, J. C. 2002. Vascular endothelial growth factor-D expression is an independent prognostic marker for survival in colorectal carcinoma. *Cancer Research,* 62**,** 1669-75.

Wilkinson, D. G., Bhatt, S. & Herrmann, B. G. 1990. Expression pattern of the mouse T gene and its role in mesoderm formation. *Nature,* 343**,** 657-9.

Wilson, A. & Trumpp, A. 2006. Bone-marrow haematopoietic-stem-cell niches. *Nat Rev Immunol,* 6**,** 93-106.

Wilson, N. K., Foster, S. D., Wang, X., Knezevic, K., Schutte, J., Kaimakis, P., Chilarska, P. M., Kinston, S., Ouwehand, W. H., Dzierzak, E., Pimanda, J. E., De Bruijn, M. F. & Gottgens, B. 2010. Combinatorial transcriptional control in blood stem/progenitor cells: genome-wide analysis of ten major transcriptional regulators. *Cell Stem Cell,* 7**,** 532-44.

Wilson, V. & Conlon, F. L. 2002. The T-box family. *Genome Biol,* 3**,** REVIEWS3008.

Wilson, V., Manson, L., Skarnes, W. C. & Beddington, R. S. 1995. The T gene is necessary for normal mesodermal morphogenetic cell movements during gastrulation. *Development,* 121**,** 877-886.

Winnier, G., Blessing, M., Labosky, P. A. & Hogan, B. L. 1995. Bone morphogenetic protein-4 is required for mesoderm formation and patterning in the mouse. *Genes & Development,* 9**,** 2105-16.

Wittler, L., Shin, E. H., Grote, P., Kispert, A., Beckers, A., Gossler, A., Werber, M. & Herrmann, B. G. 2007. Expression of Msgn1 in the presomitic mesoderm is controlled by synergism of WNT signalling and Tbx6. *EMBO Rep,* 8**,** 784-9.

Workman, C., Jensen, L. J., Jarmer, H., Berka, R., Gautier, L., Nielser, H. B., Saxild, H. H., Nielsen, C., Brunak, S. & Knudsen, S. 2002. A new non-linear normalization method for reducing variability in DNA microarray experiments. *Genome Biol,* 3**,** research0048.

Xu, F., Hazzard, T. M., Evans, A., Charnock-Jones, S., Smith, S. & Stouffer, R. L. 2005. Intraovarian actions of anti-angiogenic agents disrupt periovulatory events during the menstrual cycle in monkeys. *Contraception,* 71**,** 239-48.

Yamazaki, D., Suetsugu, S., Miki, H., Kataoka, Y., Nishikawa, S., Fujiwara, T., Yoshida, N. & Takenawa, T. 2003. WAVE2 is required for directed cell migration and cardiovascular development. *Nature,* 424**,** 452-6.

Yanagisawa, K. O., Fujimoto, H. & Urushihara, H. 1981. Effects of the Brachyury (T) mutation on morphogenetic movement in the mouse embryo. *Developmental Biology,* 87**,** 242.

Yang, X. R., Ng, D., Alcorta, D. A., Liebsch, N. J., Sheridan, E., Li, S., Goldstein, A. M., Parry, D. M. & Kelley, M. J. 2009. T (brachyury) gene duplication confers major susceptibility to familial chordoma. *Nature Genetics,* 41**,** 1176-8.

Yin, J., Ye, J. & Jia, W. 2012. Effects and mechanisms of berberine in diabetes treatment. *Acta Pharmaceutica Sinica B,* 2**,** 327-334.

Ying, Q. L., Nichols, J., Chambers, I. & Smith, A. 2003. BMP induction of Id proteins suppresses differentiation and sustains embryonic stem cell self-renewal in collaboration with STAT3. *Cell,* 115**,** 281-92.

Yoshihara, H., Arai, F., Hosokawa, K., Hagiwara, T., Takubo, K., Nakamura, Y., Gomei, Y., Iwasaki, H., Matsuoka, S., Miyamoto, K., Miyazaki, H., Takahashi, T. & Suda, T. 2007. Thrombopoietin/MPL signaling regulates hematopoietic stem cell quiescence and interaction with the osteoblastic niche. *Cell Stem Cell,* 1**,** 685-97.

Yue, R., Li, H., Liu, H., Li, Y., Wei, B., Gao, G., Jin, Y., Liu, T., Wei, L., Du, J. & Pei, G. 2012. Thrombin receptor regulates hematopoiesis and endothelial-to-hematopoietic transition. *Developmental Cell,* 22**,** 1092-100.

Zetter, B. R. 1998. Angiogenesis and tumor metastasis. *Annu Rev Med,* 49**,** 407-24.

Zhang, M., Zhang, J., Lin, S. C. & Meng, A. 2012. beta-Catenin 1 and beta-catenin 2 play similar and distinct roles in left-right asymmetric development of zebrafish embryos. *Development,* 139**,** 2009-19.